

18

# Cost Modeling and Design for Manufacturing Guidelines for Advanced Composite Fabrication

by

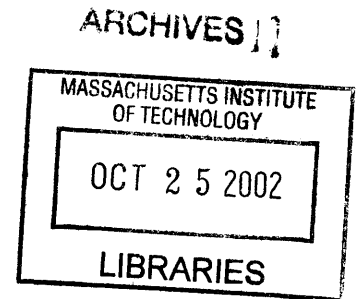
Sascha M. Haffner

Cand.-Ing. (B.S.), Mechanical Engineering

University of Kaiserslautern, 1993

Dipl.-Ing. (M.S.), Mechanical Engineering

University of Kaiserslautern, 1997



Submitted to the Department of Mechanical Engineering on May 13<sup>th</sup>, 2002 in  
Partial Fulfillment of the Requirements for the Degree of

DOCTOR OF PHILOSOPHY IN MECHANICAL ENGINEERING

at the

MASSACHUSETTS INSTITUTE OF TECHNOLOGY

June 2002

© 2002 Massachusetts Institute of Technology

All Rights Reserved

Signature of Author: .....  
Department of Mechanical Engineering  
May 13<sup>th</sup>, 2002

Certified by: .....  
Timothy G. Gutowski  
Professor, Department of Mechanical Engineering  
Chairman, Doctoral Thesis Committee

Accepted by: .....  
Ain A. Sonin  
Chairman, Department Committee on Graduate Students



# **Cost Modeling and Design for Manufacturing Guidelines for Advanced Composite Fabrication**

by  
Sascha M. Haffner

Submitted to the Department of Mechanical Engineering on May 13<sup>th</sup>, 2002 in  
Partial Fulfillment of the Requirements for the Degree of  
Doctor of Philosophy in Mechanical Engineering

## **Abstract**

Experience shows that the majority of costs are committed during the early stages of the development process. Presently, many cost estimation methods are available to the public for metal processing, but there are almost none (excluding proprietary) for advanced composite materials. Therefore, the central objective of this thesis is to provide a comprehensive overview of the costs of common composite production technologies such as Hand Layup, Resin Transfer Molding, Automated Tow Placement, Pultrusion, Forming, and Assembly. The work includes information on investment costs for production equipment and tooling as well as estimation guidelines for labor and material. Designers are presented with Design for Manufacturing guidelines (DFM) explaining how process selection and part design can lead to potential cost saving opportunities. Process based or technical cost models are well suited to quantify manufacturing costs and relate them to part design features, such as size and shape complexity. These physically based scaling principles can be easily adapted to changes in process technology and thereby reducing data requirements. In order to identify all relevant cost drivers, a detailed process plan is compiled for each composite manufacturing method. These processes can include up to 50 process steps and a total of 270 cost equations are used to calculate the cost contribution of each. A number of case studies conducted in concert with our industrial sponsors clearly identifies the best point of each production process and for example help to explain the economic benefits of co-curing versus mechanical assembly. Users can therefore study the economic consequences of design changes in detail and consequently highlight any favorable design/process combinations. To further facilitate the comparison of process performance and to promote the feedback from industry all of the models are available on the Internet at <http://web.mit.edu/lmp/www/composites/costmodel/>.

### Thesis Committee:

Dr. Timothy G. Gutowski (Chairman)  
Professor, Department of Mechanical Engineering  
Dr. Joel P. Clark  
Professor, Department of Materials Science & Engineering  
Dr. Daniel E. Whitney  
Senior Research Scientist, Center for Technology, Policy & Industrial  
Development

(This page is intentionally left blank.)

## Acknowledgements

My appreciation goes to all the people who made this work possible. I especially would like to thank my advisor, Professor Timothy Gutowski, for his guidance and commitment to the success of this study. Special thanks also to the members of my thesis committee, Professor Joel Clark and Dr. Dan Whitney, for their advice and expertise. In addition, I like to acknowledge the generous support of the National Science Foundation.

There are always a few special people who make this time worth remembering. Thanks to Sally Stiffler, Karuna Mohindra, and the administrative staff of MIT. Also, I like to mention the students who have contributed to the success of this project. Thank you, Alexandros Gorgias, Robert Lin, Anjali Goel, John Boyer, Thomas Marin, Guido Beresheim, and Joshua Pas. You have done an excellent job and it was always a pleasure working with you.

I would especially like to acknowledge my wife, Sabine, and dedicate this work to her, because she was an endless source of inspiration and strength. Thanks, also to both of our families, who believed in me and supported us throughout this exceptional phase of our lives.

(This page is intentionally left blank.)

## Table of Contents

<b>Abstract</b> .....	<b>3</b>
<b>Acknowledgements</b> .....	<b>5</b>
<b>Table of Contents</b> .....	<b>7</b>
<b>List of Figures</b> .....	<b>13</b>
<b>List of Tables</b> .....	<b>21</b>
<b>1 Introduction</b> .....	<b>25</b>
1.1 Motivation .....	26
1.2 Approach .....	27
1.3 References .....	30
<b>2 Composite Materials</b> .....	<b>33</b>
2.1 Fiber Types.....	35
2.1.1 Glass Fibers .....	36
2.1.2 Aramid Fibers.....	37
2.1.3 Carbon Fibers .....	38
2.2 Matrix Types .....	40
2.2.1 Epoxy (EP) .....	41
2.2.2 Polyester .....	42
2.2.3 Vinylester .....	42
2.2.4 Polyamide-imide (PAI) .....	42
2.2.5 Polyetheretherketon (PEEK).....	43
2.2.6 Polyethylene (PE).....	43
2.3 Material Forms .....	44
2.3.1 Continuous Rovings .....	44
2.3.2 Fabrics .....	45
2.3.3 Prepreg Fabrics.....	47
2.3.4 Unidirectional Tapes & Tows .....	48
2.4 Material Selection Guidelines .....	49
2.5 References .....	51
2.6 Appendix - Composite Materials .....	53
<b>3 Design for Manufacturing (DFM) for Composites</b> .....	<b>57</b>
3.1 Introduction .....	57

3.2	Composite Manufacturing Processes .....	59
3.2.1	Process Discriminators .....	62
3.2.2	Process Cost Drivers .....	64
3.2.3	Hand Lay-Up (HLU).....	66
3.2.4	Resin Transfer Molding (RTM).....	68
3.2.5	Automated Tow Placement Process (ATP).....	70
3.2.6	Pultrusion Process (PUL).....	72
3.2.7	Double Diaphragm Forming (DDF).....	74
3.2.8	Autoclave Curing Process .....	76
3.3	Composite Assembly Processes .....	78
3.3.1	Assembly Process Discriminators.....	78
3.3.2	Assembly Architecture and Integration of Parts .....	78
3.3.3	Assembly Cost Driver .....	79
3.3.4	Mechanical Assembly .....	81
3.3.5	Adhesive Bonding.....	85
3.3.6	Co-Curing.....	88
3.4	Reference Geometries .....	90
3.4.1	Flat Panels (C1).....	91
3.4.2	Parts with Single Curvature (C2) .....	92
3.4.3	Parts with Double Curvature (C3).....	93
3.4.4	Flange Type Parts (C4) .....	94
3.4.5	Straight L-Profiles (C5).....	95
3.4.6	Straight C-Profiles (C6) .....	96
3.4.7	Straight I-Profiles (C7).....	97
3.4.8	Straight T-Profiles (C8).....	98
3.4.9	Curved L-Profiles (C9).....	99
3.4.10	Curved C-Profiles (C10) .....	100
3.4.11	Curved I-Profiles (C11).....	101
3.4.12	Curved T-Profiles (C12).....	102
3.4.13	Straight Tubular Profiles (C13).....	103
3.4.14	Tapered Tubular Profiles (C14) .....	104
3.4.15	Straight Hollow Square Profiles (C15) .....	105
3.4.16	Rib Like Structures (C16) .....	106
3.5	Process Selection Guidelines .....	107
3.6	References .....	110
<b>4</b>	<b>Introduction into Cost Models.....</b>	<b>113</b>
4.1	Motivation for Cost Estimation.....	113
4.2	Cost Modeling Concepts .....	114
4.2.1	Rules of Thumb.....	114
4.2.2	Accounting Methods .....	114
4.2.3	Activity Based Costing.....	115
4.2.4	Process-Based Cost Models .....	115



---

4.3	Manufacturing Cost Elements .....	120
4.3.1	Operating Conditions .....	120
4.3.2	Variable Costs .....	123
4.3.3	Fixed Costs .....	125
4.3.4	Unit Costs .....	129
4.4	Time Scaling Laws .....	132
4.4.1	Process Plans .....	132
4.4.2	Cycle Time .....	132
4.4.3	Power Law Models .....	134
4.4.4	Process Physics Based Laws (1 <sup>st</sup> Order Model etc.) .....	136
4.4.5	Learning Effects .....	143
4.5	References .....	145
4.6	Appendix - Introduction into Cost Models .....	147
<b>5</b>	<b>Production Cost Models for Composites .....</b>	<b>149</b>
5.1	Complexity Scaling .....	149
5.1.1	Complexity Scaling for Fiber Composites .....	151
5.2	Cost Model Applications .....	160
5.2.1	Hand Lay-Up (HLU) .....	160
5.2.2	Resin Transfer Molding (RTM) .....	165
5.2.3	Automated Tow Placement (ATP) .....	171
5.2.4	Pultrusion (PUL) .....	179
5.2.5	Double Diaphragm Forming (DDF) .....	184
5.2.6	Autoclave Cure .....	190
5.2.7	Mechanical Assembly .....	196
5.2.8	Adhesive Assembly .....	204
5.3	References .....	207
5.4	Appendix – Production Cost Models for Composites .....	215
5.4.1	Information Theory .....	215
5.4.2	On Differential Geometry and Fibers .....	220
5.4.3	Examples of Fiber Mapping using FiberSim© .....	223
5.4.4	Process Plans & Cost Drivers .....	224
5.4.5	Composite Layup Time Estimation .....	240
<b>6</b>	<b>Production Equipment Costs .....</b>	<b>249</b>
6.1	Hand Lay-Up Equipment (HLU) .....	250
6.2	Resin Transfer Molding Machines (RTM) .....	251
6.3	Automated Tow Placement Machines (ATP) .....	254
6.4	Pultrusion Machines (PUL) .....	257
6.5	Double Diaphragm Forming Machines (DDF) .....	260

6.6	Autoclave Equipment .....	262
6.7	Vacuum Bagging Material .....	265
6.8	Assembly Equipment .....	267
6.9	References .....	277
6.10	Appendix - Production Equipment Costs .....	279
<b>7</b>	<b>Cost and Design Elements of Tooling .....</b>	<b>283</b>
7.1	Overview of Tooling for Composites .....	283
7.1.1	Tooling classified by Material .....	283
7.1.2	Tooling classified by Process .....	285
7.1.3	Material Properties and Selection Criteria .....	289
7.2	Fabrication Processes for Metal Tooling .....	296
7.2.1	Plasma Cutting .....	296
7.2.2	Metal Bending & Forming .....	298
7.2.3	Metal Casting .....	299
7.2.4	Gas Metal Arc Welding (GMAW) .....	300
7.2.5	Machining .....	302
7.2.6	Electroless Coating .....	304
7.2.7	Polishing and Finishing .....	305
7.2.8	Inspection .....	306
7.3	Open Mold Metal Tooling .....	307
7.3.1	Design Requirements .....	307
7.3.2	Material .....	308
7.3.3	Open Mold Design Features .....	308
7.3.4	Cost Components of Open Mold Tooling .....	315
7.3.5	Tooling Complexity .....	320
7.3.6	Case Study: Curing Tool for Jet Engine Caulings (Invar, Level 4) .....	322
7.3.7	Other Case Studies & Generalized Cost Model .....	335
7.4	Tooling for Resin Transfer Molding .....	339
7.4.1	Design Requirements .....	339
7.4.2	Material .....	339
7.4.3	RTM Mold Design .....	340
7.4.4	Cost Components of RTM Molds .....	343
7.4.5	Case Study: RTM Tooling .....	345
7.5	Tooling for Pultrusion .....	349
7.5.1	Design Requirements .....	349
7.5.2	Material .....	349
7.5.3	Pultrusion Die Design .....	350
7.5.4	Cost Components of Pultrusion Dies .....	351
7.5.5	Case Study: Pultrusion Die for a L-Profile .....	353
7.6	Tooling for Assembly .....	357

7.6.1	Design Requirements .....	357
7.6.2	Material .....	357
7.6.3	Assembly Fixture Design .....	358
7.6.4	Cost Components .....	359
7.7	References .....	363
7.8	Appendix - Cost and Design Elements of Tooling .....	367
7.8.1	Tooling Materials .....	367
7.8.2	Performance Data of Tool Making Processes .....	368
7.8.3	Case Study: Flat Open Mold Tool (Aluminum, Level 1) .....	371
7.8.4	Case Study: Helicopter Blade Curing Tool (Aluminum, Level 2).....	374
7.8.5	Case Study: Flat Open Mold Tool (Invar, Level 1) .....	377
7.8.6	Case Study: Horizontal Stabilizer Co-Curing Tool (Invar, Level 3) .....	379
7.8.7	Case Study: Engine Cauling Curing Tool (Invar, Level 4).....	382
7.8.8	Summary: Open Mold Tooling .....	384
7.8.9	Case Study: RTM Mold .....	386
7.8.10	Case Study: Pultrusion Die .....	388
<b>8</b>	<b>Model Implementation and WEB Design .....</b>	<b>391</b>
8.1	Excel Spreadsheet .....	392
8.2	WEB Based Cost Worksheet .....	393
8.2.1	Introduction & Navigation .....	394
8.2.2	Process Selection Matrix .....	394
8.2.3	Part Definition Interface.....	395
8.2.4	Material Costs .....	396
8.2.5	Process Plan Selection.....	397
8.2.6	Cycle Time .....	397
8.2.7	Cost Summary .....	398
8.2.8	Resource Databases.....	399
8.2.9	Programming Details.....	399
8.3	Summary of the WEB Implementation.....	401
8.4	References .....	402
8.5	Appendix .....	403
<b>9</b>	<b>Results &amp; Discussion.....</b>	<b>407</b>
9.1	Case Study 1: Component Production Processes.....	408
9.1.1	Production Scenario .....	408
9.1.2	Hand Lay-Up (HLU).....	412
9.1.3	Resin Transfer Molding (RTM) .....	416
9.1.4	Automated Tow Placement (ATP).....	420
9.1.5	Pultrusion (PUL) .....	424
9.1.6	Double Diaphragm Forming (DDF).....	428
9.1.7	Summary & Process Comparison .....	432

9.2	Case Study 2: Composite Assembly Processes.....	437
9.2.1	Production Scenario .....	437
9.2.2	Co-Cure .....	440
9.2.3	Mechanical Assembly .....	443
9.2.4	Adhesive Assembly.....	448
9.2.5	Summary & Process Comparison .....	452
9.3	Case Study 3: Assembly of a Horizontal Stabilizer.....	455
9.3.1	Design & Manufacturing Conditions .....	455
9.3.2	Co-Cured Design.....	459
9.3.3	Black Aluminum Design .....	468
9.3.4	Design & Cost Comparison.....	473
9.4	References .....	476
9.5	Appendix - Results & Discussion .....	479
9.5.1	Prices for Tooling & Equipment .....	479
9.5.2	Hand Layup (HLU) - Manufacturing Data .....	480
9.5.3	Resin Transfer Molding (RTM) - Manufacturing Data .....	481
9.5.4	Automated Tow Placement (ATP) - Manufacturing Data .....	482
9.5.5	Pultrusion (PUL) - Manufacturing Data.....	483
9.5.6	Double Diaphragm Forming (DDF) - Manufacturing Data .....	484
9.5.7	Assembly - Manufacturing Data .....	485
9.5.8	Co-Cure - Manufacturing Data .....	485
9.5.9	Mechanical Assembly - Manufacturing Data.....	486
9.5.10	Adhesive Bonding - Manufacturing Data .....	487
9.5.11	Horizontal Stabilizer - Component Manufacturing Data .....	488
9.5.12	Co-Cured Stabilizer - Assembly Data.....	489
9.5.13	Black Alu Design - Assembly Data .....	490
<b>10</b>	<b>Conclusions &amp; Outlook.....</b>	<b>491</b>

## List of Figures

Figure 1.1	Composites Use in Structural Aircraft Components.....	25
Figure 1.2	Co-Cure of B777 Empenage, JSF X-32 Cure Mold (31' x 21' x 4') [10]	26
Figure 1.3	Cost Components of Aircraft Production [9, 10].....	28
Figure 2.1	Comparison of Matrix Properties.....	41
Figure 2.2	Continuous Aramid Rovings [19].....	45
Figure 2.3	Woven Glass-, Carbon-, and Aramid Fabric [19, 21, 22, 24].....	45
Figure 2.4	a) Plain Weave, b) Basket Weave, c) Twill, d) Crowfoot Satin, e) 8-end Satin, f) 5-end Satin [1].....	46
Figure 2.5	Unidirectional Prepreg Tape and Tows [20].....	48
Figure 2.6	Material Selection Matrix for Manufacturing.....	50
Figure 2.7	Average Material Costs (G/E: \$1/lb, C/E: \$60/lb, A/E: \$50/lb).....	53
Figure 2.8	Average Glass/Epoxy Costs (G/E: \$1/lb).....	53
Figure 2.9	Glass Fiber Roving Properties.....	54
Figure 2.10	Glass Fiber Roving Properties.....	54
Figure 2.11	Carbon Fiber Roving Properties.....	54
Figure 2.12	Glass Fiber Woven Fabric (* in laminate).....	55
Figure 2.13	Aramid Fiber Woven Fabric (** approximate value).....	55
Figure 2.14	Carbon Fiber Woven Fabric (* in laminate).....	55
Figure 2.15	Various Prepregs (** properties of the dry fiber).....	55
Figure 2.16	Thermoset Neat Resins (* for laminate; ** HDT 1.82 MPa).....	56
Figure 2.17	Thermoplastic Neat Resins (***) HDT 0.455 MPa).....	56
Figure 3.1	Role of Design for Manufacturing Concepts.....	57
Figure 3.2	Cost Saving Opportunities over Project Evolution [2].....	58
Figure 3.3	Laminate Properties and Fiber Orientation.....	61
Figure 3.4	Hand Lay-Up Process (HLU).....	66
Figure 3.5	Resin Transfer Molding Process (RTM) [2, 12].....	68
Figure 3.6	Automated Tow Placement Process (ATP) [17].....	70
Figure 3.7	Pultrusion Process (PUL) [25].....	72
Figure 3.8	Double Diaphragm Forming Process (DDF) [26, 27].....	74
Figure 3.9	Autoclave Curing Process [28, 29].....	76
Figure 3.10	Skin Stringer - vs. Sandwich Composite Design [31, 32].....	78
Figure 3.11	Composite Fuselage Side Panel vs. Aluminum Baseline [31].....	79
Figure 3.12	Expected Trade-off between Investment and Variable Costs.....	80
Figure 3.13	Fastener Spacing (Fastener Diameter: d) [2].....	81
Figure 3.14	Titanium Lockbolt Fasteners [33].....	82

---

Figure 3.15	Titanium Blind Bolt Fasteners [33].....	83
Figure 3.16	Automated Fastening Machine [34].....	84
Figure 3.17	Bonded Joint Configurations [2].....	85
Figure 3.18	Schematic of Co-Curing, Co-Cured Skin Stringer Assembly [32].....	88
Figure 3.19	Overview of the Reference Geometries.....	90
Figure 3.20	Flat Panels (C1).....	91
Figure 3.21	Parts with Single Curvature (C2).....	92
Figure 3.22	Parts with Double Curvature (C3).....	93
Figure 3.23	Shrink- and Stretch Flange (C4).....	94
Figure 3.24	Straight L-Profiles (C5).....	95
Figure 3.25	Straight C-Profiles (C6).....	96
Figure 3.26	Straight I-Profiles (C7).....	97
Figure 3.27	Straight T-Profiles (C8).....	98
Figure 3.28	Curved L-Profiles (C9).....	99
Figure 3.29	Curved C-Profiles (C10).....	100
Figure 3.30	Curved I-Profiles (C11).....	101
Figure 3.31	Curved T-Profiles (C12).....	102
Figure 3.32	Straight Tubular Profiles (C13).....	103
Figure 3.33	Tapered Tubular Profiles (C14).....	104
Figure 3.34	Straight Hollow Square Profiles (C15).....	105
Figure 3.35	Rib Like Structures (C16).....	106
Figure 3.36	Process Capability Matrix.....	107
Figure 3.37	Process Selection Matrix.....	109
Figure 4.1	Process Based Cost Estimation Model.....	116
Figure 4.2	Process Flow and Scope of Model (Example: Hand Lay-Up).....	117
Figure 4.3	Manufacturing Cost Elements.....	120
Figure 4.4	Unit Costs vs. Production Volume.....	131
Figure 4.5	Power Law Model (Example Layout) [24].....	135
Figure 4.6	1 <sup>st</sup> Order Model (Velocity Response and Size Scaling).....	138
Figure 4.7	Impact of 1 <sup>st</sup> Order Parameter Increases.....	139
Figure 4.8	Hyperbolic Size Scaling Model.....	142
Figure 4.9	Comparison of Size Scaling Models.....	142
Figure 4.10	Learning Curve Effects.....	143
Figure 4.11	Derivation of the Hyperbolic Model.....	147
Figure 5.1	Manufacturing Time vs. Weight of 209 Composite Parts [45].....	150
Figure 5.2	Complexity of Composites and Information Content [35, 36, 37, 62]....	151
Figure 5.3	Discretization of a Curved Fiber.....	153
Figure 5.4	Fiber Segmented into N Pieces.....	154

Figure 5.5	Discretization of a Fiber Network.....	155
Figure 5.6	Fiber Mapping and Complexity Scaling .....	157
Figure 5.7	Process Flow of Hand Lay-Up.....	160
Figure 5.8	Complexity and Process Analogies.....	161
Figure 5.9	Model Verification (Stretch Flange) .....	163
Figure 5.10	Resin Transfer Molding [50].....	165
Figure 5.11	Process Flow of RTM .....	166
Figure 5.12	Infinitesimal Laminate Element.....	166
Figure 5.13	Automated Tow Placement .....	171
Figure 5.14	Process Flow of ATP.....	172
Figure 5.15	Machine Velocity Profile; Lengths of the Fiber Strip.....	172
Figure 5.16	Single Fiber Ply.....	174
Figure 5.17	Pultrusion .....	179
Figure 5.18	Process Flow of Pultrusion.....	180
Figure 5.19	Pultrusion Die Model .....	180
Figure 5.20	Die Cross-Section.....	181
Figure 5.21	Verification of the Scaling Law .....	182
Figure 5.22	Schematic of the Double Diaphragm Forming Process .....	184
Figure 5.23	Process Flow of Double Diaphragm Forming.....	184
Figure 5.24	Schematic of the Heating/Cooling Process .....	185
Figure 5.25	Vacuum Bagging, Autoclave Operation [65, 66].....	190
Figure 5.26	Process Flow of Autoclave Cure.....	191
Figure 5.27	Schematic of the Autoclave Heating Process.....	191
Figure 5.28	Typical Cure Cycle for Epoxy Resins.....	194
Figure 5.29	Single Lap Joint Large Assembly Fixture.....	196
Figure 5.30	Process Flow of Mechanical Assembly .....	197
Figure 5.31	Single Lap Joint, Mechanically Fastened.....	198
Figure 5.32	Process Flow of Adhesive Assembly .....	204
Figure 5.33	Single Lap Joint, Adhesively Bonded.....	205
Figure 5.34	Average Information Content vs. Probability of a Character i. ....	216
Figure 5.35	Information Content (Binary Case).....	217
Figure 5.36	Maximum Average Information Content (Equiprobable Case).....	218
Figure 5.37	Definition of Curvature .....	220
Figure 5.38	Relation of Shear Slip and Enclosed Angle .....	221
Figure 5.39	Gauss-Bonnet Theorem.....	222
Figure 5.40	Stretchflange $R = 20"$ , $90$ deg , Flange Width = $4"$ .....	223
Figure 5.41	Shrinkflange $R = 120"$ , $30$ deg , Flange Width = $2"$ .....	223
Figure 5.42	Schematic of a Wing Rib .....	223

---

Figure 5.43	Flat Panel (36" x 36" x 1/8", quasi-isotropic).....	225
Figure 5.44	Hand Layup of Flat Panel (36" x 36" x 1/8", quasi-isotropic).....	225
Figure 5.45	Curved L-Profile (R90" x 4.25" x 3.25" x 1/4 ") .....	227
Figure 5.46	RTM of a Curved L-Profile (R90" x 4.25" x 3.25" x 1/4 ").....	227
Figure 5.47	Simple Curved Part (R90" x 90" x 1/4").....	229
Figure 5.48	ATP of a Curved Part (R90" x 90" x 1/4").....	229
Figure 5.49	Straight C – Profile (4" x 3" x 1/4" x 30 ft.) .....	231
Figure 5.50	Pultrusion of a Straight C – Profile (4" x 3" x 1/4" x 30 ft.).....	231
Figure 5.51	Simple Curved Part (R90" x 90" x 1/4").....	233
Figure 5.52	Forming of a Simple Curved Part (R90" x 90" x 1/4") .....	233
Figure 5.53	Flat Panel (36" x 36" x 1/8", quasi-isotropic).....	235
Figure 5.54	Autoclave Cure of a Flat Panel (36" x 36" x 1/8") .....	235
Figure 5.55	Lap Joint Dimensions: Lx=12", Ly = 108", w = 2", s = 1", d = 1/4" .....	237
Figure 5.56	Mechanical Joining of a Single Lap Joint .....	237
Figure 5.57	Lap Joint Dimensions: Lx=12", Ly = 108", w = 2" .....	239
Figure 5.58	Adhesive Joining of a Single Lap Joint.....	239
Figure 5.59	Layup of a Flat Panel using Woven Prepreg.....	240
Figure 5.60	Comparison of Layup Times for Flat Panels .....	240
Figure 5.61	Layup of a L-Profile using Woven Prepreg .....	241
Figure 5.62	Comparison of Layup Times for L-Profiles .....	242
Figure 5.63	Layup of a Curved Panel (Small Radii) using Woven Prepreg.....	242
Figure 5.64	Layup of a Curved Panel (Large Radii) using Woven Prepreg.....	243
Figure 5.65	Layup of a Stretch Flange using Woven Prepreg.....	244
Figure 5.66	Comparison of Layup Times for Stretch Flanges .....	245
Figure 5.67	Layup of a Shrink Flange using Woven Prepreg .....	246
Figure 5.68	Comparison of Layup Times for Shrink Flanges .....	246
Figure 6.1	RTM Injection Equipment (Piston Type, Extruder Type) [20, 22].....	251
Figure 6.2	RTM Equipment vs. Mixing Ratio [29].....	252
Figure 6.3	RTM Equipment vs. Shot Size [25, 29] .....	253
Figure 6.4	ATP Machine (Viper 1200) [14].....	254
Figure 6.5	Tape Laying Machine [21].....	255
Figure 6.6	Pultrusion Equipment (Belt Type) [17].....	257
Figure 6.7	Pultrusion Equipment (Reciprocating) [19] .....	258
Figure 6.8	Pultrusion Equipment Price vs. Pulling Capacity .....	259
Figure 6.9	Pultrusion Equipment Price vs. Part Envelope Area.....	259
Figure 6.10	Custom-built Double Diaphragm Forming Machine [6].....	260
Figure 6.11	Very Large Autoclave (D18ft x 60ft) [27].....	262
Figure 6.12	Medium to Large Autoclave (D5ft x 12ft) [12] .....	263



Figure 6.13	Autoclave Price vs. Internal Volume .....	263
Figure 6.14	Vacuum Bagging [5] .....	265
Figure 6.15	Vacuum Bagging Prices vs. Part Area .....	266
Figure 6.16	Automated Fastening Machine [9].....	267
Figure 6.17	Typical One- and Two-Piece Fastener Geometries [9].....	268
Figure 6.18	Typical Automatic Fastening Cycle [8] .....	269
Figure 6.19	ESCRT™ AFS Machine Concepts [9].....	270
Figure 6.20	Airbus Assembly - 5-Axis Riveting Machines [8].....	273
Figure 6.21	Airbus Assembly - Tacking & Cleanup Fixtures [8] .....	274
Figure 6.22	Aerospatial Assembly - 5-Axis Clamping and AFS Machine [8].....	275
Figure 6.23	Boeing Assembly - 5-Axis AFS Machines [8] .....	276
Figure 7.1	Invar Layup Tool for Rocket Motor Casing [29].....	286
Figure 7.2	Design Features of a Matched-Die Mold Set for RTM [3].....	287
Figure 7.3	Aluminum Bonding Jig [29] .....	288
Figure 7.4	CNC-Plasma Cutter [42] .....	296
Figure 7.5	CNC-Press Brake [38].....	298
Figure 7.6	Metal Casting Processes [36].....	299
Figure 7.7	GMAW Welding [39] .....	300
Figure 7.8	Endmill & Facemill [37] .....	302
Figure 7.9	Electroless Nickel [41] .....	304
Figure 7.10	Power Tool & Polishing [29, 35] .....	305
Figure 7.11	CMM & Laser Tracker Inspection [29] .....	306
Figure 7.12	Welded or Electroformed Tooling Face.....	309
Figure 7.13	Tool Face with Eggcrate Support Structure .....	311
Figure 7.14	Individual Stiffener Plate w/ Cut-Outs for Air Flow.....	312
Figure 7.15	Complexity Levels of Open Mold Tooling [29] .....	321
Figure 7.16	Autoclave Tool for Engine Cauling [29].....	322
Figure 7.17	Schematic of the Engine Cauling Tool (Bottom View) [29] .....	323
Figure 7.18	Plasma Cut Invar Plates for the Substructure [29] .....	324
Figure 7.19	Welding of the Substructure [29] .....	325
Figure 7.20	Stress Relieving and Die Pen Checking Prior to Machining [29].....	329
Figure 7.21	Rough and Finish Machining on 5 Axis CNC Milling Center [29] .....	330
Figure 7.22	Install Vacuum Plumbing and Fairings [29] .....	331
Figure 7.23	Polishing to a 63 μin. Finish [29].....	332
Figure 7.24	Final Contour Inspection using a Laser Tracker [29] .....	332
Figure 7.25	Distribution of the Total Costs (excluding Profit) .....	334
Figure 7.26	Total Cost Distribution of an Average Aluminum/Invar Tool.....	336
Figure 7.27	Price Estimation Chart for Open Mold Tooling.....	337

---

Figure 7.28	Prices for Flat (Level 1) Open Mold Tooling [29].....	338
Figure 7.29	RTM Part.....	345
Figure 7.30	Male RTM Mold [5].....	346
Figure 7.31	Female RTM Mold [5] .....	346
Figure 7.32	Dimensions of the L-Profile.....	353
Figure 7.33	Design Features of a Pultrusion Die.....	354
Figure 7.34	Work Piece Dimensions .....	355
Figure 7.35	Schematic of a Locator Feature.....	358
Figure 7.36	Fixture for the Assembly of a Horizontal Stabilizer .....	361
Figure 7.37	Modern Modular Tooling System [31] .....	362
Figure 7.38	Flat (Level 1) Aluminum Tooling (Courtesy of Remmele) .....	371
Figure 7.39	Total Cost Distribution for a Flat Aluminum Tool .....	372
Figure 7.40	Manufacturing Cost Distribution of the Flat Aluminum Tool .....	372
Figure 7.41	Helicopter Blade Curing Tool (Aluminum, Level 2) [29] .....	374
Figure 7.42	Total Cost Distribution of the Helicopter Blades Tooling .....	375
Figure 7.43	Manufacturing Cost Distribution of the Helicopter Blades Tooling.....	375
Figure 7.44	Total Cost Distribution of the Flat Invar Tooling .....	377
Figure 7.45	Manufacturing Cost Distribution of the Flat Invar Tooling.....	378
Figure 7.46	Horizontal Stabilizer Co-Curing Tool (Invar, Level 3) [7].....	379
Figure 7.47	Total Cost Distribution of the Horizontal Stabilizer Tooling .....	380
Figure 7.48	Manufacturing Cost Distribution of the Horizontal Stabilizer Tooling ..	380
Figure 7.49	Distribution of the Manufacturing Costs.....	383
Figure 7.50	Schematic of the Engine Cauling Tool (Frontal View).....	383
Figure 7.51	Distribution of the Total Costs .....	384
Figure 7.52	Manufacturing Cost Distribution of the Average Aluminum Tool.....	385
Figure 7.53	Manufacturing Cost Distribution of the Average Invar Tool.....	385
Figure 8.1	Map of the WEB Based Cost Estimation Model.....	394
Figure 8.2	Estimation Flow Chart .....	395
Figure 8.3	Design and Production Data Entry Form .....	396
Figure 8.4	Material Cost Interface.....	396
Figure 8.5	Definition of Additional Process Steps .....	397
Figure 8.6	Summary of the Manufacturing Costs .....	398
Figure 8.7	Interaction of WEB Languages .....	400
Figure 8.8	Spreadsheet Based Production Cost Model (HLU) .....	403
Figure 8.9	Process for Hand Layup (Default Steps are Checked).....	404
Figure 8.10	Process Cost by Mfg. Step .....	405
Figure 8.11	Process Cost by Step (cont' from Figure 8.10).....	406
Figure 9.1	Scope of Production Model.....	409

---

Figure 9.2	Sketch of Sample Production Part.....	410
Figure 9.3	Schematic of Quasi-Isotropic Laminate.....	410
Figure 9.4	Hand Layup Manufacturing Time Distribution (Batch Size 10).....	414
Figure 9.5	Distribution of Hand Layup Costs (Total Production 500 Parts).....	415
Figure 9.6	RTM Manufacturing Time Distribution (Batch Size 10).....	418
Figure 9.7	Distribution of RTM Costs (Total Production 500 Parts).....	419
Figure 9.8	ATP Manufacturing Time Distribution (Batch Size 10).....	422
Figure 9.9	Distribution of ATP Costs (Total Production 500 Parts).....	423
Figure 9.10	Pultrusion Manufacturing Time Distribution (Batch Size 10).....	426
Figure 9.11	Distribution of Pultrusion Costs (Total Production 500 Parts).....	427
Figure 9.12	Forming Manufacturing Time Distribution (Batch Size 10).....	430
Figure 9.13	Distribution of Forming Costs (Total Production 500 Parts).....	431
Figure 9.14	Process Performance .....	432
Figure 9.15	Manufacturing Tooling Costs.....	434
Figure 9.16	Manufacturing Unit Costs (incl. Tooling, Batch Size 1).....	435
Figure 9.17	Cost Distribution of Hand Layup, ATP, RTM & Pultrusion .....	436
Figure 9.18	Scope of the Assembly Model .....	438
Figure 9.19	Mechanical and Adhesive Assembly of the Sample Structure .....	438
Figure 9.20	Distribution of Co-Curing Costs (Total Production 500 Parts) .....	442
Figure 9.21	Mechanical Assembly Time Distribution (w/o Component Production).....	445
Figure 9.22	Distribution of Mech. Assembly Costs (Total Production 500 Parts) ....	447
Figure 9.23	Adhesive Bonding Time Distribution (w/o Component Production) ....	450
Figure 9.24	Distribution of Adhesive Bonding Costs (Total Production 500 Parts)..	451
Figure 9.25	Assembly Production Time (incl. Component Production).....	452
Figure 9.26	Assembly Unit Costs (incl. Tooling, Batch Size 1) .....	453
Figure 9.27	Costs of Mechanical-, and Adhesive Assembly (500 Assemblies).....	454
Figure 9.28	Horizontal Stabilizer of a Large Cargo Plane .....	455
Figure 9.29	Main Box of the Right Stabilizer .....	456
Figure 9.30	Design Detail of Horizontal Stabilizer Main Box .....	457
Figure 9.31	Assembly Detail and Fasteners .....	458
Figure 9.32	Side & Frontal View of the Skin Cross-Section .....	459
Figure 9.33	Stringer Layup and Preparation of Skin/Stringer Co-Cure .....	460
Figure 9.34	Main Box Assembly Fixture .....	464
Figure 9.35	Evolution of Unit Costs with Cumulative Production Volume .....	474
Figure 9.36	Part Cycle Time.....	479
Figure 9.37	Schematic of an Aluminum Rib.....	488
Figure 9.38	Time Driver – Component Production.....	488
Figure 9.39	Co-Cured Design: Time Driver – Assembly.....	489

Figure 9.40 Black Alu Design: Time Driver – Assembly .....490  
Figure 10.1 Production Layout for Composite Aircraft Production.....491

## List of Tables

Table 2.1	Common Fiber Properties .....	35
Table 2.2	Common Matrix Properties .....	40
Table 4.1	Example of Power Law Models (Lay Up) [24].....	134
Table 5.1	1 <sup>st</sup> Order Parameters for Hand Layup .....	163
Table 5.2	Kinetic Cure Parameters [49, 63].....	169
Table 5.3	RTM Cost and Performance Data .....	169
Table 5.4	ATP Performance Data .....	176
Table 5.5	Resulting ATP Performance Data .....	178
Table 5.6	Pultrusion Performance Data [27, 89].....	182
Table 5.7	Thermal Material Properties [44, 64].....	187
Table 5.8	Rib Chord Forming Data [54] .....	188
Table 5.9	Kinetic Cure Parameters [49].....	194
Table 5.10	Model Parameter of dominant Mechanical Assembly Processes [28]....	203
Table 5.11	Model Parameter of dominant Adhesive Assembly Processes .....	206
Table 6.1	AFS Machine Size Categories.....	270
Table 6.2	AFS Cost Matrix .....	271
Table 6.3	RTM Equipment [25 ,29].....	279
Table 6.4	Pultrusion Equipment [16, 17, 19, 23] .....	279
Table 6.5	Autoclave Equipment [12, 27] .....	280
Table 6.6	Bagging Material [11] .....	281
Table 6.7	AFS Machine Part Size Envelopes [9].....	282
Table 6.8	AFS Machine Costs [9] .....	282
Table 7.1	Properties of Common Tooling Materials.....	294
Table 7.2	Typical Horizontal Welding Rates .....	301
Table 7.3	Typical Vertical Welding Rates .....	301
Table 7.4	Typical Machining Parameters.....	303
Table 7.5	Electroless Nickel Properties .....	304
Table 7.6	Generic Process Plan for Open Mold Tooling .....	316
Table 7.7	Material Costs for Engine Cauling Tool .....	323
Table 7.8	Processing Data for the Cutting of the Substructure Elements .....	324
Table 7.9	Processing Data for the Welding of the Substructure .....	325
Table 7.10	Processing Data for the Machining of the Substructure.....	326
Table 7.11	Processing Data for the Machining of the Substructure.....	326
Table 7.12	Processing Data for the Forming & Fitting of the Face Sheet Elements	327
Table 7.13	Processing Data for the Welding of the Tool Face .....	328

Table 7.14	Processing Data for the Deburring of the Welding Seams.....	328
Table 7.15	Processing Data for Heat Treatment .....	329
Table 7.16	Processing Data for the Machining of the Tool Face Contours .....	330
Table 7.17	Cost Estimates of the Optional Details .....	331
Table 7.18	Processing Data for the Polishing of the Tool Face .....	331
Table 7.19	Processing Data for the Contour Inspection & Leak Test.....	332
Table 7.20	Summary of the Engine Cauling Curing Tool .....	333
Table 7.21	Summary of Open Mold Tooling Prices .....	335
Table 7.22	Distribution of the Total Costs for Open Mold Tooling .....	336
Table 7.23	Aluminum Properties .....	340
Table 7.24	Aggregated Manufacturing Process Plan for RTM Molds .....	344
Table 7.25	Mold Design Parameters .....	345
Table 7.26	Aggregated Manufacturing Costs.....	347
Table 7.27	Manufacturing Costs Summary.....	348
Table 7.28	Tool Steel Properties .....	349
Table 7.29	Aggregated Manufacturing Process Plan .....	352
Table 7.30	Die Design Parameters .....	354
Table 7.31	Aggregated Manufacturing Costs.....	355
Table 7.32	Manufacturing Costs Summary.....	356
Table 7.33	Fixture Costs for Constant Curvature Assemblies (Fuselage Panels).....	360
Table 7.34	Fixture Costs for Variable Curvature Assemblies (Wing Skins) .....	360
Table 7.35	Material Selection Chart for Tooling (Part 1) .....	367
Table 7.36	Material Selection Chart for Tooling (Part 2) .....	367
Table 7.37	Typical Cutting Speeds for Plasma Cutting [42] .....	368
Table 7.38	Process Time for Metal Bending [23] .....	369
Table 7.39	Polishing Speeds using Rotary Air Power Tools .....	370
Table 7.40	Cost Details of the Flat Aluminum Tool.....	373
Table 7.41	Cost Details of the Helicopter Blade Tool .....	376
Table 7.42	Cost Details of the Flat Invar Tooling.....	378
Table 7.43	Cost Details of the Horizontal Stabilizer Tooling.....	381
Table 7.44	Cost Summary for the Engine Cauling Tool .....	382
Table 7.45	Labor and Machine Costs for Engine Cauling Tool .....	382
Table 7.46	Distribution of Material and Manufacturing Costs .....	384
Table 7.47	Detailed Process Plan for Making a RTM Mold.....	386
Table 7.48	Detailed Process Plan for Making a Pultrusion Die.....	388
Table 9.1	Sample Part Characteristics.....	411
Table 9.2	Investment Costs for Hand Layup & Autoclave Cure .....	412
Table 9.3	Hand Layup Manufacturing Time.....	413

---

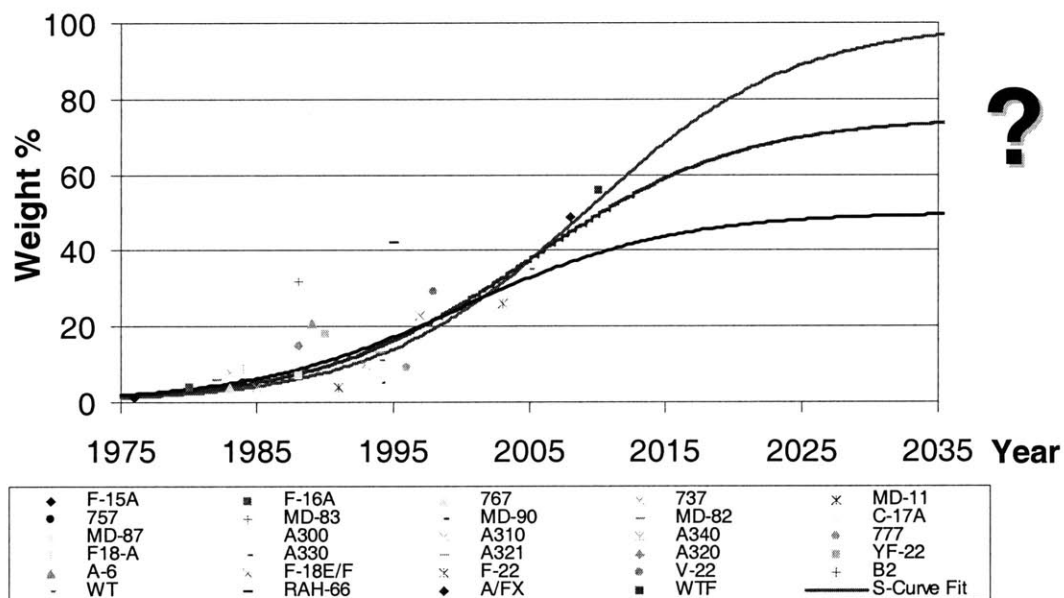
Table 9.4	Hand Layup Manufacturing Costs (Batch Size 1) .....	414
Table 9.5	Investments for Resin Transfer Molding .....	417
Table 9.6	RTM Manufacturing Time .....	417
Table 9.7	RTM Manufacturing Costs (Batch Size 1).....	419
Table 9.8	Investments for Automated Tow Placement .....	420
Table 9.9	ATP Manufacturing Time .....	421
Table 9.10	ATP Manufacturing Costs (Batch Size 1).....	423
Table 9.11	Investments for Pultrusion .....	424
Table 9.12	Pultrusion Manufacturing Time .....	425
Table 9.13	Pultrusion Manufacturing Costs (Batch Size 1).....	427
Table 9.14	Investments for Double Diaphragm Forming .....	428
Table 9.15	Forming Manufacturing Time .....	429
Table 9.16	Forming Manufacturing Costs (Batch Size 1).....	431
Table 9.17	Layup Performance without the Cure Cycle .....	433
Table 9.18	Manufacturing Unit Costs (incl. Tooling, Batch Size 1).....	434
Table 9.19	Sample Structure Characteristics (w/o Fasteners).....	439
Table 9.20	Investment Costs for Hand Layup & Autoclave Co-Cure .....	440
Table 9.21	Co-Curing Cycle Time .....	441
Table 9.22	Co - Curing Costs (Batch Size 1, incl. Component Costs) .....	442
Table 9.23	Investments for Mechanical Assembly .....	444
Table 9.24	Mechanical Assembly Cycle Time (w/o Component Production).....	445
Table 9.25	Mech. Assembly Costs (Batch Size 1, incl. Component Costs) .....	446
Table 9.26	Investments for Adhesive Bonding .....	449
Table 9.27	Adhesive Bonding Cycle Time (w/o Component Production) .....	449
Table 9.28	Adhesive Bonding Costs (Batch Size 1, incl. Component Costs).....	451
Table 9.29	Assembly Unit Costs (incl. Tooling, Batch Size 1) .....	453
Table 9.30	Summary of the Component Parameters.....	458
Table 9.31	Consolidated Process Plan for the Skin/Stringer Co-Cure.....	461
Table 9.32	Component Manufacturing Costs.....	462
Table 9.33	Manufacturing Tooling Costs (Co-Cure).....	463
Table 9.34	Consolidated Assembly Process Plan (Co-Cure Design).....	465
Table 9.35	Assembly Costs (Co-Cure Design) .....	466
Table 9.36	Manufacturing Tooling Costs (Black Aluminum Design).....	469
Table 9.37	Assembly Costs (Black Aluminum Design) .....	471
Table 9.38	Costs of Co-Cured vs. Black Aluminum Design .....	473
Table 9.39	Hourly Equipment Rates at Different Capital & Maintenance Costs ....	479
Table 9.40	Price of Production Tooling .....	479
Table 9.41	Hand Layup Manufacturing Times & Performance.....	480

Table 9.42	Hand Layup - Manufacturing Time Distribution .....	480
Table 9.43	RTM Tooling Costs.....	481
Table 9.44	RTM Manufacturing Times & Performance .....	481
Table 9.45	RTM - Manufacturing Time Distribution .....	481
Table 9.46	ATP Tooling Costs.....	482
Table 9.47	ATP Manufacturing Times & Performance .....	482
Table 9.48	ATP - Manufacturing Time Distribution .....	482
Table 9.49	Pultrusion Tooling Costs.....	483
Table 9.50	Pultrusion Manufacturing Times & Performance .....	483
Table 9.51	Pultrusion - Manufacturing Time Distribution.....	483
Table 9.52	DDF Manufacturing Times & Performance.....	484
Table 9.53	DDF - Manufacturing Time Distribution .....	484
Table 9.54	Assembly Production Time (incl. Component Production).....	485
Table 9.55	Co-Curing Costs w/o Tooling .....	485
Table 9.56	Mechanical Assembly Cycle Time (incl. Component Production).....	486
Table 9.57	Mech. Assembly - Time Distribution (w/o Component Production).....	486
Table 9.58	Mech. Assembly Costs (w/o Component Costs).....	486
Table 9.59	Adhesive Bonding Cycle Time (incl. Component Production) .....	487
Table 9.60	Adhesive Bonding - Time Distribution (w/o Component Production)...	487
Table 9.61	Adhesive Bonding Costs (w/o Component Costs).....	487
Table 9.62	Manufacturing Time Distribution .....	488
Table 9.63	Co-Cured Design: Assembly Time Distribution.....	489
Table 9.64	Black Alu Design: Assembly Time Distribution .....	490



# 1 Introduction

To fully exploit the performance benefits of modern composite materials in terms of weight, strength, and stiffness at a minimal cost, accurate cost models are necessary to guide designers and project managers. Their application assists in the evaluation of cost reduction strategies and their impact on component production and final assembly cost. Designers are facing the challenge of making important design decisions early on in the development process, while being confronted with rapidly evolving production techniques. Understanding the full impact of design modifications under these circumstances on production will aid the business to remain competitive in the market place. Therefore, the central objective of this thesis is to provide a comprehensive overview of the costs of common composite production technologies such as Hand Layup, Resin Transfer Molding, Automated Tow Placement, Pultrusion, Forming, and Assembly. Hereby it is central to generalize effectively the enormous amount of trade-off scenarios and their implementation into a computer based costing solution.



**Figure 1.1 Composites Use in Structural Aircraft Components**

## 1.1 Motivation

In general, the substitution of advanced composite materials for metals is primarily based on performance [1-6]. However, these benefits come at a cost premium and therefore efforts to reduce manufacturing cost can not entirely rely on the economy of scale, but also require the introduction of new production techniques and design concepts in order to remain economical [3]. The rapid development of production automation along with the increased integration of parts presents difficulties to cost estimators. Frequent updating of cost models without available historical production data is limited by the complexity of existing models [7-9]. However, a key element to cost reduction is the ability to provide the designer with quick information on development, investment, material and labor cost. Previous work [9-17] has shown that process based cost estimating models facilitate model maintenance due to increased transparency and the reduction of data requirements. Such an approach can be based upon size and complexity scaling laws for common composite part fabrication and assembly processes [9-11]. The models can aid process selection and give the designer information about the sensitivity of costs in terms of material, design features, and production volume. It is possible to use the new tools to assess the cost impact of new technologies, government regulations, or changes in customer preferences and market conditions. Primarily this study focuses on manufacturing cost and design for manufacturing guidelines. Future studies might address the total costs incurred during the life cycle of the product. These costs can include costs, which arise during the production, the usage and the end-of-life phase of a product and are generally borne by different entities [14].

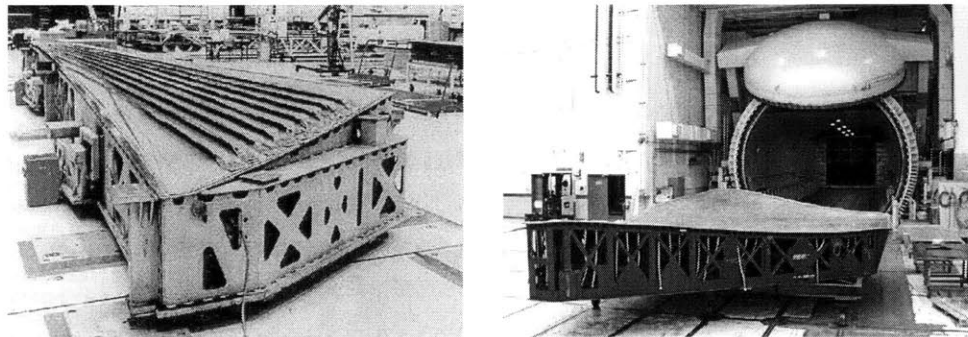


**Figure 1.2** Co-Cure of B777 Empennage, JSF X-32 Cure Mold (31' x 21' x 4') [10]

## 1.2 Approach

In order to obtain a comprehensive picture of the production costs of components and composite structures, the following topics have to be studied.

### Material Costs

Essential to any production cost model are the material costs. Selection criteria and a summary of the typical material properties, help engineers to quickly identify a suitable combination of fiber and matrix materials. In addition, a database containing around 100 entries provides information on material prices and common stock sizes.

### Design for Manufacturing Guidelines

Commonly, the design process is divided into a concept development, preliminary design, detailing, and production planning stage. Industry experience shows that the majority of component costs are committed in the first two stages of the development process. Therefore, a thorough understanding of how these costs are generated is essential to cost reduction. An analysis of the design parameters and their effects on part production can provide insight into cost / design relations. Process selection and design for manufacturing guidelines provide a general overview of available composite manufacturing methods, the major area of their application and their capabilities in terms of size, complexity and production volume [12]. They are intended to help people new to the field, to quickly narrow down the choice of processes suited for their particular manufacturing needs [19-21].

### Cost Modeling Strategies

Process based or technical cost models are well suited to relate manufacturing cost to design features, material type, and fabrication method [14-16]. Technical cost models are founded on an analysis of the process physics. These models therefore exhibit improved predictive capabilities, adapt quickly to changing process conditions, and require little user expertise and historical production data [2, 8]. Manufacturing time and cost often scale with various summary descriptors of the part design, such as size and complexity.

For example, the 1<sup>st</sup> Order Models is a model, which works well to describe extensive processes [9, 11, 16]. These processes are characterized by the movement of an endeffector in three-dimensional space. In contrast, processes dominated by the exchange of energy scale often with the 1<sup>st</sup> Law of Thermodynamics [14]. For resistive flow type applications, such as mold filling, Darcy's Law provides the scaling relationship [17].

### Cost Elements

Costs are conveniently subdivided into Fixed Costs and Variable Costs. Fixed Costs can include production equipment, auxiliary equipment, tooling, buildings, real estate, capital costs, sales-, general- and administrative expenses and are the foundation of every production. They are often related to the production volumes and the installed production capacity [14, 21]. Variable costs are calculated on a per part basis and can comprise material, direct labor and energy costs. The suggested production cost model for composites follows these separations as illustrated in Figure 1.3. One concern of this work is to effectively organize the gathering of relevant equipment and tooling for all the six production methodologies.

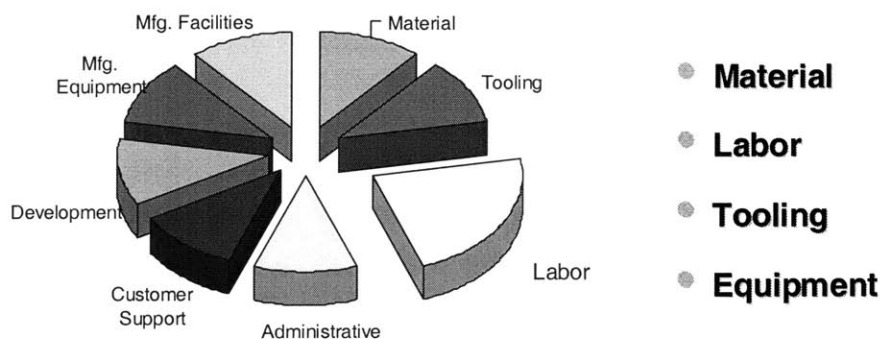


**Figure 1.3 Cost Components of Aircraft Production [9, 10]**

### WEB Implementation

Cost models for sixteen reference shapes are developed, while considering six different manufacturing processes. The models are aimed at both novice, and expert users and provide default process plans that can be modified for specific situations. All

calculations for the models use JavaScript which has been embedded into the HTML interface. XML databases store the parameters for the process description, material cost, and other production resources. In future updates of the models, the programmer will only need to refresh the databases without having to change the JavaScript code [22].

### Application of the Cost Models

The thesis concludes with several case studies of part production and assembly economics. The studies also demonstrate the capabilities of the developed cost estimation method and highlight its potential as an assessment tool for design and assembly concepts. The comparison of the individual cost elements aids the understanding of the various trade-off scenarios between process performance, part design and investment costs. A similar study is conducted to differentiate various assembly techniques and closes the gap between component production and creation of a larger, more intricate composite structure.

### Summary

The optimal manufacturing system for a given firm maximizes the return on assets by minimizing the respective costs. The characteristics of the system are a function of production volume, product design, market conditions and the overall competitive strategy of a firm. This work identifies the major cost drivers for a large portion of the presently employed composite production technologies. It also provides cost and pricing information so managers can make better choices when aligning their companies to the future challenges of technology and increased competitive pressures.

### 1.3 References

- [1] McLane, R., "Economic Issues in Composites Manufacturing", Proc. Amer. Soc. Comp., 1988.
- [2] Restar, S. A., "Advanced Airframe Structural Materials, A Primer in Cost Estimating Methodology", RAND Report # R-4016-AF, 1991.
- [3] Polland, D. R. et al., "Global Cost and Weight Evaluation of Fuselage Side Panel Design Concepts", NASA Report CR-4730, 1997.
- [4] Kassapoglou, C., "Minimum Cost and Weight Design of Fuselage Frames. Part A: Design Constraints and Manufacturing Process Characteristics", Composites, Part A, Vol. 30, 1999, pp. 887-894.
- [5] Kassapoglou, C., "Minimum Cost and Weight Design of Fuselage Frames. Part B: Cost Considerations, Optimization, and Results", Composites, Part A, Vol. 30, pp. 895-904, 1999.
- [6] Kim, P. "Comparative Study of the Mechanical Performance and Cost of Metal, FRP, and Hybrid Beams", Applied Composite Materials, Vol. 5, 1998, pp. 175-187.
- [7] Zaloom, V., Miller, C., "A Review of Cost Estimating for Advanced Composite Materials Applications", Engineering Costs and Production Economics, Vol. 7, 1982.
- [8] Northrop Corporation, "Advanced Composite Cost Estimating Manual (ACCEM)", AFFDL-TR-76-87, August 1976.
- [9] Ilcewicz, L. B., Smith, P. J., et al., "Advanced Technology Composite Fuselage - Program Overview", NASA CR-4734, 1996.
- [10] Willden, K., et al. "Advanced Technology Composite Fuselage - Manufacturing", NASA Report CR-4735, 1997.
- [11] Neoh, E. T. "Adaptive Framework for Estimating Fabrication Time", Ph.D Thesis, MIT, 1995.
- [12] Boothroyd, G.; Dewhurst, P.; Knight, W.A., "Product Design for Manufacture and Assembly", Basel, New York: Marcel Dekker, Inc., 1994.
- [13] Ashby, M. F., "Materials Selection in Mechanical Design", Butterworth Heinemann, 1992.
- [14] Clark, J. P., Roth, R., Field, F. R. III., "Techno-Economic Issues in Materials Selection", ASM Handbook Vol. 20, pp. 256-265, 1990.
- [15] Suh, N., "The Principles of Design", Oxford University Press, 1990.
- [16] Gutowski, T. G., "Advanced Composites Manufacturing", New York: John Wiley & Sons, Inc., 1997.

- [17] Kang, P. J., "A Technical and Economic Analysis of Structural Composite Use in Automotive Body-in-White Applications", M.S. Thesis, MIT, June 1998.
- [18] Reinhart, T. J. (Ed.), "Engineered Materials Handbook – Composites", Vol. 1, ASM International, 1988.
- [19] Cunningham, T. W., Mantripragada, R., Lee, D., Thornton, A., Whitney, D., "Definition, Analysis and Planning of a flexible Assembly Process", Proceedings of the Japan/USA Symposium on Flexible Automation, Boston, MA, 1996.
- [20] Niu, M. -C. -Y., "Composite Airframe Structures - Practical Design Information and Data", Hong Kong: Conmilit Press Ltd., 1992.
- [21] de Neufville, R. "Applied Systems Analysis", McGraw Hill, New York, 1990.
- [22] Pas, J. W., "WEB Based Cost Estimation Models for the Manufacturing of Advanced Composites", M.S. Thesis, M.I.T., 2001.

(This page is intentionally left blank.)



## 2 Composite Materials

The intrinsic characteristics of modern composite materials have been studied comprehensively during the past 30 years. Therefore, this chapter limits itself to the most fundamental properties and how they relate to the cost and process selection decisions. For additional information, the reader is referred to the many scientific texts, which discuss the properties of the material in detail [1-6].

The general definition of composites describes the material as a composition of at least two elements working together to produce material properties different from the ones of each constituent. Commonly, the composites consist of a reinforcement component, which provides strength and stiffness and a bulk or matrix part, which acts as a bonding agent. The composite materials discussed in this study are classified as fiber reinforced polymers, since a polymer based resin system is used as the matrix material. The reinforcements consist of either glass, aramid, or carbon fibers. Although each component possesses its own properties, the characteristics of the laminate are primarily determined by:

- Fiber & Matrix Properties
- Orientation of the Fibers
- Ratio between Fibers & Matrix (Fiber Volume Fraction)
- Strength of the Fiber-, Matrix Interface

Chapter 2.1 gives an overview of the fiber and matrix properties. The influence of the fiber orientation is depicted in Figure 3.3.

The fiber volume fraction is defined as  $\varphi = \frac{V_F}{V_F + V_M}$  where  $V_F$  represents the volume of the fibers and  $V_M$  the volume of the matrix within the composite. Since, the fibers generally exhibit superior mechanical properties, a higher fiber volume fractions results in a stronger laminate. The achievable fiber volume fraction depends on the manufacturing process and generally ranges from 30% to 70% [1, 2, 5].

Due to a decreased probability of material flaws, thin fibers exhibit exceptional properties along their length and maximize the fiber matrix interface strength too. A large interface area in connection with a compatible fiber/matrix finish improves the overall laminate strength.

Each of the above mentioned fiber types are available in various material forms. They can be procured as continuous yarns or rovings, as fabrics or already impregnated with the matrix resin of choice (prepregs). The differences between the material forms and the consequences on material and production process selection is discussed in Chapter 2.3.

## 2.1 Fiber Types

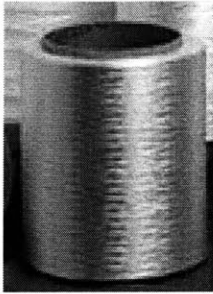
The selection of the reinforcement material primarily depends on the performance requirements and the economics of a particular part design. The part production process does usually not limit the use of any fiber type. Only when employing carbon fibers some precautions are necessary to prevent fiber damage during production. Table 2.1 lists the most common reinforcement fibers and their properties [1]. It should be noted, that the mechanical properties are measured in fiber direction only. As Figure 3.3 shows, the mechanical properties perpendicular to the fibers are even inferior to the properties of the matrix material.

**Table 2.1 Common Fiber Properties**

<i>Dry Fibers</i>	<i>Density</i> [lbs/in <sup>3</sup> ]	<i>Strength</i> [ksi]	<i>Modulus</i> [Msi]	<i>Strain</i> [%]	<i>Typical Price</i> [\$/lb]
<b>Glass</b>					
E-glass	0.094	435	10	5.0	0.8 - 1.0
C-glass	0.090	479	10	5.0	0.8 - 1.0
S2-glass	0.090	580	12	5.3	6.0 - 8.0
<b>Carbon</b>					
Carbon HS	0.065	522	32	1.6	20 - 30
Carbon IM	0.065	769	44	1.8	30 - 40
Carbon HM	0.065	508	55	0.4	45 - 90
Carbon UHM	0.072	290	64	0.8	110 - 160+
<b>Aramid</b>					
Aramid LM	0.054	522	9	3.6	20
Aramid HM	0.054	450	17	2.4	25
Aramid UHM	0.054	493	26	1.3	30

Appendix 2.6 gives more detailed information on fiber properties and commercially available fiber types [12-27].

### 2.1.1 Glass Fibers



Glass fiber filaments possess a diameter between 7 - 20  $\mu\text{m}$  and are produced by pushing liquid glass through tiny nozzles at ca. 2,900°F (1,600°C). The filaments are then drawn together into a larger bundle or roving. From these rovings, other material forms (see Chapter 2.3) are produced. The fiberglass rovings themselves are categorized according to their weight, which is measured in tex (1 tex = 1g/km).

Common weights range between 300 and 4,800 tex. However, before the fibers are wound onto spools the filaments are coated with a finish or sizing, which provides filament cohesion and facilitates fiber/matrix bonding. One differentiates mainly between 3 types of glass fibers depending on the mechanical and physical properties.

a) E-Glass

E-Glass (electrical) exhibits moderate tensile and compressive strength and stiffness. It is often used because of its outstanding dielectric properties (printed circuit boards) and relatively low costs. This glass type also features good fatigue resistance, and chemical resistance, but lacks impact strength. Depending on the material form and the purchase volume the price ranges between 0.8 – 1.0 \$/lb.

b) C-Glass

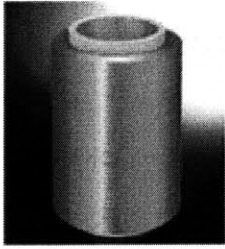
C-Glass (chemical) possesses similar mechanical properties as E-glass, however trades off the electrical properties for even better chemical resistance. Prices are similar to E-glass and are about 0.8 – 1.0 \$/lb.

c) S-Glass

S-Glass (strength) features an improved tensile strength (+40%) and stiffness (+20%). The material boasts a slightly lower density and is used where the higher performance is crucial. The price is therefore considerably higher in comparison to E-glass and is approximately 6 – 8 \$/lb.

More detailed information on glass fibers, its production and its application is available from a number of sources (e.g. Owens Corning) [22].

### 2.1.2 Aramid Fibers



Aramid fibers are easily distinguished by their bright yellow color and are produced by spinning fibers from a liquid aromatic polyamide. The filaments usually have a diameter of around  $12\ \mu\text{m}$  and are commonly available in the form of rovings ranging between 20 to 800 tex. Of course, all other material forms are available using the rovings as a base material. The finish (sizing) of the fibers is critical for the performance of aramid composites and has to be compatible with the matrix system. Aramid fibers are labeled according to their mechanical properties.

#### a) Aramid-LM

Aramid LM is a low modulus fiber and exhibits reduced stiffness properties. However, its tensile strength is extraordinarily high and it also possesses, as all aramid fibers, a high impact resistance, excellent fatigue characteristics and a low density. One of the weaknesses of Aramid is its low compression strength and its tendency to degrade under the influence of UV radiation. However, the material stands up well to abrasion, to chemical, and to thermal degradation. As opposed to glass fibers, the coefficient of thermal expansion is negative for aramid fibers. The price for the low modulus fiber is about \$20/lb depending on material form and procurement volume.

#### b) Aramid-HM

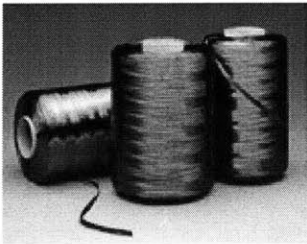
Aramid HM is a high modulus fiber with good stiffness and strength characteristics. Most other properties are similar to the lower grade Aramid LM. Prices are slightly higher however and range around \$25/lb.

#### c) Aramid-UHM

Aramid UHM consists of ultra-high modulus fibers, which not only provide excellent stiffness, but also good strength. Although the other properties are similar, the characteristic brittleness of the material is more pronounced. Material prices are around \$30/lb.

Aramid is also known under its trade names Kevlar® and Twaron®, produced by DuPont and Akzo Nobel respectively. These manufacturers along with a number of comprehensive references provide all the necessary information for designing with this type of material [12, 19].

### 2.1.3 Carbon Fibers



Carbon fibers resemble the high end of composite performance. They are among the strongest and stiffest reinforcement materials available and have a very low material density, which gives them an excellent strength- and stiffness-to-weight ratio. The black fibers are either derived from a pitch or polyacrylonitrile (PAN) precursor and are graphitized at 4,700°F (2,600°C) or 5,400°F (3,000°C) depending on their modulus. The 5 - 10  $\mu\text{m}$  thick filaments are available in roving and other material forms. In contrast to glass-, and Aramid fibers their weight is however is not measured in tex. However, the rovings are designated by the amount of filaments they contain and are produced with 1K (1K = 1,000 filaments), 3K, 6K, 12K, and 48K. As a rule of thumb one can state that the higher the filament count the lower the material price per pound. The following terminology is used to group the fibers according to their mechanical properties.

#### a) Carbon-HS

Carbon HS (high strength, modulus < 265 GPa) offers good tensile and compressive strength, but possesses lower stiffness compared to other carbon fibers. However, as all carbon fibers it features superior resistance to corrosion, creep and fatigue and possesses excellent damping properties. The thermal service limit of carbon fibers is extremely high > 3,500°F (2,000°C) and is only restricted by the thermal degradation of the matrix material. Carbon fibers also possess a negative coefficient of expansion and can therefore be used to design zero-expansion structures. However, one of the drawbacks of the fiber is its brittleness, its low impact resistance and low shear modulus. The fibers tend to

fray during handling and therefore extra care has to be taken during production in order to avoid fiber damage and equipment contamination with frayed fibers. The price ranges roughly from 20 to 30 \$/lb depending on material form and purchasing volume.

b) Carbon-IM

The Carbon IM (intermediate modulus 265-320 GPa) fibers have a stiffness and strength exceeding that of steel. However, they are still able to carry a reasonable amount of strain before failure. Prices are of course higher and are approximately 30 to 40 \$/lb.

c) Carbon-HM

Carbon-HM (high modulus 320 – 440 GPa) fibers trade off elasticity and strength for higher stiffness. The material prices are around 45 to 90 \$/lb depending on the material form and the purchasing volume.

d) Carbon-UHM

The Carbon-UHM (ultra high modulus > 440 GPa) fibers are extremely stiff, but also very brittle. They have the highest negative thermal expansion coefficient of all the carbon fiber types and because of these properties they are often used for specialized applications. The price for dry rovings can be between 110 and 160+ \$/lb.

Again, more comprehensive textbooks should be consulted before designing with carbon fibers. Manufactures such as Hexcel, Zoltek, Cytec, Toray etc also provide good guidance and many practical and technical information [20, 21, 25, 27].

## 2.2 Matrix Types

Since, the main purpose of the matrix is to bind the reinforcement fibers together an important characteristic are its adhesive properties. The matrix not only distributes the loads between the fibers it also protects them from environmental moisture and chemical corrosion. For the composite to carry the intended loads, the matrix should have at least similar strain to failure limits as the underlying reinforcement fibers. The matrix will then be able to reduce brittle failures and provide resistance to crack propagation. In most cases the properties of the matrix determines the service temperature limitations of the part and more importantly the processing conditions. The cure- or melting temperature along with their viscosity primarily influences process selection and the processing parameters. As a matter of fact, nowadays for each of the aforementioned processes special matrix compositions are available on the market. Other influential factors are the shelf-life of the matrix, its tack and its shrinkage during cure. Modern advanced composites commonly employ organic matrices, which are broadly divided in thermoset and thermoplastic resins. Table 2.2 gives an overview of the common representatives of each category [6, 13, 16, 23, 24].

**Table 2.2 Common Matrix Properties**

<i>Neat Resin</i>	<i>Density</i>	<i>Strength</i>	<i>Modulus</i>	<i>Strain</i>	<i>Typical Price</i>
	<i>[lbs/in<sup>3</sup>]</i>	<i>[ksi]</i>	<i>[Msi]</i>	<i>[%]</i>	<i>[\$/lb]</i>
<b>Thermosets</b>					
Epoxy	0.043	1.0	0.5	7.0	1.7 - 2.0
Polyester	0.040	0.9	0.4	4.5	1.6 - 2.1
Vinylester	0.040	0.8	0.3	3.0	1.7 - 2.2
<b>Thermoplasts</b>					
PAI	0.054	14.8	2.0	2.1	30 - 40
PEEK	0.047	14.9	0.8	1.6	40 - 50
PE	0.034	3.6	0.2	2.1	0.6 - 0.8

The chain-like molecules react differently to the influence of heat. Thermoplastics generally soften with rising temperature and eventually melt. The process of melting and hardening is repeatable without any consequences to the polymer. Thermosets however, are formed from a chemical reaction between a resin, a hardener, and a catalyst. Their viscosity is generally much lower and once cured the reaction cannot be reversed. When



subjected to heating most of the thermosets exhibit a certain temperature (glass transition temperature  $T_g$ ) at which their mechanical and physical properties change significantly. The following list outlines the advantage and disadvantages of thermoset and thermoplastics and how these relate to process selection.

<b><i>Thermosets</i></b>	<b><i>Thermoplastics</i></b>
<ul style="list-style-type: none"> <li>• Irreversible Chemical Curing Process</li> <li>• Low Viscosity and Good Fiber Wetting</li> <li>• Long Processing Time (hrs)</li> <li>• Limited Shelf-Life</li> <li>• Exhibit Brittleness</li> </ul>	<ul style="list-style-type: none"> <li>• Reversible Solidification Process</li> <li>• High Viscosity and Poor Fiber Wetting</li> <li>• Rapid Processing Time (sec)</li> <li>• Infinite Shelf-Life</li> <li>• Superior Toughness</li> </ul>

**Figure 2.1 Comparison of Matrix Properties**

The following paragraphs discuss the properties of the most common resin systems in more detail.

### 2.2.1 Epoxy (EP)

The large family of epoxy resins is among the highest performing thermosetting resin types. They offer good chemical resistance, superior adhesion to fibers and can be formulated to a wide range of viscosities. Due to the absence of any volatiles they exhibit low shrinkage and also prevent the formation of voids (gas bubbles). Depending on the service temperature they are either cured at around 250°F (125°C) or 350°F (175°C). However, in their unmodified form epoxies are often brittle and have to be toughened by the resin producer. They also have a tendency to absorb water, which can lead to degradations of the resin and the laminate. Epoxies are widely used and easily processed and sell for about 1.7 to 2.0 \$/lb.

### **2.2.2 Polyester**

Unsaturated polyesters are the most widely used thermosetting resin systems in the composite industry. Their low viscosity, the ease of processing combined with low costs qualifies them for a variety of applications. They can be cured at room temperature or at a temperature up to 350°F (175°C). They also offer a compromise between strength and impact resistance and is chemically resistant. However, polyesters have a limited shelf-life since they start to gel after a period of time and become unusable. Volatiles (styrenes) cannot only cause voids but also health issues. The price for polyester ranges from 1.6 to 2.1 \$/lb.

### **2.2.3 Vinylester**

Vinylesters are a subfamily of polyesters and therefore have similar curing and processing characteristics. However, due the molecular composition vinylesters are tougher and are therefore better able to absorb shock loads. For similar reasons the material is also less prone to absorb water (hydrolysis) and can be subjected to wet service conditions. Again, the styrene content can lead to health problems during open processing. This thermosetting resin retails for about 1.7 to 2.2 \$/lb.

### **2.2.4 Polyamide-imide (PAI)**

Polyamide-imide combines all the advantages of a thermoplastic resin with excellent mechanical properties. It is not only very strong and stiff it also exhibits great toughness and impact resistance. The material melts around 500°F (260°C) and starts to degrade around 530°F (280°C), which requires tight temperature control during the already difficult processing stage. Critical during processing is also the fiber wet out and the attainable interface strength between fiber and matrix. PAI is comparatively expensive at 30 to 40 \$/lb.

### **2.2.5 Polyetheretherketon (PEEK)**

Polyetheretherketon (PEEK) is a semi-crystalline thermoplastic material capable withstanding a service temperature of up to 260°F (130°C). Aside from the high service temperature the material is also flame retardant. Additionally it exhibits good strength and stiffness and has outstanding impact strength and chemical resistance. The viscosity in its molten stage at ca. 280°F (140°C) is slightly lower in comparison to PAI and it is therefore processed more easily. However, it is consider as one of the most expensive matrix systems with prices ranging from 40 to 50 \$/lb.

### **2.2.6 Polyethylene (PE)**

Polyethylene (PE) is along with Polypropylene (PP) one of the most widely used commodity thermoplastics. The material is chemically inert and exhibits a high electrical resistance. However, its melting point is with 230°F (110°C) quite low, which limits its usefulness but facilitates processing. Many derivatives of the material exist, such as Low Density and High Density Polyethylene, which feature different mechanical properties. As most thermoplastic the material comes most often in pellet form and costs about 0.6 to 0.8 \$/lb.

## 2.3 Material Forms

The composite manufacturing process not only influences the selection of the matrix material but also very much determines the material form to be used. The scope of this thesis is limited to the material forms, which are commonly used together with the studied manufacturing processes. Furthermore, the following paragraphs only talk about material forms with defined fiber directions since these material forms are mostly employed in high performance applications. The prices vary strongly depending on the amount of additional processing and the type of materials used. The prices listed in Table 2.1 and Table 2.2 apply only to the basic materials. However, prices of certain material forms such as prepregs can be considerably higher than just the sum of their basic constituents (see Appendix 2.6).

Most material forms can be obtained either “dry” or “preimpregnated” with the desired resin system. When using dry forms the matrix is applied in-situ during the production process, while the “preimpregnated” or “prepreg” forms can dispense with such a step.

### 2.3.1 Continuous Rovings

The most basic dry fiber forms used in composite production are continuous rovings. The roving is essentially a continuous fiber bundle consisting of many individual filaments. Generally, as seen Figure 2.2, rovings come on spools of various sizes. Glass- and Aramid fiber rovings are classified according to their weight measured in tex (1 tex = 1 g/km) or denier (1 denier = 1g/0.9km). Common weights range between 20 and 4,800 tex. Carbon fiber rovings are categorized with respect to the number of filaments contained in the roving and the diameter of each filament. The most widely used designations are 1K, 3K, 6K, 12K, and 48K, where 1K equals 1,000 filaments. Rovings are simple to use, but have to be impregnated with resin during processing. In particular when using carbon rovings care has to be taken in order to minimize any fiber damage during the impregnation and processing stage. Continuous rovings are most commonly employed in pultrusion, filament winding and braiding processes. With some extra effort

they can also be used in automated tape placement and resin transfer molding applications. Rovings represent the basic material to produce more advanced material forms such as fabrics and tapes.

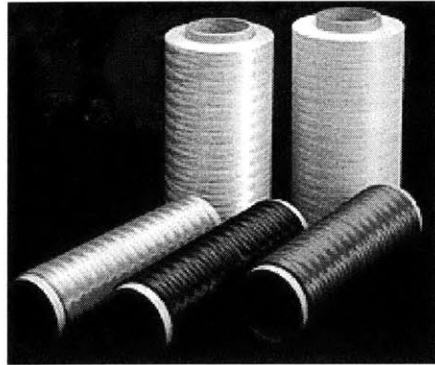


**Figure 2.2** Continuous Aramid Rovings [19]

### 2.3.2 Fabrics

All fiber types are also available in forms of dry fabrics as seen in Figure 2.3. Fabrics are commonly described by the type of weave and the number yarns per inch in the warp (along the length of the fabric) and in the fill direction. They are further classified by their weight measured in  $\text{oz/yd}^2$  or  $\text{g/m}^2$  and the weight of the yarn used in the weaving process (see Chapter 2.3.1 Rovings). Fabric weights range commonly between  $1.8 \text{ oz/yd}^2$  and  $14 \text{ oz/yd}^2$  and the fabrics are typically sold on rolls of 38 inches to 50 inches in width (97 cm to 127 cm).

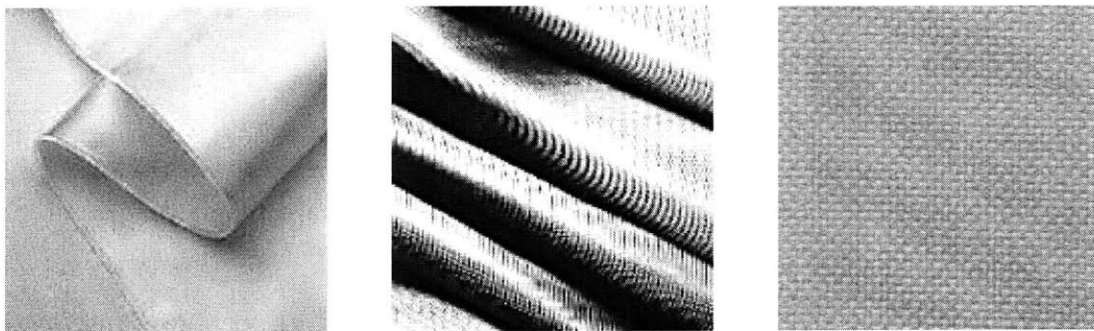


**Figure 2.3** Woven Glass-, Carbon-, and Aramid Fabric [19, 21, 22, 24]

One of the advantages of fabrics originates from the convenience of handling a broad-good versus a single fiber. The major disadvantages lie within their reduced strength due to fiber crimp and diminished fiber volume fraction. The handling and mechanical properties of a fabric are not only defined by the weight but also by the weaving style. Although many other derivatives exist, the most common styles are unidirectional fabrics, plain weaves and satin weaves [1, 24].

a) Unidirectional

Unidirectional (UD) fabrics feature mainly fibers with one single orientation (warp) and held in position by tie yarns (fill). These fabrics maximize the mechanical properties of the fibers, since they introduce as little fiber crimp as possible. They are therefore similar to unidirectional tapes in their behavior.

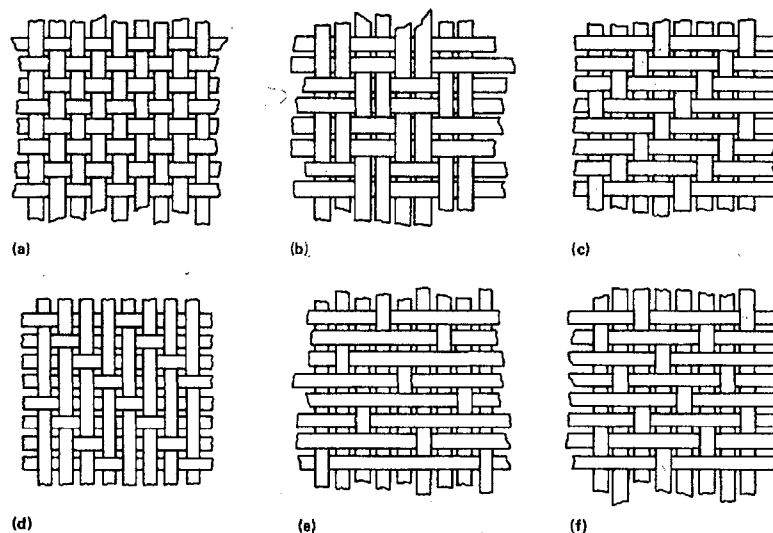


**Figure 2.4** a) Plain Weave, b) Basket Weave, c) Twill, d) Crowfoot Satin, e) 8-end Satin, f) 5-end Satin [1]

b) Plain

Plain weave fabrics as seen in Figure 2.4 are very firm in their composition and quite stable. They are therefore best suited for flat or simply curved parts. The properties are symmetric and most pronounced in  $0^\circ/90^\circ$  direction. However, due to the extensive fiber crimp some mechanical performance is sacrificed. To avoid

excessive crimping mainly thin rovings are used in the weaving process (3K or 600 tex), which can increase the price considerably.

c) **Satin**

Satin weave fabrics, as seen in Figure 2.4, are derivation of twill weaves and are typically produced in 4, 5, and 8-end (or harness) styles. The fabrics are very flat and can be draped well over complex shapes without inducing too much wrinkling. As opposed to plain weaves, satin weaves exhibit considerably less fiber crimp, which in turn gives them better mechanical properties. However, the fibers are not symmetric and display a dominant fiber and strength direction.

Fabrics are mainly used as part of manual hand lay-up operations, but are also common in resin transfer molding and pultrusion. Most fiber manufactures also offer their products in the form of fabric [19, 21, 22, 24]. Appendix 2.6 lists a selection of dry fabrics and their prices. As always, the purchasing volume can have significant influence on the actual procurement costs.

### **2.3.3 Prepreg Fabrics**

Prepreg fabrics already contain the thermoset or thermoplastic matrix and therefore their application reduces production times considerably. As long as the compatibility between fiber and matrix is assured pretty much every fiber/resin combination is feasible to produce. However, the major suppliers keep widely used combinations in stock and Appendix 2.6 gives an overview of a selected few. Prepreg fabrics are characterized by the weave of the fabric, the resin type, the amount of resin and the overall weight per square yard. For production consideration, the tack (stickiness of the resin) is a major criterion, since it determines how easily the prepreg can be handled and draped. Prepregs containing a thermoset resin system have to be kept refrigerated in order to extend their already limited shelf-life. Preimpregnated fabrics are often used during hand lay-up, but can also be introduced into pultrusion dies. Prices depend on the materials used and because of the additional prepregging step can be higher than the sum of the individual constituents.

### 2.3.4 Unidirectional Tapes & Tows

Unidirectional tapes are impregnated with resin and hold the continuous longitudinal fibers together in order to form as continuous sheet. Figure 2.5 displays carbon fiber based tapes with different widths. However, as with all preregs many fiber/matrix combinations are available in tape form. Since the fibers are oriented in only one direction the production process has to ensure the correct placement in accordance to the design requirements. Prepreg tapes facilitate production, since the fibers are already wetted by the matrix. Tapes generally come in width between 3 inches and 12 inches and are also categorized by weight and the size of the fibers used. Smaller widths of around 1/8 inch (3.2 mm) are generally described as tows. Commonly the thickness of tapes and tows ranges between 5 to 10 mils (0.127 to 0.254 mm). Tapes and tows are primarily used in automated tow placement or automated tape-laying processes. However, the tapes are sometimes used in hand lay-up and the tows are introduced into a pultrusion process. Appendix 2.6 shows a list of a few selected unidirectional tapes. Prices are similar to prepreg fabrics and can be obtained from the major suppliers [19, 21, 22, 24].

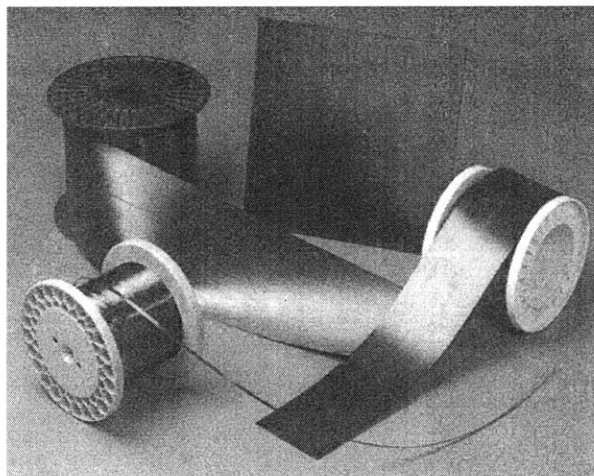


**Figure 2.5 Unidirectional Prepreg Tape and Tows [20]**



## 2.4 Material Selection Guidelines

The systematic selection of materials has been studied extensively [1, 4, 8, 9]. Material selection plays a decisive role in final production costs. Therefore, the enormous number of different materials requires a scheme to simplify selection during the early design stages. Traditionally, materials have been selected by the designers based on their specific mechanical or physical properties. However, competitive advantages can only be gained if compatibility between material and production process can be assured. That is, the material cannot be chosen independently from the manufacturing process if the overall costs are to be minimized. Even health or environment related issues can become part of the economic consideration, since any violations can lead to costly litigations. Generally, the material selection should observe the following criteria.

- Fiber & Matrix Properties
- Material & Processing Costs
- Health or Environmental Impacts

Of course, the final product has to fulfill strength, stiffness, impact, and fatigue resistance requirements. It also has to withstand any thermal or environmental influences such as chemicals and radiation. However, for economic reasons, a possible match between certain processes and groups of materials has to be determined [8, 9, 10]. The previous chapters establish, that the fiber type (glass, aramid, carbon) does not pose any limits on process selection. However, the matrix (thermoset, thermoplastic) and the material form (roving, fabric, tape, prepreg) can be used as reliable process selection criteria. The following selection chart (Figure 2.6) intends to give some preliminary guidance during the many tradeoff decisions of early design work. The selection is restricted to the processes and material forms within the scope of this study and has deliberately been kept simple.

<i>Process / Material Form</i>	<i>HLU</i>	<i>ATP</i>	<i>DDF</i>	<i>PUL</i>	<i>RTM</i>	<i>Assem.</i>
<u>Continuous Roving (Dry)</u>	0	X	0	XX	X	N/A
<u>Woven Fabric (Dry)</u>	XX	0	0	X	XX	N/A
<u>Unidirectional Tape (Prepreg)</u>	XX	X	X	X	0	N/A
<u>Woven Fabric (Prepreg)</u>	XX	0	XX	X	0	N/A
<u>Tow (Prepreg)</u>	0	XX	0	XX	0	N/A
<u>Thermoset Resin Systems</u>	XX	XX	XX	XX	XX	X
<u>Thermoplastic Resin Systems</u>	X	X	0	X	0	0

**XX = common, X = possible, 0 = not common, N/A = not applicable**

**Figure 2.6 Material Selection Matrix for Manufacturing**

## 2.5 References

- [1] Reinhart, T. J. (Ed.), "Engineered Materials Handbook – Composites", Vol. 1, ASM International, 1988.
- [2] Tsai, S. W. , "Introduction to Composite Material", Technomic Pub Co; January 1980.
- [3] Tsai, S. W. , "Theory of Composite Design", Think Composites, November 1992.
- [4] Niu, M. -C. -Y., "Composite Airframe Structures - Practical Design Information and Data", Hong Kong: Conmilit Press Ltd., 1992.
- [5] Schwartz, M. -M., "Composite Materials, Properties, Nondestructive Testing, and Repair", Vol. I & II, New Jersey: Prentice-Hall, Inc. 1997.
- [6] Strong, A. Brent, "Plastics – Materials and Processing", New Jersey: Prentice-Hall, Inc., 1996.
- [7] Boyer, J. R., "Compilation of a Material Cost Database for a WEB-Based Cost Estimator", B.S. Thesis, MIT, 2000.
- [8] Ashby, M. F., "Materials Selection in Mechanical Design", Butterworth Heinemann, 1992.
- [9] Boothroyd, G.;Dewhurst, P.; Knight, W.A., "Product Design for Manufacture and Assembly", Basel, New York: Marcel Dekker, Inc., 1994.
- [10] DoD, FAA, ASTM, "The Composite Materials Handbook-MIL 17", Vol. 1, 2, 3, Lancaster: Technomic Publishing Company Inc., 2000.
- [11] Beckwith, S. W., "Preforms, for Resin Transfer Molding (RTM) Processing", Composites Fabrication, October 1999, p. 60-74.
- [12] Akzo Nobel, Inc. <http://www.akzonobel.com/>
- [13] BASF AG, <http://www.basf.com/> .
- [14] BP Amoco Chemicals, Carbon Fibers, <http://www.bpamococarbonfibers.com/>.
- [15] BP Amoco Chemicals, Engineering Polymers, <http://www.bpamocoengpolymers.com/>.
- [16] Chevron Phillips Chemical Company, <http://www.chevronphillips.matweb.com/>.
- [17] Cytec Industries, Inc., <http://www.cytec.com/> .
- [18] Dow Chemical Company, DERAkANE®, <http://www.dow.com/derakane/> .
- [19] DuPont, KEVLAR®, <http://www.dupont.com/kevlar/> .
- [20] Hexcel Corporation, Inc., Hexcel Fibers, <http://www.hexcelfibers.com/> .
- [21] Hexcel Corporation, Inc., Hexcel Schwebel, <http://www.hexcelschwebel.com/> .

- [22] Owens Corning, Composites Solutions, <http://www.owens-corning.com/composites/> .
- [23] Reichhold Chemicals, Inc., <http://www.reichhold.com/>.
- [24] SP Systems, <http://www.spsystems.com/> .
- [25] Toray Industries, Inc., <http://www.toray.com/> .
- [26] Victrex, PEEK™ High Performance Polymer, <http://www.victrex.com>.
- [27] Zoltek Inc., <http://www.zoltek.com/>

## 2.6 Appendix - Composite Materials

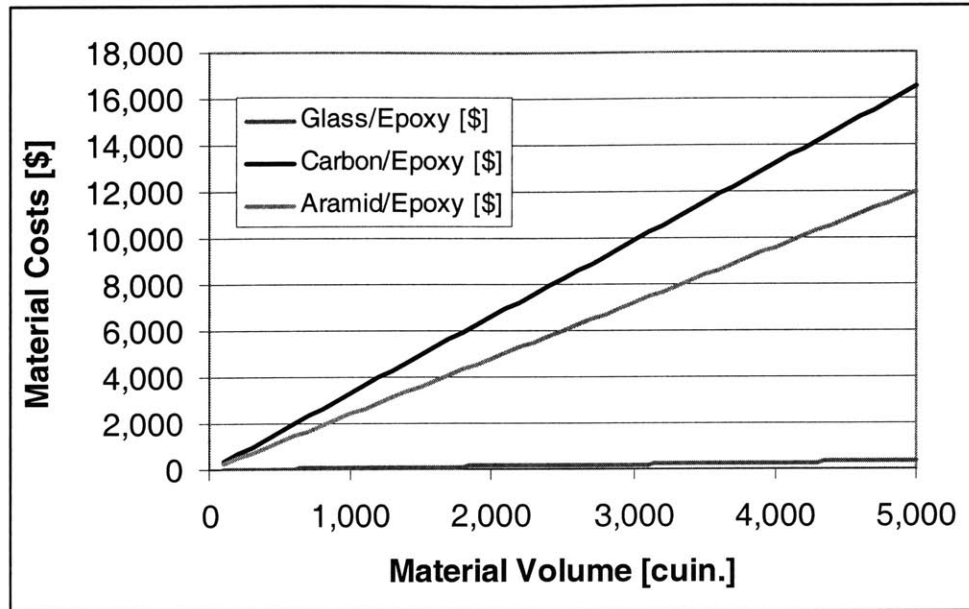


Figure 2.7 Average Material Costs (G/E: \$1/lb, C/E: \$60/lb, A/E: \$50/lb)

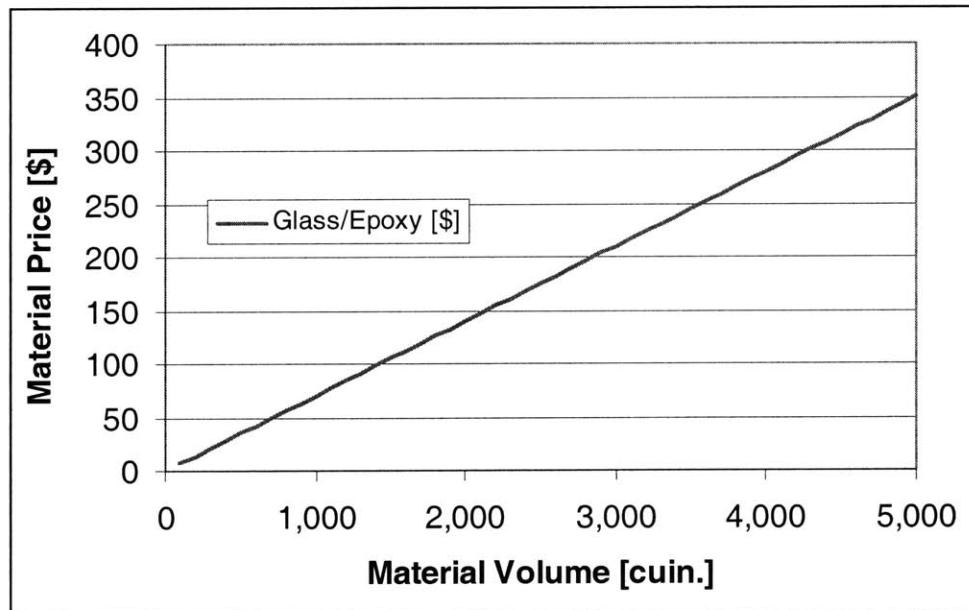


Figure 2.8 Average Glass/Epoxy Costs (G/E: \$1/lb)

	Density	Price	Modulus	UTS	Filament	Wt./Length	Strain
	[g/cm <sup>3</sup> ]	[\$/lb]	[GPa]	[MPa]	Dia. [μm]	[g/m]	[%]
<b>Glass Fiber Roving</b>							
Owens Corning 366 Type 30® Fiberglas®	2.62	1.12	80.00	3100	N/A	N/A	4.60
Owens Corning 449 S-2 Glass®	2.49	8.00	96.52	4826	10.0	N/A	5.15
PPG 1062 (TEX 1145)	2.64	1.15	72.39	N/A	13.0	1.145	N/A
PPG 1062 (TEX 2010)	2.64	1.09	72.39	N/A	13.0	2.010	N/A
PPG 1062 (TEX 4030)	2.64	1.12	72.39	N/A	13.0	4.030	N/A
PPG 1712 Multi-End (TEX 4310)	2.64	1.18	72.39	N/A	13.0	4.310	N/A
PPG 1764 Multi-End (TEX 2300)	2.64	1.01	72.39	N/A	13.0	2.300	N/A
PPG 7065 Roving (TEX 2350)	2.64	1.34	72.39	N/A	N/A	2.480	N/A
PPG Hybon® 2006 Direct-Draw (TEX 1985)	2.64	0.95	72.39	N/A	22.0	1.985	N/A
PPG Hybon® 2022 (TEX 1503)	2.64	0.99	72.39	N/A	20.0	1.503	N/A
PPG Hybon® 2022 (TEX 1722)	2.64	0.95	72.39	N/A	15.0	1.722	N/A
PPG Hybon® 2022 (TEX 2205)	2.64	0.95	72.39	N/A	17.0	2.205	N/A

**Figure 2.9 Glass Fiber Roving Properties**

	Density	Price	Modulus	UTS	Filament	Wt./Length	Strain
	[g/cm <sup>3</sup> ]	[\$/lb]	[GPa]	[MPa]	Dia. [μm]	[g/m]	[%]
<b>Aramid Fiber Roving</b>							
DuPont Kevlar® 29 Fiber (1500 denier)	1.44	22.75	70.30	2760	12.0	0.166	3.6
DuPont Kevlar® 49 Fiber (2160 denier)	1.44	22.50	112.37	2923	12.0	0.240	2.4
DuPont Kevlar® 49 Fiber (2840 denier)	1.44	22.50	112.37	3000	12.0	0.315	2.4

**Figure 2.10 Glass Fiber Roving Properties**

	Density	Price	Modulus	UTS	Filament	Wt./Length	Strain
	[g/cm <sup>3</sup> ]	[\$/lb]	[GPa]	[MPa]	Dia. [μm]	[g/m]	[%]
<b>Carbon Fiber Roving</b>							
Hexcel AS4C 3K	1.78	24.50	231.00	4205	7.0	0.200	1.82
Hexcel AS4C 6K	1.78	20.50	231.00	4205	7.0	0.400	1.82
Hexcel AS4C 12K	1.78	15.00	231.00	4205	7.0	0.800	1.82
Hexcel AS4 3K	1.79	25.50	228.00	4150	8.0	0.210	1.82
Hexcel AS4 6K	1.79	29.50	228.00	4150	8.0	0.427	1.82
Hexcel AS4 12K	1.79	29.00	228.00	4150	8.0	0.858	1.82
Hexcel IM4 12K	1.78	22.50	276.00	4480	N/A	0.723	1.60
Hexcel IM6 12K	1.76	50.00	279.00	5510	5.0	0.446	1.97
Hexcel IM7 6K	1.78	63.00	276.00	5080	5.0	0.223	1.84
Hexcel IM7 12K (5000 spec)	1.78	50.00	276.00	5530	5.0	0.446	2.01
Hexcel IM7 12K (6000 spec)	1.79	50.00	292.00	5760	5.0	0.446	1.97
Hexcel IM8 12K	1.79	65.00	304.00	5580	5.0	0.446	1.83
Hexcel IM9 12K	1.80	80.00	304.00	6120	4.5	0.335	2.01
Hexcel UHM 3K	1.87	350.00	440.00	3570	4.4	0.085	0.81
Hexcel UHM 12K	1.87	110.00	440.00	3570	4.4	0.330	0.81
Thornel® T-300 1K	1.76	128.50	231.00	3750	7.0	0.066	1.40
Thornel® T-300 6K	1.76	26.00	231.00	3750	7.0	0.395	1.40
Thornel® T-650/35 6K	1.77	28.00	255.00	4280	6.8	0.391	1.70
Thornel® T-650/35 12K	1.77	26.00	255.00	4280	6.8	0.763	1.70
Thornel® T-300C 1K	1.76	115.00	231.00	3750	7.0	0.066	1.40
Thornel® T-300C 6K	1.76	19.00	231.00	3750	7.0	0.395	1.40
Thornel® T-650/35C 12K	1.77	11.00	248.00	4280	6.8	0.763	1.70
Thornel® P-25 Pitch-Based 4K	1.90	49.50	159.00	1380	11.0	0.715	0.90
Zoltek Panex® 33 48K (45,700 filaments)	1.81	9.00	228.00	3800	7.2	3.300	N/A

**Figure 2.11 Carbon Fiber Roving Properties**

	Density [g/cm <sup>3</sup> ]	Price [\$/lb]	Modulus [GPa]	UTS [MPa]	Weight [g/m <sup>2</sup> ]	Width [cm]	Thickness [mm]
<b>Glass Fiber Woven Fabric</b>							
Hexcel® Schwebel 106 Plain Weave Fabric	2.57	74	68.94	N/A	25	96.5	0.04
Hexcel® Schwebel 112 Plain Weave Fabric	2.57	20	68.94	N/A	71	96.5	0.06
Hexcel® Schwebel 120 4H Satin Weave Fabric	2.57	20	68.94	N/A	107	96.5	0.09
Hexcel® Schwebel 1527 Plain Weave Fabric	2.57	8	68.94	N/A	417	111.8	0.38
Hexcel® Schwebel 1543 4H Satin Weave Fabric	2.57	8	68.94	N/A	292	96.5	0.20
PPG Hybon® Woven Roving Plain Weave (610 g/m <sup>2</sup> )	2.64	2	301.0*	N/A	610	106.7	N/A
PPG Hybon® Woven Roving Plain Weave (814 g/m <sup>2</sup> )	2.64	2	301.0*	N/A	814	106.7	N/A

Figure 2.12 Glass Fiber Woven Fabric (\* in laminate)

	Density [g/cm <sup>3</sup> ]	Price [\$/lb]	Modulus [GPa]	UTS [MPa]	Weight [g/m <sup>2</sup> ]	Width [cm]	Thickness [mm]
<b>Aramid Fiber Woven Fabric***</b>							
Hexcel® Schwebel 328 Plain Weave Kevlar® 49	1.44	34	124.00	2760**	217	96.5	0.30
Hexcel® Schwebel 345 4H Satin Weave Kevlar® 49	1.44	154	124.00	2760**	58	96.5	0.08
Hexcel® Schwebel 348 8H Satin Weave Kevlar® 49	1.44	85	124.00	2760**	166	96.5	0.20
Hexcel® Schwebel 351 Plain Weave Kevlar® 49	1.44	95	124.00	2760**	75	127.0	0.10
Hexcel® Schwebel 352 Plain Weave Kevlar® 49	1.44	44	124.00	2760**	173	127.0	0.25

Figure 2.13 Aramid Fiber Woven Fabric (\*\* approximate value)

	Density [g/cm <sup>3</sup> ]	Price [\$/lb]	Modulus [GPa]	UTS [MPa]	Weight [g/m <sup>2</sup> ]	Width [cm]	Thickness [mm]
<b>Carbon Fiber Woven Fabric</b>							
Hexcel® Schwebel 130 Plain Weave 1K Fabric	1.79	201	228.0	N/A	125	106.7	0.14
Hexcel® Schwebel 282 Plain Weave 3K Fabric	1.79	37	228.0	N/A	197	106.7	0.22
Hexcel® Schwebel 433 5H Satin Weave 3K Fabric	1.79	34	228.0	N/A	285	106.7	0.32
Hexcel® Schwebel 584 8H Satin Weave 3K Fabric	1.79	37	228.0	N/A	373	106.7	0.42
ThermalGraph® EWC-300x Plain Weave (4K Pitch-Based)	2.10	250	275.0*	689*	610	89.0	0.94

Figure 2.14 Carbon Fiber Woven Fabric (\* in laminate)

		Price [\$/lb]	Weight [g/m <sup>2</sup> ]	Modulus [GPa]	UTS [MPa]	Resin Content [%]	Cure Temp. [C]	Width [cm]	Cured-Ply Thickness [mm]
<b>Woven Fabric/Epoxy</b>									
NB-1100 TIP	Hexcel® Schwebel 106 Glass	54	250	69**	N/A	34	121-148	127	N/A
NB-1109	Hexcel® Schwebel 328 Kevlar® 49	84	217	124**	N/A	34	121-148	127	N/A
NB-1122	Hexcel® Schwebel 282 Carbon 3K	105	197	228**	N/A	34	148-190	127	N/A
NB-1122	Hexcel® Schwebel 348 Kevlar® 49	110	166	124**	N/A	34	148-190	127	N/A
NB-1450	Hexcel® Schwebel 433 Carbon 3K	94	285	228**	N/A	34	112-135	127	N/A
AW370-5H/3501-6	5H Satin Weave Carbon 6K	43	370	69	827	42	176	124.5	0.36
AW370-8H/3501-6	8H Satin Weave Carbon 6K	73	370	69	N/A	42	176	124.5	0.36
AW193-PW/3501-6	Plain Weave Carbon 6K	69	193	69	758	42	176	124.5	0.20
<b>UD Tape/Epoxy</b>									
NCT-106/8	Owens Corning S-2 Glass®	19	125	96**	4826**	34	112-148	30.5	N/A
NCT-303	Hexcel AS4 Carbon 3K	23	150	228**	4150**	34	121-148	30.5	N/A
NCT-306	Owens Corning S-2 Glass®	19	200	96**	4826**	34	121-140	30.5	N/A
NCT-321	DuPont Kevlar® 49 Fiber (2160 denier)	20	150	112**	2923**	34	135	30.5	N/A
NCT-1122	Hexcel AS4 Carbon 6K	23	250	228**	4150**	34	171-190	30.5	N/A
AS4/3501-6	Hexcel AS4 Carbon 6K	45	150	141	2139	36	176	30.5	0.13

Figure 2.15 Various Prepregs (\*\* properties of the dry fiber)

<b>THERMOSETS</b>							
<b>Epoxy Thermoset Resin (Bisphenol A)</b>	<b>Density</b>	<b>Price</b>	<b>Modulus</b>	<b>UTS</b>	<b>Viscosity</b>	<b>Tg</b>	<b>Heat Deflection</b>
	<b>[g/cm<sup>3</sup>]</b>	<b>[\$/lb]</b>	<b>[GPa]</b>	<b>[MPa]</b>	<b>[m Pa s]</b>	<b>[C]</b>	<b>Temp. [C]</b>
Vantico Araldite® GY 507	1.14	2.11	N/A	N/A	600	N/A	<200*
Vantico Araldite® GY 6010/GY 6010CSR	1.17	1.70	N/A	N/A	12,500	N/A	<200*
Vantico Araldite® GY 6020	1.17	1.70	N/A	N/A	18,000	N/A	<200*
Dow DERAKANE D.E.R.® 329	1.16	1.80	N/A	N/A	1100	N/A	N/A
<b>Vinyl Ester Thermoset Resin</b>							
Ashland HETRON® 922	1.04	2.01	3.17	86.20	N/A	105.00	105.00**
Ashland HETRON® 942/35	1.08	2.08	3.58	91.70	N/A	121.11	121.11**
Ashland HETRON® 980/35	1.08	2.20	3.31	87.56	N/A	132.22	132.22**
Dow DERAKANE® 411-350	1.05	1.80	3.10	79.00	350	N/A	102.00**
Dow DERAKANE® 470-300	1.08	2.00	3.60	85.00	300	N/A	152.00**
Dow DERAKANE® 8090	1.04	1.60	2.90	66.00	320	106.00	83.00**
<b>Polyester Thermoset Resin</b>							
Ashland AROPOL™ 7241T-15 Isophthalic Polyester	1.07	1.59	3.65	62.74	solid	N/A	98.88
Ashland AROPOL™ 7334T-15 Isophthalic Polyester	1.10	1.57	3.44	86.18	solid	N/A	93.88
Ashland HETRON® 700 Bisphenol A	0.97	2.12	3.17	68.94	solid	N/A	142.22

**Figure 2.16 Thermoset Neat Resins (\* for laminate; \*\* HDT 1.82 MPa)**

<b>THERMOPLASTICS</b>							
<b>Polyamide-imide Thermoplastic Resin</b>	<b>Density</b>	<b>Price</b>	<b>Modulus</b>	<b>UTS</b>	<b>Viscosity</b>	<b>Tg</b>	<b>Heat Deflection</b>
	<b>[g/cm<sup>3</sup>]</b>	<b>[\$/lb]</b>	<b>[GPa]</b>	<b>[MPa]</b>	<b>[m Pa s]</b>	<b>[C]</b>	<b>Temp. [C]</b>
BP Amoco Torlon® 4301	1.46	30.45	6.60	164.00	solid	260	279.00
BP Amoco Torlon® 5030	1.61	29.45	10.80	205.00	solid	260	282.00
BP Amoco Torlon® 7130	1.48	39.50	22.30	203.00	solid	260	282.00
<b>Polyetheretherketone Thermoplastic Resin</b>							
Victrex PEEK™ 381G, Depth Filtered Pellets	1.30	47.00	3.50	97.21	solid	142.77	160.00
Victrex PEEK™ 450G, General Purpose Pellets	1.30	44.00	3.50	97.21	solid	142.77	160.00
Victrex PEEK™ 450FC30, Lubricated Pellets	1.44	39.75	8.30	141.95	solid	142.77	276.66
<b>Polyethylene Thermoplastic Resin</b>							
Chevron Phillips Marlex® C579 High-Density	0.945	0.60	1.10	22.06	solid	N/A	72.77***
Chevron Phillips Marlex® K605	0.959	0.60	1.59	30.33	solid	N/A	N/A

**Figure 2.17 Thermoplastic Neat Resins (\*\*\* HDT 0.455 MPa)**



## 3 Design for Manufacturing (DFM) for Composites

### 3.1 Introduction

Design for Manufacturing (DFM) or Concurrent Engineering concepts are nothing new and have been employed successfully for a considerable number of years. In particular Boothroyd & Dewhurst [1] have shown in their studies how cost conscious design can save money and increase the competitiveness of a product. The concept is based on the idea, that if the decision makers within each step of the product value chain interact constructively, the overall system can be optimized instead of individual subsystems. The outcome will be an improved product depending on the design or customer requirements. These design requirements can either involve performance (strength, weight, stiffness), production costs or part quality or a balance between all three parameters. Commonly, the stages of the design process are divided into concept development, preliminary design, detailing and production planning. As illustrated in Figure 3.2, industry experience shows that the majority of costs are committed in the first two stages of the development process [2, 3]. During these early stages the cost saving opportunities are the largest and providing designer with a cost feedback of their decisions is crucial. Therefore, a thorough understanding of how these costs are generated is essential for a successful cost reduction. An analysis of design parameter and their effects on part production can provide insight into cost/design relations.

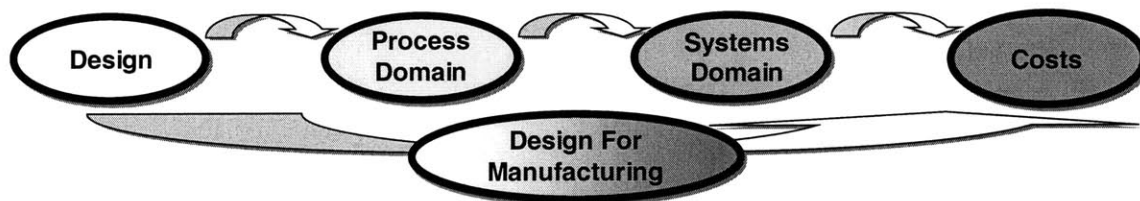


**Figure 3.1** Role of Design for Manufacturing Concepts

The derived Design for Manufacturing (DFM) and Design for Assembly (DFA) rules can serve two purposes. First, these guidelines encourage a standard of best design practice for certain materials and processes and thereby facilitate cost modeling. Secondly, DFM

rules for composites will help to shorten the path from the design to the costing phase as previous work in other areas has successfully demonstrated [1, 3, 4]. The subsequent chapters will introduce DFM guidelines for the production of advanced fiber reinforced materials. In particular guidelines will be developed in support of process selection decisions for Hand Lay-up (HLU), Automated Tow Placement (ATP), Double Diaphragm Forming (DDF), Resin Transfer Molding (RTM), Pultrusion (PUL), Autoclave Cure and Assembly processes.

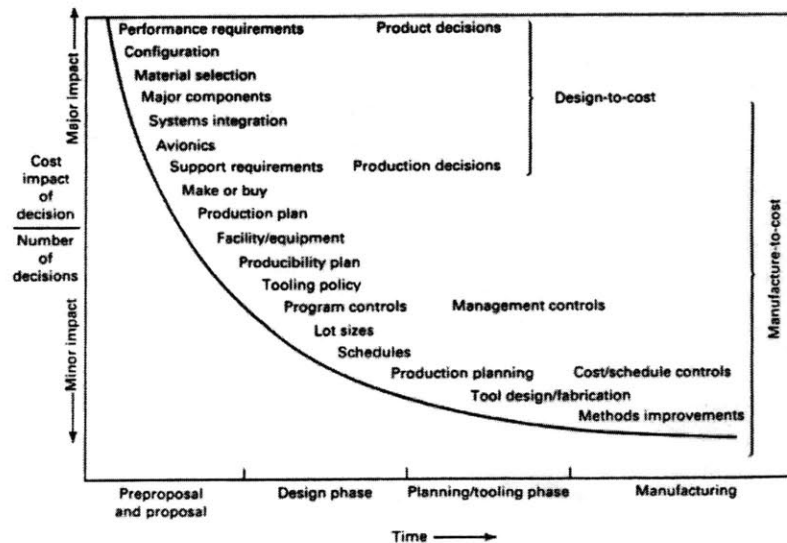


**Figure 3.2 Cost Saving Opportunities over Project Evolution [2]**

Process selection guidelines provide a general overview of available composite manufacturing methods, their major area of application and their capabilities in terms of size, complexity and production volume [6]. They are intended to help practitioners new to the field, to quickly narrow down the processes suited for their particular manufacturing needs. Process selection assistance will be given for the 7 composite manufacturing processes including assembly. For each process a comprehensive summary including illustrations highlights the process' capabilities, raw materials and equipment requirements. In general process selection can be best described as decision problem with multiple objectives [4] and a process selection matrix gives recommendations for the common usage and application of the above composite manufacturing processes.

## 3.2 Composite Manufacturing Processes

Before going into the characteristics of composite manufacturing processes an overview and classification of the available production processes will help any user to compare processes and better judge the many process variations. Conveniently, the processes can be categorized in terms of their primary shape generation, their consolidation and curing mechanisms. Finishing and quality assurance processes will not be mentioned for the sake of simplicity, but can be studied using the following references [2, 6, 8-11].

### Primary Shape Generation

#### b) Lay-Up

- Hand Lay-Up (HLU)
- Automated Tow Placement (ATP)
- Automated Tape Laying
- Contoured Tape Laying
- Filament Winding

#### c) Textile

- Braiding 2D & 3D
- Weaving
- Knitting
- Stitching

#### d) Forming

- Diaphragm Forming (DDF)
- Compression Molding
- Hot Transfer Press Molding

#### e) Impregnation/Wetting

- Pultrusion (PUL)
- Resin Transfer Molding (RTM)
- Vacuum Assisted Resin Injection (VARI)
- Reaction Injection Molding (RIM)
- Structural Reaction Injection Molding (SRIM)
- Reinforced Reaction Injection Molding (RRIM)

This study discusses one process of each category in more detail and looks at its economical characteristics. The many process derivations for special applications such as the one for Resin Transfer Molding are beyond the scope of this study.

#### Consolidation & Curing Processes

- Oven
- Vacuum Bagging
- Autoclave
- Hot Press
- UV Radiation
- Radio Frequency

Either thermal, ultraviolet or microwave radiation is employed to initiate the cross-linking mechanism of the resin systems and therefore the curing of the part. Structural integrity is achieved by compressing and consolidating the bonded layers through either vacuum or iso-static pressure.

#### General Characteristics of Composite Manufacturing Processes

The manufacturing of composite structures is more comparable to a casting process as it is to a conventional machining process. Similar to casting, composite production is an additive process in which material is added to built up the ultimate shape of the designed part. Also in many cases, a mold or tool is used to define the shape and dimensions of the part. Therefore composite production processes use material more deliberately than machining operation and have the potential to lower material waste. However, in contrast to casting, composite production is mostly performed in a sequential fashion at least at one point of the production cycle where the laminate properties are defined. The production of composites offers the great advantage to tailor the material to the expected load and performance requirements of the part. This optimization of the part's microstructure has consequences for the fabrication processes. As opposed to casting the processes have to provide the capability to accurately position each layer or fiber strand as the laminate is being built up.

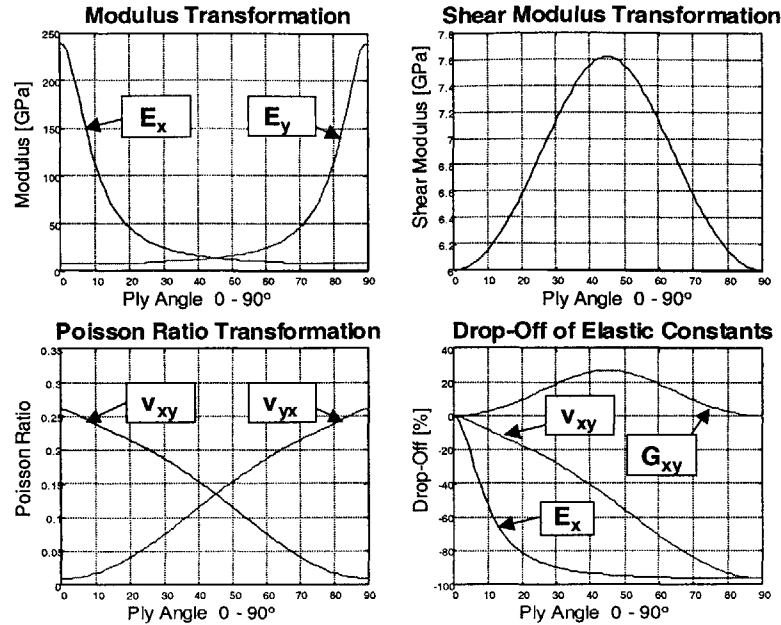


**Figure 3.3** Laminate Properties and Fiber Orientation

Figure 3.3 shows the sensitivity of the major mechanical properties to the fiber direction and therefore the lay-down angle for a unidirectional laminate. This particular process requirement also explains why automation in an effort to reduce labor and production costs has been so difficult to achieve. As it turns out automation often trades off up front investment costs with variable labor costs. Since automated process equipment is still very expensive the decision comes down to total production volume and if the investment costs can be recovered.

### 3.2.1 Process Discriminators

When selecting processes, several general factors have to be taken into account. These process discriminators describe the process' overall capabilities and determine whether a process is suitable to the specified production requirements.

- Size, Shape & Laminate Limitations
- Quality, Tolerance & Surface Finish Capabilities
- Investment & Operational Costs
- Equipment, Tooling & Labor Requirements
- Process Performance (Production Rate & Lead Time)

#### Size Limitations

The production equipment and the available facilities pose size restriction on process capabilities. Often equipment for curing, such as ovens or autoclaves, comes with certain maximum holding volumes, which cannot be exceeded. However, lay-up facilities can also pose special demands on size. As for manual lay-up station the reach of the worker is often a limit unless means to access the parts from all sides are provided. For automated equipment the size is limited by the maximum travel of the individual axis.

#### Shape & Laminate Limitations

Although a wide variety of shapes and geometries can be fabricated with composite materials, some limitations exist for individual processes. Tight radii or double curvature can often cause wrinkles in the laminate, which has deteriorating effects on the mechanical properties. In particular if fabric or woven material is used in connection with the process. Also, some processes such as Pultrusion only allow the production of straight parts, which exhibit constant cross-sections. The various processes also differentiate themselves in terms of their capability to accurately control the macroscopic properties of the laminate such as the fiber angle and the maximum fiber volume fraction. Again, the mechanical properties suffer, if either the fiber angle is inaccurate or the fiber

volume fraction is below the specified one. Eventually, the economic impact of the part complexity has to be considered and is discussed further in Chapter 5.1.

### Quality & Tolerance

The ability of a process to consistently produce a part within the specified tolerances has a major impact on process selection and manufacturing economics. Not only economic consequences associated with scrap or rework are significant, but also the reduction of overall production capacity. If capacity is limited due to quality issues the production demand cannot be satisfied. The tolerance for ply thickness lies within  $\pm 0.006$  in., however accumulation of these errors over several plies can be significant. Therefore, tooling often determines dimensional tolerances and unless a process, such as RTM, lends itself to the use of closed tooling, the accuracy of at least one dimension has to be compromised. The shrinkage of parts due to the consolidation pressures and the evaporation of the volatile resin components have also been taken into account.

### Surface Finish

Similar to the variation of the part thickness, the surface finish is very much determined by the employed tooling type. Processes which use closed tooling with polished surfaces yield the best finishes on both sides of the part. However, many components possess a visible and a non-visible side. In such cases, open mold tooling delivers satisfactory results.

### Investment & Operational Costs

Investment and operational costs, such as labor requirements, maintenance and consumables determine the economic success of a product and therefore its survival in the marketplace. Because of the vital importance of these costs subsequent chapters are dedicated solely to these decision variables.

### Equipment & Tooling Requirements

Equipment and tooling requirements have a direct impact on investment and operational costs. It is not only important to know what each process requires from a cost point of view, but also from a manufacturing planning standpoint.

### Process Performance

Process performance determines the speed with which a part can be manufactured. Given a certain annual production volume the process performance (cycle & lead time) determines how many parallel production streams are required to fulfill demand. Needless to say that each duplication of production equipment leads to higher investment costs.

### **3.2.2 Process Cost Drivers**

According to the theory of concurrent engineering or DFM the designer has to be aware of the cost consequences of his design decisions. Chapter 5 looks at process costs and their relation to design parameters with great detail.

- Production Volume & Batch Size
- Process Cycle Time (Non-recurring & recurring)
- Labor & Equipment Rates
- Learning Curves
- Productivity & Utilization
- Scrap Rate

### Production Volume & Batch Size

The cumulative production volume has a direct impact on total and unit costs. In general unit costs go down as more parts are produced since any investment is simply spread over a larger amount of parts. Also increasing batch size often reduces unit costs, because setup costs have to be born less frequently.



### Process Cycle Time

The production time of a part is directly related to its ultimate costs. For every hour equipment or labor is used, costs are accrued. From a design point of view the cycle time is directly influenced by the size of the part, its shape complexity, the laminate structure and the tolerance requirements. The subsequent Chapter 4 on cost modeling presents relationships between design parameters and process cycle time.

### Labor & Equipment Rates

All workers have to be paid their wages, but also associated benefits and any overhead costs have to be considered. A similar calculation can be conducted for machines, tools and auxiliary equipment, which also include maintenance and charges for consumables.

### Learning Curves

With each part produced workers become more efficient and processes are improved. This learning process can lead to significant cost reductions and its potential has to be estimated for each process. In general, learning is more pronounced for labor-intensive processes and less for highly automated processes. Chapter 4.4.5 on cost modeling further introduces the concept of learning curves.

### Productivity & Utilization

Idle workers and machines still have to be paid and therefore cost money, but obviously do not produce any parts. The level of productivity and machine utilization is different for every organization. It depends on the plant layout, the motivation of the work force and the processes used.

### Scrap Rate

When a part has to be scrapped because of missed quality targets the material, labor and processing costs are lost. Correct process selection in concert with reasonable tolerance requirements from designers can greatly reduce scrap. Scrap also reduces productivity and production capacity and can possibly lead to production bottlenecks.

### 3.2.3 Hand Lay-Up (HLU)

#### Process Description

Composite fibers are manually deposited layer by layer onto a tool, which gives the part its shape. The operator cuts each ply, removes possible release films and places the new ply in its predefined location. Hereby, the operator has to ensure the correct orientation of the fibers and the absence of wrinkles. The manual lay up rate generally lies between 0.002 and 2 lb/hr.

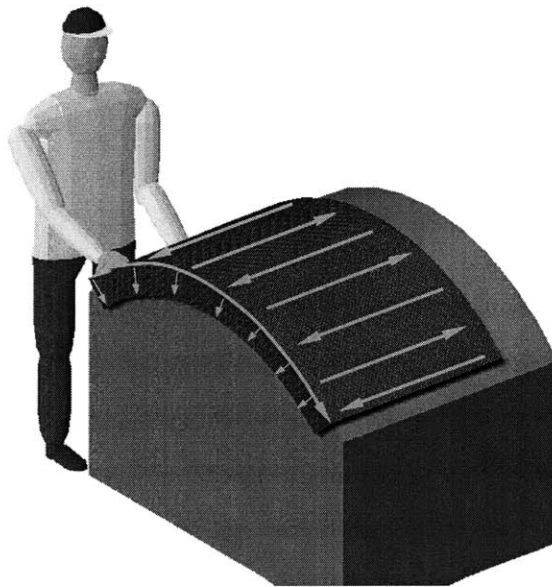


**Figure 3.4 Hand Lay-Up Process (HLU)**

#### Material

All types of materials such as unidirectional tape, woven preregs of dry fiber mats can be processed through hand lay up. Single strands and very narrow tapes of fibers are not usually economical to be layed up manually. Aside from workers safety issues, there are no restrictions regarding the resin systems that can be processed. Commonly, preimpregnated woven material is used, because it is easy to form and the tackiness of the resin prevents the material from slipping on the layup tool.

### Equipment

Only minimal investment in manufacturing equipment is required, which generally includes a layup table, storage racks and possibly templates or even laser projectors to aid in positioning the plies. In addition worker safety equipment is used, such as latex gloves, lab coats and respirators, which protect against fiber dust and resin volatiles. Carpet or electrical knives are utilized to cut the plies into their final shape. Sometimes a CNC cutter pre-cuts the plies and thus reduces labor time. Also various mechanical devices are employed to help handle and unroll the material.

### Tooling

Layup tooling can be manufactured of wood, cast epoxy and metal depending on the size of the production run and the required temperature range of the tool. If the layup tool also serves as a curing tool, it has to withstand temperatures around 350°F (175°C) and consolidation pressures on the order of 100 psi (0.7 MPa). In general open mold tooling is used for layup, although layup into an open half of a matched tooling die is possible.

### Application

There are no limits for hand layup in terms of part shape. Part size is only limited by accessibility and material shelf-life (safe usage time of material). Generally male shapes are more economical to lay up. The accuracy of the ply deposition can become an issue for certain high performance parts, but can be enhanced by layup aids such as pins, marks or even laser projections. Hand Lay-up is commonly used for low volume or prototype production of 1 to 30 parts/month depending on size. Numerous applications can be found in aerospace, and boat building [2, 9].

### 3.2.4 Resin Transfer Molding (RTM)

#### Process Description

RTM consists of a resin being injected into a sealed matched mold containing a dry fiber preform. The preform is often pre-shaped and produced by secondary processes such as hand layup, braiding or weaving etc. After tightly closing the mold, liquid resin is injected under pressure (approx. 100 psi, 0.7 MPa) to impregnate the fiber reinforcements. The part is generally cured inside the mold and features smooth surface finishes on both sides and narrow part tolerances. Several derivations of this process exist (VARI, RIM, SRIM, RRIM) and their application depends primarily on part size and shape.

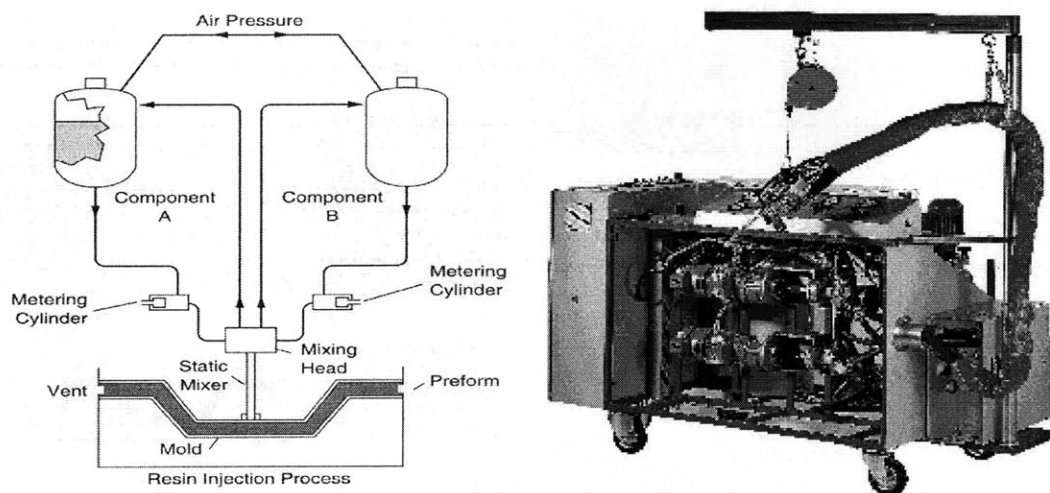


**Figure 3.5 Resin Transfer Molding Process (RTM) [2, 12]**

#### Material

All types of fiber material are used in their dry unimpregnated form to be shaped into preforms. Wovens, mats, and stitched unidirectional fabrics are processed. Mainly thermoset resin systems, such as polyester, epoxy and vinyl ester are injected, generally because of their low viscosity. Often the resin is cured at room temperature or at slightly elevated temperatures of 250°F (120°C).

### Equipment

Generally, a moderate investment is required to procure the metering apparatus, which stores and mixes 2 components of the resin (binder, catalyst) before it is injected into the tool. For higher production volumes hydraulic presses are used to quickly open and close the matched tools and prevent resin from escaping. For lower production volumes less costly mechanical clamps are employed for this purpose.

### Tooling

Closed mold RTM tooling is mainly machined out of Aluminum or steel in order to better withstand the injection pressure. However, also cast epoxy or zinc cast molds are used for less demanding, low volume production. The tooling surfaces are often coated and polished in order to attain a good surface finish of the part.

### Application

RTM is generally used for medium to high volume production of complex parts, which require a good surface finish. The application of the process for high performance products can be limited by the slightly lower fiber volume fraction inherent to the process. Production runs of 100 to 1,000 parts/month are considered economical. In terms of size there are certain limits because of insufficient impregnation. However, special derivatives of the process (SRIM) are also suitable for large structures. The process is mainly employed in the automotive, and sporting goods industries [13-16].

### 3.2.5 Automated Tow Placement Process (ATP)

#### Process Description

Automated tape or tow placement consists usually of a CNC controlled multi-axis machine, which deposits prepreg tape or tows onto the contour of a layup or curing tool. The automation allows good repeatability and accuracy when producing complex part shapes. The tows are stored on spools (reels), which are carried along with the placement head. Depending on the laminate design the tows can be placed and cut in all possible fiber directions. Limitations exist for the layup of small concave radii, which are smaller than the compression roller on the layup head. Typical placement rates are up to 10 lb/hr.

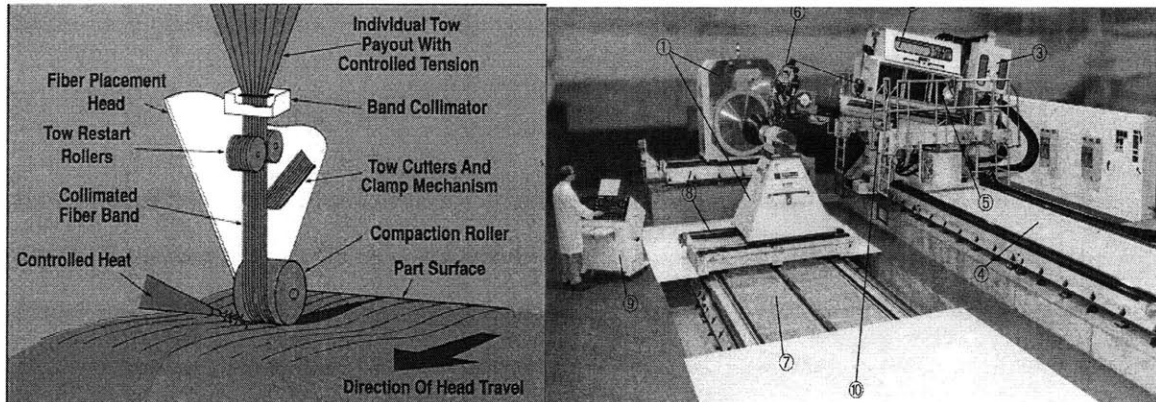


**Figure 3.6 Automated Tow Placement Process (ATP) [17]**

#### Material

Several types of reinforcement fibers are available as tows, which consist of several unidirectional strands. For the tows to stick to the tool surface, it is preimpregnated with the exact amount of resin necessary to achieve the desired fiber volume fraction. Commonly, epoxy resins are used but other types are possible and even thermoplastics can be layed up with modifications to the process. For thermosets, the out-time is important and therefore specially treated resin are employed, which exhibit several weeks of out-time. The tows are delivered on reels and come in various widths, from about 1/8" for tow placement up and 3", 6" and 12" widths for tape laying applications.

### Equipment

The investment for an ATP machine is considerable (usually \$5M). The gantry style machines are usually quite large (> 30 x 20 ft) and they often feature approximately 7 CNC controlled axes, which provide movement capabilities in space, head orientation, roller angle etc.

### Tooling

Tooling is generally manufactured out of metals since ATP is often used in large scale production and, depending on whether the tool is used for curing or not, it might be either machined out of Invar or Aluminum. For tape laying the tools are mainly flat or simply curved, whereas for tow placement they can also feature moderate double curvature. The tools should include machine reference points.

### Application

ATP is mainly used in aerospace for the production of large, simple to moderately complex parts. The typical production run lies between 5 - 100 parts/month. It is time consuming and therefore not economical to layup small, complex shaped parts. However, the process can achieve very good repeatability and accuracy [18-23].

### 3.2.6 Pultrusion Process (PUL)

#### Process Description

Pultrusion is a continuous automated process suited to the fabrication of composites featuring constant part cross-sections. Dry fibers are pulled through an impregnation station and are subsequently passed through a forming and curing die. Typical pultrusion speeds range between 1 in/min to 10 ft/min. Commonly wall thickness ranges between 0.05" and 3" and radii should not be smaller than 1/16". A part tolerance of approximately  $\pm 0.01$ " can be expected due to shrinkage effects.

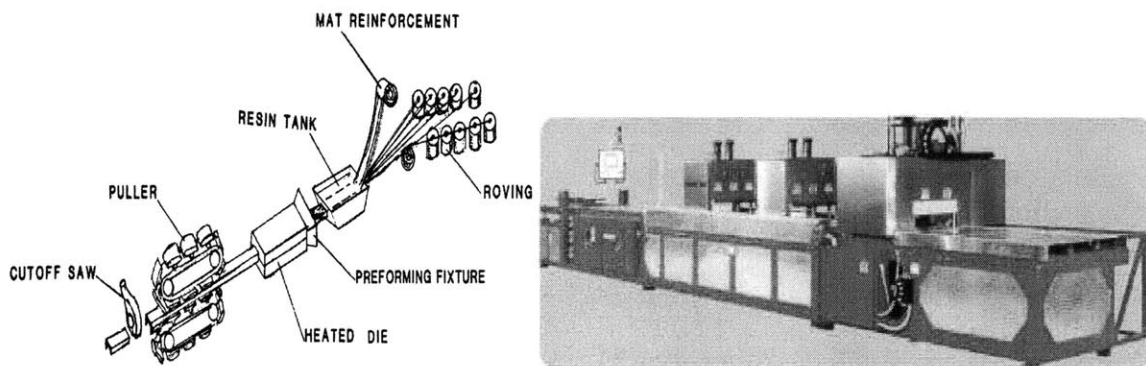


**Figure 3.7 Pultrusion Process (PUL) [25]**

#### Material

Typically glass, aramid and carbon fibers are used, which are stored in dry form on so-called creel stands. Although woven and multi-axial fibers can be introduced into the pultrusion process, the majority consists of unidirectional fibers, which take up the pulling forces. Resin systems such as epoxy, vinyl ester and polyester are employed, which are specially enhanced to promote faster curing. However, also fibers preimpregnated with thermoplastic matrix are now used. The attainable fiber volume fraction lies between 20% and 50%.



### Equipment

The investment costs for a pultrusion apparatus are moderate to high. The installation consists of several components: the storage unit for the dry reinforcement fibers or creel stand, the fiber impregnation station or resin bath, followed by a heated forming die in which the cross-section is formed and the resin is cured. The rigid profile is then grabbed by a pulling mechanism (band or reciprocating grippers), which continuously advances the profile at a pre-set speed. Finally, a cut-off station trims the profile to its precise length.

### Tooling

The heated and cooling section of the forming die have inserts, which are shaped according to the form of the produced profile. These inserts are mainly machined out of steel and are chrome-plated for wear resistance. For hollow profiles, special tooling including a floating core is required.

### Application

The pultrusion process is best suited for the mass production of profiles with constant cross-section. Pultruded composite profiles are available in nearly any shape and therefore can replace extruded aluminum. Pultruded profiles are increasingly used as structural elements of larger constructions such as buildings, bridges and electrical towers, in particular because of the insulation capabilities of pultruded glass fiber [2, 9].

### 3.2.7 Double Diaphragm Forming (DDF)

#### Process Description

The diaphragm forming process starts out with the entire laminate in a flat state, before forming it in one step into its final shape. This can significantly reduce the production time in comparison to hand layup. The process employs hydrostatic pressure to shape the stack of plies over a tool. Elastic diaphragms clamp the relatively stiff fibers with vacuum pressure and thus minimize buckling and wrinkling in the formed part. Several derivatives of the process exist, such as single - and double diaphragm forming and matched die forming. Once formed the part is usually transferred to an autoclave or oven for cure.

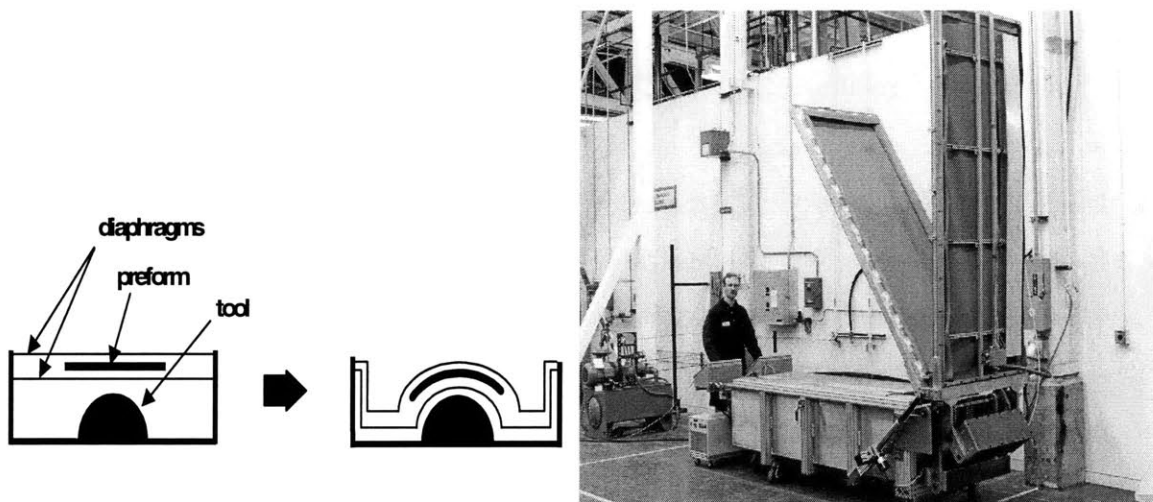


**Figure 3.8 Double Diaphragm Forming Process (DDF) [26, 27]**

#### Material

Woven prepreg material is normally used, but unidirectional tape is also possible to be formed within certain boundaries. Thermosets such as epoxy, vinylester, polyester, or thermoplastics hold the fibers together, prevent slipping during the forming and bond the material after cure.

### Equipment

Moderate investment is required to acquire forming machines, which are often custom built for a particular product line. The machine generally consists of a tank substructure, which contains the tool holder and is sealed by a silicone rubber diaphragm. A vacuum system provides the hydrostatic clamping and forming pressure. In addition, a heater/cooler system is installed to soften the resin prior to forming and stiffen it to lock in the formed shape.

### Tooling

The tooling can be made out of wood, cast epoxy or machined metal as long as it can withstand the forming pressure. The size of the production run determines the material choice for the mostly male forming tools.

### Application

The process lends itself for high volume production of mainly simply curved and slightly double curved parts. The timesavings in comparison to hand lay-up are significant, and especially for small and medium size parts the process is even more economical than, for example, automated tape laying [9, 26].

### 3.2.8 Autoclave Curing Process

#### Process Description

The autoclave promotes a chemical reaction in order to solidify the resin within the laminate. Internal autoclave pressure and vacuum assist the consolidation and bonding of the individual layers. The pressure ranges between 80 psi (0.5 MPa) to 100 psi (0.7 MPa) and the curing temperatures are between 250°F (120°C) and 450°F (230°C), depending on the resin system. Prior to the autoclave run, the part is sealed with a vacuum bag, which also includes layers of spongy material (breather, bleeder) to soak up excessive resin and carry away volatiles and moisture. The duration of the cure cycle depends on the resin and generally lasts between 3 to 8 hours.

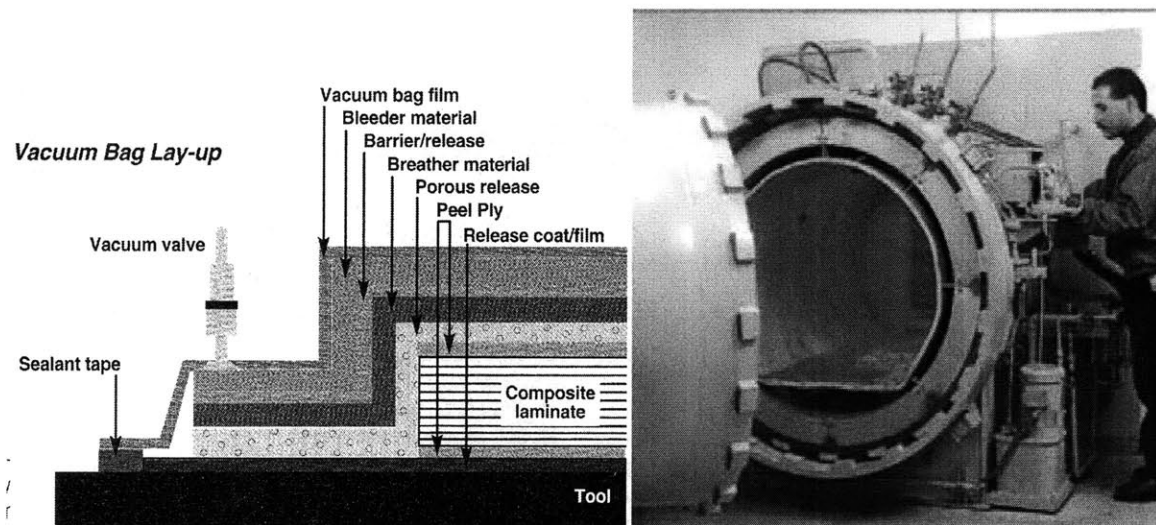


**Figure 3.9** Autoclave Curing Process [28, 29]

#### Material

A wide range of materials can be processed. Thermosets and thermoplastics are used for impregnation or bonding applications.

#### Equipment

The investment cost for an autoclave is medium to high. Aside from the actual pressure chamber the supply of compressed air and vacuum needs to be installed. Some

autoclaves even require a nitrogen atmosphere, which necessitates storage facilities for compressed nitrogen. For the heating of the autoclave chamber gas is generally used for large autoclave, whereas electricity is used for smaller systems. Also the control and data acquisition equipment for pressure, temperature control can be a major cost driver if it is computerized and fully automated.

### Tooling

Autoclave tooling is mainly made of metal or even composites, which both can withstand the high temperatures and pressures. A one sided open mold gives the part its shape, however the thickness is only loosely controlled through the consolidation pressure and the ply thickness. The part is sealed with a vacuum bag and therefore the tooling often has to be tested for its vacuum integrity before the first production run. Due to the elevated curing temperatures matching of the CTE can be crucial to achieve high dimensional accuracy and/or to ensure proper demolding of the part. Therefore often Invar or carbon fibers composites are used, which exhibit similar CTE's as the carbon fibers themselves. For curing of flat and simple parts, Aluminum tools would also work. Ultimately the material choice for the tool depends on the size of the production run and the duration of the production program.

### Application

Autoclave cure is used for a wide range of part sizes and complexities where excellent consolidation and mechanical properties are a must. In principle there are no limits in terms of part shape aside from the fact that one-sided tooling is employed and demolding has to be ensured. Autoclaves are mainly used in aerospace application of small to large production runs. The curing of laminates, but also the subsequent bonding of pre-cured parts are among common autoclave batch operations [2, 29, 30].

### 3.3 Composite Assembly Processes

#### 3.3.1 Assembly Process Discriminators

Again the process selection is mainly based on the underlying design concept and the degree of integration. A list of process discriminators helps to make the trade-off between performance and assembly cost:

- Size & Access Limitations
- Joint Quality & Tolerance
- Investment & Operational Costs
- Equipment, Tooling & Labor Requirements
- Process Performance (Production Rate & Lead Time)

#### 3.3.2 Assembly Architecture and Integration of Parts

The assembly architecture and integration of parts during concept design of the product have to be determined. While considering all the assembly cost drivers, it has to be decided whether the product will have an integral or modular design. Both concepts need to meet design requirements, which in turn will affect performance and producibility. Design for Assembly rules can be applied to help with the final decision.

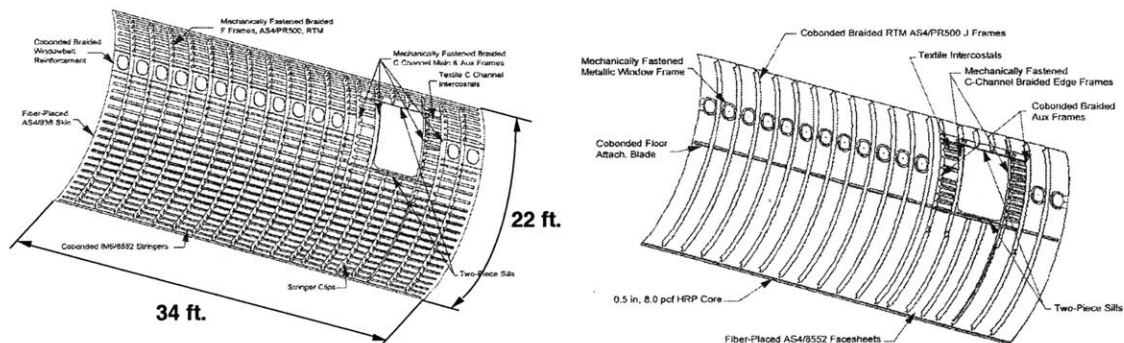
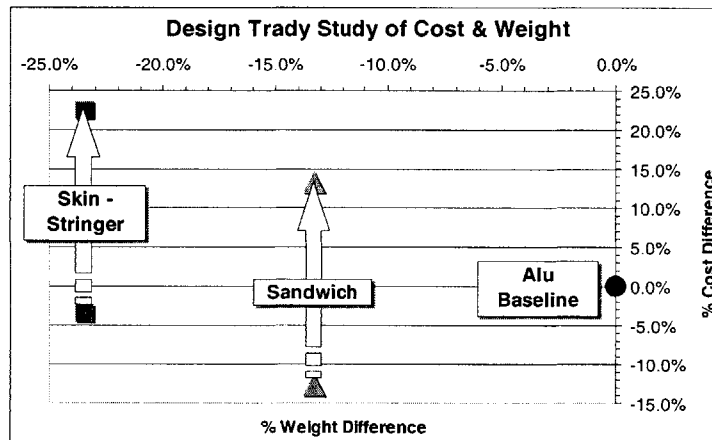


Figure 3.10 Skin Stringer - vs. Sandwich Composite Design [31, 32]

A major strategy to reduce cost in composite fabrication has been the integration of parts. While trying to keep the part performance (strength & stiffness) constant, various degrees of integration can be evaluated in terms of their costs. In general, the higher the part count, the more labor intensive is the assembly. For example the design for an aircraft fuselage shows (Figure 3.10) that the higher part count of a skin-stringer design increases the labor intensive assembly costs, which are traded off by higher tooling costs required for co-bonding the skin in the more integrated sandwich design. A further cost driver are the joining methods used to assemble composites. For example, co-cure, which also can be described as "soft" assembly because most of the components are still flexible and possess more degrees of freedom than their rigidly assembled counterparts. Co-cure are can reduce delays and costs due to over constraints and tolerance build-up [30, 32]. However, higher integration can create increased manufacturing risks since the potential scrapping of a part becomes progressively more expensive. Figure 3.11 shows the results of a NASA study, illustrating the trade-offs between weight and costs [31].



**Figure 3.11 Composite Fuselage Side Panel vs. Aluminum Baseline [31]**

### 3.3.3 Assembly Cost Driver

Minimizing assembly costs is clearly a design function and this must include proper consideration and identification of all cost drivers:

- Production Volume
- Process Cycle Time (Non-recurring & recurring)
- Number of Components
- Fastening Method
- Accessibility
- Shimming & Surface Preparation
- Dimensional Tolerance
- Labor & Equipment Rates
- Productivity & Utilization
- Quality & Rework Rate

The number of parts in an assembly has a significant impact to the total assembly cost. Generally, the goal is to generate a design with the minimum number of parts, while achieving the necessary functionality at the same time. Less parts results in reduced assembly operations and less assembly material (fasteners, adhesives). Less assembly material also contributes to weight savings. However a more integrated structure tends to create a more complex design, which makes access more difficult. Lack of accessibility can also limit the use of automatic fastener installation technology. A more complex design requires also complicated and expensive tooling [36-43].

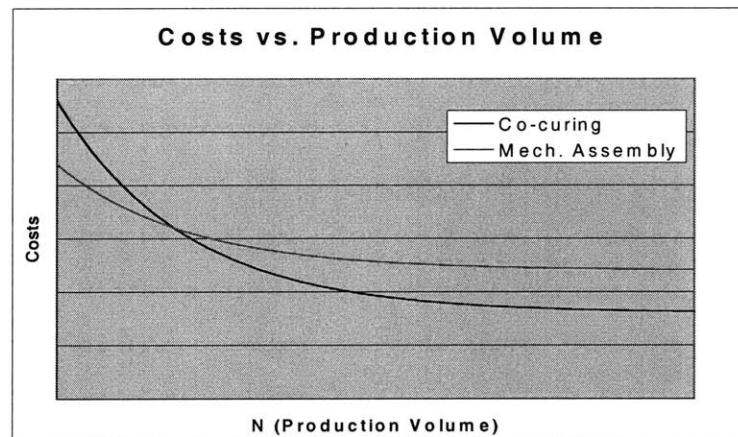


**Figure 3.12** Expected Trade-off between Investment and Variable Costs



### 3.3.4 Mechanical Assembly

#### Process Description

Mechanical fastening represents the most straightforward joining process for composites because of its similarity to metal joining. Engineers understand the design of mechanical joints very well including the associated loads and stresses [2, 11]. For composites the critical parameters are static and cyclic lap shear or bearing failure. Therefore the overlapping area should be maximized within the design envelope and a minimum amount of  $\pm 45^\circ$  and  $90^\circ$  plies should be used. In addition the strength of the composite to resist pull-through of the fastener has to be calculated carefully due to the frequently reduced mechanical properties of the laminate perpendicular to the fiber network. In order to achieve the increased reliability of mechanical joints in comparison to other methods, the spacing of the fasteners becomes another major design parameter. Fastener spacing has a considerable impact on manufacturing cost and weight of the final structure. Manufacturing costs are often driven by the cost of the fastener and the installation time for each fastener. The fastening process, however, lends itself easily to automation, which for higher volume production results in significant cost reductions. Further advantages of mechanical assembly are the reparability of large structures and the possibility of unproblematic disassembly at the end of the useful life.

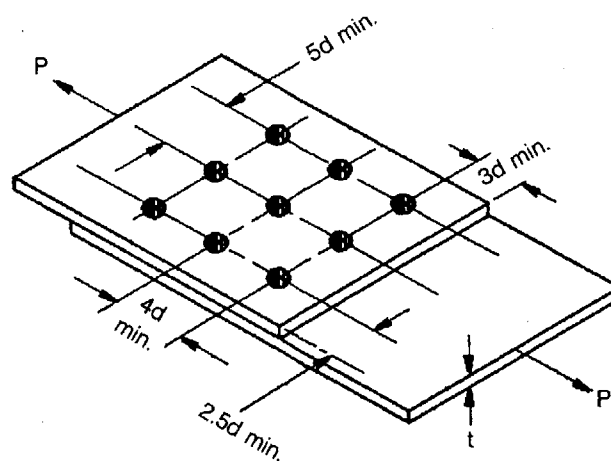


**Figure 3.13 Fastener Spacing (Fastener Diameter: d) [2]**

Although, surface treatment of the parts to be joined is generally not necessary, shimming is usually required when joining parts with large overlapping areas. The shim is a liquid or liquid-solid mixture, which is applied between the parts and cured to provide a proper match. The shimming operation is a very critical, but time-consuming process because even small gaps between mating surfaces lead to improper loading of the composite laminates, which can lead to delamination and structural failure. Also the drilling of fastener holes can lead to complications, because the severed fibers not only interrupt the transfer of loads, they also allow water to enter and possibly weaken the laminate. In order to minimize moisture adsorption, care has to be taken when drilling to avoid unnecessary fraying of fibers and to insure a perfect fit between fastener and material.

### Material

Similar to the joining of metal assemblies, composites are also joined by using rivets, pins and bolts, which however are modified in their design to accommodate the special properties of the composite material. Since composites are sensitive to crushing, the heads of any fastener should be large enough to sufficiently distribute the clamping loads. The clamping loads are limited through special design features on the fasteners, which prevent an overloading of the laminate. Another important consideration in fastener selection is the avoidance of galvanic corrosion, which is aggravated when joining carbon fiber composites.

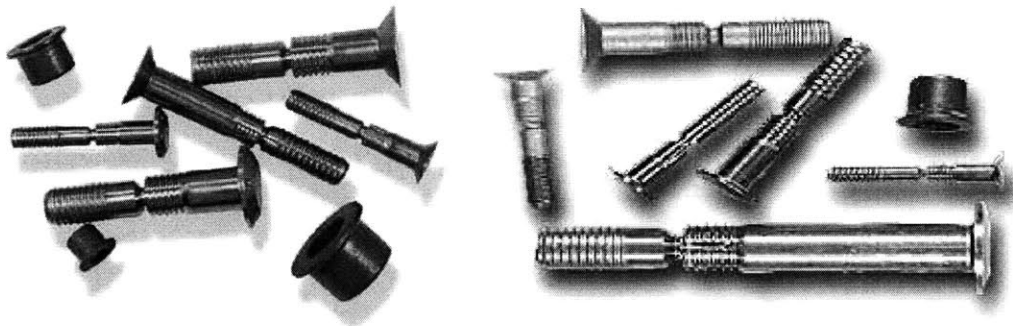


**Figure 3.14** Titanium Lockbolt Fasteners [33]

Particularly resistant are titanium fastener, but also some stainless steel types and nickel alloys are compatible with carbon fibers. Aluminum fasteners are used more for glass

fiber constructions. The combination of the different materials always leads to some thermal mismatch, which has to be taken into consideration when exposing the structure to thermal cycling. Thermal mismatch can lead to stresses and fatigue within the joint. Weight and cost considerations have to be matched to the overall design objective.

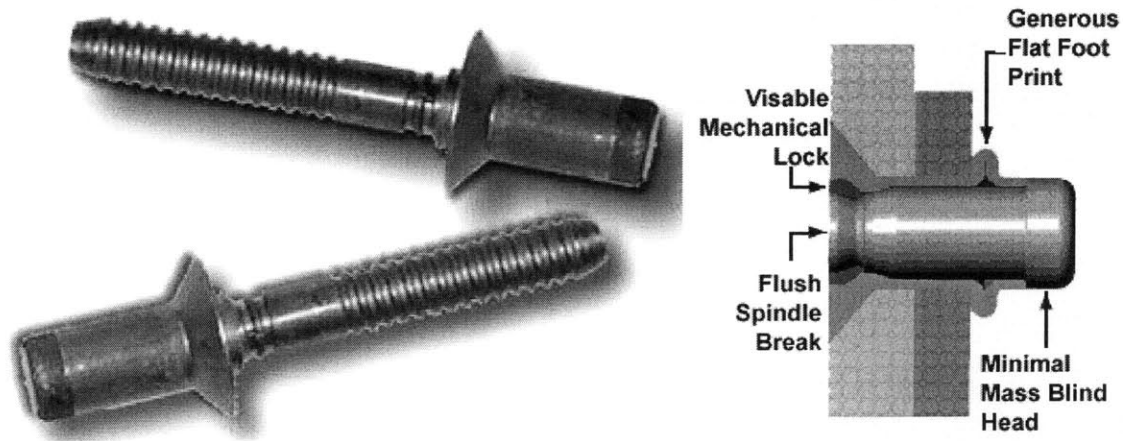


**Figure 3.15** Titanium Blind Bolt Fasteners [33]

### Equipment

Similar to metal structures, assembly fixtures are used to correctly position the individual components with reference to their counterparts. Fixture design and part tolerance are interrelated and have to be optimized in order to avoid the build-up of residual stresses in cases of over-constrained assemblies. In terms of investment cost, the designer has to minimize overall costs. There exists a trade-off between less complex assembly fixtures using higher integrated components and the potentially more complicated rigs needed to assemble structures with higher part counts.

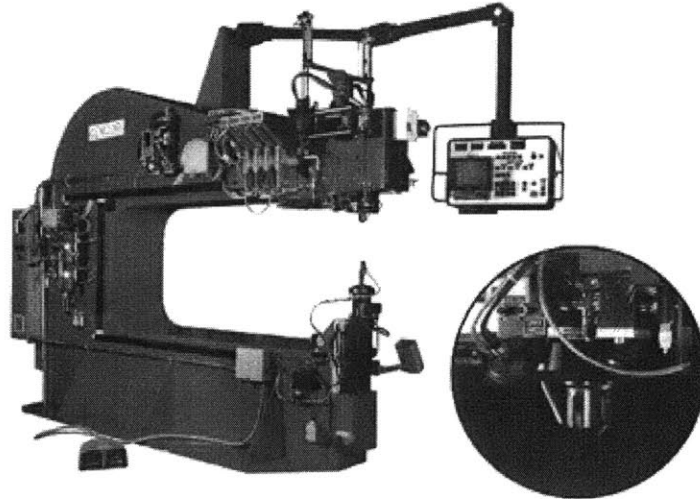


**Figure 3.16 Automated Fastening Machine [34]**

The installation of fasteners requires fairly inexpensive equipment for drilling. However, there is an opportunity for cost savings when using automated tools for the insertion and tightening of fasteners. The projected total production volume determines whether such a step is economically warranted [35].

#### Application

Due to its versatility and simplicity, mechanical joining can be used in a wide range of applications. However, one can observe some interesting trends, where the aerospace applications outnumber the use of mechanical fasteners in the automotive sector. Despite the weight disadvantage, the reliability and improved inspectability of the process gives aerospace engineers a better safety margin.

### 3.3.5 Adhesive Bonding

#### Process Description

Adhesive bonding is an assembly process where a material (adhesive) is placed between two already cured parts (adherents). Under the application of sometimes considerable consolidation forces, the adhesive is cured at either ambient or an elevated temperature. In order to achieve good bonding strength, the bonding surface has to be prepared and cleaned of any contaminations, which could negatively affect the adhesion strength. Mechanical and liquid surface preparation methods are common. Also the design of the joint can be critical for the strength. In general, the joint should be designed so normal and peeling stresses are minimized. However, some of the joint designs can require machining, which is less desirable in terms of cost and laminate integrity. Furthermore the gap width should be constant and adjusted for the viscosity of the adhesive [2,11].

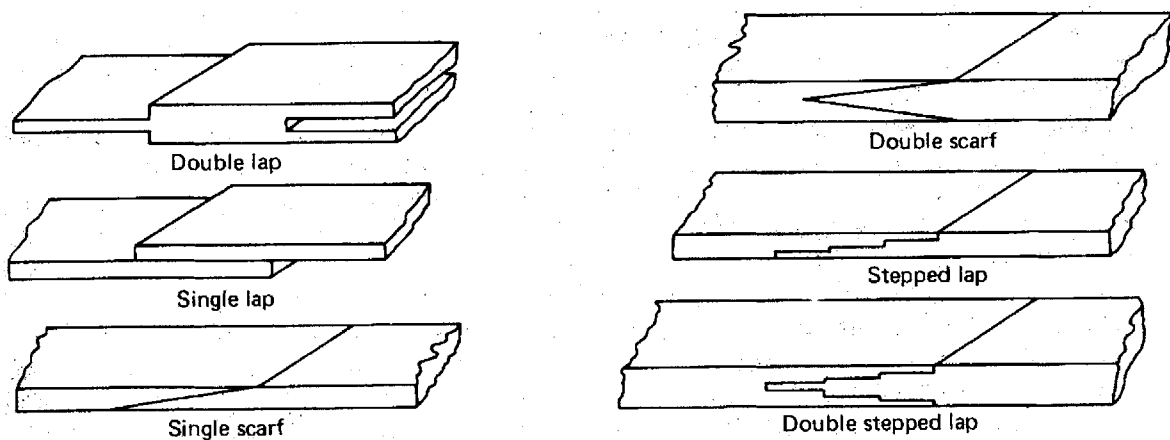


**Figure 3.17 Bonded Joint Configurations [2]**

Advantages of adhesive bonding lie within the substantial weight and cost savings when compared to other joining techniques. Due to the large bonding areas, loads are distributed evenly and stress concentrations can be minimized. The possibility to create smooth surfaces improves the aerodynamic qualities of the connection. Bonding also enables designers to easily join different types of materials. For the safe operation of bonded structures throughout their lifetime, the fatigue life of adhesive bonds has to be considered carefully. Thermal cycling and/or operation at elevated temperatures can

weaken the structural integrity. In addition to crack development and growth, the more elaborate inspectability of the bonding area can influence the life cycle cost. For damaged areas special methods for repair have to be developed in order to restore the full load carrying capability of the structure.

### Material

The selection of the adhesive is also an important part of the bonding design. The adhesive must be compatible with the adherents and must withstand the required stresses in the full range of environmental conditions to which the component may be exposed. Selection tests for adhesives should include stressed durability testing for heat, humidity and stress simultaneously. Furthermore, the viscosity of the adhesive has to be adapted for the gap width between the adherents. For a small gap, high viscous bonding agents achieve optimum performance characteristics. The adhesive costs are directly related to the required performance criteria, such as strength and operating temperature. Adhesives based on epoxies, phenolic resins, and also thermoplastic resins are available.

### Equipment

Aside from equipment for surface preparation, special clamping and curing tools are often required. Tooling is probably the most dominant cost driver since recurring material costs are relatively small in comparison to mechanical joining techniques. The tooling not only has to ensure the correct positioning of the components, but also has to provide sufficient clamping forces for the subsequent curing cycles. Since the curing of the adhesive is commonly conducted at elevated temperatures, thermal expansion has to be taken into account when requiring small tolerances and minimal residual stresses. Tooling can therefore be more expensive and the investment costs have to be assessed with respect to the total production volume.

### Application

Due to its simplicity adhesive bonding is being used increasingly, in particular as more and more advanced bonding agents become available. The advantage of combining components of different materials into a lightweight and strong structure proves very attractive for the aerospace and automotive industry. The relatively small recurring costs and weight benefits will expand the usage of this methodology once all reliability and failure issues are understood.

### 3.3.6 Co-Curing

#### Process Description

Co-curing joins two or several uncured components simultaneously during a single cure cycle to form a larger more integrated structure. The process allows designers to prescribe the fiber directions and fuse the constituents together to a coherent structure, which generally results in improved mechanical properties and superior weight performance. Since all the components are assembled in an uncured and flexible state, the soft assembly is generally not over-constrained. Therefore residual stresses are low and strength improves. In addition, the integration of parts not only reduces the part count, but also saves time and therefore decreases overall assembly costs.

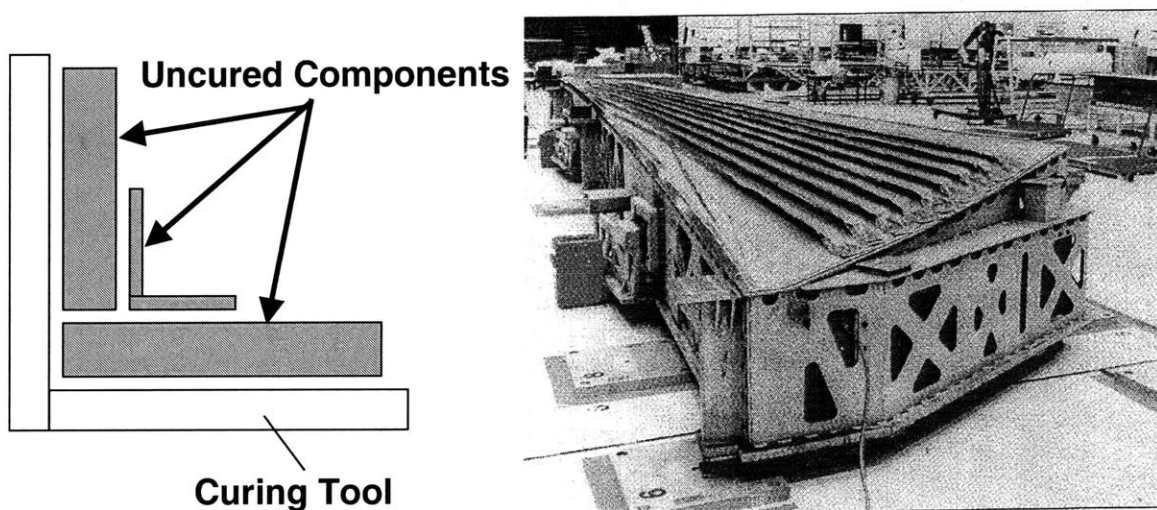


**Figure 3.18 Schematic of Co-Curing, Co-Cured Skin Stringer Assembly [32]**

As disadvantages of co-curing, one can list the increased complexity of the produced part. The increased complexity makes inspection more difficult and time consuming, in particular when accessibility is restricted. Increased tooling cost and the risk of scrap have to be taken into consideration when estimating production cost. The increased complexity also requires additional caution during design in order to avoid the locking in of thermal stresses and the resulting deformations.



### Material

Aside from the common bagging materials for curing processes, no special materials are usually required.

### Equipment

Co-curing requires more sophisticated tooling in order to define the geometry of the final part. In particular for high temperature curing resins thermal matching of tool and laminate becomes crucial. These requirements can drive up investment costs for tooling significantly. Also secondary tooling such as caul plates, which ensure uniform consolidation pressure and surface quality, can add to tooling costs. As with the curing of individual parts, autoclaves or curing ovens are commonly used. However, the oven and autoclave have to be able to handle the increased size of the more complex part.

### Application

An aircraft that makes extensive use of co-curing is the AV-8B Harrier II. Primary considerations were low cost and lightweight. The approach was to design the aircraft with as few parts and fasteners as possible. This was accomplished by co-curing large graphite/epoxy structural components. The aluminum forward fuselage consisted of 237 parts and 6,400 fasteners. The new composite structure that replaced it is made of 88 parts and 2,450 fasteners [36].

Another application is the Beech Starship I, in which the majority of the airframe is co-cured. The 54 ft. long, single piece, top and bottom wing-skin panels are mated together with spars and ribs after they are co-cured. The Starship's advanced composites guarantee a lightweight and smooth structure.

### 3.4 Reference Geometries

The introduction of reference geometries limits the otherwise infinite possibilities of shapes and dimensions to a finite amount of structural building blocks. Each reference shape has specific characteristics and represents a class of parts. Because once fabrication guidelines are established for one part of a class, they can be cautiously expanded to other geometries and applications. For our purposes, we choose the most basic shapes. For example, there are thin membrane-like structures, which mainly exhibit a two-dimensional stress distribution under load. These thin plates can be used as skins and often define the outer surface of a larger structure. Other part types represent beams and typically best resist bending moments, tensile and compression loads. These profiles can be employed as stiffening elements in combination with other stiffeners or skin type parts using the previously described assembly methods. Figure 3.19 shows a selection of the 16 shapes studied as part of this thesis.

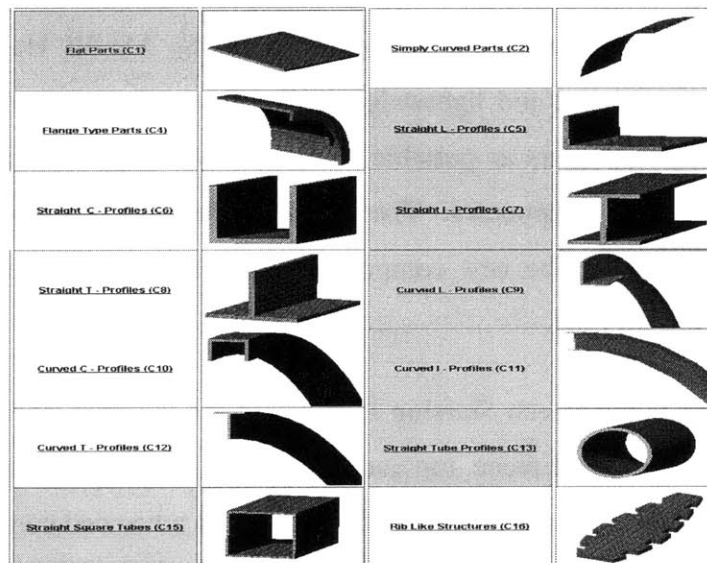


**Figure 3.19 Overview of the Reference Geometries**

The following paragraphs describe common production methods for each reference shape and highlight any frequently encountered difficulties or special requirements. However, these are recommendations based on what the process is capable off in its most conventional development stage.

### 3.4.1 Flat Panels (C1)

- a) Small Production Volumes (1 - 10 parts/month):  
Processes: Hand Lay-up, Autoclave Cure or Hot Press  
Tooling: No CTE match req., however meet temp. and pressure requirements  
Issues: For exact fiber orientation additional lay-up aids have to be installed.
  
- b) Medium to High Production Volumes (10 - to over 100 parts/month):  
Processes: Resin Transfer Molding, Pultrusion, Hot Presses  
Tooling: Metal preferred because of durability  
Issues: Limitation in width and fiber orientation exist for pultrusion  
Example: Printed Circuit Board
  
- c) Large Parts:  
Processes: Automated Tape Placement & Autoclaves, Hot Presses  
Tooling: Metal preferred because of durability  
Issues: Part size limited by processing equipment.

Comments:

Many other possibilities exist for the production of flat shapes and most will be selected in terms of availability, production volume and size considerations. In general warping can become an issue for very thin laminates, whereas for thick parts the exothermal reaction has to be controlled when using thermoset resins.

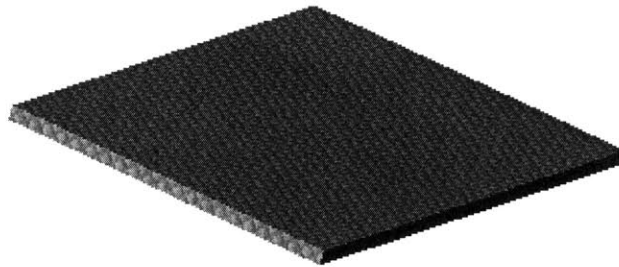


**Figure 3.20 Flat Panels (C1)**

### 3.4.2 Parts with Single Curvature (C2)

- a) Small Production Volumes (1 - 10 parts/month):  
Processes: Hand Lay-up, Autoclave Cure  
Tooling: Special attention is necessary if very high accuracy is req.  
Issues: For exact fiber orientation additional lay-up aids have to be installed.
  
- b) Medium to High Production Volumes (10 - to over 100 parts/month):  
Processes: Resin Transfer Molding, Pultrusion, Forming, Filament Winding  
Tooling: Metal preferred because of durability, special tooling for filament winding of 0 deg. fiber orientation  
Issues: Limitation in width and fiber orientation exist for pultrusion.
  
- c) Large Parts:  
Processes: Automated Tape Placement, Forming  
Tooling: Metal preferred because of durability  
Issues: The use of presses is limited to parts of less than 180 deg. curv..

#### Comments:

Again many production options exist. In general, the use Filament Winding for large parts and Pultrusion for smaller diameter parts, RTM is recommended if special surface quality is desired. Filament Winding produces rotational symmetric parts, which will have to be trimmed subsequently.



**Figure 3.21** Parts with Single Curvature (C2)

### 3.4.3 Parts with Double Curvature (C3)

a) Small Production Volumes (1 - 10 parts/month):

Processes: Hand Lay-up, Autoclave Cure

Tooling: CTE matching is required to ensure accuracy and demolding

Issues: For exact fiber orientation additional lay-up aids have to be installed.

Wrinkling can occur in areas of pronounced curvature, the introduction of darts might be necessary.

b) Medium to High Production Volumes (10 - to over 100 parts/month):

Processes: Resin Transfer Molding, Forming

Tooling: Metal preferred because of durability

Issues: see above.

c) Large Parts:

Processes: Automated Tape Placement, Hot Presses

Tooling: Metal preferred because of durability

Issues: Concave areas can result in problems for ATP.

Comments:

In general the use of hot presses is quicker and more economical than RTM. For very large structures ATP or even hand lay-up is preferable.



**Figure 3.22** Parts with Double Curvature (C3)

### 3.4.4 Flange Type Parts (C4)

a) Small Production Volumes (1 - 10 parts/month):

Processes: Hand Lay-up, Autoclave Cure

Tooling: CTE matching is required to ensure accuracy and demolding

Issues: For exact fiber orientation additional lay-up aids have to be installed.

Wrinkling can occur in areas of pronounced curvature, the introduction of darts might be necessary.

b) Medium to High Production Volumes (10 - to over 100 parts/month):

Processes: Resin Transfer Molding

Tooling: Metal preferred because of durability

Issues: see above.

c) Large Parts:

Processes: Automated Tape Placement

Tooling: Metal preferred because of durability

Issues: Care has to be taken when producing the sharp bent.

Comments:

In general it is a difficult part to fabricate, because of the potential wrinkling of fibers in the flange area. RTM works best to achieve good surface quality on both sides. Special care is required when using Forming or Hand Lay-up due to the danger of wrinkling.

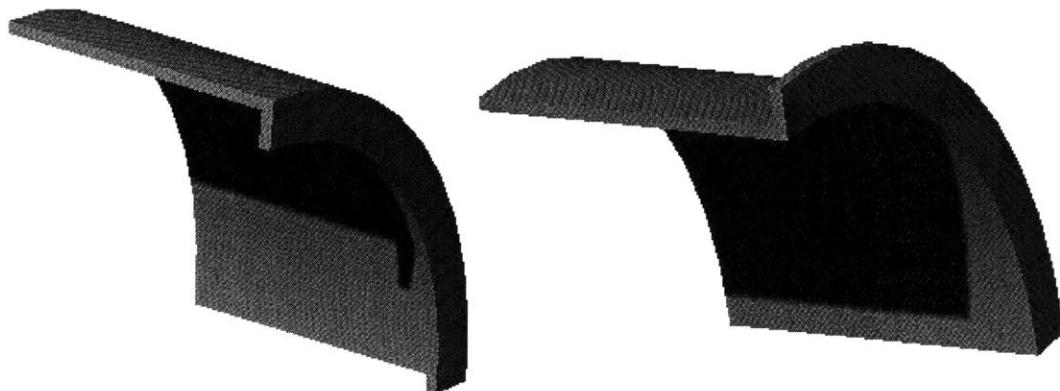


**Figure 3.23** Shrink- and Stretch Flange (C4)

### 3.4.5 Straight L-Profiles (C5)

a) Small Production Volumes (1 - 10 parts/month):

Processes: Hand Lay-up, Autoclave Cure

Tooling: CTE matching is required to only for high accuracy requirements

Issues: For exact fiber orientation additional lay-up aids have to be installed.

b) Medium to High Production Volumes (10 - to over 100 parts/month):

Processes: Pultrusion, Forming

Tooling: Metal preferred because of durability

Issues: Side length is somewhat limited unless specialized machines are used.

c) Large Parts:

Processes: Pultrusion, Resin Transfer Molding, Forming

Tooling: Metal preferred because of durability

Issues: For very high aspect ratio parts, Pultrusion might already be justified, RTM is recommended for low aspect ratio and high surface quality requirements.

Comments:

In general straight profiles of high aspect ratio are best produced by pultrusion. Only if many off-axis fiber orientation are necessary and for lower aspects ratios forming represents a good alternative.

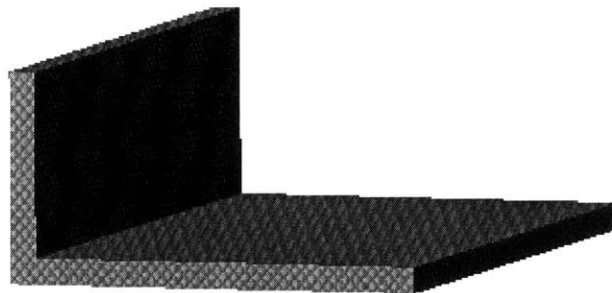


**Figure 3.24** Straight L-Profiles (C5)

### 3.4.6 Straight C-Profiles (C6)

- a) Small Production Volumes (1 - 10 parts/month):  
Processes: Hand Lay-up, Autoclave Cure  
Tooling: CTE matching is required to only for high accuracy requirements  
Issues: For exact fiber orientation additional lay-up aids have to be installed.
- b) Medium to High Production Volumes (10 - to over 100 parts/month):  
Processes: Pultrusion, Forming  
Tooling: Metal preferred because of durability  
Issues: Side length is somewhat limited unless specialized machines are used.
- c) Large Parts:  
Processes: Pultrusion, Resin Transfer Molding, Forming  
Tooling: Metal preferred because of durability  
Issues: For very high aspect ratio parts, Pultrusion might already be justified, RTM is recommended for low aspect ratio and high surface quality requirements.

#### Comments:

In general straight profiles of high aspect ratio are best produced by pultrusion. Only if many off-axis fiber orientation are necessary and for lower aspects ratios forming represents a good alternative.

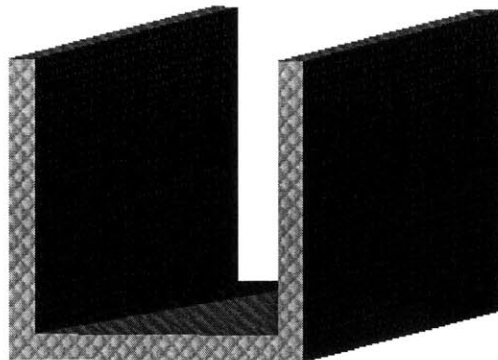


**Figure 3.25** Straight C-Profiles (C6)



### 3.4.7 Straight I-Profiles (C7)

- a) Small Production Volumes (1 - 10 parts/month):

Processes: Hand Lay-up, Autoclave Cure

Tooling: CTE matching is required to only for high accuracy requirements

Issues: Lay up of two C-Profiles and co-cure / co-bonding in autoclave is necessary.

- b) Medium to High Production Volumes (10 - to over 100 parts/month):

Processes: Pultrusion, Resin Transfer Molding, Forming

Tooling: Metal preferred because of durability

Issues: If pultrusion is not avail. two C-Channels could be formed and co-bonded / co-cured in autoclave.

- c) Large Parts:

Processes: Pultrusion, Resin Transfer Molding (SCRIMP)

Tooling: Metal preferred because of durability

Issues: For very high aspect ratio parts, Pultrusion might already be justified,

RTM is recommended for low aspect ratio and high surface quality requirements..

Comments:

In general straight profiles of high aspect ratio are best produced by pultrusion. Only if many off-axis fiber orientation are necessary and for lower aspects ratios forming is an excellent alternative. However the direct forming of I-Profiles is not possible and an intermediate step of forming C-profiles is necessary.

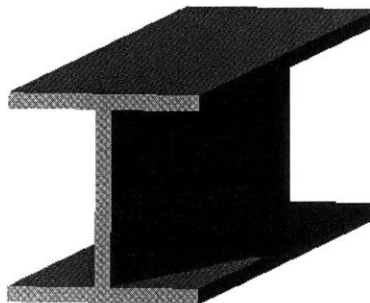


**Figure 3.26** Straight I-Profiles (C7)

### 3.4.8 Straight T-Profiles (C8)

- a) Small Production Volumes (1 - 10 parts/month):  
Processes: Hand Lay-up, Autoclave Cure  
Tooling: CTE matching is required to only for high accuracy requirements  
Issues: Lay up of two L-Profiles and co-cure / co-bonding in autoclave is necessary.
- b) Medium to High Production Volumes (10 - to over 100 parts/month):  
Processes: Pultrusion, Forming  
Tooling: Metal preferred because of durability  
Issues: If pultrusion is not avail. two L-Channels could be formed and co-bonded / co-cured in autoclave..
- c) Large Parts:  
Processes: Pultrusion, Resin Transfer Molding (SCRIMP)  
Tooling: Metal preferred because of durability  
Issues: For very high aspect ratio parts, Pultrusion might already be justified, RTM is recommended for low aspect ratio and high surface quality requirements..

#### Comments:

In general straight profiles of high aspect ratio are best produced by pultrusion. Only if many off-axis fiber orientation are necessary and for lower aspects ratios forming is an excellent alternative. However the direct forming of T-Profiles is not possible and an intermediate step of forming L-profiles is necessary.

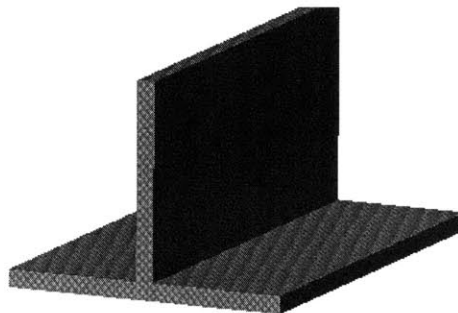


**Figure 3.27** Straight T-Profiles (C8)

### 3.4.9 Curved L-Profiles (C9)

a) Small Production Volumes (1 - 10 parts/month):

Processes: Hand Lay-up, Autoclave Cure

Tooling: CTE matching is required to ensure demolding and accuracy.

Issues: For exact fiber orientation additional lay-up aids have to be installed.

Wrinkling can occur in areas of pronounced curvature, the introduction of darts might be necessary.

b) Medium to High Production Volumes (10 - to over 100 parts/month):

Processes: Forming, RTM, Pultrusion

Tooling: Metal preferred because of durability

Issues: Pultrude with partial cure, post form and complete cure.

c) Large Parts:

Processes: Resin Transfer Molding, Forming

Tooling: Metal preferred because of durability

Issues: Forming is restricted to slight curvature parts because of wrinkling, RTM is recommended for low aspect ratio and high surface quality requirements.

Comments:

In general profiles with double curvature are prone to wrinkling and therefore hand lay-up is often the only option. However within limitation forming is economically a very good alternative if feasible. Pultrusion is in general not practical, since the parts are not straight, however exceptions exist.



**Figure 3.28** Curved L-Profiles (C9)

### 3.4.10 Curved C-Profiles (C10)

a) Small Production Volumes (1 - 10 parts/month):

Processes: Hand Lay-up, Autoclave Cure

Tooling: CTE matching is required to ensure demolding and accuracy.

Issues: For exact fiber orientation additional lay-up aids have to be installed.

Wrinkling can occur in areas of pronounced curvature, the introduction of darts might be necessary.

b) Medium to High Production Volumes (10 - to over 100 parts/month):

Processes: Forming, Resin Transfer Molding, Pultrusion

Tooling: Metal preferred because of durability

Issues: Pultrude with partial cure, post form and complete cure.

c) Large Parts:

Processes: Resin Transfer Molding, Forming

Tooling: Metal preferred because of durability

Issues: Forming is restricted to slight curvature parts because of wrinkling, RTM is recommended for low aspect ratio and high surface quality requirements.

Comments:

In general profiles with double curvature are prone to wrinkling and therefore hand lay-up is often the only option. However within limitation forming is economically a very good alternative if feasible. Pultrusion is in general not practical, since the parts are not straight, however exceptions exist.

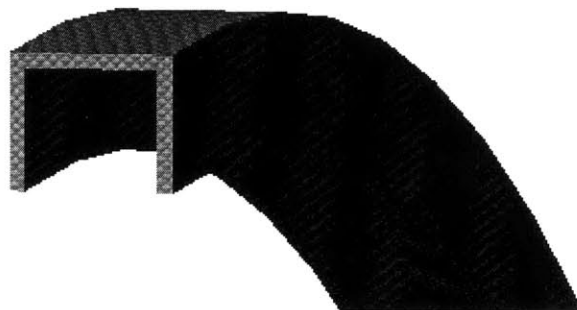


**Figure 3.29** Curved C-Profiles (C10)

### 3.4.11 Curved I-Profiles (C11)

- a) Small Production Volumes (1 - 10 parts/month):

Processes: Hand Lay-up, Autoclave Cure

Tooling: CTE matching is required to ensure demolding and accuracy.

Issues: Lay up of two C-Profiles and co-cure / co-bonding in autoclave is necessary.

- b) Medium to High Production Volumes (10 - to over 100 parts/month):

Processes: Resin Transfer Molding, Pultrusion

Tooling: Metal preferred because of durability

Issues: Pultrude with partial cure, post form and complete cure. Otherwise RTM is the only feasible & economical process.

- c) Large Parts:

Processes: Resin Transfer Molding, Forming (limited)

Tooling: Metal preferred because of durability

Issues: RTM is recommended, for large parts special care is required to ensure proper impregnation. Forming of two C-Profiles and co-cure / co-bonding in autoclave is possible.

Comments:

In general profiles with double curvature are prone to wrinkling and therefore hand lay-up is often the only option. Lay-up of two C-Profiles and co-cure / co-bonding in autoclave is necessary. However within limitation forming is economically a very good alternative if feasible. Pultrusion is in general not practical, since the parts are not straight, however exceptions exist.



**Figure 3.30** Curved I-Profiles (C11)

### 3.4.12 Curved T-Profiles (C12)

- a) Small Production Volumes (1 - 10 parts/month):  
Processes: Hand Lay-up, Autoclave Cure  
Tooling: CTE matching is required to ensure demolding and accuracy.  
Issues: Lay up of two L-Profiles and co-cure / co-bonding in autoclave is necessary.
- b) Medium to High Production Volumes (10 - to over 100 parts/month):  
Processes: Resin Transfer Molding, Pultrusion  
Tooling: Metal preferred because of durability  
Issues: Pultrude with partial cure, post form and complete cure. Otherwise RTM is the only feasible & economical process..
- c) Large Parts:  
Processes: Resin Transfer Molding, Forming (limited)  
Tooling: Metal preferred because of durability  
Issues: RTM is recommended, for large parts special care is required to ensure proper impregnation. Forming of two L-Profiles and co-cure / co-bonding in autoclave is possible.

#### Comments:

In general profiles with double curvature are prone to wrinkling and therefore hand lay-up is often the only option. Lay up of two L-Profiles and co-cure / co-bonding in autoclave is necessary. However within limitation forming is economically a very good alternative if feasible. Pultrusion is in general not practical, since the parts are not straight, however exceptions exist.

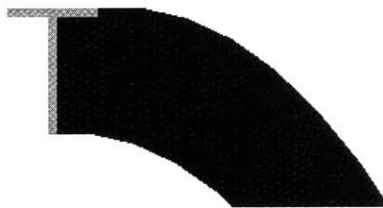


**Figure 3.31 Curved T-Profiles (C12)**

### 3.4.13 Straight Tubular Profiles (C13)

a) Small Production Volumes (1 - 10 parts/month):

Processes: Hand Lay-up, Autoclave Cure

Tooling: CTE matching is required to ensure demolding and accuracy.

Issues: Shrinkage onto the core or mandrel has to be taken into account..

b) Medium to High Production Volumes (10 - to over 100 parts/month):

Processes: Pultrusion, Resin Transfer Molding, Filament Winding, ATP

Tooling: Special tooling is required to pultrude hollow profiles.

Issues: Very large diameters require special equipment and process development.

Also large percentages of off-axis fibers can pose problems.

c) Large Parts:

Processes: Automated Tape Laying, Resin Transfer Molding (limited)

Tooling: CTE matching is required to ensure demolding and accuracy. Metal preferable. RTM would require special tooling using a removable core.

Issues: Either CTE matching or collapsible core is required.

Comments:

In general, straight profiles of high aspect ratio are best produced by pultrusion or filament winding. Only if many off-axis fibers are necessary and for lower aspect ratios RTM presents an alternative. One could also form two halves of a tube and bond them together if the situation allows this.

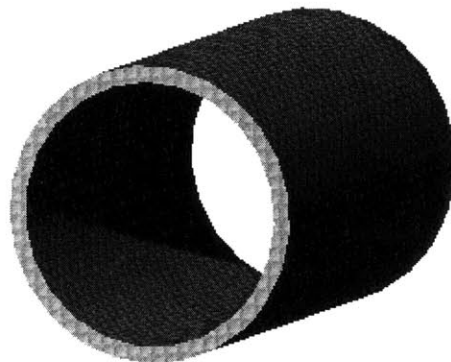


**Figure 3.32** Straight Tubular Profiles (C13)

#### 3.4.14 Tapered Tubular Profiles (C14)

- a) Small Production Volumes (1 - 10 parts/month):  
Processes: Hand Lay-up, Autoclave Cure  
Tooling: CTE matching is required to ensure demolding and accuracy.  
Issues: Shrinkage onto the core or mandrel has to be taken into account especially if tapered in both directions.
- b) Medium to High Production Volumes (10 - to over 100 parts/month):  
Processes: Resin Transfer Molding, Automated Tape Laying  
Tooling: Special winding mandrels are required for large percentage of 0 deg. fibers.  
Issues: Strong taper leads to section of non-constant wall thickness.
- c) Large Parts:  
Processes: Automated Tape Laying, Resin Transfer Molding (limited)  
Tooling: CTE matching is required to ensure demolding and accuracy. Metal is preferable. RTM would require special tooling using a removable core.  
Issues: Either CTE matching or collapsible core is required..

#### Comments:

For very high volumes filament winding and automated tow placement are most economical. RTM and ATP present good alternatives for small and large parts, respectively.

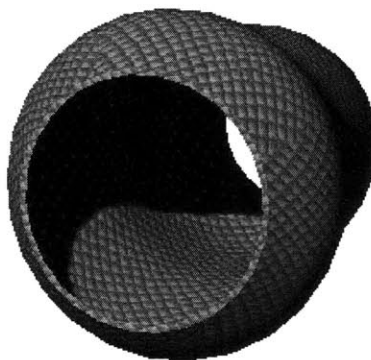


**Figure 3.33 Tapered Tubular Profiles (C14)**



### 3.4.15 Straight Hollow Square Profiles (C15)

a) Small Production Volumes (1 - 10 parts/month):

Processes: Hand Lay-up, Autoclave Cure

Tooling: CTE matching is required to ensure demolding and accuracy.

Issues: Shrinkage onto the core or mandrel has to be taken into account..

b) Medium to High Production Volumes (10 - to over 100 parts/month):

Processes: Pultrusion, Resin Transfer Molding (limited), ATP, Filament Winding

Tooling: Special tooling is required to pultrude hollow profiles.

Issues: Very large cross sections require special equipment and development.

Also large percentages of off-axis fibers can pose problems not perfectly sharp or resin rich edges can be a shortcoming.

c) Large Parts:

Processes: Automated Tape Laying, Resin Transfer Molding (limited), Filament Winding

Tooling: CTE matching is required to ensure demolding and accuracy. Metal preferable. RTM would require special tooling using a removable core.

Issues: Either CTE matching or collapsible core is required.

Comments:

In general straight profiles of high aspect ratio are best produced by pultrusion. Only if many off-axis fibers are necessary and for lower aspects ratios RTM presents a good alternative. One could also form two halves of a square tube and bond them together if the situation allows this.

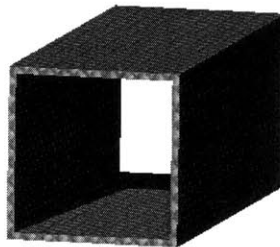


**Figure 3.34** Straight Hollow Square Profiles (C15)

### 3.4.16 Rib Like Structures (C16)

a) Small Production Volumes (1 - 10 parts/month):

Processes: Hand Lay-up, Autoclave Cure

Tooling: CTE matching is required to ensure accuracy and demolding

Issues: For exact fiber orientation additional lay-up aids have to be installed.

Wrinkling can occur in areas of pronounced curvature, the introduction of darts might be necessary.

b) Medium to High Production Volumes (10 - to over 100 parts/month):

Processes: Resin Transfer Molding

Tooling: Metal preferred because of durability

Issues: RTM is limited in its capabilities to produce high fiber volume fractions.

c) Large Parts:

Processes: Automated Tape Placement

Tooling: Metal preferred because of durability

Issues: Concave areas can result in problems for ATP and so can the sharp bents.

A combination of lay-up and subsequent trimming might become necessary.

Comments:

For very large structures ATP or even hand lay-up is preferable and might be the only feasible process to deal with the darts and possible wrinkling within the part.

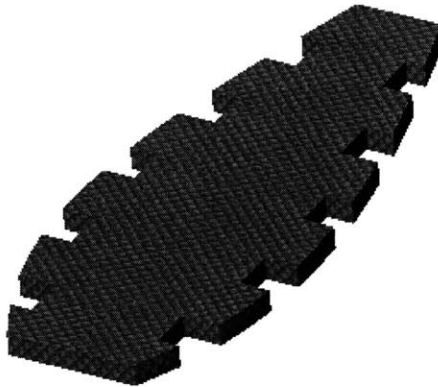


**Figure 3.35 Rib Like Structures (C16)**

### 3.5 Process Selection Guidelines

In order to take advantage of the existing cost saving opportunities early in the development stage, designers need to know how the attributes of parts are related to their costs. Part of this decision making process is the knowledge of the process capabilities. Only if the process is well matched to the designed part, economic fabrication can be achieved. Figure 3.36 shows the capability range of each process with respect to part size, the maximum complexity of the shape and degree of control over the fiber orientation. Parts of low complexity are generally flat or exhibit only slight single curvature. Highly complex parts are defined as parts, which feature extensive double curvature, tight radii and many features. The importance of accurate fiber orientation has already been illustrated in Figure 3.3.

#### Process Capability Matrix

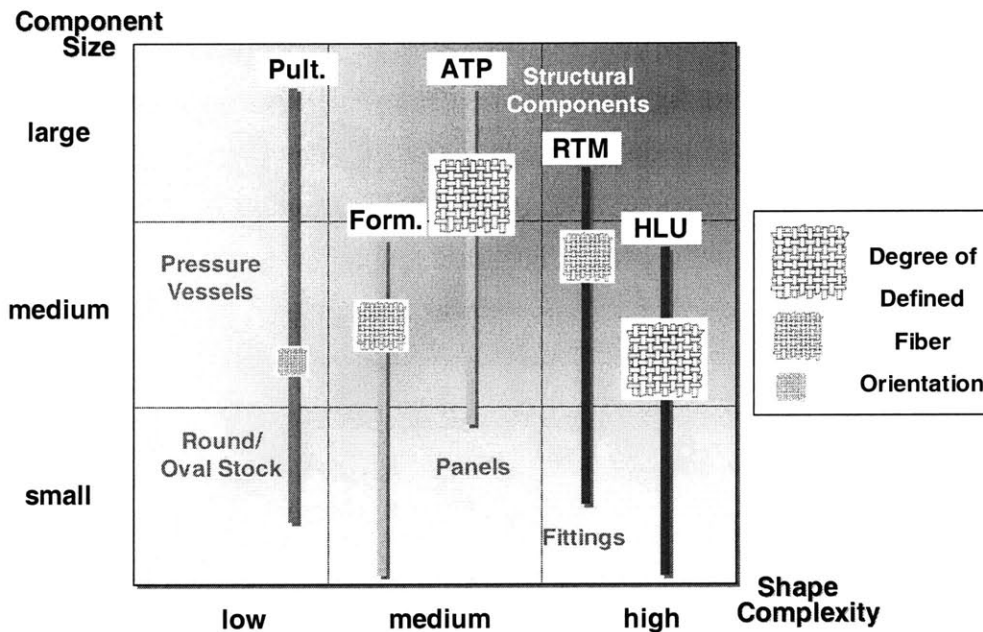


Figure 3.36 Process Capability Matrix

Of course, the process capability matrix only presents an approximate view of the actual capabilities and a more detailed analysis is necessary in order not to miss any favorable process/part combinations. Therefore the following process selection matrix seen in

Figure 3.37 has been compiled. It lists all the combinations between the previously introduced reference geometries as depicted in Figure 3.19 and the processes for composite fabrication as discussed in Chapter 3.1. The process selection matrix guides designers in their decisions by ranking process and part combination in terms of their technical and economical merit. The developed system ranks each process/part combination into the three categories, uncommon, feasible and common. The vagueness is intentional, since special process development efforts can undoubtedly produce a combination, which was previously classified as uncommon. In addition, the classification scheme also limits the possible combinations from 98 to 71. The selection matrix was compiled under the consideration of generic process capabilities and to match these to the attributes of the reference shapes. Any special development will require additional resources and will consequently shift the overall process economics.

The selection matrix also points the way for a more detailed economic analysis. Such an analysis is necessary in order to discover the economically best combination of part and process for the manufacturing situation at hand. The subsequently developed cost model for composite fabrication will further clarify the relation between design features and production costs. Obviously, there is always a price to be paid if a more complicated part has to be manufactured at a higher rate. Therefore the ultimate process choice involves many decision steps including material form, equipment, tooling and labor skill requirements.

<i>Process / Part</i>	<u><i>HLU</i></u>	<u><i>ATP</i></u>	<u><i>DDF</i></u>	<u><i>PUL</i></u>	<u><i>RTM</i></u>	<u><i>Assem.</i></u>
<u>Flat Parts (C1)</u>	<u>XX</u>	<u>XX</u>	0	<u>XX</u>	<u>X</u>	<u>X</u>
<u>Simply Curved Parts (C2)</u>	<u>XX</u>	<u>XX</u>	<u>XX</u>	<u>X</u>	<u>X</u>	<u>X</u>
<u>Double Curvature Parts (C3)</u>	X	0	X	X	XX	0
<u>Flange Type Parts (C4)</u>	<u>XX</u>	X	X	0	<u>XX</u>	X
<u>Straight L - Profiles (C5)</u>	<u>X</u>	<u>X</u>	XX	<u>XX</u>	<u>X</u>	0
<u>Straight C - Profiles (C6)</u>	<u>X</u>	X	XX	<u>XX</u>	<u>X</u>	0
<u>Straight I - Profiles (C7)</u>	<u>X</u>	0	0	<u>XX</u>	<u>XX</u>	<u>X</u>
<u>Straight T - Profiles (C8)</u>	<u>X</u>	0	0	<u>XX</u>	<u>XX</u>	<u>X</u>
<u>Curved L - Profiles (C9)</u>	X	0	<u>X</u>	X	<u>XX</u>	0
<u>Curved C - Profiles (C10)</u>	X	0	X	X	<u>XX</u>	0
<u>Curved I - Profiles (C11)</u>	X	0	0	X	<u>XX</u>	X
<u>Curved T - Profiles (C12)</u>	X	0	0	X	<u>XX</u>	X
<u>Straight Tube Profiles (C13)</u>	X	<u>XX</u>	0	<u>XX</u>	<u>X</u>	0
<u>Tapered Tubes (C14)</u>	XX	XX	0	0	X	0
<u>Straight Square Tubes (C15)</u>	X	XX	0	<u>XX</u>	<u>X</u>	0
<u>Rib Like Structures (C16)</u>	XX	X	X	0	X	X

**XX = common, X = possible, 0 = not common for Process/Part Choices**

**Figure 3.37 Process Selection Matrix**

### 3.6 References

- [1] Boothroyd, G., Dewhurst, P.; Knight, W. A., "Product Design for Manufacture and Assembly", Basel, New York: Marcel Dekker, Inc., 1994.
- [2] Reinhart, T. J. (Ed.), "Engineered Materials Handbook – Composites", Vol. 1, ASM International, 1988.
- [3] El Wakil, S. D., "Processes and Design for Manufacturing", 2nd Edition, PWS Publishing Company, Boston, 1998.
- [4] Swift, K. G., Booker, J. D., "Process Selection From Design to Manufacturing", John Wiley & Sons, Inc., New York, 1997.
- [5] Anderson, B.-W., "The Impact of Carbon Fiber Composites on a Military Aircraft Establishment", Journal of Physics, D Applied Physics (1987) 20, p. 311-321.
- [6] Coleman, R. M., "The Effects of Design, Manufacturing Processes, and Operations Management on the Assembly of Aircraft Composite Structure", M.S. Thesis, MIT, 1991.
- [7] Kandebo, S. "Manufacturers seek Reduced Costs through New Fabrication Techniques", Aviation Week & Space Technology, 1986, p. 73-77.
- [8] Niu, M. -C. -Y., "Composite Airframe Structures - Practical Design Information and Data", Hong Kong: Conmilit Press Ltd., 1992.
- [9] Gutowski, T. G., "Advanced Composites Manufacturing", New York: John Wiley & Sons, Inc., 1997.
- [10] Schwartz, M. - M., "Composite Materials, Properties, Nondestructive Testing, and Repair", Vol. I & II, New Jersey: Prentice-Hall, Inc. 1997.
- [11] Schwartz, M. - M., "Joining of Composite-Matrix Materials", Materials Park, Ohio: ASM International, 1995.
- [12] Liquid Control Corporation, N. Canton, Ohio, <http://www.liquidcontrol.com/>
- [13] Lacovara, B., "Considering Resin Transfer Molding", Composite Fabricators Association, 1995.
- [14] Silberman, A. A., "RTM, Design and Implementation", Ph.D. Thesis, University of Illinois at Urbana-Champaign, 1997.
- [15] Advani, S. G., "Manufacturing Education and Training Program in Composite Materials for the DoD and Durable Goods Industries", CCM, University of Delaware, 1999.
- [16] Veldsman, G., "Aspects of Design for Manufacturability in RTM: Design Guidelines, Composite Mould Design, and Early Cost Estimation", M.S. Thesis, University of Stellenbosch, 1995.

- [17] Cincinnati Machine Company, Cincinnati, Ohio, <http://www.cinmach.com/>
- [18] Land, I. B., "Design and Manufacture of Advanced Composite Aircraft Structures using Automated Tow Placement", M.S. Thesis, MIT, 1996.
- [19] Tsai S. W., Springer, G. S. Enders, M. L. "The Fiber-Placement Process", ICCM 8, Composites, Vol. 2, Sections 12-21, p. 14B1-14B11.
- [20] Breda, B. J., Stump, K. H., "A Case Study of Controlled Tape Laying", AHS, 52nd, June 4-6 1996, vol.1, p. 603-610.
- [21] Meason, R., Sewell, K. "Fiber Placement: Low Cost Production for Complex Composite Structures" AHS annual conference, June 4-6 1996, p. 611-622.
- [22] Evans, D. O., Vaniglia, M. M., Hopkins, P. C., "Fiber Placement Process Study", 34th SAMPE, May 8-11, 1985, p. 1822-1833.
- [23] Kitson, L., Johnson, B., "Fiber Placement Technology Advancements at Boeing Helicopters", AHS Annual Conference, May 9-11, 1995, p. 69-79.
- [24] Beresheim, G., "Part Complexity Based Time Estimation Model for the ATP Process", MIT & IVW Report, 2001.
- [25] Entec Composite Machines, Salt Lake City, Utah, <http://www.entec.com/>
- [26] Truslow, S., "Permanent Press, No Wrinkles: Reinforced Double Diaphragm Forming of Advanced Thermoset Composites", M.S. Thesis, MIT, 2000.
- [27] Gutowski, T. G., Dillon, G., Li, H., Chey, S., "Apparatus for Diaphragm Forming", US Patent # 5,648,109, July 15<sup>th</sup>, 1997.
- [28] Thermal Equipment Corporation, Torrance, California, <http://www.thermalequipment.com/>
- [29] Clements, L., "Vacuum Bagging Technology Improved," High Performance Composites January/February, 2000.
- [30] Klein, A. -J., "Cocuring Composites", Advanced Composites, 1988, Vol. 1, p. 43-53.
- [31] Willden, K., Gessel, M., Grant, C., Brown, T., "Manufacturing Scale-up of Composite Fuselage Crown Panels", NASA Report CR-4730, 1995, vol. 1, part 2.
- [32] Willden, K., et all. "Advanced Technology Composite Fuselage - Manufacturing", NASA Report CR-4735, 1997.
- [33] Huck International Inc., Tucson, Arizona, <http://www.huck.com/>
- [34] Gemcor, Inc., West Seneca, New York, <http://www.gemcor.com/>
- [35] Speller, T., "A Case Study of a Product Architecture", M.S. Thesis, SD&M, MIT, 2000.

- [36] Robinson, M. J. "A Qualitative Analysis of Some of the Issues Affecting The Cost of Composite Structures", Intl. SAMPE Techn. Conf. 23, 1991, pp. 1-14.
- [37] Berchthold, G., Klenner, J., "Optimization of Composite Aircraft Structures by Direct Manufacturing Approaches", Flight Mechanics Panel Symposium, 1993, p. 6-1 – 6-12.
- [38] Lambert, B. -K., "Find Low-cost Methodology when Machining Composites", Cutting Tool Engineering, 1987, p. 20-22.
- [39] Lee, D. -J.; Thornton, A. -C., "The Identification and Use of Key Characteristics in the Product Development Process", ASME Design Engineering Technical Conferences and Computers in Engineering Conference, 1996.
- [40] Gorgias, A., "Economic Analysis of Assembly vs. Part Integration in Composite Manufacturing", M.S. Thesis, MIT & TU Munich, 2000.
- [41] Mantripragada, R.; Whitney, D. -E., "The Datum Flow Chain-A Systematic Approach to Assembly Design and Modeling", Research in Engineering Design, Vol. 10, 1998, p. 150-165.
- [42] Noton, B. -R., "Cost Drivers and Design Methodology for Automated Airframe Assembly", International SAMPE Symposium 31, 1986, p. 1441-1455.
- [43] Thornton, A. -C., "Using Key Characteristics to balance Cost and Quality during Product Development", ASME Design Engineering Technical Conferences, 1997.
- [44] Goel, A., "Economics of Composite Material Manufacturing Equipment", B.S. Thesis, MIT, 2000.



## 4 Introduction into Cost Models

The cost models presented as part of this study follow the concepts developed previously by other researchers [1-13]. However, most of the techniques and costing strategies are repeated to clearly state any assumptions differing from the initial approach. Furthermore, the discussing of the equations facilitates the understanding of the impact of the individual cost parameters on the overall costs.

### 4.1 Motivation for Cost Estimation

The general duty of managers is to look after the interests of the organization's shareholders. Managers therefore constantly evaluate projects in terms of their ability to increase shareholder value. One of the more practical decision criteria used is the Net Present Value (NPV). It is generally accepted that investing in all projects with a positive NPV increases the shareholder value. Equation 4.1 defines the NPV and explains how future cash flows are discounted to account for the time-value of money. The discount factor depends on the opportunity costs of capital  $r$ , which again depend on the risk of the project. Several sources explain how  $r$  can be calculated, but generally  $r$  ranges between 10% and 50% for manufacturing companies [14, 15].

$$NPV = C_0 + \frac{C_1}{1+r} + \frac{C_2}{(1+r)^2} + \dots + \frac{C_n}{(1+r)^n} > 0 \quad \text{Equation 4.1}$$

The determination of the future cash flow ( $C_i$ ) is also subject to uncertainty and depends on the future sales and the related expenses. Expenses can be categorized in sales, administrative, interest, tax, research & development and operating expenses. This study focuses on the manufacturing costs, which are major part of the operating expenses for manufacturing companies. The ability to forecast a major component of the future costs is vital when attempting to identify positive NPV projects. Therefore, reliable cost estimation models can facilitate business decisions.

Cost estimation can have several objectives. Frequently, for manufacturing companies, the objective is to assess the cost impact of one or a combination of the following factors:

- Technologies
- Designs
- Materials
- Operating Conditions
- Risks

The scale of these tradeoff scenarios can encompass individual parts or entire product lines. The decision most often comes down to a tradeoff between product performance and cost. The following chapter introduces some of the concepts, which have been developed to describe the costs of products.

## **4.2 Cost Modeling Concepts**

Today there are a number of concepts being used in industry depending on the nature of the costing problem. Each model has its justification depending on the boundary conditions and the objectives of the model.

### **4.2.1 Rules of Thumb**

Rules of thumb are very simple and quick to apply. They often rely on experience about the cost impacts of certain parameters. Also, they are reasonably accurate, but require long expertise and often lack predictive qualities in situations where new elements are introduced [3].

### **4.2.2 Accounting Methods**

Accounting models take accounting data describing the financial performance of the entire company and derive costing equations. These regression based models are

comparatively simple to implement, since the data is readily available from previous financial reports. However, their reliance on statistical and historical data inhibits their capabilities when describing the impacts of major changes in the production conditions. Also, the allocation of costs to individual parts or products can be difficult if not impossible at times [15].

### **4.2.3 Activity Based Costing**

Activity based costing schemes attempt to eliminate the disadvantages of cost accounting and promote the allocation of costs to individual products and plants. As costs are incurred, they get charged to the activity, which caused them. Activity based costing is ideal to monitor the financial performance of products and plants and detect any deviations. The concept is also able to identify individual cost drivers and then develop actions to improve them. However, the disadvantages are that activity based costing still relies on historical data and is therefore not capable to determine the impact of production, design, or material changes. In particular if new technologies, design concepts or never before used materials are involved [3].

### **4.2.4 Process-Based Cost Models**

Process-based cost models are based on the observation that there exists an inherent relation between product design, process costs, and product costs. The concept distinguishes between variable and fixed costs and relates them to individual production steps [1-13]. It therefore allows a fairly accurate description of the part costs and permits evaluations of process effectiveness. Most importantly, the model can answer questions related to the cost impact of material types, process technologies, design changes, and productions conditions. The models attempt to map these factors to the part cost by establishing a relation between product design, material choice, process selection and processing costs. The equations describing the relation between the costs and the product design etc. are conveniently derived from the physics of the underlying production process. For example by employing the basic laws of physics a variety of processes can

be described whether they involve dynamic motions, thermodynamic, heat – or mass transfer phenomena. These laws often provide the scaling between part design and the processing time. One of these attempts has resulted in the 1<sup>st</sup> Order Model, which is described extensively in Chapter 4.4.4 [16-21]. The major disadvantage of process based models is that their development is often time consuming and expensive. In addition, they require some engineering knowledge of the processes and the evaluated parts. Figure 4.1 outlines the steps to develop a reliable and meaningful cost model.

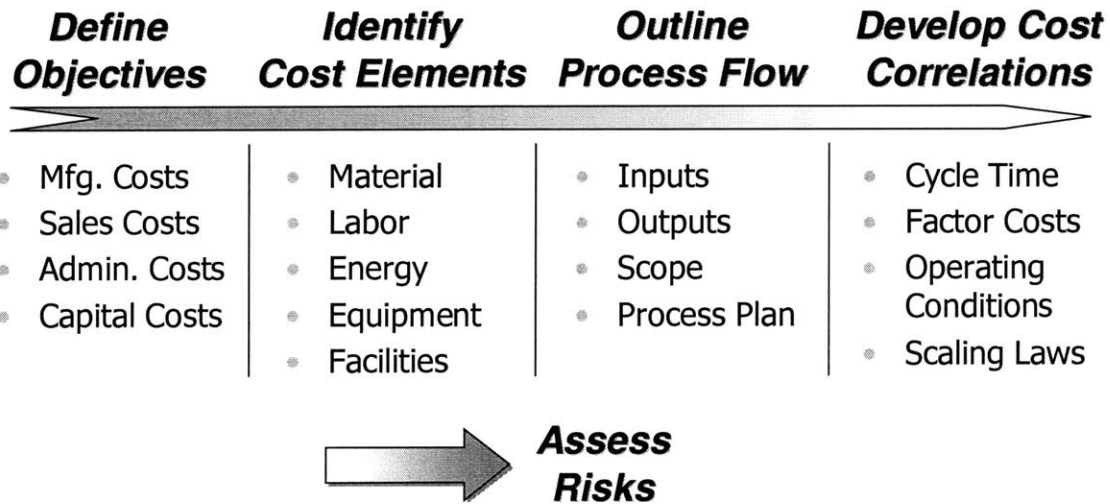


**Figure 4.1** Process Based Cost Estimation Model

#### Define Objectives of the Model

It is advisable to clearly define the objectives of the model before starting the project. Any questions the model should be able to answer and the type of costs have to be written down so no time is wasted during development. Although, the model is traditionally applied to manufacturing costs other business processes can also be modeled with this concept.

#### Identify Relevant Cost Elements

The identification of the relevant cost elements further narrows down scale of the overall efforts and forces the developers to only focus on the elements, which significantly contribute to the overall costs. Of course, sometimes several costs elements have to be

taken into account in order to fulfill the objectives of the model. If necessary, an approximate cost driver analysis can help to determine the contributing factors. The subsequent chapter shows, how a further breakdown in different cost elements facilitates the estimation of manufacturing costs.

### Outline the Process Flow

All the process steps, which contribute to the previously defined cost elements, should be described along with their inputs and outputs. A flow diagram, as depicted in Figure 4.2, helps to understand the inflow of resources, such as labor, material, and energy etc. The outflows consist of interim or finished product stages, but also of scrap, rejects, and all sorts of emissions.

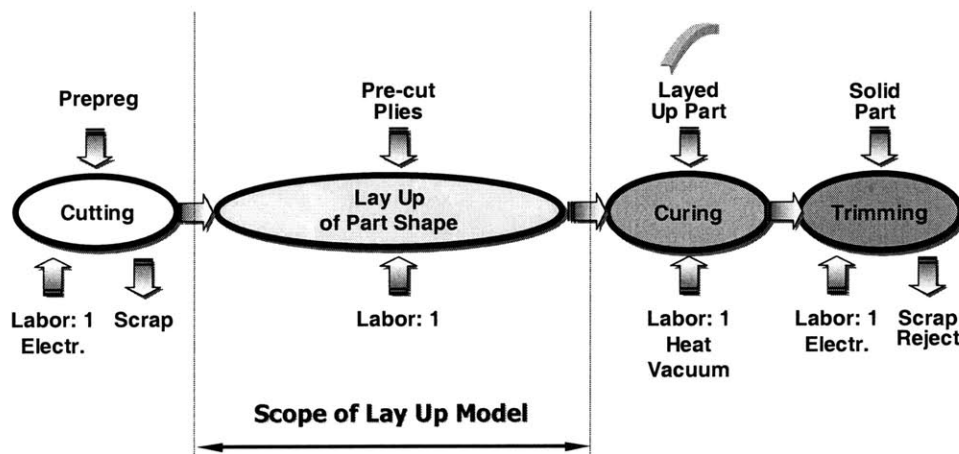


**Figure 4.2** Process Flow and Scope of Model (Example: Hand Lay-Up)

In some applications where the objectives require only a part of the entire cost generating processes to be modeled, the developer should mark the boundaries of the model. The definition of the scope of the model clarifies which costs and process steps are accounted for and what is excluded from the calculations. This clarification is vital in particular when comparing different process technologies. The results would otherwise be difficult to compare if each model encompasses different product stages or forms of raw material.

Once the scope of the model is clear, a more detailed process plan breaks down the entire operation into even smaller sub steps. The amount of detail necessary for the process

plan depends on the objectives of the cost model. In general, one should focus the modeling efforts on the major cost drivers, provided they are known, in order to keep the development time to a minimum.

#### Development of Cost Correlations

For each process step of interest, a correlation between the total cost and the cost defining factors has to be established. The nature and degree of sophistication of these relations again depend on the objectives of the cost model. For example if the impact of part design on the production costs are to be investigated the model has to reflect the effects of part size and design features. However, if only the cost consequences of changing production conditions such as volume or mix are regarded as important, the model only needs to account for these effects.

In most business environments the costs and the success of the company are directly related to the cycle time of an operation. The cycle time is usually equivalent to the time it takes to complete a process step. Expressions to describe cycle time are also known as scaling laws, which define the relations between the extent of an operation and the performance of its processes. Because of the significance of the cycle time, several chapters are dedicated to the formulation of equations for cycle time estimations (see Chapter 4.4.2).

Aside from the processing conditions such as throughput and failure rates, factor costs represent the basic input parameter of almost every cost model. These costs include wages, material costs, overhead rates and energy prices, but also fixed cost elements such as equipment and building costs. Factor costs can become important when attempting to compare production scenarios between different locations or even countries.

#### Asses the Risks and Uncertainties

Once all the equations are put into place one can start to conduct cost comparisons, and also assess the sensitivity of the result as well as the impact of uncertainties. Studies during which all or a subset of the input parameters are either varied deterministically or stochastically can lead to important insights about the reliability of the obtained cost

results. An evaluation of how costs are affected by a changing economic environment, the advent of new materials or the evolution of technology can provide managers with vital information about the risks of a certain decision.

### 4.3 Manufacturing Cost Elements

For manufacturing operations, certain costs appear regularly, independent of the particular production practice or the business. The division in several cost elements simplifies the estimation process. Commonly, practitioners distinguish between variable and fixed costs. Variable unit costs are defined as being independent of the production volume, whereas fixed unit costs often scale with the inverse of the production volume. As subsequent chapters show, in some cases the cost classification does not follow strictly the definitions of variable and fixed costs. Examples are direct labor and machine/tooling costs. For this study, the costs are categorized as shown in Figure 4.3.

<b><i>Variable Costs</i></b>	<b><i>Fixed Costs</i></b>
<ul style="list-style-type: none"><li>• Material</li><li>• Direct Labor</li><li>• Energy</li></ul>	<ul style="list-style-type: none"><li>• Machinery</li><li>• Tooling</li><li>• Facilities</li><li>• Costs of Capital</li><li>• Admin., Management</li><li>• R&amp;D, Maintenance</li></ul>

**Figure 4.3** Manufacturing Cost Elements

The individual cost elements can be expressed on an annual base, an hourly base or as unit costs per part. One should choose whatever is practical for the calculation, although this study follows the above conventions.

#### 4.3.1 Operating Conditions

##### Production Volume

All manufacturing costs are directly affected by the operating conditions and the production volume. The customer demand rate or the amount of delivered product is very much equal to the annual production rate. However, as expressed by Equation 4.2 the actual or effective production rate can be different depending on the amount of



rejected products. The reject rate describes the percentage of produced parts, which do not pass the quality specifications and have to be scrapped.

$$\text{Eff. Prod. Vol.} = \frac{\text{Annual Prod. Vol.}}{(1 - \text{Reject Rate})} = \text{Eff. Number of Runs} \times \frac{\text{Parts}}{\text{Run}} \quad \text{Equation 4.2}$$

From the annual effective production volume one can derive the effective number of runs necessary when producing at a certain run size. The run size is also known as batch size and stands for the amount of parts produced between setups.

### Productivity

Productivity is generally defined as the relation between output and input of an operation. Labor productivity can be defined in many ways, one of them is shown in Equation 4.3. Labor productivity generally amounts to about 78%.

$$\text{Labor Productivity} = \frac{\text{Ann. Prod. Time}}{\text{Ann. Avail. Time}} \quad \text{Equation 4.3}$$

The annual time available for production depends on the amount of working days per year and the daily number of hours the company is open for operations. It is approximately equivalent to the time for which each worker gets paid. Many factories are open 240 days per year and work 2 shifts a day at 8 hours each.

$$\text{Ann. Avail. Time} = \frac{\text{Working Days}}{\text{Year}} \times \frac{\text{Shifts}}{\text{Day}} \times \frac{\text{Hours}}{\text{Shift}} \quad \text{Equation 4.4}$$

In contrast, the time spent annually on actual production is always smaller or equal than the available time. The difference is made up of downtime, breaks, and idle time. In our case the annual production time can be expressed as described by Equation 4.5.

$$\text{Ann. Prod. Time} = \frac{\text{Cycle Time}}{\text{Run}} \times \text{Eff. Number of Runs} \quad \text{Equation 4.5}$$

### Capacity

The determination of the production capacity is important for planning and budgeting purposes. The size of the planned capacity affects the amount of required machinery, tooling, and floor space and therefore has a direct impact on costs. Here the capacity is described as the number of parallel production streams, which have to be installed in order to achieve the required production volume. Equation 4.6 shows how the capacity depends on other operating conditions such as the available time, the cycle time, and the labor productivity. Of course, the number of parallel streams has to be an integer. Therefore, the expression inside the straight brackets must be rounded up to the closest integer in order to provide sufficient capacity to fulfill demand.

$$\text{Number of Parallel Streams} = \left\lceil \frac{\text{Eff. Number of Runs} \times \frac{\text{Cycle Time}}{\text{Run}}}{\text{Ann. Avail. Time} \times \text{Labor Productivity}} \right\rceil \quad \text{Equation 4.6}$$

Further insights can be obtained, when solving the previous Equation 4.2 for the effective number of runs and plugging the resulting expression into Equation 4.6. Obviously, an increase in the annual production volume can increase the overall capacity requirement. However, poor quality can lead to a rise of the reject rate and consequently also increases the demand for production capacity. In contrast, when increasing the run size (parts/run) the existing capacity can be better utilized. The last conclusion however leads to frequent controversy among operations managers. The increase in run size in order to maximize utilization does not consider the adverse cost effects such as hidden quality problems and overall production flow requirements.

$$\text{Capacity Utilization} = \frac{\text{Eff. Number of Runs} \times \frac{\text{Cycle Time}}{\text{Run}}}{\text{Number of Parallel Streams} \times \text{Ann. Avail. Time}} \quad \text{Equation 4.7}$$

When defining utilization as the ratio between actual output and maximal designed output one arrives at the expression displayed in Equation 4.7. The capacity utilization is also often used as a performance measure to evaluate the effective usage of resources by

management. However, due to fluctuations and variability of the production flow there should always be an adequate amount of extra capacity in reserve if the production goals are to be achieved. Consequently, 100 percent utilization cannot be attained without jeopardizing the overall production schedule.

### 4.3.2 Variable Costs

#### Material Costs

The annual material costs are related to the annual amount of material processed and its price. Equation 4.8 describes this relation and shows how the design influences the material cost through the part weight and the material scrap rate. It becomes evident from the formula below how quality problems affecting the scrap rate can increase the material costs. In some applications the material scrap can be resold and the material costs should be adjusted accordingly, however for composites this is rarely the case.

$$\text{Ann. Matl. Cost} = \frac{\text{Part Weight} \times \text{Eff. Prod. Vol.}}{(1 - \text{Matl. Scrap Rate})} \times \text{Matl. Rate} \quad \text{Equation 4.8}$$

The material rate is generally expressed per unit weight and not only accounts for the material price but also for overhead associated with the material consumption (Equation 4.9).

$$\text{Matl. Rate} = \text{Matl. Price} \times (1 + \text{Matl. Burden Rate}) \quad \text{Equation 4.9}$$

The annual material overhead can for example involve the costs stemming from material handling, warehousing, and purchasing. These overhead costs are often expressed as a percentage of the base material costs and are called material burden rate (Equation 4.10).

$$\text{Matl. Burden Rate} = \frac{\text{Ann. Matl. Overhead}}{\text{Ann. Matl. Req.} \times \text{Matl. Price}} \quad \text{Equation 4.10}$$

Direct Labor Costs

The direct labor costs are treated in this study as variable costs. However, in many instances labor costs are regarded as fixed, since the work force cannot always be scaled in accordance to the production volume. Equation 4.11 illustrates how the annual labor costs scale with the various parameters. Evidently, the annual time spent on production plays a role, which is adjusted for the labor productivity to result in the actual time paid for the entire year.

$$\text{Ann. Labor Costs} = \frac{\text{Eff. Number of Runs} \times \frac{\text{Labor Time}}{\text{Run}} \times \text{Labor Rate}}{\text{Labor Productivity}} \quad \text{Equation 4.11}$$

For the objectives of the models presented as part of this study it proved useful to express the cycle time on a per run and not on a per part base. Chapter 4.4.2 explains the computation of the cycle time in more detail. As seen in Equation 4.12 the process performance and the number of employed workers impacts the labor costs.

$$\frac{\text{Labor Time}}{\text{Run}} = \frac{\text{Cycle Time}}{\text{Run}} \times \text{Number of Workers} \quad \text{Equation 4.12}$$

The labor rate as expressed in Equation 4.13 is subject to many different factors. First of all, the hourly wages including benefits paid to the workers strongly depends on the industry, the type of work, the skill level, and the geographic location of the operations.

$$\text{Labor Rate} = \text{Hourly Wages} \times (1 + \text{Labor Burden Rate}) \quad \text{Equation 4.13}$$

In addition, various labor related overhead costs have to be taken into account. Such overheads can include the costs for supervising managers, administrative costs and all other costs, which scale reasonably with the amount of labor employed. The annual labor overhead is then related to the base labor costs through a burden rate.

$$\text{Labor Burden Rate} = \frac{\text{Ann. Labor Overhead}}{\text{Hourly Wages} \times \text{Ann. Paid Time}} \quad \text{Equation 4.14}$$

### Energy Costs

The annual energy costs for production are computed as outlined in Equation 4.15. The price for energy can vary depending on the energy source, the region and even on seasonal variations. For industrial electricity the price is approximately \$0.08/kWh.

$$\text{Ann. Energy Costs} = \text{Ann. Energy Consumption} \times \text{Energy Price} \quad \text{Equation 4.15}$$

The energy consumption of course is related to the size of the operation and the type of equipment used. Although, the consumed energy does not always scale with the number of parts produced it is common to treat energy costs as variable anyway. For the production of composite structures the energy costs are very small in comparison to other cost elements and are therefore neglected in the subsequent estimations.

### 4.3.3 Fixed Costs

#### Machine Costs

The investment costs for machines are calculated by adding up the price and all the installation and training costs for each purchased machine. Equation 4.16 simplifies this calculation by using an average for the procurement price and the other expenses. In many cases the installation and training costs are combined and expressed as a percentage of the total machine price. Often the investment costs are obtained from quotations of equipment vendors. The amount of money invested represents an important figure for budgeting and financial planning and give manager an idea how much capital they have to commit to the new production program.

$$\text{Investment Costs} = \text{Number of Parallel Streams} \times \text{Machines/Stream} \times (\text{Machine Price} + \text{Installation Costs} + \text{Training Costs}) \quad \text{Equation 4.16}$$

Once the investment costs are known they have to be distributed in a practical way over the duration of the operations. Eventually, a certain fraction of the costs has to be charged to each produced product unit. The exact strategy on how to distribute these

costs depends on the type of operation and the company. This study however only introduces one of the many options to distribute the investment costs. Equation 4.17 annualizes the investments costs and treats them as loan, which has to be paid over the useful life  $t$  of the equipment. The potential salvage value of the equipment is assumed to be zero and the equation is derived from the calculation of an annuity [14]. Equation 4.17 considers the payments of interests and principal on the loan. These capital costs again depend on the opportunity costs of capital  $r$  for the company or the project. Any textbook on corporate financing outlines the calculation of  $r$  depending on the company and the risk of the investment [14]. For manufacturing companies  $r$  generally ranges between 10% and 50%.

$$\text{Ann. Invest. Costs} = \text{Invest. Cost} \times \left( \frac{1}{r} - \frac{1}{r \cdot (1+r)^t} \right)^{-1} + \text{Ann. Maint. Costs} \quad \text{Equation 4.17}$$

In addition to the annual capital costs the annual costs for maintaining the machinery are also included (see Equation 4.17). Sometimes it is practical to express the maintenance costs as a percentage of the annualized capital costs. However, in contradiction to the definition of fixed costs the maintenance cost can be a function of the annual production volume. The more parts are produced the more maintenance can be required. In addition, maintenance costs can be subject to quite considerable variations.

In many manufacturing situations, the equipment is not always dedicated to one specific product. The problem of correctly allocating the annual costs to each product is solved here by introducing an hourly machine rate as defined by Equation 4.18. Similar to the labor rate each product gets charged an amount proportional to the usage time of the equipment. The annual investment costs as expressed in Equation 4.17 are normalized by the annual available time for production as defined by Equation 4.4.

$$\text{Machine Rate} = \frac{\text{Ann. Invest. Costs}}{\text{Ann. Avail. Time}} \quad \text{Equation 4.18}$$

There are several other solutions to this problem and each has its advantages and disadvantages. The one introduced here is quite simple and intuitive to use, however if equipment utilization changes considerably the hourly rate might have to be recalculated.

### Tooling Costs

The distribution of tooling costs is handled in the same fashion as the machine costs. However, in reality the total investment costs are often difficult to determine. Tooling is often unique and produced in small quantities. Its production also frequently involves a considerable amount of manual labor. These factors often complicate the estimation of the investment costs for tooling and the practitioner is often forced to rely on quotations from vendors. However, after the total investment for tooling is determined, the amount is annualized over the useful life of the tooling. It has to be taken into account that the useful life of tooling can differ substantially from the useful life of machinery. In addition, annual maintenance costs for tooling are different from the maintenance costs for machinery. Furthermore tooling is always dedicated to a specific product, however the annual costs are converted into a tooling rate for the matter of convenience.

### Building Costs

The investment costs for buildings and facilities are related to the size of the manufacturing operation. As Equation 4.19 demonstrates the investment costs can be estimated by multiplying the price for a unit of floor space by the amount of space required for all the equipment, offices etc.

$$\text{Invest. Costs} = \text{Floorspace Price} \times \text{Number of Par.Streams} \times \frac{\text{Footprint}}{\text{Stream}} \quad \text{Equation 4.19}$$

Again, similar to the machine costs the investment costs for buildings are annualized and paid back over the useful life of the buildings. Accountants often use a theoretical value of 39.5 years as the useful life. The price per square foot industrial space is about \$75, which however strongly depends on the location and the local real estate market. The annual maintenance costs for the facilities have to be added in as well [3, 5].

### Costs of Working Capital

Working capital can be described as the capital, which must be invested to produce a product before the product can be sold. Working capital includes the costs for material, labor, energy, and warehousing as the product is produced and then stored before being sold. It can also include the costs to fill up the distribution channels and the total amount of the required working capital can be quite substantial. For estimation purposes the working capital is considered proportional to the variable costs as stated in Equation 4.20. The capital recovery period is the time from the beginning of the investment to the reception of the payment for the sold product.

$$\text{Working Capital} = \frac{\text{Ann. Variable Costs}}{12} \times \text{Capital Recovery Period} \quad \text{Equation 4.20}$$

The amount of the required working capital be substantial. In particular, for high value and long-term projects such as airplanes, ships the opportunity costs for the working capital can be very high. Equation 4.21 introduces a simple way to compute these costs. As discussed in the paragraph on machine costs,  $r$  represents the corporate discount rate.

$$\text{Costs of Working Capital} = \text{Working Cap.} \times \frac{r}{12} \times \text{Cap. Recov. Period} \quad \text{Equation 4.21}$$

### Overhead Costs

Overhead costs are generally costs, which are difficult to allocate to a specific product but are necessary for the operation of the business. These costs can include costs for administration, sales, management, maintenance, research & development etc. The overhead costs are however difficult to predict and estimates are generally based on historical cost data. However, in some cases it is worthwhile to attempt an allocation of these costs in order to determine the actual product costs more precisely. The allocation of the costs depends on the structure of the business and the type of operations. Frequently, the overhead costs are driven by one or several scaling factors. For example, these cost drivers can be the total amount of labor hours, the amount of machine hours, the amount of material processed or even the amount of required space. The annual



overhead costs are then normalized with these cost drivers and added as a burden rate to the variable or the fixed costs.

As a side comment, the allocation of overhead costs is often heavily contested in corporations structured as cost or profit centers. If the chosen cost driver does not accurately reflect the actual incurrence of the overhead costs, there is a danger of cross-subsidies between product lines and corporate divisions. The cross-subsidies not only cause an unfair distribution of the overhead costs they also distort the actual product costs and therefore unprofitable products can appear profitable or vice versa.

#### 4.3.4 Unit Costs

After summing up all the terms of the annual variable and fixed costs the average unit costs can be determined straightforwardly. There are more than one way to normalize the costs and Equation 4.22 expresses the cost components based on the annual production rate.

$$\text{Unit Costs} = \frac{\text{Ann. Variable Costs}}{\text{Ann. Prod. Vol.}} + \frac{\text{Ann. Fixed Costs}}{\text{Ann. Prod. Vol.}} \quad \text{Equation 4.22}$$

##### Variable Unit Costs

Each of the terms of the above equation can be analyzed further to gain a better understanding on how the unit costs vary in dependence of the different cost components and operating conditions. The variable unit costs as expressed by Equation 4.23 are obtained by introducing the respective formulas into Equation 4.22.

$$\text{Var. Unit Costs} = \frac{\text{Part Weight} \times \text{Matl. Rate}}{(1 - \text{Matl. Scrap}) \times (1 - \text{Reject})} + \frac{\frac{\text{Labor Time}}{\text{Run}} \times \text{Labor Rate}}{(1 - \text{Reject}) \times \frac{\text{Parts}}{\text{Run}} \times \text{Labor Prod.}} \quad \text{Equation 4.23}$$

Equation 4.23 shows that the contribution of the material costs to the unit costs increases with the part weight and the material rate. However, it also becomes clear that material scrap and part reject rates should be improved continuously in order to keep the unit costs as low as possible. The unit labor costs increase with rising labor time per run and labor rate. High labor productivity and a low reject rate decrease the labor unit costs. The expression for the unit labor costs also demonstrates the trade off between large run sizes (parts per run) and a short labor time per run. As Chapter 4.4.2 shows however, labor time per run does not scale linearly with run size and therefore the greater the run size the lower the labor unit costs. This is generally due to a better utilization of labor and the distribution of setup times over several parts. However, as mentioned in the previous paragraph on capacity, large run sizes can have adverse effects on quality control (reject rate) and production flow.

#### Fixed Unit Costs

The unit costs contributions of the investments in machinery, tooling and facilities are stated in Equation 4.24. The derivation follows a similar path as the one for the variable unit costs and divides the expression for the annual investments by the annual production rate. The annual production volume cancels out and the fixed unit costs are very much related to the ratio of cycle time per run and available time for production. The longer the cycle time the less parts can be produced and therefore more equipment might be needed to fulfill the annual demand. Secondly, the higher the price for one set of manufacturing equipment the higher the fixed unit costs. Slightly more difficult to see is the influence of the corporate discount rate  $r$  on the fixed unit costs. However, it is intuitively understood that the higher the discount rate and the shorter the payback period the higher the capital costs and therefore the unit costs.

$$\text{Fix. Unit Costs} = \frac{\text{Equip. Price} \times \frac{\text{Cycle Time}}{\text{Run}} \times \left( \frac{1}{r} - \frac{1}{r \cdot (1+r)^n} \right)^{-1}}{(1 - \text{Reject}) \times \frac{\text{Parts}}{\text{Run}} \times \text{Labor Prod.} \times \text{Avail. Time}} \quad \text{Equation 4.24}$$

The composition of the nominator illustrates the already familiar effects of productivity and quality on the fixed unit costs. Again, the higher the quality and the productivity, the lower the costs. As for the run size (parts per run), an increase results in lower costs mainly due to improved equipment utilization and an advantageous distribution of the setup times. This becomes particularly clear when substituting the term for the cycle time with the expression from Equation 4.25.

### General Findings

The various expressions for the variable and fixed unit costs can now be combined as described in Equation 4.22 and one can plot the influence of the many parameters on the unit costs. Figure 4.4 shows qualitatively that indeed the unit costs scale with the inverse of the production volume. Only as capacity limits are reached and an extension requires additional capital investments, one observes jumps in the otherwise steadily declining unit costs. Another interesting observation is the decreased sensitivity of the unit costs to the increasing price of one set of production equipment. Although the price per set is almost doubled along the y-axis, the unit costs do not double for larger production volumes. Of course, the exact ratios depend on the variable and total fixed costs etc. but this holds true simply as a result of the above equations and regardless of any performance improvement the more expensive equipment might offer. The downside is that, declining demand and decreasing production volume can have suddenly a more dramatic impact on unit costs and therefore on overall profitability.

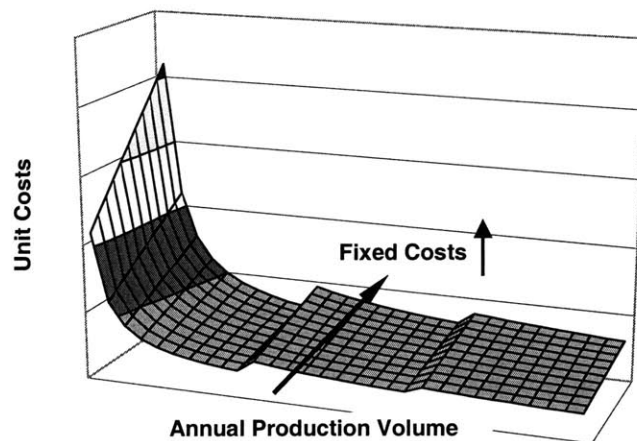


**Figure 4.4** Unit Costs vs. Production Volume

## 4.4 Time Scaling Laws

This chapter on time scaling laws introduces two methods, which are useful to estimate the production time of a product and to establish manufacturing time standards. The first method represents a statistical approach, which uses historical production time information and calculates a regression formula. The second technique is based on the physics of the production process. It shows the various possibilities to relate production time to part design features such as size and shape.

### 4.4.1 Process Plans

As stated previously, this study focuses mainly on process based cost models. These models recognize that the production of parts frequently consists of many individual process steps. Each of these steps can use different techniques, equipment and therefore differ widely in their characteristics. It is therefore practical to write down the process plan or a list of all the production steps. The degree of detail depends on the objective of the model and the information available. However, the analyst should include the most time consuming steps in order to obtain reasonably accurate results. Once the process plan is established, a time estimation model is developed for each of the most significant production steps.

### 4.4.2 Cycle Time

Initially, it is preferable to establish a convention for expressing the cycle time. The cycle time can be written for each step or for the entire manufacturing operation. In Equation 4.25, the cycle time is expressed as the sum over all individual processing steps and is comprised of a term for the setup time and the processing time for each run.

$$\frac{\text{Cycle Time}}{\text{Run}} = \frac{\text{SetupTime}}{\text{Run}} + \frac{\text{Processing Time}}{\text{Run}} \qquad \text{Equation 4.25}$$

Equation 4.26, however expresses the cycle time per run for each individual process step as indicated by the subscript  $i$ . The processing time per run further depends on the number of parts per as each part is processed separately. In some cases, a particular process step or operation is repeated several times to complete each part. One example is, the hand layup processes, which often requires numerous plies to be stacked up. Another example can be a drilling operation, which is repeated until all the designed holes are produced. The term processing time per operation describes the time it takes to drill one hole or to layup one ply. The delay time per operation considers any delay between the individual operations such as moving the drill from one hole to the next during a drilling step. The following two chapters (Chapters 4.4.3 and 4.4.4) present techniques on how to estimate standard times for processing and any delay time per operation.

$$\frac{\text{Cycle Time}}{\text{Run}}_i = \frac{\text{Setup}}{\text{Run}} + \left( \frac{\text{Delay}}{\text{Operation}} + \frac{\text{Proc. Time}}{\text{Operation}} \right) \times \left( \frac{\text{Operations}}{\text{Part}} \right) \times \left( \frac{\text{Parts}}{\text{Run}} \right)$$

**Equation 4.26**

### 4.4.3 Power Law Models

Power law models are based on a curve fit of historical production data to a power law type equation as expressed by Equation 4.27. Many of these models exist for conventional metal working operations [22, 23], but also some have been developed for composite manufacturing applications [24, 26]. In general, the processing time  $t$  is plotted versus the part size  $x$  on double log paper and then approximated with a straight line as seen in Figure 4.5. The coefficient  $A$  and the exponent  $r$  can now be determined by using Equation 4.28.

$$t = A \cdot x^r \Leftrightarrow x = \left(\frac{t}{A}\right)^{\frac{1}{r}} \quad \text{Equation 4.27}$$

$$\log(t) = \log(A \cdot x^r) \Leftrightarrow \log(t) = \log(A) + r \cdot \log(x) \quad \text{Equation 4.28}$$

These regression type models or power law models are generally quite accurate depending on the data used for the regression. However, that is also their biggest drawback, since they only yield accurate results for a specific previous manufacturing situation from which the data was collected. The regression is unable to account for any variations on the part design or process improvements.

**Table 4.1 Example of Power Law Models (Lay Up) [24]**

<i>Lay Up</i>	<i>Setup [hrs]</i>	<i>Runtime [hrs]</i>
<b>Manual</b>		
- 3" Tape (in.)	0.05	$0.00140 \cdot L^{0.6018}$
- 12" Tape (in.)	0.05	$0.001454 \cdot L^{0.8245}$
- Woven (sqin.)	0.05	$0.000751 \cdot A^{0.6295}$
<b>Automatic</b>		
- 720 IPM	0.15	$0.00063 \cdot L^{0.4942}$
- 360 IPM	0.15	$0.000058 \cdot L^{0.5716}$

#### ACCEM Reference Model

Table 4.1 shows as an example for a power law model an excerpt from the ACCEM manufacturing standard for composite production [24]. The ACCEM power law model is

widely accepted by industry and was developed by the Air Force and the Northrop Corporation. It is therefore used as a reference model to test some of the other ideas presented in this study. Many of the ACCEM time standards exhibit a convex shape when plotted on linear axis as seen in Figure 4.5. The value of the exponent  $r$  therefore lies between  $0 < r \leq 1$ .

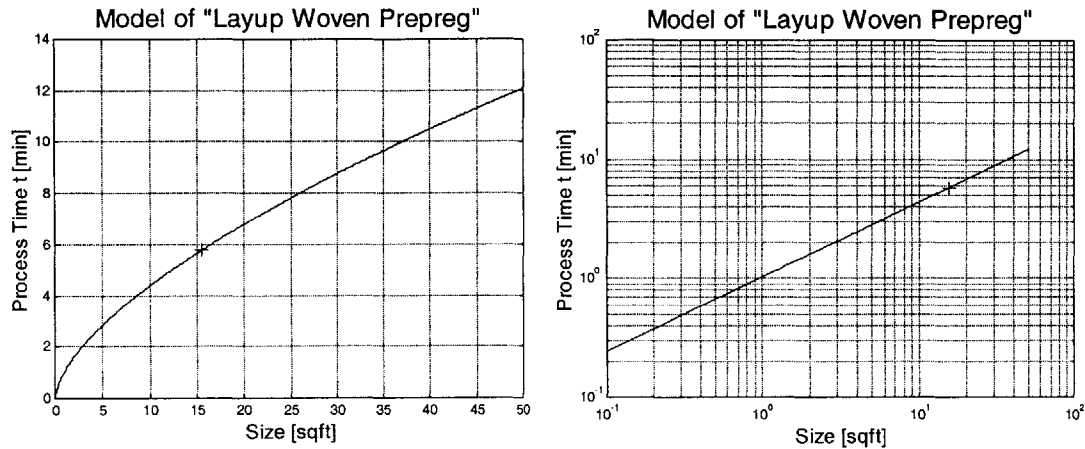


**Figure 4.5 Power Law Model (Example Layup) [24]**

As with all cost models it is important to outline the scope of the model. The relations listed in Table 4.1 include the following processing steps: unroll woven material on layup table, flatten, scribe pattern, position straight edge, cut pattern, move to flat layup tool, and smooth down.

However, regression models can be developed for many correlations between design parameters and processing time. The ACCEM model also features basic relations between part complexity and processing time [24].

#### 4.4.4 Process Physics Based Laws (1<sup>st</sup> Order Model etc.)

Process based or technical cost models are well suited to relate manufacturing cost to design features, material and fabrication processes and generally outperform both rules of thumb and accounting methods [3]. Technical cost models are based on an analysis of the process physics. These models therefore exhibit improved predictive abilities, adapt quickly to changing process conditions. They also require less user expertise and historical data, than other known techniques such as statistical methods [3, 5]. Processing time and cost often scale with various summary descriptors of the part design, such as size and complexity. One example is the 1<sup>st</sup> Order Model for extensive processes [17, 19-21]. Extensive processes are characterized by the movement of a mass in a three-dimensional coordinate frame controlled by a so-called endeffector. For example, the manual placement of a part during an assembly represents such an extensive process where the operators hand serves as the endeffector. In other applications, the behavior of machines traversing in space using a variety of tools can also be modeled using the 1<sup>st</sup> Order law. A convenient approximation of the 1<sup>st</sup> Order Law is the Hyperbolic Model, which was introduced by Boeing [19].

On the contrary, production processes dominated by the exchange of energy, are better described by the 1<sup>st</sup> Law of Thermodynamics as a scaling model [20]. To estimate the processing time of resistive flow type applications, such as mold filling, Darcy's Law provides a good scaling relationship [13].

#### Boundary Conditions of Process Based Models

Scaling laws for manufacturing processes, which express the processing time in relation to the part size, should comply with the following five boundary conditions [16]. The parameter  $L$  stands for the size capabilities of a certain process and  $f(L)$  generally describes the processing time as a function of the part size  $L$ .

1. the range of  $L$  is limited to  $L_{\min} \leq L \leq L_{\max}$ , where  $L_{\min}$  is on the order of the process accuracy, and, in some cases,  $L_{\max}$  is on the order of the machine size. Operations beyond this standard range must be considered a different process.



2.  $f(L)$  is monotonically increasing in  $L$ ,  $df(L)/dL > 0$
3.  $f(L)$  is convex,  $d^2f(L)/dL^2 \leq 0$
4. for large  $L$ ,  $f(L) \sim L$ , (a linear length dependence)
5. for small  $L$ ,  $f(L) > 0$ , (a finite time is required to perform even very small "actions").

It can easily be demonstrated that the 1<sup>st</sup> Order Model and its approximations fulfill the boundary conditions whereas the power law model violates condition number 4.

### 1<sup>st</sup> Order Model

It was found that for "extensive" processes, where "x" is the extensive variable (length, area or volume) the processing time  $t$  could be successfully described by only two factors that represent the process; the process rate  $v_0$  and a time constant  $\tau_0$  [17, 19]. These parameters are quite transparent because of their relation to the dynamic laws describing the actual process physics. Neglecting the effects of 2<sup>nd</sup> order oscillations on the processing time one can write for the step response of a 1<sup>st</sup> Order Dynamic System:

$$v = -a \cdot \tau_0 \Rightarrow v = -\frac{dv}{dt} \cdot \tau_0 \Leftrightarrow \frac{dv}{v} = -\frac{dt}{\tau_0} \Rightarrow \frac{v}{v_0} = e^{-t/\tau_0} \quad \text{Equation 4.29}$$

Under consideration of the boundary conditions, one obtains the velocity response:

$$\Rightarrow v = v_0 \cdot \left(1 - e^{-t/\tau_0}\right) \quad \text{Equation 4.30}$$

By integration follows the size scaling relation, here expressed in dimensionless form:

$$\Rightarrow \frac{x}{v_0 \cdot \tau_0} = \left[ \frac{t}{\tau_0} - \left(1 - e^{-t/\tau_0}\right) \right] \quad \text{Equation 4.31}$$

In contrast to power law and other regression models, the parameter  $v_0$  and  $\tau_0$  can at least be guessed from the characteristics of the underlying process. The value for the steady

state velocity  $v_0$  is generally in the order of the maximum process performance, whereas the time constant  $\tau_0$  represents the average time to reach the steady state performance.

The behavior of the model is displayed in Figure 4.6 where the velocity response (Equation 4.30) and the size scaling relation (Equation 4.31) are plotted in their dimensionless forms.

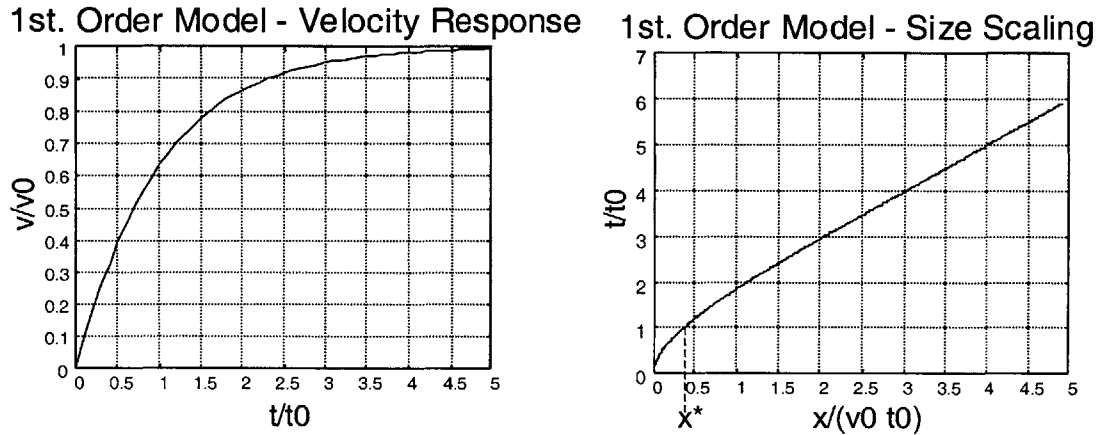


**Figure 4.6 1<sup>st</sup> Order Model (Velocity Response and Size Scaling)**

As also seen in Figure 4.6 the 1<sup>st</sup> Order Model exhibits a transient behavior before reaching steady state. The transient state can be described as follows:

1. Transient case for  $t/\tau_0 < 1$

$$e^{-t/\tau_0} \text{ is dominating and with Taylor expansion } \Rightarrow e^x = 1 + x + \frac{x^2}{2} + \dots + \frac{x^n}{n!}$$

$$\Rightarrow x = v_0 \cdot \left\{ t - \tau_0 \cdot \left[ 1 - \left( 1 - t/\tau_0 + \frac{(t/\tau_0)^2}{2} \right) \right] \right\} \quad \Leftrightarrow t = \left( \frac{2 \cdot \tau_0}{v_0} \cdot x \right)^{1/2}$$

The steady state is characterized by linear behavior and can be derived according to the following argument:

2. Steady State case for  $t/\tau_0 > 1$

$e^{-t/\tau_0}$  converges to zero

$$\Rightarrow x = v_0 \cdot (t - \tau_0) \quad \Rightarrow t = \tau_0 + \frac{x}{v_0}$$

The transition between transient and steady state occurs when  $t = \tau_0$ . The ratio  $v/v_0$  becomes equal to  $\frac{v}{v_0} = 1 - \frac{1}{e} = 0.63$ . It expresses the time after which  $v$  has reached 63% of the steady state velocity  $v_0$ . The time constant  $\tau_0$  can also be regarded as delay time. However, for  $v/v_0$  to reach the tighter 95% criteria, the ratio  $t/\tau_0$  would have to be approximately equal to  $t/\tau_0 = 3$ .

Furthermore it would be interesting to know to which extent the process has progressed before reaching steady state. Again, when setting  $t = \tau_0$  we get  $\frac{x}{v_0 \cdot \tau_0} = \frac{1}{e} = 0.37$  and solving for the size  $x$  one obtains the critical or characteristic size  $x^*$  of the process as defined in Equation 4.32.

$$\text{Characteristic Size: } x^* = \frac{v_0 \cdot \tau_0}{e} \quad \text{Equation 4.32}$$

The critical size  $x^*$  is a measure of the distance to reach 63 % of the steady state velocity  $v_0$ . For  $x < x^*$  the process has not reached its full potential yet. Only when exceeding the size  $x^*$  the process reaches steady state and becomes economical.

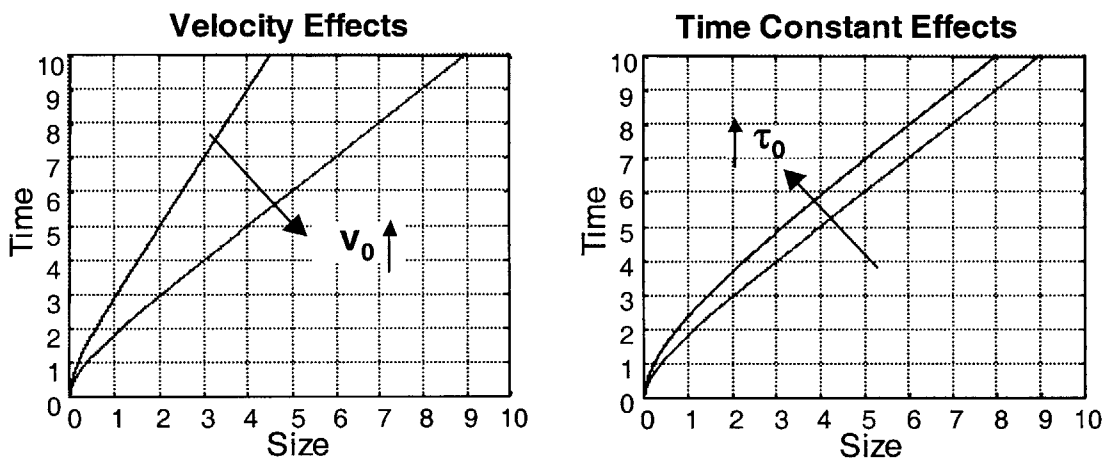


**Figure 4.7** Impact of 1<sup>st</sup> Order Parameter Increases

In order to give a better sense of the effects of parameter changes, Figure 4.7 shows how the processing time decreases with increasing  $v_0$  and increasing  $\tau_0$ . This characteristic of

the 1<sup>st</sup> Order model can be utilized to model the impact of part design features on the process performance. As explained in Chapter 5.2, certain part features can cause a reduction in processing performance or even cause a delay. The 1<sup>st</sup> Order Model therefore offers a straightforward way to not only account for size effects on the processing time but also consider the impact of part shape and complexity.

### Estimation of 1<sup>st</sup> Order Model Parameter

As mentioned previously, in contrast to power law and other regression models, the 1<sup>st</sup> Order Model parameter  $v_0$  and  $\tau_0$  can at least be guessed from the characteristics of the underlying process. The value for the steady state velocity  $v_0$  is generally in the order of the maximum process performance, whereas the time constant  $\tau_0$  represents the average time to reach the steady state performance. However, since manufacturing models based on power law relations are still used quite frequently a simple way of conversion is desirable. Therefore, the derivation of 1<sup>st</sup> Order Model parameter from Power Law parameter can facilitate the implementation of the new approach. The conversion can be conducted as outlined by Equation 4.33 and Equation 4.34.

To obtain an approximation of the steady state velocity  $v_0$  the derivative with respect to time is calculated using the original Power Law:

$$x = \left(\frac{t}{A}\right)^{1/r} \Rightarrow \frac{dx}{dt} = \frac{1}{A \cdot r} \cdot \left(\frac{t}{A}\right)^{1/r-1} \text{ and with the Power Law for } t \text{ it follows } v = \frac{x^{1-r}}{A \cdot r} \text{ and}$$

$$v_0 \approx \frac{x_{\max}^{1-r}}{A \cdot r} \text{ for } t > \tau_0 \quad \text{Equation 4.33}$$

To determine the time constant  $\tau_0$  we take advantage of  $v = 0.63 v_0$  at  $t = \tau_0$  and by using the two previous expressions for  $v$  and  $v_0$  we obtain:

$$\frac{1}{A \cdot r} \cdot \left(\frac{t}{A}\right)^{1/r-1} = 0.63 \cdot \frac{x_{\max}^{1-r}}{A \cdot r} \text{ and with } t = \tau_0 \text{ we get}$$

$$\tau_0 = 0.63^{\frac{r}{1-r}} \cdot A \cdot x_{\max}^r \quad \text{Equation 4.34}$$

Where A is the power law coefficient and r the exponent. The variable  $x_{\max}$  represents the maximum size capability of a particular process and should be much larger than the characteristic size  $x^*$ . For example,  $x_{\max}$  for a milling process would be the size of the worktable. The relations presented in Equation 4.33 and Equation 4.34 only give approximations of the actual parameters and further refinements are generally recommended. However, studies have shown that the agreement between Power Law Models and the 1<sup>st</sup> Order Law is generally better than R-Square > 99% [20].

### Hyperbolic Model

A major inconvenience of the 1<sup>st</sup> Order Model (Equation 4.31) is that it cannot be solved directly for the processing time t. However, in order to facilitate computation it is desirable to have the scaling equations in the form of  $t = f(x)$ . To solve the problem, Boeing proposed the Hyperbolic Model (Equation 4.35) as an approximation of the 1<sup>st</sup> Order Model [17, 19]. Using trial and error they came up with a factorable polynomial, which consists of a linear component and a transient component. The transient component approaches zero for large x. This study however offers a more rigorous derivation of the Hyperbolic Model, which can be found in the Appendix 4.6.

$$t = \sqrt{\left(\frac{x}{v_0}\right)^2 + \frac{2 \cdot \tau_0}{v_0} \cdot x} \quad \text{Equation 4.35}$$

Figure 4.8 displays the Hyperbolic Model plotted in its dimensionless form. Also during the course of this project extensive error studies have been conducted. The results are expressed qualitatively in Figure 4.9. The fit of the Hyperbolic Model and the 1<sup>st</sup> Order Model always proved better than R-Square > 99% [20].

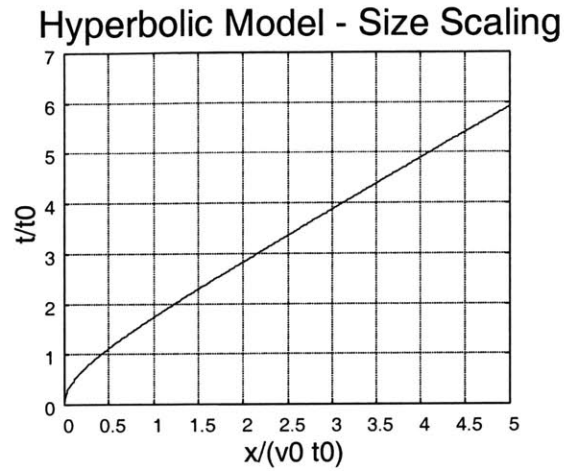


Figure 4.8 Hyperbolic Size Scaling Model

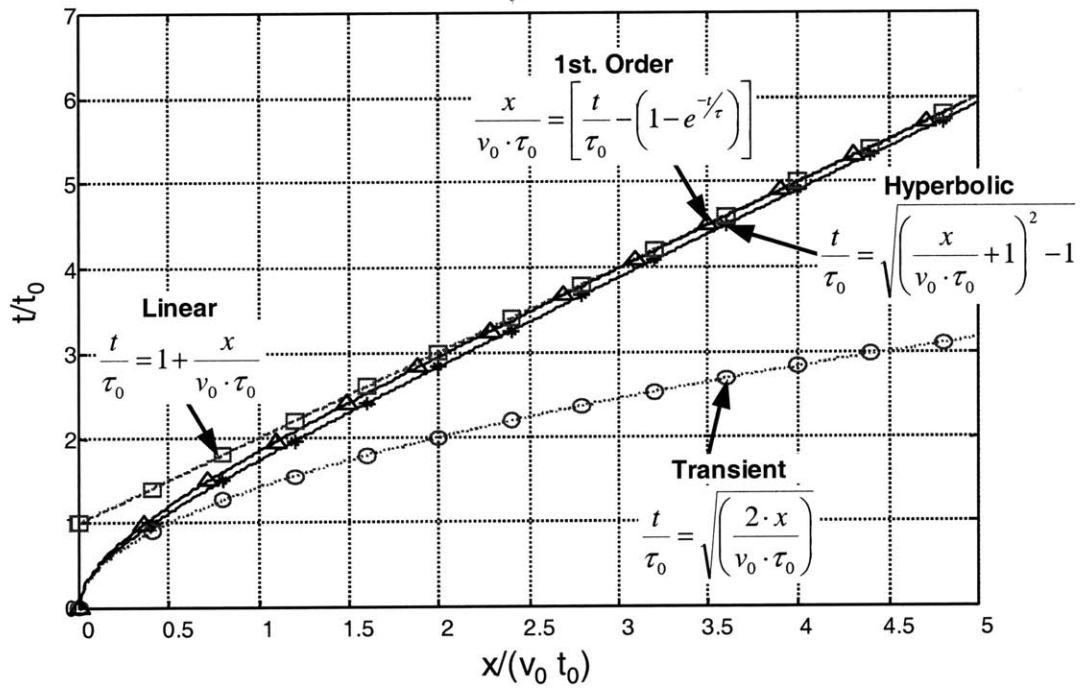
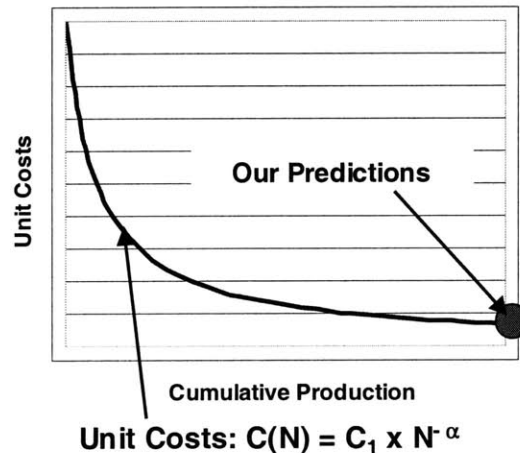


Figure 4.9 Comparison of Size Scaling Models

#### 4.4.5 Learning Effects

The previously introduced models attempt to estimate standard manufacturing times. These are the processing times after the organization has realized the majority of the possible cost savings due to learning. However, it is well established that the unit costs for the first part to be manufactured can easily differ by a magnitude from the costs further down the learning curve. Therefore, the time estimates presented as part of this study have to be adjusted in order to account for learning effects.



**Figure 4.10** Learning Curve Effects

The work of Ein Teck [17] gives an excellent overview of the various consequences and modeling approaches. Learning is generally time dependent but is commonly expressed as a function of the cumulative number of parts produced. Kivenko [18] finds that cost savings attributed to learning is mainly due to the following factors:

- Job Familiarization of Workforce
- Work Flow and Supply Organization Improvements
- Production Process Advances
- Manufacturing Friendly Parts & Assemblies

Not surprisingly, the study finds that only 25% of cost savings is achieved by direct labor improvements. Another 35% come from savings in logistics and the remaining 40% derive itself from functions such as engineering, supervision and planning. Because of

the variety of factors influencing the development of the unit costs it is difficult to generalize the evolution of corporate learning. The progress differs with the economic situation, the industry and even by the individual shop. Since, the ability to achieve operational improvements can lead to significant competitive advantages every corporation should pursue improvements continuously and attempt to develop their specific learning curves.

Commonly, the learning effects are modeled by using power law relations such as the one displayed in Figure 4.10. The costs for each part produced  $C(N)$  are expressed as a function of the cumulative production volume and the costs of the first part produced  $C_1$ . The exponent  $\alpha$  is defined according to Equation 4.36, where  $L$  represent the percentage of cost reduction each time the volume doubles. Literature often lists learning factors around  $75\% < L < 85\%$  [17, 18]. To account for the costs saving achieved by improvements in direct labor one can also model the processing time  $t$  as a function of the cumulative production volume (Equation 4.36).

$$t_N = t_1 \times N^{-\alpha} \quad \text{with } \alpha = \frac{-\ln L}{\ln 2} \quad \text{Equation 4.36}$$

However, in contrast to Equation 4.36 learning is seldom a continuous and steady function of the production volume. One observes jumps in unit cost reductions as new equipment or new operational concepts are introduced. Practitioners have therefore attempted to model reality by employing discontinuous polynoms or power law relations [24, 25].



## 4.5 References

- [1] de Neufville, R. "Applied Systems Analysis", McGraw Hill, New York, 1990.
- [2] Field, F. R. III., de Neufville, R., "Materials Selection - Maximizing Overall Utility", *Metals & Materials*, 1988, p. 378.
- [3] Busch, J. V., Field, F.R. III., "Technical Cost Modeling", *Blow Molding Handbook*, Chapter 24, Donald Rosato and Dominick Rosato, eds., Hanser Publishers, New York, 1989, p. 839-871.
- [4] Busch, J. V., "Technical Cost Modeling of Plastics Fabrication Processes", Ph.D. Thesis, MIT, May 1987.
- [5] Clark, J. P., Field, F. R. III., "Fundamentals in Process-Based Cost Modeling", MIT Course: *Dynamic Strategic Planning*, MIT, 2000.
- [6] Clark, J. P., Roth, R., Field, F. R. III., "Techno-Economic Issues in Materials Selection", *ASM Handbook Vol. 20*, pp. 256-265, 1990.
- [7] Han, Y. C., Park, J. C., Clark, J. P., Field, F. R. III., "Spreadsheet Based Cost Estimation for the P/M Fabrication Process", *Modern Developments in Powder Metallurgy*, Vol. 21, 1988, p. 723.
- [8] Nallicheri, N. V., Clark, J. P., Field, F. R. III., "Techno-Economic Assessment of Alternate Processes for the Connecting Rod", *Advances in Powder Metallurgy Proc. Powder Metall Conf Exhib.*, pp. 153-175, 1990.
- [9] Nallicheri, N. V., "A Technical and Economic Analysis of Alternate Net Shape Processes in Metals Fabrication", Ph.D. Thesis, MIT, June 1990.
- [10] Arnold, S., Hendrichs, N., Clark, J. P., Field, F. R. III., "Competition Between Polymeric Materials and Steel in Car Body Applications", *Materials and Society*, Vol. 13, No 3; 1989.
- [11] Lee Hong, Ng, Field, F. R. III., "Materials for Printed Circuit Boards: Past Usage and Future Prospects", *Materials and Society*, Vol. 13, No 3; 1989.
- [12] Poggiali, B., "Production Cost Modeling: A Spreadsheet Methodology", S.M. Thesis, MIT, August, 1985.
- [13] Kang, P. A., "A Technical and Economic Analysis of Structural Composite Use in Automotive Body-In-White Applications", S.M. Thesis, MIT, May 1998.
- [14] Bodie, Z., Kane, A., Marcus, A. J. "Investments", McGraw Hill, New York, 1999.
- [15] Pratt, J. "Financial Accounting – 4<sup>th</sup> Edition", South-Western College Publ., 2000.
- [16] Wright, T. P., "Factors Affecting the Cost of Airplanes", *J. Inst. Aeronaut. Serv.* 34-40, 1936.

- [17] Neoh, E. T. "Adaptive Framework for Estimating Fabrication Time", Ph.D Thesis, MIT, 1995.
- [18] Kivenko, K., "Predict Your Production Costs with Learning Curves", Production Engineering, August 1977.
- [19] Willden, K., et al., "Advanced Technology Composite Fuselage - Manufacturing", NASA Report CR-4735, 1997.
- [20] Haffner, S. M., Gutowski, T.G., "Manufacturing Time Estimation Laws for Composite Materials", NSF Conference, 1999.
- [21] Haffner, S. M., Gutowski, T.G., "Automated Cost Estimation for Advanced Composite Materials", NSF Conference, 1998.
- [22] Ostwald, P. F., "AM Cost Estimator", 4th Edition, Penton Publishing Inc., 1988.
- [23] Polgar, K. C. "Simplified Time Estimation for Basic Machining Operations", M.S. Thesis, MIT, 1996.
- [24] Northrop Corporation, "Advanced Composite Cost Estimating Manual (ACCEM)", AFFDL-TR-76-87, August 1976.
- [25] Restar, S. A., "Advanced Airframe Structural Materials, A Primer in Cost Estimating Methodology", RAND Report # R-4016-AF, 1991.
- [26] Politis, D., "An Economic and Environmental Evaluation of Aluminum Designs for Automotive Structures", S.M. Thesis, MIT, May 1995.
- [27] Han, H. N., "The Competitive Position of Alternative Automotive Materials", Ph.D. Thesis, MIT, May 1994.
- [28] Ashby, M. F., "Physical Modeling of Materials Problems", Materials Science and Technology, Vol. 8, February 1992, pp. 102-111.
- [29] Boothroyd, G., Dewhurst, P., Knight, W.A., "Product Design for Manufacture and Assembly", Basel, New York: Marcel Dekker, Inc., 1994.
- [30] Mundel, M. E., "Motion and Time Study: Improving Productivity", 6th edition, Prentice-Hall, New Jersey, 1985.
- [31] Niebel, B. W., "Motion and Time Study", 8th. Edition, Irwin, Illinois, 1988.
- [32] Sullivan, W. et al. "Monte Carlo Simulation Analyses Alternatives in Uncertain Economy", Industrial Engineering, November 1982, p. 205.
- [33] Brealey, R. A., Myers, S. C. "Principles of Corporate Finance – 6<sup>th</sup> Edition", McGraw Hill, New York, 2000.

### 4.6 Appendix - Introduction into Cost Models

Substituting the similarity variables

into the 
$$x^* = \frac{x}{v_0 \cdot \tau} \quad t^* = \frac{t}{\tau}$$

• 1<sup>st</sup>. Order Model

$$\frac{x}{v_0 \cdot \tau} = \left[ \frac{t}{\tau} - \left( 1 - e^{-t/\tau} \right) \right]$$
 leads to

and also 
$$x^* + 1 = t^* + e^{-t^*}$$

• Hyperbolic Model

gives 
$$\frac{x}{v_0 \cdot \tau} = \sqrt{1 + \left( \frac{t}{\tau} \right)^2} - 1$$

then choose a 
$$x^* + 1 = \sqrt{1 + (t^*)^2}$$

Factorable Polynomial of the form

$$g(t^*) = [C1 + C2 \cdot (t^*) + C3 \cdot (t^*)^2]^{C4}$$

Boundary Conditions:

1.)  $g(t^*) = 1$  for  $t^* = 0$

2.)  $\frac{dg(t^*)}{dt^*} = \frac{dx^*}{dt^*} = \frac{v_0}{v_0} = 1$  for  $t^* \rightarrow \infty$

3.)  $g(t^*) = \frac{1}{2} \cdot (t^*)^2$  for  $t^* \ll 1$

from B.C. 1.)

$$\Rightarrow g(t^*=0) = [C1 + C2 \cdot 0 + C3 \cdot 0]^{C4} = 1 \Rightarrow C1 = 1$$

from B.C. 2.)

$$\text{for } t^* \rightarrow \infty \Rightarrow \frac{dg(t^*)}{dt^*} = \frac{2 \cdot C3 \cdot C4 \cdot (t^*)^{C4-1}}{[C3 \cdot (t^*)^2]^{1-C4}} = 1$$

$$\Rightarrow C4 = \frac{1}{2} \text{ for } \frac{dg}{dt^*} \text{ to be finite and for } \Rightarrow C3 = 1$$

from B.C. 3.)

$$\Rightarrow x^* + 1 = [1 + C2 \cdot (t^*) + (t^*)^2]^{1/2} \Leftrightarrow x^* = \frac{1}{2} \cdot C2 \cdot (t^*) + \frac{1}{2} \cdot (t^*)^2$$

which has to be equal to the transient model

$$x^* = \frac{1}{2} \cdot (t^*)^2 \Rightarrow C2 = 0$$

Plugging C1=1, C2=0, C3=1 and C4=1/2 back into g(t\*) gives us back

$$g(t^*) = \sqrt{1 + (t^*)^2} \text{ and with } x^* = g(t^*) - 1$$

$$\Rightarrow x^* = \sqrt{1 + (t^*)^2} - 1$$

**Hyperbolic Model**

$$\Rightarrow \frac{x}{v_0 \cdot \tau} = \sqrt{1 + \left( \frac{t}{\tau} \right)^2} - 1 \Leftrightarrow t = \tau \cdot \sqrt{\left( \frac{x}{v_0 \cdot \tau} + 1 \right)^2 - 1}$$

Figure 4.11 Derivation of the Hyperbolic Model

(This page is intentionally left blank.)

## 5 Production Cost Models for Composites

Industry has always striven to develop production cost models for new and evolving manufacturing techniques [1-4]. Many existing models and guidelines for conventional production and assembly methods employ either statistical or process performance based algorithms. For the manufacturing of composites the ACCEM [5] and the RAND [6, 7] model are so far the only comprehensive publicly available production cost models. In addition, a number of databases exist listing the properties and costs of fibers and resins [8]. Furthermore, some aircraft manufacturers under the direction of NASA have already published some cost information on composite production processes [10-18]. In order to develop a more advanced and comprehensive cost model some of the ideas discussed in Chapter 4 are implemented as part of this study. The following chapters introduce production cost models for composites based on the physics of each process. The objective is to present transparent models for Hand Lay-Up, Automated Tow Placement, Diaphragm Forming, Pultrusion, Resin Transfer Molding, Autoclave Cure, and Assembly. As outlined in Chapter 4.4, the process based techniques such as the 1<sup>st</sup> Order model allow the cost to be related to some of the design features such as part size and complexity. However, the shape and the difficulty to manufacture a part also have a major impact on its final cost. Therefore, in connection with the size scaling, a complexity scaling model is also introduced. The newly developed models are then compared to the already existing cost information for validation purposes.

### 5.1 Complexity Scaling

As discussed previously there is a need to estimate the cost implications of all design features in order to provide feedback to designers about the economics of their decisions. Next to size, the complexity of a part is probably the single most important factor influencing the production costs. Evidence suggests that this also holds true for the production of composite parts [5, 10, 22]. For example, Figure 5.1 plots the production time versus the weight of over 200 different composite parts on a double log scale.

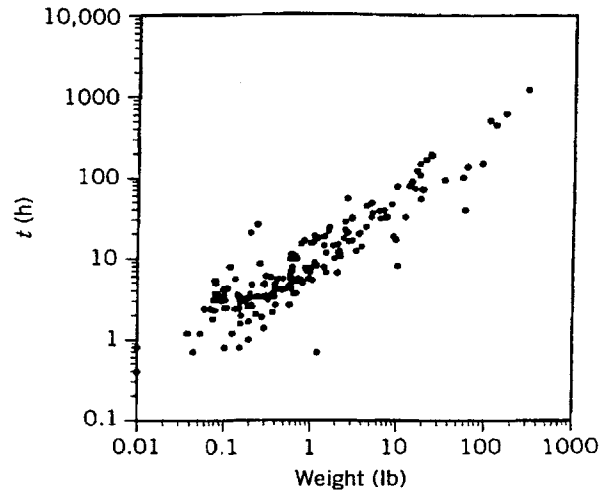


**Figure 5.1** Manufacturing Time vs. Weight of 209 Composite Parts [45]

Independent from their size, the parts distinguish themselves by different degrees of complexity. Therefore, the variation in production time for parts of similar size reflects the required production effort and thus the parts' complexity. Existing models acknowledge the relationship between part complexity and costs. The ACCEM model for example, lists power law equations for a few select part shapes, which relate the complexity to the processing time [5]. The challenge however lies in the determination of a universal complexity measurement able to quantify the complexity of a part dependably. Reality shows that each process has different capabilities to produce certain part features. The process specific capabilities have to be considered in the development of the size and complexity scaling models. For fiber composites, it turns out that the direction and curvature of the fibers present a possibility to serve as complexity indicator [22-23]. In order for the proposed complexity measure to work one has to show its independence from the size of the part. The size scaling model already accounts for size effects, whereas the complexity measure should only be influenced by part features such as geometry and shape. However, the complexity model can be linked to the parameters of the size scaling model and subsequent chapters explain the techniques in greater detail.

### 5.1.1 Complexity Scaling for Fiber Composites

Cost models are based on mathematical relations. However, to account for part complexity one has to define complexity and agree on a measure to quantify it. Previous work shows, that information theory developed by Shannon [34] provides a convenient way of quantification [36, 38, 39]. For readers not familiar with these ideas, the Appendix 5.4.1 features a very brief introduction into the theory. The question is, what exactly makes a part complex and time consuming to manufacture? Apart from the part geometry, looking at the type of material and the processes used certainly helps in finding a meaningful complexity measure. For fiber composite production, one can define a shape complexity and a tolerance complexity. The first defines the difficulty to produce a certain shape and geometry. The latter measures the difficulty of achieving a certain part tolerance.

#### Shape Complexity

As opposed to machined parts, composite part production is characterized by additive processes. Layer upon layer of fibrous material, formed and oriented in predefined ways make up the final part. On a microscopic level, one can distinguish individual fibers, which are bent, curved and intertwined in order to follow the contours of the part.

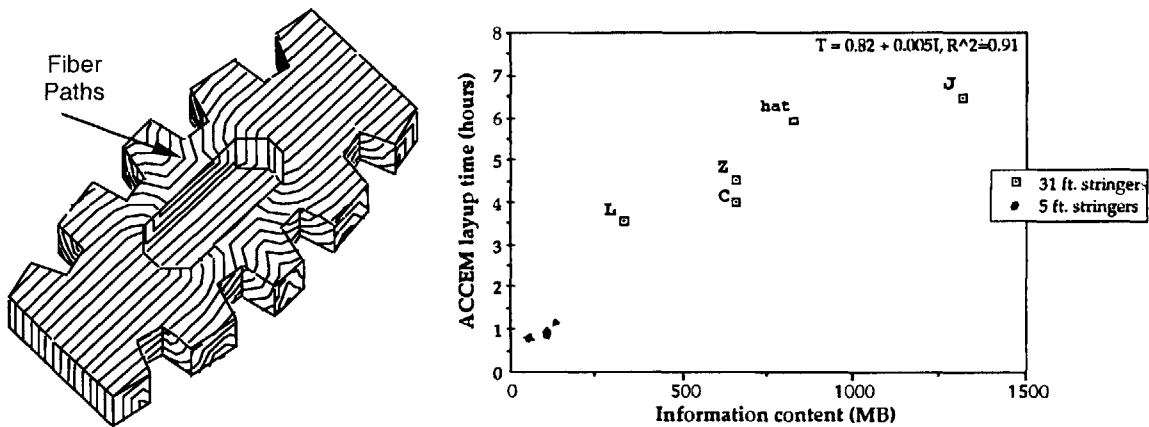


Figure 5.2 Complexity of Composites and Information Content [35, 36, 37, 62]

As a general hypothesis, the shape complexity of a composite design can be evaluated by using various measures from differential geometry. Furthermore, these same measures have a physical interpretation as to their effect on fabrication time. The principal measure, representing the complexity of a shape or a fiber path, has been the fiber deformation angle. The underlying design features directly determine the shape and the fiber path and therefore the curvature of fiber paths presents a good measure of part complexity. A worker or a machine requires time to produce this deformed fiber network. The difficulty in production can be quantified conveniently by converting fiber deformation into information content. Previous studies have shown the validity of this concept on a theoretical and experimental basis [37, 45]. Figure 5.2 demonstrates how the production time increases with the information content or complexity of some select composite parts [37]. Moreover, the figure also shows an additional feature of fiber composites structures and their relation to complexity. The effects of localized geometric features on fiber structure can be observed throughout the entire part. As seen in Figure 5.2, the fiber deformation caused by the indentation affects the entire fiber network. The complexity concept cannot only focus on individual features, but has to consider the entire structure. The exact paths, which the fibers assume is best determined by computers. The algorithms, based on the theory of differential geometry, calculate the distribution of the fibers depending on the shape and curvature of the underlying part geometry. Appendix 5.4.2 contains a brief discussion of differential geometry. The algorithms also consider the material form, since the deformation, the wrinkling, and the slippage is different for single fibers bundles than it is for a woven material [52]. The deformation mechanisms for the different material forms are slightly different. Single fibers tend to slip along non-geodesic paths whereas fabrics are prone to wrinkle when formed into shapes exhibiting double curvature [60]. The shear forces, which cause in plane bending and slippage of single fibers, are responsible for fabric to deform in a trellissing mode as illustrated in Figure 5.6. The following paragraphs introduce several models on how to treat the different scenarios and how to define a practical measure of part complexity.



Model 1.) Information Content of Single Fibers (Equal Probability)

Tse argues that a fiber can be modeled as an information storage device [37]. To illustrate the idea one can think of a sensor, which passes along a deformed fiber and detects angular changes with accuracy  $\Delta\Theta$ . Either the sensor detects a deformation or it does not. These two outcomes are assumed to occur with equal probability  $p_i = 1/2$ .

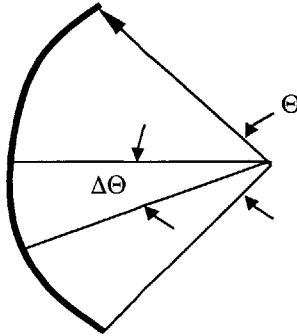


**Figure 5.3 Discretization of a Curved Fiber**

When discretizing a fiber as seen in Figure 5.3 in  $N$  different segments it represents a message with a length of  $N = \frac{\Theta}{\Delta\Theta}$  binary characters. The information stored in a fiber bent at an angle  $\Theta$  can be described as (see Appendix 5.4.1):

$$I = \frac{\Theta}{\Delta\Theta} \cdot \log_2(2) \Rightarrow I = \frac{\Theta}{\Delta\Theta} \Rightarrow I \propto \Theta \quad \text{Equation 5.1}$$

The model relates the part complexity directly to the bent angle of the fiber, a simple concept, which can be used even without computers. The validity of this approach has been tested and as Figure 5.2 shows, it is capable to rank order parts according to their complexity [35-37]. However, the concept not only works for parts exhibiting simple (or normal) curvature, but also for geometries featuring double curvature. Here according to the additive properties of information (see Equation 5.92, Appendix 5.4.1), the information components due to normal and geodesic curvature are simply added (Equation 5.2).

$$I = I_n + I_g \quad \text{Equation 5.2}$$

Model 2.) Information Content of Single Fibers (Variable Probability)

The second model is derived from the previous one and can be applied to a pre-segmented fiber. This new concept can be employed in connection with CAD programs, where 3D geometries are already subdivided in surface patches. It therefore lends itself to an automated complexity calculation, since the CAD information can be passed directly to the cost model for evaluation. The CAD software subdivides the fibers and determines the number of segments  $N$  (length of message) (see Figure 5.4). At each node, the following segment can point in  $n = \frac{\Theta_{\max}}{\Delta\Theta}$  different directions (choices) within its plane of movement.

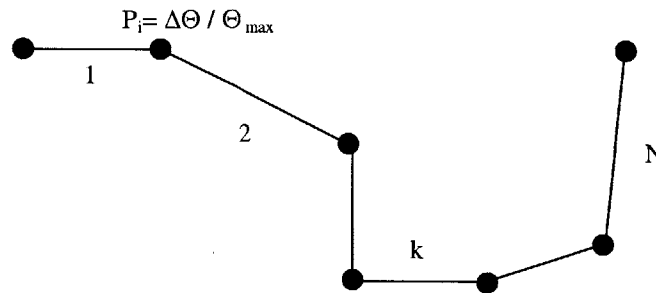


**Figure 5.4** Fiber Segmented into  $N$  Pieces

Therefore, the maximum average information stored within each node (character) of the fiber is written as:

$$H_{\max} = \log_2\left(\frac{\Theta_{\max}}{\Delta\Theta}\right) \quad \text{Equation 5.3}$$

Equation 5.3 establishes that the maximum average information  $H_{\max}$  is independent from the number of fiber segments and thus independent of the size of the fiber. However, the actual average information content  $H$  is often less than  $H_{\max}$  and can be computed by Equation 5.4:

$$H = \sum_{i=1}^n \frac{N_{\Theta_i}}{N} \cdot \log_2\left(\frac{N}{N_{\Theta_i}}\right) \quad \text{Equation 5.4}$$

The frequency  $N_{\Theta_i}$  with which a certain angle value  $\Theta_i$  occurs can be determined manually or by computer. Together with the number of nodes  $N$  (characters) the probability of each angle value to occur is  $p_{\Theta_i} = \frac{N_{\Theta_i}}{N}$ . Since, the average information content  $H$  is independent of the number of subdivisions (size) it too can be used as an information measure for composites.

Model 3.) Information Content of a Fiber Network

The third model is also new and attempts to estimate the information content of an entire fiber network. It too can be used to automatically compute complexity. This works particularly well for a part made of a woven fabric. Such a part can be characterized by a grid, in which the nodes represent the crossover points of the individual wrap and fill fibers (see Figure 5.5).

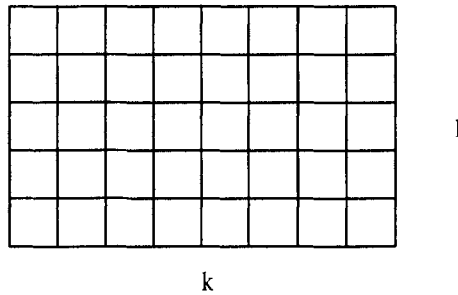


**Figure 5.5 Discretization of a Fiber Network**

The number of nodes (characters) in such a grid (message) is defined as  $N = k \cdot l$ . Again, Equation 5.4 can be applied to calculate the information content and thus the complexity of the fiber network. The fibers at each node can be bent within the osculating (normal curvature) or within the tangential (geodesic curvature) plane. In addition, the fabric can be deformed by shear forces and exhibit trellissing of the fibers. In the generic case, the fibers can assume a different set of angles for each bending mode. The maximal information for each bending mode averaged for each node can be written as:

$$\text{Normal: } H_{n_{\max}} = \log_2 n_n; \quad \text{Geodesic: } H_{g_{\max}} = \log_2 n_g \quad \text{Equation 5.5}$$

With  $n_{n/g} = \frac{\Theta}{\Delta\Theta}$  as the number of choices for either normal or geodesic bending.

However, the actual information content of a part differs from the maximum information content. The information content is determined separately for each node and then summed up over all nodes:

$$H_{n/g} = \sum_{i=1}^n \frac{N_{\Theta_i}}{N} \cdot \log_2 \left( \frac{N}{N_{\Theta_i}} \right) \quad \text{Equation 5.6}$$

Similar to the previous model, the occurrence of each angle value  $N_{\Theta_i}$  is counted and divided by the total number of nodes  $N$ . Again, the information content for in-plane (geodesic) bending can be superimposed with the information content for out-of-plane (normal) bending (Equation 5.7).

$$H = H_n + H_g \quad \text{Equation 5.7}$$

The average information content  $H$  can then be used as a complexity measure to characterize composite parts. The measure  $H$  is independent of the grid size and the subsequent chapter demonstrates how Equation 5.6 can be used in connection with the 1<sup>st</sup> Order model (Equation 5.8).

### Complexity Scaling Model

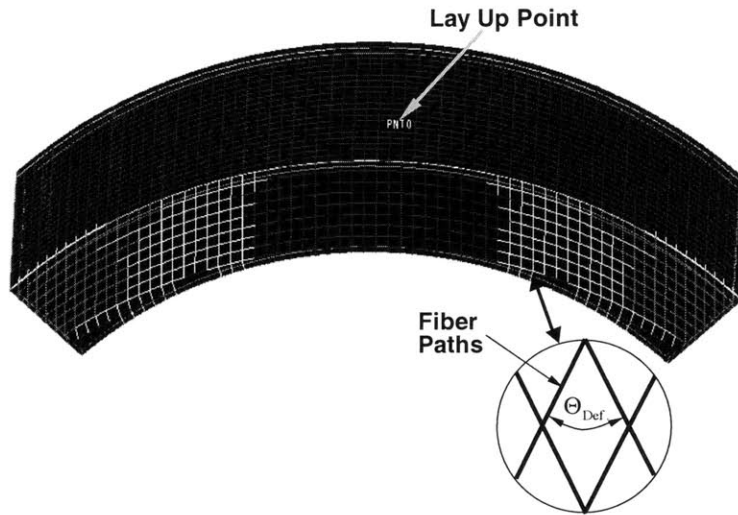
As some studies have suggested it appears, that the information stored in a deformed fiber pattern does indeed provide a measure of part complexity [36-37]. The complexity scaling model establishes the necessary relationship between the complexity measure and the processing time. One can argue that increased complexity leads either to delays or to a reduction in the processing rate or both. Human performance studies conducted by Fitts, Goldman and Ching [31-32] and studies involving the production of composites [36] suggest a linear relationship between performance and information content (see also

Figure 5.2). In general, process based cost models offer a convenient way to mathematically describe a production slow down or delay. The processing rate  $v$  and the time constant  $\tau$  of the 1<sup>st</sup> Order Model (Equation 5.8) can be related linearly to the part complexity  $I$  in order to achieve the desired effect. Equation 5.9 shows this relationship including the linear coefficients  $b$  and  $c$ . The two coefficients can be interpreted as a gain, controlling the sensitivity of the 1<sup>st</sup> Order parameters to the complexity  $I$ .

$$t = \sqrt{\left(\frac{x}{v}\right)^2 + \frac{2 \cdot \tau}{v} \cdot x} \tag{Equation 5.8}$$

Time Constant:  $\tau = \tau_0 + b \cdot I$  ; Processing Rate:  $\frac{1}{v} = \frac{1}{v_0} + \frac{I}{c}$  Equation 5.9

The parameter  $v$  and  $\tau$  carry the subscript 0 whenever the process is not affected by complexity effects, which is generally the case for flat shapes.



**Figure 5.6 Fiber Mapping and Complexity Scaling**

In order to be consistent in the calculation of part complexity the process is automated. Figure 5.6 shows the mapping of a fiber network onto a flange type shape. The mapping technique follows the principles of differential geometry and calculates the deformation of the fabric as it assumes a particular shape. FiberSim© [40] numerically outputs the fiber deformation angle  $\theta_{def}$  for each node of the predefined mesh. For fabrics, as seen in

the example above (Figure 5.6), shear forces cause the fibers to swivel around the intersection nodes. This trellessing becomes more pronounced as the fabric is draped over shapes exhibiting large areas of double surface curvature. Eventually the deformation reaches a maximum trellessing angle and wrinkling occurs. The prevention or smoothing out of any wrinkles slows down the layup rate and causes delays. In addition, FiberSim© is also capable of calculating the deformation of single fiber bundles instead of fabrics. Again, a distribution of the deformation angle is written out for further processing and calculation of the part complexity. Figure 5.40 and Figure 5.41 in the Appendix 5.4.3 provide further examples of fiber mapping and Chapter 5.2.1 describes an actual cost model based on the above concepts.

Conclusively, it should be stated that there are many ways to establish complexity relations and they might differ for every material and process. However, unless future research suggests otherwise, the general rule one should follow is to use whatever relationship works and makes sense in terms of the process behavior.

### Dimensional Complexity

A further application of information theory is the quantification of dimensional complexity. It can be described as the difficulty to achieve a certain part tolerance. Suh [38] has outlined in his book how the information content can be used to describe the dimensional complexity of machined parts. However, the theory can be easily adapted to express the complexity of positioning parts within a certain tolerance. Part of composite production not only involves the positioning of parts, but also features machining like operations such as trimming or drilling. Assuming constant probability Suh constitutes, that the total information content of a part and therefore its complexity can be described as:

$$I = \sum_{i=1}^k \log_2 \left( \frac{\text{dimension}}{\text{tolerance}} \right)_i \quad \text{Equation 5.10}$$

According to Equation 5.10, the fabrication of a long beam while complying with tight tolerances is a more difficult endeavor as if the beam would be shorter. The interpretation further says, that the tighter the tolerance the less likely it is, that one succeeds in manufacturing this particular part. Since information is additive (Shannon) [34] one can take the sum over all part dimensions  $k$ .

## 5.2 Cost Model Applications

The following chapters introduce cost models for the six most common composite production techniques. The models are built in accordance to the previously presented ideas of process based cost modeling. The most time consuming steps, size and complexity scaling laws relate the processing time to the parts' design features. Each model includes a description of the boundary conditions and a parameter set for the most common processing conditions. Verification studies and a comparison of process performance are presented in Chapter 9 and the Appendix 5.4.5.

### 5.2.1 Hand Lay-Up (HLU)

Composite fibers are manually deposited layer by layer onto a tool, which gives the part its shape. The operator takes each pre-cut ply, removes possible release films and places the ply in its predefined location. Hereby the operator has to ensure the correct fiber orientation and the absence of wrinkles.

#### Scope of the Model

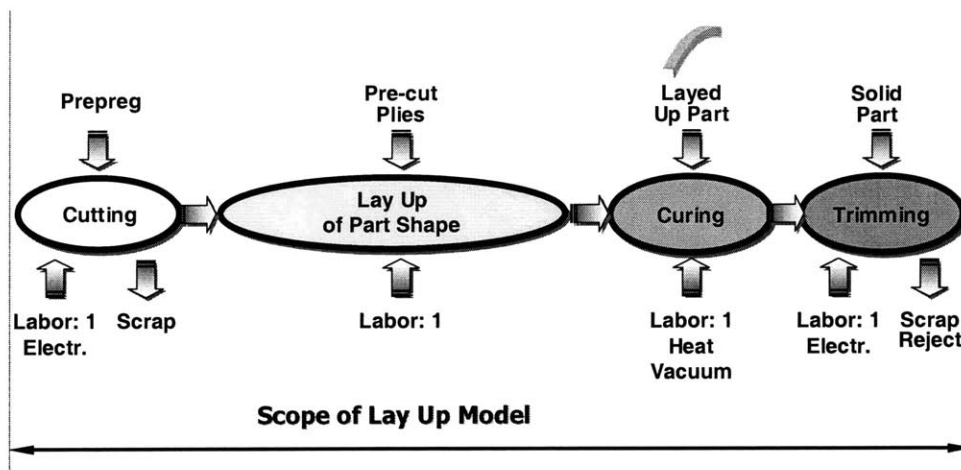


**Figure 5.7** Process Flow of Hand Lay-Up

Figure 5.7 schematically outlines the process flow of the Hand Lay-Up process. The above figure shows not only the required input of material and resources, but also the



initial and final state of the actual product. Each of the 4 shown processing stages are comprised of many individual processing steps, which are all listed in a more comprehensive process plan in Appendix 5.4.4. Chapter 5.2.6 introduces a time estimation model for the curing of the part.

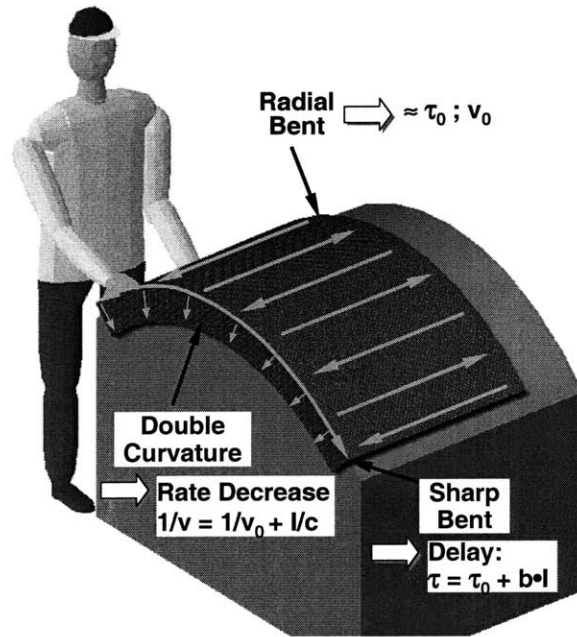


**Figure 5.8 Complexity and Process Analogies**

Scaling Model: Time per Ply

The size scaling model is based on process analogies, which suggest that sharp bends cause a delay in the layup process. In contrast, areas affected by double curvature have to be processed at a slower rate since the danger of wrinkles reduces the layup rate.

The Hand Lay-Up process of composites can be modeled by using the 1<sup>st</sup> Order Model. The processing time to layup one ply is expressed by:

$$t_{ply} = \sqrt{\left(\frac{x}{v}\right)^2 + \frac{2 \cdot \tau}{v} \cdot x} \quad \text{with } \tau = \tau_0 + b \cdot \bar{l} \quad \text{and} \quad \frac{1}{v} = \frac{1}{v_0} + c \cdot \bar{l} \quad \text{Equation 5.11}$$

Where  $t_{ply}$  is the layup time per ply or strip and  $x$  can be either the area of the layer or length of the strip. The steady state layup rate and the time constant depend on the part

complexity. According to process analogies, the information content of a fiber network affected by single or double curvature can be written as:

$$\bar{I}_n = b_n \cdot \Delta\Theta_n \cdot L_y \text{ and } \bar{I}_{n/g} = c_{n/g} \cdot \Delta\Theta_g \quad \text{Equation 5.12}$$

The information content is a linear function of the respective deformation angle for normal and geodesic bending. The coefficients  $b$  [s/bit] and  $c$  [s/m/bit] can be interpreted as information processing rates.

The effects of single curvature and double curvature are added up as seen in the following expression:

$$t_{\text{Ply}} = \left( \tau_{\text{Single}} \cdot \sqrt{\left( \frac{A_{\text{Single}}}{V_{\text{Single}} \cdot \tau_{\text{Single}}} + 1 \right)^2 - 1} \right) + \left( \tau_0 \cdot \sqrt{\left( \frac{A_{\text{Double}}}{V_{\text{Double}} \cdot \tau_0} + 1 \right)^2 - 1} \right) \quad \text{Equation 5.13}$$

#### Scaling Model: Time per Part

The total layup time is calculated by multiplying the processing time per ply and the total number of plies:

$$t_{\text{Part}} = n_{\text{Ply}} \cdot t_{\text{Ply}} \quad \text{Equation 5.14}$$

#### Process Parameters

The scaling model as described by Equation 5.13 is used to calculate the processing times for six different reference shapes. As the design parameters, such as size and degree of complexity are varied, the resulting processing times are compared to the ACCEM [5] model. The ACCEM model is introduced in Chapter 4.4.3 and is accepted by industry as a cost reference. The layup times for composite prepreg (Carbon/Epoxy Prepreg: Hercules AS4/3505-6) stemming from the 1<sup>st</sup> Order model are plotted against the ACCEM results as seen in Figure 5.9.

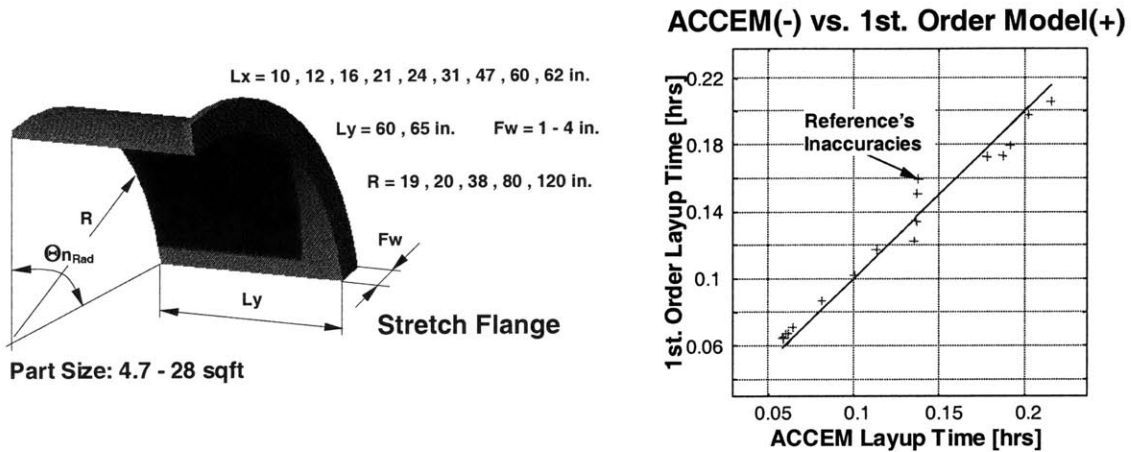


**Figure 5.9 Model Verification (Stretch Flange)**

The results for stretch flanges show that the reference model apparently does not capture all of the complexity effects. Figure 5.9 shows how 4 data points, representing the flanges with flange widths between 1” and 4”, deviate from the ACCEM results. The 1<sup>st</sup> Order Model, however accounts for the actual increase in complexity as the flange width is increased and consequently the fiber network is subjected to larger deformations.

The remainder of the results are discussed in the Appendix 5.4.5. The derived 1<sup>st</sup> Order Parameters are listed in Table 5.1.

**Table 5.1 1<sup>st</sup> Order Parameters for Hand Layup**

<i>Hand Lay-Up</i>	<i>Woven Prepreg</i>	<i>3" Tape [28]</i>	<i>12" Tape [28]</i>
<b>Time Constant:</b> $\tau_0$	5.814 min	1.146 min	0.666 min
<b>Steady State Velocity:</b> $v_0$	6.49 sqft/min	15.21 ft/min	2.63 ft/min
<b>Sharp Normal Bends:</b> $b_n$	7.56e-2 min/ft rad		
<b>Radial Normal Bends:</b> $c_n$	4.19e+3 cuft rad/min		
<b>Double Curvature:</b> $c_n$	2.53e-1 sqft rad/min		
<b>Critical Size:</b> $x^*$	13.9 sqft	6.4 ft	0.7 ft

Labor Rates

As always labor rates depend on the industry, the company overhead, the skill level, and the geographic location. Generally, it is assumed, that for a worker in the aerospace

industry a rate of \$100/hr has to be considered, including overhead and benefits. Layup of complex parts requires a great amount of skill and diligence. In addition, the risks are considerable, since errors in the layup sequence etc. can be costly and lead to structural failure. Layup tasks, which are less demanding can also be conducted by workers with less experience.

### 5.2.2 Resin Transfer Molding (RTM)

During Resin Transfer Molding (RTM) a dry fiber perform is placed into a matched mold and injected with liquid resin. The resin within the closed mold is then left to cure and solidify. Depending on the type of resin the curing process takes place at either room temperature or at an elevated temperature. All the steps including the ones preceding and succeeding the cure are listed as part of the process plan in the Appendix 5.4.4. This chapter introduces a model describing the injection and the curing time.

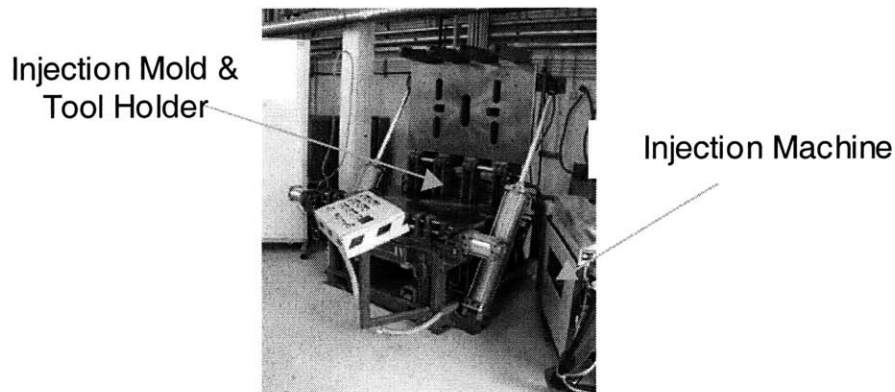


**Figure 5.10 Resin Transfer Molding [50]**

The injection of the low viscous resin can be accomplished in two different ways. The first is to inject at a constant rate and letting the injection pressure vary. The second method keeps a constant injection pressure and allows the injection rate to fluctuate.

#### Scope of the Model

The process plan describing the individual steps in detail can be found in the Appendix 5.4.4. Figure 5.11 shows, that the model encompasses all operations starting with the filling and closing of the mold. The resin is injected, cured and the finished part is taken out of the mold and trimming according to specs. However, the production of the fiber perform is not included.

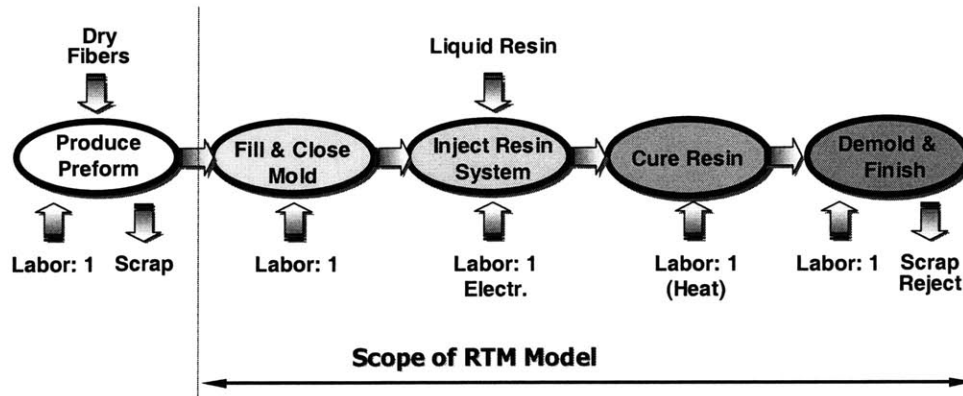


**Figure 5.11 Process Flow of RTM**

Scaling Model: Time per Mold Fill

The law of mass conservation (Equation 5.15) together with the expression for the total resin volume (Equation 5.16) leads to a simple scaling law. The assumptions include: uniform flow profile and linear pressure distribution throughout the die. The bulk velocity of the resin within the mold is denoted by the variable  $v$ .

Mass Conservation: 
$$dV_{Resin} = \dot{V}_{Resin} \cdot dt$$

Resin Injection Rate: 
$$\dot{V}_{Resin} = A_{Resin} \cdot v \quad \text{Equation 5.15}$$

Fiber Vol. Fraction: 
$$\phi = \frac{V_{Fiber}}{V_{Part}} = \frac{V_{Fiber}}{V_{Fiber} + V_{Resin}} \Rightarrow V_{Resin} = V_{Part} \cdot (1 - \phi) \quad \text{Equation 5.16}$$

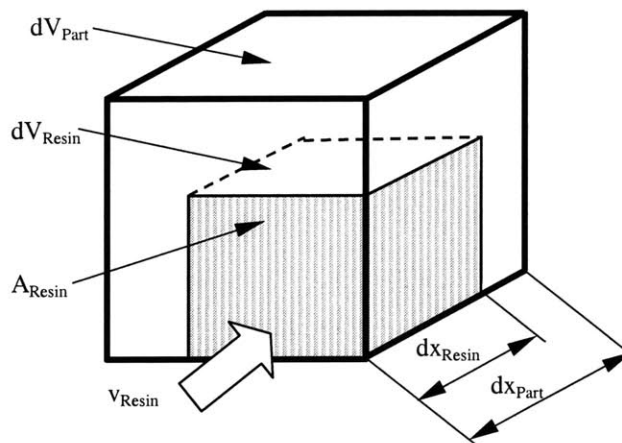


**Figure 5.12 Infinitesimal Laminate Element**

Injection Time – Constant Flow Rate

The integration of mass conservation leads to the mold filling time assuming a constant injection rate (Equation 5.17). Equation 5.18 expresses the scaling law in relation in relation to the parts size and the fiber volume fraction  $\phi$ .

Mold Filling Time (const. flow): 
$$t_{MoldFill} = \frac{V_{Resin}}{\dot{V}_{Resin}} = \frac{V_{Part} \cdot (1 - \phi)}{\dot{V}_{Resin}} \quad \text{Equation 5.17}$$

Scaling (const. flow): 
$$t_{MoldFill} \propto V_{Part} \cdot (1 - \phi) \quad \text{Equation 5.18}$$

Darcy's Law

Darcy's Law proves to be helpful when modeling the flow of viscous resin through the porous fiber preform. The law is a simple description of the bulk flow  $v$  of a fluid with a viscosity  $\mu$  through porous media, exhibiting a permeability  $S$  (Equation 5.19).

Bulk Resin Velocity: 
$$v = -\frac{S}{\mu} \cdot \frac{dp}{dx} \quad \text{Equation 5.19}$$

Injection Time - Constant Flow Rate

Introducing Equation 5.19 into the volumetric flow rate leads to:

$$\dot{V}_{Resin} = -A_{Resin} \cdot \frac{S}{\mu} \cdot \frac{dp}{dx} \quad \text{Equation 5.20}$$

and rewriting the expression considering mass conservation, results in:

$$dV_{Resin} = -A_{Resin} \cdot \frac{S}{\mu} \cdot \frac{dp}{dx} \cdot dt \quad \text{Equation 5.21}$$

One can use a modified expression of the fiber volume fraction and write for  $dV_{Resin}$ :

$$dV_{Resin} = A_{Resin} \cdot (1 - \phi) \cdot dx \quad \text{Equation 5.22}$$

By plugging Equation 5.22 into Equation 5.21 one obtains:

$$dt \cdot dp = -\left(\frac{\mu}{S}\right) \cdot (1 - \varphi) \cdot dx^2 \quad \text{Equation 5.23}$$

Under the assumption of a linear pressure profile one can integrate the above expression and solve it for the mold filling time  $t_{\text{MoldFill}}$ , where  $L$  represents the total flow length.

$$\text{Mold Filling Time (const. pressure): } t_{\text{MoldFill}} = \frac{1}{2} \cdot \left(\frac{\mu}{S}\right) \cdot \left(\frac{L^2}{\Delta p}\right) \cdot (1 - \varphi) \quad \text{Equation 5.24}$$

$$\text{Scaling Law (const. pressure): } t_{\text{MoldFill}} \propto L^2 \cdot (1 - \varphi) \quad \text{Equation 5.25}$$

The above expressions provide insight in the time scaling of the filling process with respect to the part geometry. However, Equation 5.24 has practical limitations, since the permeability of the fiber structure  $S$  is usually not readily available and a function of many parameters. The scaling law however can be used to fit a few experimental data and built a time estimation model.

#### Scaling Model: Time per Cure

The n-th Order Cure Rate expression relates the rate of cure to the resin properties of thermoset resins. Part of the formula are the frequency factor  $Z$  [1/s] and the activation energy [J/mol K] (Equation 5.26) [63].

$$\text{n-th Order Cure Rate Expr.: } \frac{d\alpha}{dt} = Z \cdot \exp\left(\frac{-E_a}{\mathfrak{R} \cdot T}\right) \cdot (1 - \alpha)^n \quad \text{Equation 5.26}$$

where  $\mathfrak{R} = 8.413 \text{ J/mol K}$  is the general gas constant.

The frequency factor  $Z$  is a strong function of the temperature  $T$  and the extent of the cure  $\alpha$  and therefore a straightforward integration is difficult if  $Z$  is not constant. To obtain a numerical solution it helps to linearize the above expression by taking the log on both sides and obtain:



$$\log\left(\frac{d\alpha}{dt}\right) = \log(Z) + \frac{1}{\ln 10} \left(\frac{-E_a}{R \cdot T}\right) + n \cdot \log(1 - \alpha) \tag{Equation 5.27}$$

The differences in curing time between resins can then be approximated as:

Scaling of Cure: 
$$\frac{t_{Cure1}}{t_{Cure2}} \propto \frac{Z_1}{Z_2} \cdot \exp\left(\frac{E_{a1} - E_{a2}}{R \cdot T}\right) \cdot \frac{(1 - \alpha_2)^{n_2}}{(1 - \alpha_1)^{n_1}} \tag{Equation 5.28}$$

The above expression can be further simplified by setting  $\alpha_1 = \alpha_2$  and  $n_1 = n_2$ .

**Table 5.2 Kinetic Cure Parameters [49, 63]**

	<i>Z</i> [1/s]	<i>E<sub>a</sub></i> [J/mol K]
<b>Polyester</b>	1.61 x 10 <sup>8</sup>	75,100
<b>Vinyl Ester</b>	8.0 x 10 <sup>7</sup>	76,550
<b>Polyurethane</b>	1.27 x 10 <sup>5</sup>	38,900

The cure time usually depends on the ratio between resin and catalyst. It can be obtained from the resin specifications of the manufacturer. Using the manufacturers' specs is far more practical for cost modeling purposes since the respective parameters such as the activation energy etc. are often time consuming to determine. Table 5.3 therefore gives an overview of the numerous published performance and costs data for RTM.

**Table 5.3 RTM Cost and Performance Data**

	<i>Krolewski</i> [27]	<i>Kang</i> [49]	<i>Moy</i> [48]	<i>Goel</i> [51]
<b>Injection Rate</b>	415 in <sup>3</sup> /min	150 in <sup>3</sup> /min	25 in <sup>3</sup> /min	16.67
<b>Injection Pressure</b>	25 psi	73 psi	1 - 5 psi	100 - 600 psi
<b>Permeabilities</b>	2 - 150 x 10 <sup>-11</sup> m <sup>2</sup>	5.34 x 10 <sup>-8</sup> m <sup>2</sup>	N/A	16.67
<b>RTM Injector</b>	\$18 K	\$150 K	N/A	\$5 K - 100 K
<b>RTM Press</b>	\$22,500	\$2,151,000	\$ 10 / hr	N/A
<b>Material / Scrap</b>	\$46.5 / 7 %	\$2.55 / 3 %	\$ 50 / 10 %	N/A
<b>Tooling</b>	7 x Open Mold	\$1,404,000	N/A	N/A
<b>Max. Parts / Year</b>	12,800	50,000	N/A	N/A
<b>Viscosity</b>	6 - 50 x 10 <sup>-3</sup> Pa s	300.0	N/A	N/A
<b>Fiber Vol. Fraction</b>	40 - 50 %	40 %	50 %	N/A
<b>Crew Size</b>	N/A	2	N/A	N/A
<b>Injection Temp.</b>	N/A	212 F	150-350 F	N/A
<b>Part Size</b>	4.1 lb	144 ft <sup>2</sup> / 121 lb	6 ft <sup>2</sup> / 100 lb	N/A
<b>Cycle Time</b>	18 min	58 min.	285 min.	N/A
<b>Floor Space</b>	144 ft <sup>2</sup> + 256 ft <sup>2</sup>	458 ft <sup>2</sup>	N/A	N/A

<b>Depreciation</b>	10 % / 8 yrs	10 % / 20 yrs	N/A	N/A
<b>Downtime</b>	N/A	15 %	N/A	N/A
<b>Depreciation</b>	10 % / 8 yrs	10 % / 20 yrs	N/A	N/A
<b>Labor / Fringe</b>	\$ 20 / 30 %	\$ 25 / 35 %	\$70 / 1%	N/A

The cycle time of Resin Transfer Molding (RTM) is dominated by the injection and chiefly by the curing time of the resin. Since the curing time strongly depends on the type of the resin system, the catalyst and the curing temperature, resin manufacturers provide tabulated data of gel and curing times. Scaling laws describing injection and cure might provide insight in the some of the mechanisms involved but are not used to estimate manufacturing times. Tabulated curing times are quite exact and can be entered directly into a cost calculation. In addition, it should be considered that production can be increased by demolding the part once the resin has gelled and putting the part in an oven to complete the cure. The effective production rate excluding post cure, trimming and inspection lies around 2lb/hr for the here discussed process. However, as seen in the Pareto charts in Appendix 5.4.4 the curing operation is the bottleneck of the process and by switching to resins with a cure time of about 60 min. or even less the production rate could be increased to about 10 lb/hr.

#### Labor Rates

As always labor rates depend on the industry, the company overhead, the skill level, and the geographic location. Generally, it is assumed, that for a worker in the aerospace industry a rate of \$100/hr has to be considered, including overhead and benefits. However, RTM process does not require such a high skill level as Hand Layup for example. Once the equipment and the resin system is set up by a supervisor the tasks are quite uniform and consists mainly of cleaning the mold, filling it with the perform, closing it and initiating the automatic injection and cure cycle. Newly hired workers can be trained quickly to perform these tasks and would probably cost less on an hourly basis.

### 5.2.3 Automated Tow Placement (ATP)

The following chapter describes the performance of Automated Tow Placement (ATP) and introduces a concept to estimate processing times. ATP machines often feature several numerical controlled axes. The performance of each engaged axis determines the overall lay down rate. Commonly, the lay up of 0 degree plies using the z-axis is more time consuming, than the placement of 90 degree plies, which activates the rotational c-axis. However, during the actual material deposition delays occur frequently. For example, the cutting of the material strip at the end of one path is one reason for delays. Furthermore, the turning of the machine head or the dead travel of the head to a new layup position can cost additional time. Also, the raising and lowering of the lay up head as well as the adding and dropping of individual tows leads to further stoppages. Under the consideration of the part geometry and the laminate properties a time estimation model should be able to account for all the above effects.

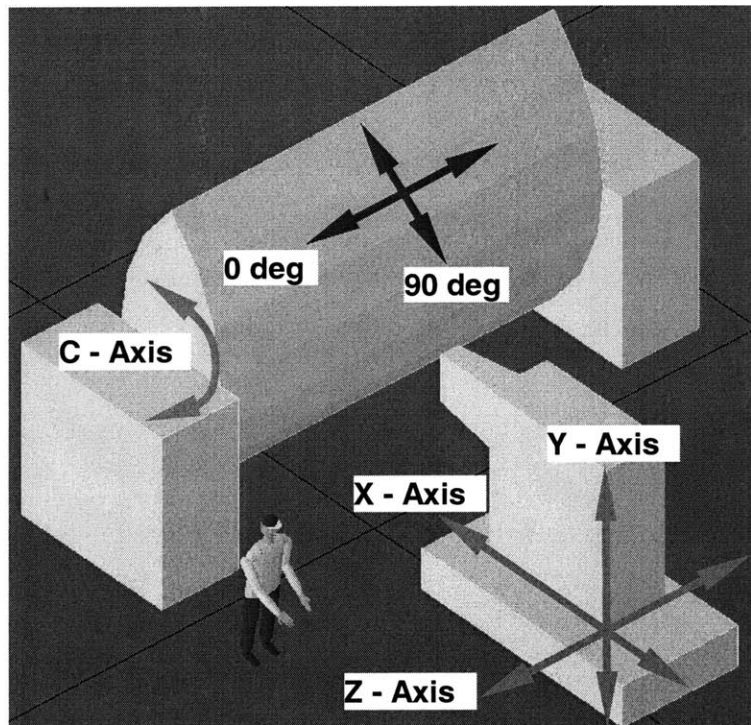
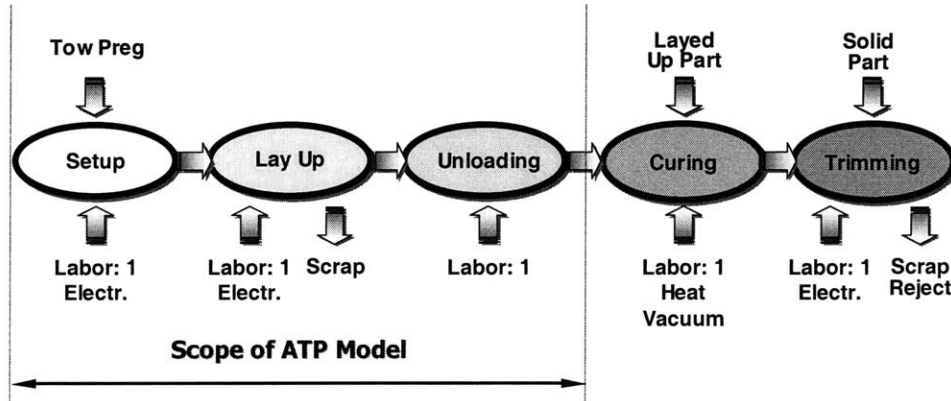


Figure 5.13 Automated Tow Placement

Scope of the Model

The process plan describing the individual steps in detail can be found in the Appendix 5.4.4. Figure 5.14 shows the general process flow of ATP excluding the curing and trimming of the part.



**Figure 5.14** Process Flow of ATP

Scaling Model

When assuming a linear acceleration profile for the placement head, one can write:

$$v = a \cdot t, x = 1/2 \cdot a \cdot t^2 \Leftrightarrow x = \frac{v_0^2}{2 \cdot a} \text{ and for steady state } x = v_0 \cdot t_0 \quad \text{Equation 5.29}$$

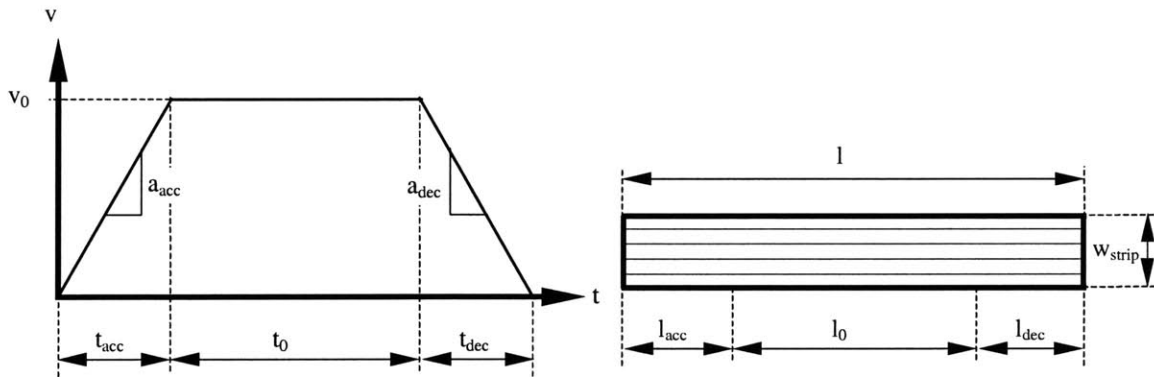


**Figure 5.15** Machine Velocity Profile; Lengths of the Fiber Strip

Geometry

The total layup length is expressed by:  $l = l_{acc} + l_0 + l_{dec}$  and with  $l_0 = v_0 \cdot t_0$ ,  $l_{acc/dec} = v_0^2 / 2a_{acc/dec}$  one gets  $l = v_0^2 / 2a_{acc} + v_0 \cdot t_0 + v_0^2 / 2a_{dec}$ . The expression can be solved for the steady state layup time:  $t_0 = l / v_0 - v_0 / 2a_{acc} - v_0 / 2a_{dec}$ .

Time per Fiber Strip

The total deposition time is written as:  $t = t_{acc} + t_0 + t_{dec} + t_{delays}$  and with  $t_{acc/dec} = v_0 / a_{acc/dec}$  and the above expression for  $t_0$  it follows:

Lay Up Time per Single Strip:

$$t_{Strip} = \frac{l_{Strip}}{v_0} + \frac{v_0}{2} (1/a_{acc} + 1/a_{dec}) + t_{Delays / Strip} \tag{Equation 5.30}$$

Where  $v_0$  represents the steady state velocity of a specific ATP axis,  $a$  denotes the axis' acceleration and  $l_{strip}$  stands for the length of the strip. The encountered delays after laying down one strip are then expressed as:

Delays per Single Strip:

$$t_{Delays / Strip} = t_{Turn180^\circ} + t_{Cut} + t_{DeadHead} + t_{Add / Drop Tow} + t_{Head Up / Down} \tag{Equation 5.31}$$

The above formulas can now be used to simulate the lay up performance for different fiber angles and machine axes. The width  $w_{strip}$  (typical 3") of a single strip can be calculated by multiplying the tow width (typical 1/8") with the number of tows (typical 24).

Time per Ply

When assuming equal acceleration and deceleration  $a_{acc} = a_{dec}$  the previous equations can be further simplified. The following graphic explains how the total material length can be calculated considering the part geometry and the fiber orientation  $\Theta_{Fiber}$ .

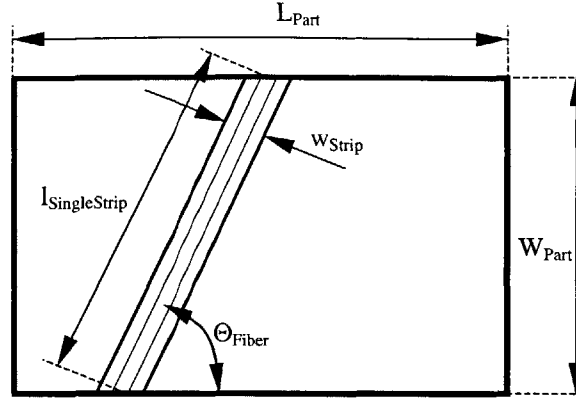


**Figure 5.16** Single Fiber Ply

The total strip length for one ply is  $l_{Strip/Ply} = \sum l_{SingleStrip} = \frac{A_{Ply}}{W_{Strip}}$  and for rectangular parts

the strip length equals  $l_{Strip/Ply} = \frac{L \cdot W}{W_{Strip}}$ . The total number of strips per ply can be

expressed as:  $n_{Strips/Ply} = \frac{L \cdot \sin \Theta}{W_{Strip}} + \frac{W \cdot \cos \Theta}{W_{Strip}}$ .

To obtain the total lay up time per ply the above expression for the total strip length  $l_{Strip/Ply}$  is introduced into Equation 5.30 and then multiplied by the number of strips per ply  $n_{Strips/Ply}$ . In addition, one can consider any initialization time  $t_{PlyInit}$  before starting the layup of a new ply. The initialization time also includes the time to move the machine head to a new starting position.

Lay Up Time per Ply:

$$t_{Ply} = \frac{A}{W_{Strip} \cdot v_0} + \frac{L \cdot \sin \Theta + W \cdot \cos \Theta}{W_{Strip}} \cdot \left( \frac{v_0}{a} + t_{Delays/Strip} \right) + t_{PlyInit} \quad \text{Equation 5.32}$$

The above model considers a non-integer number of strips per ply a reasonable approximation of reality. Also remember that the layup velocity  $v_0$  can be a function of the fiber angle  $\theta$  and part complexity  $v_0 = v_0(\Theta, \text{Curvature})$ .

Time per Part

The production time for the entire part  $t_{part}$  includes the setup time  $t_{Setup}$ , the material loading time  $t_{MatLoad}$ , and the time for the actual fiber deposition in dependence of the laminate structure.

Lay Up Time per Part:

$$t_{Part} = t_{Setup} + t_{MatLoad} + (n_{0\text{ deg}} \cdot t_{Ply0\text{ deg}} + n_{45\text{ deg}} \cdot t_{Ply45\text{ deg}} + n_{90\text{ deg}} \cdot t_{Ply90\text{ deg}} + \dots)$$

**Equation 5.33**

Tow Length per Part

One can use the following expression to calculate the total amount of material required for an entire part.

Total Tow Length per Part:

$$l_{Strip / Part} = n_{TotalPly} \cdot A_{Ply} / w_{Strip}$$

**Equation 5.34**

Effective Lay Up Rate

The effective material deposition rate and the average layup speed can serve as a valuable performance measure.

Eff. Lay Up Speed:

$$v_{Speed} = \frac{l_{Strip / Part}}{t_{Part}}$$

Eff. Deposition Rate:

$$v_{Deposition} = \frac{Part\ Weight}{t_{Part}}$$

**Equation 5.35**

Size & Complexity Scaling

The above derivation shows that the production time for a part scales with its volume. The complexity of a part however is reflected by the various ply orientations and the underlying geometry, since both affect the performance of an ATP axis.

Scaling:

$$t_{Part} = t_{Part} (Volume, Curvature, Laminate)$$

**Equation 5.36**

Performance Data

Table 5.4 lists performance data from several sources. A closer look reveals similarities between the ATCAS [14] data and the study conducted by Dan Whitney [69]. Even the quite dated information published by Susan Krolewski [27] is within range of the previous two studies. Ian Land [67] took a different approach and used a 1<sup>st</sup> Order Model to calculate the overall process performance. However, most differences can be attributed to different assumption about down times and the extent of the model. For example, the reloading of material is included in the data reported by Ian Land model and therefore reduces the effective layup speed, whereas ATCAS and Dan Whitney treat the material loading as a separate manufacturing step. Ian Land also quotes in his thesis a machine downtime of up to 80% due to breakdowns and maintenance. At the time the fiber placement heads were still experiencing difficulties with resin built up.

**Table 5.4 ATP Performance Data**

	ATCAS [14]	Whitney [69]	Land [67]	Krolewski [27]
$v_{max}$ 0 deg [in/s]	12.3	10.0	5.71	16.67
$v_{max}$ 45 deg [in/s]	12.3	10.0	4.19	16.67
$v_{max}$ 90 deg [in/s]	12.3	10.0	6.67	16.67
$v_{max}$ jog [in/s]	25.0	20.0	25.0	N/A
$a_{acc}$ [in/s <sup>2</sup> ]	30.0	40.0	N/A	8.33
$\tau_0$ 0 deg [s]	N/A	N/A	9.4	N/A
$\tau_0$ 45 deg [s]	N/A	N/A	10.4	N/A
$\tau_0$ 90 deg [s]	N/A	N/A	10.0	N/A
t Setup/Part [s]	N/A	300.0	N/A	N/A
t Head Up [s]	1.0	N/A	N/A	N/A
t Cut [s]	1.0	30.0	1.0	N/A
t Turn / Return [s]	N/A	7.5	8.75	2.0
t Curv [s/rad]	N/A	N/A	3.273	N/A
t Matl Load [s/lb]	30.0	33.0	N/A	45
Spool Size [lb]	5 lb x 32	9 lb	25 lb	10 lb
W <sub>Strip</sub> [in]	5.74	3.0 (24 tows)	3.0 (24 tows)	4.0

Overall, Dan Whitney and ATCAS present the most detailed information about the various production steps. However, Ian Land's model accounts for the influence of part shape and fiber orientation. Under the consideration of 80% machine down time Ian



Land obtains an average deposition rate of 0.72 lb/hr to 1.75 lb/hr compared to 0.84 lb/hr calculated by Dan Whitney.

Summary

For the estimation of ATP layup times a linear model is proposed. The equation involves parameters, which can be obtained easily from equipment manufacturers. Therefore, the model as summarized in the following equation is transparent and easy to use.

Lay Up Time per Ply:

$$t_{Ply} = \frac{A}{W_{Strip} \cdot v_0} + \frac{L \cdot \sin \Theta + W \cdot \cos \Theta}{W_{Strip}} \cdot \left( \frac{v_0}{a} + t_{Delays / Strip} \right) + t_{PlyInit} \quad \text{Equation 5.37}$$

Delays per Single Strip:

$$t_{Delays / Strip} = t_{Turn180^\circ} + t_{Cut} + t_{DeadHead} + t_{Add / Drop Tow} + t_{Head Up / Down} \quad \text{Equation 5.38}$$

However, it is recommended to obtain layup speeds for different fiber angles and use them in the above equation. The total production time per part can then be calculated as:

Lay Up Time per Part:

$$t_{Part} = t_{SetUp} + t_{MatlLoad} + (n_{0deg} \cdot t_{Ply0deg} + n_{45deg} \cdot t_{Ply45deg} + n_{90deg} \cdot t_{Ply90deg} + \dots) \quad \text{Equation 5.39}$$

Table 5.5 gives proposed values for the individual speeds and delays derived from the review of the four case studies.

Labor Rates

As always labor rates depend on the industry, the company overhead, the skill level, and the geographic location. Generally, it is assumed, that for a worker in the aerospace industry a rate of \$100/hr has to be considered, including overhead and benefits. The skill leveled required to operate an ATM machine can probably be compared to that of an experienced CNC machinist. In order to perform the tasks workers need special training to operate the many axes of the ATP machine and should have constant access to

engineering staff for support. The work not only involves the loading, editing and execution of programs it also requires the worker to be familiar with the properties of the prepreg material and the numerous error scenarios. The operation of an ATP machine requires workers of the highest skill level and job dedication.

**Table 5.5 Resulting ATP Performance Data**

		<i>ATP</i>
$v_{\max}$	0 deg [in/s]	10.0
$v_{\max}$	45 deg [in/s]	10.0
$v_{\max}$	90 deg [in/s]	10.0
$v_{\max}$	jog [in/s]	25.0
$a_{\text{acc}}$	[in/s <sup>2</sup> ]	30.0
t	Setup/Part [s]	300.0
t	Head Up [s]	1.0
t	Cut [s]	10.0
t	Turn 180 [s]	7.5
t	Curv [s/rad]	N/A
t	Matl Load [s/lb]	30.0
Spool Size [lb]		5 lb x 32
$w_{\text{Strip}}$ [in]		3.0 (24 tows)

### 5.2.4 Pultrusion (PUL)

Although thermoplastic matrix system can be pultruded efficiently, the model only focuses on the pultrusion of thermoset resins. Once the pultrusion process is set up, the production rate is very much determined by the actual pulling speed. The cost model considers all the major production steps, however this chapter mainly describes the scaling law for the pultrusion speed  $v_p$ . The speed  $v_p$  depends on the heating rate of the part and therefore its cross-section. Heat transfer and reaction kinetics are considered in the scaling law.

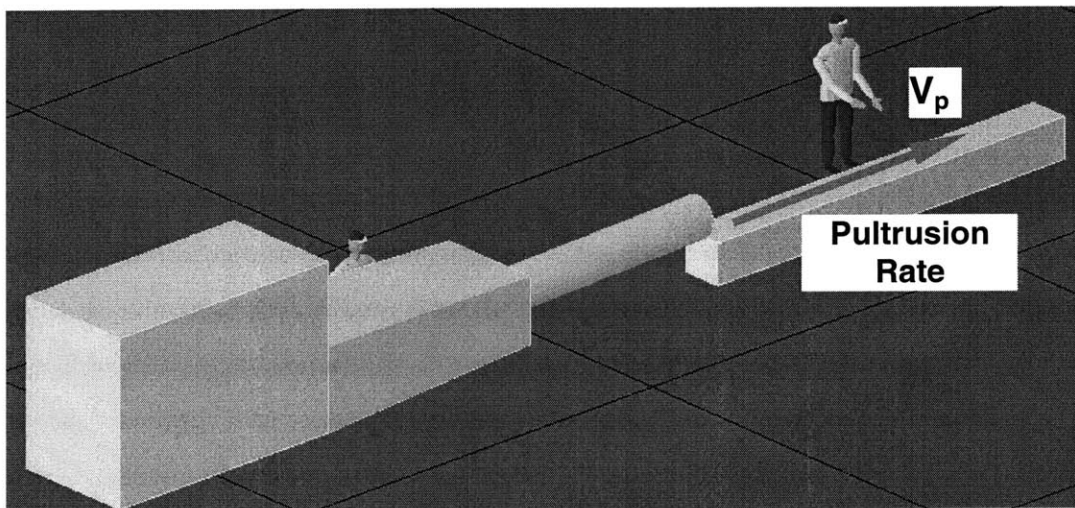


**Figure 5.17 Pultrusion**

#### Scope of the Model

The process plan describing the individual steps in detail can be found in the Appendix 5.4.4. Figure 5.18 shows, that the model encompasses all operations starting with the set up and concluding with the finishing steps. Generally, setup includes the cleaning and readying of the die and the pultrusion machine, the prefeeding of the dry fibers and the filling of the resin bath.

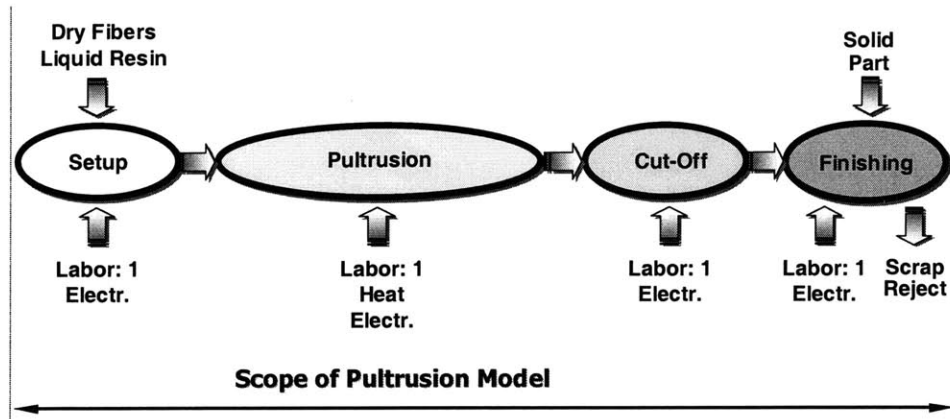


**Figure 5.18** Process Flow of Pultrusion

### Scaling Law

The scaling law for the pultrusion rate is based on a simple one-dimensional heat transfer model of the pultrusion die. It is assumed that the resin and fibers move in bulk and that the temperature is distributed uniformly over the cross-section of the die. In addition, the heat generated by the exothermal cure reaction is neglected. Of course, all the above assumptions strongly simplify the actual situation, but for the development of a scaling law, the model is sufficiently accurate. Of course, elaborate FEM models deliver results, that are more precise, however do not provide scaling laws.

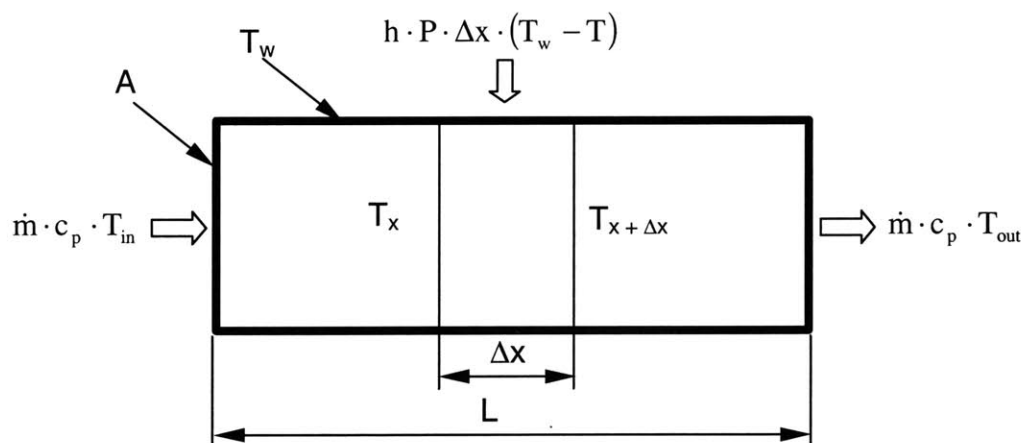


**Figure 5.19** Pultrusion Die Model

Figure 5.19 displays the pultrusion die model where  $L$  is the die length,  $A$  its cross-section, and  $P$  stands for the die perimeter. The prescribed boundary conditions (B.C.) are the die wall temperature  $T_w$  and the entry  $T_{in}$  and exit temperature  $T_{out}$ . The solution (Equation 5.41) for the pultrusion rate  $v_p$  is obtained by introducing the law of mass conservation into the energy balance of the above control volume.

Mass Flow Rate:  $\dot{m} = \rho \cdot A \cdot v_p$

Energy Balance:  $\dot{m} \cdot c_p \frac{dT}{dx} = h \cdot P \cdot (T_w - T)$  ; B.C.:  $x=0$  ,  $T = T_{in}$  ;  $x = L$  ,  $T = T_{out}$

Solution:  $\frac{T_w - T_{out}}{T_w - T_{in}} = e^{-\frac{h \cdot P \cdot L}{\dot{m} \cdot c_p}}$  with  $\Theta = \frac{T_w - T_{out}}{T_w - T_{in}}$  **Equation 5.40**

$$\Rightarrow v_p = \frac{1}{\ln(1/\Theta)} \cdot \left( \frac{h}{c_p \cdot \rho} \right) \cdot \left( \frac{P \cdot L}{A} \right) \quad \text{Equation 5.41}$$

Scaling Law:  $v_p \propto \left( \frac{P \cdot L}{A} \right)$  **Equation 5.42**

The above scaling law can be further simplified, since the die length  $L$  can be regarded as constant. The perimeter  $P$  and the cross-section  $A$  can be expressed by the wall thickness of the part  $t$  and the width  $w$  of the die (Equation 5.43).

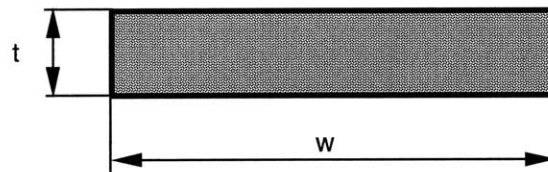


**Figure 5.20 Die Cross-Section**

$$v_p \propto \left( \frac{P \cdot L}{A} \right) = \frac{2 \cdot (t + w)}{t \cdot w} = 2 \cdot \left( \frac{1}{w} + \frac{1}{t} \right) \text{ and with } w = \text{const.} \quad \text{Equation 5.43}$$

$$v_p \propto \frac{1}{t} \quad \text{Equation 5.44}$$

One can show easily that the same scaling law  $v_p \sim 1/t$  still holds for the pultrusion of other thin walled profiles such as C-profiles, L-profiles, round, and square tubes where  $w$  would be set equal to the perimeter of the part.

### Pultrusion Performance Data

**Table 5.6 Pultrusion Performance Data [27, 89]**

Thickness $t$ [in]	Width $w$ [in]	Cross Section $A$ [sqin]	Perimeter $P$ [in]	Die Length $L$ [in]	$P^*L/A$ [1]	Ratio $P^*L/A$ [1]	Line Speed $v_p$ [in/min]	Ratio $v_p$ [1]
0.188	1.00	0.19	2.38	1.00	12.7	1.00	32	1.00
0.250	1.00	0.25	2.50	1.00	10.0	0.79	32	1.00
0.250	1.00	0.25	2.50	1.00	10.0	0.79	20	0.63
0.375	1.00	0.38	2.75	1.00	7.3	0.58	20	0.63
0.500	1.00	0.50	3.00	1.00	6.0	0.47	16	0.50
0.750	1.00	0.75	3.50	1.00	4.7	0.37	16	0.50

Table 5.6 lists performance data for the pultrusion of poly- and vinylester resins. In an attempt to verify the derived scaling law, as described by Equation 5.44 the performance data listed in Table 5.6 is plotted in the subsequent graph. Figure 5.21 shows how a curve, which scales with the inverse of the wall thickness, fits the data reasonably well ( $R^2 > 80\%$ ). The scaling law  $v_p = 9 + 9/2t_w$  however, only is valid for the above production conditions and resin types, since epoxies are expected to be processed at a slightly slower pace and the parameters of the scaling law would have to be different.

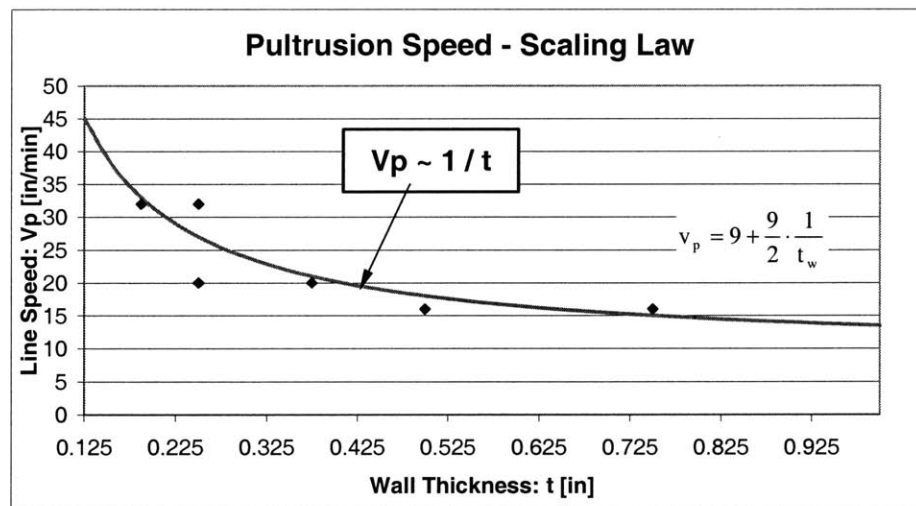


**Figure 5.21 Verification of the Scaling Law**

The effective production rate of the actual pultrusion process (time of machine usage, including setup) is about 5 lb/hr. For infinitely long parts the rate increases up to 90 lb/hr. That is if no machine downtimes due to maintenance or machine failures have to be taken into account. For Pultrusion to be economical the actual pultrusion process should be at least as long as the combined setup times. In the case shown in the Appendix 5.4.4 at least 500 ft. and not 30 ft. of the C-profile should be produced in order for the process to be economical.

### Labor Rates

As always labor rates depend on the industry, the company overhead, the skill level, and the geographic location. Generally, it is assumed, that for a worker in the aerospace industry a rate of \$100/hr has to be considered, including overhead and benefits. The required skill level is comparable to the one for RTM. Again, once the pultrusion equipment is set up and the machine is running it only requires minimal supervision from the worker. The setup is usually conducted in concert with a supervisor, while the loading of the fibers is performed by low to medium level workforce. The workers monitoring the machine also remove and stack the precut pultrusion profiles.

### 5.2.5 Double Diaphragm Forming (DDF)

The double diaphragm forming process modeled as part of this work employs two silicone diaphragms to sandwich the stacked up preform. The diaphragms provide support to the material during forming and prevent the laminate from wrinkling. Once the part matches the shape of the tool, the vacuum pressure is released and the formed material is removed from the tool. Subsequently, a curing process using an oven or autoclave solidifies the matrix.

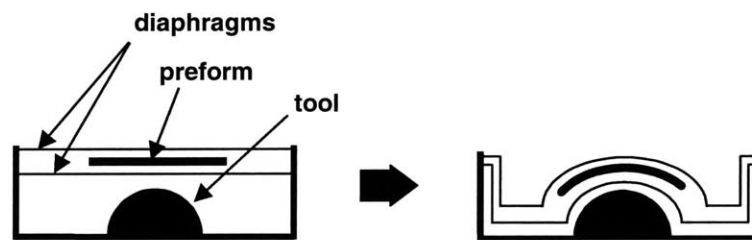


**Figure 5.22** Schematic of the Double Diaphragm Forming Process

#### Scope of the Model

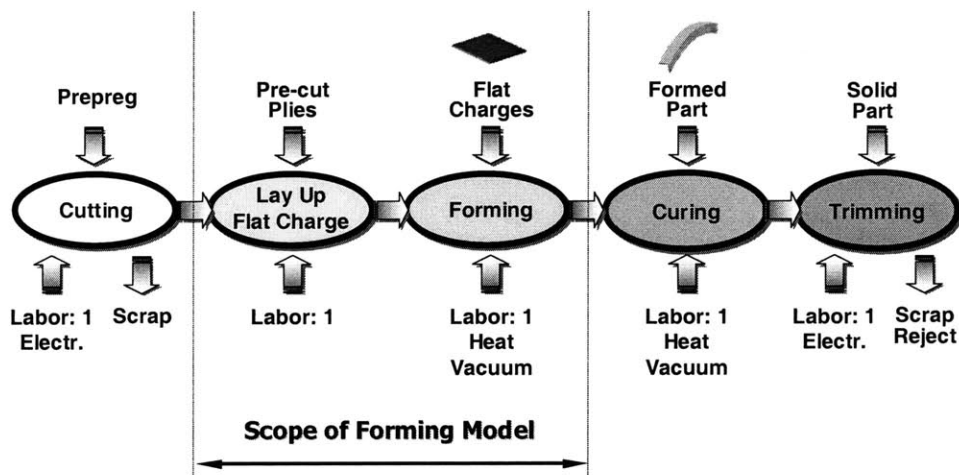


**Figure 5.23** Process Flow of Double Diaphragm Forming

The process plan describing the individual steps in detail can be found in the Appendix 5.4.4. Figure 5.23 shows how the forming process is preceded by the layup (Hand Lay-Up or ATP) of the flat charges. In general, the layup of the flat charge takes considerably



more time than the actual forming. The scaling model focuses only on the forming step, since the layup step and the curing step are discussed in other chapters.

### Scaling Model (Heating/Cooling of the Charge)

The scaling model assumes that the heating and cooling steps drive the cycle time. Figure 5.24 schematically shows the heating of the flat charge by radiation heaters. Once the forming is completed, the heat is removed by cooling the aluminum tool underneath. The material becomes rigid and once the vacuum is released, the part can be removed from the forming machine.

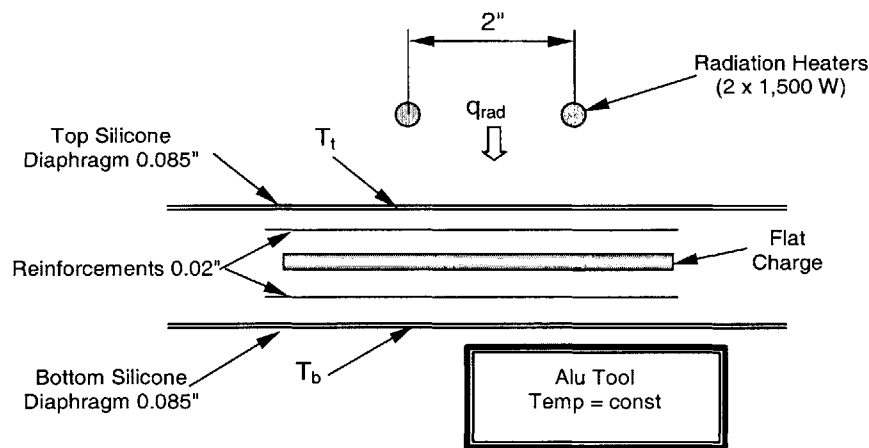


**Figure 5.24 Schematic of the Heating/Cooling Process**

### Transient Heat Transfer Model

To derive a scaling law of the processing time a simple model is generally sufficient. It is assumed that the situation can be treated as a lumped system. The assumption is a quite crude approximation, however it will give us the basic functional relations between part size and heating/cooling time. That is, no significant temperature gradient exists within the part during heating and cooling, which is generally true for thin parts and/or slow heating/cooling. To verify the assumption the Biot Number is checked subsequently ( $Bi < 1/6$ ). Furthermore, the model assumes a constant heat flux from the radiators ( $q_{rad} = \text{const.}$ ) and neglects all other heat sources and losses.

Energy conservation gets us:

$$\rho \cdot V \cdot c_p \cdot \frac{dT}{dt} = -\bar{h} \cdot A \cdot (T - T_\infty) \quad \text{Equation 5.45}$$

and integration gives us the temperature response [64]:

$$\Theta = \frac{T(t) - T_\infty}{T_0 - T_\infty} = e^{-\frac{\bar{h} \cdot A}{\rho \cdot V \cdot c_p} t} \quad \text{Equation 5.46}$$

Solving for the heating time yields:

$$\text{Time Constant: } t_c = \frac{\rho \cdot V \cdot c_p}{\bar{h} \cdot A} \quad \text{Equation 5.47}$$

where  $V$  is the part volume and  $A$  its surface area. The material properties, such as the density  $\rho$  and the specific heat  $c_p$  are averaged over the fiber prepreg and the silicone diaphragms. The average heat transfer coefficient is denoted as  $\bar{h}$ .

### Size Scaling

As seen Equation 5.48, the heating/cooling time for the part scales with its size. Assuming everything to be constant, the scaling law can be derived from Equation 5.47.

$$t \propto \frac{V}{A} \quad \text{Equation 5.48}$$

and for flat plates one can write:

$$t \propto d \quad \text{Equation 5.49}$$

That is for thin plates the cycle time is a linear function of the thickness  $d$  only. This relation might not be true for a large range of thickness and heating conditions, however one can easily fit a linear function to a number of experimental data within the practical range of the process application.

### Validity Check of Model, Bi Estimation

In order to check the validity of the previous assumptions the Biot Number has to be checked. Table 5.7 lists the required thermal properties for the test.

**Table 5.7 Thermal Material Properties [44, 64]**

	<i>Density</i> [kg/m <sup>3</sup> ]	<i>Spec. Heat</i> [J/kg K]	<i>Conductivity</i> [W/m K]
Carbon Fiber	1,800	750	10 - 300
Epoxy Resin	1,200	1,850	0.34
Teflon (Si-Rubber)	2,200	1,050	0.40

The Biot Numer should be smaller than 1/6 in order to model the situation as a lumped system.

$$\text{Biot: } Bi = \frac{\bar{h} \cdot d}{k} \leq \frac{1}{6} \text{ with } d \approx 0.16'' \text{ and } k \approx 0.3 \text{ W/mK} \quad \text{Equation 5.50}$$

Plugging in all the values and solving the maximum heat transfer coefficient comes out to be  $\bar{h} \approx 10 \text{ W/m}^2$ .

From literature, one can get a thumb rule to estimate the average heat transfer coefficient for radiation  $\bar{h}_{rad}$  [64].

$$\text{Radiation Heat Transfer Coeff.: } \bar{h}_{rad} = 6 \cdot \varepsilon_1 \text{ W/m}^2 \text{K} \quad \text{Equation 5.51}$$

Where the emissivity is  $\varepsilon_1 \leq 1$  and the view factor  $F_{12} = 1$ . In our case  $F_{12}$  would be even smaller than 1, actually around 1/2 and therefore one can safely assume that  $\bar{h}_{rad}$  will not exceed  $10 \text{ W/m}^2 \text{K}$ . Given this situation  $\bar{h}_{rad}$  is probably around  $\bar{h}_{rad} \leq 3 \text{ W/m}^2 \text{K}$ . Now Equation 5.50 can be solved for the thickness d. The maximum thickness for which the model is valid can be calculated and is approximately  $d_{max} = 1/2''$ .

$$\text{Max. Part Thickness: } d \leq \frac{1}{6} \cdot \frac{k}{\bar{h}_{rad}} = 0.65 \text{ in. using } \bar{h}_{rad} \approx 3 \text{ W/m}^2 \text{K} \text{ and } k \approx 0.3 \text{ W/m K.}$$

For cases where a significant temperature difference within the part is observed, one can use the one-dimensional model of a slab [64]. There the heating/cooling time is related to the Fourier number, which is defined as  $Fo = \frac{\alpha \cdot t}{L^2}$ . The size scaling for this case turns out to be  $t \propto d^2$ . However, for small changes in thickness this relation can also be linearized.

#### Experimental Time - Temperature Data

**Table 5.8 Rib Chord Forming Data [54]**

<b>Time [min]</b>	<b>T Diaphr. Top [F]</b>	<b>T Part Top [F]</b>	<b>T Heater [F]</b>
0	70	70	70
3	129	71	525
5	146	78	525
6	150	82	575
7	158	87	575
8	168	93	575
9	166	100	575
10	178	106	575
11	177	113	575
12	185	120	590
13	185	127	590

The experimental data describes the forming of a 0.16" thick structural part of an airplane. The part is around 48" x 3" and is made off plain woven carbon fiber prepreg with a toughened epoxy matrix.

#### Summary of the Scaling Law for Double Diaphragm Forming

According to the scaling law and the above data, a relation for the heating and cooling time can be derived for the above production scenario. The heating and cooling times scales linearly with the part thickness d:

$$t_{heat} = \frac{8 \text{ min}}{0.16 \text{ in}} \cdot d = 50 \text{ min/in} \cdot d \quad ; \quad t_{cool} = \frac{18 \text{ min}}{0.16 \text{ in}} \cdot d = 112.5 \text{ min/in} \cdot d \quad \text{Equation 5.52}$$

### Labor Rates

As always labor rates depend on the industry, the company overhead, the skill level, and the geographic location. Generally, it is assumed, that for a worker in the aerospace industry a rate of \$100/hr has to be considered, including overhead and benefits. Aside from the layup of the flat charges, the required skill level is comparable to RTM. The work is quite uniform and new workers can be trained quickly to perform the basic tasks. The work involves the loading of the machine with new charges, which need to be aligned properly, the closing of the diaphragms and the starting of the automated forming cycle. Once complete the formed parts are then removed and stacked onto another tool for final cure. The cycle repeats itself and workers of a low to medium labor category can run the operation.

### 5.2.6 Autoclave Cure

The pressure and heat inside an autoclave consolidates the laminate and solidifies the resin. The pressure ranges between 80 psi (0.5 MPa) to 100 psi (0.7 MPa) and the curing temperatures are between 250°F (120°C) and 450°F (230°C), depending on the resin system. Prior to the autoclave run, the part is sealed into a vacuum bag, which also includes layers of spongy material (breather, bleeder) ready to soak up excessive resin and carry away volatiles and moisture (see Figure 5.25). The duration of the cure cycle depends on the resin but generally lasts between 3 to 8 hours.

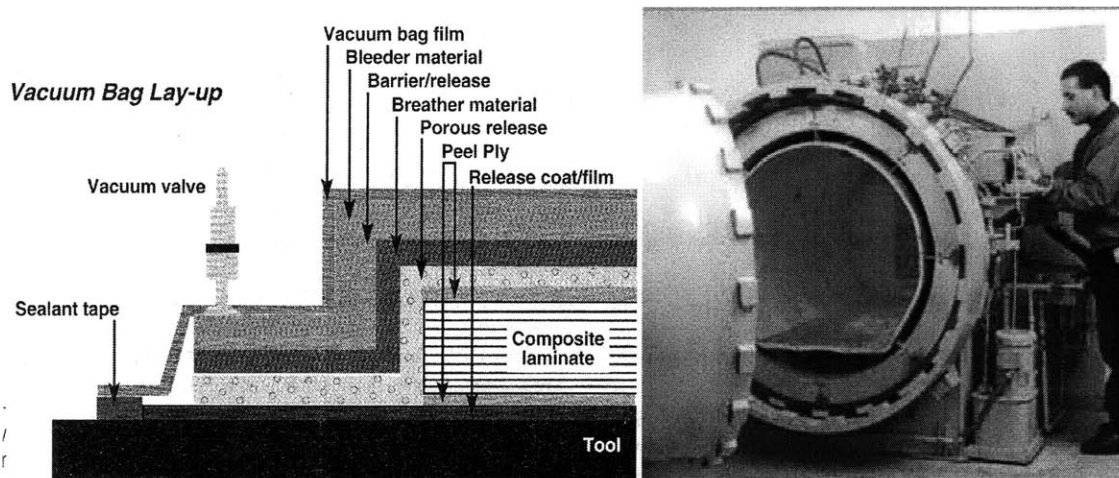


**Figure 5.25 Vacuum Bagging,**

**Autoclave Operation [65, 66]**

#### Scope of the Model

The process plan describing the individual steps in detail can be found in the Appendix 5.4.4. Figure 5.26 outlines the process flow of the autoclave curing process. The model describes the vacuum bagging of the part, the setup of the autoclave and the subsequent cure cycle. Once, the part is cured the bagging materials are removed and the part is released from the curing tool. The initial layup of the laminate can be performed by Hand Lay-Up or ATP, which are described in Chapter 5.2.1 and Chapter 5.2.3, respectively.

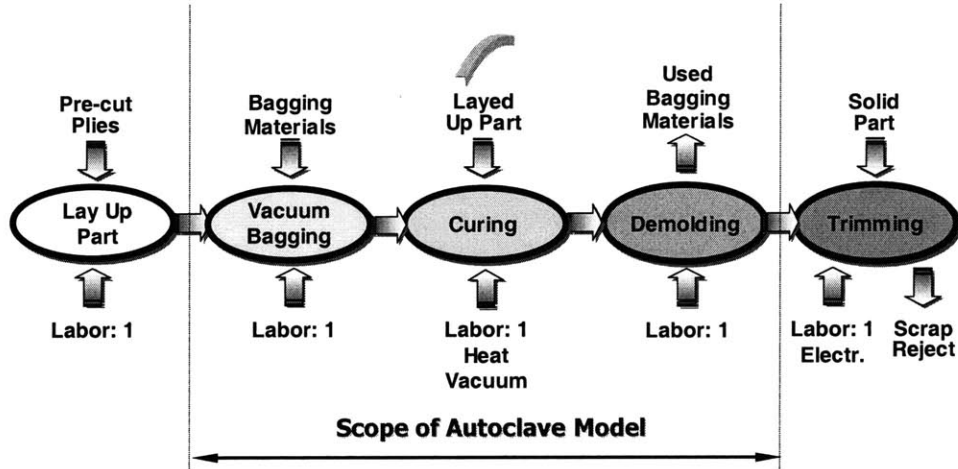


Figure 5.26 Process Flow of Autoclave Cure

Scaling Model

The scaling model assumes that the heating, curing, and cooling steps are the time drivers of this process. Figure 5.27 displays schematically the heat transfer between the autoclave and the part. The heaters located in the outer shell of the autoclave heat up the composite part and the surrounding air or nitrogen atmosphere.

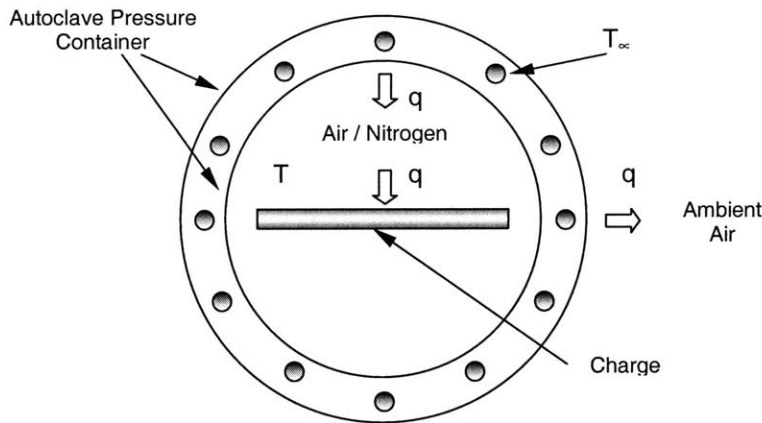


Figure 5.27 Schematic of the Autoclave Heating Process

Transient Heat Transfer Model

In order to simplify calculations, the heat transfer is modeled as a lumped system. The assumption is a quite crude approximation, however it will give us the basic functional relations between part size and heating/cooling time. That is, no significant temperature gradient exists within the part during heating and cooling, which is generally true for thin parts and/or slow heating/cooling. To verify the assumption the Biot Number is checked subsequently ( $Bi < 1/6$ ). Furthermore, the model assumes a constant heat flux from the radiators ( $q_{\text{rad}} = \text{const.}$ ) and neglects all other heat sources and losses.

Energy conservation gets us:

$$\rho \cdot V \cdot c_p \cdot \frac{dT}{dt} = -\bar{h} \cdot A \cdot (T - T_\infty) \quad \text{Equation 5.53}$$

and integration gives us the temperature response [64]:

$$\Theta = \frac{T(t) - T_\infty}{T_0 - T_\infty} = e^{-\frac{\bar{h} \cdot A}{\rho \cdot V \cdot c_p} \cdot t} \quad \text{Equation 5.54}$$

Solving for the heating time yields:

$$\text{Time Constant: } t_c = \frac{\rho \cdot V \cdot c_p}{\bar{h} \cdot A} \quad \text{Equation 5.55}$$

where  $V$  is the part volume and  $A$  its surface area. The material properties, such as the density  $\rho$  and the specific heat  $c_p$  are averaged over the fiber prepreg and vacuum bagging. The average heat transfer coefficient is denoted as  $\bar{h}$ .

Size Scaling

As seen in Equation 5.56, the heating/cooling time for the part scales with its size. Assuming everything to be constant, the scaling law can be derived from Equation 5.55.

$$t \propto \frac{V}{A} \quad \text{Equation 5.56}$$



and for flat plates one can write:

$$t \propto d \quad \text{Equation 5.57}$$

That is for thin plates the cycle time is a linear function of the thickness  $d$  only. This relation might not be true for a large range of thickness and heating conditions, however one can easily fit a linear function to a number of experimental data within the practical range of the process application.

For cases where a significant temperature difference within the part is observed, one can use the one-dimensional model of a slab [64]. There the heating/cooling time is related to the Fourier number, which is defined as  $Fo = \frac{\alpha \cdot t}{L^2}$ . The size scaling for this case turns out to be  $t \propto d^2$ . However, for small changes in thickness this relation can also be linearized.

Scaling Model: Time per Cure

The  $n$ -th Order Cure Rate expression relates the rate of cure to the resin properties of thermoset resins. Part of the formula are the frequency factor  $Z$  [1/s] and the activation energy [J/mol K] (Equation 5.26) [63].

$$\text{n-th Order Cure Rate Expr.: } \frac{d\alpha}{dt} = Z \cdot \exp\left(\frac{-E_a}{\mathfrak{R} \cdot T}\right) \cdot (1 - \alpha)^n \quad \text{Equation 5.58}$$

where  $\mathfrak{R} = 8.413 \text{ J/mol K}$  is the general gas constant.

The frequency factor  $Z$  is a strong function of the temperature  $T$  and the extent of the cure  $\alpha$  and therefore a straightforward integration is difficult if  $Z$  is not constant. To obtain a numerical solution it helps to linearize the above expression by taking the log on both sides and obtain:

$$\log\left(\frac{d\alpha}{dt}\right) = \log(Z) + \frac{1}{\ln 10} \left(\frac{-E_a}{\mathfrak{R} \cdot T}\right) + n \cdot \log(1 - \alpha) \quad \text{Equation 5.59}$$

The differences in curing time between resins can then be approximated as:

$$\text{Scaling of Cure: } \frac{t_{\text{Cure 1}}}{t_{\text{Cure 2}}} \propto \frac{Z_1}{Z_2} \cdot \exp\left(\frac{E_{a1} - E_{a2}}{\mathfrak{R} \cdot T}\right) \cdot \frac{(1 - \alpha_2)^{n_2}}{(1 - \alpha_1)^{n_1}} \quad \text{Equation 5.60}$$

The above expression can be further simplified by setting  $\alpha_1 = \alpha_2$  and  $n_1 = n_2$ .

**Table 5.9 Kinetic Cure Parameters [49]**

	$Z [1/s]$	$E_a [J/mol K]$
<b>Polyester</b>	$1.61 \times 10^8$	75,100
<b>Vinyl Ester</b>	$8.0 \times 10^7$	76,550
<b>Polyurethane</b>	$1.27 \times 10^5$	38,900

The cure time usually depends on the ratio of resin and catalyst. It can be obtained from the resin specifications of the manufacturer. Using the manufacturers' specs is far more practical for cost modeling purposes since the respective parameters such as the activation energy etc. are often difficult to determine.

#### Process Performance

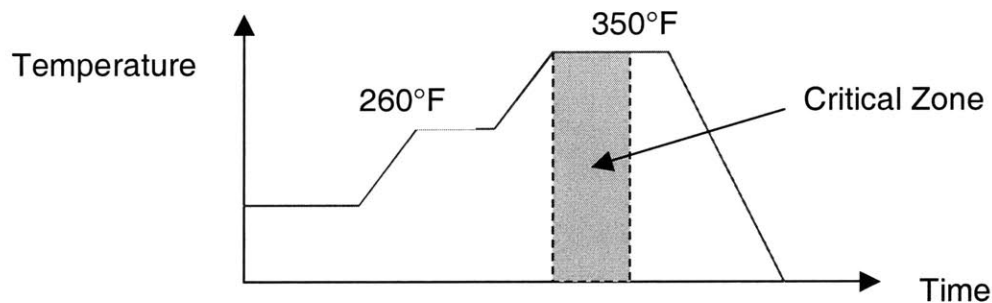


**Figure 5.28 Typical Cure Cycle for Epoxy Resins**

The process performance primarily depends on the cure characteristics of the resin system and the thermal inertia of the autoclave. In general, the specifications of the autoclave have to match the required cure cycle time of the resin. The actual cure takes about 90 minutes at 350°F (175°C) for a typical epoxy resin system. However, the entire cycle to heat up and cool down can last up to 10 hours. The performance can be affected

by for example a vacuum bag failure during the cure cycle. However, only if the leakage occurs during the critical period before the resin has sufficiently gelled (critical zone) damage to the part such as voids and insufficient consolidation can occur. Hot air leaking into the bag from somewhere in the middle is generally stopped by the caul plate and the breather. In case the leakage is on the side of the part, a manifold draws the hot air away from the laminate. The critical zone, during which a bag failure can damage the part, is relatively short and therefore the amount of risk and rework is generally small.

Costs for autoclave cure consist of machine operating cost (depreciation, nitrogen, energy) and labor for monitoring the process. Some manual labor is required to set up the autoclave and vacuum bag the part. A labor rate between \$60/hr and \$100/hr depending on overhead and benefits can be assumed. The operation of the autoclave and the curing process requires skilled personal. However, one operator can monitor several autoclaves or an entire batch of parts. Automation and investment in measurement devices affects this capability. In general, the process is most economical when the autoclave is filled to capacity and a batch of parts is cured. According to an industry source, the hourly operating cost for large and centrally controlled autoclaves is only about \$20/hr excluding labor [5].

### Labor Rates

As always labor rates depend on the industry, the company overhead, the skill level, and the geographic location. Generally, it is assumed, that for a worker in the aerospace industry a rate of \$100/hr has to be considered, including overhead and benefits. The vacuum bagging process requires workers with medium to high work skills, which are also able to assume some responsibility. Although the bagging process is not too complicated, it has to be conducted very diligently, because a vacuum leak or bag failure can result in the loss of the entire part. The workers are within a similar labor category as the ones responsible for the hand layup of complicated parts. As for the monitoring of the autoclave cycle profound knowledge of the autoclave and the often computerized control systems are required. In smaller firms, process engineers often setup the cure cycle, whereas in larger companies specially trained operators perform this task.

### 5.2.7 Mechanical Assembly

Mechanical joining of composites is generally the best understood joining methodology, because of its similarity to the assembly of metal components. Commonly the components are loaded into a fixture or assembly jig for positioning. Once positioned and securely locked into place, holes for the fasteners are drilled in preparation of the fastening step.

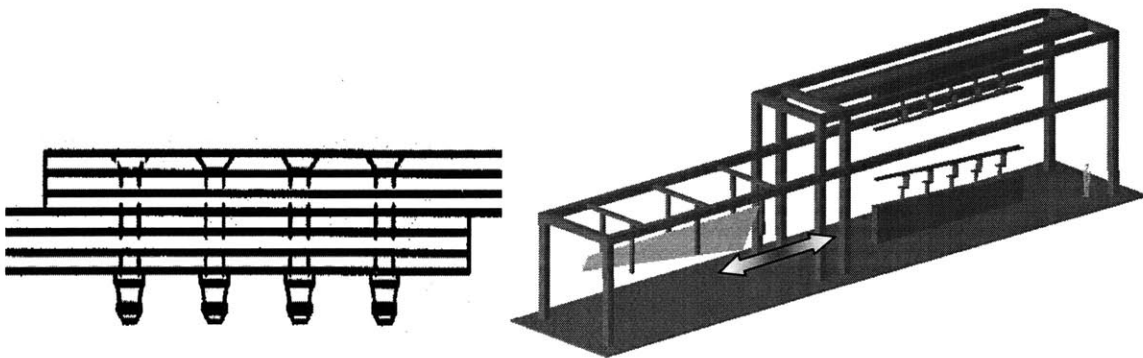


**Figure 5.29** Single Lap Joint

**Large Assembly Fixture**

Precise joints inducing a minimum of residual stresses often require shimming. The shimming can be a liquid compound, which has to be cured or thin strips of material intended to bridge any unevenness within the joint. Eventually the fasteners are installed and tensioned. The tensioning or riveting is conducted by using either manual or automatic tools.

#### Scope of the Model

The process plan describing the individual steps in detail can be found in the Appendix 5.4.4. Figure 5.30 outlines the process flow of the mechanical assembly. The model only estimates the processing times for the assembly steps. A time scaling law is derived for the most time consuming operations, such as positioning, shimming, and fastening. Shimming is generally optional and depends on the assembly requirements. The model considers the use of either liquid or rigid shims. The scaling models for the fastening step mainly look at operations such as manual drilling, manual insertion, and manual tightening of two-piece or one-piece fasteners.

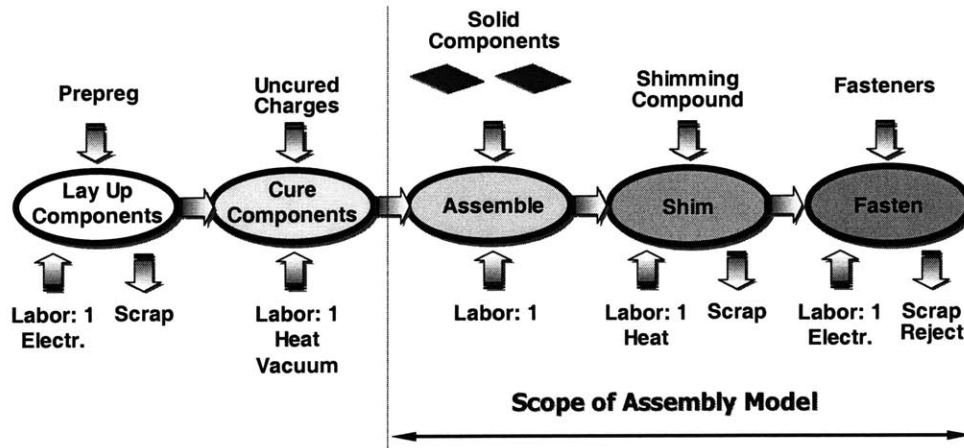


**Figure 5.30 Process Flow of Mechanical Assembly**

Scaling Model: Shimming

The shimming process is very much determined by the type of shim used. For liquid shims the application and the curing of the compound are the dominant steps, whereas for rigid shims the cutting and fitting are most time consuming. Both these operations involve extensive manual labor and are therefore best modeled by the 1<sup>st</sup> Order Model (Equation 5.61). The model parameter  $v_0$  and  $\tau_0$  are empirically obtained or can be derived from similar already known processes.

$$t = \sqrt{\left(\frac{A}{v_0}\right)^2 + \frac{2 \cdot \tau_0}{v_0} \cdot A} \tag{Equation 5.61}$$

The variable  $x$  in the generic 1<sup>st</sup> Order Model (Equation 5.61) is replaced with the size of the interface area, which according to Figure 5.31 can be described as:

$$A = L_y \times w \tag{Equation 5.62}$$

The model treats the setup time and delays between the shimming of different interface areas separately and therefore  $\tau_0 = 0$ . Thus, the shimming time can be expressed as:

Shimming Time: 
$$t = \frac{A}{v_0} \tag{Equation 5.63}$$

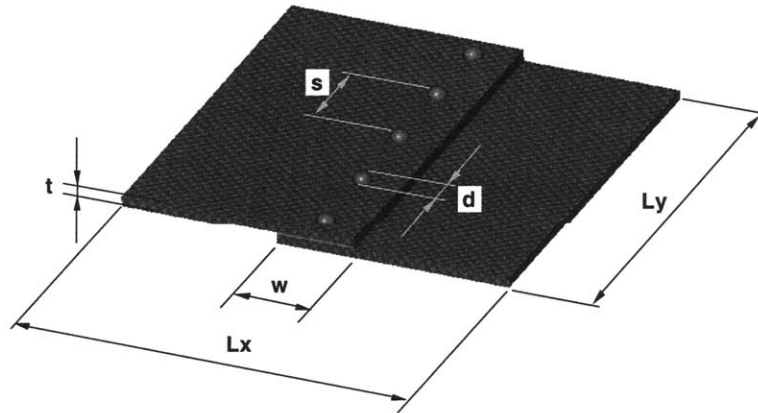


**Figure 5.31 Single Lap Joint, Mechanically Fastened**

### Cure Liquid Shimming

A similar argument as described in Chapter 5.2.6 can be followed when deriving the size scaling for the curing process of liquid shim. From the chapter on Autoclave Cure one obtains:

$$\text{Heating/Cooling Time: } t \propto \frac{V}{A} \text{ and for flat plates one can write: } t \propto d \quad \text{Equation 5.64}$$

That is the cycle time is a linear function of the part thickness  $d$  only.

For the actual cure, a simplified cure model can be employed as demonstrated before:

$$\frac{t_{Cure 1}}{t_{Cure 2}} \propto \frac{Z_1}{Z_2} \cdot \exp\left(\frac{E_{a1} - E_{a2}}{\mathfrak{R} \cdot T}\right) \quad \text{Equation 5.65}$$

However, for all practical reasons the curing time specified by the manufacturer of the liquid shim is used in the time estimation model.

### Scaling Model: Install Fasteners

The drilling of the holes and tightening of the fasteners represent another significant step of the assembly process. As both these steps are labor intensive the 1<sup>st</sup> Order is well suited for estimating the processing times.

Drill Holes

The time required to drill the holes is of course related to the number of holes and the volume of each hole. The 1<sup>st</sup> Order Model gives the drilling time per part:

$$t_{Drill / Part} = \left( t_{delay} + \sqrt{\left(\frac{V}{v_0}\right)^2 + \frac{2 \cdot \tau_0}{v_0} \cdot V} \right) \times \text{Number of Holes/Part} \quad \text{Equation 5.66}$$

In contrast to the previous convention, Equation 5.66 actually includes the delay between the individual drilling operations. The delay time can easily be of the same magnitude as the actual drilling time and therefore has to be considered in the model. The total time per part scales mainly with the number of holes to be drilled and ultimately with the part size. The volume of each hole is a function of the hole diameter  $d$  and the overall thickness of the joint  $2 \times t$ .

$$V = \frac{\pi \cdot d^2}{4} \cdot 2 \cdot t \quad \text{Equation 5.67}$$

Size Scaling: Installation and Tightening of Fasteners

The time estimates for the installation and tightening of the fasteners is solely based on empirical data. The time can vary depending on the assembly conditions and whether automatic or manual tools are employed. In addition, the access to the fastener itself can have a significant impact on the overall installation time.

Therefore, a very simple model is used to estimate the time of this step. It might be inaccurate, however can be adjusted easily to each individual situation.

Installation Time:  $t_{Install / Part} = t_{delay} \times \text{Number of Holes/Part}$  **Equation 5.68**

### Number of Fasteners

The amount of fasteners in each joint is calculated by multiplying the fastener rows by the number of fasteners per row. The number of fasteners per row can be approximated by Equation 5.69:

$$\text{Number of Fasteners per Row: } n = \left\lfloor \frac{L_y}{s} - 1 \right\rfloor \quad \text{Equation 5.69}$$

where  $L_y$  is the length of the joint and  $s$  the spacing of the fasteners.

### Scaling Model: Part Handling and Positioning

Estimating the time to handle and position parts of various shapes and sizes is probably the most challenging aspect of this research. What makes it difficult is the interdependence of the numerous variables affecting the positioning time. As already mentioned, the size and the shape along with the weight can have a significant impact. It simply takes longer to handle heavier and more bulky components. In addition, the use of handling equipment can make a considerable difference. Furthermore, the assembly time is affected by the required positioning tolerance of the individual components. Of course, tooling and fixtures can greatly simplify the operation, however often at the expense of higher investment cost.

The manual handling of parts has been studied previously by others and many have attempted to devise a model. Neoh offers a comprehensive summary of all the previous research results and presents a model based on process physics and some actual experimental data [28]. The results look promising, however one has to ensure the assembly situation is similar to one described by the underlying model. Many of these models are based on physics and ergonomics and some are briefly presented in the following paragraphs. However, for the sake of practicality a model is chosen based on empirical data in connection with the 1<sup>st</sup> Order Model.



Transport

The transportation time is expressed in dependence of the speed at which a certain distance is covered:

$$\text{Transportation Time: } t_{Transport} = \frac{\text{distance}}{v_{Transport}} \quad \text{Equation 5.70}$$

The model accounts for the difference in performance between mechanical and manual transportation. For manual transportation, the velocity  $v_{Transport}$  ranges between 2.5 mph (3.7 ft/s) and 4.5 mph (6.6 ft/s) depending on the weight to be carried. For mechanical transportation, the values can be obtained from the technical specifications of the transportation device.

Positioning

The positioning of a part is conducted either manually or mechanically within a certain tolerance. The process can be modeled by a generic spring-mass-damper system. If the target is a distance of  $x_0$  away from the current position and has to be hit with an accuracy of  $\Delta x$  the positioning time can be described as [28]:

$$\text{Positioning Time: } t_{Positioning} = T \cdot \ln\left(\frac{x_0}{\Delta x}\right) \text{ with the}$$

$$\text{First Order Time Constant: } T = \frac{1}{\zeta \cdot \omega} \quad \text{Equation 5.71}$$

The Eigenfrequency  $\omega$  and the damping ratio  $\zeta$  can be written as:

$$\omega = \sqrt{k/m} \text{ and } \zeta = \frac{d}{2 \cdot \sqrt{m \cdot k}} \text{ for translational positioning and}$$

$$\omega = \sqrt{k/J} \text{ and } \zeta = \frac{d}{2 \cdot \sqrt{J \cdot k}} \text{ for rotational positioning.} \quad \text{Equation 5.72}$$

where  $m$  is the mass,  $J$  the mass moment of inertia,  $k$  the stiffness, and  $d$  the damping coefficient.

Thus, the equation for the positioning time be rewritten to:

$$t_{Trans.Pos} = \frac{2 \cdot m}{d} \cdot \ln\left(\frac{x_0}{\Delta x}\right) \text{ for translational positioning} \quad \text{Equation 5.73}$$

$$t_{Rot.Pos} = \frac{2 \cdot J}{d} \cdot \ln\left(\frac{\Theta_0}{\Delta \Theta}\right) \text{ for rotational positioning} \quad \text{Equation 5.74}$$

The scaling of the positioning time can be derived from the above equations and is written as:

$$t_{Positioning} \sim \text{weight} \quad \text{Equation 5.75}$$

#### Combined Scaling Law: Transportation and Positioning

Equation 5.70, Equation 5.73, and Equation 5.74 can be united to one simple model expressing the handling time of a part:

$$t_{Handling} = \text{delay} + \frac{\text{distance}}{v_{Transport}} + \text{coeff.} \times \text{weight} \quad \text{Equation 5.76}$$

Any delay associated with the operation is considered and the coefficient (coeff.) has to be chosen depending on the sensitivity of the task relative to the weight. In some cases, tabulated data might be available, but more often than not, the coefficient has to be determined empirically.

#### Alternative Size Scaling: Transportation and Positioning

Alternatively, the 1<sup>st</sup> Order Model can be applied, since it offers similar scaling characteristics and the respective parameters can be derived from factory observations.

$$\text{Positioning Time: } t = \text{delay} + \frac{x}{v_0} \quad \text{Equation 5.77}$$

Here the size variable  $x$  can represent the part weight, the part area or its length, whatever is practical. This study uses the part area as the scaling variable  $x$  for bulky parts and the

length for parts exhibiting a high aspect ratio. The time constant  $\tau_0$  is observed to be equal to zero and typical values for  $v_0$  are presented in Table 5.10.

Summary of the Model Parameter

**Table 5.10 Model Parameter of dominant Mechanical Assembly Processes [28]**

	<i>Setup</i>	<i>Delay</i>	$v_0$	$\tau_0$
	[min/run]	[min/oper]	[size unit/min]	[min]
Apply Clamping Force using Straps	20	0.13	5 in/min	0
Remove Clamping Straps	10	0.13	9.88 in/min	0
Position Long Part into the Assembly Jig	1	1	14.38 in/min	0
Position Bulky Part into the Assembly Jig	2	0	1575 sqin/min	0
Apply Liquid Shimming Compound	5	1	40 sqin/min	0
Cure Liquid Shim	480	0	0	0
Fabricate Solid Shimming	3	1	5 sqin/min	0
Manually Drill Countersunk Holes	10	0.062	0.246 cuin/min	0.039
Install Lockbolt Fastener	3	0.5	0	0

The above table lists a few selected assembly steps and their respective 1<sup>st</sup> Order parameter. Most of them can be derived indirectly from process physics and their corresponding scaling laws. However, some are solely based on empirical findings and have to be reviewed when they are used in connection with different assembly scenarios.

Labor Rates

As always labor rates depend on the industry, the company’s overhead structure, the skill level, and the geographic location. Generally, it is assumed, that for a worker in the aerospace industry a rate of \$100/hr has to be considered, including overhead and benefits. The mechanical assembly of large structures definitely requires an advanced skill set. Although, the actual fastening process is quite repetitive, the positioning of the individual components requires care and some ingenuity in case problems arise. The work can also be physically demanding, depending on the size of the parts and the access to the fastening points. The shimming process requires a similar if not even higher skill set, since very small tolerances have to be observed in the operation.

### 5.2.8 Adhesive Assembly

When joining components adhesively, the bonding is established by the cross-linking reactions of the polymeric adhesive. Similar to mechanical assembly the individual components are positioned with respect to one another and held in place by clamps, straps, and fixtures. However, the shimming step is generally not required because the adhesive compound acts as a liquid shim and evens out any unevenness along the bonding interface. Since the positioning and handling steps are already described in the previous chapter, their scaling laws are not repeated here.

#### Scope of the Model

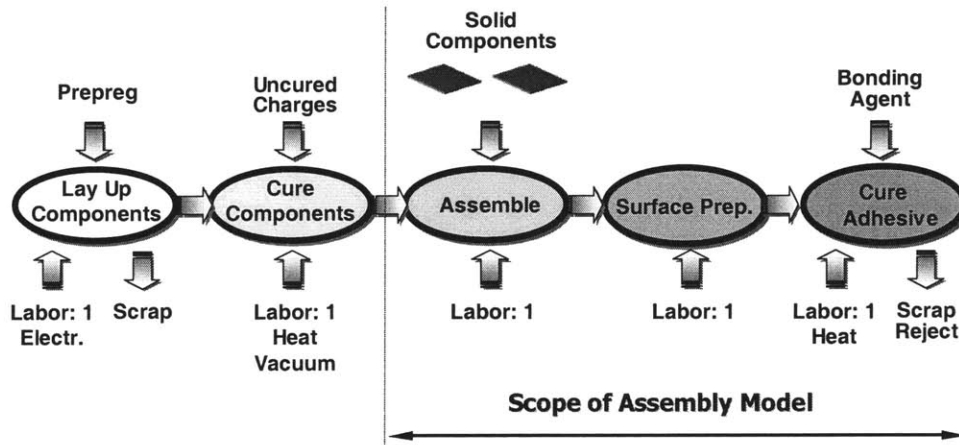


**Figure 5.32 Process Flow of Adhesive Assembly**

The process plan describing the individual steps in detail can be found in the Appendix 5.4.4. Figure 5.32 outlines the process flow of adhesive assembly and the models estimate the time to position the individual components. However, the joining time is determined by the time to prepare the surface, to apply and to cure the adhesive.

#### Scaling Model: Adhesive Bonding

The bonding process is very much determined by the type of the employed adhesive. The application and the curing of the compound represent the most time consuming steps. Both these operations involve extensive manual labor and are therefore best modeled by

the 1st Order Model (Equation 5.78). The model parameter  $v_0$  and  $t_0$  are empirically obtained or can be derived from similar and already known processes.

$$t = \sqrt{\left(\frac{A}{v_0}\right)^2 + \frac{2 \cdot \tau_0}{v_0} \cdot A} \tag{Equation 5.78}$$

The variable  $x$  in the generic 1<sup>st</sup> Order model (Equation 5.78) is replaced with the size of the interface area, which according to Figure 5.33 can be described as:

$$A = L_y \times w \tag{Equation 5.79}$$

The model treats the setup time and delay between the different interface areas separately and therefore  $\tau_0 = 0$ . Thus, the time to apply the adhesive to each interface can be expressed as:

Adhesive Application Time:  $t = \frac{A}{v_0}$  Equation 5.80

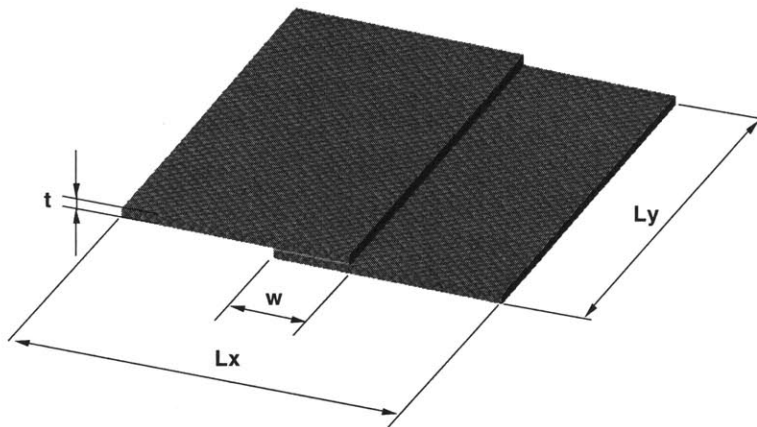


**Figure 5.33 Single Lap Joint, Adhesively Bonded**

Cure Adhesive Bonding

The procedure is identical to the curing of liquid shimming described in Chapter 5.2.7. From the chapter on Mechanical Assembly one obtains:

Heating/Cooling Time:  $t \propto \frac{V}{A}$  and for flat plates one can write:  $t \propto d$  **Equation 5.81**

That is the cycle time is a linear function of the part thickness  $d$  only.

For the actual cure, a simplified cure model can be employed as demonstrated before:

$$\frac{t_{Cure 1}}{t_{Cure 2}} \propto \frac{Z_1}{Z_2} \cdot \exp\left(\frac{E_{a1} - E_{a2}}{\mathfrak{R} \cdot T}\right) \quad \text{Equation 5.82}$$

However, for all practical reasons the curing time specified by the manufacturer of the adhesive is used in the time estimation model.

#### Summary of the Model Parameter

**Table 5.11 Model Parameter of dominant Adhesive Assembly Processes**

	<i>Setup</i>	<i>Delay</i>	$v_0$	$\tau_0$
	[min/run]	[min/oper]	[size unit/min]	[min]
Apply Clamping Force using Straps	20	0.13	5 in/min	0
Remove Clamping Straps	10	0.13	9.88 in/min	0
Position Long Part into the Assembly Jig	1	1	14.38 in/min	0
Position Bulky Part into the Assembly Jig	2	0	1575 sqin/min	0
Apply Adhesive Compound	5	1	40 sqin/min	0
Cure Adhesive Compound	480	0	0	0

The above table lists a few selected assembly steps and their respective 1<sup>st</sup> Order parameter. Most of them can be derived indirectly from process physics and their corresponding scaling laws. However, some are solely based on empirical findings and have to be reviewed when they are used for different assembly scenarios.

#### Labor Rates

As always labor rates depend on the industry, the company's overhead structure, the skill level, and the geographic location. Generally, it is assumed, that for a worker in the aerospace industry a rate of \$100/hr has to be considered, including overhead and benefits. The work skills required are comparable to the ones for mechanical assembly.

### 5.3 References

#### Cost Models General

- [1] Ostwald, P. F., "AM Cost Estimator", 4th Edition, Penton Publishing Inc., 1988.
- [2] Polgar, K. C. "Simplified Time Estimation for Basic Machining Operations", M.S. Thesis, MIT, 1996.
- [3] de Neufville, R. "Applied Systems Analysis", McGraw Hill, New York, 1990.
- [4] Boothroyd, G., Dewhurst, P.; Knight, W. A., "Product Design for Manufacture and Assembly", Basel, New York: Marcel Dekker, Inc., 1994.

#### Composites Cost Model

- [5] Northrop Corporation, "Advanced Composite Cost Estimating Manual (ACCEM)", AFFDL-TR-76-87, August 1976.
- [6] McLane, R., "Economic Issues in Composites Manufacturing", Proc. Amer. Soc. Comp., 1988.
- [7] Restar, S. A., "Advanced Airframe Structural Materials, A Primer in Cost Estimating Methodology", RAND Report # R-4016-AF, 1991.
- [8] Composites Fabricators Association, Arlington, Virginia, <http://www.cfa-hq.org/>
- [9] Wright, T. P., "Factors Affecting the Cost of Airplanes", J. Inst. Aeronaut. Serv. 34-40, 1936.
- [10] Freeman, W. T., Ilcewicz, L. B., Swanson, G. D., Gutowski, T. G., "Designers' Unified Cost Model," Proceedings 9th DoD/NASA/FAA Conference, Fibrous Composites in Structural Design, DOT/FAA/CT-92-25, Vol. II, Lake Tahoe, Nevada, Nov., 1991, pp. 601-620.
- [11] Freeman, W. T., Vosteen, L. F., Siddiqi, S., "A Unified Approach for Composite Cost Reporting and Prediction in the ACT Program", First NASA Advanced Composites Technology Conference, NASA CP-3104, Part 1, 1991, pp. 357-369.
- [12] Ilcewicz, L. B., Walker, T. H., et al., "Application of a Design-Build-Team Approach to Low Cost and Weight Composite Fuselage Structure", NASA CR-4418, 1991.
- [13] Polland, D. R. et al., "Global Cost and Weight Evaluation of Fuselage Side Panel Design Concepts", NASA Report CR-4730, 1997.
- [14] Ilcewicz, L. B., Smith, P. J., et al., "Advanced Technology Composite Fuselage - Program Overview", NASA CR-4734, 1996.
- [15] Willden, K., et al. "Advanced Technology Composite Fuselage - Manufacturing", NASA Report CR-4735, 1997.

- [16] Mabson, G. E., Ilcewicz, L. B., et al., "Cost Optimization Software for Transport Aircraft Design Evaluation - Overview," NASA CR-4736, 1996.
- [17] Ilcewicz, L. B. et al., "Cost Optimization Software for Transport Aircraft Design Evaluation", NASA Report CR-4737, 1996.
- [18] Willden, K., Gessel, M., Grant, C., Brown, T., "Manufacturing Scale-up of Composite Fuselage Crown Panels", Vol. 1, Part 2, NASA Report, 1995.
- [19] Kassapoglou, C., "Minimum Cost and Weight Design of Fuselage Frames. Part A: Design Constraints and Manufacturing Process Characteristics", Composites, Part A, Vol. 30, 1999, pp. 887-894.
- [20] Kassapoglou, C., "Minimum Cost and Weight Design of Fuselage Frames. Part B: Cost Considerations, Optimization, and Results", Composites, Part A, Vol. 30, pp. 895-904, 1999.
- [21] Harmon, B. and Arnold, S. A. "Cost Implications of Composite Materials in Military Airframes", Advanced Composite Materials: New Developments and Applications Conference Proceedings, Detroit, Michigan, Sept. 30 - Oct. 3, 1991.
- [22] Gutowski, T. G., Neoh, E. T. , Dillon, G. , "Design Scaling Laws for Advanced Composites Fabrication Cost", Proc. 5<sup>th</sup> NASA/DoD Advanced Composites Technology Conf., Seattle, Aug. 22-25, 1994.
- [23] Gutowski, T. G., Neoh, E. T. , Dillon, G. , "Framework for Estimating Fabrication Time of Advanced Composites Manufacturing Processes", Proc. 40<sup>th</sup> Intl. SAMPE Symp. And Exhibition, Anaheim, CA, May 8-11, 1995.
- [24] Haffner, S. M., Gutowski, T. G., "Manufacturing Time Estimation Laws for Composite Materials", NSF Conference, 1999.
- [25] Haffner, S. M., Gutowski, T. G., "Automated Cost Estimation for Advanced Composite Materials", NSF Conference, 1998.
- [26] Haffner, S. M.; "Comparison of Size Scaling and Complexity Models", MIT Internal Report, Cambridge, 1998.
- [27] Krolewski, S. "An Economic Based Model to Evaluate Advanced Composite Fabrication Technologies", Ph.D. Thesis, MIT, 1989.
- [28] Neoh, E. T. "Adaptive Framework for Estimating Fabrication Time", Ph.D Thesis, MIT, 1995.
- [29] Kim, P. "Comparative Study of the Mechanical Performance and Cost of Metal, FRP, and Hybrid Beams", Applied Composite Materials, Vol. 5, 1998, pp. 175-187.
- [30] Zaloom, V., Miller, C., "A Review of Cost Estimating for Advanced Composite Materials Applications", Engineering Costs and Production Economics, Vol. 7, 1982.



## Complexity

- [31] Fitts, P. M., Posner, M. I., "Human Performance", Basic Concepts in Psychology Series, Brooks/Cole Publishing Co., 1967.
- [32] Sheridan, T. B., Ferrell, W. R., "Man-Machine Systems: Information, Control, and Decision Models of Human Performance", MIT Press, Cambridge, 1974.
- [33] Casti, J., "Complexification", Harper, 1994.
- [34] Shannon, C. E., Weaver, W., "The Mathematical Theory of Communication", University of Illinois Press, Urbana, 1949.
- [35] Muter, S., "Cost Comparisons of Alternate Designs: An Information Based Model", M.S. Thesis, MIT, 1993.
- [36] Kim, C. E., Composites Cost Modeling: Complexity, M.S. Thesis, Department of Mechanical Engineering, Massachusetts Institute of Technology, May 1993.
- [37] Tse, M., "Design Cost Model for Advanced Composite Structures", M.S. Thesis, MIT, 1992.
- [38] Suh, N., "The Principles of Design", Oxford University Press, 1990.
- [39] Wilson, D. R., "An Exploratory Study of Complexity in Axiomatic Design" Ph.D. Thesis, MIT, 1980.
- [40] VISTAGY, Inc, Waltham, Massachusetts, <http://www.vistagy.com/>

## Differential Geometry

- [41] Stoker, J. J., "Differential Geometry", Wiley-Interscience, New York, 1969.
- [42] Struik, D. J., "Lectures on Classical Differential Geometry", 2nd. Edition, Addison-Wesley, Reading, 1961.

## Manufacturing

- [43] Kalpakjian, S., Manufacturing Engineering and Technology, 2nd ed., Addison-Wesley Publishing Co. 1992.

## Composites General

- [44] Reinhart, T. J. (Ed.), "Engineered Materials Handbook – Composites", Vol. 1, ASM International, 1988.
- [45] Nui, M. C. Y., "Composite Airframe Structures", Conmilit Press, 1992.
- [46] Gutowski, T. G., "Advanced Composites Manufacturing", New York: John Wiley & Sons, Inc., 1997.

## RTM

- [47] Potsch, G., Michaeli, W., "Injection Molding: An Introduction", Hanser Publishers, Munich, 1995.
- [48] Moy, E. "Design Tradeoffs for Advanced Composite Manufacturing Using Cost Modeling", M.S. Thesis, MIT, 1997.
- [49] Kang, P. J., "A Technical and Economic Analysis of Structural Composite Use in Automotive Body-in-White Applications", M.S. Thesis, MIT, June 1998.
- [50] Institute for Composite Materials, Kaiserslautern, Germany, <http://www.ivw.uni-kl.de/>
- [51] Goel, A. , "Economics of Composite Material Manufacturing Equipment", M.S. Thesis, MIT, 2000.

## Forming

- [52] Li, H., "Forming of Advanced Thermoset Composites: Process Development and Deformation Study", Ph.D. Thesis, M.I.T, 1998.
- [53] Mandosa, N., "The Buckling Behavior of Graphite Epoxy Composites under Simulated Diaphragm Forming Conditions", B.S. Thesis, MIT, 1997.
- [54] Truslow, S., "Permanent Press, No Wrinkles: Reinforced Double Diaphragm Forming of Advanced Thermoset Composites", M.S. Thesis, MIT, 2000.
- [55] Lamas, P., "The Formation of Advanced Composite Materials over Complex Geometric Shapes using Inflated Diaphragms", B.S. thesis, Dept. of Mechanical Engineering, M.I.T., 1997.
- [56] von Waldburg, A. R., "Diaphragm Control in Inflated Tool Forming of Composites", B. S. Thesis, MIT, 1997.
- [57] Gutowski, T. G., Dillon, G., Chey, S., Li, H., "Laminate Wrinkling Scaling Laws for Ideal Composites", Composite Manufacturing, Vol. 6, 1995, p. 123-134.
- [58] Gutowski, T. G., Dillon, G., Li, H., Chey, S., "Method and system for forming a composite product from a thermoformable material", United States Patent Number 5,578,158, 1996.
- [59] Gutowski, T. G., Dillon, G., Li, H., Chey, S., "Apparatus and Method for Diaphragm Forming", United States Patent Number 5,648,109, 1997.
- [60] Tam A. S., Gutowski, T. G., "The Kinematics for Forming Ideal Aligned Fiber Composites", Composites Manufacturing, Vol.1, No. 4, 1990.
- [61] Tam, A. S., "A Deformation Model for the Forming of Aligned Fiber Composites", Ph.D. Thesis, MIT, June 1990.

- [62] Gonzalez-Zugasti, J., "Computer Modeling of Advanced Composites Forming", M.S. Thesis, MIT, 1991.

#### Curing

- [63] Roylance, D. K., "Reaction Kinetics for Thermoset Resins", MIT Paper, MIT, March 2000.
- [64] Mills, A. F., "Heat Transfer", Prentice-Hall, New York, 1998.
- [65] Thermal Equipment Corporation, Torrance, California, <http://www.thermalequipment.com/>
- [66] Clements, L., "Vacuum Bagging Technology Improved," High Performance Composites January/February, 2000.

#### ATP

- [67] Land, I. B., "Design and Manufacture of Advanced Composite Aircraft Structures using Automated Tow Placement", M.S. Thesis, MIT, 1996.
- [68] Beresheim, G. "Part Complexity Based Time Estimation Model for the ATP Process", MIT & IVW Report, 2001.
- [69] Whitney, D. "Performance Model for ATP", MIT Internal Report, MIT, 1990.
- [70] Kitson, L., Johnson, B. "Fiber Placement Technology Advancements at Boeing Helicopters", AHS Annual Conference, May 9-11, 1995, p. 69-79.
- [71] Evans, D. O., Vaniglia, M. M., Hopkins, P. C., "Fiber Placement Process Study", 34<sup>th</sup> SAMPE, May 8-11, 1985, p. 1822-1833.
- [72] Enders, M. L., Hopkins, P. C. "Developments in the Fiber Placement Process", 36<sup>th</sup> Intl. SAMPE Symposium, April 15-18, 1991, p. 778-790.
- [73] Evans, D. O., "Fiber Placement", Cincinnati Milacron, 1995.
- [74] N.N.: "Cincinnati Machine – FPS Viper 1200", [http://www.cinmach.com/products/adva\\_set.htm](http://www.cinmach.com/products/adva_set.htm) , 2001.
- [75] N.N.: "Viper FPS-3000 specifications", Cincinnati Machine Product Information, Publication No. SP-191-1, Ohio, 2000.
- [76] Tsai, S. W., Springer, G. S., Enders, M. L., "The Fiber-Placement Process", ICCM 8, Composites, Vol. 2, Sections 12-21, p. 14B1-14B11.
- [77] Breda, B.J., Stump, B. J., "A Case Study of Controlled Tape Laying", AHS, 52<sup>nd</sup>, Vol.1, June 4-6, 1996, p. 603-610.
- [78] Carlson, D., Breda, B. J., "Fabrication of the BA 609 Wing Skin", AHS, May 25-27, 1999, p. 777-782.

- [79] Meason, R., Sewell, K. "Fiber Placement Low Cost Production for Complex Composite Structures", AHS Annual Conference, June 4-6, 1996, p. 611-622.
- [80] Kisch, R., "Automated Fiber Placement", In: Mamidala Ramulu (Supervisor): Seminars in Manufacturing Management, Lecture at the University of Washington, ME518 Seminar 2, 6th April, 2000.
- [81] Kanbeo, S. W., "V-22 Modifications focus on cost, productivity", Aviation Week & Space Technology, May 22<sup>nd</sup>, 1995, p. 35-36.
- [82] Berchthold, G., Klenner, J. "Optimization of Composite Aircraft Structures by Direct Manufacturing Approaches", Flight Mechanics Panel Symposium, 1993, p. 6-1 – 6-12.
- [83] Sawicki, A., Schulze, E., et al., "Structural Qualification of V-22 EMD Tow Placed Aft Fuselage", AHS, Vol.2, May 9-11, 1995, p. 1641-1653.
- [84] McCloy, M., Deckers, M., Benson, V. "Fabrication of an Isogrid Fan Containment Case", SAMPE Journal, Vol.35, No.1, J/F, 1999.
- [85] Jones, S., Raciti, R., Steiner, K. V., et al., "A Hybrid Methodology for Quantifying the Cost and Productivity of Manufacturing Scenarios for Automated Fiber Placement of Aircraft Skins", 43<sup>rd</sup> International SAMPE Symposium, 5/31 – 6/4, 1998, p. 44-55.
- [86] Neddo, R., Kogstrom, K., "Automated Tow Placement of Fan Cowl Door Skins", 28<sup>th</sup> Intl. SAMPE Symposium, Nov. 4-9, 1996, p. 979-993.
- [87] Pirrung, P. F., "Machines Automate Tape Layup", Advanced Materials and Processes, Dec., 1989, p. 43-47.
- [88] Anderson, R. L., Grant, C. G. "Advanced Fiber Placement of Composite Fuselage Structures", NASA-LARC Conference, part 2, 1993, p. 817-830.

#### Pultrusion

- [89] Gutowski, T. G. , "Pultrusion Workbook", GLCC, Lemay Center for Composite Technology, July 1998.
- [90] Meyer, R. W. , "Handbook of Pultrusion Technology", Chapman & Hall, NY, 1985.

#### Assembly

- [91] Redford, A., Chal, J., "Design for Assembly: Principles and Practice", McGraw-Hill, 1994.
- [92] Keeney, R. L., Raiffa, H., "Decisions with Multiple Objectives", John Wiley, 1976.
- [93] Ulrich, K., "Design for Manufacturing", Product Design and Development, 1999, pp.181-205.

- 
- [94] Ulrich, K., Eppinger, S., "Product Architecture", Product Design and Development, 1999, pp. 131-150.
- [95] De Fazio, T., Whitney, D., Rhee, S., "A Design-Specific Approach to Design for Assembly (DFA) for Complex Mechanical Assemblies", Proc. IEEE International Symposium on Assembly and Task Planning, 1997.
- [96] Cunningham, T. W., "Chains of Function Delivery: A Role for Product Architecture in Concept Design", Ph.D. Thesis, MIT, 1998.
- [97] Cunningham, T. W., Mantriaprada, R., Lee, D., Thornton, A., Whitney, D., "Definition, Analysis and Planning of a flexible Assembly Process", Proceedings of the Japan/USA Symposium on Flexible Automation, Boston, MA, 1996.
- [98] Mantriaprada, R., "Assembly Oriented Design: Concepts, Algorithms and Computational Tools", Ph.D. Thesis, MIT, 1998.
- [99] Lee, D., Thornton, A., "The Identification and Use of Key Characteristics in the Product Development Process", Proceedings of the ASME Design Engineering Technical Conference, Irvine, CA, 1996.
- [100] Noton, B. "Cost Drivers and Design Methodology for Automated Airframe Assembly", 31<sup>st</sup> International SAMPE Symposium, 1986.
- [101] Noton, B. "Manufacturing Cost/Design Guide (MC/DG) for Metallic and Composite Structures", Battelle's Columbus Laboratories, American Institute of Aeronautics and Astronautics, 1981.

(This page is intentionally left blank.)

## 5.4 Appendix – Production Cost Models for Composites

### 5.4.1 Information Theory

In an attempt to quantify complexity the information theory developed by Shannon and Weaver in 1949 [34] proves to be quite useful. To obtain an intuitive understanding, one could say that for example an elaborate painting containing many details and variations in colors is very time consuming to produce. No doubt, the artist conveys a lot of information and everyone would agree on how complex the painting really is.

Shannon defines the total information content of a message as:

$$I = \log_2 \left( \frac{1}{p} \right) \tag{Equation 5.83}$$

where  $p$  is the total probability of this particular message to occur. Consider a message, which consists of  $N$  characters (symbols, digits, etc.) and each character can be chosen out of a set of  $n$  characters. The probability of such a message can be expressed as:

$$p = p_1^{p_1 \cdot N} \cdot p_2^{p_2 \cdot N} \cdot p_3^{p_3 \cdot N} \cdot \dots \cdot p_n^{p_n \cdot N} \tag{Equation 5.84}$$

The probability of each individual character to appear is  $p_i$  to the power of its average number of appearance within the whole message  $p_i \cdot N$ . Since all the characters are assumed independent from each other, the individual probabilities are simply multiplied to obtain the probability of the entire message.

Introducing  $p$  back into Equation 5.83 gives us:

$$I = -\log_2 \left( p_1^{p_1 \cdot N} \cdot p_2^{p_2 \cdot N} \cdot p_3^{p_3 \cdot N} \cdot \dots \cdot p_n^{p_n \cdot N} \right) \Leftrightarrow I = -\sum_{i=1}^n p_i \cdot N \cdot \log_2 p_i$$

$$I = N \cdot \sum_{i=1}^n p_i \cdot \log_2 \left( \frac{1}{p_i} \right) \tag{Equation 5.85}$$

Dividing the total information content of a message  $I$  by the amount of characters it contains, results in the average information content per character (symbol), which is denoted as  $H$ :

$$H = \frac{I}{N} = \sum_{i=1}^n p_i \cdot \log_2 \left( \frac{1}{p_i} \right) \quad \text{Equation 5.86}$$

The probability of each individual character  $p_i$  to occur can be calculated easily by counting all the characters of one type  $N_i$  and relating them to the total number of characters in the entire message  $N$ . Thus, the probability of each character is:

$$p_i = N_i / N \quad \text{Equation 5.87}$$

Once this is accomplished, the average information content can be plotted as seen in Figure 5.34. The graph can be used to calculate the total information content of the entire message by adding up the individual results  $-p_i \cdot \log_2 p_i$  for each of the  $n$  different characters. The sum is then multiplied by the total number of characters  $N$  in the message (or length of the message). The maximum information is conveyed if each character occurs with the probability  $p_i = 1/e = 0.3679$  and  $H_{\max} = 1/e \cdot \log_2(e) = 0.5307$ .

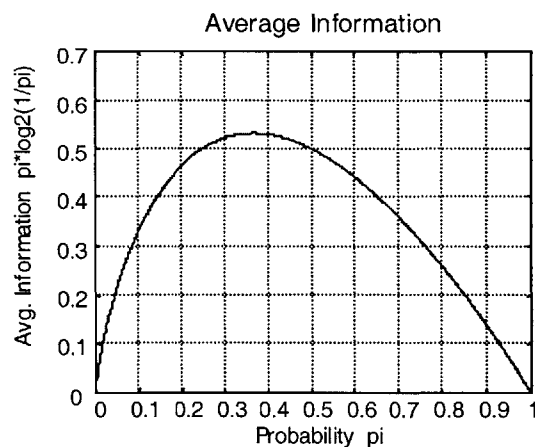


**Figure 5.34** Average Information Content vs. Probability of a Character  $i$ .



Example 1: Information Content of a Binary Character Set

Using Equation 5.86, the average information stored by of a set of two characters (for example 0 and 1) can be written as:

$$H = -p \cdot \log_2 p - (1 - p) \cdot \log_2 (1 - p) \quad \text{Equation 5.88}$$

The following graph plots the average information content of a binary set versus the probability of their occurrence. A maximum of information is stored when each character (event) is equally likely to occur  $p_i = 1/2$ .

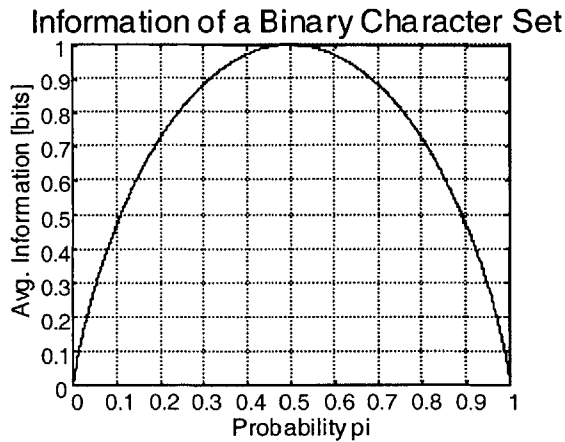


**Figure 5.35 Information Content (Binary Case)**

Equiprobable Case

The average information content per character in a message approaches its maximum when every character out of set of  $n$  characters can occur with equal probability. Now the probability for each character is  $p_i = \frac{1}{n}$  where  $n$  is the number of characters in the particular set. It can also be regarded as the number of choices. For this equiprobable case the equation for the average information content  $H$  simplifies to:

$$\Rightarrow H_{\max} = \sum_{i=1}^n \frac{1}{n} \cdot \log_2 n \quad \Rightarrow H_{\max} = \log_2 n \quad \text{Equation 5.89}$$

Figure 5.36 shows the maximum average amount of information contained per character for a set of  $n$  different but equally probable characters. Again to obtain the maximum amount of information stored in a message  $I_{\max}$  of equiprobable characters  $H_{\max}$  is multiplied by the number of characters  $N$ .

$$I_{\max} = H_{\max} \cdot N \quad \text{Equation 5.90}$$

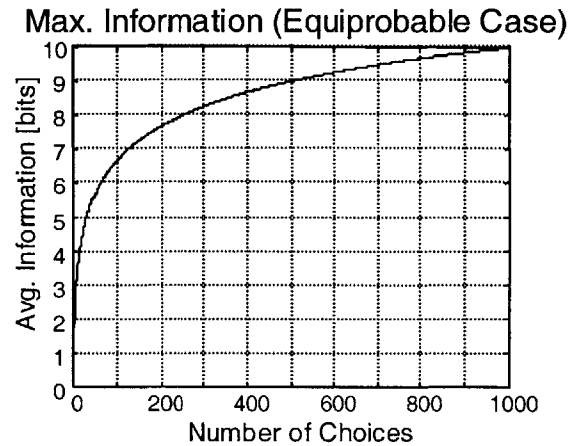


**Figure 5.36** Maximum Average Information Content (Equiprobable Case)

Example 2: Binary Array with Equal Character Probabilities

In binary array there are  $n = 2$  choices (0,1) and each occurring with a probability of  $p_i = 1/2$ . The array is  $N$  characters long. Therefore the total information stored in the array is:

$$I = N \cdot \sum_{i=1}^2 \frac{1}{2} \cdot \log_2 2 = N \text{ bits} \quad \text{Equation 5.91}$$

Example 3: Binary Grid of 256 x 256 Datapoints (Pixels)

The length of the message is  $N = 256 \times 256 = 65,536$  data points and the total information according to Equation 5.91 is equal to 65,536 bits. This can be verified by creating a binary image (black & white) of this size and storing it in a pixel format on a computer's harddisk. The required storage space equals 8,192 byte, which is identical to 65,536 bits, since 1 byte = 8 bits.

Example 4: 24 Bit Grid of 256 x 256 Datapoints (Pixels)

Again we have  $N = 65,536$  data points, but this time there are 24 bit of information stored per character. Multiplication gives 1,572,864 bits or 196,608 bytes, which is confirmed by saving the previous picture in 24 bit format and checking the required disk space. In such pictures each pixel can assume a color out of  $2^{24} = 16,777,216$  possible colors (choices).

Information Arithmetic

The information content of several messages, characters etc. can be added in order to gain the information content of the new combined message. The rule states:

$$I = I_1 + I_2 + I_3 + \dots + I_M \quad \text{Equation 5.92}$$

Redundancy

A further measurement of information is the redundancy, which is defined as follows:

$$R = 1 - \frac{H_{actual}}{H_{max}} = 1 - \frac{I_{actual}}{I_{max}} \quad \text{Equation 5.93}$$

Application for Part Complexity

The somewhat theoretical concept of information theory can indeed be applied to quantify the complexity of parts. As described in this chapter the number of different choices is a measurement of complexity. This idea can be applied to actual parts by assessing how many different shapes, characteristics, dimensions a part can assume. Also, any part geometry can be subdivided into grids as many CAD and FEM meshing programs do and each node can be treated as a character in a message as described by Example 4. The possibilities are endless and for each scenario, the defining descriptor of part complexity has to be determined.

### 5.4.2 On Differential Geometry and Fibers

The following few paragraphs are intended to provide a brief overview of differential geometry in order to aid a better understanding of the deformation of fibers. For further reading references [41] and [42] are recommended. Differential geometry theory describes any curve in three-dimensional space by its curvature and torsion. If the curvature is known at every point, then torsion is not independent. Hence, curvature lends itself as an information measure for fibers.

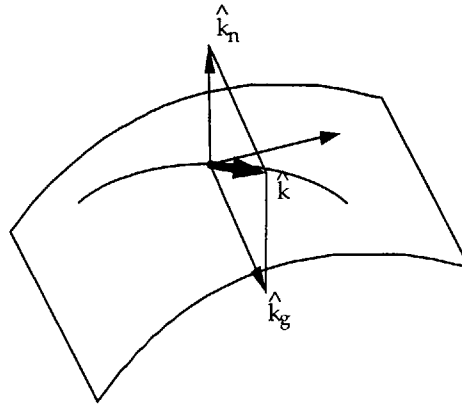


**Figure 5.37** Definition of Curvature

The curvature at any point can be represented by a vector pointing along the direction of the fiber. As shown in Figure 5.37 this curvature vector has two components, one normal to the surface of the part and the other in the plane of the part. It can be written as:

$$\hat{k} = \hat{k}_n + \hat{k}_g = \kappa \hat{n} = \kappa_n \hat{N} + \kappa_g \hat{u} \quad \text{Equation 5.94}$$

with  $\kappa_n$  describing the normal (out-of-plane) and  $\kappa_g$  expressing the geodesic (in-plane) curvatures. In general the larger the magnitude of the geodesic curvature  $\kappa_g$  the more pronounced is the double curvature of the underlying part shape. The magnitude of the normal curvature  $\kappa_n$  is a measure of the single curvature of the underlying shape. The above relation demonstrates how the geometry of the surface influences the fiber, which follows it. Integration of the curvatures  $\kappa_n$  and  $\kappa_g$  along the fiber direction  $s$  gives an

expression of the enclosed angles normal  $\theta_n$  and perpendicular  $\theta_g$  to the surface (see Equation 5.95).

$$\theta_n = \int \kappa_n ds \quad \text{and} \quad \theta_g = \int \kappa_g ds \quad \text{Equation 5.95}$$

Substitution of the above expressions into Equation 5.94 results in Equation 5.96 where  $\theta$  represents the total enclosed angle [42].

$$\theta^2 = \theta_n^2 + \theta_g^2 \quad \text{Equation 5.96}$$

The two enclosed angles  $\theta_n$  and  $\theta_g$  have clear physical interpretations. They are related to the out-of-plane and in-plane shear slip required to deform an initially flat laminate, as is demonstrated by Tam [60, 61]. Figure 5.38 illustrates the shear between two adjacent fibers (layers) and the total enclosed deformation angle  $\theta$ .

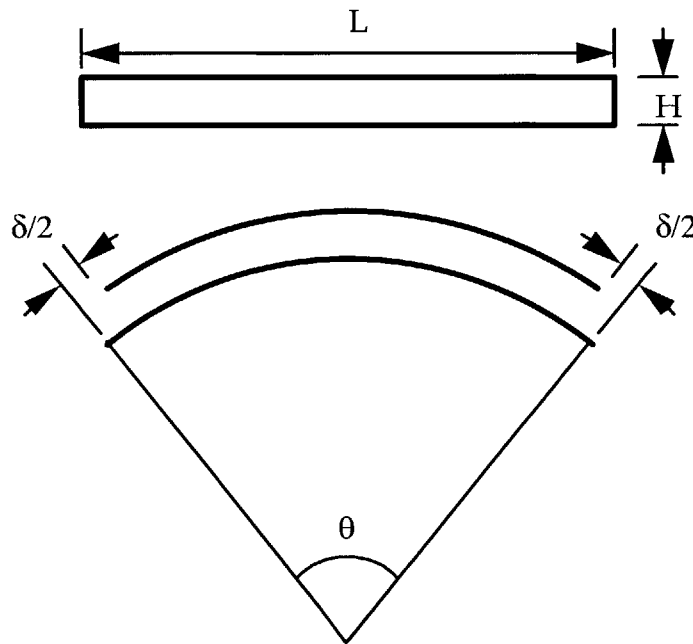


**Figure 5.38 Relation of Shear Slip and Enclosed Angle**

Another important relationship is the Gauss-Bonnet theorem. It simplifies the calculation of the geodesic curvature  $\kappa_g$  and its attendant enclosed angle  $\theta_g$  depending on the to part curvature. As illustrated in Figure 5.39, the Gauss-Bonnet theorem relates the geodesic

curvature  $\kappa_g$  for the piecewise line segments  $C_i$  to the double curvature (Gaussian curvature)  $K$  of the enclosed region  $R$  and the angles of intersection  $\theta_i$ .

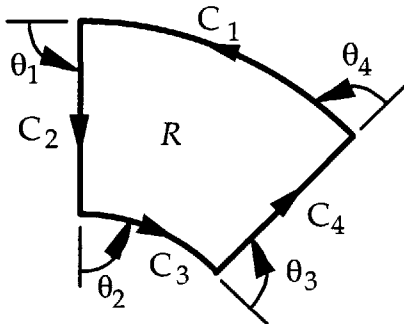


**Figure 5.39 Gauss-Bonnet Theorem**

The actual theorem is stated in Equation 5.97:

$$\int_C \kappa_g ds + \iint_R K dA = 2\pi - \sum \theta_i \quad \text{Equation 5.97}$$

For some shapes, the calculation can be done quickly by selecting line segments  $C_i$ , which follow non-geodesic paths. In that case  $\kappa_g = 0$  and the first integration term can be discarded. Since, the angles  $\theta_i$  can simply be measured the value of the area integral is then known. In some cases, the double curvature  $K$  is also a constant and the equation can easily be solved for  $K$  by dividing the right part by the area  $A$ . Tam [61] in his work gives many examples of parts and geometries where the above technique is successfully applied.

### 5.4.3 Examples of Fiber Mapping using FiberSim©

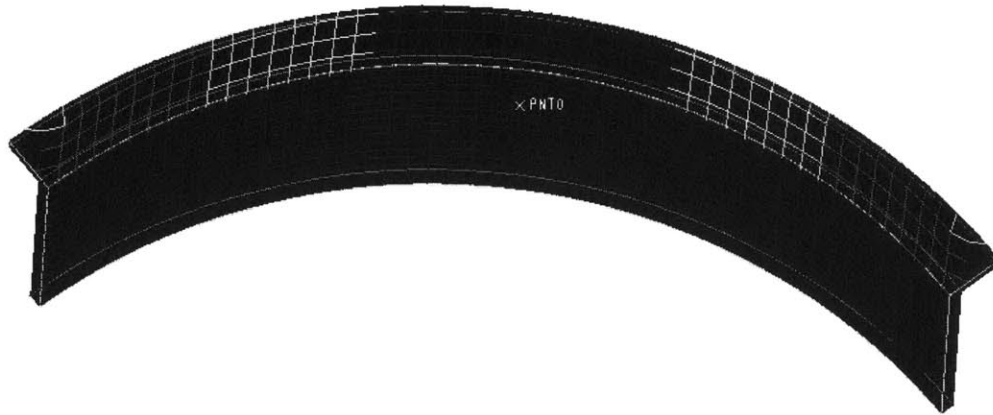


Figure 5.40 Stretchflange R = 20" , 90 deg , Flange Width = 4"



Figure 5.41 Shrinkflange R = 120" , 30 deg , Flange Width = 2"

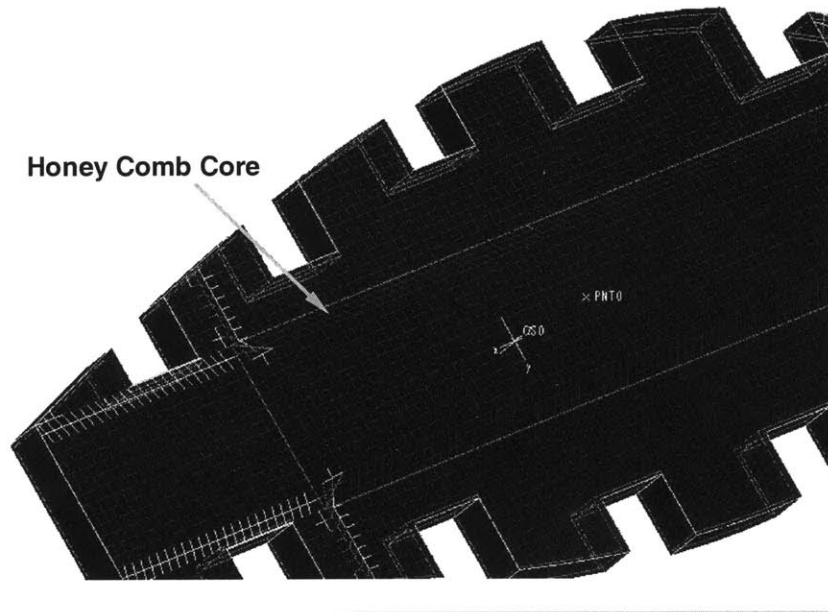


Figure 5.42 Schematic of a Wing Rib

### 5.4.4 Process Plans & Cost Drivers

#### Hand Lay-Up (HLU)

<b>Tool Setup</b>	1	Clean Tool
	2	Tool Setup
	3	Apply Release Agent
	4	Apply Barrier Film
<b>Material Setup</b>	5	Setup Prepreg
	6	Cut Prepreg
	7	Cut Bleeder
	8	Cut Breather
	9	Cut Vacuum Bag
<b>Layup</b>	10	Layup
<b>Debulking</b>	11	Debulk
	12	Remove Compaction Bag
<b>Vacuum Bagging</b>	13	Apply Bleeder
	14	Apply Breather
	15	Apply Cork Dams
	16	Apply Sealant Tape
	17	Apply Vacuum Bag
	18	Connect Vacuum Line
	19	Apply Vacuum
	20	Check Seals
	21	Disconnect Vacuum Lines
	22	Apply Peel Plies
	23	Install Caul Plate
<b>Autoclave Setup</b>	24	Transfer to Autoclave
	25	Connect Vacuum Line
	26	Connect Thermocouples
	27	Apply Vacuum
	28	Check Seals
	29	Setup Autoclave
<b>Cure Cycle</b>	30	Start Autoclave Cycle
	31	Disconnect Vacuum Lines
	32	Disconnect Thermocouples
	33	Remove Part from Autoclave
<b>Finishing</b>	34	Remove Vacuum Bagging
	35	Demold Part
	36	Clean Part
	37	Abrade Part
	38	Trim Part
	39	Deflash Part
	40	Deburr Part



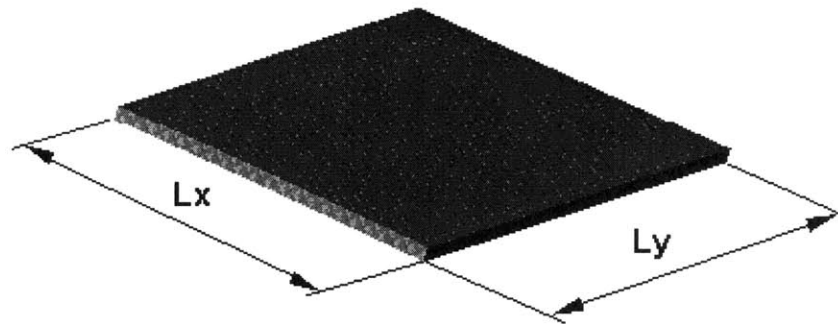


Figure 5.43 Flat Panel (36'' x 36'' x 1/8'', quasi-isotropic)

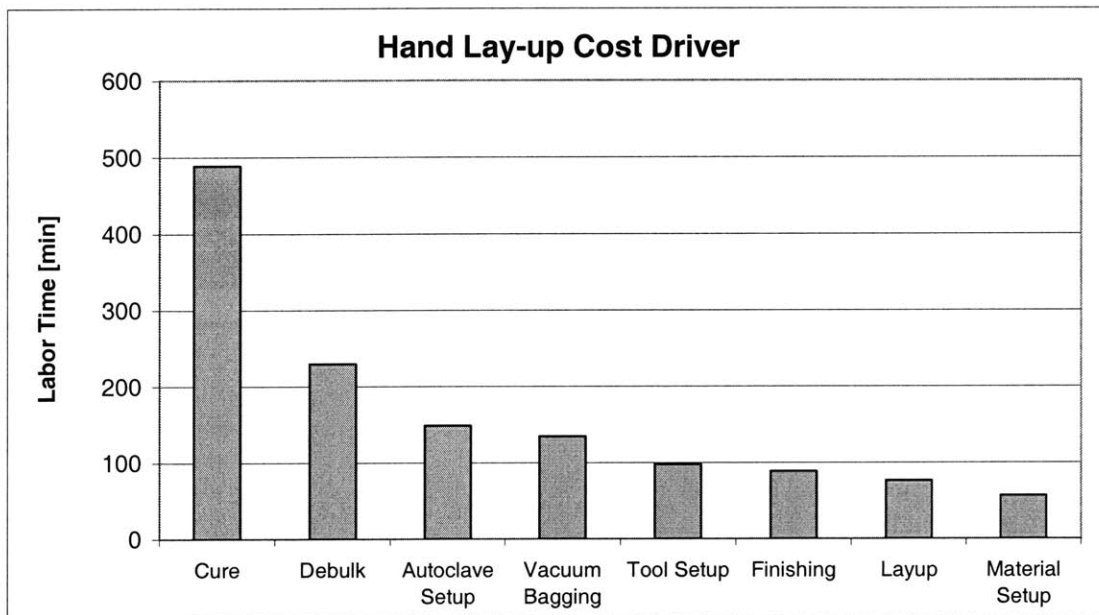
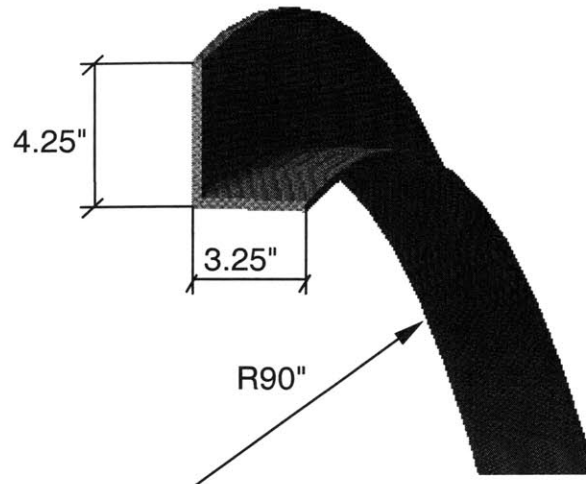


Figure 5.44 Hand Layup of Flat Panel (36'' x 36'' x 1/8'', quasi-isotropic)

Resin Transfer Molding (RTM)

<b>Tool Setup</b>	1	Clean resin transfer mold
	2	Apply mold release to resin transfer mold
<b>Material Loading</b>	3	Position braided preform into mold
	4	Fold frame flange
<b>Close Mold</b>	5	Position "O" ring mold seal
	6	Close off resin transfer mold
	7	Attach vacuum lines to resin transfer mold
	8	Attach thermocouple lines to resin transfer mold
	9	Attach resin injection lines to resin transfer mold
<b>Machine Setup</b>	10	Setup resin injection machine
	11	Load two part resin onto injection machine
<b>Inject &amp; Cure</b>	12	Pull vacuum on resin transfer mold
	13	Cure frame blank in resin transfer mold
<b>Demolding</b>	14	Remove injection lines to resin transfer mold
	15	Remove thermocouple lines to resin transfer mold
	16	Remove vacuum lines to resin transfer mold
	17	Remove resin transfer mold lid
	18	Remove resin transfer mold seal
	19	Remove frame blank from resin transfer mold
<b>Post Cure</b>	20	Post cured frame blank
<b>Finishing</b>	21	Trim manual edge gr/ep
	22	Setup NC trimming equipment
	23	Position part into NC trimming equipment
	24	Trim automated edge gr/ep
	25	Remove finished part from NC trimming equipment
	26	Deflash cured frame blank
	27	Manual deburr edge



**Figure 5.45** Curved L-Profile (R90" x 4.25" x 3.25" x 1/4 ")

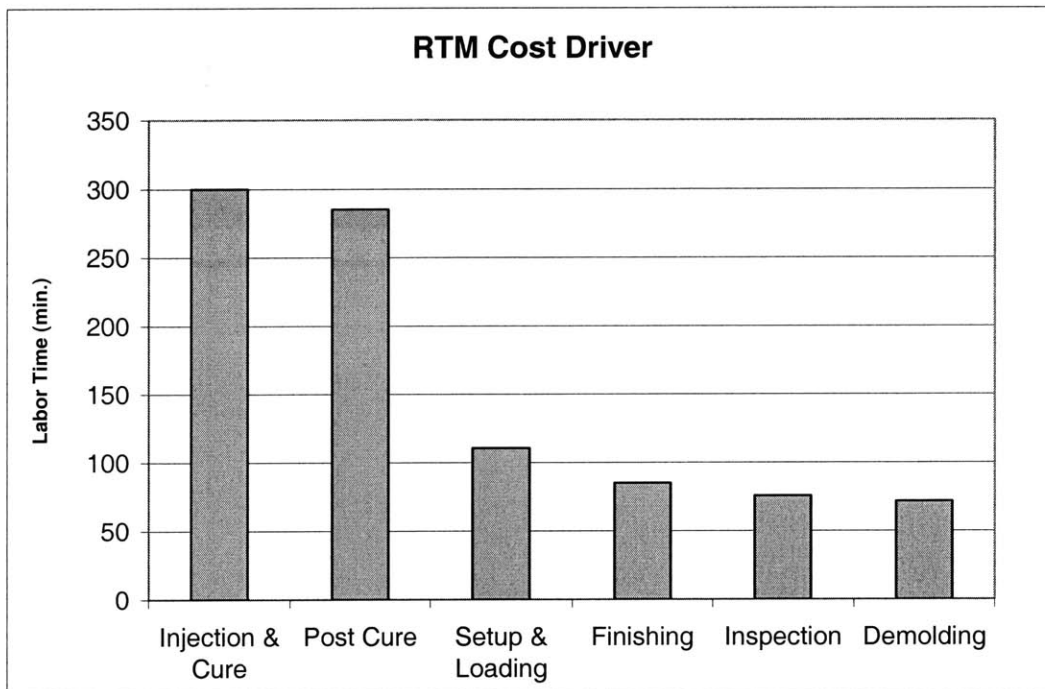


**Figure 5.46** RTM of a Curved L-Profile (R90" x 4.25" x 3.25" x 1/4 ")

Automated Tow Placement (ATP)

<b>Part &amp; Tool Setup</b>	1	Identify required items for TPM
	2	Position winding tool into staging area
	3	Apply separation film to winding tool surface
	4	Hand lay up fabric ply over winding tool
	5	Position skin debulk bag
	6	Debulk hand layed up fabric ply
	7	Remove debulk bag from skin
	8	Load winding tool onto TPM
<b>Machine Setup</b>	9	Setup TPM equipment for skin layup
<b>Material Setup</b>	10	Load prepreg tow onto ATP equipment as required
<b>Layup</b>	11	Layup 0 degree plys onto winding tool using TPM
	12	Layup 15 degree plys onto winding tool using TPM
	13	Layup 30 degree plys onto winding tool using TPM
	14	Layup 45 degree plys onto winding tool using TPM
	15	Layup 60 degree plys onto winding tool using TPM
	16	Layup 75 degree plys onto winding tool using TPM
	17	Layup 90 degree plys onto winding tool using TPM
<b>Unload</b>	18	Unload winding tool with skin layup from TPM cell
<b>Protection</b>	19	Hand lay up fabric ply over winding tool
	20	Position skin debulk bag
	21	Debulk hand layed up fabric ply
	22	Remove debulk bag from skin
	23	Protect skin layup on winding tool
	24	Identify skin layup on winding tool
<b>Transport</b>	25	Transport to next used on

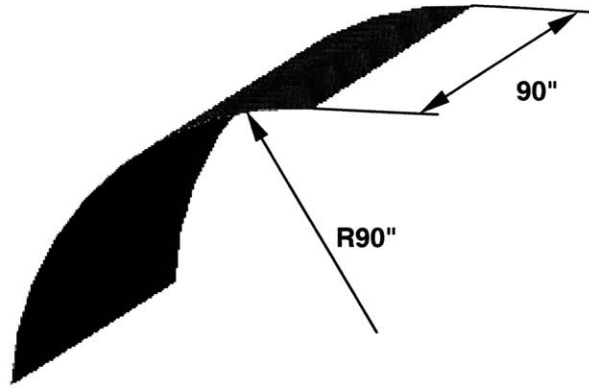


Figure 5.47 Simple Curved Part (R90" x 90" x 1/4")

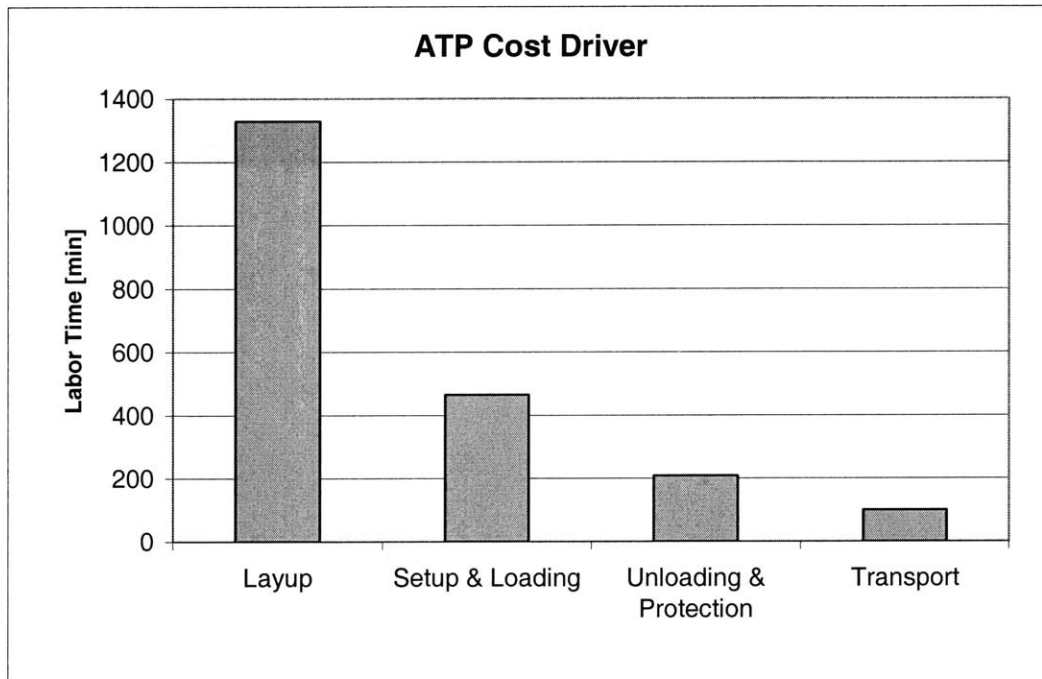
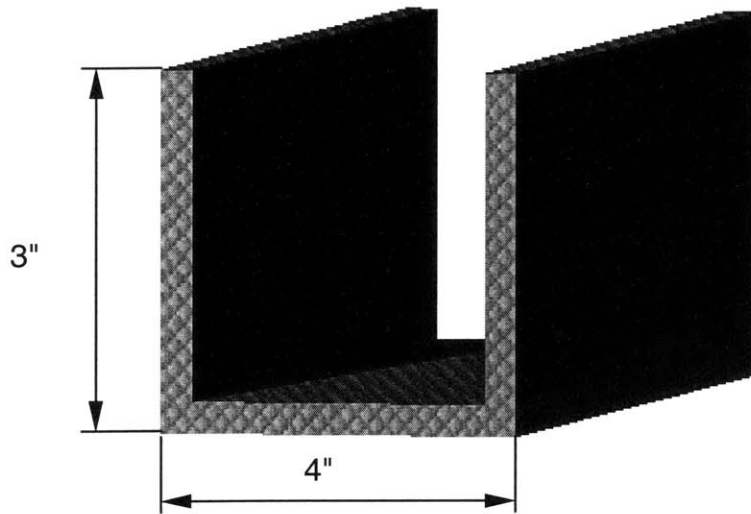


Figure 5.48 ATP of a Curved Part (R90" x 90" x 1/4")

Pultrusion (PUL)

<b>Setup</b>	1	Identify required items for pultrusion
	2	Setup pultrusion equipment
	3	Setup inline ultra-sonic inspection equipment
	4	Load form die onto pultrusion equipment
	5	Attach thermocouple lines to pultrusion die
<b>Fiber Prep.</b>	6	Load dry fiber material onto pultrusion equipment
<b>Resin Prep.</b>	7	Setup resin bath
	8	Load resin into resin bath
<b>Resin Prep.</b>	9	Setup pultrusion resin injection machine
<b>(alternatively)</b>	10	Load two part resin onto pultrusion injection machine
	11	Attach resin injection lines to pultrusion die
<b>Pultrusion</b>	12	Run pultrusion equipment(including cut-off)
	13	Remove form die from pultrusion equipment
	14	Clean pultrusion form die
<b>Trimming</b>	15	Setup NC trimming equipment
<b>&amp; Finishing</b>	16	Position part into NC trimming equipment
	17	NC drill indexing holes c/t pultruded section(optional)
	18	Trim automated edge gr/ep
	19	Remove finished part from NC trimming equipment
	20	Manual deburr edge



**Figure 5.49** Straight C – Profile (4" x 3" x 1/4" x 30 ft.)

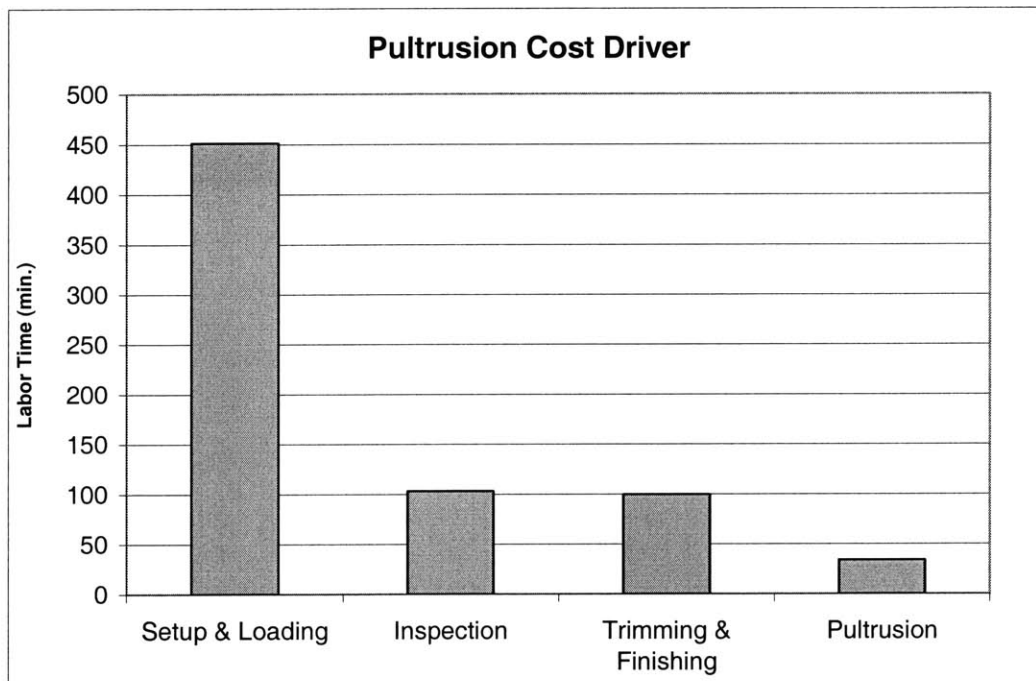
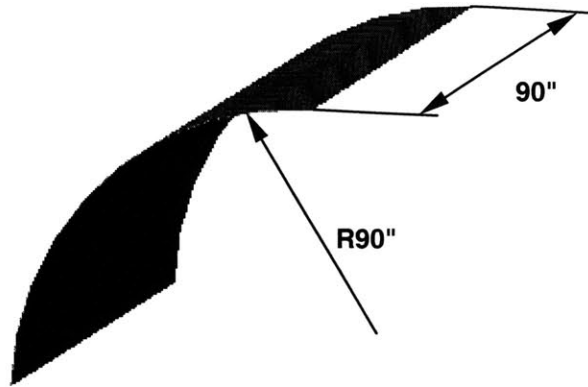


**Figure 5.50** Pultrusion of a Straight C – Profile (4" x 3" x 1/4" x 30 ft.)

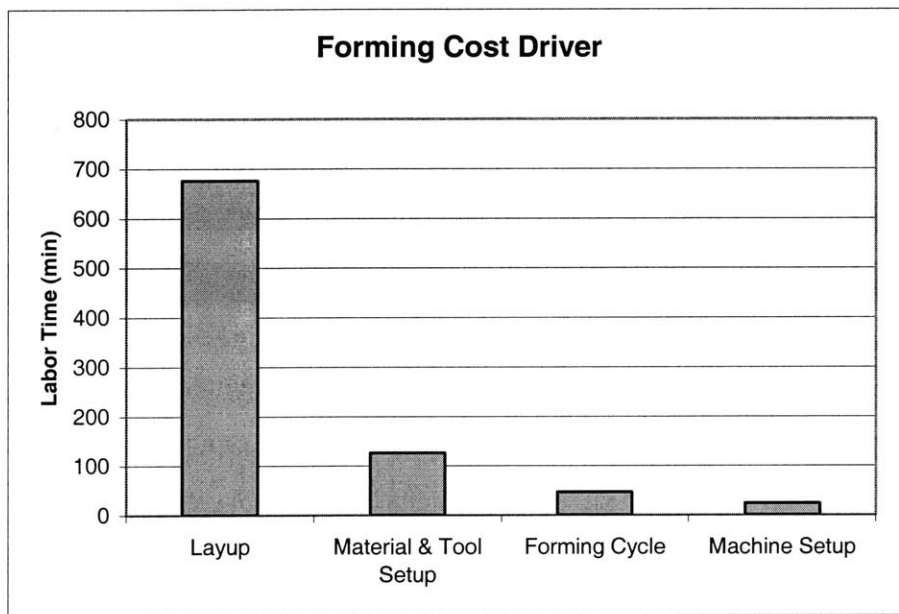
Double Diaphragm Forming (DDF)

<b>Material &amp; Tool Setup</b>	1	Cut Material
	2	Clean Tool
	3	Tool Setup
	4	Apply Release Agent
<b>Layup</b>	5	Hand Layup Flat Charge
<b>Machine Setup</b>	6	Setup Forming Machine
	7	Reset Tooling
	8	Load Parts
	9	Lower Upper Diaphragm Frame
	10	Lock Frames
<b>Forming Cycle</b>	11	Preheat Charges
	12	Apply Vacuum
	13	Cool Parts
	14	Open Upper Frame
	15	Remove Part





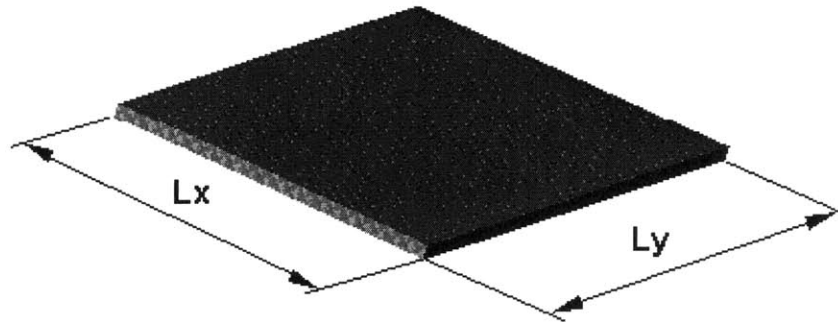
**Figure 5.51 Simple Curved Part (R90" x 90" x 1/4")**



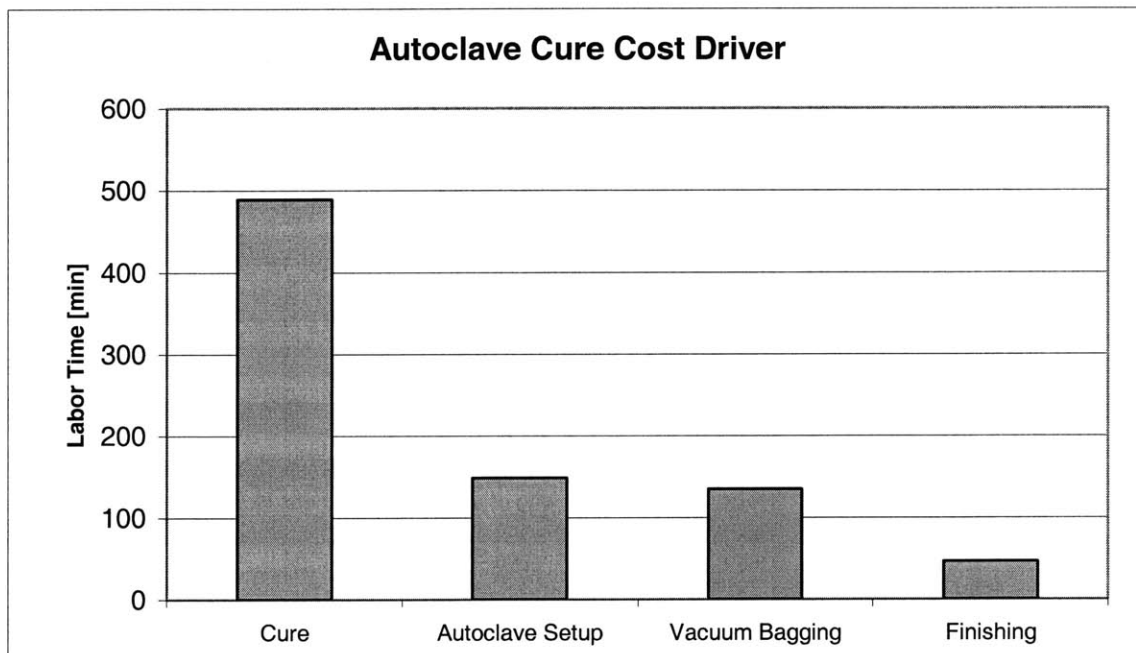
**Figure 5.52 Forming of a Simple Curved Part (R90" x 90" x 1/4")**

Autoclave Cure

<b>Vacuum Bagging</b>	1	Apply Bleeder
	2	Apply Breather
	3	Apply Cork Dams
	4	Apply Sealant Tape
	5	Apply Vacuum Bag
	6	Connect Vacuum Line
	7	Apply Vacuum
	8	Check Seals
	9	Disconnect Vacuum Lines
	10	Apply Peel Plies
	11	Install Caul Plate
<b>Autoclave Setup</b>	12	Transfer to Autoclave
	13	Connect Vacuum Line
	14	Connect Thermocouples
	15	Apply Vacuum
	16	Check Seals
	17	Setup Autoclave
<b>Cure Cycle</b>	18	Start Autoclave Cycle
	19	Disconnect Vacuum Lines
	20	Disconnect Thermocouples
	21	Remove Part from Autoclave
<b>Demold Part</b>	22	Remove Vacuum Bagging
	23	Demold Part
	24	Clean Part



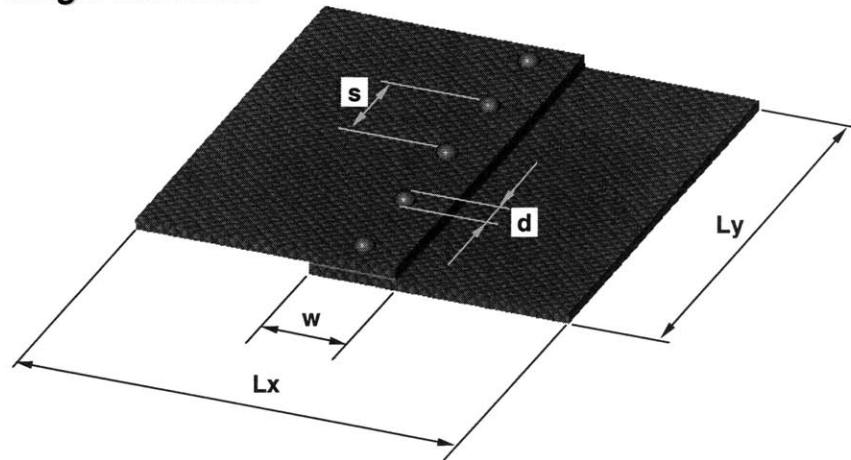
**Figure 5.53** Flat Panel (36'' x 36'' x 1/8'', quasi-isotropic)



**Figure 5.54** Autoclave Cure of a Flat Panel (36'' x 36'' x 1/8'')

Mechanical Assembly

<b>Generic Assembly Process Plan</b>			
Setup Assembly	1	Ready Workplace	
	2	Setup Assembly Jig	
Load Parts	3	Position Manually a Long Part into Jig	
	4	Position Manually a Bulky Part into Jig	
	5	Position Manually a Bulky Part w/ Index Holes into Jig	
	6	Hoist Assisted Positioning of a Long Part w/ Index Holes into Jig	
	7	Apply Clamping Force using Clamps	
	8	Apply Clamping Force using Straps	
	9	Inspect Manually Interface Gaps w/ Feeler Gage	
	10	Identify Interface Area	
	Shimming	11	Remove Clamping Straps
		12	Remove Manually a Long Part from Jig
13		Remove Manually a Bulky Part from Jig	
14		Trim Manually the Edge of the Separation Film	
15		Layup Manually the Separation Film	
16		Fabricate Kapton Shim	
17		Abrade Joint Surface	
18		Clean Part	
19		Position Manually the Kapton Shim	
20		Mix Liquid Shimming Compound	
21		Apply Liquid Shimming Compound	
22		Position Manually a Long Part into Jig	
23		Position Manually a Bulky Part into Jig	
24		Position Manually a Bulky Part w/ Index Holes into Jig	
25		Hoist Assisted Positioning of a Long Part w/ Index Holes into Jig	
26		Apply Clamping Force using Clamps	
27		Apply Clamping Force using Straps	
28		Remove Manually the Liquid Shim Squeeze Out	
29		Position Manually the Heating Lamps	
30		Cure Liquid Shim	
31		Remove Manually the Heating Lamps	
32		Remove Clamping Straps	
33	Remove Manually a Long Part from Jig		
34	Remove Manually a Bulky Part from Jig		
35	Remove Manually the Separation Film		
36	Inspect Visually the Cured Liquid Shim		
37	Position Manually a Long Part into Jig		
38	Position Manually a Bulky Part into Jig		
39	Position Manually a Bulky Part w/ Index Holes into Jig		
40	Hoist Assisted Positioning of a Long Part w/ Index Holes into Jig		
41	Apply Clamping Force using Clamps		
42	Apply Clamping Force using Straps		
Drilling	43	Position Manually the Drill Template	
	44	Drill Automated Gr/Ep Holes c/t indexing holes	
	45	Drill Manually Gr/Ep Countersunk Holes	
	46	Drill Manually Gr/Ep Through-Holes	
	47	Remove Manually the Drill Template	
	48	Inspect Visually the Drilled Holes	
Install Fasteners	49	Install Fastener Clecos	
	50	Install Lockbolt Fastener	
	51	Install Torqued Fasteners	
	52	Inspect Visually the Fasteners	
Unload Assembly	53	Remove Clamping Straps	
	54	Remove Manually a Long Part from Jig	
	55	Remove Manually a Bulky Part from Jig	

**Single Lap Joint**

**Figure 5.55** Lap Joint Dimensions:  $L_x=12''$ ,  $L_y = 108''$ ,  $w = 2''$ ,  $s = 1''$ ,  $d = \frac{1}{4}''$

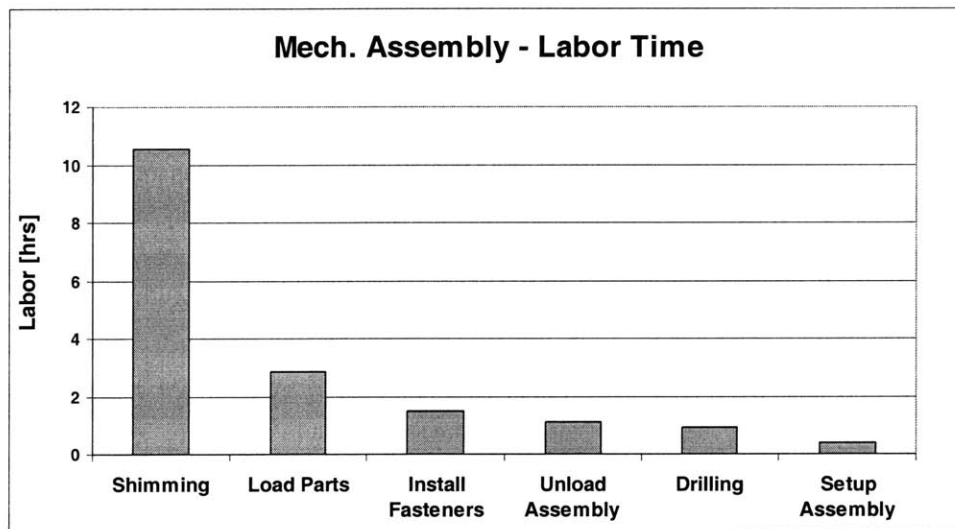


**Figure 5.56** Mechanical Joining of a Single Lap Joint

Adhesive Assembly

<b>Generic Assembly Process Plan</b>		
Setup Assembly	1	Ready Workplace
	2	Setup Assembly Jig
Load Parts	3	Position Manually a Long Part into Jig
	4	Position Manually a Bulky Part into Jig
	5	Position Manually a Bulky Part w/ Index Holes into Jig
	6	Hoist Assisted Positioning of a Long Part w/ Index Holes into Jig
	7	Apply Clamping Force using Clamps
	8	Apply Clamping Force using Straps
	9	Inspect Manually Interface Gaps w/ Feeler Gage
Surface Preparation	10	Identify Interface Area
	11	Remove Clamping Straps
	12	Remove Manually a Long Part from Jig
	13	Remove Manually a Bulky Part from Jig
	14	Trim Manually the Edge of the Separation Film
	15	Layup Manually the Separation Film
	16	Fabricate Kapton Shim
	17	Abrade Joint Surface
	18	Clean Part
	19	Position Manually the Kapton Shim
Adhesive Bonding	20	Mix Liquid Adhesive Compound
	21	Apply Liquid Adhesive
	22	Position Manually a Long Part into Jig
	23	Position Manually a Bulky Part into Jig
	24	Position Manually a Bulky Part w/ Index Holes into Jig
	25	Hoist Assisted Positioning of a Long Part w/ Index Holes into Jig
	26	Apply Clamping Force using Clamps
	27	Apply Clamping Force using Straps
	28	Remove Manually the Liquid Adhesive Squeeze Out
	29	Position Manually the Heating Lamps
	30	Cure Liquid Adhesive
	31	Remove Manually the Heating Lamps
	32	Remove Clamping Straps
	33	Remove Manually a Long Part from Jig
Unload Assembly	34	Remove Manually a Bulky Part from Jig
	35	Remove Manually the Separation Film
	36	Inspect Visually the Cured Adhesive

**Single Lap Joint**

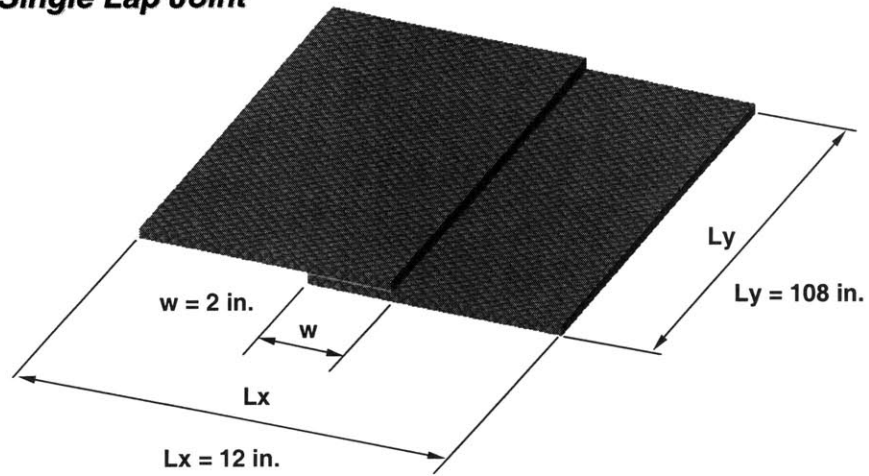


**Figure 5.57 Lap Joint Dimensions:  $L_x=12''$ ,  $L_y = 108''$ ,  $w = 2''$**

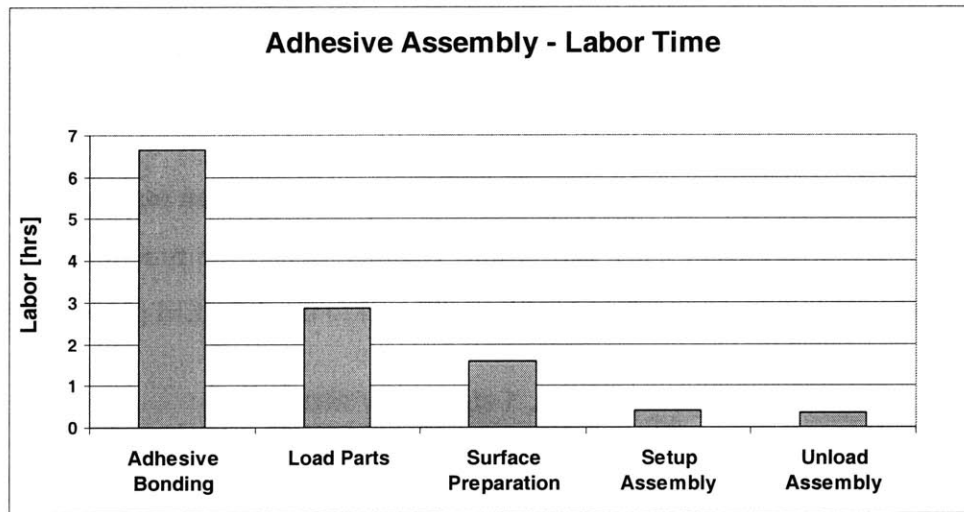


**Figure 5.58 Adhesive Joining of a Single Lap Joint**

### 5.4.5 Composite Layup Time Estimation

#### Flat Panel

$L_x = 10, 12, 16, 21, 24, 31, 47, 60, 62$  in.

$L_y = 60, 65$  in.

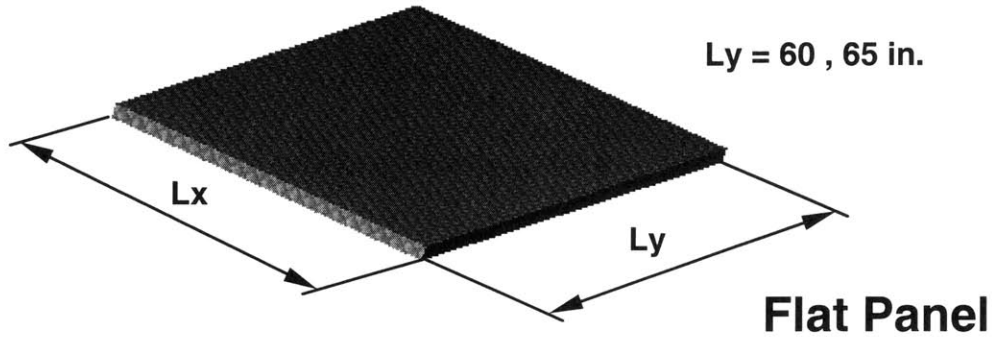


**Figure 5.59** Layup of a Flat Panel using Woven Prepreg

$$t_{ply} = \left( \tau_0 \cdot \sqrt{\left( \frac{A_{Total}}{v_0 \cdot \tau_0} + 1 \right)^2 - 1} \right) \text{ with } \tau_0 = 5.81 \text{ min. and } v_0 = 6.48 \text{ sqft/min.}$$

In this set of experiments the total layup time for one layer of woven material is estimated for various sized Flat Panels. The processing velocity  $v_0$  and the time constant  $\tau_0$  have been determined by curvefitting the Hyperbolic Model to the ACCEM [5] benchmarks.

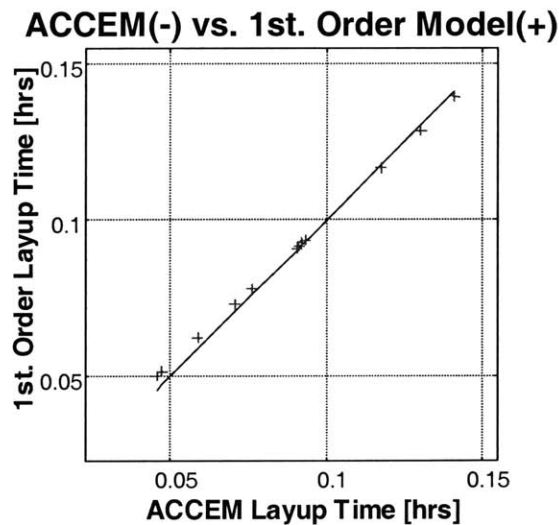


**Figure 5.60** Comparison of Layup Times for Flat Panels



The size of the parts ranged between 680 - 4080 sqin (4.7 - 28 sqft), which is well below the max. range of ACCEM (50 sqft.), but also in the transition region of the critical area  $A^* = 2250$  sqin. (15.63 sqft.). The accuracy of the correlation is  $R^2 = 0.99$  and the max. error = 9.7%.

L-Profile

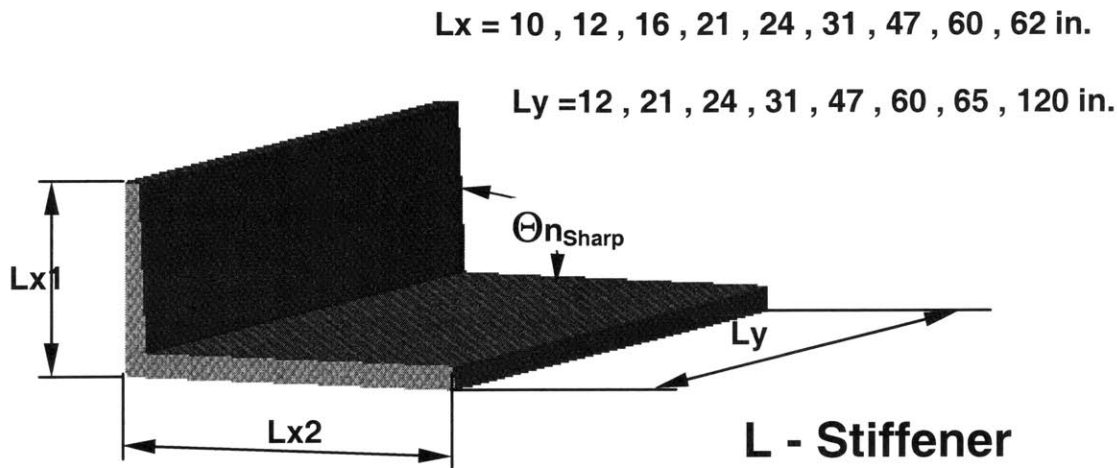


**Figure 5.61 Layup of a L-Profile using Woven Prepreg**

$$t_{ply} = (\tau_0 + b_n \cdot I) \cdot \sqrt{\left(\frac{A_{Total}}{v_0 \cdot (\tau_0 + b_n \cdot I)} + 1\right)^2 - 1} \quad \text{with by } \tau = \tau_0 + b_n \cdot I \quad \text{and}$$

$I = \Delta\Theta_{nSharp} \cdot Ly$  where  $Ly$  represents the length of the bend. The previously determined 1<sup>st</sup> Order parameters  $\tau_0 = 5.81$  min. and  $v_0 = 6.48$  sqft/min are also used. The coefficient  $b_n$  equals  $b_n = 7.6e-2$  min/(ft rad).

It is understood, that sharp bends with radii smaller than the endeffector's size ( $R < 12"$ ) are best modeled by an additive time penalty by means of modification of  $\tau$ . The experiments are based on a set of 40 differently sized stiffeners. The size of the parts ranges between 120 – 4,080 sqin (0.83 - 28 sqft), which is well below the max. range of ACCEM (50 sqft.). The best fit yields a R-Square value of  $R^2 = 0.9956$  and the maximum estimation error is 28%. The consideration of the bent length  $Ly$  as part of the

complexity scaling model reflects the effort of an operator to move along the bent and deform of the fabric.

**ACCEM(-) vs. 1st. Order Model(+)**

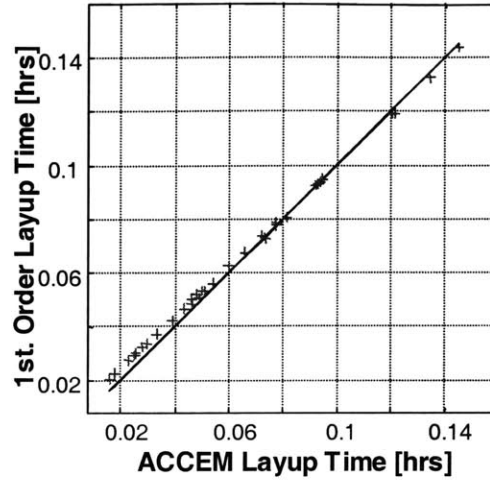


**Figure 5.62 Comparison of Layup Times for L-Profiles**

Curved Panel with Small Bent Radii

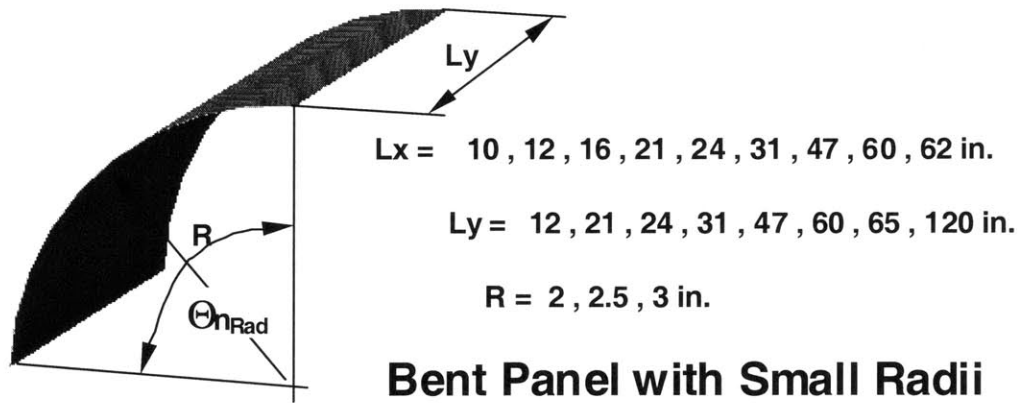


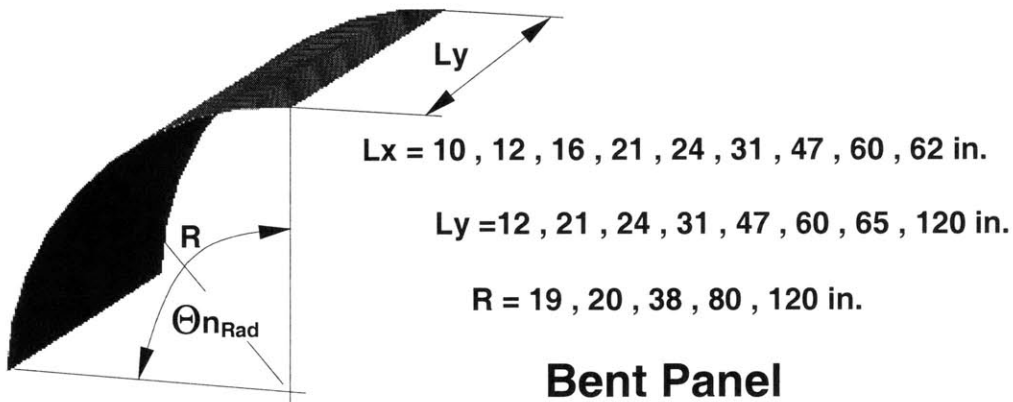
**Figure 5.63 Layup of a Curved Panel (Small Radii) using Woven Prepreg**

The modeling approach is the same as for the previously discussed L-Profile. Again, the processing (layup) time per ply is expressed by:

$$t_{ply} = (\tau_0 + b_n \cdot I) \cdot \sqrt{\left(\frac{A_{Total}}{v_0 \cdot (\tau_0 + b_n \cdot I)} + 1\right)^2 - 1} \quad \text{with by } \tau = \tau_0 + b_n \cdot I \quad \text{and}$$

$I = \Delta\Theta_{nSharp} \cdot Ly$  where  $Ly$  represents the length of the bend. The previously determined 1<sup>st</sup> Order parameters  $\tau_0 = 5.81$  min. and  $v_0 = 6.48$  sqft/min are also used. The coefficient  $b_n$  equals  $b_n = 7.6e-2$  min/(ft rad).

Curved Panel with Large Bent Radii

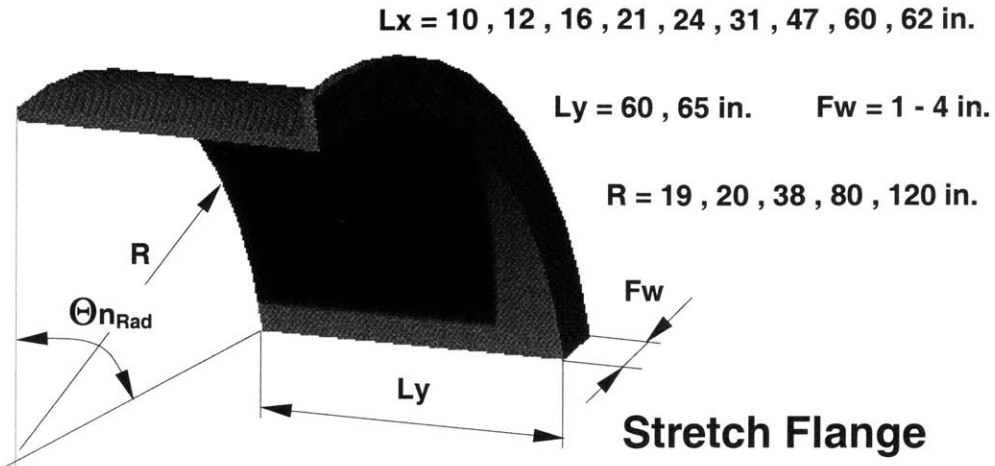


**Figure 5.64 Layup of a Curved Panel (Large Radii) using Woven Prepreg**

$$t_{ply} = \left( \tau_0 \cdot \sqrt{\left(\frac{A_{Single}}{v_{Single} \cdot \tau_0} + 1\right)^2 - 1} \right) \quad \text{with } v_{Single} = \frac{v_0}{1 + (v_0/cn) \cdot I}, \quad I = \Theta_n \cdot Ly \quad \text{and with } \tau_0$$

= 5.81 min. and  $v_0 = 6.48$  sqft/min. The coefficient  $c_n$  equals  $c_n = 1.8e+4$  (cuft rad.)/min.

Here processing velocity is affected by the shape of the part. It is assumed, that for bent radii larger than the endeffector size ( $R > 12''$ ), the machine/operator has to slow down in its movements. The experiments are based on a set of 40 differently sized panels ranging in size between 120 – 4,080 sqin (0.83 - 28 sqft). The R-Square value equals  $R^2 = 0.99447$  and the maximum error is 33%. However, the incredibly high value of  $c_n$  suggests, that the influence of bent radii ( $R > 12''$  Endeffector Size) on the layup time is almost insignificant.

Stretch Flange**Figure 5.65** Layup of a Stretch Flange using Woven Prepreg

$$t_{Ply} = \left( \tau_{Single} \cdot \sqrt{\left( \frac{A_{Single}}{v_{Single} \cdot \tau_{Single}} + 1 \right)^2} - 1 \right) + \left( \tau_0 \cdot \sqrt{\left( \frac{A_{Double}}{v_{Double} \cdot \tau_0} + 1 \right)^2} - 1 \right)$$

$$\tau_{Single} = \tau_0 + b_n \cdot \Delta\Theta_{nRad} \cdot Ly, \quad v_{Single} = \frac{v_0}{1 + (v_0/c_n) \cdot \Theta_{nRad} \cdot Ly}, \quad v_{Double} = \frac{v_0}{1 + (v_0/c_g) \cdot \Delta\Theta_g}$$

$$\Delta\Theta_g = \left| 90^\circ - \Theta_{FiberDef.} \right|$$

with  $\tau_0 = 5.81$  min.,  $v_0 = 6.48$  sqft/min.,  $c_n = 1.8e+4$  (cuft rad.)/min., and  $b_n = 7.6e-2$  min/(ft rad) determined from the previous experiments. Here  $\Theta_n$  [rad] stands for the normal bent angle and  $\Theta_g$  [rad] represents a measure of the geodesic bent angle. The missing coefficient turns out to be equal to  $c_g = 2.5e-1$  (sqft rad.)/min.

The model is based on the assumption that sharp bend ( $R < \text{Endeffector size}$ ) causes a simple time delay, which is accomplished here by an additive time penalty. In contrast a smoothly bent section ( $A_{single}$ ) or an area affected by double curvature ( $A_{double}$ ) is processed at an overall slower processing velocity  $v_{single}$  and  $v_{double}$  respectively. The size of the 20 parts ranges between 680 – 4,080 sqin (4.7 - 28 sqft) and the area affected by double curvature varies between 21 - 125 sqin (0.15 - 0.87 sqft.), which represents 3% to 6% of the total area. The best fit yields a R-Square value of  $R^2 = 0.95612$  and the max.

error equals 15%. Insignificantly better fits have been achieved by using the 2<sup>nd</sup> Moment or Std. Deviation of the deformation angle as an information measure. However, for simplicity reasons the mean of the deformation angle as an information measure is employed.

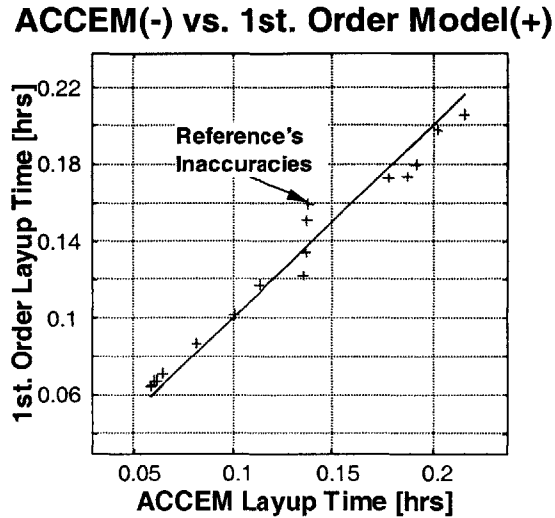


**Figure 5.66 Comparison of Layup Times for Stretch Flanges**

Interesting is the deviation of three data points around 0.14 hrs layup time, which actually account for the maximum error. The maximum errors of the rest of the data points lie within  $\pm 10\%$ , which is considered sufficiently good. Closer investigation reveals, that these are the data points representing the parts, where the flange width was varied between 1" and 4". FiberSim© records higher deformation angles with increased flange width, however the ACCEM model for woven material does not account for such an effect. This is surprising, in particular since the ACCEM model for tape layup clearly includes these obvious effects in its complexity model. It is therefore assumed, that the ACCEM benchmark for Woven Material has some shortcomings whereas the new 1<sup>st</sup> Order Model accounts for the described effects.

Shrink Flange

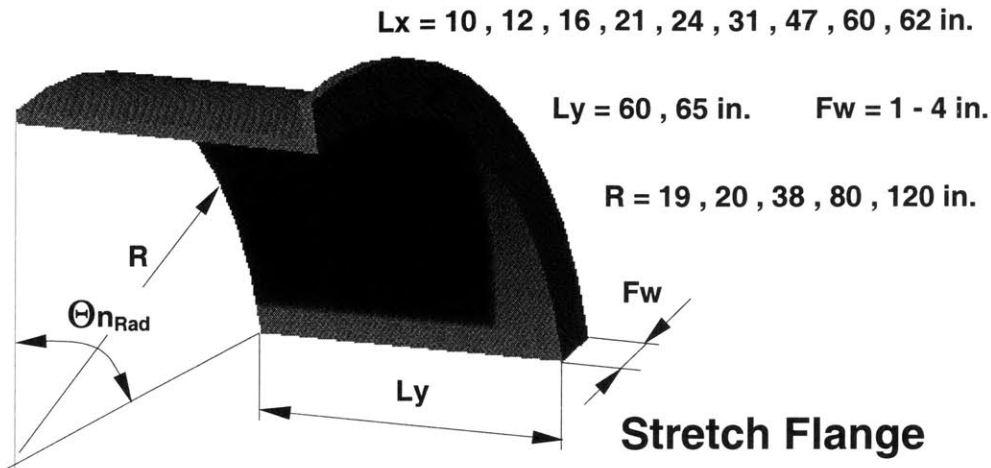


**Figure 5.67 Layup of a Shrink Flange using Woven Prepreg**

All the parameters are now known and when using the same 1<sup>st</sup> Order Model as described in the previous paragraph the hand layup time for a part can be estimated. The model accounts for size and the complexity caused by single and double curvature. The new model is tested by calculating the production layup times for a family of 20 different shrink flanges and comparing the results to the ACCEM reference model. As seen in Figure 5.68 the new model is reasonably accurate. The comparison to the ACCEM model results in a R-Square value of  $R^2 = 0.96261$  and a maximum error of 15.5%.

**ACCEM(-) vs. 1st. Order Model(+)**

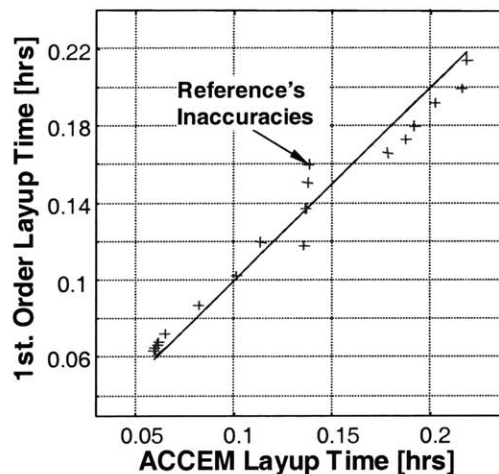


**Figure 5.68 Comparison of Layup Times for Shrink Flanges**

### Summary of the Time Estimates for Hand Lay-Up

The newly developed model for the layup time estimation of woven material proved to be reliable and accurate. The layup times per ply for simple parts such as flat panels, radially bent panels and L-Profiles have been calculated. These parts were also used to determine the factors for reduced processing time ( $c_n$ ) and increased time constants ( $b_n$ ) for radial and sharp bents, respectively. Anyway, as seen from the data, the influence of large radial curvature on the total layup time can be neglected. This is reflected in the very high value for  $c_n$ .

The obtained parameters were introduced into the new model and the according parameter ( $c_g$ ) for double curved part was determined by means of the stretch flange data. A total of 80 different ACCEM parts were used to determine the required parameters. Subsequently, the complete model was employed to calculate layup times for 20 different shrink flanges and it was found, that the model could verify the ACCEM [5] benchmarks. However, future studies have to fine tune the model to actual production parts. Here it could become necessary to incorporate more sophisticated information measures or even calculate the layup time for each discrete element based on the mesh provided by FiberSim©.

(This page is intentionally left blank.)

4430-61



## 6 Production Equipment Costs

Initially much of the production equipment was custom-built, however as the composite industry evolved, standards for the machinery have been developed. As more suppliers enter the market, the determination of equipment prices becomes easier. However, pricing information is still difficult to obtain and is subject to wide variations. The apparent inconsistent pricing data is mainly due to the competitive situation within a specific equipment market and depends on the strategy of each supplier. Since, the number of customers for composite production equipment is still limited, producers segment the market and give different pricing concessions to different customers. Sometimes, there are only 2 to 3 producers for one equipment type and even these few differentiate themselves by focusing either on the market for small, medium, or large size machines. As a result, many producers enjoy a small monopoly within their niche and the relatively small market size often prevents further competition from entering. Therefore, the collected pricing information should be treated with some caution and new quotes should be requested if necessary. Also as some of the machines are still custom-built, prices can be negotiated individually in particular if several workstations are ordered. Another major price driver are built-in features, such as computerized process control, and monitoring systems. The electronics are mainly of the shelf, but are adapted specifically for the application at hand. Therefore, the most commonly requested equipment configuration was identified during conversations with manufacturers in an attempt to make the pricing information comparable and practical to use. The prices are then listed in dependence of the major process discriminators, such as equipment size, capacity, or performance. In the cases where plentiful and distinct pricing information is available, the prices are plotted in graphs versus the major cost driver. The Internet and buyer guides [1-4] are used extensively to identify suppliers for Hand Lay-Up, Resin Transfer Molding, Automated Tow Placement, Pultrusion, Double Diaphragm Forming, and Autoclave equipment. Some suppliers have requested confidentiality, however the majority was willing to share pricing information openly. The Reference section 6.9 lists the various suppliers in alphabetical order.

## **6.1 Hand Lay-Up Equipment (HLU)**

Since the Hand Lay-Up of composites is dominated by manual process steps, only a minimal amount of equipment is required. The costs for compaction rollers and worker protection gear such as coats, gloves and in some cases respirators is negligible and therefore not listed as part of this study. Tooling for the layup of composites is considered separately and is discussed in Chapter 7.3. Future studies should include the costs for laser projection equipment, which is employed increasingly in layup operation of complex parts and laminates. The projector beams the position, the ply number and the fiber direction onto the tool and thus aides the operator with the layup.

## 6.2 Resin Transfer Molding Machines (RTM)

The costs of RTM injection equipment can vary greatly depending on the capabilities of the machine. The basic equipment version will mix and inject the resin mechanically at pre-set mixing ratios. More advanced models also store the binder and catalyst, feature adjustable mixing ratios, or include monitoring devices to check the pressure and temperature of the resin. An RTM machine can dispense resin from a storage unit as small as 2,100 cubic centimeters up to 500 gallons tanks. The Resin is injected at pressures between 100 psi (0.7 MPa) and 600 psi (4.1 MPa). In general, there are two types of injection machines in use today. The first type is flow rate controlled and uses spindle extruder mechanisms powered by an electrical motor. The second type of machines injects resin at a constant pressure and is based on a piston type apparatus driven by compressed air. The simplicity of the latter type is often reflected in the price, however they have a limited shot size, whereas extruder type machines do not possess such limitations. Prices for the piston type machines range around \$8,000 whereas extruder types cost around \$60,000. The hourly costs can be calculated according to Equation 4.18 and Chapter 9.1.3 presents an actual calculation example.

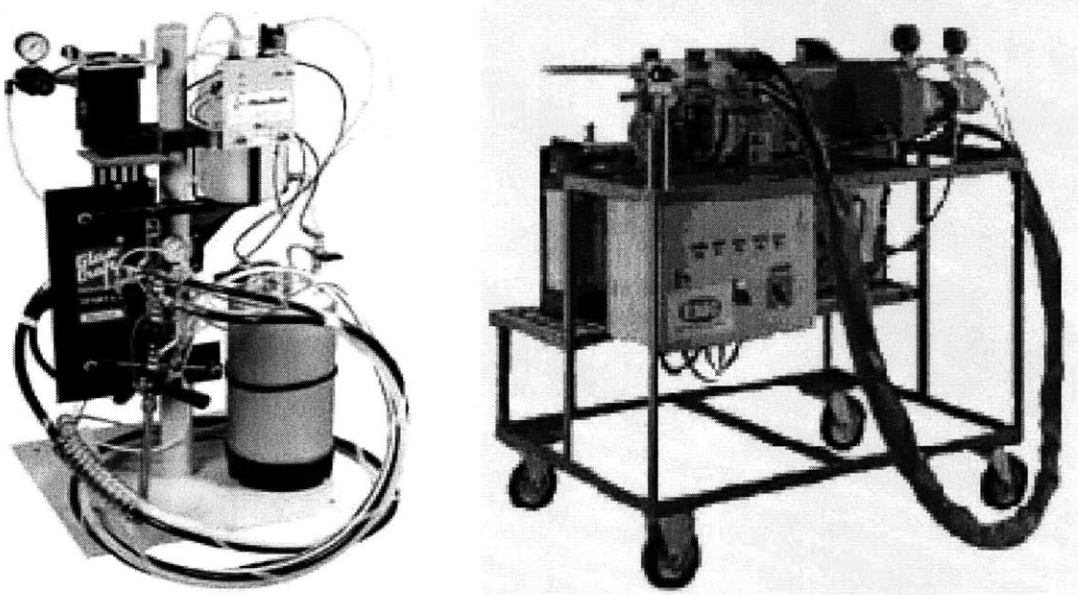
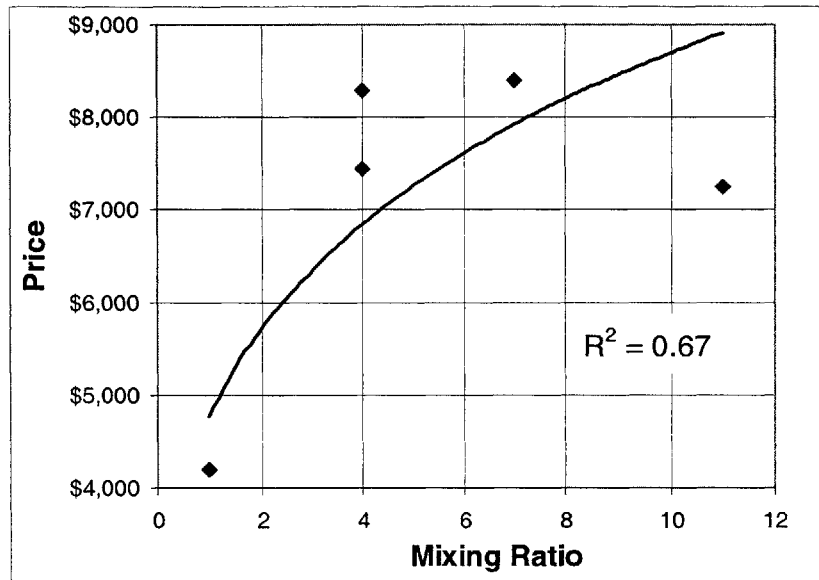


Figure 6.1 RTM Injection Equipment (Piston Type, Extruder Type) [20, 22]

Aside from these basic differences the prices of RTM equipment can also vary due to differences in resin storage capacity, automation features, mixing ratio, temperature range and pressure capacity. The costs of piston driven RTM dispenser are plotted in Figure 6.2 versus the varying mixing ratios (Manufacturers A & B). These very basic machines do not boast any data acquisition, automated pressure, or temperature monitoring features.



**Figure 6.2 RTM Equipment vs. Mixing Ratio [29]**

In contrast, Figure 6.3 mainly shows the prices for extruder type RTM equipment. The machines generally include the dispenser, the mixer and alternatively come with or without data acquisition capabilities (Manufacturer C). For comparison, the prices for both a pneumatic pressure-controlled device and an electric flow-controlled device are shown. The figure shows how the prices fluctuate with the injector shot size, which is generally measured in cubic centimeter ( $\text{cm}^3$ ). The base price of the basic machine is about \$29,000 and for each  $1,000 \text{ cm}^3$  of shot size an additional \$5,650 have to be taken into account. When furnished with the data acquisition equipment \$10,000 have to be added to the original base price.

Manufacturer I has submitted two quotes for custom-made machine. The first quote for an RTM metering, mixing and dispensing system is approximately \$55,000. The

machine includes two 5-gallon tanks for the component materials (resin & catalyst), has a maximum temperature range of 350°F (175°C) and 600 psi (4.1 MPa) maximum output pressure. Shot size and ratio of component mixing can be adjusted manually in this machine.

The second custom-made machine, with the same basic capabilities as the one described above additionally features a digital, metering, mixing, and dispensing system. The system allows the injection parameter to be preset and to be kept in memory for various molds. The controlled parameters include the mixing ratio, shot-size, output rate, and mixer speed. The system is fully automatic and adjustable and costs from \$150,000 to \$225,000 depending on its complexity. Options such as a vacuum chamber sized at 5,500 in<sup>3</sup> would cost an additional \$40,000. The vacuum chamber is used to degas the resin and therefore prevents the forming of voids within the part, resulting in improved part quality. Pressure transducers can be added to the metering pump in order to maintain the preset pressure for a cost of \$5,000 to \$10,000.

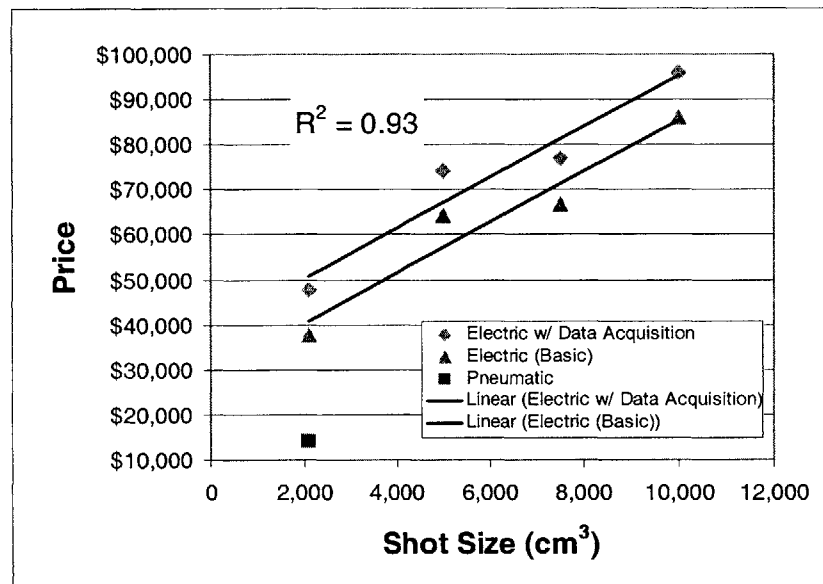
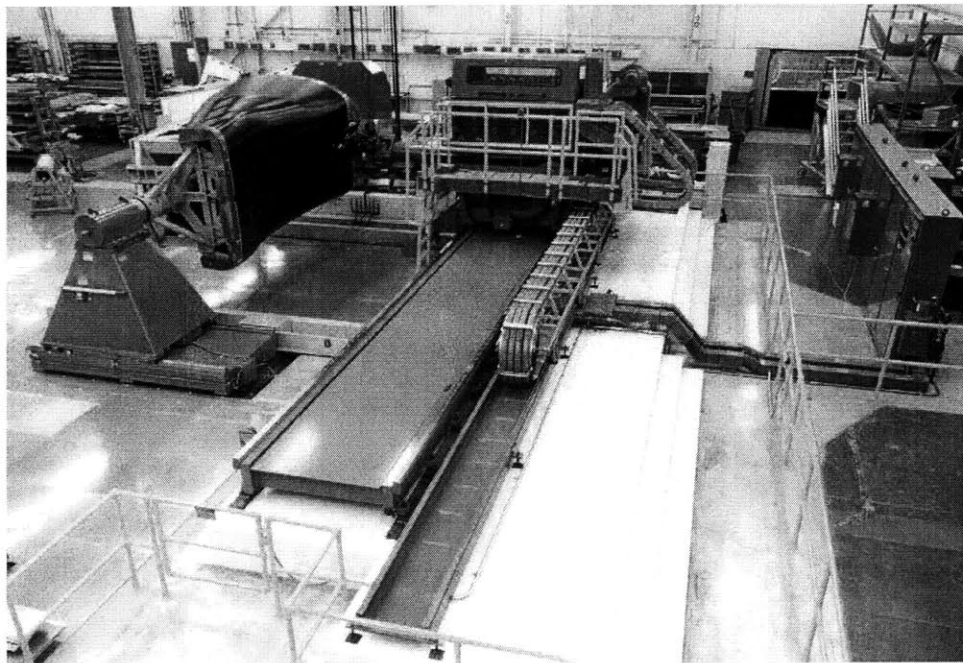


Figure 6.3 RTM Equipment vs. Shot Size [25, 29]

Manufacturers and suppliers of RTM equipment are Venus-Gusmer, Radius Engineering, Advanced Process Technology, Liquid Control Corporation, RTM Systems, GS Manufacturing, and Glas-Craft.

### 6.3 Automated Tow Placement Machines (ATP)

The market for ATP machines is still quite small and therefore it is difficult to determine a reliable price for these enormous machines. Because of their similarity, prices have been collected for both Automated Tow Placement machines and Tape Laying machines. The former are generally more complex, since they commonly lay down 3 to 24 individual fiber tows with a width of 1/8" to 1" each (see Figure 6.4). Tape Laying machines use only a single tape with a width of commonly 3" to 12" (see Figure 6.5). The machines are typically 30 feet by 20 feet or greater and have the capability of making parts as large as 26 feet by 140 feet. They are equipped with multiple tape or tow cutters and are fully automated with seven to eleven CNC axes.



**Figure 6.4** ATP Machine (Viper 1200) [14]

Automated tow placement is primarily used in the aerospace industry for large and expensive parts. Currently, there are approximately 40 - 45 operational machines of this type worldwide [28], and because of the small market, the machines are typically custom-built. An individual manufacturer may produce between 0.5 to 3 machines per year. The limited production volume and the high specialization further complicates the pricing of

these machines. The main cost driver are the engineering costs due to the technical complexity and performance requirements of the machines. Added features to the basic version will further increase the price of the machine. Changes that are customarily made to the standard machine are changes in length, changes in width, or changes specific to national safety regulations. Also the user interface and CNC programming is often adapted according to customer preferences. The cost to change the capabilities of length for the manufactured parts is minimal. However, the incremental cost for adding 10 feet in the width of the machine is approximately \$100,000. Sample pricing quotes promote the understanding of how custom-built machines are priced. The hourly costs can be calculated according to Equation 4.18 and Chapter 9.1.4 presents an actual calculation example.

Manufacturer A has provided pricing information for automated tow placement (ATP) equipment. The machine is capable of placing as many as 32 tows each 1/8 of an inch wide with a maximum speed of 1,200 in/min. The machine features a seven-axis CNC placement system and achieves a ply orientation accuracy of  $\pm 0.5$  degrees. The travel of the machine is 30ft x 28.5ft x 5ft. A machine of this type costs between \$4.5 Million to \$6 Million. However, tow placement machines that are capable of making smaller parts can be found for as low as \$3 Million.

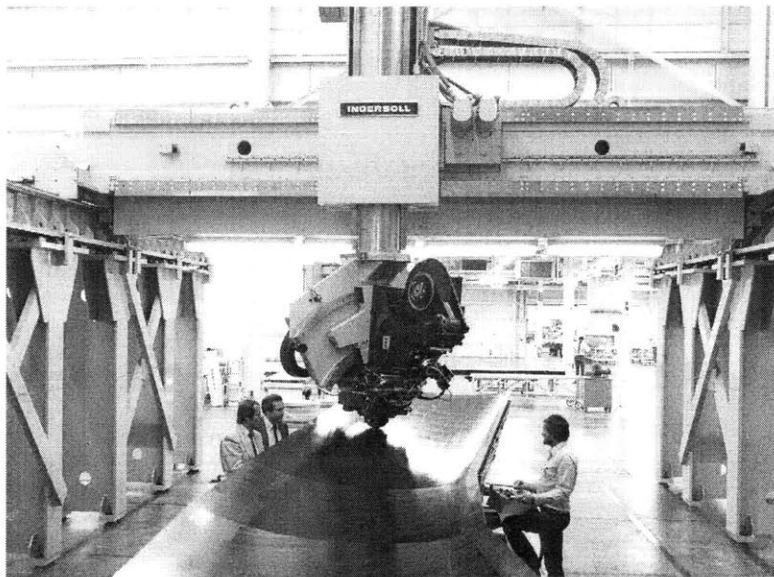


**Figure 6.5** Tape Laying Machine [21]

The tape laying machine from Manufacturer B and has the capability of making parts as large as 25ft x 120ft with an accuracy of  $\pm 0.02$  inches, and was quoted with a base price of \$3.5 Million. The machine boasts an 11-axis CNC control system and can hold 6 in. and 12 in. wide tapes. It also detects tape defects, features a tape lineup system, and cuts tapes with two ultrasonic knives. Adding software, postprocessor, part history recording, and installation costs to the same machine would raise the cost to approximately \$4.2 Million. To make the same machine at half the size would cost approximately 5% to 7% less than the price quoted above.

The second tape laying machine quoted comes from Manufacturer C and is 16 feet wide and can make parts as long as 140 feet. The machine is priced at a total of approximately \$2.5 - \$2.6 Million. However, the same machine with all features, including software, safety sensors, and two traveling shears, would cost \$4.25 - \$4.8 Million. An addition of 20 ft in width would increase the cost by \$200,000.

The major producer of ATP machines is the Cincinnati Machine Company. Tape laying machines can also be procured from M. Torres (Spain) and Ingersoll Milling Machine Company (USA).



## 6.4 Pultrusion Machines (PUL)

The equipment for thermoset pultrusion consists of several subcomponents. Firstly, the creel stand holds the spools of dry fibers, which are subsequently passed through the resin bath for impregnation. The wet fibers are then led through the heated forming and curing die where the part cross-section is created and the resin is solidified. Next follows the cooling section of the die from which the finished profile exits and is gripped by the pulling mechanism. In general, two types of puller mechanisms are common. The reciprocating puller is usually less expensive and features two grippers, which intermittently grab the profile and pull it continuously through the die (see Figure 6.7). The other approach is features two continuous belts, which clamp the part from both sides and move it forward (see Figure 6.6). Electrical and hydraulic systems are in service to drive the pullers. The reciprocating has a slight advantage when pulling parts of complex cross-sections, whereas the continuous belts exert less damaging force onto the profile. At the end, a cut-off saw parts the continuous profile into individual pieces.

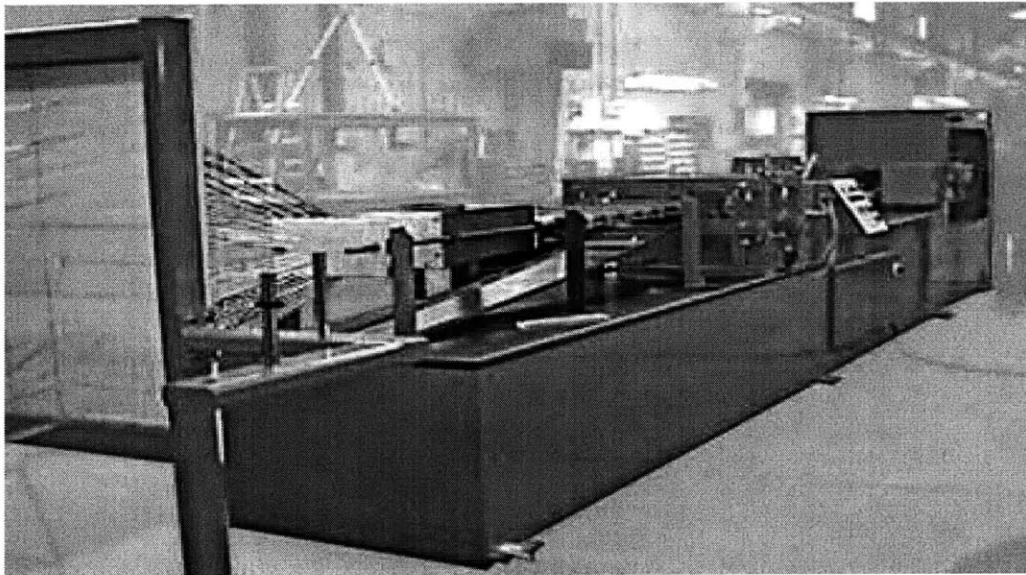


**Figure 6.6 Pultrusion Equipment (Belt Type) [17]**

The required pulling force increases with the part cross-sectional area and can be as little as 500 lbs for a machine with an envelope area of 1 in<sup>2</sup>. For cross-section as large as 1,440 in<sup>2</sup> the pulling force can easily reach 50,000 lbs. The machine prices range

between \$100,000 and \$400,000. Aside from the pulling mechanism the costs for pultrusion equipment is mainly driven by the maximum pulling capacity generally measured in pounds (lbs). Due to the correlation between part cross-section and pulling force, one observes an increase in prices for machines, which are able to handle larger parts and therefore require higher pulling strength. Figure 6.8 plots the equipment prices versus their maximum pulling force. The base price for commercial pultrusion equipment is approximately \$120K and one has to spend an additional \$3,700 for every 1,000 lbs of pulling force. The hourly costs can be calculated according to Equation 4.18 and Chapter 9.1.5 presents an actual calculation example.

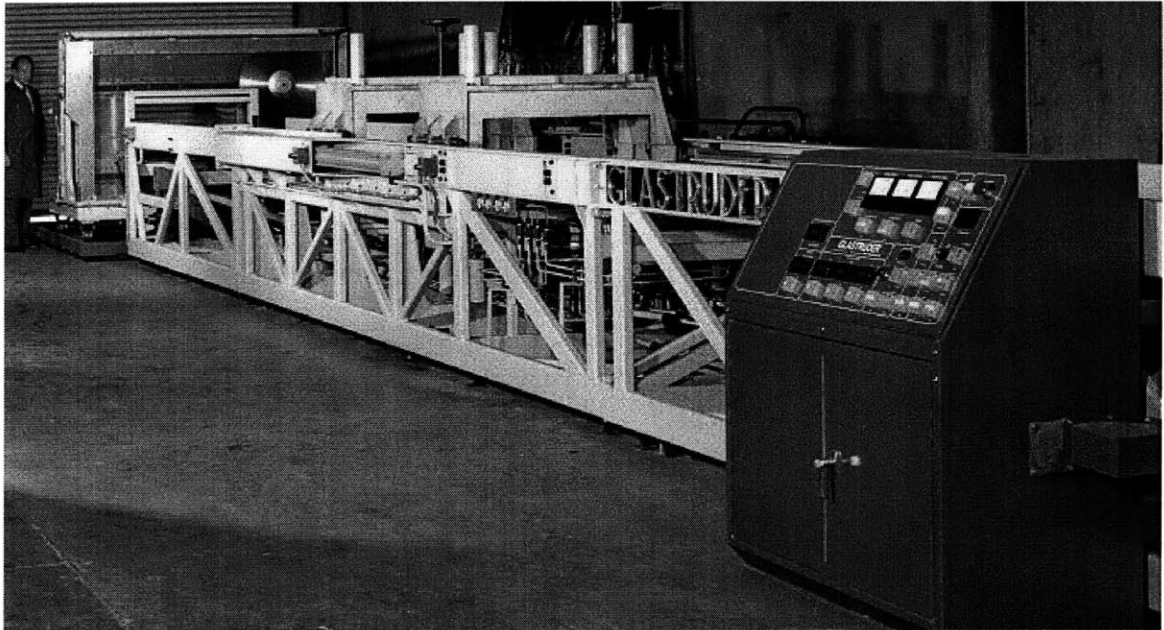


**Figure 6.7 Pultrusion Equipment (Reciprocating) [19]**

In addition, the prices are plotted versus the maximum part envelope, which can be accommodated by the machine. Figure 6.9 displays the relationships for machines with reciprocating and with belt driven pulling systems. The data shows that a machine featuring the belt system costs approximately \$15,000 to \$35,000 more than the same puller with a reciprocating pulling mechanism. The base price for the machines is around \$132K, however one has to pay around \$750/in<sup>2</sup> envelope area for a belt driven versus \$390/in<sup>2</sup> for a reciprocating type.

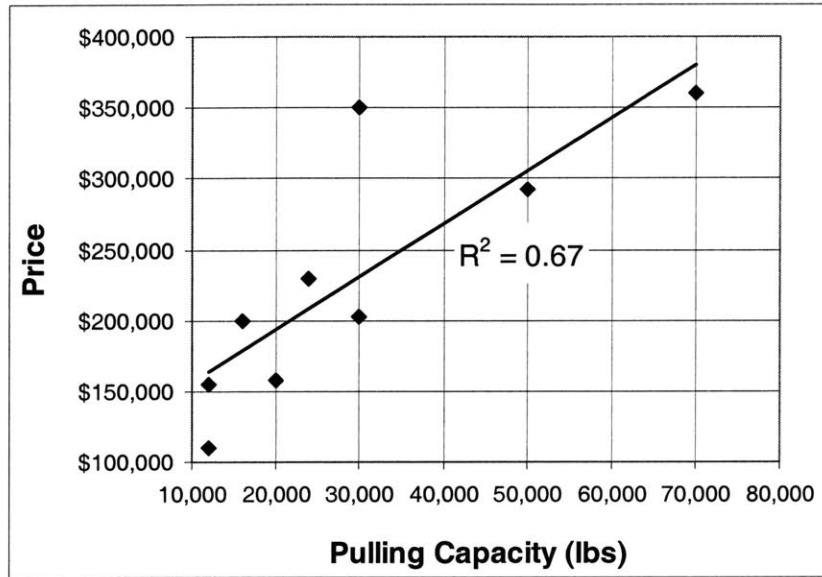


**Figure 6.8 Pultrusion Equipment Price vs. Pulling Capacity**

Manufacturers of pultrusion equipment include Martin Pultrusion Group, Strongwell Machinery & Licensing, Entec Composite Machines.

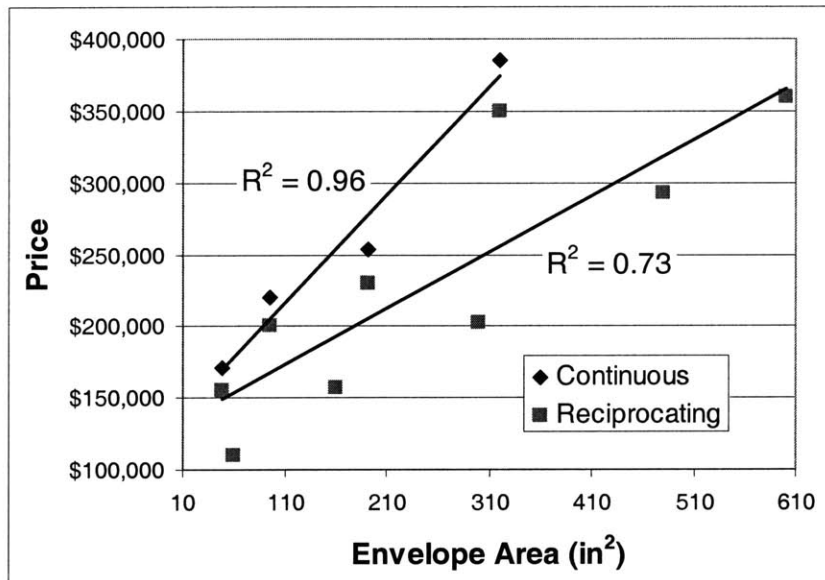


**Figure 6.9 Pultrusion Equipment Price vs. Part Envelope Area**

## 6.5 Double Diaphragm Forming Machines (DDF)

Although, economically very promising the double diaphragm forming process is not yet installed on a large industrial base. Only recently, a major aircraft manufacturer introduced a newly developed machine into their production facilities [6]. Therefore, the few machines in production are mainly custom-built and often undergo many iterations and improvements. Reliable pricing information is consequently not available. Figure 6.10 shows the custom-built machine used for the production of structural aircraft components.

The machines generally consist of a tank substructure, which is airtight and contains the vacuum during forming. A tank substructure is needed to encase the tool holder and is sealed by the diaphragms. Furthermore, a vacuum pump provides the forming and clamping pressure in connection with the two elastic diaphragms. The heater/cooler system serves to soften the resin prior to forming and to stiffen the part in order to lock it into its formed shape.

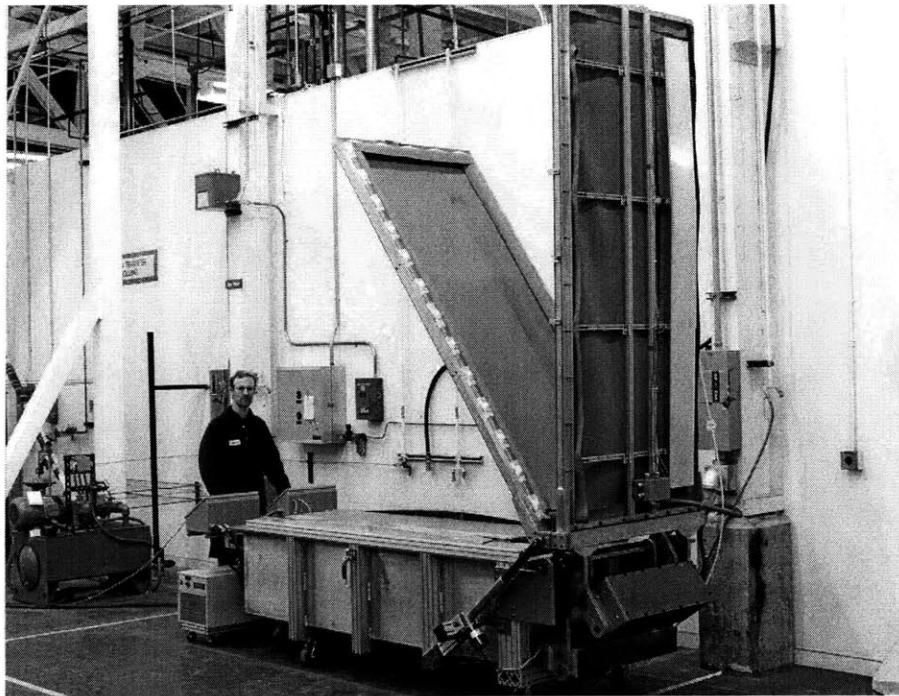


**Figure 6.10** Custom-built Double Diaphragm Forming Machine [6]

The machine seen in Figure 6.10, features a forming area of about 8 feet by 3 feet. Since the machine was produced for research purposes at MIT, various design changes were carried out. However, the creator of the machine estimated the cost to manufacture the machine to be between \$80,000 and \$100,000. The hourly costs can be calculated according to Equation 4.18 and Chapter 9.1.6 presents an actual calculation example.

One manufacturer of composite manufacturing equipment, Radius Engineering, is in the initial stages of finding investors in order to manufacture diaphragm-forming equipment. The Radius representative anticipated that if the proposal is accepted, they will be manufacturing equipment within a few years.

## 6.6 Autoclave Equipment

Autoclaves have become quite common for the consolidation and cure of advanced fiber reinforced composites. A number of suppliers produce these pressurized ovens at various sizes and performance characteristics. For composites consolidation pressure ranges between 80 psi (0.5 MPa) to 100 psi (0.7 MPa) and curing temperatures from 250°F (120°C) and 850°F (450°C) depending on the resin system. The investment cost for an autoclave lies between \$80,000 and \$2,500,000. The major cost driver is size among the maximum temperature and pressure capability. Optionally, computerized control, monitoring and data acquisition equipment can also add significantly to the procurement costs. Autoclaves come in dimensions of approximately 3 feet in length and 1 foot in diameter up to 60 feet length and 20 feet diameter, if not larger. Figure 6.11 shows a photograph of such a large autoclave. In addition, compressed air and vacuum have to be supplied including the necessary auxiliary equipment. Air, nitrogen, or carbon dioxide are commonly employed as pressurizing media and often require special storage cylinders. Autoclaves are further differentiated by the way they are heated. Gas is usually used for large autoclaves while electricity is employed for smaller systems.

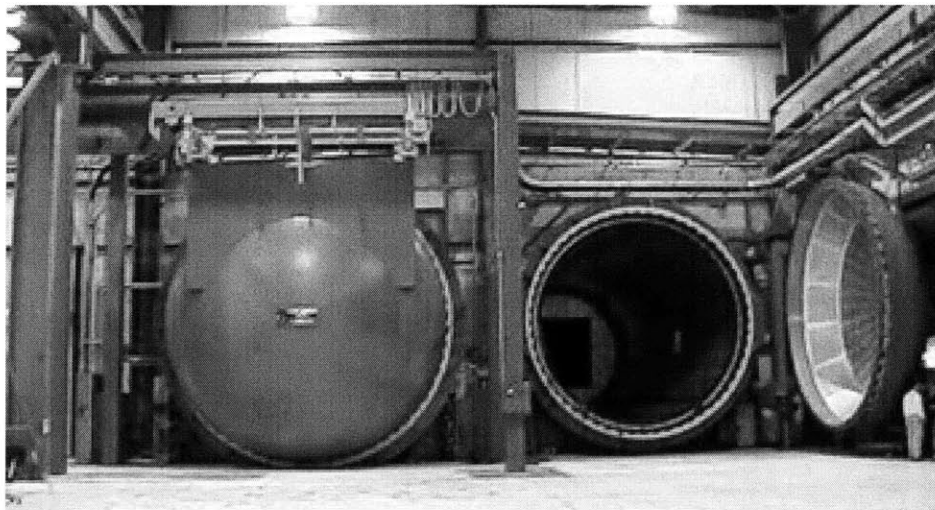


**Figure 6.11** Very Large Autoclave (D18ft x 60ft) [27]

Prices have been collected from 5 different manufactures and are listed in Table 6.5 in the Appendix 6.6. In order to retain anonymity, capital letters in parentheses indicate the

different suppliers. A closer look at Table 6.5 shows the effects of the previously identified cost drivers. Generally, the diameter has a stronger effect on the price than length of the autoclave.

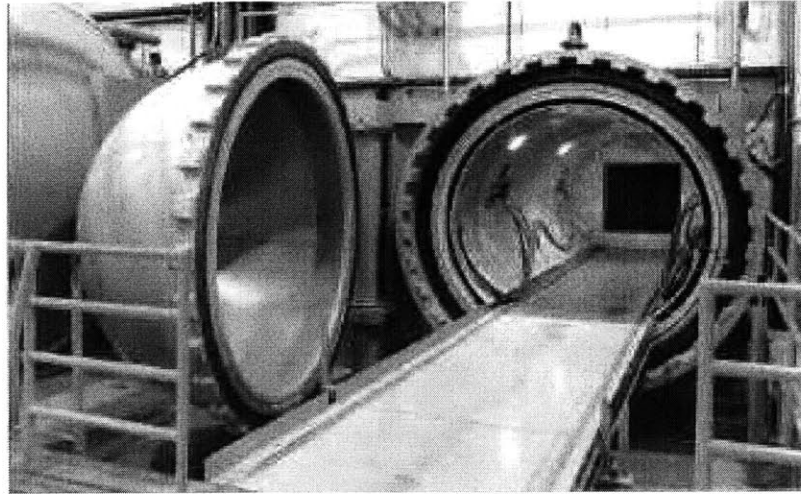


**Figure 6.12 Medium to Large Autoclave (D5ft x 12ft) [12]**

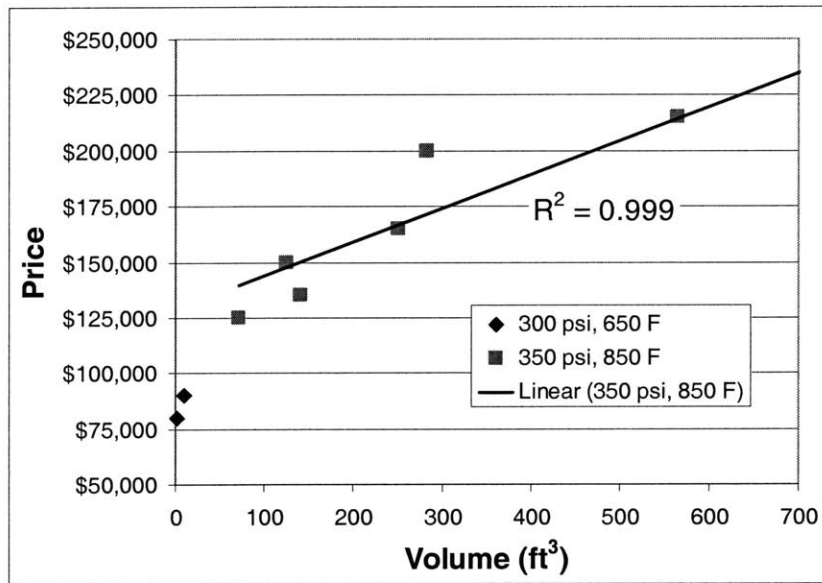


**Figure 6.13 Autoclave Price vs. Internal Volume**

Figure 6.13 plots the price versus the internal volume of an autoclave considering various temperature and pressure constraints. Any price differences due to optional computerized control or data acquisition equipment are not considered in the plot. The data point for

Model 7 (7,000ft<sup>3</sup>, \$1.2M) is not shown but correlates well with the other data. The results indicate a strong relationship between volume and price for an autoclave with a maximum working pressure of 350 psi (2.4 MPa) and a temperature range of up to 850°F (450°C). From regression, one can derive a base price of approximately \$130K. As a rule of thumb every 1,000 ft<sup>3</sup> of internal volume cost an additional \$150,000. The hourly costs can be calculated according to Equation 4.18 and Chapter 9.1.2 presents an actual calculation example.

ASC Autoclave Division, Thermal Equipment Corporation, McGill Air Pressure Corporation, and Melco Steel are some of the leading autoclave manufacturers.



## 6.7 Vacuum Bagging Material

The vacuum bagging of parts before cure in an autoclave or oven requires a variety of different films, cloth and other materials. One has the choice between reusable and non-reusable bagging material. Non-reusable material is used in applications of small to medium production volumes or whenever complex shapes have to be bagged. It is by far the most commonly used method for vacuum bags. The material consists mainly of breather plies and bleeder plies, which absorb the excess resin. Peel plies or release films are used to ensure the part does not stick to the tool. The actual vacuum bagging film covers the part and special sealant tape seals the perimeter [5]. Figure 6.14 schematically shows a cross-section of a vacuum bagged composite.

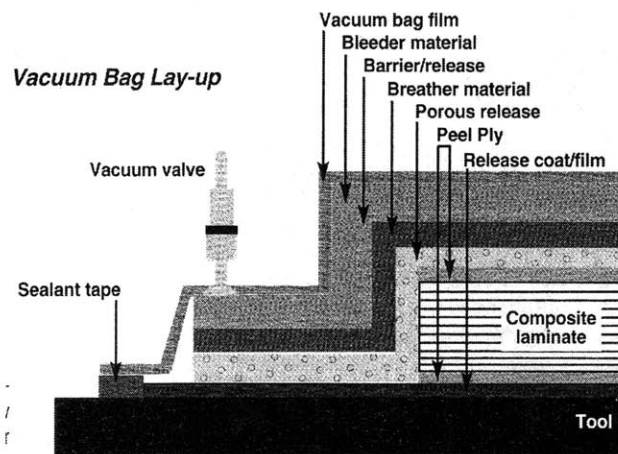


**Figure 6.14 Vacuum Bagging [5]**

Table 6.6 in the Appendix 6.10 lists the prices for the most commonly used materials. Each cost item is then added up and normalized by the area while considering about 10% material waste. The costs per square foot of part area range between  $\$2.30/\text{ft}^2$  and  $\$2.50/\text{ft}^2$ . Figure 6.15 plots the maximum and minimum prices for hand lay up equipment versus the part area. The costs for manual cutting equipment, lab coats, gloves, and respirators can be neglected.

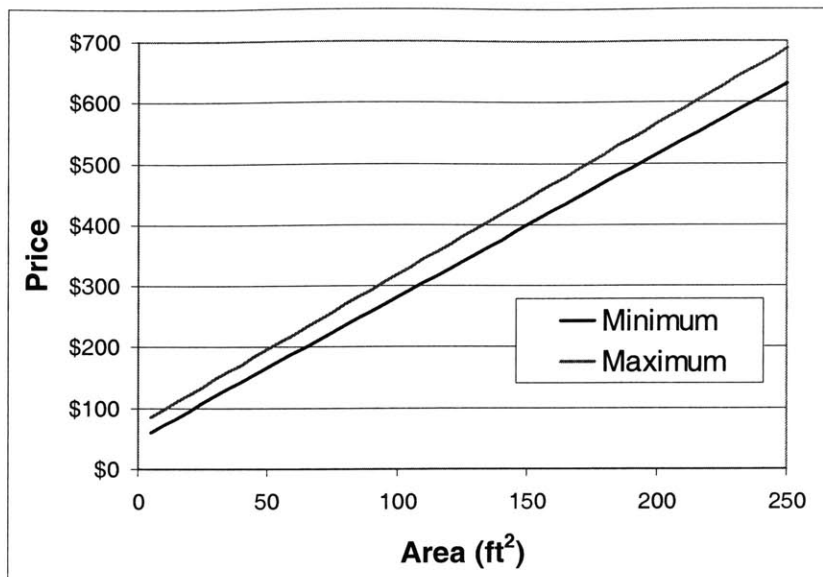


**Figure 6.15 Vacuum Bagging Prices vs. Part Area**

The major suppliers for bagging material are Airtech, Richmond Aircraft Products, Torr Technology, and Bond Pro USA.

## 6.8 Assembly Equipment

As the use of composite materials becomes more widespread, the equipment used for assembly will become more sophisticated and efficient. Currently, most composite structures are assembled manually using bolts and rivets identical to the ones described in Chapter 3.3.4. Some applications use adhesive bonding, but so far aerospace designs have relied on mechanical techniques for safety reasons. Composites are generally assembled by workers with powered hand tools used to tighten the connections. These power tools are not dedicated to a particular task and their costs are mostly negligible compared to the overall production costs.

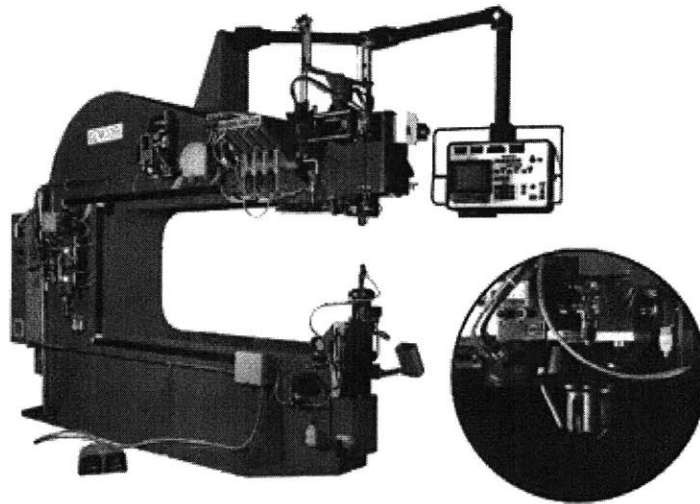


**Figure 6.16** Automated Fastening Machine [9]

However, with increasing production volume of assembled composite structures the implementation of Automated Fastening Systems (AFS) can shift the assembly economics. These systems have been used extensively in the assembly of metal (aluminum) aircraft structures. The production volumes seen in the commercial aircraft market justify the high initial investment in these machines, which speed up the fastening process considerably. So far, the newness and the low volume of composite assemblies have prevented the use of AFS beyond the lab scale according to an industry expert [8]. Since technical feasibility does not appear to be an issue, the following paragraphs outline the costs if AFS are considered in future composite production. Information

provided by a leading AFS supplier gives an overview of how costs are driven by the size and the complexity of the machines.

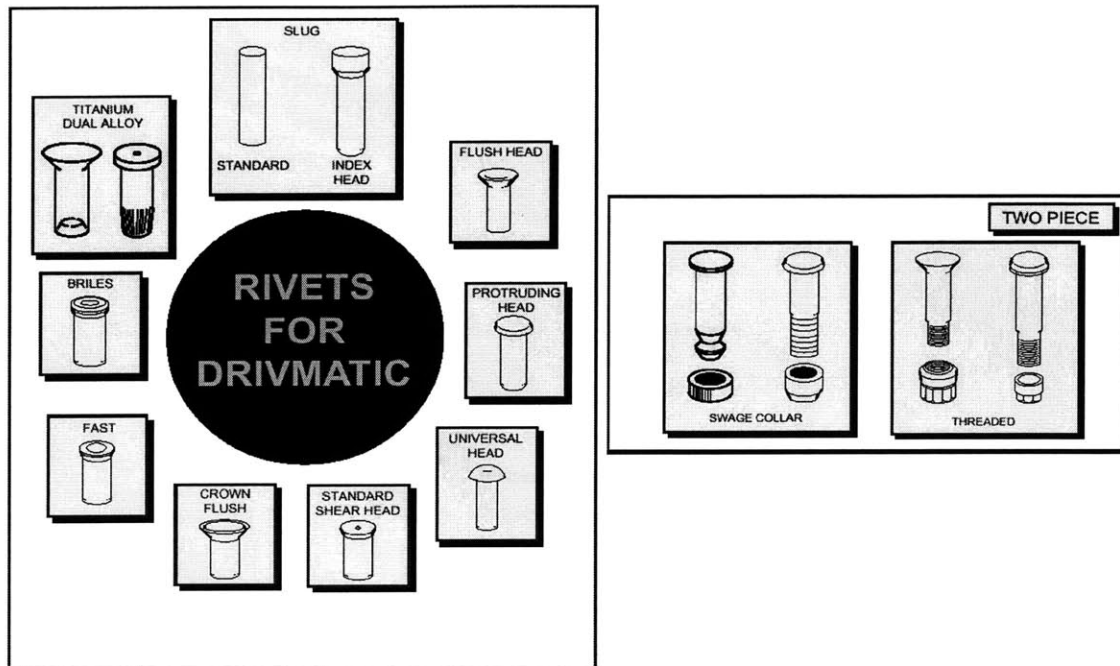


**Figure 6.17** Typical One- and Two-Piece Fastener Geometries [9]

### AFS Performance

Before discussing the costs in detail, a brief description of the machines' functionality provides a better understanding of their performance and ultimately their cost drivers. The machines drill and countersink the burr-free holes for the fasteners according to very tight tolerances. The metal chips from drilling and deburring are removed during the operation. The fasteners are then automatically fed to the machine head and installed into the holes. Because of the tight tolerances and the interference fits required in metal assembly a computerized sensor and control system monitors insertion force among other process parameters. Once installed the fasteners are tightened before the machines moves to the next position. Figure 6.18 schematically outlines the basic fastening cycle for one- and two-piece fasteners. Generally, the application of sealant is only used in connection with metal assemblies and protects against corrosion and fuel leaks. Regardless, whether the fastener is a threaded bolt or a blind rivet the specialized

machine heads can execute the assembly speedily. Speed is one of the major advantages of the Automated Fastening Systems, but also the consistency and the quality of the joint lead to higher factory throughput. Once the workpiece is moved into the machine, the system installs about 10 to 15 fasteners per minute, including drilling, fastening, and repositioning. Experience shows that the machines generally have an uptime in excess of 90% [8]. Sensors and data acquisitions systems monitor and document the joining process and contribute to product safety. Figure 6.16 shows an example of such an Automated Fastening Machine. For a more in-depth description of the fastening process and its economics, the reader is referred to the thesis of T. Speller [8].

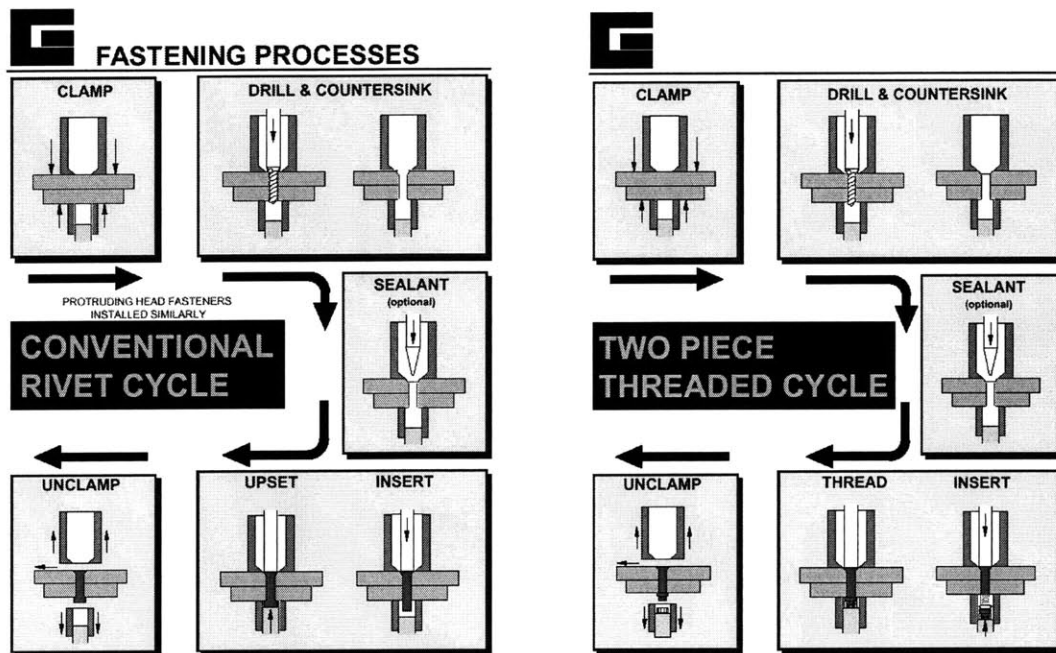


**Figure 6.18** Typical Automatic Fastening Cycle [8]

### AFS Costs

The costs of the AFS machines are primarily determined by their size and their performance capabilities. Not surprisingly the cost drivers for the machines are similar to the generic cost drivers for assembly as discussed in Chapter 5.2.7. Apart from the size of the structure to be assembled, the number and the complexity of the components can influence the machines' specifications and ultimately its price. Furthermore, the fastener type determines the head design of the machine and therefore the costs. Machines

require a higher degree of sophistication to perform the installation of complex threaded two-piece fasteners as opposed to rivets. Also as the joining speed increases, in order to fulfill higher throughput requirements, the design becomes more demanding and consequently more expensive. Lastly, the costs of computerized sensors and process control equipment also contribute considerably to the total costs. Admittedly, the resulting combinations and cost consequences can be numerous and therefore the machines are divided into different size and complexity categories. The size classification into small, medium and large relates to the machine envelope and the lengths of the various axes. Derived from Table 6.7 in the Appendix 6.10, Table 6.1 defines the dimensional boundaries of these categories.

**Table 6.1 AFS Machine Size Categories**

<i>Small</i>			<i>Medium</i>			<i>Large</i>		
Length [ft]	Depth [ft]	Height [ft]	Length [ft]	Depth [ft]	Height [ft]	Length [ft]	Depth [ft]	Height [ft]
40	8	6	50	10	8	65	13	10

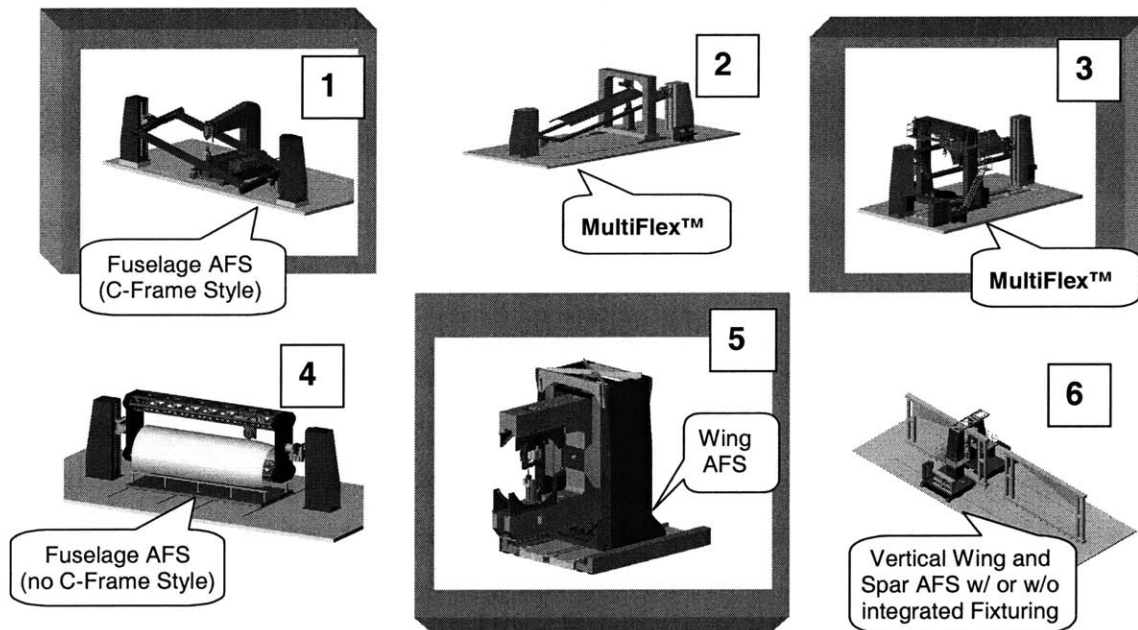


**Figure 6.19 ESCRT™ AFS Machine Concepts [9]**

The complexity definition follows the illustrations in Figure 6.19 and considers the major costs drivers such as fastener type, throughput performance, electronics, and part complexity.

From the information listed in Table 6.8 of the Appendix 6.10, a matrix is derived showing the costs of AFS machines. Table 6.2 lists the prices per machine without installation costs depending on the size and the complexity. Of course, the data only gives a limited picture of the actual cost structure and therefore it is recommended to request individual quotes from AFS manufacturers for specific assembly scenarios.

**Table 6.2 AFS Cost Matrix**

<b>Complexity / Size</b>	<b><i>Small</i></b>	<b><i>Medium</i></b>	<b><i>Large</i></b>
<b><i>Low</i></b>	<b>\$1.5M to \$3.5M</b>	<b>\$2.2M to \$4.0M</b>	<b>\$3.0M to \$10.0M</b>
<b><i>Average</i></b>	<b>+10% to +20%</b>	<b>+10% to +20%</b>	<b>+10% to +20%</b>
<b><i>High</i></b>	<b>+20% to +30%</b>	<b>+20% to +30%</b>	<b>+20% to +30%</b>

The investment costs of the AFS machines can be spread over several years. In particular, since the machines are adaptable to various production programs. Therefore, a less aggressive depreciation schedule can be adopted as opposed to assembly fixtures, which are generally dedicated to a specific program. The costs for newly setting up the machines and reprogram them for different assembly scenarios are only a fraction of the initial investment. In general, AFS machines are in service for about 10 years after which they usually undergo a major overhaul and upgrade of their electronics. The hourly costs can be calculated according to Equation 4.18.

AFS in Composite Assembly

For the mechanical joining of composite components the machines will have to be adapted slightly to the specific requirements. According to industry sources, such an adaptation could be performed within a reasonable time period. In general, composite assembly involves more complex fasteners, such as the two-piece threaded fasteners seen

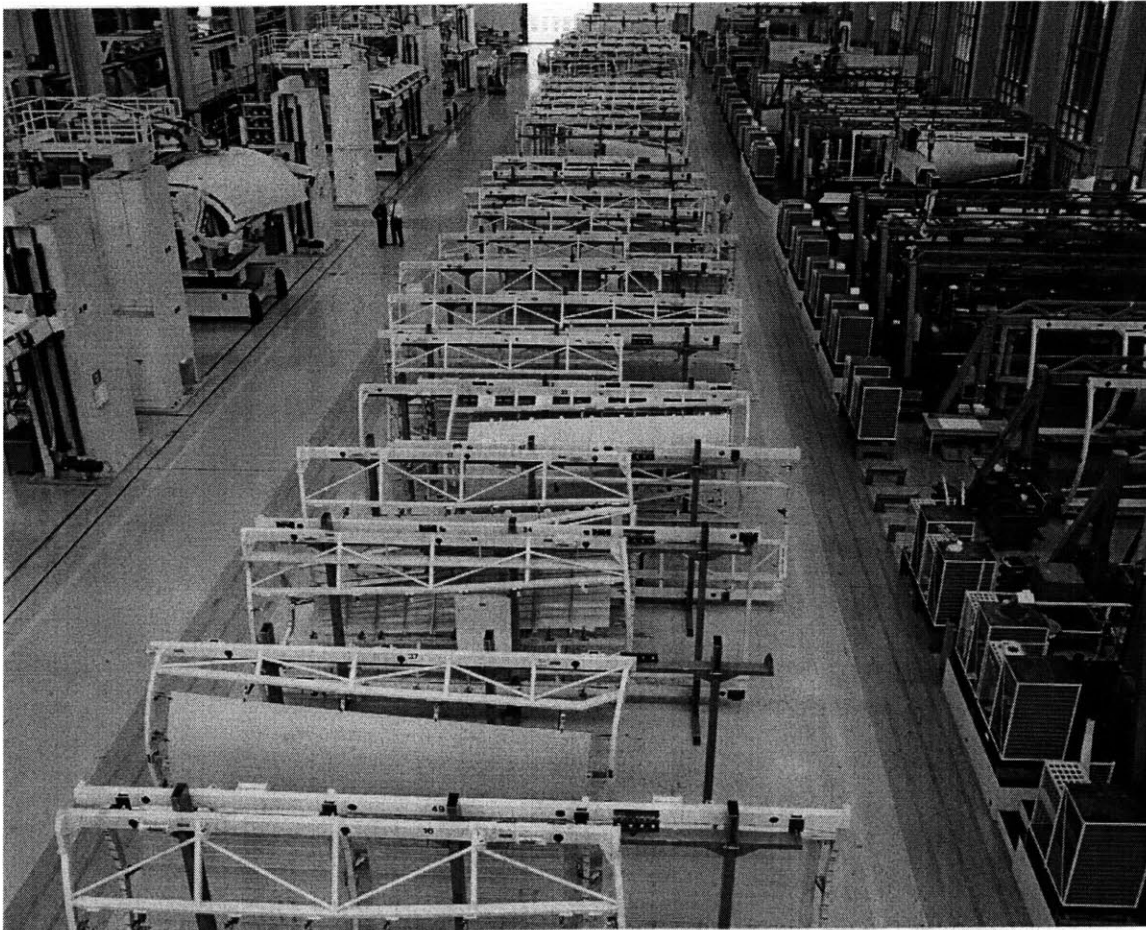
in Figure 6.17. Also, the depth of the countersink needs to be within certain tolerances, which however is more of a challenge for human workers than it is for a machine. The torque on the bolts has to be controlled by the bolt design or by electronic means to avoid crushing and delaminations within the laminate. However, the actual task of inserting the fastener is accomplished more easily when dealing with composites, because composite joints do not require an interference fit as opposed to their metal counterparts. Again, there are no technical hurdles for using AFS in composite assembly only the volume has to be high enough for such a decision to be economical.



### AFS Examples

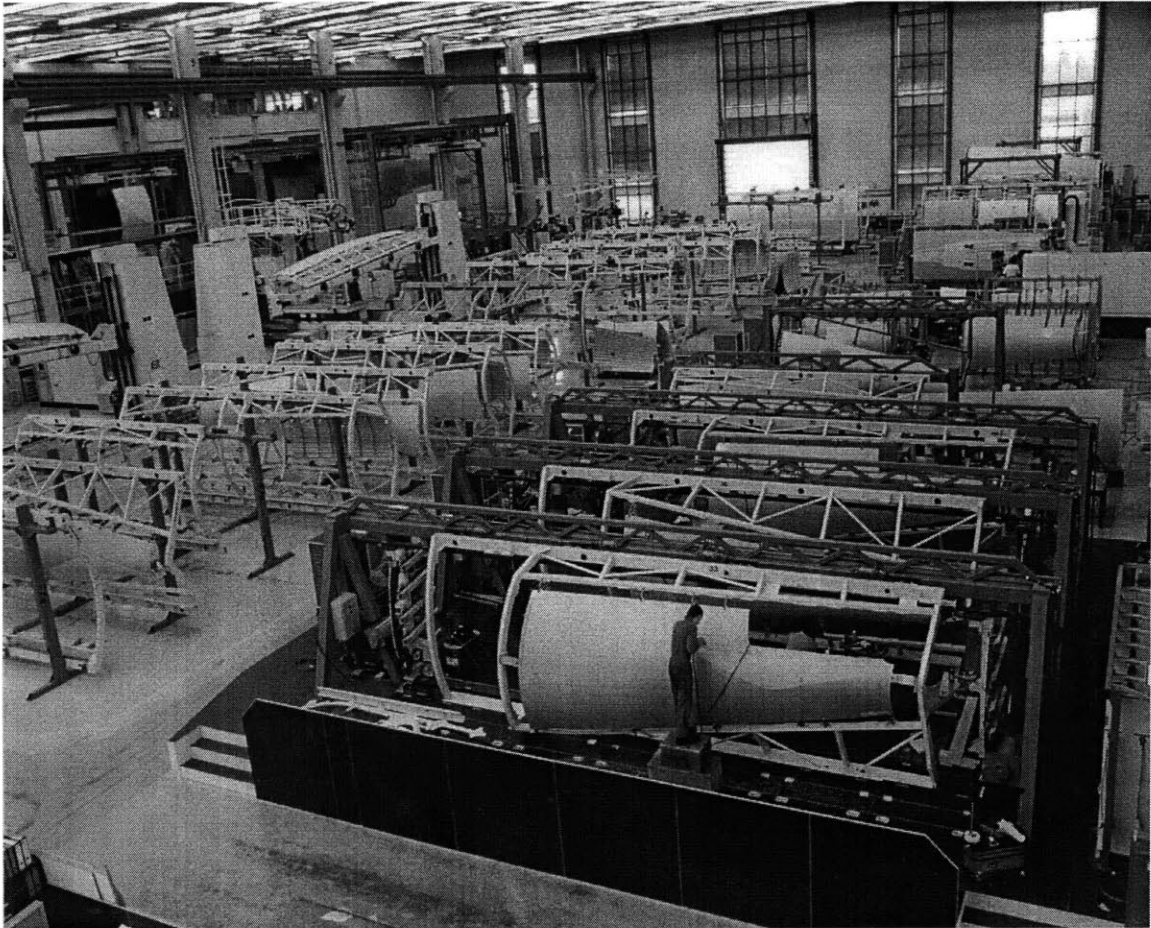
In order to give a better impression of the tasks performed by today's AFS machines the following paragraphs describe a few cases of aluminum aircraft assembly in more detail [9].

Figure 6.20 and Figure 6.21 shows one of the most modern assembly plants located in Augsburg, Germany. The plant is devoted to the fuselage panel assembly of the aft section of the entire Airbus fleet. The first photo shows six 5-Axis AFS machines including assembly fixtures. The entire AFS installation is worth approximately \$18M-\$20M in today's dollars including installation and setup. However, the machines were not purchased all at once, but rather procured incrementally as production volume increased.



**Figure 6.20** Airbus Assembly - 5-Axis Riveting Machines [8]

The second photograph clearly shows the stationary blue fixtures and the white removable fixtures, which are used for tacking the components prior to the final automatic fastening operation. The parts are located on the white fixtures to hold the assembly's geometry and are then moved on the removable frames over to the AFS stations. The AFS machines position and clamp the white frames automatically before it commences with the joining operation.



**Figure 6.21** Airbus Assembly - Tacking & Cleanup Fixtures [8]

The following example describes the center wing box assembly for Airbus at Aerospatiale in Nantes, France. Figure 6.22 shows the tackless automatic fastening operation, which dispenses with the tacking step and therefore saves time and assembly costs. The parts are located in a rigid fixture featuring a removable inner frame, which in turn is placed into the outer workframe of the AFS. The machine clamps the fixture automatically and begins the joining process. The machine shown in the photograph has special force/position sensors to insert the fasteners without damaging the aluminum panels. Similar to the Augsburg plant the facility in Nantes includes six AFS machines procured over time at a total of approximately \$20M.

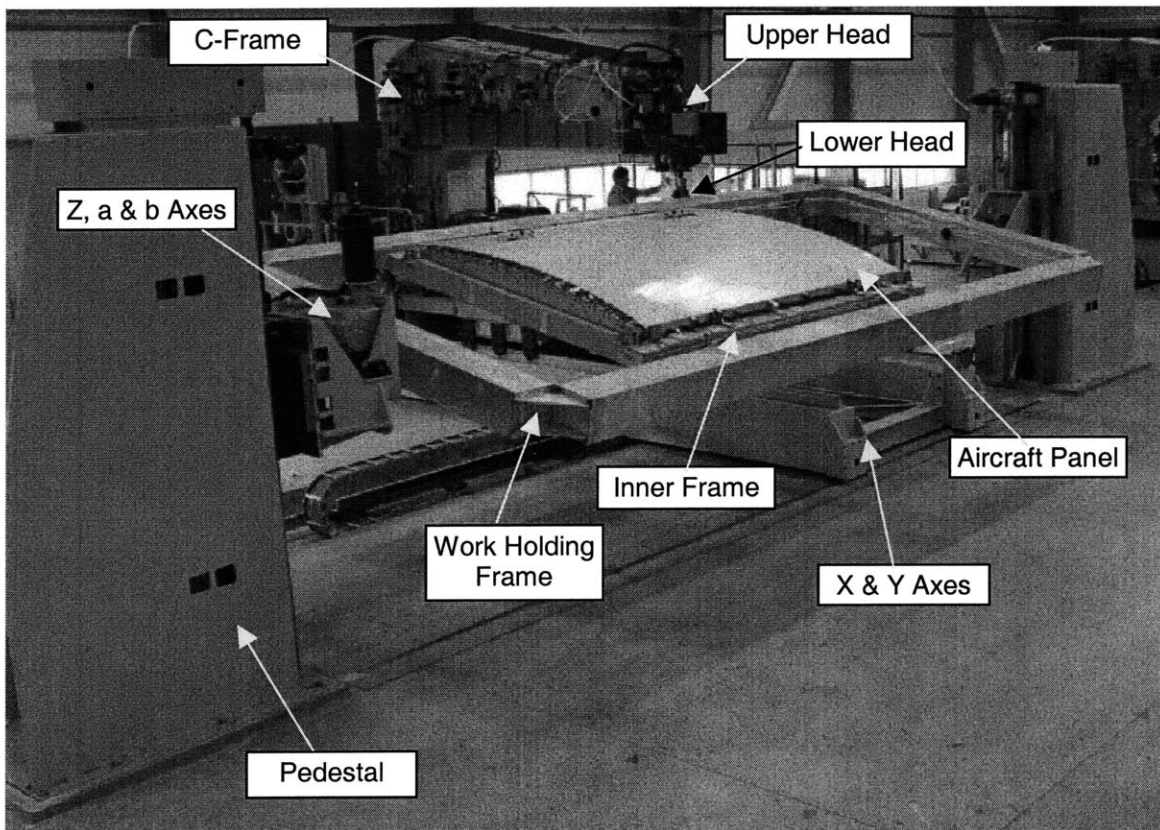


**Figure 6.22** Aerospace Assembly - 5-Axis Clamping and AFS Machine [8]

Figure 6.23 shows the Boeing 777 wing assembly. The assembly envelope would be considered large in our size category scheme. The photograph shows the tacking fixtures in the background and the AFS systems in the foreground. The six AFS machines would cost approximately \$60M in today's dollars.

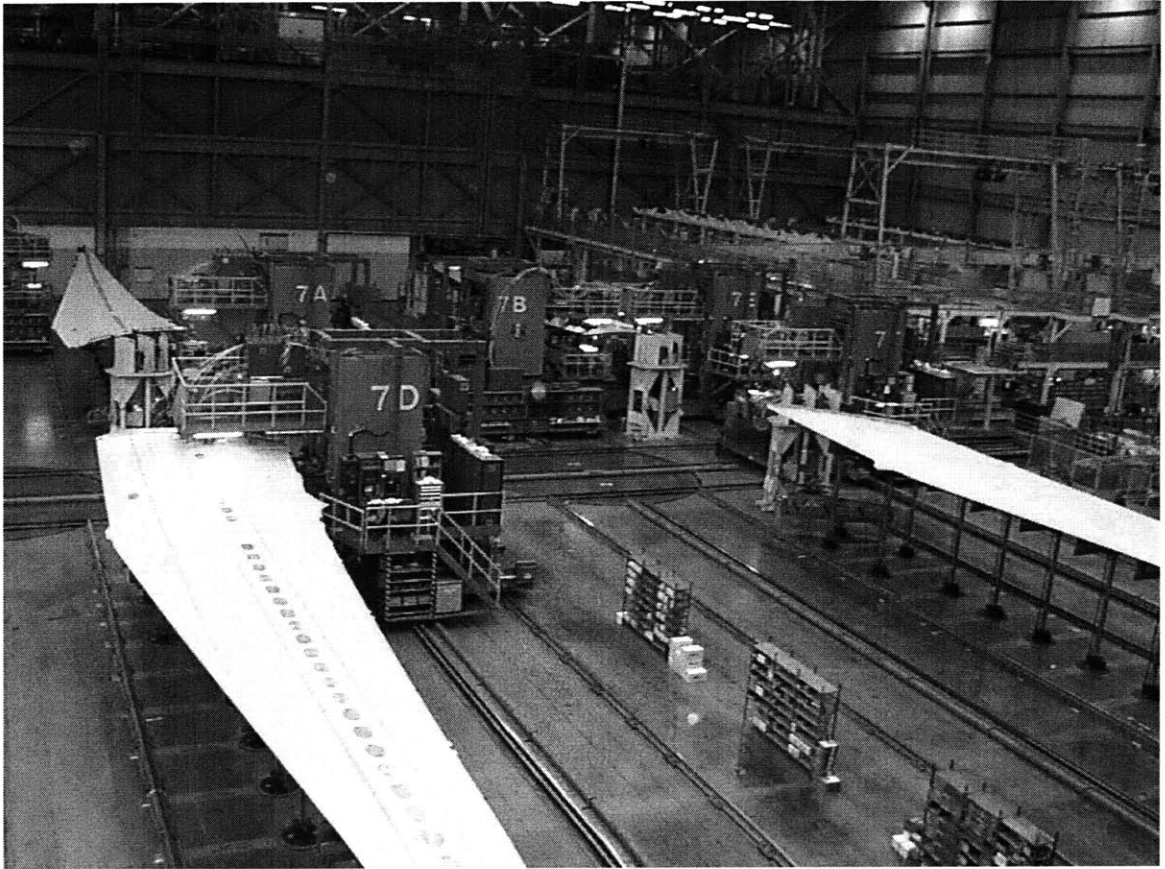


**Figure 6.23 Boeing Assembly - 5-Axis AFS Machines [8]**

## 6.9 References

- [1] Reinhardt, R. J., ed. "Engineered Materials Handbook Vol. 1 – Composites", ASMF International, 1987.
- [2] FRP Materials, Manufacturing Methods, and Markets" Composites Technology Yellow Pages 2000.
- [3] Composite Fabricators Association (CFA), "Membership Directory & Buyer's Guide", CFA, Arlington, 2000.
- [4] Thomas Register of American Manufacturers, "Products & Services", Thomas Publ. Company, New York, 2001.
- [5] Clements, L., "Vacuum Bagging Technology Improved," High Performance Composites, January/February 2000.
- [6] Truslow, S. "Permanent Press, No Wrinkles: Reinforced Double Diaphragm Forming of Advanced Thermoset Composites."
- [7] Goel, A. , "Economics of Composite Material Manufacturing Equipment", M.S. Thesis, MIT, 2000.
- [8] Speller, T., "A Case Study of a Product Architecture", M.S. Thesis, SD&M, MIT, 2000.
- [9] Gemcor, Inc., <http://www.gemcor.com/> , Interviews with Tom Speller, March 2002.
- [10] Advanced Process Technology Inc., Middlesex, New Jersey, <http://www.advancedprocess.com/>
- [11] Airtech International, Huntington Beach, California, <http://www.airtechintl.com/>
- [12] ASC Autoclave Division, Chatsworth, California, <http://www.aschome.com/>
- [13] Bondline Products, Norwalk, California, <http://www.bondlineproducts.com/>
- [14] Cincinnati Machine Company, Cincinnati, Ohio, <http://www.cinmach.com/>
- [15] Comasec Safety, Inc., Enfield, Connecticut, <http://www.comasecsafety.com/>
- [16] Composite & Wire Machinery Inc., North Kingstown, Rhode Island.
- [17] Entec Composite Machines, Salt Lake City, Utah, <http://www.entec.com/>
- [18] Gemcor, Inc., West Seneca, New York, <http://www.gemcor.com/>
- [19] Glas-Craft, Indianapolis, Indiana, <http://www.glascraft.com/>
- [20] GS Manufacturing, Costa Mesa, California, <http://www.gsmfg.com/>
- [21] Ingersoll Milling Machine Company, Rockford, Illinois, <http://www.ingersoll.com/>

- [22] Liquid Control Corporation, N. Canton, Ohio, <http://www.liquidcontrol.com/>
- [23] Martin Pultrusion Group, Twinsburg, Ohio, <http://pultrude.ne-ohio.net/>
- [24] Melco Steel, Azusa, California, <http://www.melcosteel.thomasregister.com/olc/melcosteel/>
- [25] Radius Engineering, Salt Lake City, Utah, <http://www.radiusengineering.com/>
- [26] Strongwell Machinery & Licensing, Bristol, Virginia, <http://www.strongwell.com/>
- [27] Thermal Equipment Corporation, Torrance, California, <http://www.thermalequipment.com/>
- [28] M. Torres, Navarra, Spain, <http://www.mtorres.es/>
- [29] Venus-Gusmer, Kent, Washington

### 6.10 Appendix - Production Equipment Costs

**Table 6.3 RTM Equipment [25 ,29]**

<i>Mechanical Models (A &amp; B)</i>	<i>Mixing Ratio</i>	<i>Price</i>
5 - 55 gallon drum capacity	4	\$8,284
	7	\$8,399
	11	\$7,250
	4	\$7,450
	1	\$4,200
	Variable Ratio	\$6,090
<i>Automated Models (C)</i>	<i>Shot Size [cm<sup>3</sup>]</i>	<i>Price</i>
pneumatic-pressure controlled	2,100	\$14,200
electrical - flow controlled	2,100	\$47,800
all incl. dispenser & mixer	5,000	\$74,200
	7,500	\$76,800
	10,000	\$95,900

**Table 6.4 Pultrusion Equipment [16, 17, 19, 23]**

<i>Part Envelope</i>	<i>Envelope Area [in<sup>2</sup>]</i>	<i>Pulling Capacity [lbs]</i>	<i>Gripper Type</i>	<i>Gripper Length [in]</i>	<i>Price</i>
4" x 8"	32	n/a	Reciprocating	n/a	\$60,000
4" x 8"	32	n/a	Reciprocating	n/a	\$75,000
12" x 10'	1,440	n/a	Reciprocating	n/a	\$1,000,000
10" x 6"	60	12,000	Reciprocating	24"	\$110,000
20" x 8"	160	20,000	Reciprocating	24"	\$157,500
30" x 10"	300	30,000	Reciprocating	24"	\$202,500
40" x 12"	480	50,000	Reciprocating	30"	\$292,500
50" x 12"	600	70,000	Reciprocating	30"	\$360,000
8" x 6"	48	12,000	Reciprocating	24"	\$155,000
8" x 6"	48	8,000	Continuous	n/a	\$170,500
16" x 6"	96	16,000	Reciprocating	24"	\$200,000
16" x 6"	96	16,000	Continuous	n/a	\$220,000
24" x 8"	192	24,000	Reciprocating	24"	\$230,000
24" x 8"	192	16,000	Continuous	n/a	\$253,000
40" x 8"	320	30,000	Reciprocating	24"	\$350,000
40" x 8"	320	20,000	Continuous	n/a	\$385,000

**Table 6.5 Autoclave Equipment [12, 27]**

<i>Model</i>	<i>Max. Press. [psi]</i>	<i>Max. Temp. [F]</i>	<i>Diameter [ft]</i>	<i>Length [ft]</i>	<i>Heating/Cooling Rate</i>
1	150 psi	650 F	3	3	15F/min
2	150 psi	650 F	3	3	10F/min
3	200psi	650 F	3	5	15F/min
4	120 psi	500 F	5	10	15F/min
5	300 psi	650 F	1	3	15F/min
6	300 psi	650 F	2	3	15F/min
7	350 psi	850 F	15	40	15F/min
8	350 psi	850 F	3	20	15F/min
9	350 psi	850 F	4	20	15F/min
10	350 psi	850 F	6	20	15F/min
11	350 psi	850 F	3	10	15F/min
12	350 psi	850 F	4	10	15F/min
13	350 psi	850 F	6	10	15F/min

<i>Model</i>	<i>Base Price (A)</i>	<i>Price w/ Computer (A)</i>	<i>Price w/ Computer (B)</i>	<i>Base Price (C)</i>
1	\$80,000	\$120,000	\$375,000	\$43,000
2	\$80,000	\$120,000	\$365,000	
3	\$83,000	\$123,000	\$400,000	\$75,000
4	\$160,000	\$195,000	\$500,000	\$170,000
5	\$80,000	\$120,000	\$150,000	
6	\$90,000	\$145,000	\$200,000	
7	\$1,200,000	\$1,240,000	\$2,500,000	
8	\$135,000	\$175,000	\$500,000	
9	\$165,000	\$205,000	\$600,000	
10	\$215,000	\$255,000	\$750,000	
11	\$125,000	\$165,000	\$600,000	
12	\$150,000	\$190,000	\$700,000	
13	\$200,000	\$245,000	\$800,000	



**Table 6.6 Bagging Material [11]**

<i>Name</i>	<i>Type</i>	<i>Material</i>	<i>Quantity, Size</i>	<i>Price</i>
Wrightlon 5400	Vacuum Bagging Film	Nylon	1 Roll, 60" x 200'	\$75.00
Stretchlon 200	Vacuum Bagging Film	Urethane	1 Roll, 60" x 200'	\$129.00
Release 125	Release Film		1 Roll, 60" x 200'	\$75.00
AT-199	Sealant Tape		1 Roll, 3/8" x 50'	\$44.00
Stitch Ply A	Peel Ply	Nylon w/ red tracer	1 Roll, 60" x 25 yds	\$148.00
Stitch Ply G	Peel Ply	Polyester w/ black tracer	1 Roll, 60" x 25 yds	\$128.00
Bleeder Lease B	Peel Ply	Nylon w/ release agent	1 Roll, 60" x 25 yds	\$156.00
Econoweave 44	Breather		1 Roll, 60" x 25 yds	\$58.00
AS-2400	Heavy Duty Cutters		9.5 in	\$69.00
AS-2100	Heavy Duty Cutters		8.3 in	\$53.85
AS-1800	Heavy Duty Cutters		7.1 in	\$45.20

**Table 6.7 AFS Machine Part Size Envelopes [9]**

AFS Concept	<i>Small</i>			<i>Medium</i>			<i>Large</i>		
	Length X-Axis [in]	Depth Y-Axis [in]	Height Z-Axis [in]	Length X-Axis [in]	Depth Y-Axis [in]	Height Z-Axis [in]	Length X-Axis [in]	Depth Y-Axis [in]	Height Z-Axis [in]
1	240	96	93	480	120	116	840	168	161
2	240	96	93	480	120	116	840	168	161
3	240	96	93	480	120	116	840	168	161
4	400	96	120	400	120	156	400	144	192
5	900	96	36	900	120	42	900	144	48
6	900	96	36	900	120	42	900	144	48

**Table 6.8 AFS Machine Costs [9]**

AFS Concept	<i>Small</i>	<i>Medium</i>	<i>Large</i>	<i>Very Large</i>	<i>Variation due to Complexity</i>
1 (Sm. Wing)	\$1.5M	\$2.2M	\$3.0M	\$4.5M	+20 to +30%
2 (Fuselage)	\$1.5M	\$2.2M	\$3.0M	\$4.5M	+10 to +20%
3 (Fuselage)	\$1.5M	\$2.2M	\$3.0M	\$4.5M	+10 to +20%
4 (Fuselage)	\$1.5M	\$2.2M	\$3.0M	\$4.5M	+10 to +20%
5 (Wing)	\$3.5M	\$4.0M	\$5.0M	\$7.0M	+20 to +30%
6 (Wing Spar)	\$3.5M	\$4.0M	\$5.0M	\$10.0M	+20 to +30%

## 7 Cost and Design Elements of Tooling

The costs for tooling represent a significant portion of the overall investment for composite production. Therefore, an outline of the tooling types, the materials used and the manufacturing methods provides some insight about the issues involved and the required investments. Similar to composites, the costs for tooling can also be determined following a process based cost estimation strategy. Material, fabrication, and design costs drive the overall tooling cost in dependence of its size and complexity. However, tooling is generally a unique product, which is only produced at very low volumes and is specifically designed according to customer specification. All these circumstances complicate cost estimation efforts and large uncertainties and variations in the results are to be expected. The following paragraphs discuss typical tool designs, and common process plans for open mold metal tooling, closed mold matched tooling and tooling for assembly. For each of these tooling types one or several case studies are conducted and the cost results are compared to the data provided by industry sources.

### 7.1 Overview of Tooling for Composites

Conveniently, composite tooling is organized into two categories. The first category distinguishes tooling by its construction material. This category includes for example, tools made of composites or metal. The second category characterizes tooling by the process and by the function the tools serve. Examples encompass, layup tools, pultrusion dies, and assembly fixtures.

#### 7.1.1 Tooling classified by Material

##### Composite Tools

Tools produced out of reinforced composites are commonly used for low to medium production volumes. The tools cost less than comparable metal tools and can be tailored to match the thermal expansion of the actual part. In particular, for curing tools used in

connection with autoclaves and ovens, the control of thermal expansion leads to better dimensional accuracy. Therefore, composites are mainly employed to fabricate layup, forming, and curing tools and are rarely found in resin transfer molding and pultrusion application. In the few cases where composites are used for making RTM molds, the composite surface is often backfilled with cast resin or other polymeric foams for support. The fabrication of the composite tooling surface mainly involves the hand layup of woven prepreg onto a previously constructed core, which can be made of wood, cast resin, or foam. Since, the production process is similar to the manufacture of an actual composite part the costing process can follow the concepts discussed in previous chapters. The shortcoming of composite tools is their generally limited life span and reduced durability. Therefore, the costs of repairing or replacing the tool have to be weighted against the cost of a more expensive metal tool.

### Metal Tools

Common materials for metal tools include tool steel, aluminum, and Invar. The production of metal tools can follow different paths. A common approach is to cut and form sheet stock and then weld it together to build the tool face and the supporting egg-crate structure. A machining step generally creates the final contours of the tooling surface. Other tools are machined directly out of solid metal blocks or from near net cast pieces. In some a variety of different manufacturing processes, such as machining, casting, forming and welding are used throughout the production of a single tool. As a special process, electroformed nickel is employed to fabricate a large and thin tooling surface without the necessity of further machining operations.

The advantages of metal tools lie obviously in their increased durability and strength. The surfaces are considerably more scratch resistant, especially when coated with chrome. The structures can take more abuse without going out of tolerance and are well suited for large production runs of about 1,000 to 10,000 parts annually. The inherent disadvantage of metal, in particularly aluminum, is its generally high coefficient of expansion. For tools, which are subjected to the elevated curing temperatures encountered during the curing of thermoset resins, the adverse effects of thermal

expansion have to be considered. Alternatively the use of Invar, a nickel based alloy, allows the fabrication of tools, which exhibit almost zero thermal expansion. However, Invar comes at a price and is considerably more expensive than other materials. Which material is most suited however, is a decision, which depends on the part design and the production conditions.

### **7.1.2 Tooling classified by Process**

#### Autoclave & Layup Tooling

Frequently, the tools used to cure the laminate are also used to layup the individual plies. Figure 7.1 shows such a tool for the automated layup and subsequent curing of a rocket motor casing. These open mold or one-sided tools consist of a relatively thin tooling face, which is supported by a backup structure to provide stiffness. Open mold tooling accurately defines one dimension of the part, while attempting to compensate for inaccuracies, thermal effects, and material shrinkage during cure. In applications where designers demand an A1 surface finish, the tooling face has to be highly polished and is sometimes even coated for extra scratch protection. Tools used for autoclave cure have to sustain vacuum integrity and have to maintain their dimensions at the elevated curing temperatures. For these types of tooling, the tool designer has to either compensate for the thermal mismatch and expansion of materials or a special tooling material has to be chosen. Ideally, the tool should be made of carbon fiber composites, which can be tailored to eliminate any thermal effects. However, if good durability is required, Nickel alloys (Invar) and cast iron can be used, since these metals exhibit low coefficients of thermal expansion (CTE). Fabricated metal tooling gains increased attention from manufacturers of precision and medium to high volume parts. The high durability of the tool significantly reduces subsequent maintenance costs. Metal tooling for autoclave cure withstands a minimum of 500 cure cycles without repair and quite often easily exceed this basic requirement.

Some applications however employ separate layup and curing tools. An example is the layup of uncured components prior to the assembly in a co-curing tool, as described in Chapter 9.2.2. Of course, the co-curing tool has to meet similar requirements as

described above, but the layup tool can be fabricated cheaply out of cast resin, aluminum, or even wood. Additional features, which facilitate the curing process, such as integrated vacuum plumbing or thermocouples, can also be found in current designs.

To facilitate the demolding of parts exhibiting undercuts or pronounced features with negative double curvature, tools need to be collapsible in order to be removed from the cured part. Collapsible tools become particular expensive, when simultaneously the vacuum integrity of the tool has to be ensured. The design challenges include the assurance of an airtight seal along the parting lines and the preservation of dimensional accuracy at elevated temperatures.

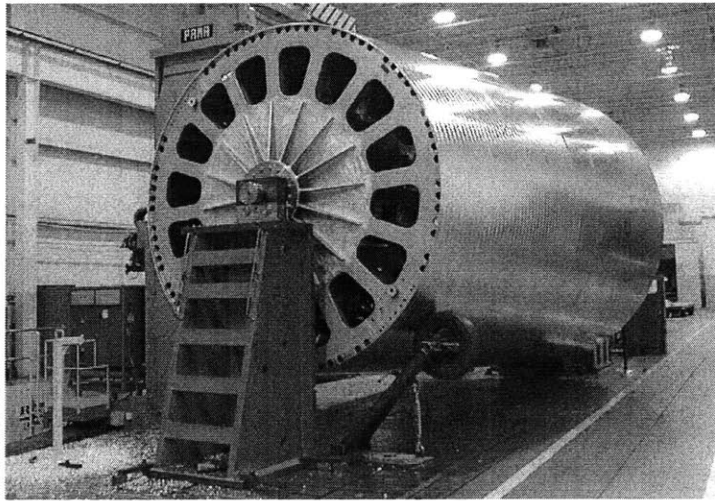


**Figure 7.1 Invar Layup Tool for Rocket Motor Casing [29]**

### Diaphragm Forming Tooling

Diaphragm forming tools are similar to layup tools and form a one-sided replica of the part to be produced. However, CTE matching and a minimization of the thermal mass are not top priorities, since the forming process takes place at lower temperatures. The surface, however, should be coated to provide resistance against premature wear caused by the abrasive shear forces during forming.

### RTM & Closed Mold Tooling

The injection of resin under pressure into a mold previously filled with reinforcement fibers necessitates a closed tool. As opposed to open mold tooling, the closed molds used for RTM define all the part surfaces in terms of their dimensions and their finish. Since a high fiber volume fraction is critical to attain good mechanical properties, the two die halves must be manufactured to tight tolerances. Also, the tool has to be sturdy enough to withstand the high injection pressure and should provide adequate sealing to prevent resin from escaping. RTM tools can be compared with tools for injection molding and are often made out of metal. In rare cases, other tooling materials are employed, such as composites, cast resins and ceramics [4, 10]. Prominent design features include injection ports, seals, positioning elements and sometimes heating/cooling channels.

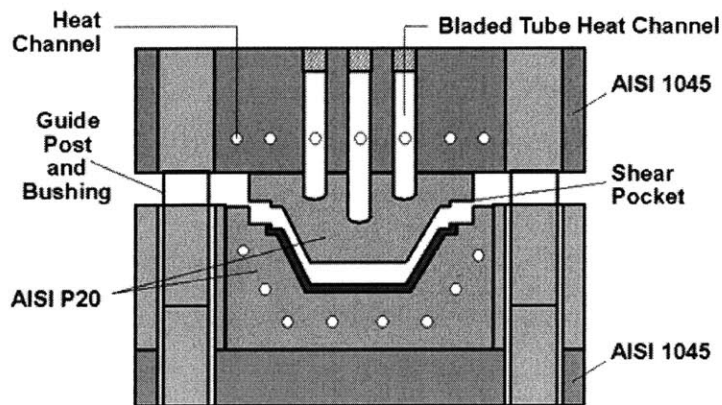


**Figure 7.2** Design Features of a Matched-Die Mold Set for RTM [3]

### Pultrusion Tooling

Pultrusion dies can also be described as matched tooling, however the tools are open on the two opposite sides for the fibers to pass through. Most commonly, the wet and impregnated fibers enter the heated tool and assume the shape of the pultruded profile before being cured. To survive the enormous forces and friction at the entrance and on inside of the die, the tool is generally fabricated out of steel. The features are often machined from a solid or a near-net cast block. Surface coating reduces wear and friction and prolongs the useful life of the tool.

### Assembly Fixtures and Bonding Jigs

The main purpose of these tools is to fixture part for subsequent assembly, bonding, or trimming operations. Previously cured parts are positioned by these tools using integrated reference points. Also some tools are used to fixture the parts for the routing and shaping of honeycomb cores before a second skin is bonded on top.

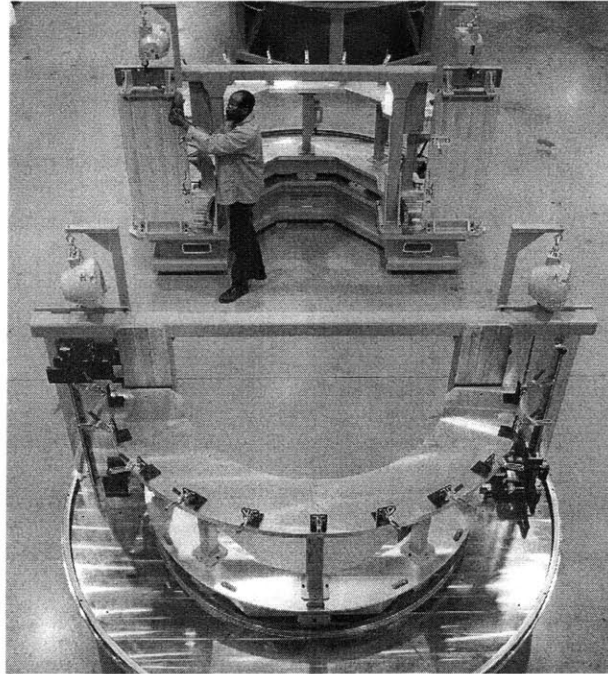


**Figure 7.3 Aluminum Bonding Jig [29]**

Bonding jigs have a similar function as fixture tools, since for example the precise location of stiffeners or other structural elements has to be insured before the bonding operation can commence. Bonding jigs include additional features such as clamps in order to exert sufficient pressure onto the part during the cure of the bonding agent.

In both cases regular clamps can be used as fixture elements, however to securely hold parts featuring complex shapes, vacuum or hydraulic chucking can become necessary. In some instances, the layup tool and curing tool also serves as a fixture tool for trimming.



### 7.1.3 Material Properties and Selection Criteria

The decision regarding the tooling material depends on how performance and economic aspects of the tool are valued by the designers. The selection process can be approached by first defining the expected life-span of the tool and then decide what type of tool (lay-up & cure or fixture tooling) is required. Secondly, the temperature range and the process conditions have to be assessed in order to estimate potential thermal expansion effects.

If thermal effects are not an issue, Aluminum (e.g. AISI 6061) or even Fiberglass or Wood is probably a good material choice. All these materials are inexpensive, exhibit good machinability, and are lightweight for easier tool handling.

However, many applications require limited and/or matched thermal expansion of the tool at high temperatures. Under these conditions controlled expansion Nickel Alloys (i.e. Invar™ or Nilo 36™) are the most suitable materials. Less durable alternatives are non-metallic materials such as Carbon/Epoxy or even Graphite. However, the better thermal performance comes at a considerable price and if economic aspects overwrite tolerance requirements, steel or cast iron (e.g. AISI P-20) might be considered possible alternatives.

#### Tooling Materials

##### a) Polymers (Neat)

Polymers refer to both thermosetting and thermoplastic materials and they all find various uses in tooling production. For cheap and prototype tooling, resins are often cast into the desired tooling shape and the surface is treated for better durability and release properties. Often fillers are incorporated into the resins to reduce overall cost and enhance the properties of the polymers. Tooling materials include epoxies, polyesters, polyimide, and thermoplastics. The most common polymer material used in casting is based on polyester type resins. Isophthalic resins and vinyl ester resins exhibit especially good mechanical properties and chemical resistance. Other

polymers including PTFE, nylons, syntactic foams, and methacrylic polymers are used for filling or for surface treatment [10, 11].

b) Glass Fiber Reinforced Polymers

Glass fiber reinforced polymers (GFRP) are generally employed for layup and cure tooling used in prototype or low volume production. E-glass fibers are the most commonly used fibers, because of their favorable cost to performance ratio. The fibers enhance the mechanical properties while the matrix supports and distributes the stresses among fibers. Since, its coefficient of thermal expansion and other material properties are similar to aluminum it is rarely used for curing tools subjected to temperatures higher than 100°F (38°C).

c) Carbon Fiber Reinforced Polymers

Carbon fiber reinforced polymers (CFRP) are frequently used for layup and cure tooling for low to medium production volumes. Although more expensive than GFRP, carbon composites offer excellent mechanical properties and a negative coefficient of thermal expansion in fiber direction. Proper laminate design allows the construction of tooling with zero thermal expansion. The temperature range is only limited by the properties of the matrix.

d) Aluminum (AISI 6061-T6)

Because of its low density and easy machinability, aluminum is often used for the fabrication of assembly fixtures, layup tools, and RTM tools. However, because of its high coefficient of thermal expansion the service range is limited to room temperature unless thermal affects can be neglected because of wide tolerances or favorable geometries. Aluminum AISI 6061-T6 is probably the most commonly available aluminum alloy, which contains some Chromium, Manganese and Titanium for heat treatment purposes and for boosting tensile strength and fatigue life. The material is mainly used in its harder T6 temper state, which also facilitates machining. The machinability is very good and very high cutting speeds can be achieved. The alloy possesses excellent welding characteristics. Gas metal arc welding is generally

used for heavier sections (GMAW), whereas Tungsten Inert Gas Welding (TIG) is employed for smaller details. Annealing for stress relief is performed at 775°F (413°C) for 2 to 3 hours followed by controlled cooling at 50°F (10°C) per hour down to 500°F (260°C), then air cool. The alloy is easily formed in annealed condition. Castings are not common in tool making, since internal porosity might result in poor surface finishes after the machining steps.

e) Tool Steel (AISI – 4140, P – 20, AISI – 1045)

Because of their strength and toughness, tool steels are commonly used to fabricate closed mold tooling for RTM and Pultrusion applications. The tool steels contain Nickel and Chromium as alloying elements for heat treatment purposes and to boost their machinability and other mechanical properties. In addition, the material offers good scratch and wear resistance, and is readily available on the market and inexpensive. Since many tools involve machining operations, the material is mainly used in its hot rolled and annealed condition. The machinability is good and the material removal rates reach about 80% of the rates for cutting common water hardening steels. Tool steels are weldable by conventional methods such as gas metal arc welding (GMAW). Annealing for stress relief takes place at 1,300°F (700°C) to 1,500°F (815°C). Hold for 1 hour per inch thickness, cool at 20°F (7°C) per hour to 1,000°F (538°C) and equalize. Then leave the part in open air to cool down to room temperature. In annealed condition, the alloy may also be formed by conventional methods. The material can be cast easily into more complex shapes.

f) Nickel Alloys (Invar 36™, Nilo 36™, Alloy 36™, Ametek 936™)

These controlled expansion alloys are generally used for complex layup and cure tooling, which can withstand the wear of high volume production. The coefficient of thermal expansion (CTE) is only about 10% of the value for standard carbon steels. The low CTE makes it the ideal metallic material when it comes to tools requiring tight part tolerances at high temperatures. The alloys are commonly known under one of their numerous trade names, Invar 36™. Only Super Invar™ and Alloy 32-6™, exhibit an even lower CTE, however the material is rarely stocked and therefore more

difficult to procure. It is also notable that increasing hardness further decreases the CTE in all temperature ranges. However, for tooling applications the material is generally used in its hot rolled and annealed condition to facilitate subsequent machining. However, cutting speeds are considerably slower in comparison to steel. Future development of cutting inserts will increase the material removal rates significantly. The material is welded as easily as steel and aluminum when employing common welding techniques such as GMAW. Annealing is performed at 1,450°F (788°C) for 30 minutes for every inch of thickness followed by air-cooling. In order to obtain maximum dimensional stability, soak at 1,500°F (815°C) and water quench, and then reheat to 600°F (316°C) for 1 hour and then air cool. The alloy can be formed by most common methods. Casting does not present any unusual problems and can be used to produce complex tool shapes. Layup tooling often uses stock plate or profiles. The high material price and the reduced material removal rates contribute to the generally high costs of Invar tooling.

g) Electroformed Nickel

The process is generally used to create accurate and complex tooling face sheets. Nickel ions are deposited onto the conductively coated surface of a master model. The process permits the reproduction of small details and fine features with a high degree of accuracy, since the master model is copied without any losses. Another advantage is that no heat is generated and therefore thermal distortions are of no concern, however the master model has to be accurate. Immersed in tanks (size up to 34 x 8 x 15 feet) and at a deposition rate of 0.0005 to 0.001 inch per hour it takes about 4 to 11 days in order to build up a tool face between 0.1 to 0.125 inches. The process can result in non-uniform material deposition in corners and edges and only reversing the polarity avoids these shortcomings, but also doubles the manufacturing time. Although Invar as a Nickel Alloy has a low thermal expansion coefficient pure Nickel does not exhibit such behavior. As seen in Table 7.1, Electroformed Nickel possesses a slightly higher CTE than steel. However, the major disadvantage is the fabrication of the master model (cathode), which has to be highly accurate and

requires a perfect surface finish. The possibility of producing more than one tool face for rate tooling is often overridden by the elaborate fabrication of the master model.

h) Others

Materials such as concrete and plaster make durable and less expensive tools compared to cast iron. The cure time is rather short in comparison to other materials. The major advantages include good castability for versatile tooling, high stiffness to weight ratio, and thermal stability. Toolmakers usually post-machine the cast structures.

### Material Selection Criteria

The materials are selected according to the tooling requirements. Primarily, the durability is traded off against costs and the materials are selected accordingly. A material has to be selected so the tool can function properly within the intended temperature range and can withstand the strain of the production needs. Layup and curing tools have to hold the dimensions at elevated temperatures whereas RTM and Pultrusion tools need to resist the forces exerted on them. The material selection is closely linked to the type of tool and to the fabrication process and consequently the cost. The following list shows the ideal properties of a tooling material:

- High Specific Stiffness & Strength
- Low Thermal Expansion
- Low Heat Capacity & High Conductivity
- Good Manufacturability
- Impermeability
- Good Availability & Low Price

Consequently, the resulting trade-off scenarios have to be resolved depending on the above criteria. Table 7.1 lists the major properties of tooling materials. The effects of

the properties on material selection are discussed in the subsequent paragraphs and are illustrated in more detail in Table 7.35 and Table 7.36 in the Appendix 7.8.1.

**Table 7.1 Properties of Common Tooling Materials**

	<i>Tensile Strength</i> [ksi]	<i>Density</i> [lbs/in <sup>3</sup> ]	<i>Thermal Diffusivity</i> [x 10 <sup>-6</sup> m <sup>2</sup> /s]	<i>Thermal Expansion</i> [x 10 <sup>-6</sup> 1/K]	<i>Typical Price</i> [\$/lb]
Tool Steel (P20)	130	0.285	13.8	11.5	0.3 - 0.6
Cast Iron (Class 60)	20	0.249	6.7	10.8	0.15 - 0.3
Aluminum (6061-T6)	45	0.098	84	23.4	2.5 - 4.5
Nickel (Electroformed)	50	0.300	16.8	13.0	9 - 18
Nickel Alloy (Invar 36)	74	0.293	2.5	1.6	5 - 15
Monolithic Graphite	8	0.065	30.8	2.7	2 - 7
Graphite/Epoxy (AS4)	82	0.058	2.8	1.4	50 - 100

a) Strength & Stiffness

The tensile strength and stiffness of a material affects the durability of the surface and structural integrity of the structure. Here Graphite is at the low end of the range and should only be considered for low volume or prototype production. Although exhibiting high tensile strength Graphite/Epoxy provides only very limited scratch resistance and surface hardness.

b) Density

A comparison of the material density allows estimates of the final weight of the tool. Proper handling and transportation has to be considered for large and heavy tools.

c) Heat Capacity & Diffusivity

In addition to the thermal mass (density x spec. heat capacity) of a material the thermal diffusivity (conductivity / (density x spec. heat capacity) provides additional information about how quickly a material heats up and how quickly temperature gradients are equalized. High diffusivity values are advantageous.

d) Coefficient of Thermal Expansion (CTE)

Low thermal expansion coefficients assure tight manufacturing tolerances if the tool is subjected to temperature fluctuations. A tool structure made out of Graphite/Epoxy (e.g. AS4), or Invar (e.g. Invar 36) matches the expansion coefficient of a carbon fiber composite the closest. However, one has to bear in mind that the CTE for Graphite/Epoxy is an average value and can vary widely depending on the laminate design (approx.  $0.5 - 25 \times 10^{-6} \text{ 1/K}$ ).

e) Costs

The specific cost or cost per unit mass represents the most obvious economic criteria when determining the cost of a composite tool. However, one should consider that not only the price of the raw material but also the subsequent manufacturing costs have to be taken into account.

f) Available Sizes

When designing and planning the production of a tool the available stock sizes are as important as anything else. The use of non-standard stock sizes can possibly render a design unfeasible or not economic.

g) Manufacturability

Cost effective production has to take the manufacturability of a material into account. For example, the material removal rate is a representative measure for manufacturability of fabricated metallic tooling. Complex shapes in tools are mainly realized by machining even if cast materials serve as a basis. Considering high machine and labor rates, the machining of these shapes can quickly become one of the major cost drivers.

## 7.2 Fabrication Processes for Metal Tooling

Many fabrication processes for metal tooling share similar production processes. Therefore, all metal working processes are discussed, which might have a significant impact on the production costs of tooling. The functionality is described briefly and performance data is listed in support of the subsequent process based cost models.

### 7.2.1 Plasma Cutting

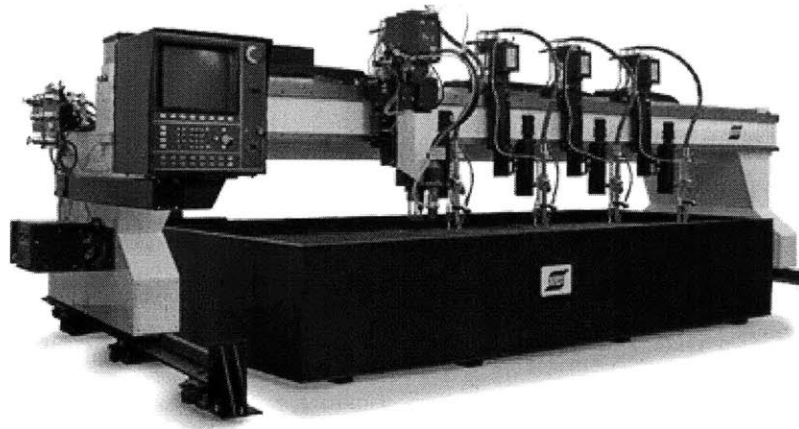


**Figure 7.4** CNC-Plasma Cutter [42]

Plasma Arc Cutting (PAC) has become a popular cutting process for stock plate. It uses an arc struck between the electrode and the surface of the workpiece to cut through various types of nonferrous and stainless-/steel panels. The high temperature plasma arc burns at temperatures of 25,000 - 50,000°F (14,000 - 28,000°C) and melts the material, which is instantly blown away by the shielding or plasma gas. Due to the much higher energy density in comparison to oxy-fuel cutting, the heating of the workpiece and consequently the warpage is reduced. Also cutting speeds are considerably higher and the kerf-widths are smaller than with oxygen torches. Plasma cutting also produces very clean cuts with little or no dross.



### Plasma Cutting Formulas

The following formula estimates the ideal cutting speed in meters per second, with the energy of the plasma arc in watts (AE), the thickness of the plate in meters (PT), the width of the cut in meters (KW), the latent heat for melting in Joules per kilogram and the material density in kilograms per cubic meter (RO).

$$CS = AE / PT / KW / LH / \text{Density} \qquad \text{Equation 7.1}$$

### CNC-Controls

The process is often employed in connection with automation equipment such as robots or CNC controlled cutting gantries. The CNC controller allows the import of CAD data and such quickly creates complex cutting paths with virtually no additional programming. In addition, these automated machines can directly bevel stock plate while cutting and therefore reduce weld seam preparation time.

### Cutting Speeds

The Table 7.37 in the Appendix 7.8.2 lists various cutting speeds for different types of materials and is based on data from the Hypertherm, Inc. [42]. The data represents heavy duty industrial plasma cutter. Smaller handheld devices only achieve about 35 in./min. for 0.25" steel plate. Larger more powerful machines can go as fast as 55 in./min. for 1.25" steel.

For cost estimating purposes, one can assume an average of 30 to 90 in./min. for all plates between 0.5" and 1" thickness.

### 7.2.2 Metal Bending & Forming



**Figure 7.5** CNC-Press Brake [38]

Press brakes are used to bend, form, seam, trim, and punch light-gage sheet metal. The process time is determined by the material, the length of the work piece, the thickness of the metal, and the radius of the bend. The inside radius of a bend is usually limited to the material thickness. Conventional power press brakes may be either hydraulic or mechanical although hydraulic presses are more popular for larger tonnages. Figure 7.5 shows a more modern type 350 ton CNC press-brake.

#### Time Estimates (AM Cost Estimator) [23]

According to Table 7.38 in the Appendix 7.8.2, setup hours depend on brake length and number of stops. The setup standards apply to conventional machines. The first process step is the transfer of the material to the machine. In addition to forming, other steps include the reposition of the material.

### 7.2.3 Metal Casting



**Figure 7.6 Metal Casting Processes [36]**

Pouring molten metal into a mold of the required form easily produces complex parts. Molds are made of refractory materials such as sand, graphite, ceramic, or metal. Sand molds are formed around a pattern or replica of the part to be produced. The molds are usually made of wood and tough plastics, or out of metals for high volume production. Material shrinkage during cooling has to be taken into account (Cast Iron: 0.83 to 1%, Alu. 1.3 to 2.1%) and patterns require draft angles between 0.5 and 2 degrees

#### Casting Formulas

To estimate the solidification time of a part in minutes (ST), enter the Part Volume (PV) and the surface area of the part (SA) into Equation 7.2 (Chvorinov's Rule).

$$ST = C \times (PV / SA)^2 \quad \text{with} \quad C = \frac{\pi}{4 \cdot k_s \cdot \rho_s \cdot c_{ps}} \left( \frac{\rho_M \cdot h_m}{T_m - T_0} \right) \quad \text{Equation 7.2}$$

#### Time Estimates

The production of high part volumes is determined by the solidification time. However, for small volumes the pattern and mold making process are the most time consuming steps.

### 7.2.4 Gas Metal Arc Welding (GMAW)

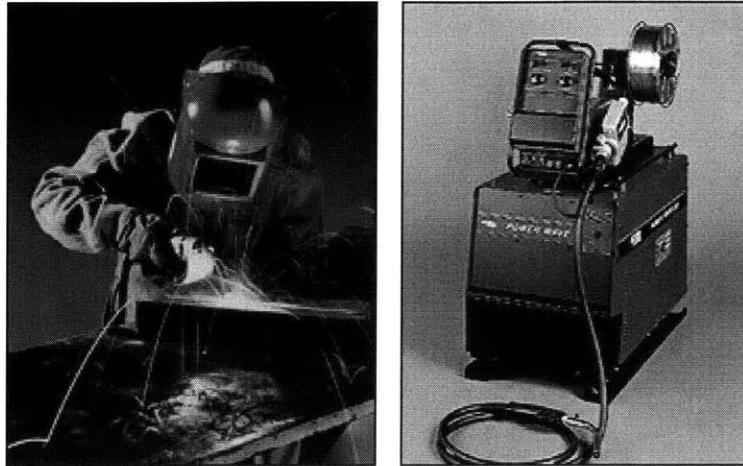


**Figure 7.7** GMAW Welding [39]

Gas Metal Arc Welding (GMAW) (also known as Metal Inert Gas or MIG Welding) and Flux Cored Arc Welding (FCAW) are the two most cost-effective manual arc welding processes, which account for the consumption of over 50% of all welding material. Both processes feed the welding wire (electrode) automatically into the welding gun, where it is molten and shielded by the welding gas (Argon/CO<sub>2</sub>/O<sub>2</sub>).

#### Welding Rate

Equation 7.3 expresses the welding rate per minute (WR), with the cross section of the welding wire in square inches ( $A_w$ ), the wire feed rate in inches per minute (WFR), and the cross section of the weld seam in square inches ( $A_s$ ).

$$WR = A_w \times WFR / A_s \quad \text{Equation 7.3}$$

#### Electrode Diameters

Typical electrode diameters are 0.030 in., 0.035 in., 0.045 in., 0.052 in. and 0.062 in. For weld seams larger than 0.5 in. electrodes larger and equal to 0.045 in. are employed.

Welding Rates

By using Equation 7.3, one can calculate the approximate welding rates for different seam types and welding positions. The average welding rate for horizontal welding is about 7 in./min. and for vertical welding it is approximately 4 in./min.

**Table 7.2 Typical Horizontal Welding Rates**

<i>Wire Diameter [in.]</i>	<i>Butt Seams [in./min.]</i>	<i>V-Seam [in./min.]</i>	<i>Fillet [in./min.]</i>
0.045	6-8	4.4-5.7	4-5.1
0.062	6.8-10	4.8-7.2	4.3-6.5

**Table 7.3 Typical Vertical Welding Rates**

<i>Wire Diameter [in.]</i>	<i>Butt Seams [in./min.]</i>	<i>V-Seam [in./min.]</i>	<i>Fillet [in./min.]</i>
0.045	2.1-3.6	1.5-2.5	1.4-2.3
0.062	2.7-6.8	1.9-4.8	1.7-4.3

Generally, higher welding rates are achieved when using larger diameter electrode wire. Depending on the ratio for horizontal versus vertical welds in the construction of a certain structure one can estimate the average welding rate for the entire design.

The AM Cost Estimator [23] (p.344) lists 3.6 in./min. for a V-Seam (0.5” steel plate, horiz.), 0.8 in./min. (0.5” plate, overhead) and 6.7 in./min. for a Fillet (0.5” plate, horiz.). These documented values are close to the values listed in Table 7.2 and Table 7.3.

### 7.2.5 Machining

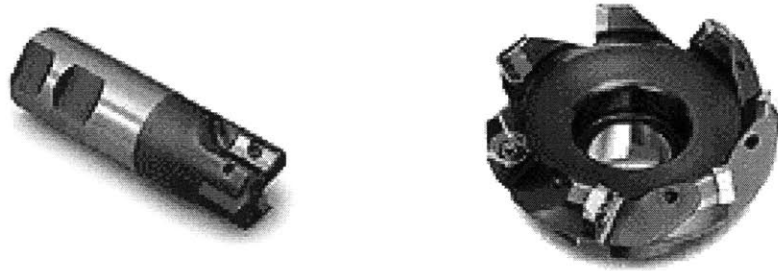


**Figure 7.8 Endmill & Facemill [37]**

Multi axis CNC-Milling processes are now frequently used to cut complex shapes out of solid blocks or plate stock. Commonly 5-axis CNC Milling machines are utilized for machining the intricate surfaces of molding tools. The programming prior to the actual cutting process is often done on the computer using CAD data directly from the designer. Modern insert technology produces cutting tools, which withstand very high abrasive forces and thus enable high cutting speeds. Multiple layers of titanium nitride coatings or polycrystalline diamond enhance tool life.

#### Feed Per Tooth

To calculate the feed per tooth (in inches) of a cutter, enter the feed in inches per minute (IPM), the number of Teeth (Z) and the RPMs of the spindle into the following formula.

$$\text{FPT} = \text{IPM} / (\text{Z} \times \text{RPM}) \quad \text{Equation 7.4}$$

#### Feed in Inches Per Minute

Equation 7.5 expresses the feed in inches per minute (IPM), with the feed per tooth (FPT), the number of teeth of face milling cutter (Z), and the RPMs of the spindle.

$$\text{IPM} = \text{FPT} \times \text{Z} \times \text{RPM} \quad \text{Equation 7.5}$$

The machining parameters are based on data from Valenite (Milpro) and reflect averages for facemilling operations. The linear feed rates are based on a  $\text{Ø}4''$  facemill. Other feed rates can be derived from these values. For the calculation of the material removal rates,

a cutting depth of 0.125 inches is assumed for a roughing and 0.04 inches for a finishing cut. However, the performance limits (horsepower) of smaller machine tools are quickly exceeded when cutting tool steel or Invar at these rates. The parameters and material removal rates for contour milling can be considerably lower, since the cutting speed is often limited by the strength of the tooling shaft. The linear feed rates have to be adjusted for these cases. The milling inserts are all CVD coated with an 11 degree relief angle and chip breaker grooves. The core material consists mainly of carbide steel.

**Table 7.4 Typical Machining Parameters**

	<i>Cutting Speed [ft./min.] Rough/Finish</i>	<i>Feed [in./tooth] Rough/Finish</i>	<i>Linear Feed [in./min.] Rough/Finish</i>	<i>Mat. Removal [in<sup>3</sup>/min.] Rough/Finish</i>
<b>Tool Steel (P20)</b>	427-760 950	0.005-0.01 0.04-0.009	19-48 (∅ 4") 43-58	7.9-48 1.7-7
<b>Cast Iron (Class 60)</b>	495-630 585-765	0.005-0.01 0.004-0.009	26-33 (∅ 4") 31-40	10-33 1.2-4.8
<b>Aluminum (6061-T6)</b>	2000-2600 2250-2727	0.007-0.016 0.005-0.009	99-238 (∅ 4") 111-208	40-238 4.4-25
<b>Nickel Alloy (Invar 36)</b>	125-200	0.004-0.009	3-10	1.2-10 0.12-1.2

### 7.2.6 Electroless Coating

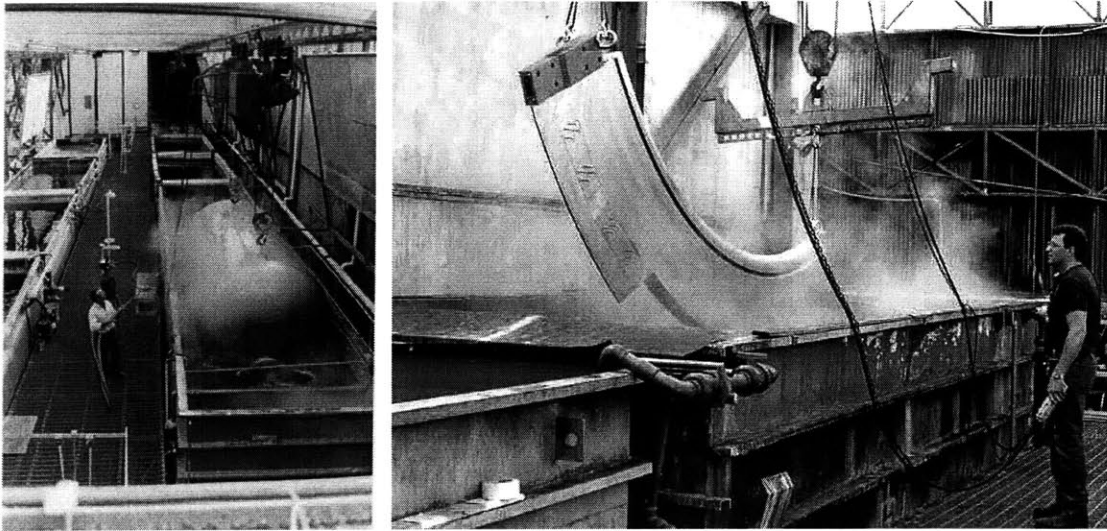


**Figure 7.9 Electroless Nickel [41]**

Electroless (autocatalytic) nickel (EN) provides a hard and uniform surface coating to tools. The coating also protects lower grade tooling materials against corrosion and abrasion. Electroless nickel is chemically deposited, making the coating exceptionally uniform in thickness. Careful process control can faithfully reproduce the surface finish, eliminating the need for costly machining after plating.

EN is a dense, nonporous, and crack-free metal-glass alloy of nickel and phosphorus, which has the appearance of polished stainless steel. EN can be applied to most metals such as steel and stainless steel, iron, aluminum, titanium, magnesium, copper, brass, bronze, and nickel. For composite tooling an EN coating is often applied to aluminum tools to improve release properties and wear resistance. The EN process is quite economical and has minor impact on the cost of composite tooling.

**Table 7.5 Electroless Nickel Properties**

	<i>Hardness</i>	<i>Density</i> [lbs/in <sup>3</sup> ]	<i>Thermal Diffusivity</i> [x 10 <sup>-6</sup> m <sup>2</sup> /s]	<i>Thermal Expansion</i> [x 10 <sup>-6</sup> 1/K]
<b>Electroless Nickel</b>	50-70C 550-1000 Vickers	0.300	13.8	13



### 7.2.7 Polishing and Finishing

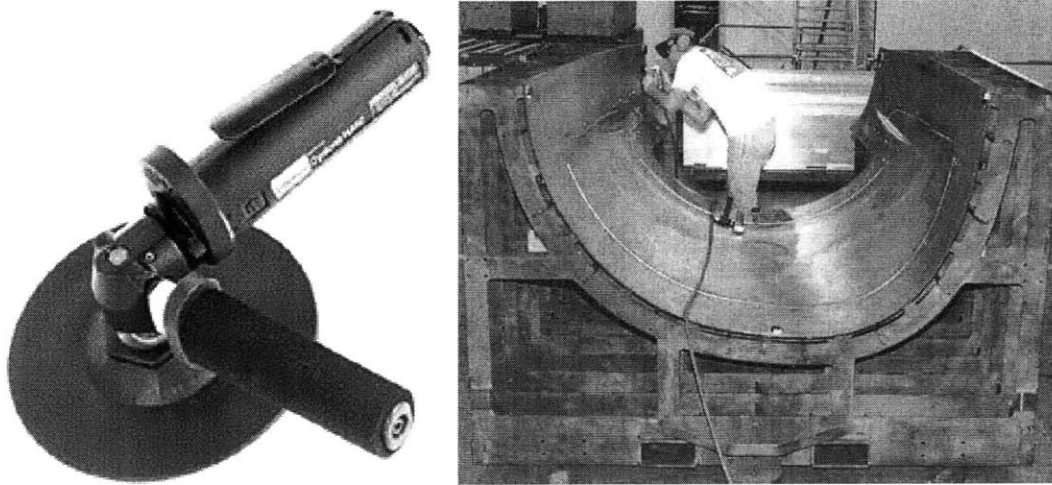


**Figure 7.10 Power Tool & Polishing [29, 35]**

Polishing is a process that produces a smooth and shiny surface finish. Two basic mechanisms are involved in the polishing process: (a) fine-scale abrasive removal, and (b) softening and smearing of surface layers by frictional heating during polishing. The shiny appearance of polished surfaces results from the smearing action. Polishing is performed with disks or belts, which are made of fabric, leather, or felt, and are coated with fine powders of aluminum oxide or diamond.

#### Time Estimates (AM Cost Estimator)

There are a variety of portable tools on the market for deburring and polishing, which are powered by compressed air or electricity. Portable-tools allow flexibility and mobility of the operator and are available at low cost.

The time estimation Table 7.39 in the Appendix 7.8.2 (AM Cost Estimator) [23] lists polishing times as a function of path length. It is assumed that an air-driven rotary flat sander is used together with an abrasive aluminum oxide grid of 50. The polishing performance in square inches per minute can be obtained by multiplying the polishing length with the disk diameter and the number of passes required. However, parts featuring irregular shapes, sharp corners, deep recesses, and sharp projections take longer to polish.

### 7.2.8 Inspection

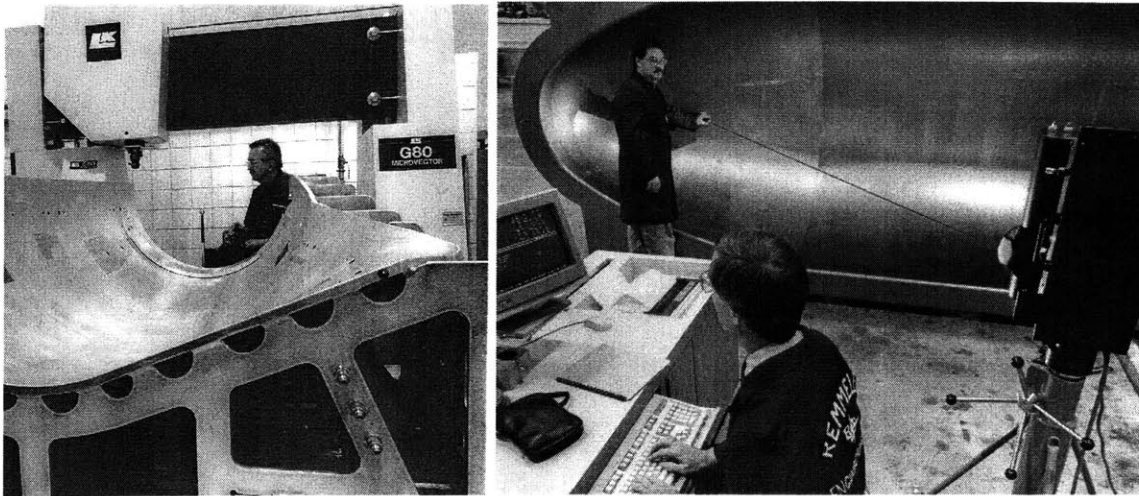


**Figure 7.11 CMM & Laser Tracker Inspection [29]**

For small to medium size tools, which require a high accuracy, a coordinate measurement machine (CMM) is used to probe the surface contours and record its dimensional accuracy. The operator steers the machine to certain reference points after which the numerical control completes the scan on its own. Due to the very stiff gantry style design a CMM machine is highly accurate.

For large tools, a Laser Tracker measurement system is employed to verify the contours of the tooling and to determine any deviation from the design specifications. In comparison to Coordinated Measurement Machines the system is slightly less accurate, but much more versatile and mobile. As seen in Figure 7.11, the surface of the part is probed with a steel ball, which contains prismatic mirrors. The laser inspection head follows the ball and triangulates constantly the distance between the stationary unit and the probing ball. The information is acquired by a computer system and after the entire surface is probed by the operator, the software depicts the actual 3D surface geometry. The 3D measurement data can then be overlaid with the CAD surface information in order to visualize any deviations. Unit costs are approximately \$100,000 and the inspection takes about 20% to 40% of the time it takes to machine the surface.

## 7.3 Open Mold Metal Tooling

### 7.3.1 Design Requirements

The layup tool can be described as an open mold, which resembles the inverted shape of the part to be produced. The main objective of the tool is therefore to match the size and shape of the part as closely as necessary under the conditions of the part manufacturing process. The designer should also strive to optimize the weight and the moment of inertia of the tool in order to facilitate its positioning and transportation. All tools have to survive the daily rigors of medium to high volume production. The surface should be polished and scratch resistant to continuously ensure high product quality and surface finishes. Autoclave tools often serve as layup tools, but they also provide dimensional stability and accuracy at the common curing temperatures of 250°F to 350°F (125°C to 175°C). The surface of the tool serves as the fixed, and the vacuum bag as the floating boundary of a vacuum container and therefore both have to be airtight. The flow of hot air inside the autoclave must not be restricted by the tool in order to promote a uniform temperature distribution. The energy and the time required to bring the tool up to curing temperature are each proportional to the mass of the tool times the specific heat capacity of its material. Consequently, a weight reduction, accomplished by means of a more efficient design, not only decreases the cycle time, but also facilitates the handling of the tool. All the design requirements have to be viewed in relations to the overall economics including the investment and maintenance costs. The following list summarizes the major design requirements.

- Durability & Accuracy of Structure
- Polished & Scratch Resistant Tooling Face
- Optimized Thermal Mass & Weight
- Minimal Thermal Expansion
- Low Resistance to Airflow
- Vacuum Integrity
- Optimized Economics

### 7.3.2 Material

Layup and Autoclave tooling generally consists of a face sheet and a support structure. The material selection criteria are linked to the design requirements and the function of the tool. Aluminum works well for tools, which are only used at room temperature. Tool steel is generally too heavy and does not possess the low thermal expansion of Invar, however steel might be used for some structural elements. Many metal Autoclave tooling is made of Invar, which keeps its dimensions at the elevated curing temperatures and can endure over 500 curing cycles without maintenance. The face sheet is generally constructed of plate stock ranging between 0.5 inches and 1 inch in thickness. The support structure is also built out of plate stock, but can also include square or cylindrical tube stock. The plate stock is available in panel sizes of up to 120 inches by 400 inches. Larger sizes also exist but generally have to be ordered specially at higher prices. The general properties are summarized in Table 7.1 and the costs are approximately \$0.5/lb for tool steel, \$5/lb for aluminum, and \$10/lb for Invar. Prices are very much dependent on the volume procured and can easily double for small orders.

### 7.3.3 Open Mold Design Features

The design of most layup and autoclave tools is similar and consists of a tool face and a support structure. Every tool possesses certain design features, which fulfill the basic requirements of the tool design. The following paragraphs introduce a generic open mold tool design and explain the major design parameters. In addition, optional features, which can be ordered by the customers, are also discussed in terms of their functionality and benefits.

#### Tool Face

The shell like structure of the tool face represents the most crucial component of the tool, since it is in direct contact with the composite part and therefore determines the quality. Accuracy under all process condition is therefore an essential functional requirement as well as a good surface finish. Small uniform wall thickness facilitates the heat transfer

between the laminate the surroundings and ensures uniform thermal expansion. The vacuum integrity is necessary for obvious reasons in an autoclave tool. Figure 7.12 shows a schematic of a face sheet.

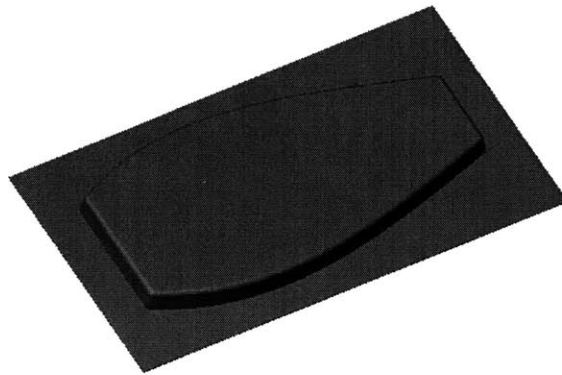


**Figure 7.12 Welded or Electroformed Tooling Face**

The design parameters associated with the above functional requirements such as the actual tool contour tolerance and face sheet's thickness are dependent on the manufacturing process. Commonly, three different methods can be used for face sheet fabrication:

a) Formed Bonded Thin Sheet

Thin sheets (0.04 to 0.125") of metal are formed by conventional forming methods. The sheets are then stacked and bonded together to give the tool face more rigidity. The process is quite labor intensive and has some limitations. Only tools for small and simple shapes can be produced economically. Larger tool sizes pose stability problems for the thin sheet metal and complex shape require expensive forming dies. Also in order to achieve acceptable accuracy several iterations between measuring and forming station are required, which too adds to the manufacturing time.

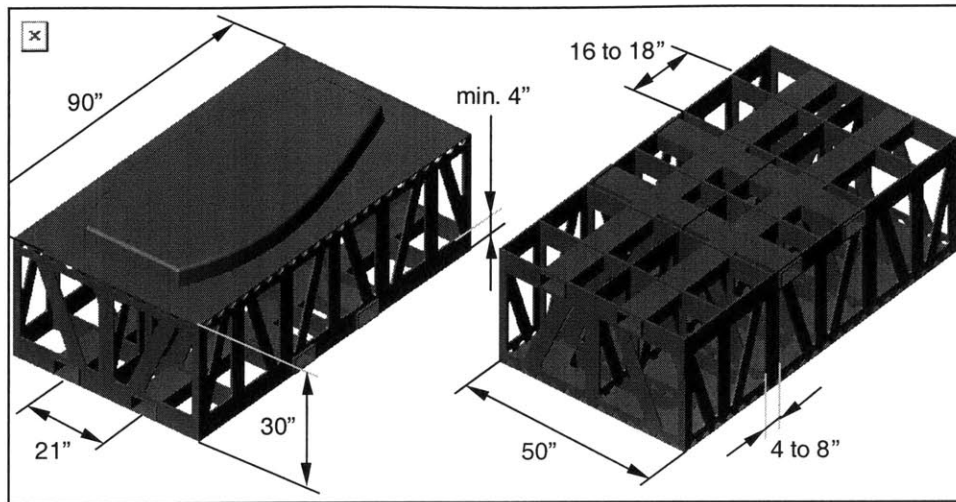
b) Electroformed Nickel

The process is generally used to produce accurate and complex tooling face sheets and is described in detail in Chapter 7.1.3. Advantages are the accurate production of numerous face sheets. To provide sufficient composite production capacity several

identical tools might be required and the initial costs for the master model can be spread out. However, the slow deposition rate of 4 to 11 days per face sheet can drive up costs and the leadtime of the tool. Also, electroformed nickel does not possess the favorable thermal expansion properties of the nickel alloy Invar. Accuracies better than  $\pm 0.01$  inches can be achieved.

c) Machining

Machined tool faces can be very accurately produced and can include complex features and up are up to 100 ft. long if not larger. Stock plate is used, which has to be sufficiently thick for machining. The thickness generally ranges between 0.5 inches to 1 inch. When possible a single plate is formed into the approximate shape and is attached to the substructure before being machined. However, in some cases the surface is too complex and has to be welded together from individually shaped plate sections. In the case of the tool face, as shown in Figure 7.12, the splits are placed along the edges, which results in 6 smaller pieces. The bending is accomplished by using common forming techniques as described in Chapter 7.2.2 and by pressing the plates into the contours of the support structure. CNC controlled machine tools programmed with CAD data achieve contour tolerances of at least  $\pm 0.01$ ". The process is also universal and not restricted to a certain material. Some complex tools require a uniform face sheet thickness to ensure an even temperature distribution. In these cases, both sides of the face sheet are machined starting with the backside. After machining the rear, the face sheet is detached from the sacrificial support structure, turned over, and attached to the regular substructure. Now the profiling of the front can commence. The process of machining both sides is very time consuming and an electroformed nickel face sheet might be an economic alternative.

Support Structure

**Figure 7.13 Tool Face with Eggcrate Support Structure**

Independently from the fabrication method of the face sheet a support structure is necessary to provide dimensional stability and stiffness to the thin tool face. The support structure for metal tooling is mainly plasma cut out of 0.375 inch to 0.75 inch stock plate and then welded together. Since in some cases, the plates of the face sheet are formed by pressing them into the substructure, the design has to be sturdy enough to withstand these forces. The thickness, the spacing of the plates and the width of the support struts have to be chosen accordingly. However, the tool should also be lightweight, since otherwise it is more difficult to handle and exhibits a high thermal mass. At least 50% of each side of the substructure has to be open to facilitate the airflow in the autoclave. As a guideline, the width of the support struts should be between 4 to 8 inches depending on the size of the tool. In addition, the stiffening plates should be spaced 16 inches to 18 inches apart.

To further enhance the heat exchange between the tool face and the ambient hot air, half circles with a radius between 1 inch and 2 inches are cut out of the stiffening plates as seen in Figure 7.14. The smaller and fewer the contact points between tool face and support the more uniform the temperature distribution within the tool face, since the substructure acts as a heat capacitor or heat source/sink.

Autoclave tooling is regularly moved from the layup areas to the Autoclave and back. Unevenness in the shop floor can cause deformation of the precise surface. To provide additional stiffness, strips of stock plate can be welded diagonally into the rectangular sections formed by the individual contour plates. Also, sections of 7 inches by 4 inches square tubing strengthen the tool and serve as jack points for forklifts and pallet jacks. The tubing is spaced 21 inches apart to accommodate the lifting forks. Eventually, the face sheet is attached either by welding or by using brackets and bolts.

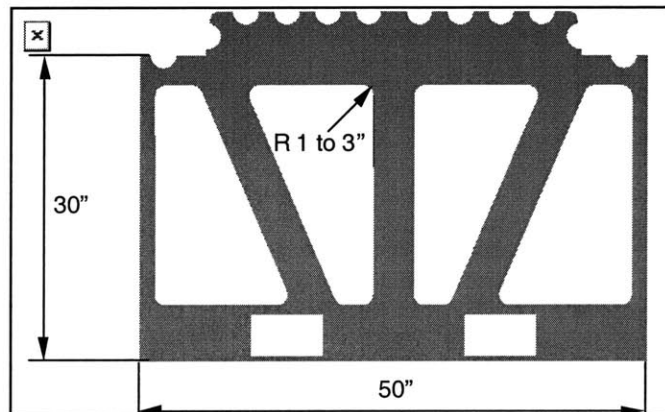


**Figure 7.14 Individual Stiffener Plate w/ Cut-Outs for Air Flow**

#### Casters

Tools the size of the one depicted in Figure 7.13 weigh about 2,500 lbs when fabricated out of steel or Invar. For additional mobility and to move even larger size tools, spring-loaded casters are attached to the substructure. They not only support the weight of the tool, but also minimize any forces transmitted to the tool by an uneven production floor. Since, in most cases the casters stay attached to the tool they need to withstand the high curing temperatures inside the oven or autoclave. To securely mount the tool onto the fasteners, special welding constructions are required, which transfer the forces into the tool structure.



### Cutting & Trimming Grooves

Optionally, cutter and trim grooves can be incorporated into the tool face. Some parts are trimmed right on the tool, which simplifies positioning and ensures precision. Although the trimming increases the turn around time of the tool, it saves a separate trimming tool.

### Fairings

Fairings are attached to the tool surface to serve as a boundary for the composite laminate during lay-up and cure. They prevent thinning of the laminate along its edges caused by the pressure exerted by the vacuum bag. These dams are machined out of solid stock and bolted to the tool face. The vacuum integrity of the tool must not be compromised when tapping the attachment holes.

### Vacuum Plumbing

Bag failure during cure can lead to poor part quality or even the loss of the part and therefore poses an economical risk. To minimize the risk, the vacuum fitting can be permanently installed into the tool instead of being attached to the more vulnerable bagging film. Openings placed in the correct location on the tool surface ensure even vacuum pressure throughout the bagged part. These holes are drilled during the machining of the face sheet and the threads for the fittings are tapped manually from the back of the tool. Copper or stainless steel pipes connect all the openings to a central terminal. Common pipe sizes range from ¼" to ½" (OD 0.540" to 0.840") with a wall thickness between 0.035" and 0.065". The installation includes the tapping of the connecting holes, the cutting and fitting of the pipes and connecting them to the fittings on the rear of the tool face.

### Thermocouples

During the cure cycle, the temperature within the laminate is monitored constantly to ensure sufficient cross-linking of the resin. However, attaching thermocouples before every Autoclave run is time consuming and inevitably leads to bad connections and false readings. Thermocouples integrated into the tool solve this problem and increase turn

around time. The thermal junction is located approximately 0.025" to 0.05" underneath the surface and the wiring is protected by tubing and connected to a central terminal. To maintain vacuum integrity the attachment holes for the thermocouples are carefully drilled by hand from the back of the tool.

### Summary of the Design Features

The following list summarizes the design features of open mold metal tooling:

#### Tooling Face

- Accuracy approx.  $\pm 0.01$ "
- Plate Thickness: 0.5"-1"
- Polished approx.  $\leq 63 \mu\text{in}$
- Uniform Thickness & Vacuum Tight

#### Support Structure

- Plate Thickness: 0.375"-0.5"
- Cut-Outs: 50%
- Half-Circle Cut-Outs: 1"-2" diameter
- Stiffener Plate Spacing: 16"-18"
- Support Elements: 4"-8" wide
- Jacking Points: 7" x 4" tubing

#### Options

- Casters
- Trimming & Cutting Grooves
- Fairings
- Central Vacuum Plumbing
- Integrated Thermocouples

### 7.3.4 Cost Components of Open Mold Tooling

In an effort to apply the methods of process based cost estimation to open mold tooling, a visit to a large tooling manufacturer helped to understand the major cost elements [29]. It is important to note, that the costs and prices quoted in this study refer to the costs of the first copy of a specific tool. All additionally produced tools would be discounted accordingly. Open mold tools can be quite large and expensive and contain a number of optional details depending on the customer specifications. The material, fabrication, and design costs, which generally drive the overall costs, are related to the size and the complexity of the tool. Despite of the uniqueness of each tool, it is possible to establish a generic fabrication process, which simplifies all cost modeling efforts. The major cost components derived from the case study are listed below:

- Material
- Tool Size & Complexity
- Detailing & Polishing
- Inspection & Leak Check
- Design & Engineering
- Order & Batch Size
- Capital Costs & Profit

#### Material Costs

Material costs scale directly with the size and the weight of the tool. In particular, for Invar tooling their contribution to the overall costs can be in excess of 30%. The general material properties are summarized in Table 7.1. The metal prices are approximately \$0.5/lb for Tool Steel, \$5/lb for Aluminum, and \$10/lb for Invar. However, one has to consider that prices are strongly dependent on the purchased volume and might easily be half or twice the average price. Also the scrap resulting from the many cut-outs can be sold, which again reduces the costs. In the subsequent case studies, an average price is assumed, which factors in the revenue of scrap material.

### Manufacturing Costs

To estimate the manufacturing costs it helps to investigate the production steps of a tool. The resulting manufacturing process plan describes the order and the type of each operation. After calculating the time for each step, the process plan serves as the base for comparing the cost of various designs. It also facilitates the development of a more generic cost model, because it allows the identification of the most cost and time-consuming operations. In the case of open mold metal tools, the process plan is similar regardless of the size or shape complexity of the tool. The basic process plan is presented in Table 7.6.

**Table 7.6 Generic Process Plan for Open Mold Tooling**

1.	<b>Plasma Cut Substructure</b>
2.	<b>Weld Substructure</b>
3.	<b>Machine Contours of Substructure</b>
4.	<b>Plasma Cut Face Sheets</b>
5.	<b>Form Face Sheets</b>
6.	<b>Weld Face Sheets</b>
7.	<b>Heat Treatment</b>
8.	<b>Straighten Face Sheet</b>
9.	<b>Machine Face Sheet</b>
10.	<b>Mount Accessories</b>
11.	<b>Polish Face Sheet</b>
12.	<b>Final Inspection</b>
13.	<b>Box and Ship Tool</b>

The costs for labor and machine usage are calculated by estimating the processing times for each step and multiplying it by the respective labor and machine rates. For an experienced machinist and welder the labor rate is approximately \$100/hr on average including overhead.

The production process requires large 5-Axis CNC controlled milling machines. These machines cost between \$200K and \$800K and depending on the depreciation schedule \$200/hr to \$300/hr are charged for their usage. The machining costs however can jump as the size of the tool increases and the next larger equipment types have to be used for the fabrication of the tool. The cutting performance is generally slightly below the

average material removal rate because of the complex contour milling operations during tool production. In accordance with the values presented in Table 7.4 the material removal rate lies in the lower third of the quoted range.

The plasma or oxy-fuel cutting machines used to trim the stock plate generally boast a 2 to 3 Axis CNC controller and cost between \$100K and \$300K. Their hourly rate lies in the range of \$100/hr to \$150/hr.

Heat treatment of the welded structure is also a major cost driver and is often outsourced by the tooling manufacturer. The costs scale with the weight of the tool, which has to be shipped to the heat treatment facility and is processed for approximately 15 to 30 hours, depending on the material and the objective. Boothroyd lists a price between \$1/lb and \$2/lb for heat treatment [29].

Welding, forming and polishing in comparison only require relatively small and inexpensive machinery. The process costs are generally driven by labor as the welding requires significant setup times and polishing is a slow and tedious process.

The costs of moving and transporting the tool around the production floor are generally larger for a shop job environment. These costs are commonly expressed as a percentage of the total manufacturing costs and depend on the efficiency of the part flow throughout the shop. As an estimate, 5% to 15% of the total manufacturing time is spent on moving the unfinished tool. For heavy tools 2 to 8 workers can be involved to handle the lifting gear and to direct the movement.

### Detailing Costs

Detailing costs can be significant and are often responsible for variations in tooling costs. Industry sources acknowledge the difficulty to generalize the estimation of detailing costs but have provided some guidelines. The detailing costs vary between 5% and 15% of the total costs depending on the options requested by the customer. However, the more detailed cost information available is outlined in the following paragraphs.

Optional casters for moving the tool on the production floor cost approximately \$500 each including the welded construction to attached them to the tool's substructure.

For integrated thermocouples the installation times ranges between 40 and 80 man-hours for a medium size tool. The material costs are insignificant compared to the labor costs as thermocouple wire prices lie between \$1/ft and \$1.50/ft for J- and K-Types. Accessories, such as jacks, connectors and fittings, sum up to about \$20 per TC-connection.

The installation of vacuum plumbing takes also between 40 hours and 80 man-hours depending on the size and the complexity of the system including the final leak checks. Again, material costs for tubing are marginal (approx. \$1/ft for copper 122 and \$2/ft for stainless steel 304) compared to the labor cost for the installation.

#### Inspection & Leak Check

The dimensional accuracy of each tool is tested by a final inspection of its contours. Depending on the size of the tool and the available equipment, a computer controlled coordinate measurement machine (CMM) or a laser tracker are employed. The systems cost are about \$100K and generally require an engineer or a specially trained operator. The time however is difficult to estimate, since unexpected problems can prolong the process considerably. Additionally, the complexity and the size of the tooling surface affect the inspection time. Therefore, as a first order approximation it takes about 10% to 50% of the machining time to measure the surface contours. This approximation is an attempt to somehow reflect the size and complexity effects of the part.

Tooling furnished with integrated vacuum plumbing or collapsible tooling is generally subjected to a leak test to ensure vacuum integrity. In some cases, the leak test is performed inside an oven to simulate the curing process and the possible effects of thermal expansion. The tests can be quite expensive for a large tool, since the testing requirements are usually beyond the capability of the tooling manufacturer. However, no pricing information could be obtained from our industry source.

### Design & Engineering Costs

Design and engineering costs make up about 30% to 50% of the total costs according to several manufacturers [28, 29]. The support structure and the face sheet have to be designed in accordance with the production requirements for each tool. Much of the engineering time is spent on customer interaction, defining the best tooling solution and on iterative design changes.

Complex curved surfaces result in time consuming CNC programs and slow machining operations. They also might require separately designed inserts for areas of pronounced double curvature and dramatic transition in the geometry. Although, generated directly from the CAD drawings approximately 10% of the machining time are required to produce and optimize the CNC code. A similar amount can be assumed for generating the CNC file for the plasma cutter.

For complex tools, Finite Element Analysis (FEM) of the thermal and mechanical loads serves as an insurance policy for the tooling manufacturer. The deformation of the tool under its own weight can be assessed reliably as well as the effects of thermal expansion. The average costs of \$5,000 to \$20,000 per analysis are still small compared to the cost of the entire tool and the costs of possible manufacturing problems.

### Batch Size

Because of the generally small batch sizes in which they are produced, the tooling costs are a strong function of the order size ( $\sim 1/n$ ). However, most costs and prices quoted in this study refer to the costs of the first copy of a specific tool. All additionally produced tools would be discounted accordingly to spread out the high fixed cost of engineering.

The production of left- and right hand tooling pairs has become easy with the advent of CAD and CNC technology. Although, slightly different the costs can almost be treated as if an extra copy of the original tool is produced.

### Capital Costs & Profit

The expenses and the time to delivery can be considerable for large open mold tooling. Therefore, capital costs have to be considered in the overall cost calculation. In general, opportunity costs of capital are in the order of 10% to 20% for the industry and the capital recovery period can be several months.

The profit margin is highly variable and depends on the pricing policy, the economic situation, and the customers bargaining power. For our calculations, the profit is assumed to be between 5% and 30%.

### **7.3.5 Tooling Complexity**

The complexity of a tool affects the manufacturing costs significantly. Complexity can be defined in many ways, however it is practical to relate complexity to the employed manufacturing process. In the case of machined metal tooling the curvature of the tool face represents a good measure of complexity. Simply speaking stronger curved surfaces result in longer CNC code, slower machining operations, and require more time to be joined and welded together. Complex tools also might require separately machined inserts for areas of pronounced levels of double curvature and dramatic transition in the geometry. Therefore, Remmele Engineering has established four major categories of complexity for the purpose of scaling the manufacturing cost. Of course, one could introduce more levels, however simplicity of the model is important so adjustments can be made quickly and user friendliness is guaranteed [28]. Figure 7.15 depicts representative tools for each of the four complexity categories.

Complexity level 1 (upper left) represents the simplest type of tools. Tools in this category are relatively flat and consist of a single piece face sheet that requires a minimum amount of forming/machining.

Complexity level 2 (upper right) tooling features more pronounced single curvature and thus requires more effort to bend and to machine the tool surface. Depending on the size



and the nature of the transition, face sheets may need to be assembled using several smaller pieces, which require additional forming/machining.

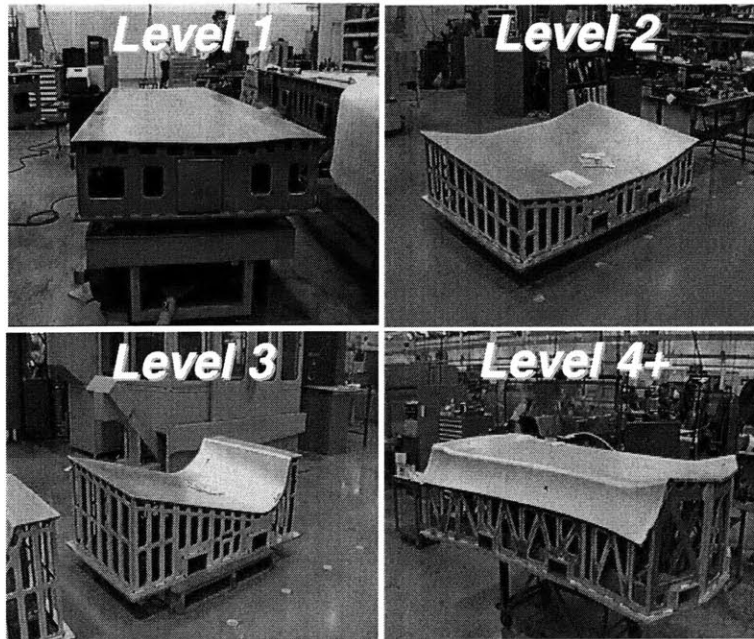


**Figure 7.15 Complexity Levels of Open Mold Tooling [29]**

Complexity level 3 tooling (lower left) is characterized by pronounced single curvature or slight double curvature. Face sheets will generally be made from more than one sheet, and plenty of forming and bending is required. Also to achieve more dramatic transitions within the tool face, pre-machined inserts are welded into the tool face in these areas before the surface is given its final contour.

Complexity level 4 (lower right) tooling exhibits bends and contours in more than one direction with dramatic transitions. Face sheets are produced by a combination of pre-machined inserts, formed plate and in some cases may require castings.

### 7.3.6 Case Study: Curing Tool for Jet Engine Caulings (Invar, Level 4)

The previous insights are applied to estimate the costs of an autoclave curing tool for jet engine caulings. The case study leads through each production step and demonstrates how process based costing works. The eggcrate type support structure of the tool, as seen in Figure 7.16, is constructed of ½ inch thick Invar plate. The tool face is welded together out of many elements of ¾ inch plate. The basic dimensions are 10ft x 10ft x 7ft. and the entire tool weighs approximately 9,400lbs. The radius of the half cylindrical tooling face varies along the length of the tool. Therefore, the geometry exhibits a significant amount of double curvature and the tool is classified as complexity level 4. The ratio of surface to projected area is approximately 140%. The manufacturer tells us that the tool also features vacuum plumbing and has fairings installed along the part's boundaries. Although several copies of the tool have been produced, in order to provide sufficient production capacity, the price for the first copy is \$750,000.

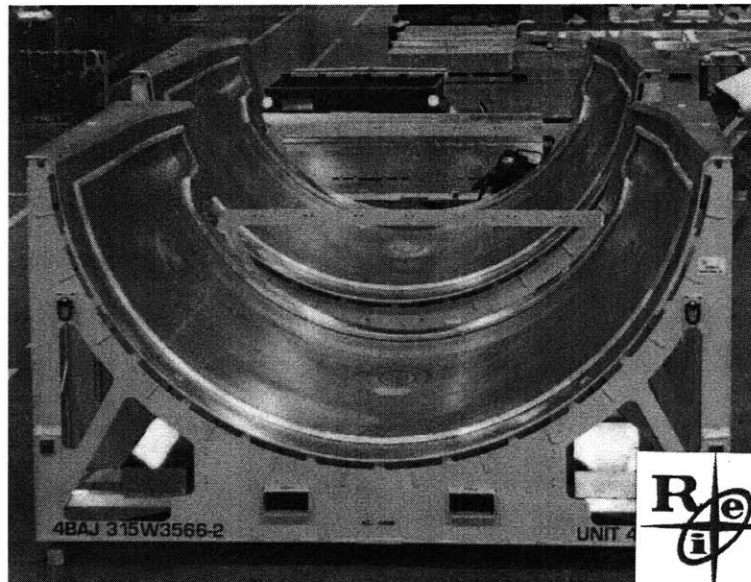
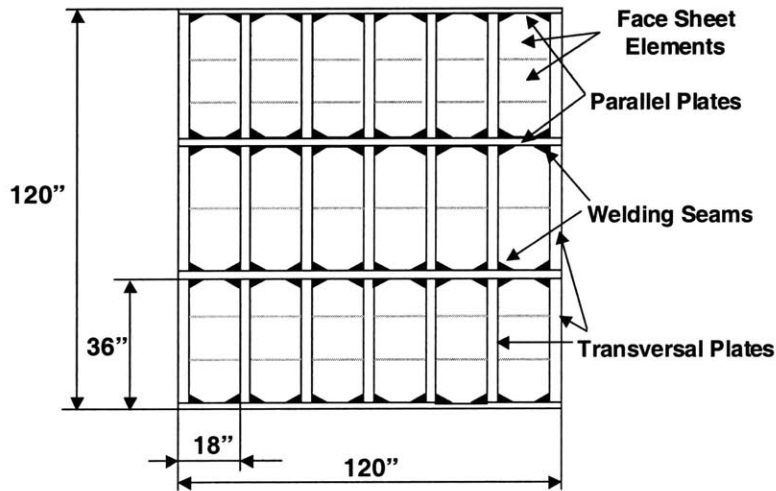


Figure 7.16 Autoclave Tool for Engine Cauling [29]

<i>Dimensions</i>	<i>Material</i>	<i>Weight</i>	<i>Surface Area</i>	<i>Options</i>	<i>Price</i>
10ft x 10ft x 7ft.	Invar 36	9,400 lbs	20,100 in <sup>2</sup>	Vac. Plumbing, Fairings	<b>\$750K</b>

Material Costs

Figure 7.17 shows a schematic of the tool as seen from the bottom (see Figure 7.50 in the Appendix 7.8.7 for a frontal view). The parallel and transversal plates, which make up the support structure, can be seen along with the welding seams. The material costs are calculated without considering any revenue from selling the scrap material from the cutouts.



**Figure 7.17 Schematic of the Engine Cauling Tool (Bottom View) [29]**

The support structure is constructed of 1/2" thick Invar stock plate, whereas the face sheet elements are made of 3/4" plate. Table 7.7 outlines the calculation of the material costs for the support structure and the face sheet assuming an Invar price of \$10/lb.

**Table 7.7 Material Costs for Engine Cauling Tool**

<i>Items</i>	<i>Values</i>
Spacing of Parallel Plates	36 in.
Number of Parallel Plates	4
Volume of 1 Parallel Plate w/o Cutouts	4,536 in <sup>3</sup>
Spacing of Transversal Plates	18 in.
Number of Transversal Plates	7
Volume of 1 Transversal Plate w/o Cutouts	4,385 in <sup>3</sup>
Material Volume (Substructure)	48,842 in <sup>3</sup>
Material Weight (Substructure)	14,311 lbs
Material Volume (Face Sheet)	12,092 in <sup>3</sup>
Material Weight (Face Sheet)	3,543 lbs
<b>Total Material Costs</b>	<b>\$178,538</b>

### Plasma Cutting of the Substructure Elements

Prior to cutting, engineering lays out the pattern and produces the CNC burn file on the computer. Given the high cost of Invar efficient nesting is paramount to keep the amount of scrap low. However, according to the design guidelines in Chapter 7.3.3 and as seen in Figure 7.17, the parallel and transversal plates features many cutouts.

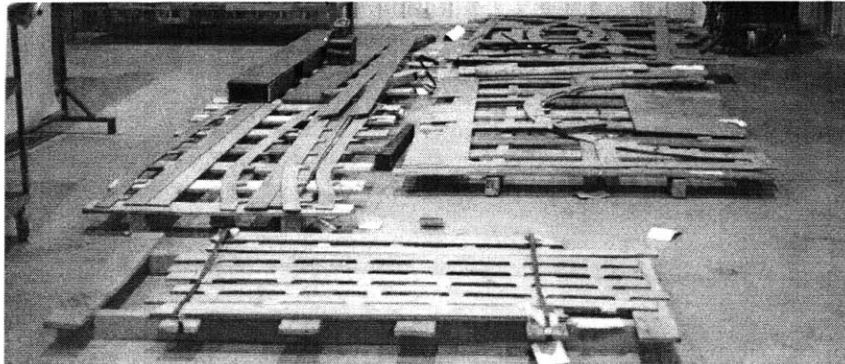


**Figure 7.18 Plasma Cut Invar Plates for the Substructure [29]**

Table 7.8 outlines the time calculation assuming 2 hours for setting up the machine, loading the program and readying the material. For the ½ inch plate stock an average cutting speed of 60 in/min is assumed, which is in accordance with the values presented in Chapter 7.2.1. In addition, a 15 min. delay between the cutting of individual part is assumed to remove the part and load the next plate onto the machine. The cost estimate for cutting is obtained by multiplying the cycle time with the respective labor (\$100/hr) and machine rates (\$150/hr).

**Table 7.8 Processing Data for the Cutting of the Substructure Elements**

<i>Items</i>	<i>Values</i>
Remaining Width	4 in.
Number of Cutouts in Parallel Plates	6
Cutting Length per Parallel Plate	1,266 in.
Number of Cutouts in Transversal Plates	3
Cutting Length per Transversal Plate	1,026 in.
Total Cutting Length	12,246 in.
<b>Plasma Cutting Time</b>	<b>12.4 hrs</b>
<b>Plasma Cutting Cost (Labor &amp; Equip.)</b>	<b>\$3,100</b>

Welding of the Substructure

It takes about 4 hours to setup the welding and to correctly position all the pieces. As seen in Figure 7.19 access can be difficult and the welder has to deal with vertical and even overhead seams. Under these circumstances, an average speed of 2.5 inches is assumed for GMAW welding of Invar. Once a seam is completed, the welder positions and rechecks the location of the plate and prepares the new seam. A delay of 30 min is considered for these preparations.

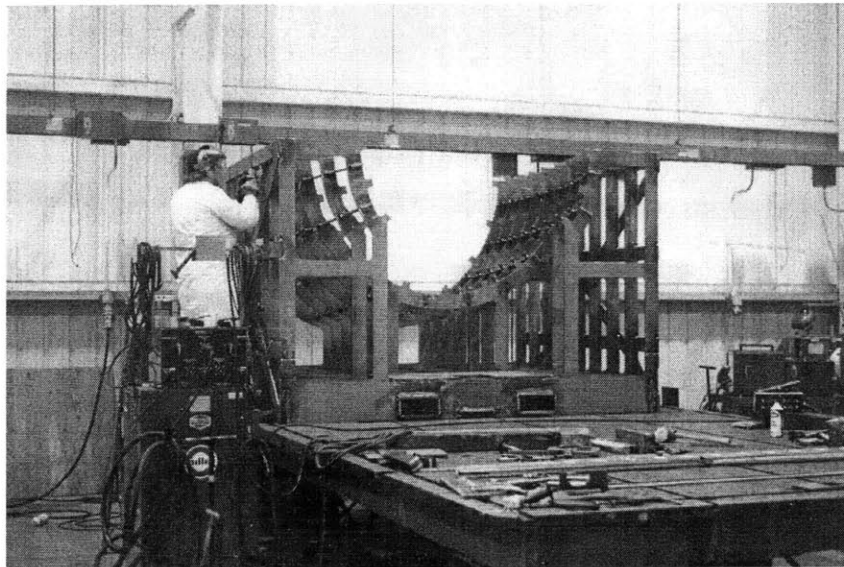


**Figure 7.19 Welding of the Substructure [29]**

The costs for welding are mainly dominated by labor and are obtained by multiplying the cycle time with the respective labor (\$100/hr) and machine rates (\$50/hr).

**Table 7.9 Processing Data for the Welding of the Substructure**

<i>Items</i>	<i>Values</i>
Number of Welding Seams	72
Length of each Seam	63 in
Total Seam Length	4,536 in
<b>Welding Time</b>	<b>70.2 hrs</b>
<b>Welding Costs (Labor &amp; Equip.)</b>	<b>\$10,536</b>

### Machining the Foot and the Contours of the Substructure

After the substructure is assembled, it is brought to a machining center for the facing of the underside. This establishes a reference plane on which the tool will rest during future machining operation. As outlined in Table 7.4, the feed for roughing operations is about 5 in/min for Invar, if not faster. To setup the heavy structure on the machine, load the program and ready the milling machine takes approximately 4 hours. The operation takes off material along each of the 4 parallel and 7 transversal plates. Following the machining of the foot the substructure is turned around and repositioned with the new reference plane now resting on the machine bed. A process, which takes about 2 hours including the setup of the machine to cut the inner contours of the substructure. Again, to compute the costs, the cycle time is multiplied by the labor rate for the machinist (\$100/hr) and the machine rate for a large 5-axis CNC milling center (\$200/hr).

**Table 7.10 Processing Data for the Machining of the Substructure**

<i>Items</i>	<i>Values</i>
Total Machining Length	2,640 in
Number of Repositionings	1
<b>Machining Time</b>	<b>16.8 hrs</b>
<b>Machining Costs (Labor &amp; Equip.)</b>	<b>\$5,040</b>

### Plasma Cutting of the Face Sheet Elements

The 18 face sheet elements are plasma cut out of  $\frac{3}{4}$  inch thick plate at a speed of 60 inches per minute. The number of face sheet elements primarily depends on the shape complexity of the tool, since the surface is subdivided in smaller elements. All process and cost parameters are identical to the ones used for cutting the substructure.

**Table 7.11 Processing Data for the Machining of the Substructure**

<i>Items</i>	<i>Values</i>
Perimeter of Each Face Element	108 in
Number of Face Elements	18
<b>Plasma Cutting Time</b>	<b>7.0 hrs</b>
<b>Plasma Cutting Costs (Labor &amp; Equip.)</b>	<b>\$1,760</b>

Forming & Fitting of the Face Sheet Elements

The forming and fitting of the individual face sheet elements is an iterative process, which makes it difficult to estimate the cycle time. The operator uses a press brake to perform each element before checking its fit on the substructure. It is assumed, that the operator returns to the press brake a second time for adjustments in the shape. Each one of these forming operations takes supposedly 15 minutes and maybe even longer. The worker then positions the face sheet element weighing about 140 lbs. using hoisting gear. In some cases, a hydraulic press is used to press the face sheets onto the contours of the substructure in order to give them their final shape and to hold them in place for tacking with the welding gun. For the tool to be fabricated in such a way, the substructure has to provide some rigidity to withstand the forces exerted by the hydraulic press. The final fitting, positioning and tacking also takes about 15 minutes. Once more, the costs are calculated by multiplying the cycle time with the respective rates for labor (\$100/hrs) and equipment (\$50/hr). The cycle time for the entire operation very much depends on the shape complexity of the tool. Not only does the number of elements increase with complexity, but also the time to form each one of them. Therefore, for very dramatic transitions pre-machined inserts or even castings can become part of the face sheet puzzle.

**Table 7.12 Processing Data for the Forming & Fitting of the Face Sheet Elements**

<i>Items</i>	<i>Values</i>
Number of Face Elements	18
<b>Forming &amp; Fitting Time</b>	<b>13.5 hrs</b>
<b>Forming &amp; Fitting Costs (Labor &amp; Equip.)</b>	<b>\$2,025</b>

According to the industry source, approximately 5 to 6 working days (ca. 100 hrs) have gone by up until this point, not including the plasma cutting [29]. Our time estimates sum up to about 108 hours, which is considered reasonably close.

Welding & Deburring of the Tool Face

The GMAW welding of the face sheet elements joins them together and closes the gaps in between. Each seam has to be airtight and free of porosity in order to ensure vacuum integrity. In addition, the 18 elements are also securely welded from the inside to the eggcrate like support structure. Sometimes two welders are working on the same tool simultaneously. The process takes about 2 to 3 working shifts for a medium size tool. The process and cost parameter are identical to the welding of the substructure.

**Table 7.13 Processing Data for the Welding of the Tool Face**

<i>Items</i>	<i>Values</i>
Number of Welding Seams	36
Length of each Seam	108 in
Total Seam Length	3,888 in
<b>Welding Time</b>	<b>23.1 hrs</b>
<b>Welding Costs (Labor &amp; Equip.)</b>	<b>\$3,462</b>

Upon completion of the welding, the seams are cleaned of slack, dross and metal droplets. A rotary air tool is used to grind away the burr on the outside of the tooling face at a speed of about 4 inches per minute. A 30 minutes setup time is taken into account.

**Table 7.14 Processing Data for the Deburring of the Welding Seams**

<i>Items</i>	<i>Values</i>
Deburring Length	1,944 in
<b>Deburring Time</b>	<b>8.6 hrs</b>
<b>Deburring Costs (Labor)</b>	<b>\$860</b>

Heat Treatment for Stress Relief

Prior to contour machining the tooling face the entire tool is fully annealed in order to relieve the residual welding stresses and to avoid any later unexpected deformation. For Invar the annealing takes place at 1,450°F for 30 minutes for every inch of thickness followed by air cooling. In order to obtain maximum dimensional stability, the tool is then soaked at 1,500°F and quenched with water, reheated to 600°F for 1 hour before cool



down in open air. The entire process takes between 12 and 48 hours depending on the thickness and total material mass. Generally, tooling manufacturers outsource the heat treatment and ship the tool to a nearby facility. Subsequently, the tool is checked for micro cracks using a die pen as seen in Figure 7.20.

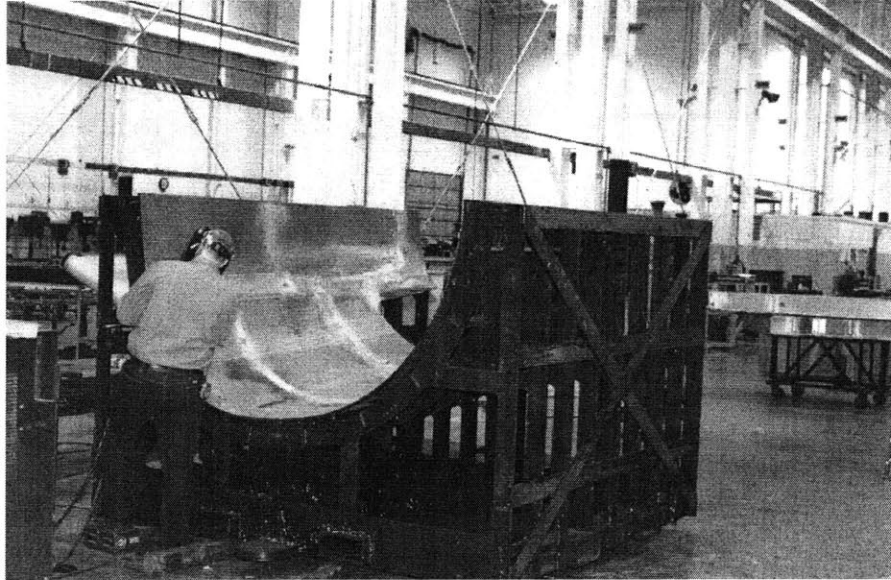


**Figure 7.20 Stress Relieving and Die Pen Checking Prior to Machining [29]**

Table 7.15 shows, that our model overestimates the actual weight of the tool by approximately 450 lbs. An average of \$1.5/lb is charged for heat treatment including shipping and handling.

**Table 7.15 Processing Data for Heat Treatment**

<i>Items</i>	<i>Values</i>
Tool Weight	9,848 lbs
<b>Heat Treatment Costs (Labor &amp; Equip.)</b>	<b>\$14,772</b>

Machining of the Tooling Face

For giving the tool face its final contours the tool again is setup on the 5-axis CNC milling center as seen in Figure 7.21. This process takes about 4 hours, which includes the probing of the tool surface, the accurate positioning, and the loading of the CNC

code. A first roughing pass machines away approximately  $\frac{1}{4}$  inch of the Invar face at a material removal rate of  $4 \text{ in}^3/\text{min}$ . The following finishing pass proceeds at a surface speed of  $10 \text{ in}^2/\text{min}$ .

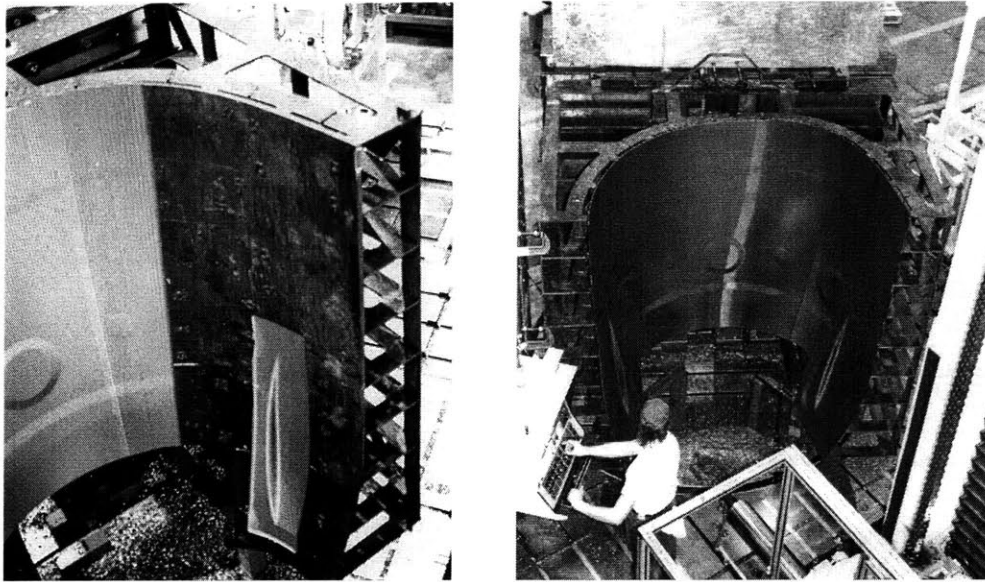


**Figure 7.21** Rough and Finish Machining on 5 Axis CNC Milling Center [29]

Table 7.16 lists the processing parameters in connection with costs for machining. Labor (\$100/hr) and machining rates (\$200/hr) are unchanged.

**Table 7.16** Processing Data for the Machining of the Tool Face Contours

<i>Items</i>	<i>Values</i>
Surface Area	20,154 in <sup>2</sup>
Cutting Depth (Roughing)	0.25 in
Material Volume	5,038 in <sup>3</sup>
<b>Rough Machining Time</b>	<b>25.0 hrs</b>
<b>Finish Machining Time</b>	<b>33.6 hrs</b>
<b>Machining Costs (Labor &amp; Equip.)</b>	<b>\$17,575</b>

### Mount Details

Before the tool face is polished, all the custom specified details are installed. As shown Figure 7.22, the engine cauling tool is furnished with a central vacuum system and fairings around the edges.

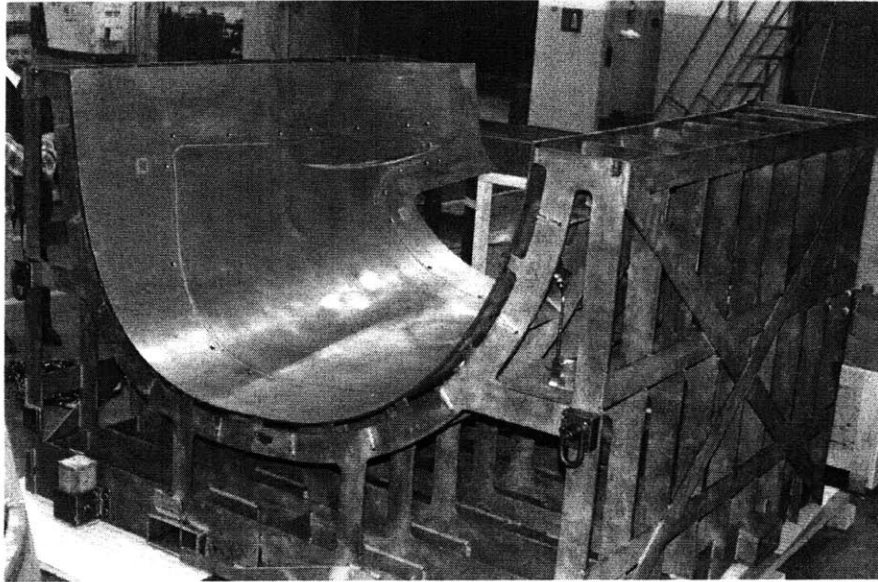


**Figure 7.22 Install Vacuum Plumbing and Fairings [29]**

It is assumed that the fabrication and installation make up about 10% of the total manufacturing time. Table 7.17 lists the time and the costs under the assumption of the usual labor and equipment rates.

**Table 7.17 Cost Estimates of the Optional Details**

<i>Items</i>	<i>Values</i>
Time 10 % of Total Mfg. Time	27.7 hrs
<b>Detailing Costs (Labor &amp; Equip.)</b>	<b>\$4,161</b>

Polishing of the Tooling Face

A rotary air tool is employed to finish the tool face and polish it to a 63 micro inch surface. The polishing is carried out by one or two workers at a speed of about 5 in<sup>2</sup>/min. The labor rate is approximately \$100/hr as evident from Table 7.18.

**Table 7.18 Processing Data for the Polishing of the Tool Face**

<i>Items</i>	<i>Values</i>
Surface Area	20,154 in <sup>2</sup>
<b>Polishing Time</b>	<b>67.2 hrs</b>
<b>Polishing Costs (Labor)</b>	<b>\$6,718</b>

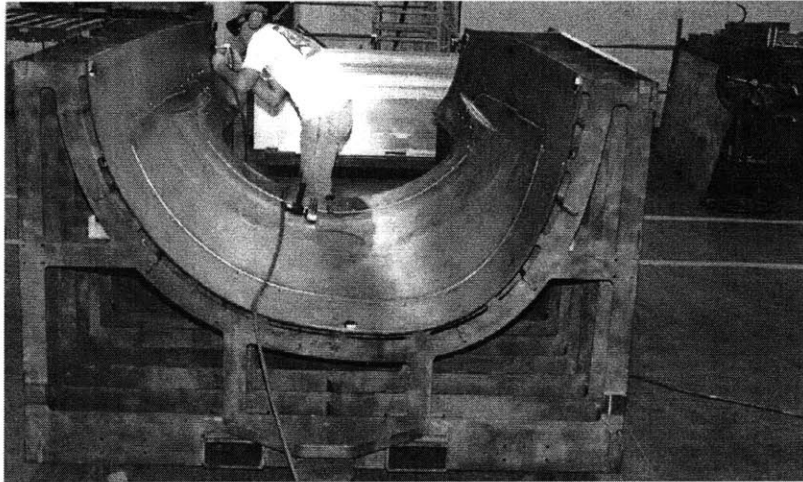


**Figure 7.23 Polishing to a 63  $\mu\text{m}$ . Finish [29]**

### Final Inspection

The final inspection includes a contour check with a laser tracker and a test of the vacuum integrity of the tooling face. To perform these tests it takes approximately 40% of the time to machine the surface of the tool. The rate for the laser tracker is \$200/hr.

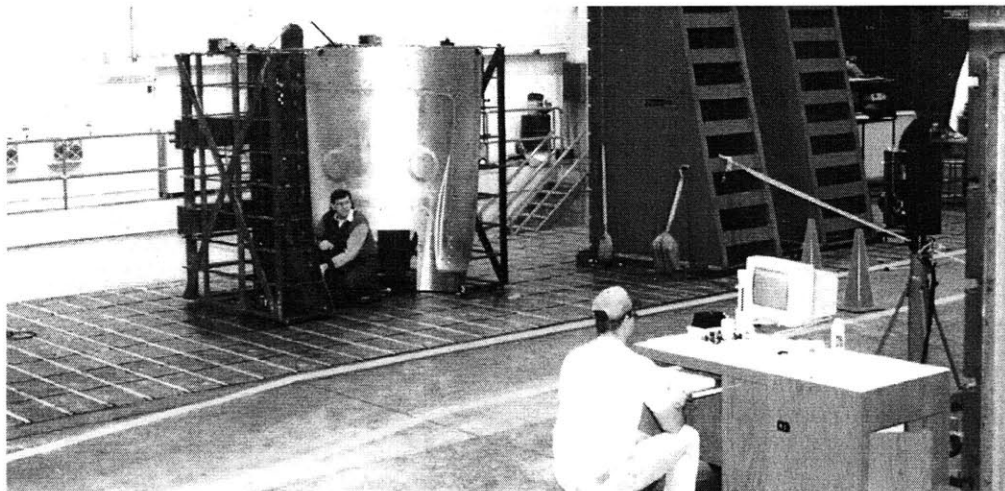


**Figure 7.24 Final Contour Inspection using a Laser Tracker [29]**

**Table 7.19 Processing Data for the Contour Inspection & Leak Test**

<i>Items</i>	<i>Values</i>
Time 50 % of Machining Time	23.4 hrs
<b>Inspection Costs (Labor &amp; Equip.)</b>	<b>\$7,030</b>

Cost Summary & Discussion

The remainder of the cost items, such as engineering costs, boxing and shipping, and capital costs are calculated in a straightforward way as outlined in Chapter 7.3.4. The costs plus an assumed 20% profit are summarized in Table 7.20 including the manufacturing and material costs. However, the closeness of the estimated price of \$742K to the actual price is misleading since the entire cost model is subject to variations and uncertainties.

**Table 7.20 Summary of the Engine Cauling Curing Tool**

<i>Cost Items</i>	<i>Time [hrs]</i>	<i>Costs [\$]</i>	<i>Comments</i>
Manufacturing Costs	430.4	\$ 90,183	
Material Costs		\$ 178,538	
Design and Engineering		\$ 268,721	50% of mfg. costs
Boxing and Shipping		\$ 26,872	5% of total costs
Optional FEM Analysis		\$ 10,000	high complexity
Capital Costs		\$ 19,144	4 months at 10%
Profit		\$ 148,365	20% profit margin
<b>Estimated Total Price</b>		<b>\$ 741,823</b>	<b>vs. \$750K actual Price</b>

Figure 7.25 shows the dominant cost drivers rank ordered according to their contribution. The engineering costs contribute 47% to the total costs or 50% of the manufacturing costs. Given, that the engineering costs are very difficult to predict and can vary between 30% and 50%, only emphasizes the potential for errors. Secondly, the total costs are also very sensitive to a fluctuation of the material costs as they make up approximately 30% of the total costs of Invar tooling. As seen in Table 7.1, the Invar price can vary up to ±50% from its average. Because of the high Invar costs, the efficiency with which scrap material is avoided or resold adds another source for variation. Thirdly, the actual manufacturing costs (excluding material) contribute about 15% to the total costs and as demonstrated in the previous paragraphs, many of the costs components can be estimated reasonably well. As depicted in Figure 7.49 in the Appendix 7.8.7, the major contributor to the manufacturing costs are the costs for machining (25%) followed by the costs for heat treatment (16%) and welding (16%). The major source of uncertainty are the costs for heat treatment, since their contribution is considerable and depend strongly on the

price negotiated with the heat treatment facility. Therefore, the variation of the manufacturing costs is assumed to be in the range of  $\pm 10\%$ , which is the generally accepted accuracy of process based cost models. Lastly, the influence on the total costs of the remaining 8% of the cost components can be neglected for now. However, in order to arrive at a price estimate, a profit between 0% and 30% is added to the total costs depending on the economics of the market and the pricing strategy of the vendor. Considering all these variations, one arrives at \$1.2M as an upper and \$290K as a lower boundary for a price estimate, which is equivalent to a deviation of +54% and -64% from the actual price. Remarkably, the median of \$745K is in line with the estimated and the actual prices and experience shows that on average the existing variations often cancel each other out. Conclusively, it should be noted that this type of cost estimation generally gets one within an order of magnitude of the actual price, although one should be aware of the potentially large errors.

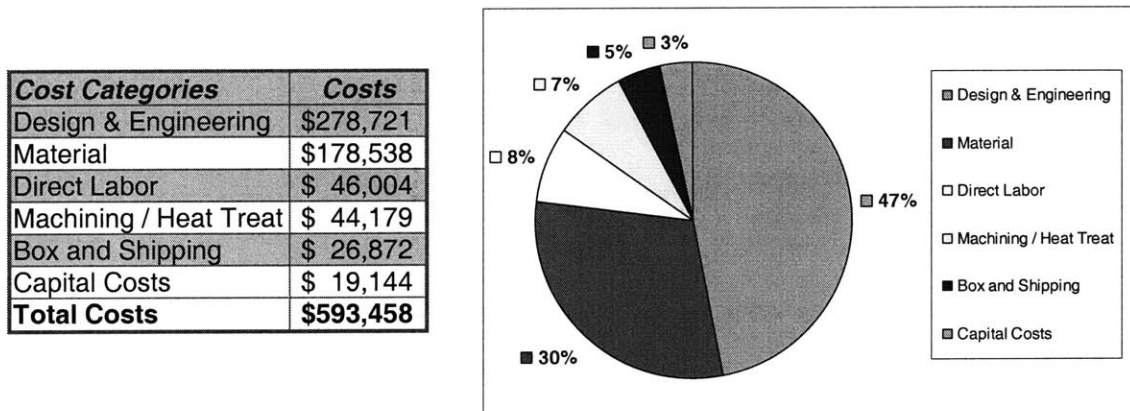


**Figure 7.25** Distribution of the Total Costs (excluding Profit)

**7.3.7 Other Case Studies & Generalized Cost Model**

Several other case studies have been conducted following a similar approach as outlined in the previous chapter. The details of these studies can be viewed in the Appendix 7.8 and the results are summarized in Table 7.21. Two of the five tools investigated are made out of Aluminum, whereas the remaining three are fabricated from Invar. The size of the tools ranges from approximately 40 ft<sup>2</sup> to about 450 ft<sup>2</sup> while the weight varies from 600 lbs. to 24,000 lbs. Generally, Aluminum tools only cost about a half of comparable Invar tools, simply because of the large difference in material price. However, as the data shows, size and weight are not the sole factors, which drive the price of open mold tooling. The shape complexity of the tooling face also affects the actual price. The data listed in Table 7.21 suggests a correlation between the qualitative complexity measure as defined in Chapter 7.3.5 and the price normalized by the projected tooling area. In addition, the ratio between the actual surface area of the tool and its projected area also seems to lend itself as a more quantitative complexity definition. The ratio successfully rank orders the tools according to their complexity, however in many situations early in the design process the actual surface area is not known and therefore the ratio has a only limited practical.

**Table 7.21 Summary of Open Mold Tooling Prices**

	<i>Flat Aluminum</i>	<i>Helicopter Blades</i>	<i>Flat Invar</i>	<i>Horizontal Stabilizer</i>	<i>Engine Cauling</i>
Complexity Level	1	2	1	3	4
Material	Aluminum	Aluminum	Invar	Invar	Invar
Surface Area	6,000in <sup>2</sup>	17,010in <sup>2</sup>	6,000in <sup>2</sup>	66,355in <sup>2</sup>	20,154in <sup>2</sup>
Projected Area	6,000in <sup>2</sup>	16,200in <sup>2</sup>	6,000in <sup>2</sup>	51,840in <sup>2</sup>	14,400in <sup>2</sup>
Surface/Projected Area	100%	105%	100%	128%	140%
Weight	566 lbs	2,812 lbs	1,691 lbs	23,729 lbs	9,848 lbs
Actual Price	\$21,500	\$175,000	\$55,000	\$1,000,000	\$750,000
Price/Projected Area	\$4/in <sup>2</sup>	\$11/in <sup>2</sup>	\$9/in <sup>2</sup>	\$19/in <sup>2</sup>	\$52/in <sup>2</sup>
<b>Estimated Price</b>	<b>\$24,657</b>	<b>\$182,603</b>	<b>\$63,405</b>	<b>\$1,060,330</b>	<b>\$741,823</b>
<b>Price Deviation</b>	<b>15%</b>	<b>4%</b>	<b>15%</b>	<b>6%</b>	<b>-1%</b>

The prices estimated by the process based cost models are within reasonable limits of the actual prices provided by the manufacturers. Although, the model is subject to a number of uncertainties it seemed to be able to capture the cost effects of size and complexity.

However, as discussed in the individual case studies listed in the Appendix 7.8, it can be expected that estimates might differ as much as  $\pm 30\%$  from the actual price. An analysis of the cost drivers helps to pinpoint the sources of these variations and provides insights in how the cost estimation process might be simplified. The total costs are defined here as the price minus the manufacturer's profit and include all costs to finance, to fabricate, and to deliver the respective tool. The distribution of the total costs is listed in Table 7.22 for each major cost category. The averages of these values are plotted in Figure 7.26 for Aluminum and Invar tools, respectively.

**Table 7.22** Distribution of the Total Costs for Open Mold Tooling

<i>Cost Categories</i>	<i>Flat Aluminum</i>	<i>Helicopter Blades</i>	<i>Flat Invar</i>	<i>Horizontal Stabilizer</i>	<i>Engine Cauling</i>
Design & Engineering	28%	46%	28%	47%	47%
Material	9%	5%	40%	29%	30%
Direct Labor	36%	24%	15%	9%	8%
Machining / Heat Treat	21%	17%	11%	8%	7%
Box and Shipping	5%	5%	5%	5%	5%
Capital Costs	2%	3%	2%	3%	3%
Total Costs	100%	100%	100%	100%	100%

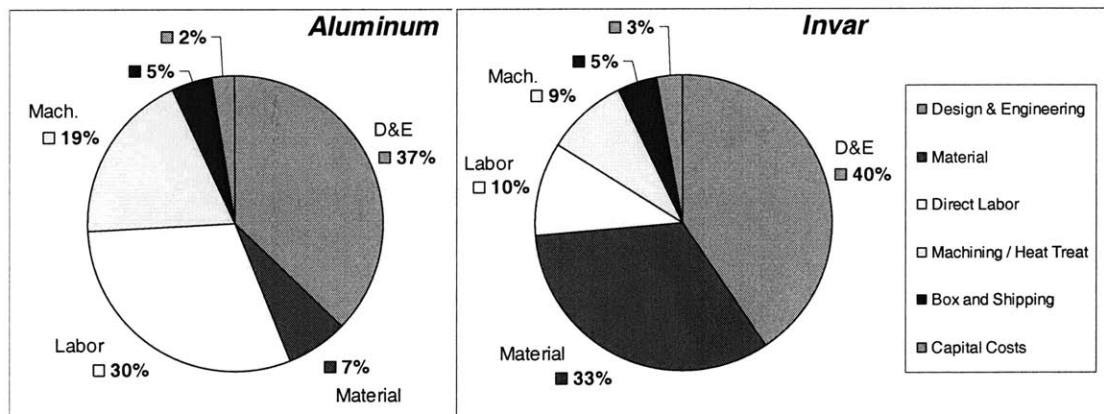


**Figure 7.26** Total Cost Distribution of an Average Aluminum/Invar Tool

The above data shows that on average 40% of the costs are incurred by the design and engineering process regardless of the type of material used. However, the cost contribution varies between 30% and 50% as the tool's complexity increases which is in accordance to the information obtained from manufacturers. The difficulty to accurately estimate the engineering costs and their large impact and can lead to considerable



fluctuations in the estimates of the total costs. Another major cost driver and source of uncertainty are the material costs. On average 33% of the total costs of Invar tools are attributed to material costs as opposed to 7% for the average Aluminum tool. Also, material prices can easily differ by as much as  $\pm 50\%$  and in particular in the case of Invar tools affect the outcome of the calculations. The manufacturing costs, here defined as the sum of the labor and equipment costs, can generally be estimated quite accurately. Experience shows that errors of about  $\pm 10\%$  are to be expected as long as the model does not deviate considerably from the actual process plan. For Aluminum tools, the manufacturing costs are the major cost driver and contribute about 50% to the total costs. However, for Invar tools only about 20% of the total costs come from manufacturing mainly because of the large impact of the material costs. An analysis of the data presented in the Appendix 7.8.8, shows however that in all cases the manufacturing costs increase as the tool becomes more complex. For Aluminum tools, this is generally reflected in the increase of the welding costs, which on average make up 26% of the manufacturing costs. Invar in contrast is much more difficult to machine and therefore the machining costs, which on average contribute 23% to the manufacturing costs, rise with increasing complexity. The latter outcome is not too surprising, since the actual surface area grows as the shape of the surface becomes more complex.

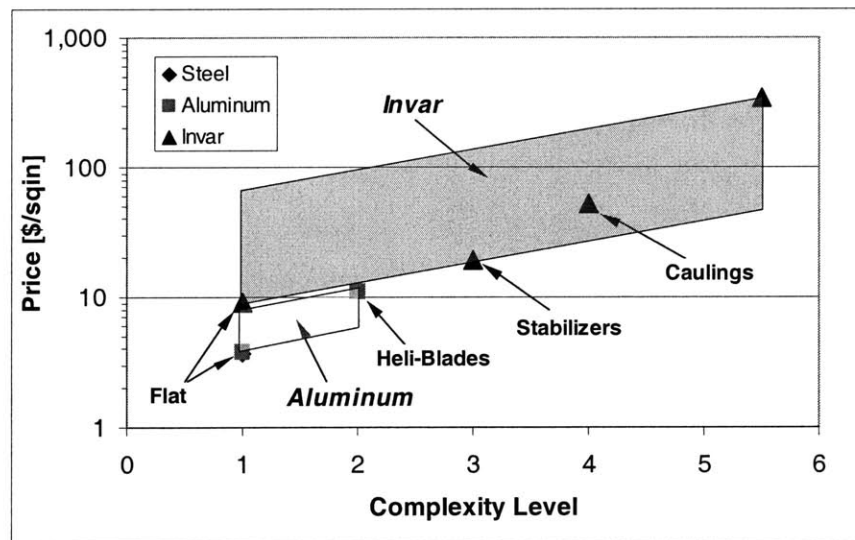
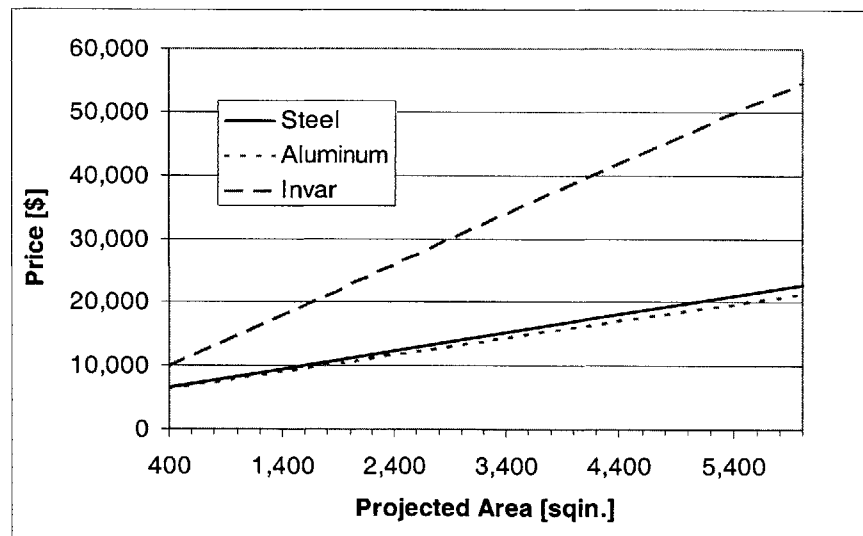


Figure 7.27 Price Estimation Chart for Open Mold Tooling

One can derive a simple rule of thumb for the costing of tools based on their material costs and ultimately their weight. Both parameters are relatively easy to guess and are therefore good candidates for a quick approximation. For example, an Aluminum tool would cost on average about 10 times its material costs whereas an Invar tool would cost on average about 3 times its material costs. However, the disadvantage is that when scaling the tooling costs by the weight only size but not complexity is considered. It is better to normalize the tooling prices by the respective projected area of each tool and use the previously introduced complexity definition to establish a ranking system. This approach accounts for both, the size and the complexity of a tool and can work because of the observed correlation between the two parameters. For cost estimation purposes, one can quickly calculate the projected tooling area, since it is closely related to the part size, and use Figure 7.27 to approximate the actual price.

In addition, Figure 7.28 can be used to read off the price for flat tools up to  $42\text{ft}^2$  in size. The graph is based on historical data from Remmele Engineering [29], however only holds for the specified size range and for flat tools, which are fabricated according to the previously described methods. The base price for flat Aluminum tooling is about \$5,400 and costs go up by  $\$385/\text{ft}^2$  ( $\$2.7/\text{in}^2$ ) per square foot. A base price of \$6,700 and  $\$1,150/\text{ft}^2$  ( $\$8/\text{in}^2$ ) per square foot have to be paid for flat Invar tooling.



**Figure 7.28** Prices for Flat (Level 1) Open Mold Tooling [29]

## 7.4 Tooling for Resin Transfer Molding

### 7.4.1 Design Requirements

The RTM process employs a closed matched mold to accurately control the dimensions and the surface finish of the produced composite part. Therefore, each half of the mold has to line up precisely with its counterpart as the mold is readied for the injection of the resin. Once closed, the mold needs to prevent any resin from escaping by providing adequate sealing against the injection pressure of 100 psi to 600 psi. The locking mechanism and the mold are designed to withstand these pressures without deforming or yielding. Since, the quality of the part depends on the proper impregnation of the fiber network, the mold design must prevent the occurrence of dry spots, voids, or resin rich areas. The solidification of the resin takes place inside the mold and the thermal energy to start the process has to flow into the mold at the beginning of the cure cycle and escape from it during the cooling period. The tool not only has to compensate for the thermal expansion during cure but also for the part shrinkage due to the escape of some volatile constituents. Depending on the production requirements, the mold must survive many of these production cycles without compromising the tolerances or the surface finish.

### 7.4.2 Material

The material selection is determined by the production volume and the required life span of an RTM mold. For prototype production (<100 parts), molds fabricated out of cast polymers generally suffice. Larger production runs dictate molds made of either cast or machined metal. Aluminum tools generally have a life span of about 5,000 parts whereas Steel molds can produce about 10,000 parts without being serviced. Both, Aluminum and Steel possess adequate strength to resist the injection pressure and can be machined quickly into any shape with modern CNC technology. Commonly, for steel molds either AISI-4140, 1045 or P-20 tool steel is used in a pre-hardened state (Rockwell C28-30), which allows for favorable cutting conditions. Aluminum, however exhibits a higher coefficient of thermal expansion but has a higher thermal conductivity, which can reduce

the production cycle time. In general, the 6er series of Aluminum is used for tool making since it provides good strength and machining characteristics. Table 7.1 gives a general overview of tooling materials, whereas Table 7.23 lists some selected properties of Aluminum.

**Table 7.23 Aluminum Properties**

	Price [\$/lb]	MRR [in <sup>3</sup> /min]	Strength [ksi]	Density [lbs/in <sup>3</sup> ]
Aluminum(6061-T6)	2.5-4.5	40-238 Rough Facing 4.4-25 Finish Facing 2-8 Contour Milling	45	0.098

### 7.4.3 RTM Mold Design

The matched molds used in the RTM process feature a few basic design elements necessary for the proper performance of the production process. Commonly, the tool is fabricated from two solid metal blocks representing the male and the female section of the mold. Certainly, the molds need to withstand the rigors and the thermal strain of the production cycle. Metals generally stand up well under to these circumstances and mold life's of 1,000 to 10,000 cycles can be achieved. Another advantage of matched tool molding is that all part sides and dimensions can be controlled by the tool. Therefore, all internal mold surfaces should be polished in particular if a superior part finish is desired. Secondly, the mold halves have to be designed to tight tolerances of at least  $\pm 0.005''$  to prevent any mismatch of the two mold halves and cause deviations from the actual part dimensions. Since the mold has to be opened and closed at each cycle, guiding systems have to be built in to ensure the proper alignment of the two mold halves. Precisely located pins or guide posts in one halve, which line up with corresponding holes in the other, represent one possible solution. The other is to incorporate accurately machined interlocking slots as seen in Figure 7.30 and Figure 7.31.

Once closed, sturdy locking and clamping mechanisms are required to resist the injection pressure. Each die is furnished with bolting holes to attach it to the tool holder of the mechanical or hydraulic locking system. These holes also serve to keep the two mold

halves securely locked together during transportation or storage and therefore prevent any damage of the internal features. Preferably, a uniform clamping pressure over the entire die surface is applied in order to prevent any deformations of the tool.

The resin injection is carried out at pressures between 100 psi and 600 psi however a well-designed injection and runner system is essential to the proper impregnation of the dry fiber network inside the mold. The location of the injection port is critical and for symmetric geometries should be located at the volumetric center of the part. For large or complex parts several injections ports might be required to guarantee sufficient filling of the mold. The system also features vents to allow the enclosed air to escape and prevent any voids or air pockets from forming. Since, the resin is generally quite viscous it tends to flow at a much higher rate in the center of the part than at the outside. The resulting non-uniformity of the velocity profile can lead to unexpected dislocations of the fiber network and ultimately to uneven fiber distribution. Properly placed gates connected with runners facilitate an even filling of the mold. In difficult cases, FEM flow models can help to optimize the design of the injection and gate system [2, 4, 13-17].

Different sealing designs are in use to prevent resin from escaping the mold. Most commonly, a gasket or o-ring is placed in a groove surrounding the perimeter of the main cavity (see Figure 7.31). Other methods involve solid features such as a pinch ring or a resin trough to either pinch off any resin flow or trap it in a small groove.

In most cases, heat is applied to start the cross-linking reaction within the polymer and to cure the part inside the mold. The simplest way is to clamp heating platens to the top and the bottom of the mold. A more uniform temperature distribution is achieved by placing the entire die into an oven. However, none of these methods is as effective as built-in heating and cooling channels, which quickly heat up the mold and cool it down in the pursuit of a speedy turnaround. Complex internal heating channels might have to be cast if they cannot be drilled from the outside, which of course affects the ultimate costs of the mold.

The cured and solidified part is then removed from the mold. However, to avoid the part from getting damaged, sometimes elaborate ejector systems are built into the die. Ejector

pins either directly push the part out of the mold or they activate so-called jackpads to apply a more uniform pressure to the part. Some of these features can be seen in Figure 7.31.

Other features involve locator holes for any hardware, which is to be molded into the part. Again, Figure 7.31 depicts some inserts, which are placed into the mold prior to closing and are being held in place during injection and subsequent cure.

Deformations caused by the thermal affect and by uneven part shrinkage during cure have to be compensated in the tool design. The allowance for shrinkage is generally about 1% of the respective part dimension. The part tolerance is then to be expected within  $\pm 0.01''$ . The following list summarizes the design guidelines.

#### Design Guidelines Summary

- Aluminum 6061, Toolsteel AISI 4140, 1045 or P - 20
- Part Wall Thickness  $> 0.05''$ , Internal Radii  $> 1/16''$ .
- Consider Part Shrinkage Factor of ca. 1%
- Clamping & Locking System
- Interlock Slots or Guide Pins for Alignment
- Injection Port, Runner System, Gates & Vents
- O-Ring, Pinch Ring or Resin Trough Sealing
- Polished Surface

#### Optionally

- Ejector Pins or Jackpads for Demolding
- Integrated Heating or Cooling Elements

#### 7.4.4 Cost Components of RTM Molds

##### Material Costs

The cost of the material is simply determined by calculating the volume and weight of the workpieces for each die half. The price for tool steel approximately ranges between \$0.32/lb and \$0.59/lb whereas Aluminum prices vary between \$2.5/lb and \$4.5/lb. However, one has to consider material overhead and possibly accept higher prices when purchasing in small volumes. For this study, a material overhead of approximately 30% is assumed.

##### Manufacturing Costs

The manufacturing costs correspond to the amount of labor and the type of machine tools required to produce the molds. For a qualified machinist approximately \$100/hr including overhead have to be considered. The majority of the work will most likely be carried out by a mid-size 3 to 5 axis CNC vertical mill. These machines cost between \$150K and \$400K. Their hourly rate lies between \$60/hr and \$160/hr depending on the depreciation schedule, the cutting tool costs, the costs of the cutting liquid, the maintenance costs and other overhead costs.

The total manufacturing costs are then estimated by calculating the time for each individual production step while considering labor and machining times. The following generic process plan gives an overview of the production steps, which are involved in the production of the RTM mold. Of course, the process plan, as seen in Table 7.24, has to be adjusted if the production of special features and shapes require additional fabrication steps. The hourly rates listed above are including overhead and therefore overhead is not treated separately in this study.

**Table 7.24 Aggregated Manufacturing Process Plan for RTM Molds**

Setup Milling Center
Square Off Male Mold
Machine External Features (Male Mold)
Contour Mill Male Mold
Square Off Female Mold
Machine External Features (Female Mold)
Contour Mill Male Mold
Machine Internal Features (Female Mold)
Polish All Surfaces
Final Inspection
Box & Shipping

### Design Costs

The design costs for RTM molds can vary widely depending on the complexity of the mold. Complex part shapes, demolding and locking mechanisms add to the costs as well as any integrated heating or cooling elements. However, for standard shapes the design costs should range between 30% and 50% of the overall costs. In general, the CNC code for the milling machines is easily derived from the generated CAD drawings. Only in rare and complicated situations, one would conduct a Finite Element (FEM) analysis of the heat and resin flow distribution inside the mold. However, such a calculation can easily add \$10,000 to the entire costs.

### Detailing Costs

Detailing costs are the most difficult to estimate and of course depend on the extras built into the die. These additional features can range from special surface treatment to built-in heating or cooling channels, thermocouples, or ejector pins. As a rule of thumb however, detailing costs cover approximately 3% to 5% of the total costs.



**7.4.5 Case Study: RTM Tooling**

Mold Design Features

The production of a half open curved profile serves as an example to introduce the cost estimation concept for RTM molds. The part shown in Figure 7.29 is 10” long, has a radius of 4” and exhibits a wall thickness of ½” resulting in a cross-section of approximately 6 in<sup>2</sup>.

***Curved Part***

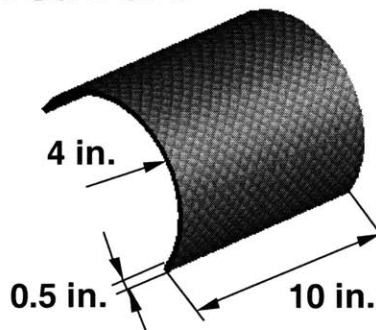


**Figure 7.29 RTM Part**

Each mold is 20 inches long, 15 inches wide and 8 inches high and is made out of Aluminum. When machined to its final shape, the male mold weighs about 142 lbs. whereas the female mold weighs approximately 211 lbs. Bolting holes keep each halve attached to the clamping and heating plates during production. When the die is moved, both halves are bolted together to protect the internal features. To align the mold halves with respect to each other interlock slots are used as seen in Figure 7.30. The features serving the demolding of the part and the injection of the resin are best seen in Figure 7.31. Other major design parameters are summarized in Table 7.25.

**Table 7.25 Mold Design Parameters**

	<i>Work P. Weight</i> [lbs]	<i>Mold Weight</i> [lbs]	<i>Mach. Matl.</i> [in <sup>3</sup> ]	<i>Surface</i> [in <sup>2</sup> ]
<b>Male Mold</b>	20x15x8x0.098 = 235 lbs	142	251	396
<b>Female Mold</b>	20x15x8x0.098 = 235 lbs	211	949	396

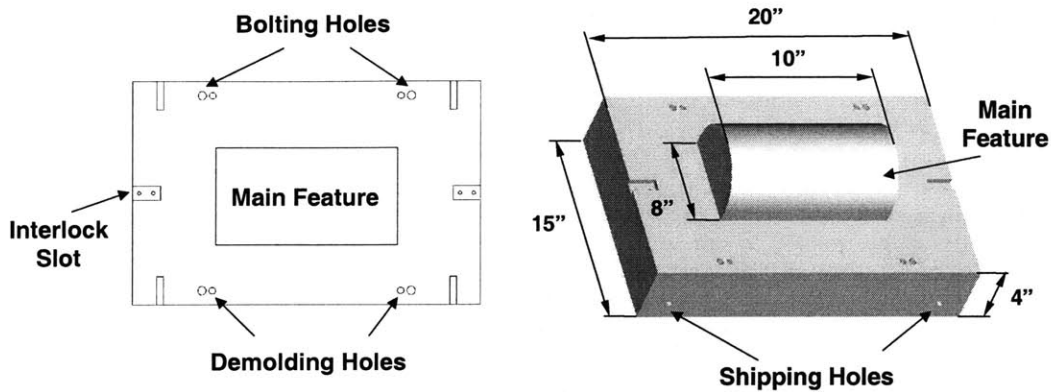


**Figure 7.30** Male RTM Mold [5]

### Material Costs

Before calculating the material costs, the size of the initial work piece has to be determined. Each mold half is machined out of Aluminum block measuring 20 x 15 x 8 inches. Figure 7.30 and Figure 7.31 show the open molds and the outlines of the work pieces. The material weight for both blocks totals 470 lbs. and using the prices listed in Table 7.23 the total material cost averages around \$2,140 including 30% for overhead.

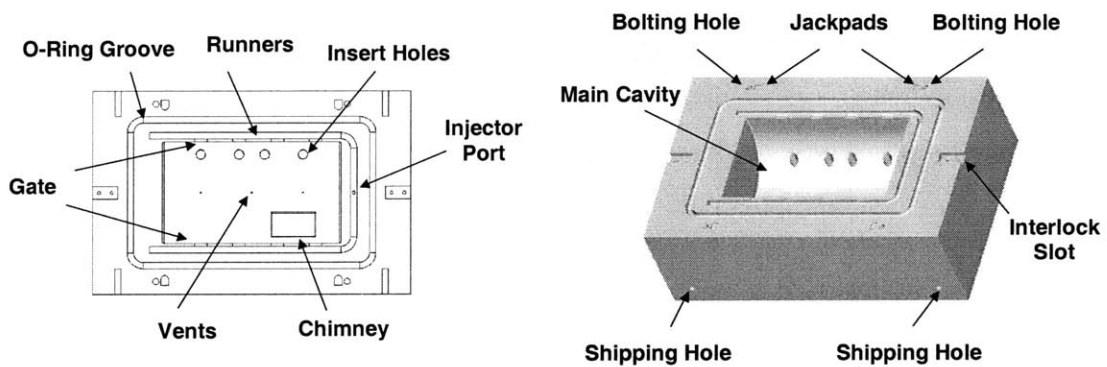


**Figure 7.31** Female RTM Mold [5]

### Manufacturing Costs

The manufacturing costs are determined by estimating the cycle time for each process step. Conventional metalworking processes are employed in the production of the RTM molds. Therefore, references such as the AM Cost Estimator by P. F. Ostwald [23] are useful to estimate the cycle times. The estimates can of course be replaced with actual

data where available. The detailed process plan for this particular die can be viewed in Appendix 7.8.9 and consists of 106 single steps. As previously mentioned the polishing of the surface is conducted with special care. Therefore it was assumed, that the worker goes over the surface 3 times to achieve the required finish. Table 7.26 lists the aggregated costs over several steps as well as the cost distribution. The total manufacturing costs add up to approximately \$4,440.

**Table 7.26 Aggregated Manufacturing Costs**

<b>Aggregated Process Plan</b>	<b>Labor [\$]</b>	<b>Machine [\$]</b>	<b>Total [\$]</b>	<b>Distrib.</b>
Machining	1,316	1,316	2,632	59%
Surface Polishing	1,607	0	1,607	36%
Final Inspection	100	100	200	5%
<b>Total Manufacturing Costs</b>	<b>\$ 3,023</b>	<b>\$ 1,416</b>	<b>\$ 4,438</b>	<b>100%</b>

Design Costs

The design costs make up about 40% of the overall costs. The costs include the generation of drawings and the CNC program and amount to roughly \$4,800 for this particular RTM tool.

Detailing Costs

The detailing costs come out to be approximately \$660 and contribute about 5% to the overall costs. In our example, these costs include shipping expenses, the costs for small parts etc. Again, detailing costs can take on considerable proportions for more complicated dies with many additional features.

Cost Summary

Summing up all the individual cost components one obtains a total cost of estimated \$12,100. This number should be regarded as an average estimate of the production costs. The error in these cost estimation techniques can however be around  $\pm 20\%$ . Also, the

actual price to be paid when the mold is procured from an outside vendor can be 10% to 40% higher depending on the profit margin and the overhead structure. Given these uncertainties, one can estimate conservatively that the tool would actually price at around \$13,450 to \$20,200. The estimated price (\$17,230) is then 14% below the actual quoted price of \$20,000, which however is still within the expected limits.

**Table 7.27 Manufacturing Costs Summary**

<i><b>RTM Mold - Cost Summary</b></i>		
Design Costs	\$ 4,824	40%
Material Costs	\$ 2,140	18%
Manufacturing Costs	\$ 4,438	37%
Detailing Costs	\$ 658	5%
<b>Total Cost</b>	<b>\$ 12,060</b>	<b>100%</b>
<b>Estimated Price</b>	<b>\$ 17,230</b>	<b>30%</b>

## 7.5 Tooling for Pultrusion

### 7.5.1 Design Requirements

During the pultrusion process, fibers wetted with resin are pulled through a die to define the shape of the part and to cure the matrix. The die is kept at the curing temperature of the resin (approximately 250°F to 350°F) and therefore must survive these conditions without any deformation. In addition, the die is subjected to abrasive forces stemming from the moving fibers. The pulling speed primarily depends on the resin system and the part cross-section. That is, the higher the pulling speed (or the slower the curing process) the longer the die. In addition, the designer has to consider whether a single or a multiple cavity die should be used. Employing several single cavity dies instead of one multi cavity die, allows production to continue in the event, that one die wears out and requires maintenance. As for the general die design, it is recommended that each pultrusion shop establishes design standards in order to facilitate the setup and exchange of dies among its machines.

### 7.5.2 Material

Tool steel is the preferred material to be used in order to provide wear resistance and to ensure a maximum life-span. Both, AISI-4140 and P-20 are used in their pre-hardened state (Rockwell C28-30) and therefore can be machined efficiently. For further resistance they can eventually be surface hardened before the chrome plating is applied. However, the additional hardening step adds costs and requires the dies to be handled with more care due to the brittleness of the surface. Aluminum or cast iron is generally not suitable for pultrusion dies. Table 7.28 lists some selected properties of tool steel.

**Table 7.28 Tool Steel Properties**

	Price [\$/lb]	MRR [in <sup>3</sup> /min]	Strength [ksi]	Density [lbs/in <sup>3</sup> ]
Tool Steel	0.32 - 0.59	7.9-48 Rough Facing 1.7-7 Finish Facing 0.3-0.7 Contour Milling	130	0.285

### 7.5.3 Pultrusion Die Design

The process conditions have to be considered in the design of a pultrusion die. The abrasive forces wear out the die surface and therefore hardened tool steel is a cost effective and durable solution. In addition, a 0.0015" - 0.0020" layer of hard chrome should be applied to the surface to minimize friction and pulling force and to provide improved wear resistance. In general, the tool is machined out of two blocks of steel, each representing the male and the female section of the die. Any machining or polishing operations should be conducted in the direction of the longitudinal axis of the die for better production results. Of course, for the pultrusion of cylindrical stock the die can simply be made out of a single piece, which is then gun drilled and honed. The total cross-section of the steel blocks is determined by the part to be pultruded. For sufficient heat capacity and to promote a uniform temperature distribution the cross-section of the tool should be at least 10 times the cross-section of the part. The two halves of the die have to be located precisely with respect to each other. Dowel pins located as depicted in Figure 7.34 often serve this function. The length of the die commonly lies between 1ft. and 3ft, but ultimately depends on the resin system and the pultrusion speed. As for the internal profile, the designer should avoid radii smaller than 1/16" and keep the part wall thickness between 0.05" to 3". In addition, large transitions in wall thickness should be avoided, since it can lead to deformations of the pultruded profile. The deformations are caused by uneven shrinkage as the resin is cured. To compensate for the shrinkage, the dimensions of the profile should be enlarged by approximately 1%. The typical part tolerance is then to be expected within  $\pm 0.01$ ". As the fibers converge at the entrance of the die, it is desirable to lead them through a smooth transition in order to avoid any fiber damage. Therefore, each die features a so-called "bell mouth" at the die entrance. The die entrance exhibits a radius between 1/16" for small parts and 1/4" for larger parts. No additional internal taper is required and can actually impede the flow of the fibers. Several methods have become common practice for mounting die halves into the pultrusion machine. The first is to fasten the die to the machine using high strength 1/2" bolts. This method is simple and allows several dies to be mounted in parallel. The second, more expensive, method requires machined ledges along the length axis of each die half in order to provide gripping space for clamps and brackets. Regardless which

system is chosen it should securely hold the die in place and be able to withstand the considerable pulling forces. The following list summarizes the design guidelines.

#### Design Guidelines Summary

- Prehardened Toolsteel AISI – 4140 or P - 20
- Internal Radii at least 1/16”.
- Part Wall Thickness between 0.05” and 3”.
- Die Cross-section approx. 10 times the part cross-section
- Simple Clamping Mechanism
- Tapped Holes to accommodate Thermocouples
- Hard Chrom Plated and Polished Surface
- Bell Mouth Entrance of ca. 1/16” – ¼ “ Radius
- Consider Part Shrinkage Factor of ca. 1%

#### **7.5.4 Cost Components of Pultrusion Dies**

##### Material Costs

The material costs are simply determined by calculating the total volume and weight of both work pieces. The price for tool steel approximately ranges between \$0.32/lb and \$0.59/lb. However, one has to consider material overhead and possibly accept higher prices when purchasing in small volumes. For this study, a material overhead of approximately 30% is assumed.

##### Manufacturing Costs

The manufacturing costs correspond to the amount of labor and the type of machine tools required to produce the dies. For a qualified machinist approximately \$100/hr including overhead have to be considered. The majority of the work will most likely be carried out by a mid-size 3 to 5 axis CNC vertical mill. These machines cost between \$150K and \$400K. Their hourly rate lies between \$60/hr and \$160/hr depending on the depreciation

schedule, the cutting tool costs, the costs of the cutting liquid, the maintenance costs and other overhead costs.

The surface grinding machine only requires a fraction of the investment cost of the milling center. However, the running costs are higher, since the grinding wheel has to be profiled specifically for each shape and wears out rapidly. Therefore, a machine rate of \$60/hr to \$150/hr is assumed for this calculation.

The dies are chrome plated for wear resistance. The costs of hard chrome plating for the required thickness is approximately \$60/sqft. In addition, according to industry sources the final polishing of the die surface and in particular the entrance takes up a considerable amount of time and labor. The total manufacturing costs are then estimated by calculating the time for each individual production step while considering labor and machining times. The following generic process plan gives an overview of the production steps, which are involved in the production of a pultrusion die. Of course, the process plan as seen in Table 7.29 has to be adjusted if the incorporation of special features and shapes require additional fabrication steps. The hourly rates listed above are including overhead and therefore overhead is not treated separately in this study.

**Table 7.29 Aggregated Manufacturing Process Plan**

Setup Milling Center
Square Off Male Die
Tap Holes (Male Die)
Square Off Female Die
Tap Holes (Female Die)
Drill Through Both Halves
Contour Mill Male Die
Contour Mill Female Die
Profile Grind Male Die
Profile Grind Female Die
Hard Chrome Both Halves
Polish Die Surfaces
Final Inspection
Box & Shipping



### Design Costs

The design costs for pultrusion dies can vary widely depending on the profile to be pultruded. However, for standard shapes the design costs range between 20% and 40% of the overall costs. In general, the CNC program for the milling machines is derived from CAD drawings. Only for complicated cases, one conducts a Finite Element (FEM) analysis of the heat distribution within the die. However, such a calculation can easily add \$10,000 to the entire costs.

### Detailing Costs

Detailing costs are the most difficult to estimate and of course depend on the extras built into the die. These additional features can include special surface treatment, built-in heating or cooling channels and thermocouple junctions. As a rule of thumb however, detailing costs cover approximately 3% to 5% of the total costs.

## 7.5.5 Case Study: Pultrusion Die for a L-Profile

### Die Design Features

The pultrusion of a common L-Profile serves as an example to introduce the cost estimation concept for pultrusion dies. The 1½" x 1½" profile shown in Figure 7.32 exhibits a wall thickness of ¼" and has a cross-section of approximately 0.7 sqin. The profile is manufactured by pulling fibers through a die as seen in Figure 7.33.

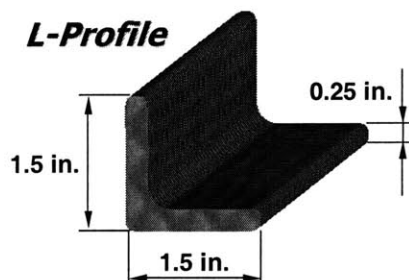


**Figure 7.32** Dimensions of the L-Profile

The die measures 2ft. in length and has a cross-section of  $3 \times 4 \text{ in}^2$  and is made out of tool steel. When subtracting the cross-section of the L-Profile one obtains the actual die cross-section of  $11.3 \text{ in}^2$ , which is more than 10 times the cross-section of the part. In terms of its design features the die exhibits a bell-mouth entrance with a radius of  $\frac{1}{4}$ ", tapped holes for attaching thermocouples and  $\frac{1}{2}$ " mounting holes. The die halves are located with respect to each other by  $\frac{1}{4}$ " dowel pins as seen in Figure 7.34. The major design parameters are summarized in Table 7.30.

**Table 7.30 Die Design Parameters**

	<i>Work P. Weight</i> [lbs]	<i>Die Weight</i> [lbs]	<i>Mach. Matl.</i> [in <sup>3</sup> ]	<i>Surface</i> [in <sup>2</sup> ]	<i>Cross-Sec.</i> [in <sup>2</sup> ]
<b>Male Die</b>	2x4x24x0.285 = 55 lbs	30	88	281	4.4
<b>Female Die</b>	2.5x4x24x0.285 = 68 lbs	47	77	345	6.9

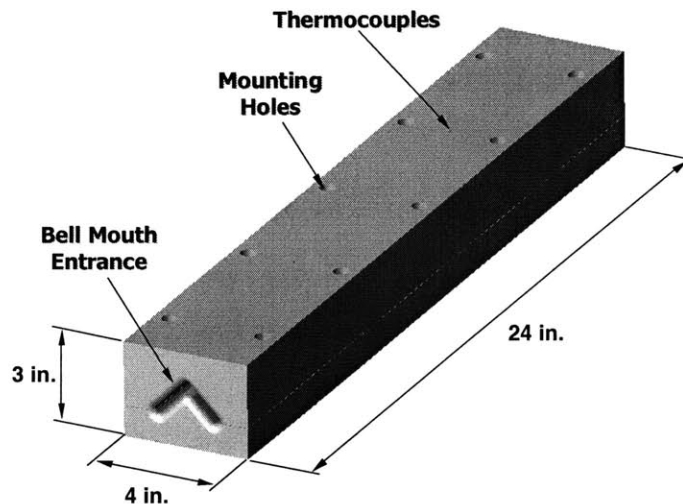


**Figure 7.33 Design Features of a Pultrusion Die**

### Material Costs

Before calculating the material costs the size of the initial work piece has to be determined. For the upper female die, a steel block of  $2.5 \times 4 \times 24 \text{ in}^3$  is required and for the lower male die, a block of  $2.0 \times 4 \times 24 \text{ in}^3$  is used. Figure 7.34 shows the open die and the outlines of the initial work pieces. The material weight for both the steel blocks

totals 123 lbs. Using the prices listed in Table 7.28, the total material cost averages around \$73 including 30% for overhead.

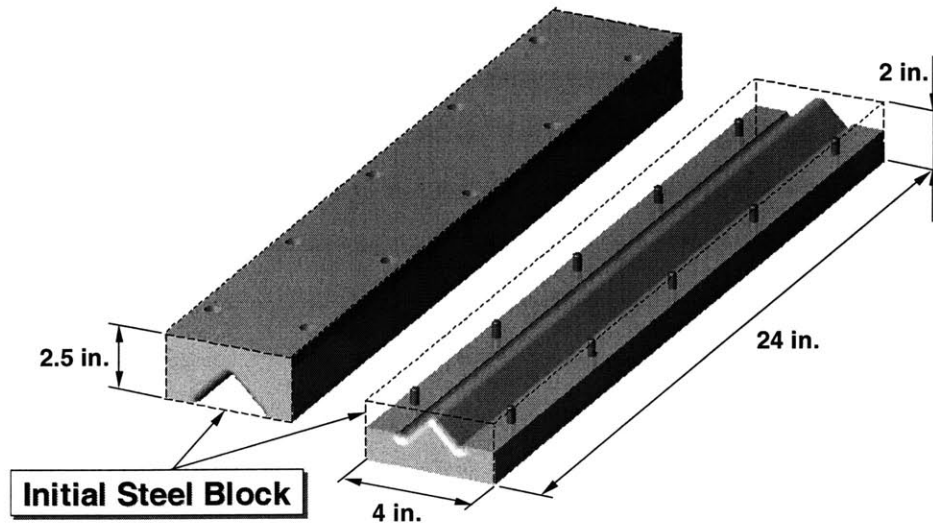


**Figure 7.34 Work Piece Dimensions**

Manufacturing Costs

The manufacturing costs were determined by estimating the production time for each process step. Conventional metalworking and treatment processes are employed in the production of pultrusion dies. Therefore, references such as the AM Cost Estimator by P. F. Ostwald can be used to estimate the cycle times for the various steps [23]. The estimated values can be replaced with actual data where available. The detailed process plan for this particular die is listed in Appendix 7.8.10 and consists of 99 single steps. It is assumed that the worker polishes the surface 3 times to achieve the required finish. Table 7.31 lists the aggregated costs over several steps as well as the cost distribution. The total manufacturing costs add up to approximately \$3,800.

**Table 7.31 Aggregated Manufacturing Costs**

<i>Aggregated Process Plan</i>	<i>Labor [\$]</i>	<i>Machine [\$]</i>	<i>Total [\$]</i>	<i>Distrib. [%]</i>
Machining	1,082	1,082	2,163	57%
Profile Grinding	299	299	598	16%
Chrome Plating	287	17	304	8%
Surface Polishing	622	100	722	19%
<b>Total Manufacturing Costs</b>	<b>\$ 2,290</b>	<b>\$ 1,497</b>	<b>\$ 3,787</b>	<b>100%</b>

### Design Costs

The design costs are estimated to make up about 30% of the overall costs. These costs include the generation of drawings and the CNC program. These costs are estimated to amount to roughly \$1,100 for this particular die.

### Detailing Costs

The detailing costs come out to be approximately \$180 and contribute about 5% to the overall costs. In our example, these costs include shipping expenses, the costs for small parts etc. Again, detailing costs can take on considerable proportion for more complicated dies with many additional features.

### Cost Summary

Summing up all the individual cost components one obtains a total cost of estimated \$6,000. This number should be regarded as an average estimate of the actual production costs. The error in these cost estimation techniques can however be around  $\pm 20\%$ . Also, the actual price to be paid when the die is procured from an outside vendor can be 10% to 50% higher depending on the profit margin and the overhead structure. Given these uncertainties, one can estimate conservatively that the die would actually price at around \$6,600 to \$9,000, which is within the limit of the actual price of about \$7,000.

**Table 7.32 Manufacturing Costs Summary**

<i><b>Pultrusion Die - Cost Summary</b></i>		
Design Costs	\$1,800	30%
Material Costs	\$ 73	1%
Manufacturing Costs	\$3,787	64%
Detailing Costs	\$ 300	5%
<b>Total Cost</b>	<b>\$ 5,960</b>	<b>100%</b>
<b>Estimated Price</b>	<b>\$ 7,450</b>	<b>20%</b>

## **7.6 Tooling for Assembly**

### **7.6.1 Design Requirements**

The most basic aspect of an assembly fixture is to hold the structural components firmly in place before they are joined permanently. Obviously, the fixture has to comply with the accuracy requirements and the tool should facilitate the accurate positioning of the individual components. The tool design also needs to consider the sequence of assembly and grant access to areas where fasteners or adhesive need to be applied. A significant problem of large-scale assembly pose the thermal expansion of the components and the tool throughout the course of the assembly process. Despite air-conditioning of production facilities, even small temperature changes can cause a misalignment of parts. In addition, there is a danger of the entire assembly being overconstrained, which can also lead to deformations due to a built-up of residual stresses. If overconstraints can be avoided by the fixture design, it is certainly beneficial. Lastly, since some joining operations are performed automatically the tool has to accommodate the special requirement of automatic fastening and be compatible with the machine's tool holding mechanism.

### **7.6.2 Material**

Since, every fixture has to provide a certain stiffness, metals are generally the construction material of choice. For the construction of gantry or frame like jigs, aluminum or construction steel are used because they can easily be welded or bolted together. Where possible, standard stock, such as profiles or tubing should be employed to keep costs down. For locator or hard points, which might wear out, especially hardened tool steel or even ceramics are used.

### 7.6.3 Assembly Fixture Design

Conventionally, each fixture is designed specifically for a certain assembly task and therefore represents a unique structure, which is only built at very low volumes. The design of fixtures requires experience and it is beyond the scope of this work to capture all aspects of fixture design. However, a general account of the major tooling features serves as an introduction into the field. The mechanical assembly of composites requires very similar tooling as the assembly of metal components and therefore many of the design guidelines apply in both cases. The only difference according to an industry source is, that in particular carbon composites possess a greater stiffness and exhibit a thermal expansion coefficient close to zero. The increased stiffness simplifies the handling of the component in many cases however might lead to constraining problems once the part is clamped. The smaller thermal expansion reduces the probability of deformation as long as the tool itself adequately compensates for it by its design. By using steel and aluminum, tools can be designed so the movement of locators due to temperature changes is minimized. The general tooling frame is constructed of standard profiles requiring little and only basic machining. However, the locators are always precision machined and are often made of hardened steel. They not only provide precise reference points for the components but also support the structure and need to bear any occurring forces with a minimal amount of deformation. Each locator is also fitted out with some type of adjustment mechanism. Once the tool is completed, an initial calibration is performed during which all locators are moved into their precise positions.

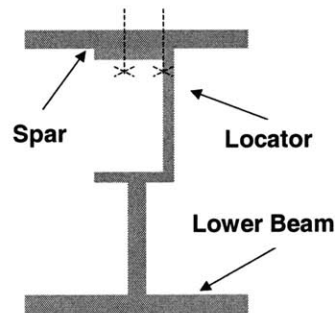


**Figure 7.35 Schematic of a Locator Feature**

Tools for adhesive bonding operations, which often take place at room temperature, also might be furnished with special clamping mechanisms to apply consolidating pressure onto the bonding interfaces. In all cases however, the designer has to consider the accessibility of the joint in order to apply the adhesive or to install any fasteners. Many of these described characteristics are realized in different ways depending on the exact production requirements, the size of the components, the complexity of the structure, and the industry. The following list summarizes the most basic design features for assembly tooling, however the reader has to refer to more in depths literature for more specific guidance.

- Facilitate Locating and Positioning
- Accuracy approx.  $< \pm 0.01''$
- Hardened and Adjustable Locator Features
- Compensation of Thermal Expansion
- Avoidance of Unnecessary Constraints
- Provide Clearance and Access
- Compatibility with Automatic Assembly

#### **7.6.4 Cost Components**

The costs of assembly tools are foremost driven by its size. However, there is also a complexity component, which influences the costs. For assembly fixtures the complexity of a tool is generally defined by the amount of locators, the accuracy requirements, and the amount of any movable sub fixtures. The high costs for locators are due to their exact and elaborate production. In addition, the precise adjustment mechanism, also add to their costs. Of course the number of locators somewhat scales with the size of the tool, but also scales with the complexity and the part count of the assembly. Therefore, relatively small fixtures for the assembly of fighter aircraft wings can be very complex and expensive [31]. In particular, access requirements and assembly sequence might necessitate several smaller fixtures, which attach modularly to the main work holding frame. Very large tools are often installed permanently. They are not only expensive to

produce because of their bulkiness but include costly measures for thermal compensation and precision keeping. In some cases, hoisting equipment or cranes are also incorporated to facilitate the movement of the large structural components.

Once it is understood what makes a tool complex and what drives the costs it is easy to comprehend that the actual material costs are only a very small cost component in the construction of assembly fixtures. Considerably more to the total cost is contributed by the manufacturing and installation costs of the tool. Since, each tool is uniquely manufactured, direct labor costs are one of the biggest contributors. However, because of its complexity and uniqueness, design and engineering costs make up at least 30% to 60% of the total costs. Tools generally undergo many iterations and test cycles before being put into production. All these changes require input from the customer's engineers and the designers alike.

**Table 7.33 Fixture Costs for Constant Curvature Assemblies (Fuselage Panels)**

<b>Complexity / Size</b>	<b><i>Small</i></b>	<b><i>Medium</i></b>	<b><i>Large</i></b>
<b><i>Low</i></b>	<b>\$4,500/ft</b>		
<b><i>Average</i></b>		<b>\$8,500/ft</b>	
<b><i>High</i></b>			<b>\$12,500/ft</b>

**Table 7.34 Fixture Costs for Variable Curvature Assemblies (Wing Skins)**

<b>Complexity / Size</b>	<b><i>Small</i></b>	<b><i>Medium</i></b>	<b><i>Large</i></b>
<b><i>Low</i></b>	<b>\$30,000/ft</b>		
<b><i>Average</i></b>		<b>\$50,000/ft</b>	
<b><i>High</i></b>			<b>\$70,000/ft</b>

According to an industry source, the assembly fixtures for the mechanical assembly of metal or composite components are similar in their design and cost. Of course, one can



develop a process based cost model, add all the component costs and come up with an estimate within 10% of the actual price. However, as an expert in tooling, Gene Vaughn has collected historic cost information and derived some basic rules to quickly estimate the costs of assembly fixtures [31]. The cost data presented in Table 7.33 and Table 7.34 considers size and complexity effects. One simply multiplies the respective figure from the respective table with the length of the fixture and arrives at an estimate of the actual fixture price. Once familiar with the classification scheme of the model the user obtains results, which are generally within  $\pm 20\%$  of the actual price.

Example: Fixture for Wing Assembly

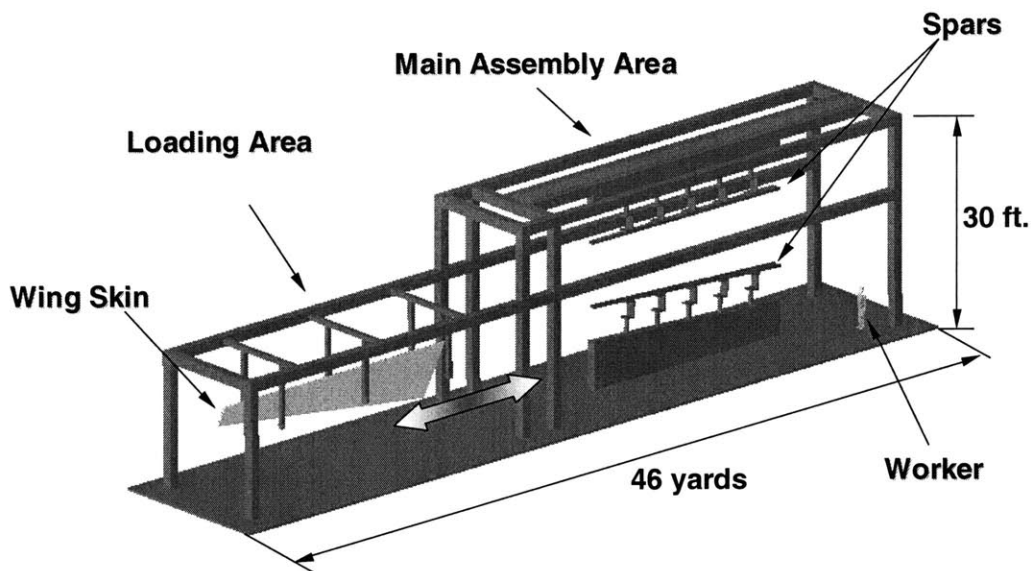


**Figure 7.36** Fixture for the Assembly of a Horizontal Stabilizer

For example, the fixture depicted schematically in Figure 7.36 is used to assemble one half of a horizontal stabilizer for a large cargo aircraft. It consists of a loading area, which holds the wing skin before it is moved on tracks into the main assembly area. The main area includes locators for the positioning of the front and rear spar. It is also furnished with integrated movable scaffolding for the workers to stand on. Once the spars are in place, the wing ribs are attached followed by the wing skins. The tool is in total about 46 yards (138ft) long and 30 feet high. The fixture represents a perfect example of a medium sized and average complex tool. Table 7.34 lists a price of

\$50,000/ft, which leads to an estimated price of approximately \$6.9M. The quoted price by the manufacturer is about \$6M. The estimate is only about 15% above the actual price and therefore within the expected boundaries.

### Future Developments

Future assembly tools are planned to be more versatile and adaptable to changing product configurations and assembly tasks. One approach pursued by Paul W. Marino Gages, Inc involves a whole set of modular components which can be combined to accommodate any assembly [31]. The advantage is that once the production program is discontinued the fixture can be disassembled and the pieces can be reused to build other fixtures. Also, changes in design can be quickly implemented, as only some components of the fixture have to be exchanged and readjusted. The concept is currently tested for small to medium size assemblies and promises a reduction in tooling costs of about 40% in the case of the Joint Strike Fighter [31].

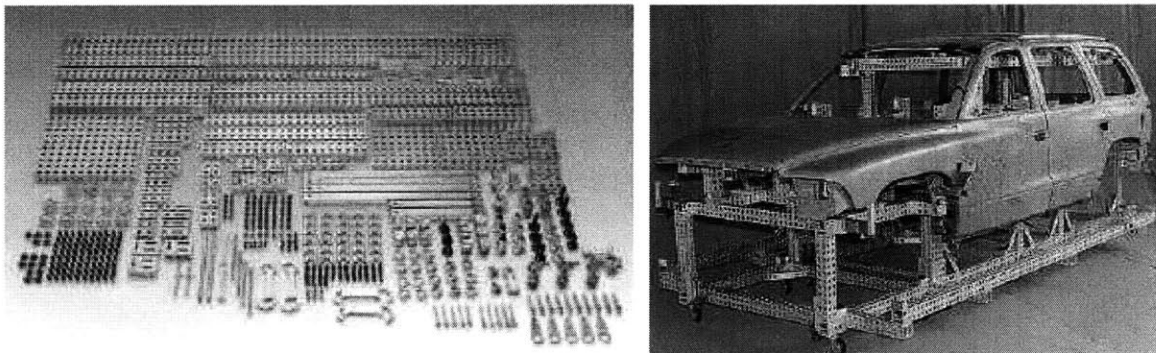


**Figure 7.37** Modern Modular Tooling System [31]

## 7.7 References

- [1] Alting, L. "Manufacturing Engineering Processes", New York: Marcel Dekker, Inc., 1994.
- [2] Reinhart, T. J. (Ed.), "Engineered Materials Handbook – Composites", Vol. 1, ASM International, 1988.
- [3] Beckwith, S. W. , "RTM Tutorial", SME, 1993.
- [4] Clark, J. "Process Based Cost Modeling: Understanding the Economic of Technical Decisions", Class Notes Course 3.57, MIT, 2000.
- [5] Lin, R. W. "Early Cost Estimation for Metal Fabricated Tooling in RTM", B.S. Thesis, MIT, 2000.
- [6] Meyer, R. W., "Handbook of Pultrusion Technology", Chapman & Hall, London, 1985.
- [7] Gorgias, A., "Economic Analysis of Assembly vs. Parts Integration in Composite Manufacturing", M.S. Thesis, Technical University of Munich & MIT, May, 2000.
- [8] Gutowski, T. G., "Pultrusion Workbook", Center of Excellence for Composites, Lemay Center for Composite Technology, July 1998.
- [9] Niu, M. -C. -Y., "Composite Airframe Structures - Practical Design Information and Data", Hong Kong: Conmilit Press Ltd., 1992.
- [10] Morena, J. J. "Advanced Composite Mold Making", New York: Van Nostrand Reinhold Company, 1988.
- [11] Hogg, P. J., Woolstencroft, D. H., "Composite Tooling II Proceedings", Elsevier Adv. Techn., Oxford, 1989.
- [12] Lambert, B.-K. "Find Low-cost Methodology when Machining Composites", Cutting Tool Engineering, 1987, p. 20-22.
- [13] Veldsman, G., "Aspects of Design for Manufacturability in RTM: Design Guidelines, Composite Mould Design, and Early Cost Estimation", M.S. Thesis, University of Stellenbosch, 1995.
- [14] Ashby, M. F., "Materials Selection in Mechanical Design", Butterworth Heinemann, 1992.
- [15] Becker, W., "RTM: Simultaneous Design and Tooling Reduces Cost and Lead-time", 23rd Intl. SAMPE Technical Conference, Oct. 21-24, 1991, pp. 601-608.
- [16] El-Amin, H., "In Resin Transfer Molding: Tooling is the Key to Success", Plastics Technology, Vol. 27 No. 12, Nov. 1981, pg. 97-99.

- [17] Gintert, L. A., "Rapid Prototype Tooling considerations for RTM", Society of Manufacturing Engineers, 1997.
- [18] Haffner, S. M., Gutowski, T. G., "Tooling for Manufacturing of Composites- Fabricated Metallic Tooling", MIT Report, September 1999.
- [19] Haffner, S. M., Gutowski, T. G., "Cost Elements of Autoclave Tooling", NSF Conference Paper, 2000.
- [20] Harper, A. R., "Proven Composite Tooling Technology for RTM", Composites Tooling II Proceedings, pp. 109-122.
- [21] Kalpakjian, S., "Manufacturing Engineering and Technology", 3rd Ed., Addison-Wesley Publishing Company, Inc., 1995.
- [22] Marsh, H. N. Jr., Griffith, T. E., Spitale, J. V. Jr., "RTM Tooling and Molding for Corrosion Resistant Applications", SPI Reinforced Plastic Composites Institute Annual Conference Proceedings 34th, New Orleans, La, Jan 30-Feb 2, 1979, Sect 3-A, p. 1-3.
- [23] Ostwald, P. F., "AM Cost Estimator: Cost Estimating Database", 4th Ed., Penton Publishing, Inc., 1988.
- [24] Polgar, K. C., "Simplified Time Estimation for Basic Machining Operations", Laboratory for Manufacturing and Productivity, M.S. Thesis, MIT, 1994
- [25] Tiffin, N., Marchbank, I., "Composites Tooling for High Specifications RTM", Composites Tooling II Proceedings, pg. 160-175
- [26] Hallum, D. L., "Copper Molds: a Cost-effective Alternative", American Machinist, v. 139 n4, Apr., 1995, p. 39-41.
- [27] Boothroyd, G., Dewhurst, P., Knight, W.A., "Product Design for Manufacture and Assembly", Basel, New York: Marcel Dekker, Inc., 1994.
- [28] Marin, T. , "Economic Analysis of Metal Fabricated Tooling for Composites Parts", M. S. Thesis, MIT & TU Munich, 2000.
- [29] Remmele Engineering, Inc., <http://www.remmele.com/> , Site Tour and Interviews with Tom Sobcinski, 1999.
- [30] Everett Pattern and Manufacturing, <http://www.everettpattern.com/> , Site Tour and Interview with Jay Jacobs, Everett, Jan. 2000.
- [31] Paul W. Marino Gages, Inc., <http://www.pmargage.com/> , Interviews with Gene Vaughn, April 2002.
- [32] Gemcor, Inc., <http://www.gemcor.com/> , Interviews with Tom Speller, April 2002.

- [33] Kazak Composites, Inc. <http://www.kazakcomposites.com/> , Interviews with Jerry Fanucci, March 2002.
- [34] Fiberspar, Inc. <http://www.fiberspar.com/> , Interviews with Steve Nolet, 2000.
- [35] Ingersoll Rand, Inc. <http://ingersoll-rand.com/>
- [36] Enterprise Foundry, Inc. <http://www.enterprisefoundry.com/>
- [37] Valenite, Inc. <http://www.valenite.com/>
- [38] Fischer, Inc., Durapress, <http://www.fischerna.com/> .
- [39] Lincoln Electric Company, Inc., <http://www.lincolnelectric.com/>
- [40] ESBA Welding, Inc., <http://www.esab.com/>
- [41] PVI Industries, Inc. <http://www.pvi.com/>
- [42] Hypertherm, Inc, Hanover, NH, <http://www.hypertherm.com/>

(This page is intentionally left blank.)

## 7.8 Appendix - Cost and Design Elements of Tooling

### 7.8.1 Tooling Materials

Table 7.35 Material Selection Chart for Tooling (Part 1)

	<i>Polymers</i>	<i>GFRP</i>	<i>CFRP</i>	<i>Nickel Electroforms</i>
<b>Toughness</b>	Prone to Chipping; easily scratched	Pretty robust, but gel coats scratch easily	Pretty robust, but gel coats scratch easily	Problems with denting, but scratch and impact resistant
<b>Tolerance</b>	moderate tolerances due to shrinkage	Moderate tolerances due to shrinkage and thermal expansion	Good tolerance	Good tolerance, depends on Master
<b>Surface Finish</b>	can be polished, easily scratched	can be polished, easily scratched	can be polished, easily scratched	can be polished, very durable
<b>Longevity</b>	reduced durability, used for prototyping	reduced durability, used for prototyping	better than GRP, but not as long as metallic tools	Very long life
<b>Gage Limits</b>	very thin machined; 1/2" for cast systems	nothing less than 1/8"	1/4" - 1/2" tool face thickness	1/8" to 1/4" tool face thickness
<b>Repairs and Modifications</b>	Easily repaired and modified	Minor repair on tool; small modifications	Minor repair on tool; small modifications	Easy to repair, modifications are limited
<b>Chemical Compatibility</b>	Has to be checked, requires release agent	No problems	No problems	No problems

Table 7.36 Material Selection Chart for Tooling (Part 2)

	<i>Ceramic</i>	<i>Aluminum</i>	<i>Tool Steel</i>	<i>Cast Metals</i>
<b>Toughness</b>	Great hardness, prone to chipping	Pretty robust, prone to scratching	Very robust; difficult to scratch, dent, or break	Hard, very scratch resistant tool faces; strength to resist most handling damage.
<b>Tolerance</b>	moderate tolerance due to shrinkage	Moderate tolerances due to thermal expansion	Machined to very fine tolerances; will hold them over time	Machined to close tolerances; stable material; holds dimensions with time
<b>Surface Finish</b>	can be polished, very scratch resistant	can be polished, easily scratched	can be polished, very durable	can be polished, very durable, porosity can cause problems
<b>Longevity</b>	Chipping is major problem	May wear out	Almost infinite lifetime for RTM processes	Excellent
<b>Gage Limits</b>	Needs to be thick	1/4" - 3/4" tool face thickness	1/4" - 3/4" tool face thickness	1/2" - 3/4" tool face thickness
<b>Repairs and Modifications</b>	Easily repaired, limited modifications	Easy to repair, modifications are limited	Easy to repair, modifications are limited	Easy to repair, modifications are limited
<b>Chemical Compatibility</b>	No problems	No problems with solvents; can corrode due to acid catalysts	No problems with solvents; can corrode due to acid catalysts; rust from damp storage	Caution of the porous casting; problems with acid catalysts

## 7.8.2 Performance Data of Tool Making Processes

Table 7.37 Typical Cutting Speeds for Plasma Cutting [42]

Material	Thickness		Current (amps)	Approximate Travel Speed	
	Inches	(mm)		(ipm)	(mm/min)
Mild Steel	1/4	6	200	135	3,400
	3/8	10	200	105	2,700
	1/2	12	200	85	2,200
	3/4	19	200	55	1,400
	1	25	200	35	900
	1 1/4	32	200	20	500
	1 1/2	38	200	13	330
	2	50	200	6	150
	3/16	5	200	220	5,600
Aluminum	1/4	6	200	190	4,800
	3/8	10	200	145	3,700
	1/2	12	200	110	2,800
	3/4	19	200	65	2,200
	1	25	200	35	900
	1 1/4	32	200	20	500
	1 1/2	38	200	12	300
	3/16	5	200	220	5,600
	1/4	6	200	195	5,000
Stainless	3/8	10	200	145	3,700
	1/2	13	200	105	2,700
	3/4	19	200	55	1,400
	1	25	200	30	760
	1 1/4	32	200	15	380
	1 1/2	38	200	10	250



Table 7.38 Process Time for Metal Bending [23]

Brake										
A. First Brake, L + W					B. Add'l Brake, L + W					
Lip In.					Min	Lip In.				
1	2	4	8	16		16	8	4	2	1
2.0					.05					
3.6	3.5				.06					2.9
5.3	5.2				.07				5.5	5.7
9.2	9.1	9.0			.08		10.3	11.5	12.1	12.3
11.5	11.4	11.2	10.9		.09		14.1	15.3	15.9	16.1
14.0	13.9	13.7	13.4		.10		18.3	19.4	20.0	20.3
16.7	16.6	16.5	16.2		.11	20.5	22.9	24.0	24.6	24.9
19.7	19.7	19.5	19.2	18.5	.12	25.5	27.9	29.1	29.7	30.0
23.1	23.0	22.8	22.5	21.9	.13	31.1	33.5	34.7	35.3	35.6
26.7	26.6	26.5	26.1	25.5	.14	37.2	39.6	40.8	41.4	41.7
30.7	30.6	30.5	30.2	29.5	.16	44.0	46.3	47.5	48.1	48.4
35.1	35.1	34.9	34.6	33.9	.17	51.4	53.8	54.9	55.5	55.8
40.0	39.9	39.8	39.4	38.8	.19	59.5	61.9	63.1	63.7	64.0
45.4	45.3	45.1	44.8	44.2	.21	68.5	70.9	72.0	72.6	72.9
51.2	51.2	51.0	50.7	50.0	.23	78.4	80.7	81.9	82.5	82.8
57.7	57.6	57.5	57.2	56.5	.25	89.2	91.6	92.8	93.3	93.6
64.8	64.8	64.6	64.3	63.6	.28	101.1	103.5	104.7	105.3	105.6
72.7	72.6	72.4	72.1	71.5	.30	114.3	116.6	117.8	118.4	118.7
81.3	81.2	81.0	80.7	80.1	.34	128.7	131.1	132.3	132.8	133.1
90.8	90.7	90.5	90.2	89.6	.37	144.6	146.9	148.1	148.7	149.0
101.2	101.1	100.9	100.6	100.0	.41	162.0	164.4	165.6	166.2	166.5
112.6	112.6	112.4	112.1	111.4	.45					
125.3	125.5	125.0	124.7	124.1	.49					
139.1	139.0	138.9	138.6	137.9	.54					
154.4	154.3	154.1	153.8	153.2	.59					
171.2	171.1	170.9	170.6	170.0	.65					

**Table 7.39** Polishing Speeds using Rotary Air Power Tools

## Rotary sand, 5, 7-in. disk, air motor

<i>L</i>	<i>Min</i>	<i>L</i>	<i>Min</i>	<i>L</i>	<i>Min</i>
1.1	.15	3.7	.71	15.9	3.40
1.3	.19	4.5	.89	19.7	4.25
1.5	.23	5.5	1.11	24.5	5.31
1.8	.29	6.8	1.39	30.5	6.64
2.1	.36	8.3	1.74	38.0	8.30
2.5	.46	10.3	2.18	47.4	10.37
3.0	.57	12.8	2.72	Add'l	.23

## Rotary sand, 2, 3-in. disk, air motor

<i>L</i>	<i>Min</i>	<i>L</i>	<i>Min</i>	<i>L</i>	<i>Min</i>
1.0	.77	1.8	1.40	3.2	2.30
1.3	1.00	2.0	1.50	3.3	2.50
1.4	1.10	2.2	1.70	3.7	2.80
1.6	1.20	2.5	1.90	4.1	3.10
1.7	1.30	2.8	2.10	Add'l	.77

### 7.8.3 Case Study: Flat Open Mold Tool (Aluminum, Level 1)

A flat aluminum tool, similar in design as the one depicted in Figure 7.38, is generally used for curing or bonding operations at curing temperatures below 150°F. The high coefficient of thermal expansion of aluminum does not affect the dimension of a flat tooling face as long as the support structure expands evenly. The dimensions of the tool are approximately 8.3ft x 5ft x 1ft resulting in a surface area of 6,000 in<sup>2</sup> (42ft<sup>2</sup>). The tool is constructed of ½ inch plate stock and weighs about 570 lbs. This simple tool does not have any of the optional features and the flat surface classify it as complexity level 1 tooling. Its quoted price is \$21,500 [29].

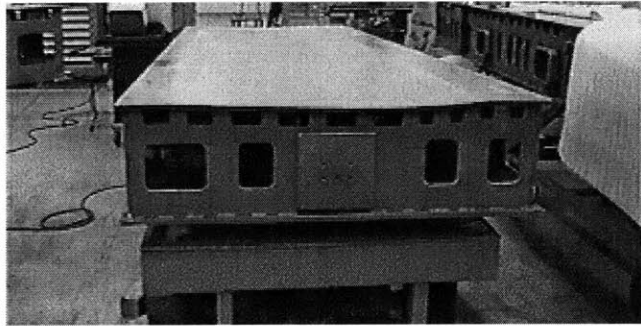


**Figure 7.38 Flat (Level 1) Aluminum Tooling (Courtesy of Remmele)**

The process based cost model estimates the total costs at \$19.8K considering only about 30% engineering costs due to the simplicity of the design. Because of the relatively low price for Aluminum (avg. \$2.5lb), material costs only make up about 9% of the total costs, whereas direct labor and equipment costs contribute over 55% (see Figure 7.39). The estimation error of the manufacturing costs should be within  $\pm 10\%$ . Assuming a profit margin of about 20% the estimated price turns out to be \$24.7K and is 15% above the actual price. All the assumptions for the model are slightly on the conservative side and therefore the estimated result is within acceptable limits. However, one always has to bear in mind that the estimated price can be as far of as  $\pm 30\%$  because of the existing uncertainties about pricing policy and engineering costs.

<b>Cost Categories</b>	<b>Costs</b>
Design & Engineering	\$ 5,544
Material	\$ 1,705
Direct Labor	\$ 7,086
Machining / Heat Treat	\$ 4,144
Box and Shipping	\$ 924
Capital Costs	\$ 323
<b>Total Costs</b>	<b>\$ 19,726</b>

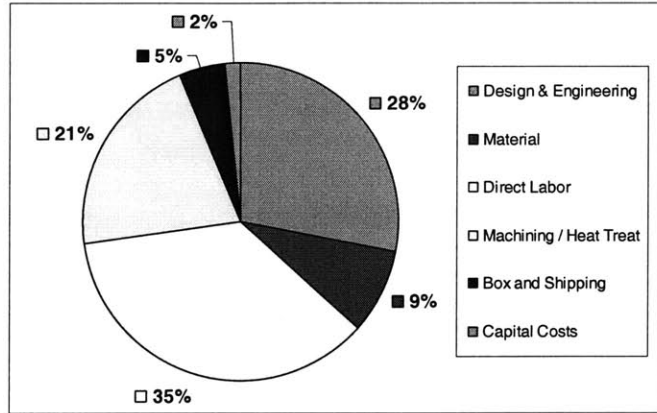


**Figure 7.39 Total Cost Distribution for a Flat Aluminum Tool**

A Pareto chart (see Figure 7.40) is constructed from the detailed cost information listed in Table 7.40. It shows that the majority of the manufacturing costs (w/o material) are incurred by the construction of the egg-crate support structure. The flat surface is made of a single piece and only requires a finishing machining step.

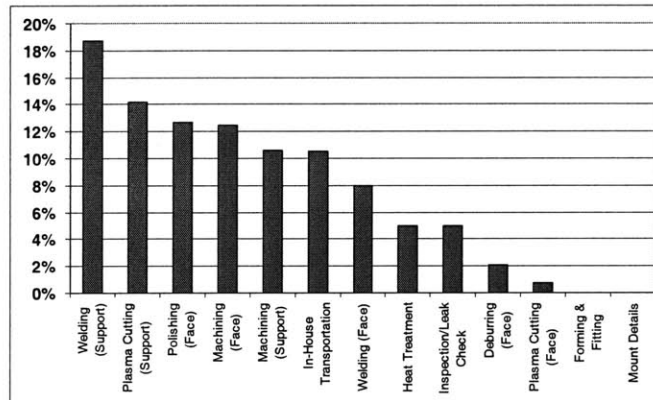


**Figure 7.40 Manufacturing Cost Distribution of the Flat Aluminum Tool**

**Table 7.40 Cost Details of the Flat Aluminum Tool**

Step	Time [hrs]	Costs	Comments
<b>Support Structure</b>			
Support Structure Material Cost		\$ 970	
Plasma Cutting	6.4	\$ 1,590	
Welding	14.0	\$ 2,100	
Machining	5.9	\$ 1,187	
<b>Total Support Structure Costs</b>	<b>26.3</b>	<b>\$ 5,847</b>	
<b>Face Sheet</b>			
Material Cost		\$ 735	
Plasma Cutting	0.3	\$ 85	
Forming	0.0	\$ -	
Fitting Sheet to Substructure	0.0	\$ -	
Welding	6.0	\$ 900	
Deburring (Face)	2.3	\$ 233	
Heat Treatment		\$ 566	
Rough Machining	0.0	\$ -	
Finish Machining	7.0	\$ 1,400	
Polishing	14.3	\$ 1,429	
Mount Details	0.0	\$ -	0%
Inspection/Leak Check	2.8	\$ 560	40%
In-House Transportation	5.9	\$ 1,181	10%
<b>Total Face Sheet Costs</b>			
<b>Manufacturing Costs</b>	<b>91.2</b>	<b>\$ 11,230</b>	
<b>Material Costs</b>		<b>\$ 1,705</b>	
<b>Overhead + Profit</b>			
Design and Engineering		\$ 5,544	30%
Boxing and Shipping		\$ 924	5%
Optional FEM Analysis		\$ -	no complexity
Capital Costs, 2 months	2	\$ 323	10%
Profit		\$ 4,931	20%
<b>Estimated Price</b>		<b>\$ 24,657</b>	

#### 7.8.4 Case Study: Helicopter Blade Curing Tool (Aluminum, Level 2)

The Aluminum tool seen in the far left of Figure 7.41 is one of a pair of left and right-handed tools used for the curing of helicopter blade skins. The surface exhibits very slight double curvature to accommodate the shape of the blades however is still machined out of only two sheets welded together. It can therefore be classified as a complexity level 2 tool. The tool's dimensions are 25ft x 4.5ft x 1ft resulting in a projected area of 16,200in<sup>2</sup> (112.5ft<sup>2</sup>). The egg-crate is constructed of ½ inch Aluminum plate whereas ¾ inch plate is used for the face sheet. One tool weighs approximately 2,800lbs. The price for the first copy of one tool is \$175,000 according to the manufacturer. The price is exclusive of any of the secondary tooling seen in Figure 7.41 but includes the costs for the casters, the integrated vacuum plumbing, and the thermocouples.

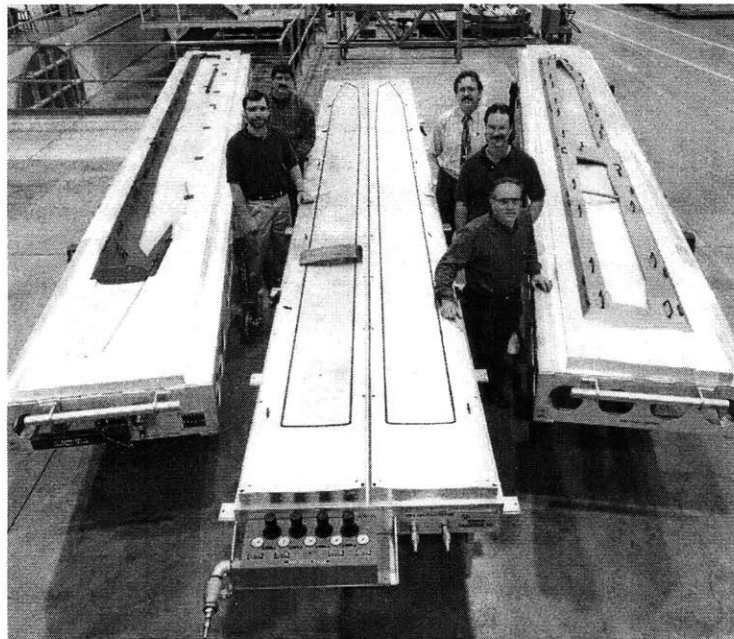


**Figure 7.41 Helicopter Blade Curing Tool (Aluminum, Level 2) [29]**

The cost model assumes that 50% of the manufacturing costs are related to engineering because of the higher complexity and the many optional design features. The estimated total costs of the tool are approximately \$146K. Material costs contribute about 5% and labor & machining about 41% to the total costs. When adding a 20% profit to the total costs the estimated price comes out to be \$182K and is 4% about the quoted price. The

result is well within the expected limits, considering the large uncertainties regarding the profit margin, the engineering and the material costs.

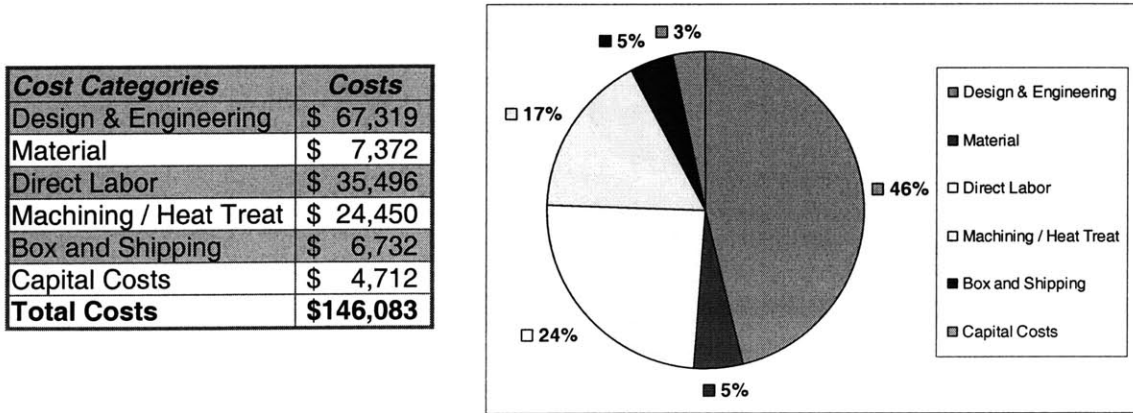


**Figure 7.42 Total Cost Distribution of the Helicopter Blades Tooling**

As seen in Table 7.41 the manufacturing costs for the curing tool (w/o material) are approximately \$60K. The Pareto chart depicted in Figure 7.43 shows that the costs for welding (support & tooling face) contribute about 26% to the manufacturing costs followed by the costs for machining 22% (support & tooling face). The almost equal costs for welding and machining are due to the increased complexity of the tooling face, which requires proportionally more machining.

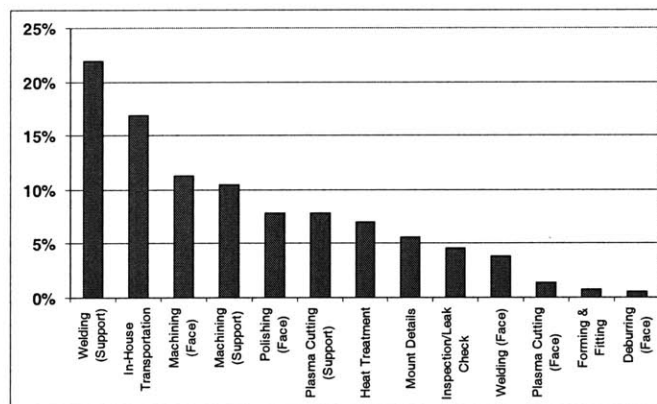


**Figure 7.43 Manufacturing Cost Distribution of the Helicopter Blades Tooling**

**Table 7.41 Cost Details of the Helicopter Blade Tool**

Step	Time [hrs]	Costs	Comments
<b>Support Structure</b>			
Support Structure Material Cost		\$ 4,247	
Plasma Cutting	18.8	\$ 4,695	
Welding	87.5	\$ 13,128	
Machining	20.8	\$ 6,252	
<b>Total Support Structure Costs</b>	<b>127.1</b>	<b>\$ 28,321</b>	
<b>Face Sheet</b>			
Face Sheet Material Costs		\$ 3,126	
Plasma Cutting	3.4	\$ 848	
Forming	2.0	\$ 300	
Fitting Sheet to Structure	1.0	\$ 150	
Welding	15.4	\$ 2,316	
Deburring	3.5	\$ 345	
Heat Treatment		\$ 4,218	
Rough Machining	8.4	\$ 2,529	
Finish Machining	14.2	\$ 4,253	
Polishing	47.3	\$ 4,725	
Mount Details	22.2	\$ 3,334	10%
Inspection/Leak Check	9.0	\$ 2,713	40%
In-House Transportation	25.4	\$ 10,142	10%
<b>Total Face Sheet Costs</b>	<b>151.8</b>	<b>\$ 38,998</b>	
<b>Manufacturing Costs</b>	<b>278.9</b>	<b>\$ 59,947</b>	
<b>Material Costs</b>		<b>\$ 7,372</b>	
<b>Overhead + Profit</b>			
Design and Engineering		\$ 67,319	50%
Boxing and Shipping		\$ 6,732	5%
Optional FEM Analysis		\$ -	simple
Capital Costs, 4 months	4	\$ 4,712	10%
Profit		\$ 36,521	20%
<b>Estimated Price</b>		<b>\$ 182,603</b>	



**7.8.5 Case Study: Flat Open Mold Tool (Invar, Level 1)**

The flat Invar curing tool is identical in its basic design to the flat Aluminum tool discussed in Chapter 7.8.3. The use of Invar as design material result in a construction, which exhibits almost no thermal expansion, but weighs considerably more and is more difficult to machine. The outer dimensions are 8.3ft x 5ft x 1ft resulting in a surface area of 6,000 in<sup>2</sup> (42ft<sup>2</sup>). The tool is constructed of ½ inch plate stock and weighs with 1,700lbs about three times as much as its Aluminum counterpart. This simple tool does not have any of the optional features and the flat surface classify it as complexity level 1 tooling. Its quoted price is \$55,000 [29].

The total costs are \$51K, which brings the estimated price to \$63K assuming a 20% profit margin. Again, similar to the aluminum counterpart the estimate is about 15% above the actual price, which could cautiously be interpreted as a systematic error in the model. The major uncertainty lies within the assumption of ca. 30% engineering costs. It is therefore perceivable that the actual engineering costs are lower for such a simple tool. Another major cost driver are the material costs, which contribute 39% to the total costs because of the high price for Invar (\$10/lb). Therefore, direct labor plus the costs for machines make up only 26% of the total costs, which are mainly driven by material costs. Because of the additional uncertainty regarding the precise material price the fluctuation of the estimate are potentially higher than the previously assumed ±30%.

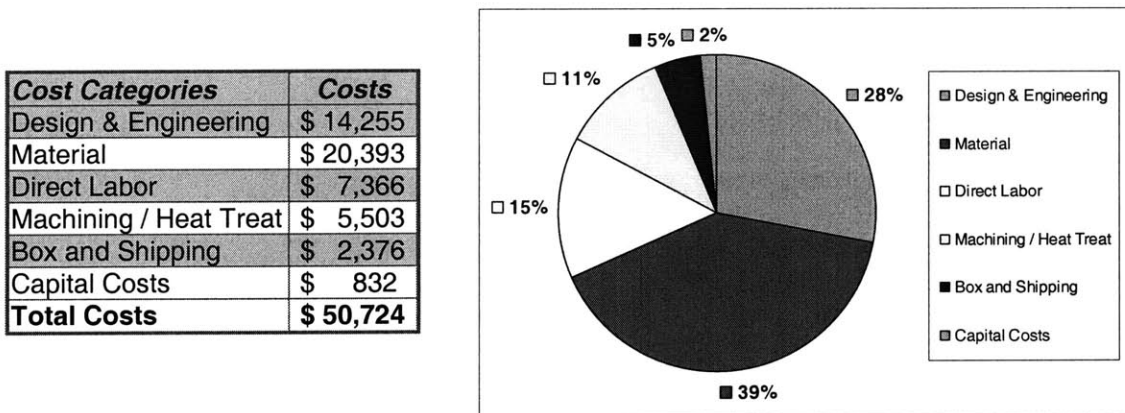


**Figure 7.44 Total Cost Distribution of the Flat Invar Tooling**

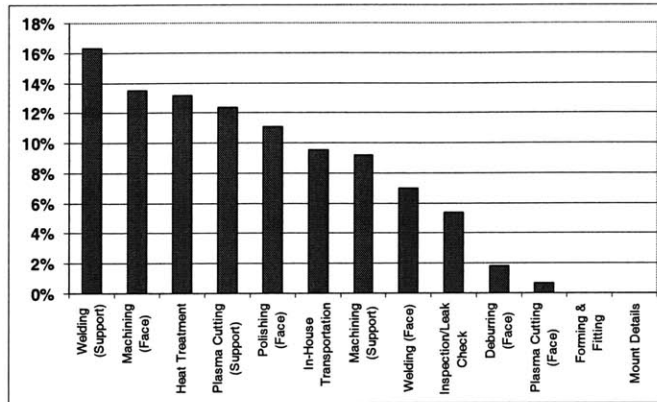


**Figure 7.45 Manufacturing Cost Distribution of the Flat Invar Tooling**

Figure 7.45 shows the distribution of the manufacturing costs (w/o material). The increased difficulty of machining Invar results in an overall larger cost contribution (22%). The costs for welding are with 23% about equal to the machining costs.

**Table 7.42 Cost Details of the Flat Invar Tooling**

Step	Time [hrs]	Costs	Comments
<b>Support Structure</b>			
Support Structure Material Cost		\$ 11,603	
Plasma Cutting	6.4	\$ 1,590	
Welding	14.0	\$ 2,100	
Machining	5.9	\$ 1,187	
<b>Total Support Structure Costs</b>	<b>26.3</b>	<b>\$ 16,479</b>	
<b>Face Sheet</b>			
Face Sheet Material Costs		\$ 8,790	
Plasma Cutting	0.3	\$ 85	
Forming	0.0	\$ -	
Fitting Sheet to Structure	0.0	\$ -	
Welding	6.0	\$ 900	
Deburring	2.3	\$ 233	
Heat Treatment		\$ 1,691	
Rough Machining	0.0	\$ -	
Finish Machining	8.7	\$ 1,733	
Polishing	14.3	\$ 1,429	
Mount Details	0.0	\$ -	0%
Inspection/Leak Check	3.5	\$ 693	40%
In-House Transportation	6.1	\$ 1,228	10%
<b>Total Face Sheet Costs</b>	<b>41.2</b>	<b>\$ 16,782</b>	
<b>Manufacturing Costs</b>	<b>67.5</b>	<b>\$ 12,869</b>	
<b>Material Costs</b>		<b>\$ 20,393</b>	
<b>Overhead + Profit</b>			
Design and Engineering		\$ 14,255	30%
Boxing and Shipping		\$ 2,376	5%
Optional FEM Analysis		\$ -	no complexity
Capital Costs, 2 months	2	\$ 832	10%
Profit		\$ 12,681	20%
<b>Estimated Total Price</b>		<b>\$ 63,405</b>	

### 7.8.6 Case Study: Horizontal Stabilizer Co-Curing Tool (Invar, Level 3)

The Invar tool shown in Figure 7.46 is one out of four tools used to co-cure stringers and the wing skin of a horizontal stabilizer. The tool is fabricated by a different manufacturer than the other examples and because of its enormous size (45ft x 8ft x 4ft) is constructed with an Electroformed Nickel tooling face instead of a machined one. Therefore, about five manufacturing steps can be eliminated from the process plan. In addition, the Electroformed Nickel process produces a very uniform part thickness, which minimizes any thermally induced deformations during curing. A further benefit is that the egg-crate support structure can be designed lighter and still can use ½ inch plate stock, since it does not have to withstand the forces exerted by the forming of the face sheet. With a tool weighing about 24,000 lbs. any weight savings reduces costs and improves the handling on the shop floor. The tool is given a complexity level 3 (to 3.5) to reflect the manufacturing difficulty caused by the double curvature of the tooling face. The high complexity of tooling face can also be observed in the difference between the actual surface area of 66,400 in<sup>2</sup> (460 ft<sup>2</sup>) and the projected area of 51,800 in<sup>2</sup> (360 ft<sup>2</sup>). The price paid for all four tools was a special deal (\$1M), since design and engineering was done entirely by the customer and the producer could probably negotiate a good Invar price from its supplier. However all industry experts consent that the actual price for the first copy of one such tool should be at least \$1,000,000. The tool also does not feature any optional design elements and the construction taught the producer new fabrication and design techniques.

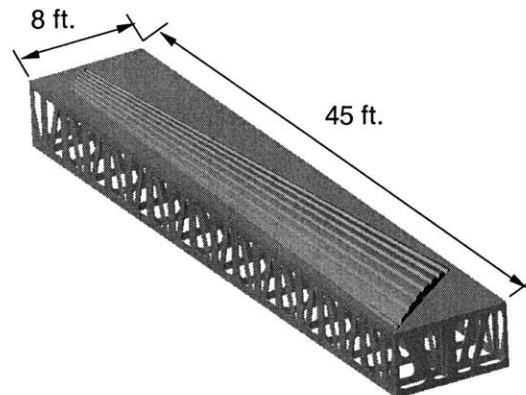


**Figure 7.46** Horizontal Stabilizer Co-Curing Tool (Invar, Level 3) [7]

<b>Cost Categories</b>	<b>Costs</b>
Design & Engineering	\$ 396,143
Material	\$ 245,304
Direct Labor	\$ 74,813
Machining / Heat Treat	\$ 66,026
Box and Shipping	\$ 38,614
Capital Costs	\$ 27,363
<b>Total Costs</b>	<b>\$ 848,264</b>

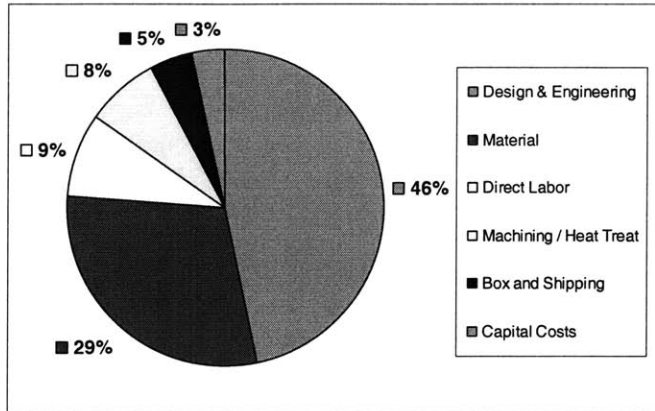


**Figure 7.47 Total Cost Distribution of the Horizontal Stabilizer Tooling**

As displayed in Figure 7.47, the model estimates the total costs excluding profit to be \$850K. Because of the complexity of the tool around 50% of the total costs are incurred by design and engineering. The costs for the Invar are approximately 30% of the total costs followed by 17% for the combined costs of direct labor and production processes. Including a 20% profit margin the estimated price for the first copy of one tool is about \$1.1M or 6% above the actual price. The calculation assumes that the producer pays a price close to the lower range for Invar (\$5/lb) because of the large order volume. Using the average of \$10/lb for Invar increases the estimated tooling price to 1.5M, which demonstrates the sensitivity of the model to the material price. Again, given the previously mentioned uncertainties regarding engineering costs, material costs, and profit margin, the estimated price can potentially deviate by at least  $\pm 30\%$  from the actual price.

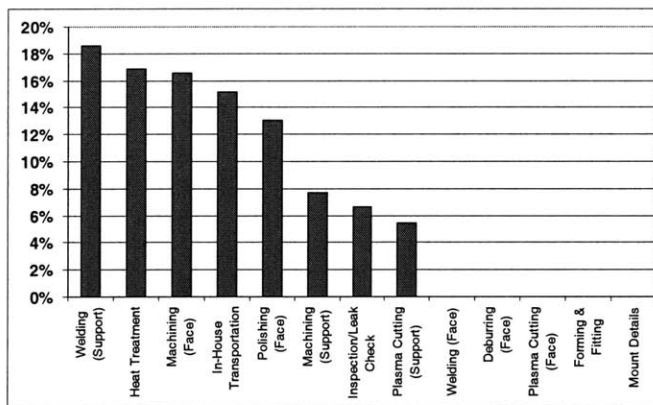


**Figure 7.48 Manufacturing Cost Distribution of the Horizontal Stabilizer Tooling**

Looking at the manufacturing cost (w/o material costs) distribution depicted in Figure 7.48 and Table 7.43, one recognizes the savings due to the use of Electroformed Nickel for the fabrication of the tooling face. Only a finishing pass is required which together with machining of the support structure make up 25% of the manufacturing costs. Again, since the welding of the face sheet is no longer required, the process step for joining the egg-crate now only contributes 18% to the manufacturing costs.

**Table 7.43 Cost Details of the Horizontal Stabilizer Tooling**

Step	Time [hrs]	Costs	Comments
<b>Support Structure</b>			
Support Structure Material Cost		\$ 148,094	
Plasma Cutting	30.6	\$ 7,649	
Welding	174.6	\$ 26,184	
Machining	36.1	\$ 10,824	
<b>Total Support Structure Costs</b>	<b>241.2</b>	<b>\$ 192,751</b>	
<b>Face Sheet</b>			
Face Sheet Material Costs		\$ 97,210	
Plasma Cutting	0.0	\$ -	
Forming	0.0	\$ -	
Fitting Sheet to Structure	0.0	\$ -	
Welding	0.0	\$ -	
Deburring	0.0	\$ -	
Heat Treatment		\$ 23,729	
Rough Machining	4.0	\$ 1,200	
Finish Machining	73.7	\$ 22,118	
Polishing	184.3	\$ 18,432	
Mount Details	0.0	\$ -	0%
Inspection/Leak Check	31.1	\$ 9,327	40%
In-House Transportation	53.4	\$ 21,375	10%
<b>Total Face Sheet Costs</b>	<b>346.6</b>	<b>\$ 193,392</b>	
<b>Manufacturing Costs</b>	<b>587.8</b>	<b>\$ 140,839</b>	
<b>Material Costs</b>		<b>\$ 245,304</b>	
<b>Overhead + Profit</b>			
Design and Engineering		\$ 386,143	50%
Boxing and Shipping		\$ 38,614	5%
Optional FEM Analysis		\$ 10,000	high complexity
Capital Costs	4	\$ 27,363	10%
Profit		\$ 212,066	20%
<b>Estimated Total Price</b>		<b>\$ 1,060,330</b>	

## 7.8.7 Case Study: Engine Cauling Curing Tool (Invar, Level 4)

Table 7.44 Cost Summary for the Engine Cauling Tool

Step	Time [hrs]	Costs	Comment
<b>Support Structure</b>			
Support Structure Material Costs		\$ 143,108	
Plasma Cutting	12.4	\$ 3,100	
Welding	70.2	\$ 10,536	
Machining	16.8	\$ 5,040	
<b>Total Support Structure Costs</b>	<b>99.4</b>	<b>\$ 161,784</b>	
<b>Face Sheet</b>			
Face Sheet Material Costs		\$ 35,430	
Plasma Cutting	7.0	\$ 1,760	
Forming	9.0	\$ 1,350	
Fitting Sheet to Structure	4.5	\$ 675	
Welding	23.1	\$ 3,462	
Deburring	8.6	\$ 860	
Heat Treatment		\$ 14,772	
Rough Machining	25.0	\$ 7,498	
Finish Machining	33.6	\$ 10,077	
Polishing	67.2	\$ 6,718	
Inspection/Leak Check	23.4	\$ 7,030	40%
In-House Transportation	30.1	\$ 13,144	10%
Mount Details		\$ 4,161	10%
<b>Total Face Sheet Costs</b>	<b>231.5</b>	<b>\$ 102,775</b>	
<b>Manufacturing Costs</b>	<b>430.4</b>	<b>\$ 90,183</b>	
<b>Material Costs</b>		<b>\$ 178,538</b>	
<b>Overhead + Profit</b>			
Design and Engineering		\$ 268,721	50%
Boxing and Shipping		\$ 26,872	5%
Optional FEM Analysis		\$ 10,000	high complexity
Capital Costs, 4 months	4	\$ 19,144	10%
Profit		\$ 148,365	20%
<b>Total Costs</b>		<b>\$ 741,823</b>	

Table 7.45 Labor and Machine Costs for Engine Cauling Tool

	Labor Cost [\$]	Machine Cost [\$]	Labor Rates [\$/hr]	Equipment Rates [\$/hr]
Plasma Cutting (Support)	1,240	1,860	100	150
Welding	7,024	3,512	100	50
Machining	1,680	3,360	100	200
Plasma Cutting (Face)	704	1,056	100	150
Forming	900	450	100	50
Fitting Sheet to Support Structure	450	225	100	50
Welding	2,308	1,154	100	50
Deburring (Face)	860	0	100	0
Heat Treatment		14,772		
Rough Machining	2,499	4,999	100	200
Finish machining Time	3,359	6,718	100	200
Polishing	6,718	0	100	0
Inspection Time/Leak check	2,343	4,687	100	200
In-House Transportation	13,144	0	100	0
Mount Details	2,774	1,387	100	50
<b>Total Manufacturing Costs</b>	<b>\$ 46,004</b>	<b>\$ 44,179</b>		

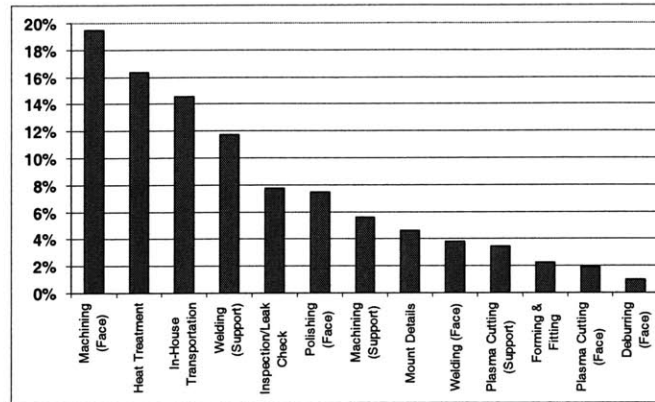


Figure 7.49 Distribution of the Manufacturing Costs

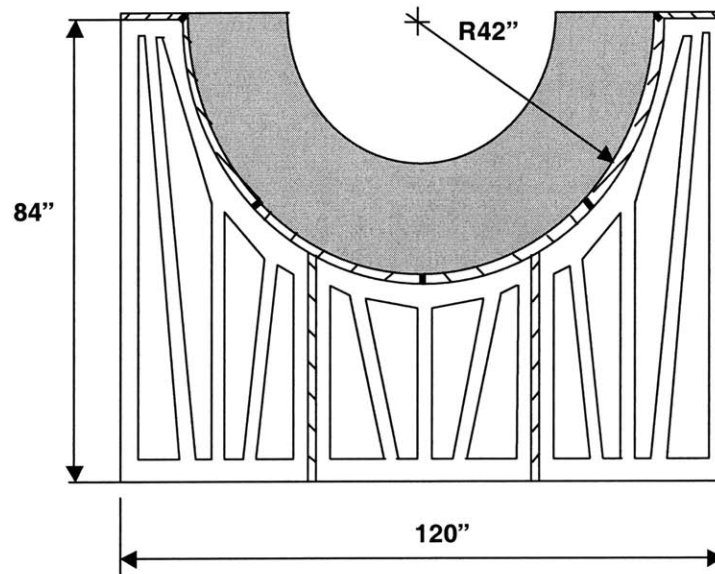
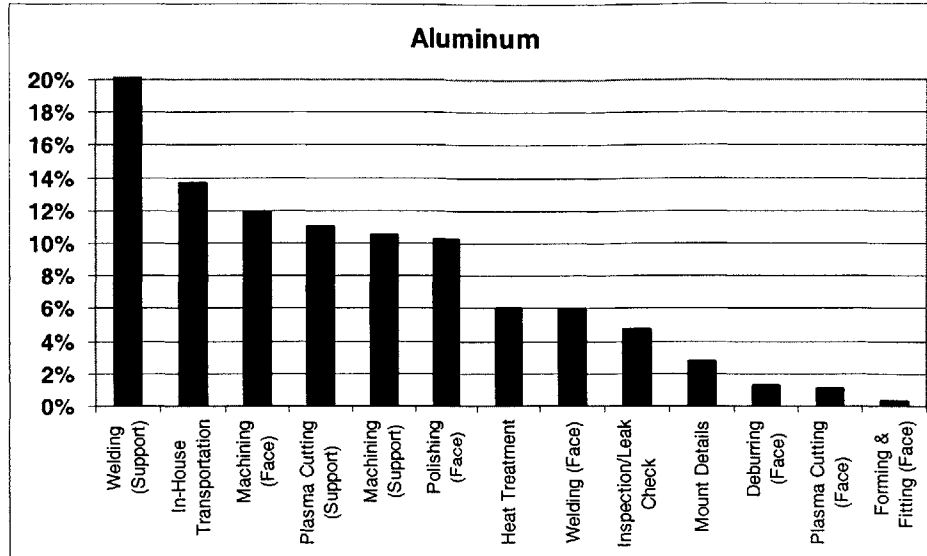


Figure 7.50 Schematic of the Engine Cauling Tool (Frontal View)







**Figure 7.52 Manufacturing Cost Distribution of the Average Aluminum Tool**

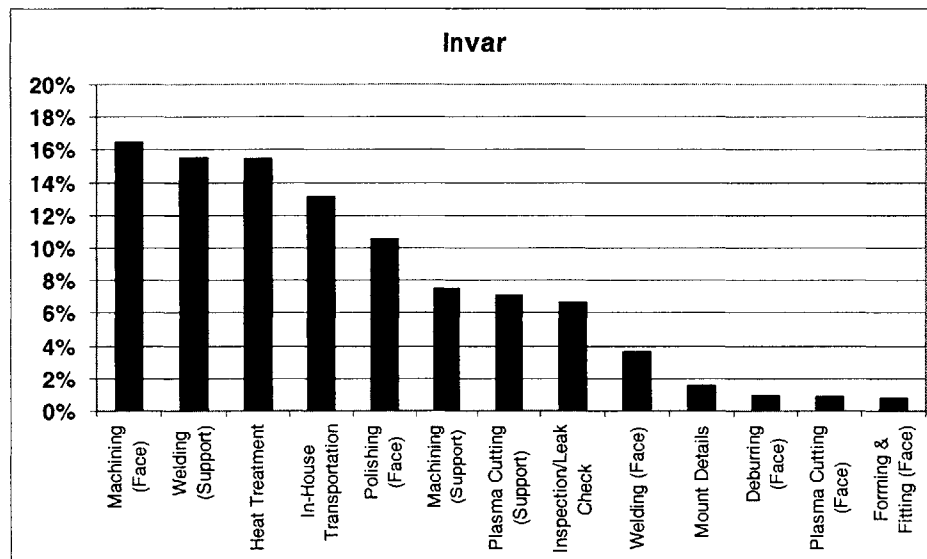


**Figure 7.53 Manufacturing Cost Distribution of the Average Invar Tool**

## 7.8.9 Case Study: RTM Mold

Table 7.47 Detailed Process Plan for Making a RTM Mold

Process Plan for a RTM Mold			ProcTime	ProcTime
Aggregated Steps	PlanStep	AM Cost	Non-Rec.	Rec.
		Est. Ref.	[min]	[min]
Setup Milling Center	1	7.1	87.0	0.0
Square Off Male Mold	2	8.1-1	7.2	0.0
	3	8.1-3	1.2	0.0
	4	11.3-1	0.0	20.0
	5	18.5-4	0.0	1.2
	6	8.1-1	9.3	0.0
	7	11.3-1	0.0	10.7
	8	18.5-4	0.0	0.9
	9	8.1-1	9.3	0.0
	10	11.3-1	0.0	10.7
	11	18.5-4	0.0	0.9
	12	8.1-1	9.3	0.0
	13	11.3-1	0.0	20.0
	14	11.3-1	0.0	8.0
	15	11.3-1	0.0	8.0
	16	18.5-4	0.0	0.9
	17	8.1-S6	1.8	0.0
	Machine External Features Male Mold	18	8.1-3	1.2
19		11.2-4	0.0	0.8
20		8.1-3	1.2	0.0
21		11.2-8	0.0	0.4
22		8.1-1	9.3	0.0
23		8.1-3	1.2	0.0
24		11.2-4	0.0	0.8
25		8.1-3	1.2	0.0
26		11.2-8	0.0	0.4
27		8.1-1	9.3	0.0
28		8.1-3	1.2	0.0
29		11.2-4	0.0	3.2
30		8.1-3	1.2	0.0
31		11.2-8	0.0	1.6
32		8.1-3	1.2	0.0
33		MRR for Alu	0.0	0.2
34		8.1-S6	1.8	0.0
35	8.1-3	1.2	0.0	
36	11.2-4	0.0	0.4	
37	8.1-3	1.2	0.0	
38	11.2-8	0.0	0.2	
39	8.1-S6	1.8	0.0	
Contour Mill Male Mold	40	8.1-3	1.2	0.0
	41	MRR for Alu	0.0	271.1
Square Off Female Mold	42	8.1-S6	1.8	0.0
	43	8.1-1	7.2	0.0
	44	8.1-1	7.2	0.0
	45	8.1-3	1.2	0.0
	46	11.3-1	0.0	20.0
	47	18.5-4	0.0	1.2
	48	8.1-1	9.3	0.0
	49	11.3-1	0.0	10.7
	50	18.5-4	0.0	0.9
	51	8.1-1	9.3	0.0
	52	11.3-1	0.0	10.7
	53	18.5-4	0.0	0.9
	54	8.1-1	9.3	0.0

	55	11.3-1	Machine 4th Surface	0.0	20.0
	56	11.3-1	Machine 5th Surface	0.0	8.0
	57	11.3-1	Machine 6th Surface	0.0	8.0
	58	18.5-4	Deburr Part Perimeter	0.0	0.9
	59	8.1-S6	Inspect Part	1.8	0.0
Machine External Features	60	8.1-3	Set Up Drill	1.2	0.0
Female Mold	61	11.2-4	2 x Drill Shipping Holes	0.0	0.8
	62	8.1-3	Set Up Tapping Tool	1.2	0.0
	63	11.2-8	2 x Tap Shipping Holes	0.0	0.4
	64	8.1-1	Reload, Position & Clamp Work Piece	9.3	0.0
	65	8.1-3	Set Up Drill	1.2	0.0
	66	11.2-4	2 x Drill Shipping Holes	0.0	0.8
	67	8.1-3	Set Up Tapping Tool	1.2	0.0
	68	11.2-8	2 x Tap Shipping Holes	0.0	0.4
	69	8.1-1	Reload, Position & Clamp Work Piece	9.3	0.0
	70	8.1-3	Set Up Drill	1.2	0.0
	71	11.2-4	4 x Drill Bolting Holes	0.0	3.2
	72	8.1-3	Set Up Tapping Tool	1.2	0.0
	73	11.2-8	4 x Tap Bolting Holes	0.0	1.6
	74	8.1-3	Set Up End Mill 1/4"	1.2	0.0
	75	MRR for Alu	Machine Interlock Slots	0.0	0.2
	76	8.1-S6	Inspect Part	1.8	0.0
	77	8.1-3	Set Up End Mill 1/8"	1.2	0.0
	78	MRR for Alu	Machine O-Ring Groove	0.0	2.4
	79	MRR for Alu	Machine Gates & Jackpads	0.0	0.1
	80	8.1-S6	Inspect Part	1.8	0.0
	81	8.1-3	Set Up Drill	1.2	0.0
	82	11.2-4	4 x Drill Interlock Holes	0.0	0.4
	83	8.1-3	Set Up Tapping Tool	1.2	0.0
	84	11.2-8	4 x Tap Interlock Holes	0.0	0.2
	85	8.1-3	Set Up Drill	1.2	0.0
	86	11.2-4	1 x Drill Injection Port	0.0	1.6
	87	8.1-S6	Inspect Part	1.8	0.0
Contour Mill Female Die	88	8.1-3	Set Up Ball End Mill 1/4"	1.2	0.0
	89	MRR for Alu	Machine Profile	0.0	71.7
	90	8.1-S6	Inspect Part	1.8	0.0
Machine Internal Features	91	8.1-3	Set Up Drill	1.2	0.0
Female Mold	92	11.2-4	4 x Drill Vent Holes	0.0	2.0
	93	8.1-3	Set Up Drill	1.2	0.0
	94	11.2-4	4 x Drill Insert Holes	0.0	1.6
	95	8.1-3	Set Up End Mill 1/4"	1.2	0.0
	96	MRR for Alu	Machine Chimney	0.0	1.5
	97	8.1-S6	Inspect Part	1.8	0.0
	98	8.1-1	Unload & Unclamp Work Piece	7.2	0.0
Polish Mold Surfaces	99	8.1-1	Handle Work Piece	5.1	0.0
	100	18.4-5	Polish Surface	0.0	456.9
	101	8.1-1	Handle Work Piece	5.1	0.0
	102	8.1	Final Inspect Part	30.0	0.0
	103	8.1-1	Handle Work Piece	5.1	0.0
	104	18.4-5	Polish Surface	0.0	456.9
	105	8.1-1	Handle Work Piece	5.1	0.0
	106	8.1	Final Inspect Part	60.0	0.0

	ProcTime Non-Rec.	ProcTime Rec.
Cycle Time / Run [min]	369.1	1,444.4
Cycle Time / Run [hrs]	6.2	24.1
<b>Total Cycle Time / Run [min]</b>	<b>1,813.6</b>	
<b>Total Cycle Time / Run [hrs]</b>	<b>30.2</b>	

## 7.8.10 Case Study: Pultrusion Die

Table 7.48 Detailed Process Plan for Making a Pultrusion Die

Process Plan for a Pultrusion Die			ProcTime	ProcTime
Aggregated Steps	PlanStep	AM Cost Est. Ref.	Non-Rec. [min]	Rec. [min]
Setup Milling Center	1	7.1	87.0	0.0
Square Off Male Die	2	8.1-1	7.2	0.0
	3	8.1-3	1.2	0.0
	4	11.3-1	0.0	6.4
	5	18.5-4	0.0	0.9
	6	8.1-1	9.3	0.0
	7	11.3-1	0.0	3.2
	8	18.5-4	0.0	0.9
	9	8.1-1	9.3	0.0
	10	11.3-1	0.0	3.2
	11	18.5-4	0.0	0.9
	12	8.1-1	9.3	0.0
	13	11.3-1	0.0	6.4
	14	11.3-1	0.0	0.5
	15	11.3-1	0.0	0.5
	16	18.5-4	0.0	0.9
	17	8.1-S6	1.8	0.0
Tap Holes for Male Die	18	8.1-3	1.2	0.0
	19	11.2-4	0.0	3.3
	20	8.1-3	1.2	0.0
	21	11.2-8	0.0	1.7
	22	8.1-3	1.2	0.0
	23	11.2-4	0.0	0.8
	24	8.1-3	1.2	0.0
	25	11.2-8	0.0	0.6
	26	11.2-3	0.0	0.5
	27	8.1-S6	1.8	0.0
Square Off Female Die	28	8.1-1	7.2	0.0
	29	8.1-1	7.2	0.0
	30	8.1-3	1.2	0.0
	31	11.3-1	0.0	6.4
	32	18.5-4	0.0	0.9
	33	8.1-1	9.3	0.0
	34	11.3-1	0.0	3.2
	35	18.5-4	0.0	0.9
	36	8.1-1	9.3	0.0
	37	11.3-1	0.0	3.2
	38	18.5-4	0.0	0.9
	39	8.1-1	9.3	0.0
	40	11.3-1	0.0	6.4
	41	11.3-1	0.0	0.5
	42	11.3-1	0.0	0.5
	43	18.5-4	0.0	0.9
	44	8.1-S6	1.8	0.0
Tap Holes for Female Die	45	8.1-3	1.2	0.0
	46	11.2-4	0.0	3.3
	47	8.1-3	1.2	0.0
	48	11.2-8	0.0	1.7
	49	8.1-3	1.2	0.0
	50	11.2-4	0.0	0.8
	51	8.1-3	1.2	0.0
	52	11.2-8	0.0	0.6
	53	11.2-3	0.0	0.5
	54	8.1-S6	1.8	0.0

Drill Through Both Die Halves	55	8.1-1	Reload, Position & Clamp Work Piece	9.3	0.0
	56	8.1-3	Set Up Drill 1/4"	1.2	0.0
	57	11.2-4	10 x Drill 1/4" x 4" Holes	0.0	13.2
	58	8.1-3	Set Up Reaming Tool 1/4"	1.2	0.0
	59	11.2-7	10 x Ream 1/4" x 4" Holes	0.0	13.4
	60	8.1-S6	Inspect Part	1.8	0.0
	61	8.1-1	Unload & Unclamp Work Piece	7.2	0.0
Profile Mill Male Die	62	8.1-3	Set Up Ball End Mill 1/4"	1.2	0.0
	63	MRR for Toolsteel	Machine Profile	0.0	176.4
	64	8.1-S6	Inspect Part	1.8	0.0
	65	8.1-1	Unload & Unclamp Work Piece	7.2	0.0
Profile Mill Female Die	66	8.1-1	Load, Position & Clamp Work Piece	7.2	0.0
	67	8.1-3	Set Up Ball End Mill 1/4"	1.2	0.0
	68	MRR for Toolsteel	Machine Profile	0.0	153.2
	69	8.1-S6	Inspect Part	1.8	0.0
Surface & Profile Grind Male Die	70	8.1-1	Unload & Unclamp Work Piece	7.2	0.0
	71	13.4-1	Set Up Surface Grinding Machine	36.0	0.0
	72	13.4-12	Change & Dress Grinding Wheel	16.0	0.0
	73	8.1-1	Load, Position & Clamp Work Piece	7.2	0.0
	74	13.4-5	Surface Grind	0.0	10.9
	75	8.1-S6	Inspect Part	1.8	0.0
	76	13.4-12	Change & Dress Grinding Wheel	16.0	0.0
	77	13.4-5	Profile Grind	0.0	10.9
	78	8.1-S6	Inspect Part	1.8	0.0
	79	8.1-1	Unload & Unclamp Work Piece	7.2	0.0
Surface & Profile Grind Female Die	80	13.4-12	Change & Dress Grinding Wheel	16.0	0.0
	81	8.1-1	Load, Position & Clamp Work Piece	7.2	0.0
	82	13.4-5	Surface Grind	0.0	10.9
	83	8.1-S6	Inspect Part	1.8	0.0
	84	13.4-12	Change & Dress Grinding Wheel	16.0	0.0
	85	13.4-5	Profile Grind	0.0	10.9
	86	8.1-S6	Inspect Part	1.8	0.0
	87	8.1-1	Unload & Unclamp Work Piece	7.2	0.0
Hard Chrome Plate both Die Halves	88	8.1-1	Handle Work Piece	5.1	0.0
	89	Steve Nolet	Chrome Plate Surface	0.0	72.0
	90	8.1-1	Handle Work Piece	5.1	0.0
	91	Steve Nolet	Chrome Plate Surface	0.0	90.0
Polish Die Surfaces	92	8.1-1	Handle Work Piece	5.1	0.0
	93	18.4-5	Polish Surface	0.0	129.2
	94	8.1-1	Handle Work Piece	5.1	0.0
	95	8.1	Final Inspect Part	30.0	0.0
	96	8.1-1	Handle Work Piece	5.1	0.0
	97	18.4-5	Polish Surface	0.0	133.8
	98	8.1-1	Handle Work Piece	5.1	0.0
	99	8.1	Final Inspect Part	60.0	0.0

	ProcTime Non-Rec.	ProcTime Rec.
Cycle Time / Run [min]	487.8	886.0
Cycle Time / Run [hrs]	8.1	14.8
<b>Total Cycle Time / Run [min]</b>	<b>1,373.8</b>	
<b>Total Cycle Time / Run [hrs]</b>	<b>22.9</b>	

(This page is intentionally left blank.)

## 8 Model Implementation and WEB Design

The concepts and ideas of the introduced process based cost estimation models (CEM) have been combined into computer models and are now accessible through the Internet. The goal of the computer-based version is to manage all the information and facilitate the computation of the production time and cost estimates. The computer therefore can assist the designer in evaluating cost reduction strategies. The Internet and computers are important tools for an integrated production and design environment that enhances all levels of decision-making. Information sharing about product and process design, process and production planning, and shop floor control are vital practices to extent the competitive position of companies. The CEMs developed as part of this study prove these objectives can be achieved for the production of composite structures. In the future, they might form the basis for resource requirement planning and economic evaluation. Cost models for the previously described sixteen reference shapes have been made available on the Internet considering six different manufacturing processes (Hand Lay-Up, Automated Tow Placement, Forming, Pultrusion, Resin Transfer Molding, and Assembly). Because the CEM facilitates the assessment of production volume and batch size effects, the user can easily compare processes for their particular production situation. The CEMs are developed for both novice and expert users by providing default values that can be modified. The expert user can easily overwrite the default values and modify the process plans and the support databases. In particular, the web-based model has been developed with the objective to efficiently communicate with industry experts, obtain feedback, and calibrate the underlying algorithms. For that reason and to win over new users a great amount of effort was directed towards the development of an intuitive user-interface. The challenge has been to find the right balance between simplicity for novices and providing enough flexibility to suit the expectations of expert users. Despite the multitude of programming languages, JavaScript, HTML, and XML have been selected because of their suitability to these objectives and their simplicity. Finally, the CEMs were tested and compared to accepted industry cost standards and can now be accessed at <http://web.mit.edu/lmp/www/composites/costmodel/> [1, 4, 5].

## 8.1 Excel Spreadsheet

All process cost models have been implemented as Excel spreadsheets. The spreadsheets offer great flexibility and allow quick changes in the user interface, data presentation, and estimation algorithms. These calculations served as a test bed for all costs models before broader, web based solutions were rolled out.

Figure 8.8 in the Appendix 8.5 gives an idea about the user interface and the multiple input options. The user starts the computation by providing part geometry and material information. Next, data regarding production conditions, capital costs, wages and overhead structure is entered, followed by information describing productivity, quality and expected investments. The extensive process plans described in Chapter 5.2 and the time estimation algorithms are located on a separate spreadsheet but receive the necessary input information from the input form. The process plans on average consists of about 30 to 40 individual steps. The estimated cycle time of each step is summed up and fed back to the user interface. As a result, the total production costs are displayed subdivided in their variable and fixed portions. The variable costs entail material, labor, and energy costs on an annual and on a per part basis. The fixed include costs machine, tooling, overhead, capital, building, and maintenance costs. All this information can facilitate the economic assessment of each individual process.

To establish a cost estimation framework for industry, in particular small and medium sized corporation, the spreadsheet based approach certainly presents a powerful tool. The information can be shared easily throughout the company by networking the individual worksheets and only a minimum of programming experience is required. This lowers the introduction cost and increases the acceptance of the newly developed estimation algorithms. Also as some preliminary tests have shown the spreadsheets can be linked to other Windows based software such as CAD programs [4] to receive part geometry information or enterprise wide planning systems to simulate the cost effects on a larger scale.



## 8.2 WEB Based Cost Worksheet

The Internet is a very important tool and provides a standardized protocol for the exchange of information. The sharing of design, production and economic data throughout a large and globally represented corporation is essential for managerial decision making. The exchange of preliminary cost information early in the planning phase enhances all levels of decision-making and improves product and process design, process planning, production planning, and shop floor control. The incorporation of cost models into company wide resource planning systems can be accomplished quicker and economically when all modules use standardized interfaces for communication.

To prove the feasibility of the concept all the initially spreadsheet based costs models have been transferred into the WEB environment. An additional benefit of this exercise is, that research results can be made public as they become available, which prompts quicker feedback and accelerated evolution of the models. It also facilitates the conduction of case studies concerning the user-friendliness of the man-machine interface. Engineering students have been asked to perform a cost calculation using the developed WEB sites without support or previous training. The comments and the results were implemented and tests with another group showed that the worksheets required little effort to understand and can be used quite intuitively [1].

After the development of a first prototype, Joshua Pas took over the programming, perfected the user interface and completed the coding for 34 individual cost worksheets [1]. All the models use JavaScript to control the program flow and to calculate the numerous parameters. The JavaScript is embedded into the HTML interface, which details the user interface and handles the in and output of data. All other parameters such as process, material and equipment information are stored in XML databases. This allows users quick and easy access to the cost data and simplifies future updates of the cost models. Finally, the web models are crosschecked with the spreadsheet based calculations and compared to accepted industry standards [7].

### 8.2.1 Introduction & Navigation

The navigation bar located on the left side of the screen leads the user through an introduction of the cost model and its functionalities. If desired more detailed instruction on the usage of the model can be accessed through an Instruction page. Subsequently, all 14 reference shapes are described in more detail, including design for manufacturing guidelines for each geometry. In addition, the characteristics and basic capabilities of all 7 composite production processes are summarized on a Process Description page. However, the entire model revolves around the process selection matrix as outlined in Figure 8.1.

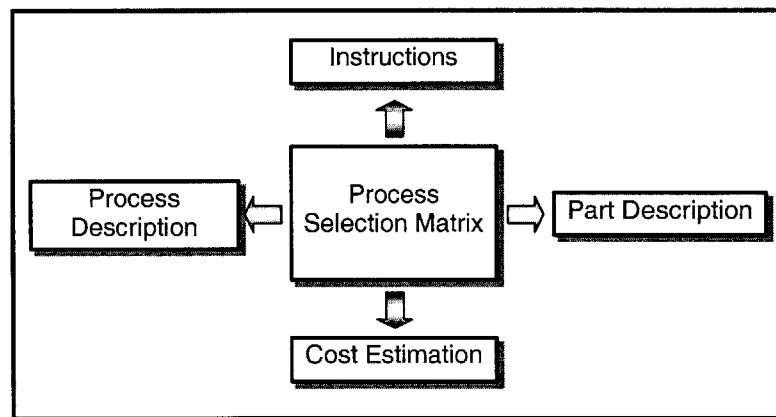


**Figure 8.1** Map of the WEB Based Cost Estimation Model

### 8.2.2 Process Selection Matrix

The process selection matrix (see Chapter 3.5) directs the user towards feasible combinations of reference shapes and production process. It therefore reduces the 98 possible part/process combinations to 71 and classifies each choice according to its practicality. A single cross symbolizes that the process/part combination is technically possible, whereas a double cross indicates that this combination is common and therefore preferable. The links on to the part and process description pages on each axis of the selection matrix links allow the user to quickly obtain more background information without leaving the process selection page. Once the user has decided on the desired

process/part combination, a click onto the underlined matrix elements (X and XX) automatically opens one of the currently installed 41 cost estimation worksheets.

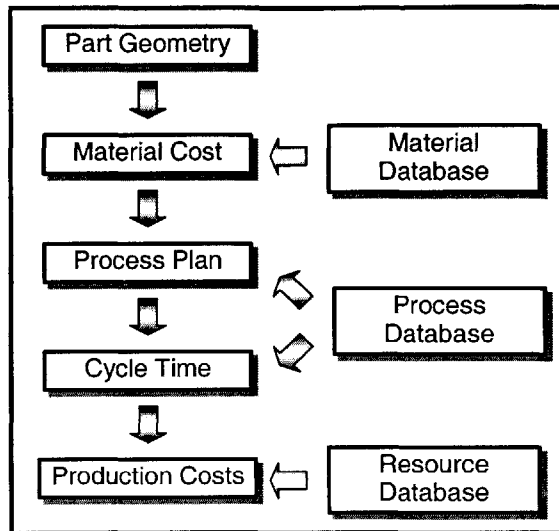


**Figure 8.2 Estimation Flow Chart**

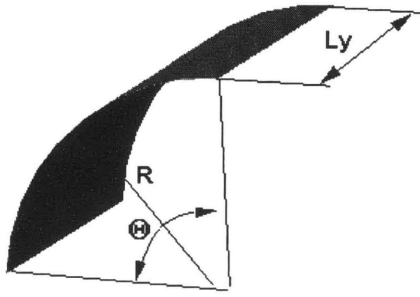
Each worksheet follows a similar path to arrive at the total production cost. Figure 8.2 outlines how the information about the part geometry is used to calculate the material cost, the cycle time, and finally the total production costs. The following chapters outline each step in more detail.

**8.2.3 Part Definition Interface**

The estimation process starts with the entry of the part design parameter such as the material type and the dimensions. The pull-down menu for the material selection is linked to the material database containing information on 107 different materials and their properties. Secondly, as depicted in Figure 8.3 the user provides information on the production volume. The data entry mask uses the batch size (parts/setup) and the number of runs (setups) to calculate the total production volume.

## Hand Lay-up: Simply Curved Parts (C2)

! using XML (View only with Internet Explorer 4.0 or higher) !

	<b>Materials:</b> Please pick your prefer material. <input type="text" value="Fabric std. mod-3K-70-PW, 42\"/>									
	<b>Dimensions:</b> Please give dimension to your part. <table border="1"> <tr> <td>Width(Ly):</td> <td><input type="text" value="108"/> inch</td> </tr> <tr> <td>Radius:</td> <td><input type="text" value="23"/> inch</td> </tr> <tr> <td>Angle:</td> <td><input type="text" value="30"/> degree</td> </tr> <tr> <td>Part thickness:</td> <td><input type="text" value="0.125"/> inch</td> </tr> <tr> <td><input type="button" value="Enter"/></td> <td>Volume = <input type="text" value="163"/> cu.in</td> </tr> </table>	Width(Ly):	<input type="text" value="108"/> inch	Radius:	<input type="text" value="23"/> inch	Angle:	<input type="text" value="30"/> degree	Part thickness:	<input type="text" value="0.125"/> inch	<input type="button" value="Enter"/>
Width(Ly):	<input type="text" value="108"/> inch									
Radius:	<input type="text" value="23"/> inch									
Angle:	<input type="text" value="30"/> degree									
Part thickness:	<input type="text" value="0.125"/> inch									
<input type="button" value="Enter"/>	Volume = <input type="text" value="163"/> cu.in									

**Quantity:** Please give the production quantity information.

Part Made per Setup:  parts / setup    Number of setup:

**Figure 8.3 Design and Production Data Entry Form**

### 8.2.4 Material Costs

Depending on the material selection the respective database entries are shown in the material cost calculation form as seen in Figure 8.4. The material costs are then calculated from the part dimension, the material density, and the price under the consideration of the material scrap rate. If necessary, all parameters can be overwritten by the user and the material costs can be recalculated.

**Materials:** Materials Information.

Material rate:  \$/lb    Density:  lb/cu.in    Scrap:  %

Thickness:  in    Width:  in of plies

Material cost = \$  for total of  part

**Figure 8.4 Material Cost Interface**

### 8.2.5 Process Plan Selection

Often, different manufacturers adapt the underlying processes to fit their particular operations. Therefore, the individual process plans differ for the same process depending on the situation. Of course, these changes can have effects on the overall cost structure and therefore have to be considered in the cost model. The web-based interface presents the user with a default process plan, which can be modified easily. Process steps can be added or excluded and the impact on costs can be observed. As seen in Figure 8.5, the interface even allows the definition of 4 additional process steps. On average, the model considers about 30 to 40 individual process steps for each process. Figure 8.9 in the Appendix 8.5 displays the process plan for Hand Lay-Up and shows how each step is identified by its unique process ID number. The number allows the user to look up the performance parameters stored in the process database.

User Additional Step: [Description of variables](#)

<input type="checkbox"/> Estimated Variables: Area setup= [ ] min, delay= [ ] min <input type="checkbox"/> Required Machine Vo1= [ ] in/min or sq.in/min, Tau= [ ] min, Crew size= [ ]	<input type="checkbox"/> Estimated Variables: Area setup= [ ] min, delay= [ ] min <input type="checkbox"/> Required Machine Vo1= [ ] in/min or sq.in/min, Tau= [ ] min, Crew size= [ ]
<input type="checkbox"/> Estimated Variables: Area setup= [ ] min, delay= [ ] min <input type="checkbox"/> Required Machine Vo1= [ ] in/min or sq.in/min, Tau= [ ] min, Crew size= [ ]	<input type="checkbox"/> Estimated Variables: Area setup= [ ] min, delay= [ ] min <input type="checkbox"/> Required Machine Vo1= [ ] in/min or sq.in/min, Tau= [ ] min, Crew size= [ ]

**Figure 8.5** Definition of Additional Process Steps

### 8.2.6 Cycle Time

As outlined in Chapter 5, size and complexity scaling models describes the relation between part size, shape complexity, and production cycle time. Once the time for each individual step is known, labor and machine costs are calculated separately, using the rate information stored in the resource database. As shown in Figure 8.10 and Figure 8.11,

the user is then presented with an overall cost distribution, which facilitates the identification of the cost driver for the underlying process.

### 8.2.7 Cost Summary

At the bottom of the cost estimation worksheet a summary of all the costs is presented showing the contribution of the material, the labor, and the machine costs to the total manufacturing costs.

The direct labor costs are broken down into non-recurring and recurring cost. One can use this information to better organize the workforce or to plan the manufacturing systems. In some cases, it might be practical to assign specially trained worker to perform the non-recurring tasks, whereas a different crew than executes the recurring jobs. A similar argument can be made for machine costs. In addition, the distinction between non-recurring and recurring machine costs gives an overview of how effectively the process uses the machinery for production. Changes in batch sizes and production flow strategy might have significant impact on the utilization of expensive equipment. Figure 8.6 shows the entire cost summary including the total costs for the entire production run as well as the unit costs.

Calculate Total Cost = Material Cost + Labor Cost + Machine Cost		
<b>Material Cost</b>	<b>Labor Cost</b>	<b>Machine Cost</b>
	Non-Recurring Cost: \$1246	Non-Recurring Cost: \$2737
\$: 506	Recurring Cost: \$678	Recurring Cost: \$316
	Total: \$1925	Total: \$3053
<b>Total cost = \$5483</b>		
<b>Average cost = \$5483 /part</b>		

**Figure 8.6 Summary of the Manufacturing Costs**

### **8.2.8 Resource Databases**

Three main databases based on the XML database definition language store the many parameters involved in the calculation of the production costs. The materials database contains information of about 100 different materials and their relevant cost and physical properties. Its entries entail the material description, the density, the price, the typical scrap rate, and where applicable the thickness and the size of the stock material.

The process database stores the parameter for approximately 270 individual process steps, which are used throughout the entire model and are part of different manufacturing settings. The database contains all the information needed to calculate the process cycle time. These performance parameters include the process velocity, the time constant, the type of scaling law to be used, and the crew size for each step.

The resource database supplies the model with information on labor rates as well as machine and tooling rates. The rates for capital equipment are calculated from their initial investment costs and their common depreciation time. The database for capital equipment and labor consists currently of approximately 50 entries [1, 6].

### **8.2.9 Programming Details**

The following four programming languages are used in the coding of the cost estimation model. HTML, JavaScript, XML, and XSL all work in concert to receive the input data, perform the calculations, and write out the results for each of the 41 cost estimation worksheets. The benefit of choosing these languages is, that the created web pages do not require any special server extensions or cgi routines. These little programs run on some web servers to support the web page functions. Since the developed code does not use any of these routines the resulting web page works independent of the underlying server configuration. Therefore, it is very easy to use the cost model on any computer platform with a modern web browser and even allows the user to run the calculations without being connected to the Internet at all. However, the disadvantage is, that if the model is accessed through the Internet the code for each worksheet has to be downloaded

onto the local terminal. So if the model would grow even larger than the currently 1,700 lines of code per worksheet, increased data traffic might burden the local network.

Figure 8.7 shows the conceptual interaction of the different programming languages. The HTML (HyperText Markup Language) is used to display information and interact with the user. The JavaScript code is part of the HTML file. Both, HTML code and the JavaScript are loaded onto the local machine each time a particular web page is accessed. The JavaScript program controls the data flow and performs all the mathematical calculations. For example, a button on the HTML-page activates a specific JavaScript routine to read the value of an user entry (a). If required, the JavaScript program requests additional information from an XML database (b,c) before executing the calculation and passing the result back to HTML to be displayed (d). Another possibility is to have the HTML code call up an XSL styles sheet (e), which displays the contents of an XML database in a special predefined format (f). For an in-depth description of the web based cost model the reader is referred to the thesis of Joshua Pas [1].

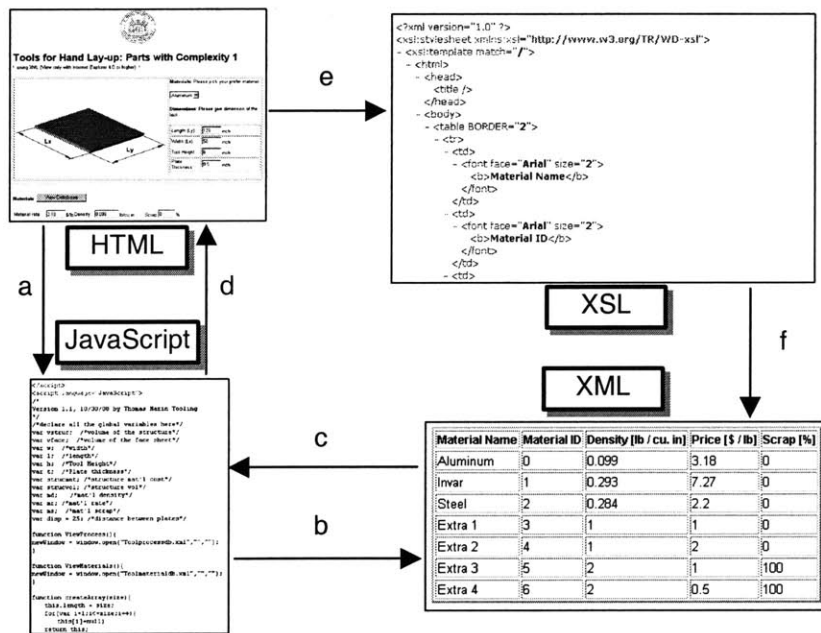


Figure 8.7 Interaction of WEB Languages



### 8.3 Summary of the WEB Implementation

The aim of CEMs is to assist the advanced composites designer in evaluating cost reduction strategies so that s/he can confidently make decisions early during the design phase using the information obtained from the models. Also the CEMs offer support in the selection of the composites manufacturing processes. They calculate the process time and costs for different production volumes, show default process plans, and make the underlying data more transparent. According to [8], Internet applications in manufacturing have the potential to transform and improve significantly all stages of manufacturing operations - from technology and market assessments to design for manufacturability, R&D, and after-sales support. The Internet has improved the competitiveness of many manufacturing organizations by publishing best manufacturing practices, knowledge bases, product information, and training materials. It minimizes the risk of a manufacturing organization of being isolated and be prevented from interacting with other companies, suppliers, and customers in a timely and cost effective manner. In manufacturing, both efficient and effective management as well as the manipulation and use of information are essential to economic vitality and growth. The most effective web sites are the ones with access to corporate databases. To improve as an industry, each manufacturer should learn from the others by means of communication. For the manufacturing organization, five basic Internet strategies are suggested:

- Communication with Customers & Distributors
- Interaction with Suppliers & Vendors
- Communication within the Organization
- Collaborating with other Organizations
- Learning from Outsiders

Chapter 9 presents a number of case studies, which demonstrate the abilities of the cost estimation model in the above-mentioned context.

## 8.4 References

- [1] Pas, J. W., "WEB Based Cost Estimation Models for the Manufacturing of Advanced Composites", M.S. Thesis, M.I.T., 2001.
- [2] Northrop Corporation, "Advanced Composite Cost Estimating Manual (ACCEM)", AFFDL-TR-76-87, August 1976.
- [3] Neoh, E. T., "Adaptive Framework for Estimating Fabrication Time", Ph.D Thesis, M.I.T, 1995.
- [4] Haffner, S. M., Gutowski, T. G. "Automated Cost Estimation for Advanced Composite Materials", NSF Conference Paper, 1998.
- [5] Haffner, S. M., Gutowski, T. G. "Manufacturing Time Estimation Law for Composite Materials", NSF Conference Paper, 1999.
- [6] Marin, T., Haffner, S. M., Gutowski, T. G. "Cost Elements of Autoclave Tooling", NSF Conference Paper, 2000.
- [7] Pas, J., Haffner, S. M., Gutowski, T. G. "Web Based Cost Estimation Model for Advanced Composites", NSF Conference Paper, 2001.
- [8] Mathieu, R. G. "Manufacturing and the Internet", Engineering and Management Press, Norcross, GA, 1996.
- [9] Nielsen, J. "Designing Web Usability", New Riders Publishing, Indianapolis, 1999.
- [10] Norman, D. A., Draper, S. W., "User Centered System Design", Erlbaum, Hillsdale, 1986.
- [11] Graham, I. S., "HTML Sourcebook", John Wiley & Sons, Inc., New York, NY, 1995.
- [12] Wagner, R., "JavaScript Unleashed", Sams.net Publishing, Indianapolis, 1997.
- [13] Heinle, N., "Designing with JavaScript – Creating Dynamic Web Pages", Sebastopol: Songline Studios, Inc. and O'Reilly & Associates, 1997.
- [14] Pardi, W. J. "XML in Action", Microsoft Press, Redmond, 1999.
- [15] Holzner, S., "XML Complete", New York: Mc Graw-Hill, Inc., 1998.

### 8.5 Appendix

HAND LAY UP TECHNICAL COST MODEL MIT- Course 3.57 Assignment		HAND LAY UP TECHNICAL - COST SUMMARY			
<b>PART MATERIAL INPUTS</b>		<b>VARIABLE COSTS</b>			
Material	1	<i>Material Cost</i>	per piece	per year	percent
Length	48.00 in		\$115.21	\$364,982	50.14%
Width	3.00 in	<i>Energy Cost</i>	\$0.00	\$0	0.00%
Thickness	0.16 in < 0.6 in	<i>Labor Cost</i>	\$104.27	\$347,752	47.77%
Projected Area	144 sqin	<b>Total Variable Cost</b>	<b>\$219.48</b>	<b>\$712,735</b>	<b>97.92%</b>
<b>EXOGENOUS DATA</b>		<b>FIXED COSTS</b>			
Annual Production Volume	3,168 (000/yr)	<i>Main Machine Cost</i>	per piece	per year	percent
Product Life	10 yrs		\$0.88	\$2,929	0.40%
Direct Wages (w/ benefits)	\$40.00 /hr	<i>Auxiliary Equipment Cost</i>	\$0.04	\$122	0.02%
Working Days/Yr	240	<i>Tooling Cost</i>	\$0.66	\$2,197	0.30%
Working Hours/Day	16	<i>Fixed Overhead Cost</i>	\$0.80	\$2,680	0.37%
Capital Recovery Rate	10%	<i>Building Cost</i>	\$0.72	\$2,408	0.33%
Working Capital Period	3 months	<i>Maintenance Cost</i>	\$0.11	\$362.82	0.05%
Price, Building Space	\$140 /sqft	<i>Cost of Working Capital</i>	\$1.34	\$4,454.59	0.61%
Building Recovery Life	39.5 yrs	<b>Total Fixed Cost</b>	<b>\$4.55</b>	<b>\$15,173</b>	<b>2.08%</b>
Price of Electricity	\$0.080 /kWh	<b>Total Fabrication Cost</b>	<b>\$224.03</b>	<b>\$727,908</b>	<b>100.00%</b>
Accounting Life of Machine	10 yrs	<b>RELATED VARIABLES</b>			
Overhead Burden (%fc)	35.0%	<b>Material Requirements</b>			
<b>PROCESS INPUTS</b>		Raw Material Price	\$50.00 /lb		
Productive Time (% total time)	78.0%	Trim Scrap Rate	40.0%		
Material Scrap Rate	40.0%	Annual Material Input	7,300 lb		
Reject Rate	5.0%	<b>Process Calculations</b>			
Direct Laborers Per Machine	1	Effective Production Volume	3,335		
Dedicated Equipment (1/0)	1 (1=y;0=n)	Run-Time for One Machine	226.4%		
Number of Parts/Cycle	2	Capacity Utilization	75.5%		
Auxiliary Equip. Cost (% mmch)	5.0%	Number of Parallel Streams	3		
Installation Cost (% mmch)	20.0%	Number of tools required	3		
Maintenance Cost (% invc)	5.0%	Required Building Space	168 sqft		
Tooling Cost	\$4,500 /tool	Energy Adjustment Factor	1.00		
Baseline Tool Life	1,000,000 cycles	<b>Cycle Time Calculations</b>			
Electricity Requirement	0 kWh/cycle	Set Up Time (min)	Predicted	Used	
<b>HAND LAY UP OVERRIDES</b>		Total Cycle Time (min)	6.0	6.0	
Actual Plant Capacity			244.0	244.0	
Annual Production Capacity	0 (000/yr)	<b>Workstation &amp; Tool Characteristics &amp; Costs</b>			
<b>Cycle Time &amp; Tool Costs</b>		Machine Size	Predicted	Used	
	0	Workstation Cost	\$5,000	\$5,000	
	0	Tool Cost	\$4,500	\$4,500	

Figure 8.8 Spreadsheet Based Production Cost Model (HLU)

Process Time: (Time: minutes, Dimension: inch)

View Database

Individual Parameters

Tool setup:

<input checked="" type="checkbox"/> 1. Clean tools(240)	<input checked="" type="checkbox"/> 2. Tool setup(2160)	<input checked="" type="checkbox"/> 3. Apply release agent(50)	<input checked="" type="checkbox"/> 4. Apply barrier film(880)
---	---	--	--

Material setup:

<input checked="" type="checkbox"/> 1. Setup prepreg	<input checked="" type="checkbox"/> 2. Cut prepreg(2280)	<input checked="" type="checkbox"/> 3. Cut bleeder(2280)	<input checked="" type="checkbox"/> 4. Cut breather(2280)
<input checked="" type="checkbox"/> 5. Cut vacuum bag(2280)			

Layup:

<input checked="" type="checkbox"/> 1. Layup(5000)			
--	--	--	--

Debulk:

<input checked="" type="checkbox"/> 1. Debulk(340)	<input checked="" type="checkbox"/> 2. Remove compaction bag (1610)		
--	---	--	--

Vacuum bagging:

<input checked="" type="checkbox"/> 1. Apply bleeder(851)	<input checked="" type="checkbox"/> 2. Apply breather(1040)	<input checked="" type="checkbox"/> 3. Apply cork dams(1210)	<input checked="" type="checkbox"/> 4. Apply vacuum/sealant tapes(4000)
<input checked="" type="checkbox"/> 5. Apply vacuum bag(1100)	<input checked="" type="checkbox"/> 6. Connect vacuum line(150)	<input checked="" type="checkbox"/> 7. Apply vacuum(80)	<input checked="" type="checkbox"/> 8. Check seals(4010)
<input checked="" type="checkbox"/> 9. Disconnect vacuum(1560)	<input checked="" type="checkbox"/> 10. Apply peel plies(851)	<input type="checkbox"/> 11. Caul plate(190,1120,1650)*	

Autoclave Setup:

<input checked="" type="checkbox"/> 1. Transfer to autoclave(2160)	<input checked="" type="checkbox"/> 2. Connect to vacuum line (150)	<input checked="" type="checkbox"/> 3. Connect thermocouples (130,1270)	<input checked="" type="checkbox"/> 4. Apply vacuum(80)
<input checked="" type="checkbox"/> 5. Check seals(4010)	<input checked="" type="checkbox"/> 6. Setup autoclave (300,940,2050)		

Cure:

<input checked="" type="checkbox"/> 1. Start autoclave cycle(350)	<input checked="" type="checkbox"/> 2. Disconnect vacuum(1560)	<input checked="" type="checkbox"/> 3. Disconnect thermocouples (1540)	<input checked="" type="checkbox"/> 4. Remove part from autoclave (4020, 4030, 4040)
---	--	--	--

Finishing:

<input checked="" type="checkbox"/> 1. Remove vacuum bagging (1630,1570,1800)	<input checked="" type="checkbox"/> 2. Demold part(1740,1800)	<input checked="" type="checkbox"/> 3. Clean part(180)	<input type="checkbox"/> 4. Abrade part(10)*
<input type="checkbox"/> 5. Trim part(2280)*	<input type="checkbox"/> 6. Deflash(2350)*	<input type="checkbox"/> 7. Debur(2340)*	

Figure 8.9 Process for Hand Layup (Default Steps are Checked)

Calculate Process Time

Time Breakdown:

	Process Time (min)	Labor Time (min)	Labor Rate (\$/hr)	Machine Time (min)	Labor & Machine Cost %(Total Cost)
<b>Tool Setup:</b>	Non-Recur: 44	Non-Recur: 79	100	Non-Recur: 0	\$166
	Recur: 18	Recur: 21		Recur: 0	3 %
	<b>Total:</b> 61	<b>Total:</b> 100		<b>Total:</b> 0	
<b>Material Setup:</b>	Non-Recur: 24	Non-Recur: 24	100	Non-Recur: 0	\$105
	Recur: 39	Recur: 39		Recur: 0	2 %
	<b>Total:</b> 63	<b>Total:</b> 63		<b>Total:</b> 0	
<b>Layup:</b>	Non-Recur: 0	Non-Recur: 0	100	Non-Recur: 0	\$128
	Recur: 77	Recur: 77		Recur: 0	2 %
	<b>Total:</b> 77	<b>Total:</b> 77		<b>Total:</b> 0	
<b>Debulk:</b>	Non-Recur: 10	Non-Recur: 10	100	Non-Recur: 0	\$156
	Recur: 42	Recur: 83		Recur: 0	3 %
	<b>Total:</b> 51	<b>Total:</b> 93		<b>Total:</b> 0	
<b>Vacuum Bagging:</b>	Non-Recur: 23	Non-Recur: 36	100	Non-Recur: 0	\$207
	Recur: 71	Recur: 88		Recur: 0	4 %
	<b>Total:</b> 94	<b>Total:</b> 124		<b>Total:</b> 0	
<b>Autoclave Setup:</b>	Non-Recur: 65	Non-Recur: 99	100	Non-Recur: 65	\$869
	Recur: 57	Recur: 57		Recur: 57	16 %
	<b>Total:</b> 122	<b>Total:</b> 156		<b>Total:</b> 122	
<b>Cure:</b>	Non-Recur: 483	Non-Recur: 483	100	Non-Recur: 483	\$3262
	Recur: 8	Recur: 8		Recur: 6	59 %
	<b>Total:</b> 491	<b>Total:</b> 491		<b>Total:</b> 489	

Figure 8.10 Process Cost by Mfg. Step

<b>Finishing:</b>	Recur: <input type="text" value="12"/> Non-	Recur: <input type="text" value="17"/> Non-	<input type="text" value="100"/>	Recur: <input type="text" value="0"/> Non-	<input type="text" value="\$84"/>	
	Recur: <input type="text" value="32"/>	Recur: <input type="text" value="34"/>		Recur: <input type="text" value="0"/>		<input type="text" value="2"/> %
	<b>Total:</b> <input type="text" value="43"/>	<b>Total:</b> <input type="text" value="50"/>		<b>Total:</b> <input type="text" value="0"/>		
<b>User Additional:</b>	Recur: <input type="text" value="0"/> Non-	Recur: <input type="text" value="0"/> Non-	Labor Rate:	Recur: <input type="text" value="0"/> Non-	<input type="text" value="\$0"/>	
	Recur: <input type="text" value="0"/>	Recur: <input type="text" value="0"/>	<input type="text" value="\$/hr"/> <input type="text" value="100"/>	Recur: <input type="text" value="0"/>		<input type="text" value="0"/> %
	<b>Total:</b> <input type="text" value="0"/>	<b>Total:</b> <input type="text" value="0"/>	Machine Rate:	<b>Total:</b> <input type="text" value="0"/>		
			<input type="text" value="\$/hr"/> <input type="text" value="0"/>			
<b>Total:</b>	Recur: <input type="text" value="659"/> Non-	Recur: <input type="text" value="748"/> Non-		Recur: <input type="text" value="547"/> Non-	<input type="text" value="\$4977"/>	
	Recur: <input type="text" value="343"/>	Recur: <input type="text" value="407"/>		Recur: <input type="text" value="63"/>		<input type="text" value="91"/> %
	<b>Total:</b> <input type="text" value="1002"/>	<b>Total:</b> <input type="text" value="1155"/>		<b>Total:</b> <input type="text" value="611"/>		

**Figure 8.11 Process Cost by Step (cont' from Figure 8.10)**

## 9 Results & Discussion

Three case studies are introduced, discussing the economics of 7 composite production processes. The first case study leads the reader through the systematic application of the previously developed cost modeling techniques. By means of a generic composite part and equal processing boundaries the study results in comparable cost and cycle time information for the different processes. Hereby, the work illustrates the capabilities of every production process and discusses the various existing trade-off scenarios between process performance and investment requirements. The first part of the study solely focuses on component production processes and describes how their performance, tooling, and equipment influences part unit costs. Although the results may only apply directly to the investigated part shape, the example provides insight in how process selection and operational aspects can influence the outcome of design decisions.

The second case study applies the same concepts to the three major assembly techniques. Again, by using a simple example the study evaluates the processing performance and economic differences between mechanical assembly, co-bonding, and co-curing. The comparison teaches how the models are applied and lays the foundation for the more comprehensive third case study.

The third study serves as an example of the economic consequences of part integration strategies. The work is based on the real-life mainbox assembly of a horizontal stabilizer of a large cargo aircraft. Formerly, the design consisted of the manual assembly of numerous aluminum components. As the aluminum was mostly substituted with better performing composites, the design also moved toward a more integrated concept. This decision of the design team was based on the more favorable economics of the integrated design as opposed to simply replacing the existing aluminum parts with composite elements. The study shows the effect of material, labor, and tooling on the unit costs of each stabilizer under varying production volumes and offers an opinion on how well the results can be applied to other part assemblies.

## 9.1 Case Study 1: Component Production Processes

The first case study compares the cycle time, production performance, and part unit costs of Hand Layup, Automated Tow Placement, Resin Transfer Molding, Pultrusion and Double Diaphragm Forming. It hereby considers the necessary investments in the appropriate size equipment and the required production tooling. The study investigates the effects of batch size on process performance and production volume on part costs.

### 9.1.1 Production Scenario

#### Conditions & Scope of Production

All the processes possess some inherent differences, which can make their objective comparison more problematic. In order to simplify the application of the various cost models, a few basic assumptions are introduced. Firstly, it is assumed that the entire business is a continuing operation and that none of the equipment and machinery is dedicated to a specific part or production program. That is, the equipment is already in place and is used for other production programs or will be so in the future. Table 9.39 shows the supposed depreciation period for each machine and shows that except for the Automated Tow Placement machine all machinery is fully utilized for 2 shifts each working day or the equivalent of 400 hours per month. In contrast, however production tooling is dedicated to the fabrication of a specific part. Also, the production program runs for 5 years and all tooling is linearly depreciated over this period. The costs of capital in connection with the investments into machinery and tooling are taken into account. It is presumed that the business faces opportunity costs of capital of 15%. Chapter 4.3.3 describes, how changes to all these assumptions can be factored in.

To study the effects of various production batch sizes all other parameters are held constant while the batch size is varied from 1 to 10 and up to 100. The batch size must not be confused with the cumulative or annual production volume. The batch size can affect how often the operation has to go through particular setup steps. In some cases, these non-recurring production steps drive the process cycle time, whereas other scenarios are dominated by the recurring processing steps. The maximum batch size is



often limited by equipment and tooling capacity, but in composite production can also be curtailed by the geltime of the resin systems or the out-time of prepreg material. The equipment considered as part of this study is large enough to allow the production of parts in batches larger than 1. In the investigated example, the realistic batch size limit is probably lies probably around 10 parts per run. The results derived for a batch size of 100 parts represents the theoretical value against which the process performance and production time converge.

The annual production volume is varied between 1 part and 100 parts per year. Over a period of 5 years this results in a cumulative production of 5, 50 and 500 parts. Admittedly, the production volume can easily be larger in real-life production scenarios, however as the production volume is increased above 500 the actual unit costs only change insignificantly. More interesting is the evaluation of the behavior for low volumes, as it describes the ramp-up of production and how quickly the economic objectives can be met.

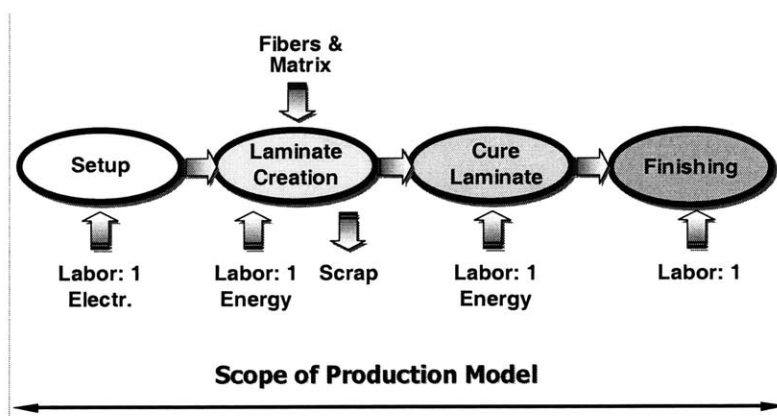


**Figure 9.1** Scope of Production Model

In order to compare process performance and part costs each process model starts and ends at comparable product stages. As seen in Figure 9.1, each process involves an initial setup of machinery and tooling including the preparation of the raw materials. This step is generally followed by a laminate creation process, which establishes the fiber structure and generates the shape of the part. The process flow is concluded by the cure and solidification of the resin plus some minor finishing operations. In some processes,

laminate creation and cure happen sequentially whereas in others the two steps occur almost simultaneously.

### Part Characteristics

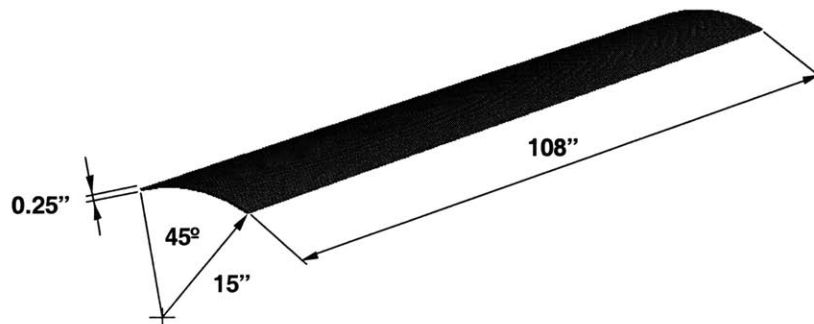


**Figure 9.2** Sketch of Sample Production Part

The 9 ft long and slightly curved sample part is depicted in Figure 9.2. It features an arc length of 1 ft, a bend radius of 15 inches and stretches over a  $45^\circ$  angle. The geometry was chosen under the condition, that all of the 7 production processes are capable to produce the part. The part exhibits a  $\frac{1}{4}$  inch wall thickness and is laid up of 36 layers of carbon fibers and epoxy resin. The entire part weighs around 20 lbs total considering an average density of  $0.057\text{lbs/in}^3$ .

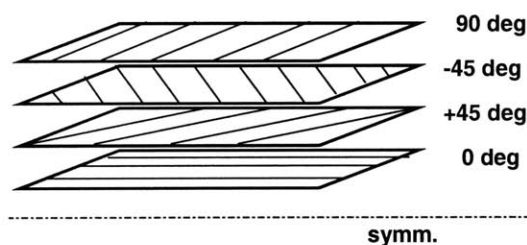


**Figure 9.3** Schematic of Quasi-Isotropic Laminate

It is inevitable, that during production some of the material has to be discarded and is considered scrap. The total material costs amount to about \$1,250 per part, assuming a constant material scrap rate of 15% and a material price of \$60/lb. Only in the case of Resin Transfer Molding (RTM), a slightly higher price of \$80/lb is assumed in order to account for the more costly production of a fiber preform. However, because of the

simplicity of the geometry, a knitted and pre-stitched fiber mat can be used as a preform. The material costs for RTM then amount to around \$1,670 per part.

The laminate is designed to exhibit quasi-isotropic properties. The 36 plies assume a  $[90^\circ, \pm 45^\circ, 0^\circ]_s$  fiber orientation and are stacked as depicted in Figure 9.3. Overall, the laminate consists of 9 x  $0^\circ$  plies, 9 x  $90^\circ$  plies, and 18 x  $\pm 45^\circ$  plies. A balanced and quasi-isotropic laminate is often used when the part is subjected to many different loading conditions. Tsai and other references discuss the theory of laminate design in more detail [1, 2]. Table 9.1 summarizes the major part characteristics.

**Table 9.1 Sample Part Characteristics**

<i>Dimensions</i>	<i>Plies</i>	<i>Surface Area</i>	<i>Weight</i>	<i>Material Costs</i>
108 x 12 x ¼ in <sup>3</sup>	36 x 0.007 in	1,300 in <sup>2</sup>	19 lbs	\$1,250/part RTM: \$1,668/part

### 9.1.2 Hand Lay-Up (HLU)

Hand Lay-Up produces the part by manually laying up the plies onto a curing tool. The operator cuts each individual ply and orients it according to the prescribed fiber direction. Before moving on to the next ply the worker smooths out any wrinkles and consolidates the laminate.

#### Material

A woven carbon/fiber epoxy prepreg is used in the construction of the part and costs about \$60/lb. The total material costs per part therefore amount to \$1,250 including 15% scrap due to cutting and other waste.

#### Labor

The workers are paid \$100/hr, which includes the overhead burden and all benefits. It is assumed, that operators work 2 shifts at 8 hours each. The monthly total adds up to 400 hours.

#### Equipment & Tooling

For the subsequent cure, an Autoclave is employed with the capacity of curing a batch of at least 10 parts at once. Such a system must have an internal volume of 2,000 ft<sup>3</sup> and according to Chapter 6.6 costs about \$430K. Considering an additional 10% for installation one arrives at total investment of \$470K. As shown in Table 9.39 in the Appendix 9.5.1, the Autoclave is utilized 400 hours per month and is depreciated aggressively over 7 years. The hourly operational costs average about \$29/hr including about 25% for maintenance and consumables and assuming a corporate discount rate of about 15% (same as opportunity costs of capital).

**Table 9.2 Investment Costs for Hand Layup & Autoclave Cure**

<i>Autoclave Investment</i>	<i>Autoclave [\$/hr]</i>	<i>Cure Tooling Investment</i>
\$ 470,000	29	\$ 30,000

Longer, less aggressive depreciation schedules or lower capital costs lead to lower hourly rates. Chapter 4.3.3 describes how to implement any changes to the above assumptions.

The layup and curing tool has a size of about 120 in. x 20 in. x 12 in. The tool is entirely fabricated out of Invar and weighs approximately 800 lbs. The tool is regarded as a complexity level 1 tool, because of the subtle curvature of the tool face. Therefore, Figure 7.28 can be used to obtain an estimate for its price. The tool exhibits a surface area of 2,900 in<sup>2</sup> and thus costs about \$30K. The \$30K are depreciated over the 5 year duration of the production program. Under the consideration of 15% capital costs and 5% annual maintenance costs, the business has to book expenses of almost \$9,400 per year for tooling. Table 9.40 in the Appendix 9.5.1 summarizes the main tooling parameters.

### Process Cycle Time

The previously developed process based cost models are harnessed to compute the production cycle time. Table 9.3 shows the setup and other non-recurring production times. The recurring portion of the production time is computed for a batch size of 1, 10, and 100 parts. The table also shows how much of the production time is dedicated to the use of the Autoclave. As the batch size increases the part cycle time drops from initially almost 24 hours to less than 13 hours. This drop in the part cycle time is caused assumption that the whole batch of parts are cured in the Autoclave at once. At the same time, the production rate for the entire process increases from 0.8 lbs/hr to 1.4 lbs/hr. It should be noted, that this performance rate calculation considers the all production steps and therefore is considerably lower than the expected production rate for layup alone.

**Table 9.3 Hand Layup Manufacturing Time**

<i>HLU Mfg. Time</i>	<i>Non-Rec.</i>	<i>Recurring</i>	<i>Recurring</i>	<i>Recurring</i>
<i>Batch Size</i>		<i>1</i>	<i>10</i>	<i>100</i>
Labor [hrs]	11	13	127	1,271
Machines [hrs]	9	1	11	111
Part Cycle Time [hrs]		23.6	13.8	12.8
Performance [lbs/hr]		0.8	1.3	1.4

In addition to Table 9.3, Table 9.41 lists the cycle times for each major production step individually. When plotting each contribution into a Pareto chart it becomes evident, that debulking, layup, and vacuum bagging take up about 73% of the total production time. In this case, it is assumed that after every fourth ply a debulking step is introduced. A different debulking policy can change the production time considerably. Figure 9.4 and Table 9.42 show that cure and Autoclave setup only contribute about 13%. The above results are based on a batch size of 10 parts.

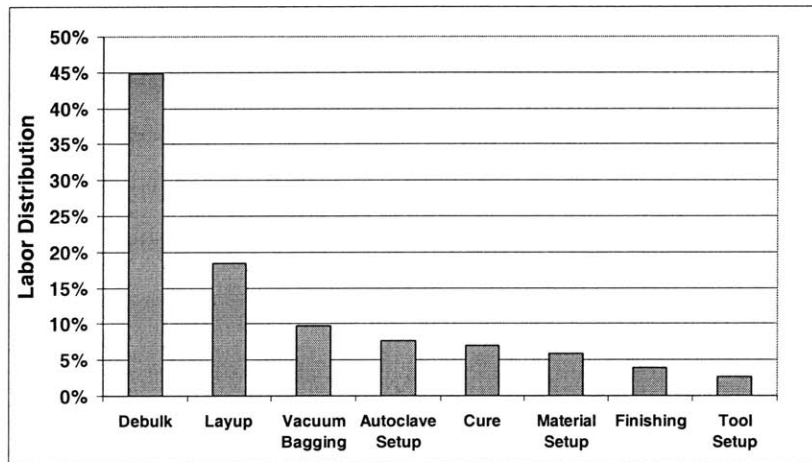


**Figure 9.4 Hand Layup Manufacturing Time Distribution (Batch Size 10)**

#### Part Production Costs

When multiplying the respective production times with the previously listed labor and machine rates one arrives at the labor and machine costs to produce a single part. Hereby, a batch size of 1 is assumed which also only requires 1 set of tools.

**Table 9.4 Hand Layup Manufacturing Costs (Batch Size 1)**

<i>HLU Mfg. Costs</i>			
<i>Ann. Prod. Vol.</i>	<i>1</i>	<i>10</i>	<i>100</i>
Material	\$ 1,251	\$ 1,251	\$ 1,251
Labor	\$ 2,358	\$ 2,358	\$ 2,358
Machine	\$ 294	\$ 294	\$ 294
Tooling	\$ 9,397	\$ 940	\$ 94
<b>Unit Costs [\$/part]</b>	<b>\$ 13,301</b>	<b>\$ 4,852</b>	<b>\$ 4,097</b>

However, as the annual production volume increases from 1 to 100 parts, Table 9.4 shows how the contribution per part to the tooling costs decreases inversely from 71% to 23%. The unit costs thereby drop from \$13,300 per part to around \$4,100 per part of which 60% are now made up by labor costs. The pie chart, seen in Figure 9.5, shows the cost distribution for an annual production rate of 100 parts equaling 500 parts over the planned production period of 5 years. The figure shows that for larger production volumes, labor and material costs drive the overall costs. These two cost elements therefore present the largest lever in any cost reduction strategy. For prototype and small volume production however, tooling clearly drives the overall costs and one might want to look into cheaper and maybe less durable alternatives.

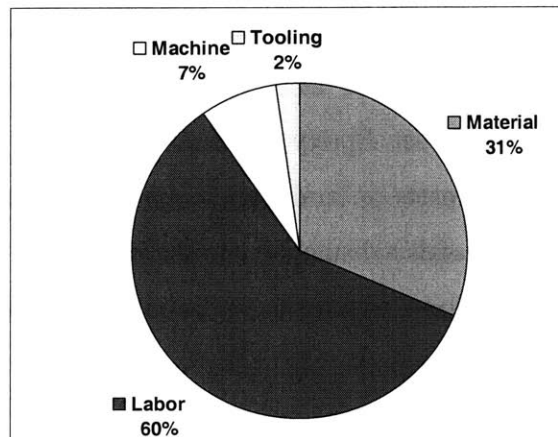


**Figure 9.5** Distribution of Hand Layup Costs (Total Production 500 Parts)

### 9.1.3 Resin Transfer Molding (RTM)

An operator places the dry fiber preform into the open RTM mold. After closing and sealing the tool, the resin is injected and cured. Once the resin has solidified, an operator takes out the part and removes any flash around the edges of the part.

#### Material

Only a very simple fiber preform is required to produce the curved panel and therefore no elaborate preform production step is required. A carbon fiber pre-stitched and knitted fabric can be bought from suppliers, cut into shape and placed into the RTM mold. The pre-stitched fabric costs approximately \$80/lb and is therefore slightly more expensive as the material used for Hand Lay-Up. The material costs are around \$1,670 per part assuming a scrap material scrap rate of 15% and a fiber volume fraction of about 45%. As a matrix material a thermoset Epoxy resin is used. In general, fiber pre-form production for more elaborate parts or laminate designs can make up the majority of the production time and therefore adds substantially to the part costs. To account for the pre-form costs of different production scenarios an additional model has to be developed.

#### Labor

The workers are paid \$100/hr, which includes overhead and benefits. It is assumed, that operators work in 2 shifts at 8 hours each. The monthly total adds up to 400 hours.

#### Equipment & Tooling

A RTM machine featuring a shot size of around 8,000 cm<sup>3</sup> has to be considered when producing large parts. Derived from actual vendor prices, Figure 6.3 shows that approximately \$80K have to be paid for such a machine. When adding another 10% for installation and training the investment totals about \$88K. Assuming an equipment write-off over 5 years and utilizing the machine for 400 hours each month, an average rate of \$7/hour is charged to the program. This figure also includes a 25% burden for consumables and maintenance. Table 9.39 provides more detailed information and



Chapter 4.3.3 describes how capital costs different from the 15% average can be factored in.

**Table 9.5 Investments for Resin Transfer Molding**

<i>RTM Mach. Investment</i>	<i>RTM Mach. [\$/hr]</i>	<i>RTM Tooling Investment</i>
\$ 88,000	7	\$ 70,000

The RTM mold is not subjected to high curing temperatures in contrast to Autoclave tools. The mold is therefore built out of Aluminum in order to limit its overall weight. The 120 in. x 20 in. x 12 in. tool however, still weighs about 2,800 lbs and costs approximately \$70K according to the process based model described in Chapter 7.4.5. Table 9.43 lists the costs results as computed by the model. Each mold half exhibits 1,300 in<sup>2</sup> of polished surface area and 4,300 in<sup>3</sup> of Aluminum have to be machined away to create the required shape. As seen in Table 9.40, the \$70K investment is depreciated over 5 years at a capital rate of 15%. Therefore, the annual expenses for tooling amount to almost \$22,000 including 5% for maintenance.

#### Process Cycle Time

RTM does not lend itself to batch operation such as other composite production processes. This characteristic is reflected in the processing times listed in Table 9.6, which show almost no improvement as the batch sizes increase. As seen in Table 9.44, the overall cycle time is clearly driven by the curing time of each part. Because each part has to be cured separately, the 4 hours curing time are considered as a recurring processing time.

**Table 9.6 RTM Manufacturing Time**

<i>RTM Mfg. Time</i>	<i>Non-Rec.</i>	<i>Recurring</i>	<i>Recurring</i>	<i>Recurring</i>
<i>Batch Size</i>		<i>1</i>	<i>10</i>	<i>100</i>
Labor [hrs]	1	7	73	729
Machines [hrs]	1	6	63	630
Part Cycle Time [hrs]		8.3	7.4	7.3
Performance [lbs/hr]		2.2	2.5	2.5

Consequently, the process performance remains almost constant at about 2.2 lbs/hr, which however is still more than twice as the one for Hand Lay-Up. Batch sizes larger than 1 however, result in additional costs for tooling.

In the contrary, the dominance of the curing step presents many opportunities for process improvements and productivity increases. By using resin systems with a faster curing time, the performance can be improved significantly. The distribution of the manufacturing time as plotted in Figure 9.6 and listed in Table 9.45 should then also become more evenly distributed.

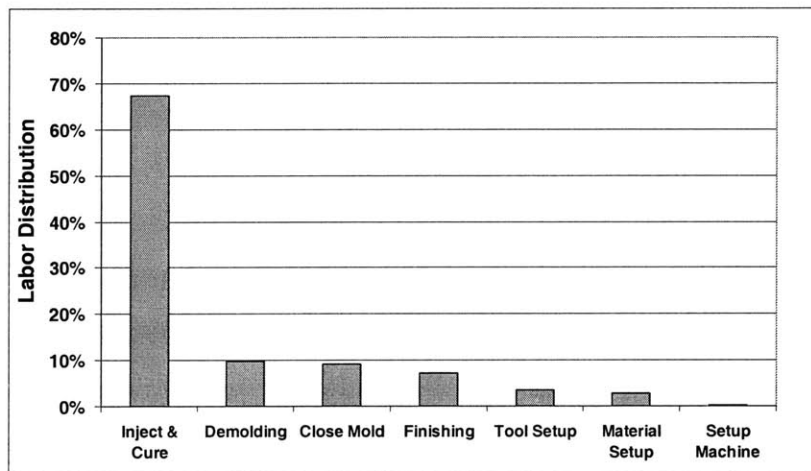


**Figure 9.6 RTM Manufacturing Time Distribution (Batch Size 10)**

### Part Production Costs

The part unit costs can be derived from the manufacturing time in dependence of the annual production volume and the tooling costs. Because of the high costs for tooling, the unit costs reach almost \$24,500 when producing only 5 parts within the 5 year production period. Table 9.7 shows however, that as the production volume increases, the contribution of the tooling costs drops quickly from the initial 90% to less than 8%. When producing about 500 parts in total, the material costs contribute roughly \$1,670 or 60% to the unit costs. The results seem to suggest, that the comparably higher investments into tooling yield in a better process performance when compared to Hand Lay-Up for example. Generally, a higher process performance leads to a greater

reduction in unit costs for large production volumes. When producing a total of 500 parts, the unit costs are reduced by over \$1,000 per part in comparison to Hand Lay-Up.

**Table 9.7 RTM Manufacturing Costs (Batch Size 1)**

<i>RTM Mfg. Costs</i>			
<i>Ann. Prod. Vol.</i>	<i>1</i>	<i>10</i>	<i>100</i>
Material	\$ 1,668	\$ 1,668	\$ 1,668
Labor	\$ 827	\$ 827	\$ 827
Machine	\$ 46	\$ 46	\$ 46
Tooling	\$ 21,926	\$ 2,193	\$ 219
<b>Unit Costs [\$/part]</b>	<b>\$ 24,468</b>	<b>\$ 4,743</b>	<b>\$ 2,860</b>

Figure 9.7 plots the cost distribution for a total production volume of 500 parts and evidently material and labor are the main levers, which have to be considered in any cost reduction strategies. However, since the RTM process is inherently simple, the employment of workers with a lower skill lever might save labor costs. Nonetheless, an efficient production of the fiber preform is paramount, if one wants to take advantage of the superior economics displayed by RTM for high production volumes.

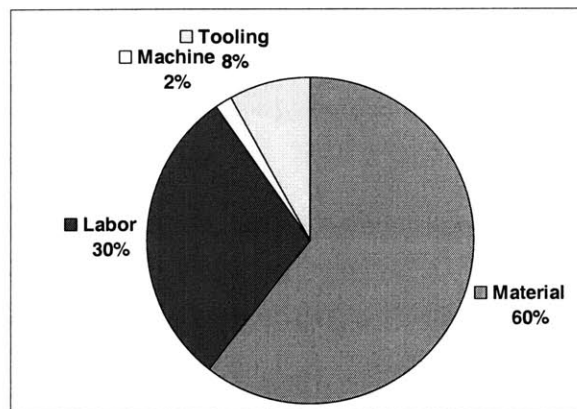


**Figure 9.7 Distribution of RTM Costs (Total Production 500 Parts)**

### 9.1.4 Automated Tow Placement (ATP)

The Automated Tow Placement machine lays down the various plies of the laminate before the produced part is moved into an Autoclave for curing. An operator loads the raw material into the ATP machine and supervises the tow placement process.

#### Material

Commonly, ATP machines lay down a 3 inch wide strip consisting of 24 individual tows. Each of these unidirectional (UD) tows is about 1/8 inch wide and is already pre-impregnated with an Epoxy matrix system. Prepreg out-times vary for each material type, but can easily exceed 5 days. Again, assuming a material price of \$60/lb the material costs add up to \$1,250 per part including 15% for scrap.

#### Labor

The workers are paid \$100/hr, which includes overhead and benefits. It is assumed, that operators work in 3 shifts at 8 hours each. The monthly total adds up to 600 hours.

#### Equipment & Tooling

The investment costs for an ATP machine are substantial and according to information listed in Chapter 6.3, one looks at \$5M price tag for the machine plus another 10% for installation and operator training. As seen in Table 9.39, such an expensive piece of machinery needs to be utilized as much as possible and therefore it is assumed, that the machine runs for 3 shifts each day or 600 hours a month. The equipment is linearly depreciated over a period of 10 years. Considering 15% capital costs and an extra 25% for maintenance and consumables, one obtains an hourly rate of \$188/hr.

**Table 9.8 Investments for Automated Tow Placement**

<i>ATP Mach. Investment</i>	<i>ATP Mach. [\$/hr]</i>	<i>Cure Tooling Investment</i>
\$ 5,500,000	188	\$ 60,000

In addition to the ATP machine an Autoclave for curing of the part is also part of the production facilities. As described in Chapter 9.1.2, the Autoclave costs about \$29/hr to operate.

Since the part is also cured on the layup tool, the tool has to be fabricated out of Invar. Although the ATP tool is similar in size as the Hand Lay-Up tool, it is however specially designed to meet the requirements of the ATP process. The tool is rotated in the ATP machine and therefore exhibits some degree of rotational symmetry. Due to the symmetry, the tool generally features 2 tooling faces, which require additional material and machining to be fabricated. Although no specific cost model for ATP tools has been developed, one can approximate the costs in this case by simply doubling the costs of the Hand Lay-Up and curing tool. Another, approach is to expand the existing cost model for open mold tooling by the required manufacturing steps to produce the second tooling face. In either case, the costs for this 1,000 lbs tool are about \$60K, as seen in Table 9.40 and Table 9.46. Under the consideration of 15% capital costs and 25% annually in maintenance, \$18,800 are due each year for tooling over the 5 year depreciation period.

### Process Cycle Time

Similar to Hand Lay-Up, over 60% of the manufacturing time is spent on the creation of the actual laminate structure. Again, as the parts are cured in batches larger than 1, Table 9.9 shows how the 8 hour curing time is distributed over several parts and the part cycle time decreases considerably. In addition, the long setup time for the ATP equipment is also better utilized and leads to an overall performance improvement with increasing batch size.

**Table 9.9 ATP Manufacturing Time**

<i>ATP Mfg. Time</i>	<i>Non-Rec.</i>	<i>Recurring</i>	<i>Recurring</i>	<i>Recurring</i>
<i>Batch Size</i>		<i>1</i>	<i>10</i>	<i>100</i>
Labor [hrs]	11	14	138	1,379
Machines [hrs]	11	11	108	1,082
Part Cycle Time [hrs]		25.2	14.9	13.9
Performance [lbs/hr]		0.7	1.2	1.3

However, the actual performance is surprisingly low and actually similar to the technologically less sophisticated Hand Layup process. The poor productivity of about 1 lbs/hr is mainly due to the many off-axis layers. The relatively small size and high aspect ratio of the part is not well suited to the ATP process. In particular, 27 of the 36 plies are not longer than 1 ft to 1.8 ft, which causes frequent stops in the process. The critical size, as defined in Chapter 4.4.4, shows that for the process to be economical the minimum path length has to be least 4 to 8 feet. Of course, the economic path length would be reduced if the maximum lay down speed of currently 10 inch per second is further improved or the process delays can be reduced. Table 9.47 and Table 9.48 list the manufacturing time and its distribution in more detail.

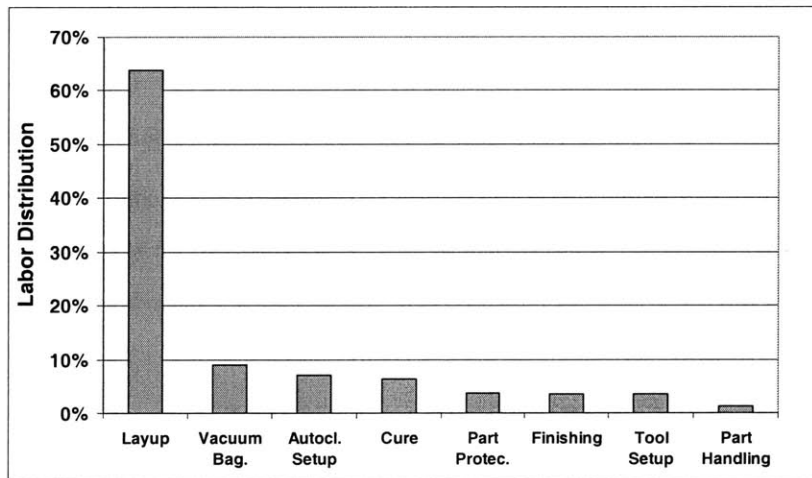


**Figure 9.8 ATP Manufacturing Time Distribution (Batch Size 10)**

### Part Production Costs

At low production volumes, 75% of the unit costs are contributed from tooling. If one were to produce only 1 part per year using ATP, the unit costs are as high as \$25,000. These are almost twice the costs of Hand Lay-Up, primarily because of the higher ATP tooling costs. As expected, at higher production volumes the situation shifts as the tooling costs are distributed over a larger number of parts. Table 9.10 shows that in this example material and labor costs are almost identical to Hand Lay-Up. When producing 500 units of the curved panel the difference between ATP and Hand Lay-Up is reduced to

\$2,500 per part. The majority of these costs are incurred by the charges for the ATP equipment itself and amount to approximately 40% of the total costs.

**Table 9.10 ATP Manufacturing Costs (Batch Size 1)**

<i>ATP Mfg. Costs</i>			
<i>Ann. Prod. Vol.</i>	<i>1</i>	<i>10</i>	<i>100</i>
Material	\$ 1,251	\$ 1,251	\$ 1,251
Labor	\$ 2,522	\$ 2,522	\$ 2,522
Machine	\$ 2,416	\$ 2,416	\$ 2,416
Tooling	\$ 18,794	\$ 1,879	\$ 188
<b>Unit Costs [\$/part]</b>	<b>\$ 24,984</b>	<b>\$ 8,079</b>	<b>\$ 6,477</b>

However, for parts more suitable to the characteristics of ATP the cost situation is quite different. When the part is large enough and the process can operate outside the critical regime, the performance goes up and less machine and labor costs are incurred. The part unit costs are then expected to drop below the ones for Hand Lay-Up even for medium volumes. The example however, illustrates, that parts for ATP have to be selected carefully and that the machine utilization should be maximized in order to keep production costs down.

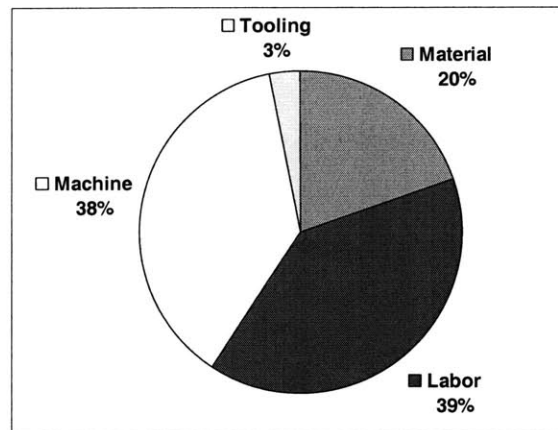


**Figure 9.9 Distribution of ATP Costs (Total Production 500 Parts)**

### 9.1.5 Pultrusion (PUL)

Once the material is loaded and the pultrusion equipment is prepared, the pulling mechanism advances the part production continuously, as the fibers are pulled through the forming and curing die.

#### Material

The dry rovings, placed onto creel stands, are led through the resin bath, the forming die and the pulling mechanism. The price for carbon fiber rovings, plus the thermoset epoxy system is around \$60/lb. Again, assuming a 45% fiber volume fraction and 15% scrap, the material costs amount to \$1,250 per part.

#### Labor

The workers are paid \$100/hr, which includes the overhead and benefits. It is assumed, that operators work in 2 shifts at 8 hours each. The monthly total adds up to 400 hours.

#### Equipment & Tooling

To produce a 12 inch wide part a pultrusion machine with an envelope area of about 220 in<sup>2</sup> is required. Such a machine is capable of pulling up to 25,000 lbs. and according to Chapter 6.4 costs approximately \$300K. Adding another 10% for installation and training and the total investment costs are around \$330K. As listed in Table 9.39, the machine is depreciated over 7 years and used for about 400 hours per month. The hourly charges to operate the machine then amount to about \$20/hr. In these hourly costs, maintenance and consumables make up about 25% and the investment is discounted at 15%.

**Table 9.11 Investments for Pultrusion**

<i>Pult. Mach. Investment</i>	<i>Pult. Mach. [\$/hr]</i>	<i>Pult. Tooling Investment</i>
\$ 330,000	20	\$ 42,000



The process based tooling model, introduced in Chapter 7.5, estimates the costs of the 36 in. x 20 in. x 6 in. steel die to be around \$42,000. Table 9.40 and Table 9.49 present more details of this 1,230 lbs tool.

Process Cycle Time

The time estimation model for pultrusion shows that for thin parts the pultrusion speed scales approximately linearly with the part thickness. The data suggests that a ¼ inch thick part can be pultruded as fast as 20 to 25 inches per minute. However, in our example it takes about 6 hours to load the tool, prepare the material and startup the machine. Therefore, when producing only a single part at a time, the process performance of 2.5lbs/hr is not much better than the one for RTM. Once the pultrusion is running, it can easily produce parts in batch sizes of up to 100 or even more as long as enough material is available and no machine failures occur. Then, the performance jumps to over 23 lbs/hr. As seen in Table 9.50, for large batch sizes, the cycle time is actually dominated by the finishing of the part. If the finishing step would be taken out a part can even be produced every 12 minutes and the performance would increase to about 90 lbs/hr. It shows the importance of properly matching the design of the part to the manufacturing process. The high aspect ratio and the constant cross-section of the curved panel is ideally suited to the characteristics of the pultrusion process.

**Table 9.12 Pultrusion Manufacturing Time**

<i>Pultrusion Mfg. Time</i>	<i>Non-Rec.</i>	<i>Recurring</i>	<i>Recurring</i>	<i>Recurring</i>
<i>Batch Size</i>		<i>1</i>	<i>10</i>	<i>100</i>
Labor [hrs]	6	1	7	72
Machines [hrs]	6	0	2	20
Part Cycle Time [hrs]		7.2	1.4	0.8
Performance [lbs/hr]		2.5	13.3	23.1

According to Figure 9.10 and Table 9.51, the setup of the machine still takes up more than 25% of the production time when producing 10 part each run. However, as the batch size further increases, the portion of the setup time declines to 5% and 95% of the production time are attributed to the actual pultrusion and finishing process. It seems quite absurd that the finishing operations take such a long time in comparison to the other

production steps. However in order to make the result comparable to the other production processes, in all cases about ½ hour is allocated to the finishing of the part.

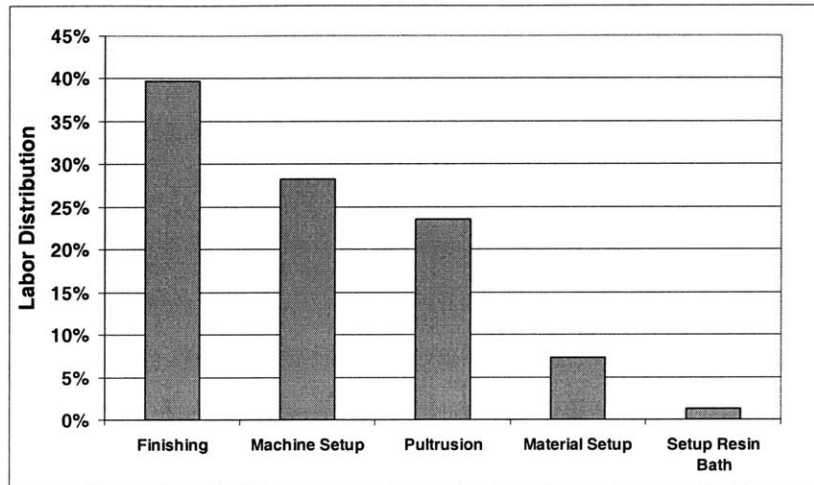


**Figure 9.10 Pultrusion Manufacturing Time Distribution (Batch Size 10)**

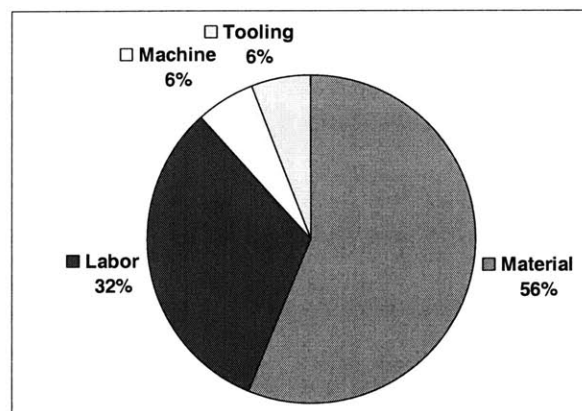
#### Part Production Costs

When assuming the most unfavorable production scenario for pultrusion and producing only one part per setup (batch size 1), one notes that the unit costs for small production volumes are mainly driven by the tooling costs. Again, the generally better overall performance of the process in comparison to Hand Lay-Up is somewhat offset by the higher tooling costs. However, as the production volume increases the good process performance can be leveraged and Table 9.3 shows how the unit costs quickly drop below the ones of Hand Lay-Up and even RTM. Because of the nature of the process the production capacity is only limited by the pultrusion machine and not by the number of tools.

**Table 9.13 Pultrusion Manufacturing Costs (Batch Size 1)**

<i>Pultrusion Mfg. Costs</i>			
<i>Ann. Prod. Vol.</i>	<i>1</i>	<i>10</i>	<i>100</i>
Material	\$ 1,251	\$ 1,251	\$ 1,251
Labor	\$ 720	\$ 720	\$ 720
Machine	\$ 130	\$ 130	\$ 130
Tooling	\$ 13,156	\$ 1,316	\$ 132
<b>Unit Costs [\$/part]</b>	<b>\$ 15,258</b>	<b>\$ 3,427</b>	<b>\$ 2,333</b>

Figure 9.11 shows the distribution of the part costs under the consideration of producing a total of 500 parts over a 5 year period. Comparable to the other production processes, which exhibit a high process performance, the material costs become increasingly important aside from the costs for labor. Of course, as almost 60% of the total costs are incurred by material, any cost reduction strategy has to evaluate how to lower the material price or minimize the use of material. However, unless a better price can be negotiated with the supplier or a volume discount can be obtained, there is only very little one can do about these costs. Only when switching to less expensive glass fiber the material costs can be significantly reduced however at the expense of specific part strength and stiffness.

**Figure 9.11 Distribution of Pultrusion Costs (Total Production 500 Parts)**

### 9.1.6 Double Diaphragm Forming (DDF)

An operator or a machine lay up a flat charge of the laminate before it is transferred into the forming equipment. The machine then forms the charges over a tool into their final shape. Once formed, the parts are removed and placed onto a curing tool for a subsequent autoclave cure.

#### Material

Similar to Hand Lay-Up, a woven carbon/fiber epoxy prepreg is used costing about \$60/lb. The total material costs per part therefore amount to \$1,250 including 15% scrap due to cutting and other waste.

#### Labor

The workers are paid \$100/hr, which includes the overhead and benefits. It is assumed, that operators work in 2 shifts at 8 hours each. The monthly total adds up to 400 hours.

#### Equipment & Tooling

A Double Diaphragm Forming machine, featuring a forming area of roughly 12 ft x 3 ft, goes for approximately \$135K. The machine is generally custom-built and when adding another 10% for installation and operator training one has to budget around \$150K. As listed in Table 9.39, the equipment is depreciated over 7 years and is in operation for 400 hours each month. The average hourly rate is then about \$9/hr including 25% for consumables and maintenance. In addition to the forming equipment, it is also required to have an Autoclave available for the curing of the part. As described in Chapter 9.1.2, the Autoclave costs about \$29/hr to operate.

**Table 9.14 Investments for Double Diaphragm Forming**

<i>DDF Mach. Investment</i>	<i>DDF Mach. [\$/hr]</i>	<i>DDF Tooling Investment</i>
\$ 150,000	9	\$ 43,000

The actual forming tool can be made of Aluminum in order to keep the weight down and facilitate the positioning and handling of the tool. Figure 7.28 in Chapter 7.3 can be used to obtain an price estimate for the 120 in x 24 in size tool. The tool classifies as a complexity 1 tool, since it only exhibits a very slight curvature and its price is approximately \$13,000. The annual expenses for the tool when depreciating the investment costs over 5 years are about \$4,100. However, as outlined in Table 9.40, on top of the costs for the forming tool one has to add the \$30,000 investment for the Invar curing tool. This brings the total annual expenses to \$13,500 considering 15% capital costs and 5% for maintenance.

### Process Cycle Time

As seen in Table 9.52, only the first 4 fabrication steps actually differ from the process plan for Hand Lay-Up. Generally, forming speeds up the creation of the part shape by simplifying the layup of the laminate and by dispensing with the time consuming debulking steps. The layup of flat charges can be accomplished more easily and can even be automated if necessary. The forming not only gives the part its final shape but also consolidates the laminate so debulking is no longer required. The results presented in Table 9.15, together with the information from Table 9.52, show that the batching of parts for curing leads to a significant improvement in processing performance. The process performance for single part flow (batch size 1) is with 1 lb/hr slightly better than for Hand Lay-Up, however doubles as more parts are formed and cured at once.

**Table 9.15 Forming Manufacturing Time**

<b>Forming Mfg. Time</b>	<b>Non-Rec.</b>	<b>Recurring</b>	<b>Recurring</b>	<b>Recurring</b>
<b>Batch Size</b>		<b>1</b>	<b>10</b>	<b>100</b>
Labor [hrs]	11	7	69	692
Machines [hrs]	10	3	25	253
Part Cycle Time [hrs]		17.6	8.0	7.0
Performance [lbs/hr]		1.0	2.3	2.6

Figure 9.12 and Table 9.53 show the distribution of the manufacturing time for the major production steps. It is surprising, that although the actual layup process is significantly simpler in comparison to Hand Lay-Up, it is still with 32% the largest contributor to the

total fabrication time. Consequently, any attempts to further boost the productivity of Double Diaphragm Forming should focus on the layup of the flat charges and carefully evaluate the benefits of a complete or partial automation of this step.

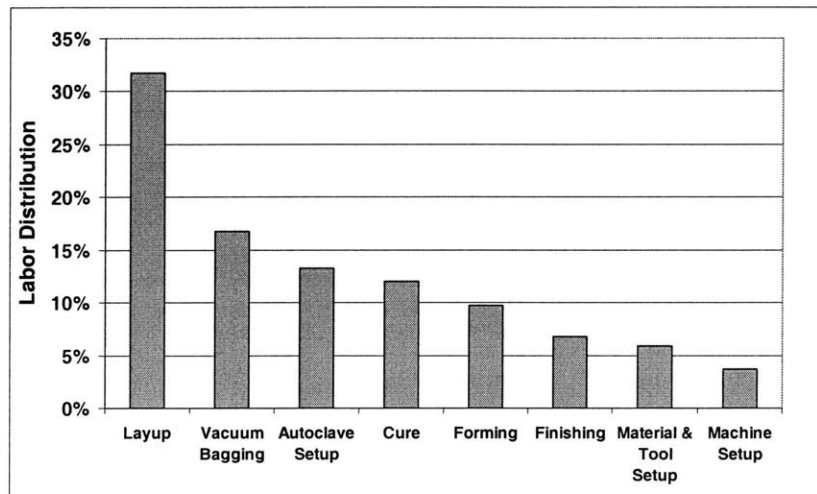


**Figure 9.12 Forming Manufacturing Time Distribution (Batch Size 10)**

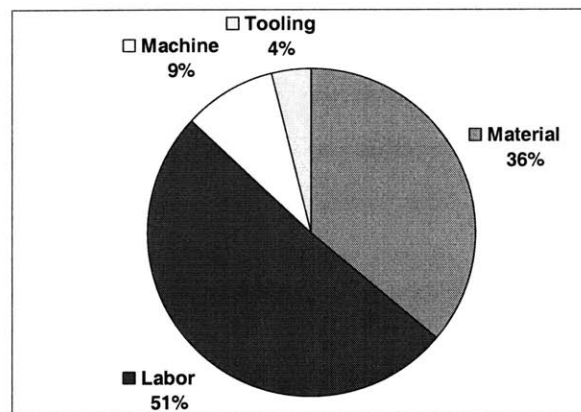
### Part Production Costs

For small production volumes the unit costs are with \$16,800 about \$3,500 higher in comparison to Hand Lay-Up because of the additional tooling requirement. Table 9.16 lists the unit costs for a total production volume of 5, 50 and 500 parts while considering a batch size 1 production. The table shows, that already at an annual production of 10 parts, the part unit costs drop below the costs for Hand Lay-Up. When producing a total of 500 parts, the costs saving in comparison to Hand Lay-Up pay easily for the additional forming machine.

**Table 9.16 Forming Manufacturing Costs (Batch Size 1)**

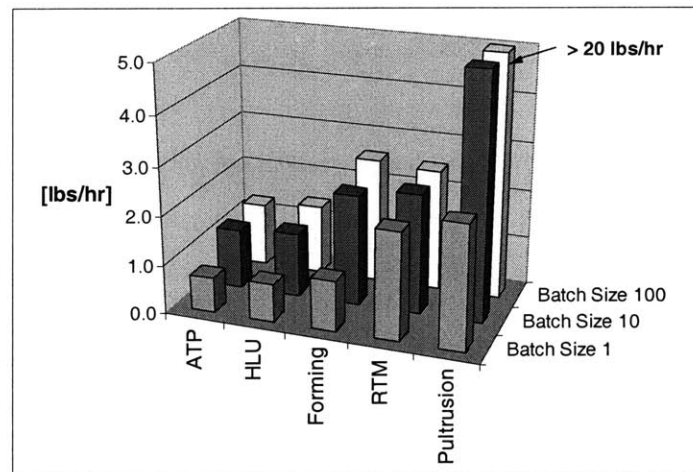
<i>Forming Mfg. Costs</i>			
<i>Ann. Prod. Vol.</i>	<i>1</i>	<i>10</i>	<i>100</i>
Material	\$ 1,251	\$ 1,251	\$ 1,251
Labor	\$ 1,760	\$ 1,760	\$ 1,760
Machine	\$ 315	\$ 315	\$ 315
Tooling	\$ 13,469	\$ 1,347	\$ 135
<b>Unit Costs [\$ /part]</b>	<b>\$ 16,796</b>	<b>\$ 4,683</b>	<b>\$ 3,561</b>

Figure 9.13 shows the cost distribution for high volume production. As the previous data on the process cycle time suggests, a majority (51%) of the costs is incurred by labor mainly because of the manual layup of the flat charges. As mentioned in a previous paragraph, an improvement of the layup process would not only increase productivity but also reduce costs efficiently. The second largest cost driver is material. It appears also, that the larger the total production volume, the more significant become the costs for material.

**Figure 9.13 Distribution of Forming Costs (Total Production 500 Parts)**

### 9.1.7 Summary & Process Comparison

Hand Lay Up and Automated Tow Placement and Forming experience large economies of scale as the batch size increases. The reason lies within the dominating equipment setup times. This non-recurring time is eventually spread out over the larger amount of parts being produced during one setup. The largest efficiency improvements are realized by the Pultrusion process. Once the machinery is setup, the line can produce parts continuously, which only have to be cut to length. In contrast, Hand Layup, ATP and Forming still require additional vacuum bagging for each additional part produced and therefore exhibit less pronounced scaling effects. For RTM, scaling effects are almost non-existent. The production cycle time is driven by the cure cycle, which has to be repeated for each part. Of course, performance could be improved if a multi cavity mold would be used, however at the expense of higher investment costs. Generally, costs are also the limiting factor when curing a larger batch of parts in an Autoclave. In most cases a separate tool is required for each part, which also leads to higher costs. However, when looking only at performance, Figure 9.14 shows how the processes rank according to their production capabilities.



**Figure 9.14 Process Performance**

The performance defines the hourly production rate of all necessary production steps, including cure and finishing. However, an extrapolation of the results to other production situations is only possible if none of the assumed boundary conditions are violated.



Clearly, Pultrusion stands out as the most efficient production process for composites. On the other hand, the small difference between Hand Layup and ATP is a somewhat surprising result. Obviously, one would expect that the automated process would perform considerably better than its manual counterpart. It turns out, that the major factor for the slow performance of ATP is the high aspect ratio of the investigated part. Since the majority of the laminate contains non-zero degree plies, the machine has to lay down many short courses. The placing of the  $\pm 45^\circ$  and the  $90^\circ$  layers causes frequent delays and prevents the ATP machine from operating at its full potential. The machine is forced to stop after approximately 12 inches, cut the tows, turn the placement head and start over. These operations take time and reduce the performance of the overall process. A thumb rule for calculating the minimum economic placement length is to multiply the maximum speed (here ca. 10 in/second) by the time delay at the end of each path (here ca. 5 second).

**Table 9.17 Layup Performance without the Cure Cycle**

<i>Layup Performance Only</i>	<i>Batch Size 1</i>	<i>10</i>	<i>Comments</i>
Hand Layup	1.7 lbs/hr	1.9 lbs/hr	w/o cure
ATP Small Parts	1.6 lbs/hr	1.8 lbs/hr	w/o cure
ATP Large Parts	4.3 lbs/hr	6.1 lbs/hr	w/o cure

The real potential of ATP becomes clear when focusing on the layup performance only and without the curing and the other processing steps. Table 9.17 shows that for small parts (< 3 ft) the performance for ATP is similar to Hand Lay-Up and barely improves as more parts are laid up in one setting. However, when producing large parts (> 6 ft) ATP clearly outperforms Hand Lay-Up by a factor of 2 to 3. A factor 2 difference in performance is the least one has to achieve, because the ATP process is approximately twice as expensive as Hand Lay-up on a hourly basis. An advantage of ATP however, is the consistency and accuracy with which the laminate is produced. The process allows better control of the fiber angle and is unlikely to miss the layup of a ply.

The study further shows, that the most efficient process is not always the most cost effective process for all production situations. To compute the total manufacturing costs

and to provide a meaningful comparison of the individual composite fabrication processes, one needs to consider the tooling costs. Figure 9.15 plots the total investments into tooling for the 5 investigated production processes. The results presented in Figure 9.15 already predict, that the highest performing process does not necessarily features the lowest costs.

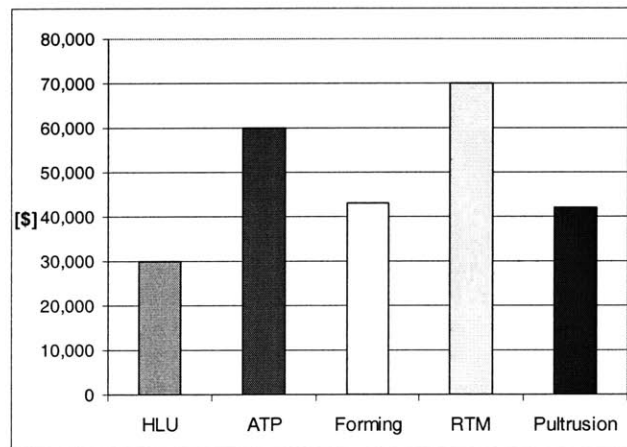


**Figure 9.15** Manufacturing Tooling Costs

When depreciating the costs for tooling over 5 years and calculating the total unit costs to produce the curved panel at varying production volumes, one arrives at the results presented in Table 9.18.

**Table 9.18** Manufacturing Unit Costs (incl. Tooling, Batch Size 1)

<i>Costs per Part</i>	<i>Prod. Vol. 5</i>	<i>Prod. Vol. 50</i>	<i>Prod. Vol. 500</i>
<b>ATP</b>	\$ 24,983	\$ 8,069	\$ 6,377
<b>HLU</b>	\$ 13,300	\$ 4,842	\$ 3,997
<b>Forming</b>	\$ 16,795	\$ 4,673	\$ 3,461
<b>RTM</b>	\$ 24,467	\$ 4,733	\$ 2,760
<b>Pultrusion</b>	\$ 15,257	\$ 3,417	\$ 2,233

Figure 9.16 takes the above results and presents them in a more accessible way. All the costs are based on the worst-case scenario of producing one part at a time (batch size 1). The unit costs drop as the investment in tooling is distributed over up to 500 parts in total during the 5 years of the production program. It is therefore not surprising that for small production volumes (here 5 in total) the unit costs are ranked according to the tooling

costs. As seen in Figure 9.16, RTM and ATP exhibit the largest costs with almost \$25,000 per part. Hand Lay-Up in contrast is the most economical solution for small volumes, since the tooling costs are the lowest. As the total production volume increases, the cost situation shifts and the most efficient process becomes also the most economical one. At 500 parts, the part unit costs are rank ordered identically to the process performance presented in Figure 9.14.

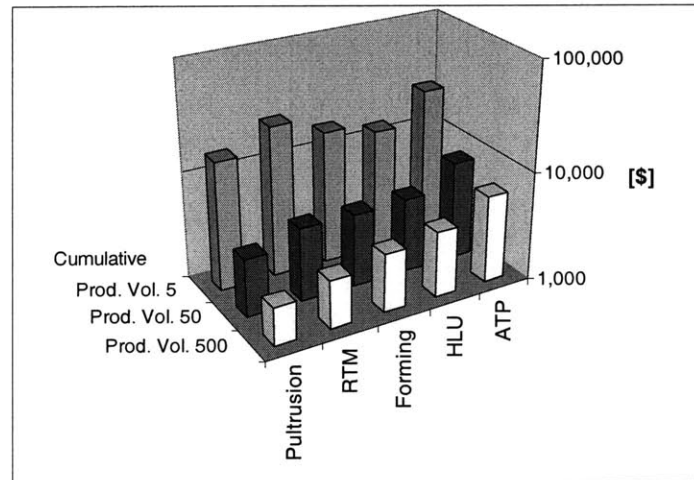


**Figure 9.16** Manufacturing Unit Costs (incl. Tooling, Batch Size 1)

As a guideline for choosing the most economic production method, one can derive the following conclusions from the above results. For low volume production, the process with the lowest tooling costs is generally the best choice. For high volume production, one should select the process with the best performance provided the process is capable of producing the part. Tooling and other investment costs are secondary, since the better performing process will eventually generate a positive return. Of course, in every case this break-even volume has to be determined individually.

Another process selection criterion, are the distribution of the costs. As presented in Figure 9.17, the cost distribution can give hints towards the best cost saving opportunities and the future economic potential of a particular process. For the production of 500 units of the curved panel, Figure 9.17 describes the cost contribution of Hand Lay-Up, Automated Tow Placement, Resin Transfer Molding, and Pultrusion. The first observation is that material costs become increasingly significant for high volume

production. This is particularly the case for processes, where automation has already replaced labor to a large extent and which exhibit a high performance. In the contrary, the lower performing processes such as Hand Lay-Up and Forming still require a large portion of labor. The ATP process partially substitutes labor with a costly machine. Therefore, high volume production with labor-intensive processes can only be economical in an environment with low wages. However, one has to factor in possible other costs such as increased transportation, production coordination, and possible quality issues.

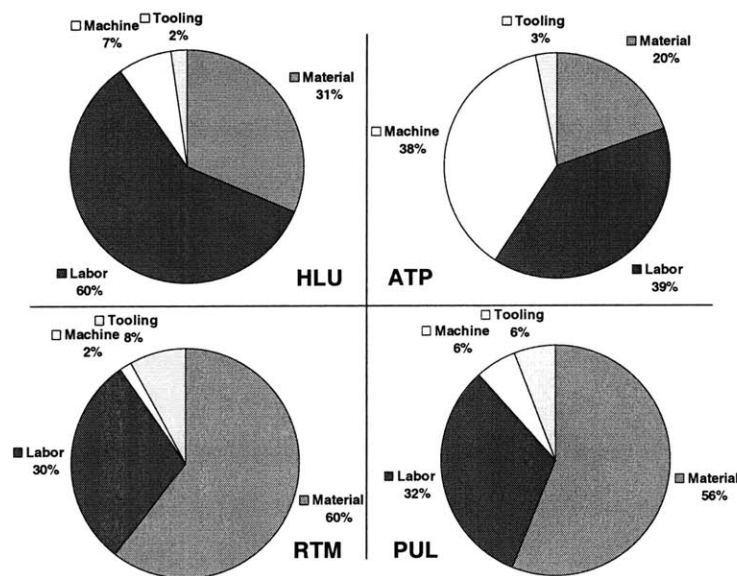


**Figure 9.17** Cost Distribution of Hand Layup, ATP, RTM & Pultrusion

Another large contributor to the unit costs, are the high material costs stemming from the application of carbon fibers. Here only volume discounts and negotiation with suppliers can effectively lower the overall costs, since machine and tooling costs become less relevant. Especially for RTM and Pultrusion where about 60% of the costs are incurred by material.

## 9.2 Case Study 2: Composite Assembly Processes

The second case study compares the productivity and part unit costs of Co-Cure, Mechanical Assembly and Co-Bonding. The study also lists the necessary investments for the assembly fixtures, the component tools, and the Autoclave. The work illustrates the impact of varying batch sizes and production volume on performance and unit costs.

### 9.2.1 Production Scenario

#### Conditions & Scope of Production

The production conditions are assumed identical to the first case study in order to provide consistency and comparability. With the exception of tooling and fixturing, the manufacturing machinery (here Autoclave) is already in place and is not dedicated to a specific production program. Table 9.39 shows the assumed depreciation period for the Autoclave, which is utilized for about 400 hours per month. It is further assumed, that the production program runs for 5 years and that tooling and fixtures are depreciated linearly over this period. The costs of capital are 15% and a certain fixed percentage for maintenance and consumables is charged to each tool and piece of machinery. Chapter 4.3.3 describes, how changes to these assumptions can be factored in.

To study the effects of various production batch sizes, all other parameters are held constant, while the batch size is varied from 1 to 10 and up to 100 parts. This method produces results, which show if the initial setup time can be effectively spread out over the production of several parts. The maximum batch size is often limited by equipment and tooling capacity, and realistically the limit for the assembly case study is probably around 1 to 2 parts depending on the process. However, the results for larger batch sizes show, how close the cycle time converges with the recurring production time.

The value for the annual production volume ranges between 1 part per year and 100 parts per year. Over a period of 5 years, this results in a cumulative production of 5, 50 and 500 parts in total. Admittedly, the production volume can easily be larger in real-life production scenarios, however as the production volume is increased above 500 the

actual unit costs only change insignificantly. More interesting is the evaluation of the behavior for low volumes, as it describes the ramp-up of production and how quickly any economic objectives can be met.

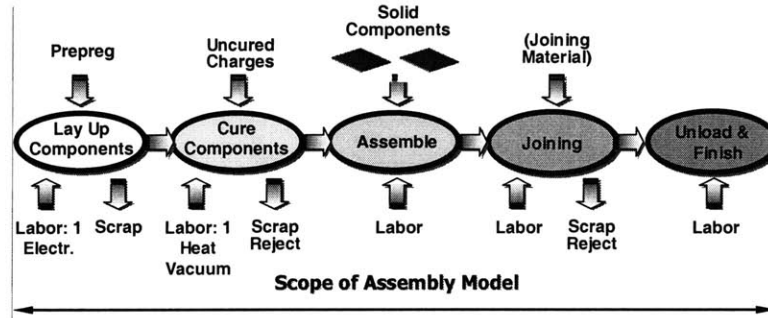


**Figure 9.18** Scope of the Assembly Model

In order to compare process performance and part costs, each process model starts and ends at similar product stages. As seen in Figure 9.18, each process starts with the production of the components, which are to be assembled. This step is generally followed by the actual assembly and fastening operations. The entire process concludes with the unloading of the assembled structure including some minor finishing operations. Some examples in the case study only list the cycle time and the costs for the actual assembly and joining process in order to better compare the performance of the various methods.

### Part Characteristics

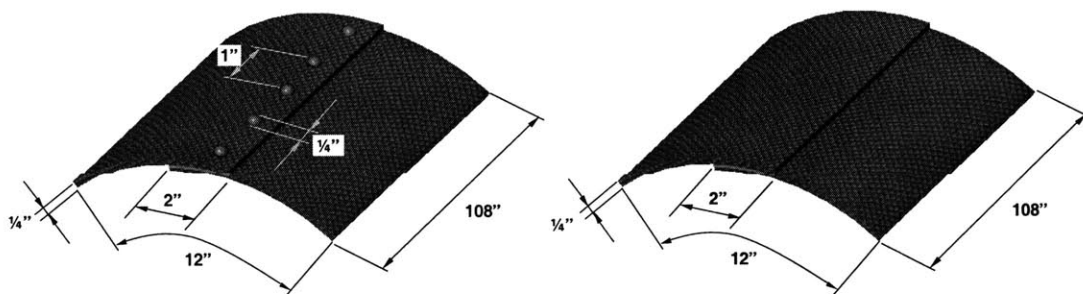


**Figure 9.19** Mechanical and Adhesive Assembly of the Sample Structure

The sample structure is almost identical to the one used for Case Study 1. Here however, the same 9 ft long and slightly curved part is created through the assembly of two separate components. The illustrations depicted in Figure 9.19, show on the left the mechanical fastening of the components, whereas its counterpart on the right, is joined by adhesive bonding. The entire structure features an arc length of 1 ft, a bend radius of 15 inches and exhibits a 2-inch single lap joint. Each component has a thickness of  $\frac{1}{4}$  inch and consists of 36 layers of carbon fiber/epoxy prepreg. All the plies assume a  $[90^\circ, \pm 45^\circ, 0^\circ]_s$  fiber orientation and are stacked according to the schematic depicted in Figure 9.3. In total the two components weigh approximately 24 lbs. considering an average density of  $0.057 \text{ lbs/in}^3$ .

Inevitably, some of the cut material has to be discarded during production. Assuming a constant material scrap rate of 15% and a material price of \$60/lb the total material costs amount to about \$1,700 per part. Table 9.19 summarizes the major part characteristics.

**Table 9.19 Sample Structure Characteristics (w/o Fasteners)**

<i>Dimensions</i>	<i>Overlap Joint</i>	<i>Total Surface</i>	<i>Weight</i>	<i>Material Costs</i>
108 x 12 x $\frac{1}{4}$ in <sup>3</sup>	108 x 2 in <sup>2</sup>	1,300 in <sup>2</sup>	24 lbs	\$1,700/structure

### 9.2.2 Co-Cure

The Co-Cure of parts has similarities to Hand Lay-Up or other layup techniques. In general, each component is laid up individually and then transferred in its un-cured and soft state to the curing tool. There it is assembled together with the other components before the whole structure is finally cured in an Autoclave. However, because of the simplicity of the structure, in this case the two components are laid up directly onto the curing tool and therefore a transfer of the parts is not required.

#### Material

The component material is a carbon fiber/prepreg material costing about \$60/lb. Because of the 2 inch overlap and some extra allowance for trim, the total material costs for the component comes to \$1,699. This is about \$450 more than for the similar sized panel presented in Case Study 1.

#### Labor

The workers are paid \$100/hr, which includes the overhead and benefits. It is assumed, that operators work in 2 shifts at 8 hours each. The monthly total adds up to 400 hours.

#### Equipment & Tooling

For component production and co-cure the only machinery required is an Autoclave. According to Chapter 6.6, such an Autoclave with 2,000 ft<sup>3</sup> of internal volume costs about \$430K. Considering an additional 10% for installation, one arrives at total investment of \$470K. As shown in Table 9.39, the Autoclave is utilized 400 hours per month and is depreciated over 7 years. Including about 25% for maintenance and consumables and assuming a corporate discount rate of about 15%, the Autoclave costs about \$29/hr on average to operate.

**Table 9.20 Investment Costs for Hand Layup & Autoclave Co-Cure**

<i>Autoclave Investment</i>	<i>Autoclave [\$/hr]</i>	<i>Cure Tooling Investment</i>
\$ 470,000	29	\$ 30,000



The same Invar 120 in. x 20 in. x 12 in. tool can be used as described in Chapter 7.8.6 to co-cure the simple structure. The 800 lbs tool with a surface area of 2,900 in<sup>2</sup> costs about \$30K. The \$30K are depreciated over the 5 year duration of the production program. Under the consideration of 15% capital costs and 5% annually for maintenance, the business books \$9,400 per year for tooling. Table 9.40 in the Appendix summarizes the main tooling parameters.

### Process Cycle Time

The previously developed process based cost models are employed to compute the production cycle for each component. Table 9.21 shows the non-recurring part of the cycle time, which is generally associated with setup and the recurring portion of the production time for a batch size of 1, 10, and 100 component sets. That is, a component batch size of 1 describes the production of the two components during one setup. The process plan is almost identical to Hand Lay-Up. The time difference of about 10 hours in comparison to the part produced by Hand Lay-Up alone, is largely due to extra the debulking steps. As outlined in Chapter 9.1.2, debulking takes up the majority of the process time and in the case of co-curing, each component goes through the debulking steps separately. The results presented in Table 9.21 show, that it takes about 35 hours in total to produce the curved panel as a co-cured assembly of two components. Certainly, a revision and improvement of the debulking strategy can have a significant impact on process cycle time and performance.

**Table 9.21 Co-Curing Cycle Time**

<i>Co-Curing Mfg. Time</i>			
<i>Batch Size</i>	<i>1</i>	<i>10</i>	<i>100</i>
Non-Recurring	650	650	650
Recurring	1,430	14,297	142,970
Labor [min]	2,080	14,947	143,620
Labor per Set [hrs]	35	24.9	23.9

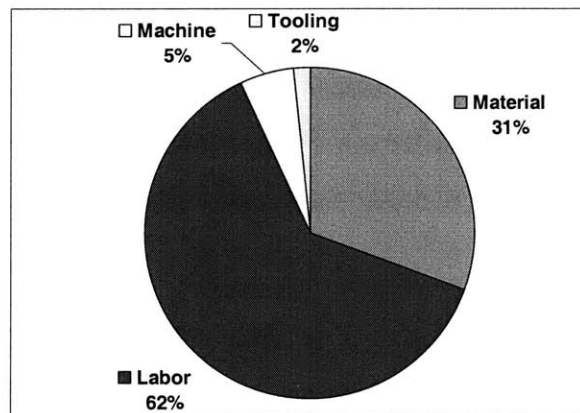
Part Production Costs

Table 9.22 lists the total unit costs. The labor and machine costs are easily derived from the previously computed cycle times. The cost results are based on the assumption, that one co-cured structure is produced during one setup. The material costs and component production costs are all included in the calculation.

**Table 9.22 Co - Curing Costs (Batch Size 1, incl. Component Costs)**

<i>Co-Curing Costs</i>			
<i>Ann. Prod. Vol.</i>	<i>1</i>	<i>10</i>	<i>100</i>
Material	\$ 1,699	\$ 1,699	\$ 1,699
Labor	\$ 3,466	\$ 3,466	\$ 3,466
Machine	\$ 294	\$ 294	\$ 294
Tooling	\$ 9,397	\$ 940	\$ 94
<b>Unit Costs [\$/part]</b>	<b>\$ 14,856</b>	<b>\$ 6,409</b>	<b>\$ 5,553</b>

The cost of tooling is distributed over an increasing number of parts as the annual production volume rises from 1 to 100 parts. For small production volumes, tooling is the major cost driver with about 64%. As the production volume increases to 500 units in total, the contribution of tooling goes down to about 2%, whereas labor shoots up to 62% of the total costs. As depicted in Figure 9.20, labor and material are the major cost drivers and any cost reduction strategies have to either look at material prices or at streamlining the production process. As discussed in the previous paragraph, debulking adds substantially to the overall production time and therefore the costs. Different, less stringent consolidation requirements can thus have a huge impact on costs.



**Figure 9.20 Distribution of Co-Curing Costs (Total Production 500 Parts)**

### 9.2.3 Mechanical Assembly

Mechanical Assembly employs rivets or bolts to join individual components together to a larger, more complex structure. The process generally involves the correct positioning of the parts, the drilling of the holes, and the installation of the fasteners. In some cases, a shimming step is added to achieve an even and tight joint interface. The example introduced as part of this work is quite simple and considers the costs for shimming, component production and the additional costs of an assembly fixture.

#### Assembly Material & Component Costs

To avoid corrosion, fasteners for joining carbon fiber composite are often made out of Titanium and are therefore quite expensive. At about \$10/pc for a two-piece fastener the total costs for fasteners alone add up to \$1,101. About 107 fasteners are need to join the 108 inch long part and considering that approximately 2.5% have to be scrapped, a total of 110 pieces has to be procured for each assembly.

The costs for liquid shimming are marginal in comparison. The compound cures in about 8 hours and only about 0.1 lb are required for each assembly. Approximately 25% of that amount is allowance for squeeze out and scrap. The price of shimming is assumed to be \$25/lb.

In addition to the assembly material, the costs for the production of the components have to be accounted for. Independently of the ultimate joining process the components have to be layed up and cured before being placed into the assembly fixture for fastening. It is assumed, that the components are produced two at a time using Hand Lay-Up and Autoclave cure. Therefore, the values listed in Table 9.22 represent a very good estimate of the actual production costs. Including tooling, the costs for one set of components ranges from \$14,860 to \$5,555, depending on the total production volume.

#### Labor

The workers are paid \$100/hr, which includes the overhead and benefits. It is assumed, that operators work in 2 shifts at 8 hours each. The monthly total adds up to 400 hours.

### Equipment & Tooling

The present example does not consider the use of any automated equipment for fastener installation. However, aside from the investment in layup and curing tools it is necessary to also invest in an assembly fixture. Component tooling is very similar in its size and design to the tools used for co-curing. This situation is somewhat of an exception, because the produced parts exhibit such a simple shape. In general, one would expect that component tooling and tooling for co-cure are different while the latter features a higher degree of complexity. However, in the present case, one can take the same Invar tool (120 in. x 20 in. x 12 in., 800 lbs), which is used for co-curing and use it for component production. The tool costs about \$30K and when depreciating this amount over 5 years and adding 15 % capital costs and 5% maintenance, the annual expenses come out to be around \$9,400.

The assembly fixture used to position the parts only has to be able to handle components exhibiting a constant radius of curvature. For such a tool, Chapter 7.6.4 quotes a price of about \$4,500 per foot. Conservatively speaking, the total investment for the assembly fixture is about \$50,000, which is equivalent to a \$15,700 annual payment given the above financing conditions. Table 9.40 summarizes the main tooling parameters.

**Table 9.23 Investments for Mechanical Assembly**

<i>Component Tooling Investment</i>	<i>Assem. Fixture Investment</i>
\$ 30,000	\$ 50,000

### Process Cycle Time

The process cycle time can include the time necessary to produce the components or it can simply express the production time for the assembly stage alone. In order to simplify the actual comparison between mechanical and adhesive bonding Table 9.24 lists the assembly times excluding the time for component production. However, to better compare all three assembly methods, Table 9.56 shows the times of all process steps.

**Table 9.24 Mechanical Assembly Cycle Time (w/o Component Production)**

<i>Mech. Assembly Mfg. Time</i>			
<i>Batch Size</i>	<i>1</i>	<i>10</i>	<i>100</i>
Non-Recurring	666	666	666
Recurring	283	2,831	28,310
Labor [min]	949	3,497	28,976
Labor per Set [hrs]	16	5.8	4.8

When focusing on the assembly only, Table 9.24 shows that it takes about 16 hours to produce a part. A total of 11 hours are due to setup only and other non-recurring operations. Of these 11 hours, 8 hours alone are incurred by curing the liquid shim of the part. This step can be executed in parallel and by batching several assemblies together and the production time can be reduced to about 5 hours per set.

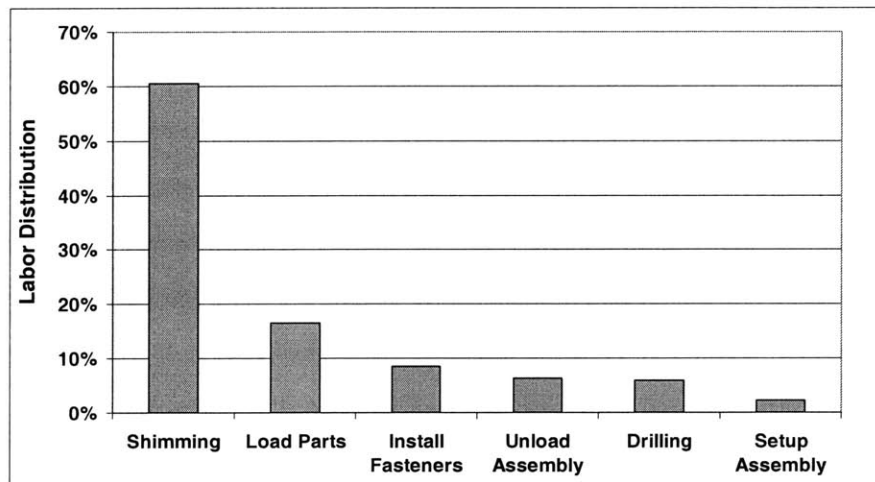
**Figure 9.21 Mechanical Assembly Time Distribution (w/o Component Production)**

Figure 9.21 shows that the shimming step contributes about 60% to the overall production time, followed by the loading and positing of the parts with about 17%. The exact distribution of the production time is listed in Table 9.57. As mentioned previously, the shimming of the components necessary in some cases. Without the shimming step, the contributions for loading and fastening would go up to 42% and 35% respectively from now around 17%. From a cost standpoint, liquid shimming is quite inexpensive, since the 8 hrs of cure does not require the supervision of a worker.

Loading and fastening however can prove to be a much larger driver of labor costs, since these steps might involve several workers depending on the size and weight of the part.

### Part Production Costs

The labor costs are derived from the production times and are listed among other costs in Table 9.25. The table shows the unit costs for one assembly, which include the costs for the production of the components. It is evident that the contribution of the fixturing costs to the unit costs decreases with increasing production volume. In addition, the tooling costs for the component production are also distributed over an increasing number of parts. The shown cost elements for labor and material are only related to actual assembly and not the production of the components. In the present example, component production represents the major cost driver. However when looking at the numbers listed in Table 9.58, which exclude the component costs, one notes that it costs about \$2,680 per assembly to join the two parts mechanically.

**Table 9.25 Mech. Assembly Costs (Batch Size 1, incl. Component Costs)**

<i>Mech. Assembly Costs</i>			
<i>Ann. Prod. Vol.</i>	<i>1</i>	<i>10</i>	<i>100</i>
Components	\$ 14,856	\$ 6,409	\$ 5,553
Material	\$ 1,101	\$ 1,101	\$ 1,101
Labor	\$ 1,582	\$ 1,582	\$ 1,582
Machine	\$ -	\$ -	\$ -
Fixturing	\$ 15,662	\$ 1,566	\$ 157
<b>Unit Costs [\$/part]</b>	<b>\$ 33,201</b>	<b>\$ 10,658</b>	<b>\$ 8,393</b>

Hereby the ratio between labor and material costs remains constant, since these costs generally scale with the number of fasteners per part, only. Figure 9.22 shows that for the mechanical assembly of this curved carbon fiber panel, about 40% of the costs are incurred by material, whereas 55% are due to labor. The costs for fixturing and tooling decrease with increasing production volume.

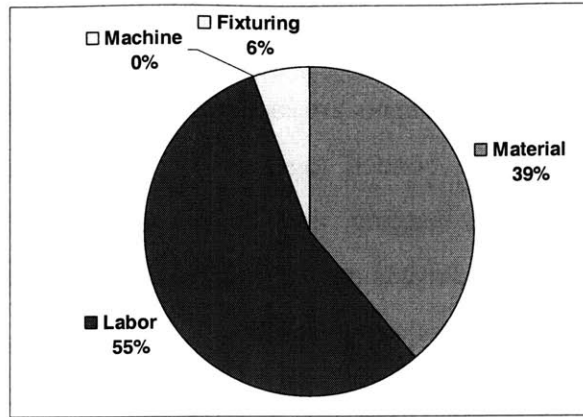


**Figure 9.22** Distribution of Mech. Assembly Costs (Total Production 500 Parts)

### 9.2.4 Adhesive Assembly

The already cured and rigid components are loaded into an assembly fixture, which holds them into position as they are bonded together by an adhesive. Depending on the technique, clamps, or vacuum bagging, provide the necessary consolidation pressure. The applied adhesive compound evens out any irregularities in the bonding interface and therefore shimming is generally not a requirement.

#### Assembly Material & Component Costs

The costs for the adhesive compound are generally small in comparison to other costs. The compound cures in about 8 hours and only about 0.1 lb are required for each assembly. Approximately 25% of the material is considered allowance for squeeze out and therefore scrap. The price of the adhesive is assumed to be \$25/lb.

In addition to the assembly material, the costs for the production of the components have to be accounted for. The components have to be layed up and cured before being placed into the assembly fixture for joining. It is assumed, that the components are produced two at a time using Hand Lay-Up and Autoclave cure. Therefore, the values listed in Table 9.22 represent a very good estimate of the actual production costs of the components. Including tooling, the costs for one set of components ranges from \$14,860 to \$5,555, depending on the total production volume.

#### Labor

The workers are paid \$100/hr, which includes the overhead and benefits. It is assumed, that operators work in 2 shifts at 8 hours each. The monthly total adds up to 400 hours.

#### Equipment & Tooling

Following a similar argument as presented in Chapter 9.2.3, one can take the same Invar tool (120 in. x 20 in. x 12 in., 800 lbs), which is used for co-curing and use it for component production. The tool costs about \$30K and when depreciating this amount over 5 years and adding 15 % capital costs and 5% maintenance, the annual expenses come out to be around \$9,400.



The assembly fixture used to position the parts only has to be able to handle components exhibiting a constant radius of curvature. For such a tool, Chapter 7.6.4 quotes a price of about \$4,500 per foot. Conservatively speaking, the total investment for the assembly fixture is about \$50,000, which is equivalent to a \$15,700 annual payment given the above financing conditions. Table 9.40 summarizes the main tooling parameters.

**Table 9.26 Investments for Adhesive Bonding**

<i>Component Tooling Investment</i>	<i>Assem. Fixture Investment</i>
\$ 30,000	\$ 50,000

### Process Cycle Time

Table 9.27 lists the time for co-bonding the two curved components to a larger panel. In addition, the values listed in Table 9.59 also include the time required for the production of the components. When comparing the results shown in Table 9.27 with the ones for mechanical assembly seen in Table 9.24, one notes, that the production time for batch size 1 production only differs by 3 hours between the two processes. This is mainly because in both cases the production time is driven by the 8 hour cure of the adhesive and the shimming compound respectively. However, as more and more parts are cured at once the cycle time for co-bonding drops to 2.6 hours, which is almost half the time spent on the mechanical assembly of the parts.

**Table 9.27 Adhesive Bonding Cycle Time (w/o Component Production)**

<i>Co-Bonding Mfg. Time</i>			
<i>Batch Size</i>	<i>1</i>	<i>10</i>	<i>100</i>
Non-Recurring	609	609	609
Recurring	152	1,523	15,230
Labor [min]	761	2,132	15,839
Labor per Set [hrs]	13	3.6	2.6

Figure 9.23 plots the distribution of the production times for the major assembly steps. The bar chart shows that aside from the application and the curing of the adhesive, the loading and positioning of the components are the most time consuming steps. Bonding

takes up about 50%, loading 23%, and the preparation of the interface area about 13% of the time. In order to streamline the process, one can foremost try to obtain a faster curing adhesive with similar strength properties. Other options are more difficult and basically come down to a careful planning of the assembly sequence and minimize unnecessary movements and work.

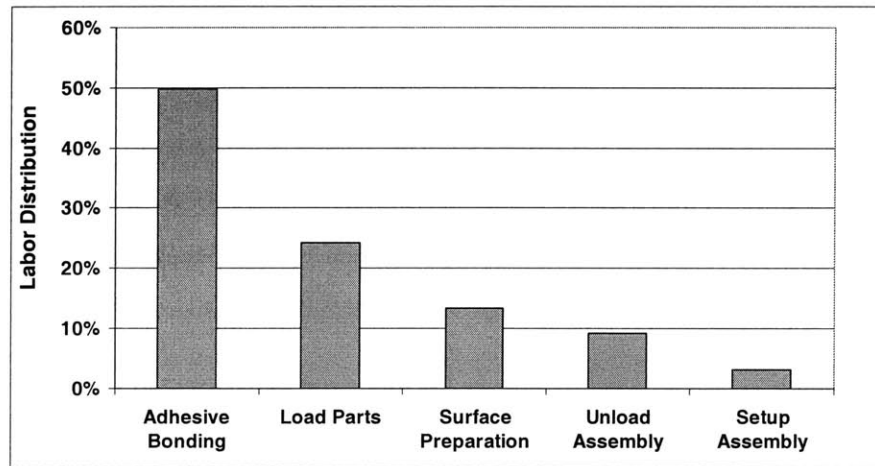


**Figure 9.23 Adhesive Bonding Time Distribution (w/o Component Production)**

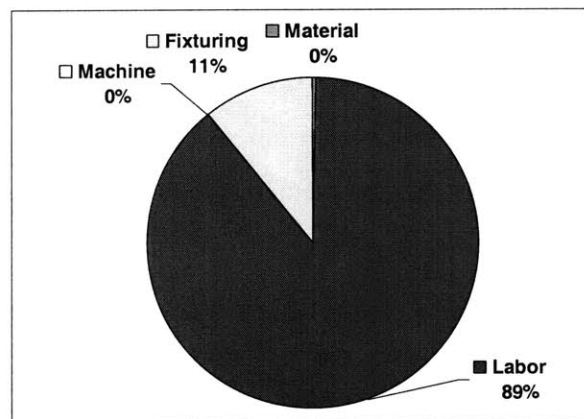
#### Part Production Costs

A quick look at the assembly costs listed in Table 9.28 reveals that aside from the dominant component costs, the major contribution to the variable costs stem from labor. Material costs are insignificant and the fixturing costs decline as the total production volume increases. The costs for co-bonding costs are around \$1,272 and are therefore about \$1,400 below the costs for mechanical fastening. The difference is mainly attributed to the very expensive Titanium fasteners and their more time consuming installation.

**Table 9.28 Adhesive Bonding Costs (Batch Size 1, incl. Component Costs)**

<i>Co-Bonding Costs</i>			
<i>Ann. Prod. Vol.</i>	<i>1</i>	<i>10</i>	<i>100</i>
Components	\$ 14,856	\$ 6,409	\$ 5,553
Material	\$ 3	\$ 3	\$ 3
Labor	\$ 1,269	\$ 1,269	\$ 1,269
Machine	\$ -	\$ -	\$ -
Fixturing	\$ 15,662	\$ 1,566	\$ 157
<b>Unit Costs [\$/part]</b>	<b>\$ 31,790</b>	<b>\$ 9,247</b>	<b>\$ 6,982</b>

As illustrated by Figure 9.24, for high volume production the costs for co-bonding are almost entirely driven by labor costs. Since the cure of the adhesive is conducted at room temperature or under heating blankets, there is no need for any expensive capital equipment such as an oven or an autoclave. The cost savings potential however is more limited in comparison to mechanical assembly. Only a difference in the wage structure or a meticulous tuning of the process plan can reduce the labor costs and therefore the variable unit costs. Both measures however have to be pursued under the careful consideration of their impact on quality and overall system performance.

**Figure 9.24 Distribution of Adhesive Bonding Costs (Total Production 500 Parts)**

### 9.2.5 Summary & Process Comparison

As seen in Figure 9.25, all three assembly processes exhibit some economies of scale as the batch size increases. The main reason is, that the curing process for the production of the components mainly drives the overall production time of co-cure, co-bond, and even mechanical assembly. The scaling effect for mechanical assemblies however would be lessened if instead of a liquid shim a solid shim would be employed.

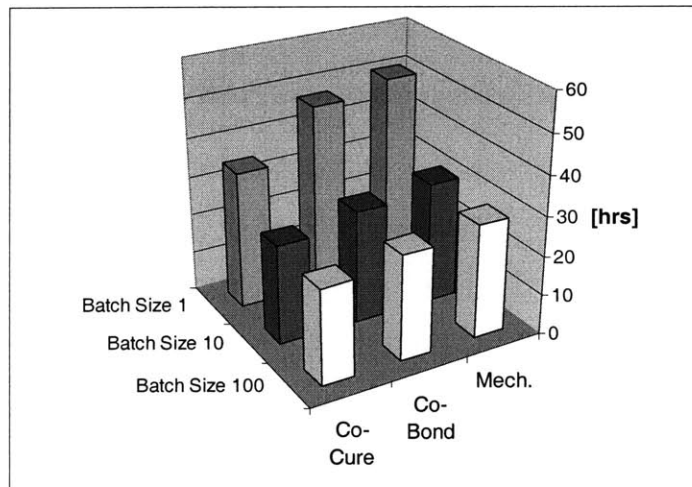


**Figure 9.25 Assembly Production Time (incl. Component Production)**

The second major finding is that in this particular case study, co-cure happens to clearly outperform the other two assembly methods. Because of the simplicity of the assembly and its components, it is possible that the production of the individual components takes about as long as the co-cure of the entire structure. In that respect, the chosen example is not very instructive, since different assembly scenarios might exist where the situation is reversed. However, the benefit of this case study is that it not only applies the developed costs models and demonstrates their potential, but it particularly facilitates the understanding of the economic differences between adhesive- and mechanical assembly.

The comparison of the unit costs as listed in Table 9.29 presents a similar picture as Figure 9.25. Co-cure represents the most economical process regardless of the total production volume. Although the gap between co-cure and the other two processes clearly narrows, in this example the costs for component production have to be borne by

co-bonding and mechanical assembly on top of the individual assembly costs. In addition to the component costs, which are here comparable to the costs for co-curing, the assembly of rigid parts also requires an investment into special assembly fixtures.

**Table 9.29 Assembly Unit Costs (incl. Tooling, Batch Size 1)**

<i>Costs per Part</i>	<i>Prod. Vol. 5</i>	<i>Prod. Vol. 50</i>	<i>Prod. Vol. 500</i>
<b>Mech.</b>	\$ 33,201	\$ 10,658	\$ 8,393
<b>Co-Bond</b>	\$ 31,790	\$ 9,247	\$ 6,982
<b>Co-Cure</b>	\$ 14,856	\$ 6,409	\$ 5,553

Consequently, for small production volumes, the unit costs for adhesive- and mechanical assembly turn out to be more than twice as high as the ones for co-curing. Of course, as the production volume increases, both the costs for fixturing and layup tooling are distributed over a larger number of units. The large amount of investment in tooling and fixtures explains the dramatic drop in unit costs as seen in Table 9.29 and Figure 9.26.

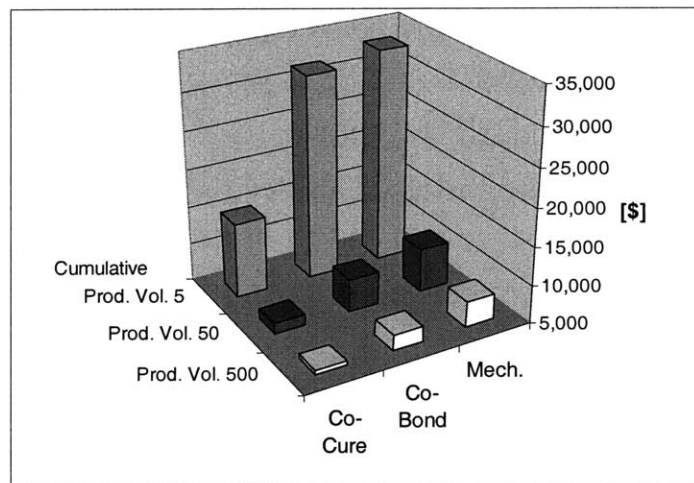


**Figure 9.26 Assembly Unit Costs (incl. Tooling, Batch Size 1)**

The case study therefore demonstrates, that any economic decision on the selection of assembly processes, is largely dependent on the costs of curing tools and assembly fixtures. This result further underlines the necessity to develop reliable cost models for tooling and fixture production. Only then, one can accurately evaluate the trade-off between building a complex co-curing tool and buying several simple curing tools plus

an assembly fixture. To solve the problem, one simply compares the costs of each scenario and can then decide which approach is most economical given the certain production volumes.

Until the cost estimation models for assembly fixtures will have become more sophisticated, one can take the present example and learn more about the differences between adhesive bonding and mechanical assembly. Regardless of the large differences in material costs for the assembly of carbon fiber composites, Figure 9.27 clearly shows that assembly processes are generally very labor intensive. For example, it is difficult to automate the positioning and location of the parts as encountered during the assembly of aircrafts or other large structures. Because of their tactile and problem solving abilities, humans generally do a great job in putting together structures, which might be overconstraint or involve a large amount of repositioning until the puzzle is complete. Therefore, it is paramount to design the structure and the process efficiently in order to minimize the labor content and control assembly costs. In addition, the generally high labor content in connection with the inflation of wages, explains that manager might be tempted to resort to a less labor intensive assembly process, which however might require larger up front investments. From this perspective, the co-curing of parts might be economic in particular for large production volumes, as the potentially higher tooling costs are distributed over numerous parts. The subsequent, third case study investigates this issue further by analyzing the assembly costs of a horizontal stabilizer.

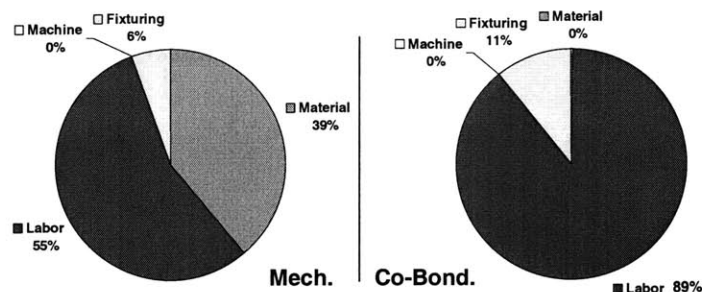


**Figure 9.27** Costs of Mechanical-, and Adhesive Assembly (500 Assemblies)

### 9.3 Case Study 3: Assembly of a Horizontal Stabilizer

To further evaluate the economic merits of co-curing versus mechanical assembly our team conducted an extensive on-site study at a large aircraft manufacturer [15, 16]. The assembly of a horizontal stabilizer of a large cargo plane serves as an example to study the effects of part integration efforts on costs. By comparing the investment and the variable costs for co-curing with the ones for mechanical assembly, one can decide which approach might be more economical under certain manufacturing conditions. The ultimate goal is then to formulate general guidelines, which support designers and managers in their endeavor to find the optimum degree of part integration. The study also qualitatively discusses the risks related to the investment, the manufacturing, and to structural failure.

#### 9.3.1 Design & Manufacturing Conditions

On average about 15 cargo planes are produced annually as part of a 5 year production program. The horizontal stabilizer consists of a port and a starboard assembly, similar to the schematic depicted in Figure 9.28. Therefore, the production facilities have to provide capacity to assemble about 30 stabilizer halves each year. The stabilizer for this cargo plane resembles a small wing and consists of a nose section, a mainbox, and a trailing edge including the control surfaces.

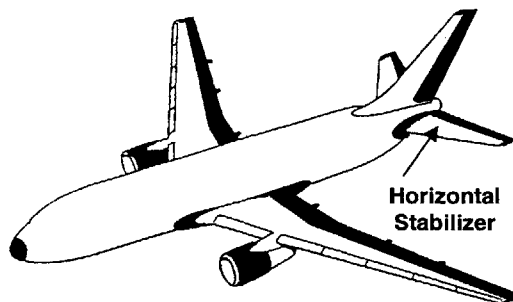


**Figure 9.28** Horizontal Stabilizer of a Large Cargo Plane

This study is mainly concerned with the production and assembly of the main box as shown in Figure 9.29. The inboard end of the mainbox is about 9 feet wide and then

tapers down to 3 feet at the outboard end. The total span of the stabilizer stretches over 70 feet and exhibits a  $27^\circ$  sweep, which results in a 43 feet long main box for each half. The total surface area of each section covers approximately  $400 \text{ ft}^2$ .

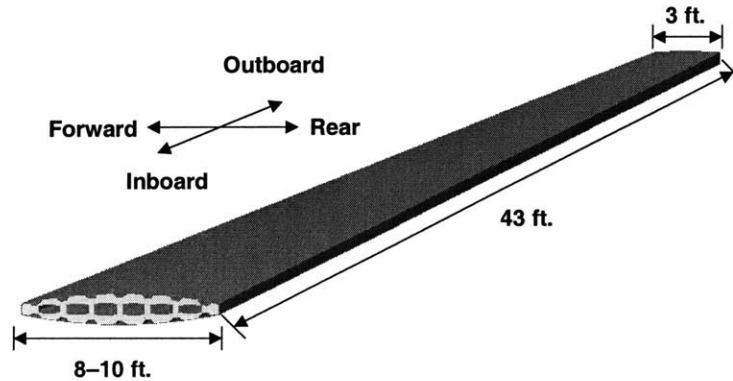


**Figure 9.29** Main Box of the Right Stabilizer

Initially the stabilizer had been constructed entirely out of Aluminum, however as part of a design revision, the manufacturer decided to switch to carbon fiber composites as the major construction material. At the time, two options presented themselves to the design team. The first was to simply substitute the Aluminum components with composite and create a so-called Black-Aluminum design. The second possibility was to reduce the overall part count by integrating several components and co-curing them together during one manufacturing step. In the subsequent paragraphs, the study discusses why the designers chose the integrated Co-Cured Design.

The mainbox assembly of the horizontal stabilizer comprises the following components. Two spars, a front-, and a rear spar make up the leading and trailing edges of the assembly. The spars are made of carbon fiber prepreg, which is laid up manually and then cured in an Autoclave. Each of the 43 feet long elements weighs approximately 50 lbs. As seen in Figure 9.30, 22 ribs are located in between the spars in order to provide torsional stiffness to the structure. The ribs are high speed machined out of Aluminum, because machining is more economical for complex and diverse shapes than composites, since it dispenses with expensive tooling. Figure 9.37 displays a schematic of such a rib, which weighs on average about 10 lbs. The upper and lower composite skins serve primarily as an aerodynamic surface, but also give the structure additional stiffness.



Because of the non-symmetric design of the wing and its backward sweep, each wing skin is slightly different and therefore a total 4 different skins make up an entire stabilizer. Each carbon fiber composite skin is laid up automatically and weighs about 323 lbs. To provide additional bending stiffness 7 longitudinal stringers are attached to each skin. Therefore, one main box encompasses 14 stringers, which are also made of carbon fiber composites and weigh approximately 40 lbs each.

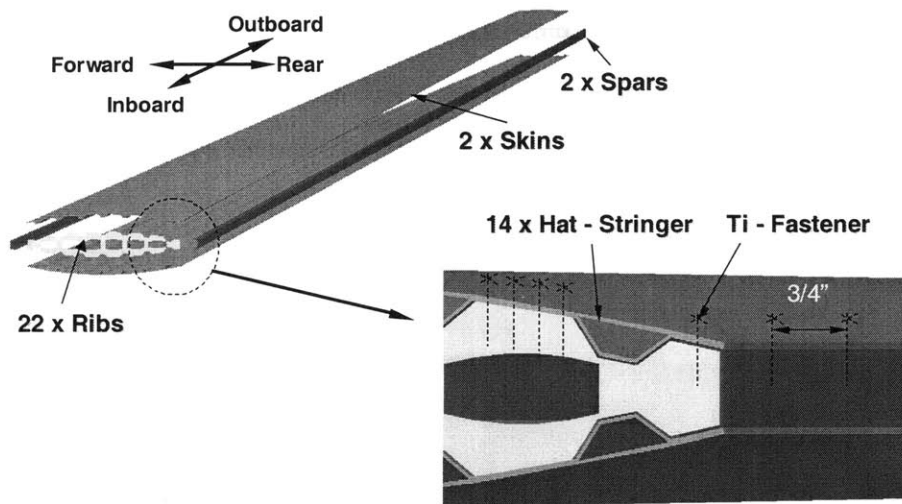


**Figure 9.30** Design Detail of Horizontal Stabilizer Main Box

In the case of the integrated design, the stringers are directly cured together with the wing skins forming a stiff and durable component. The subsequent Chapter 9.3.2 discusses the exact design features in more detail. The rest of the structure is held together by corrosion resistant Titanium fasteners each spaced about  $\frac{3}{4}$  inches apart. Figure 9.30 and Figure 9.31 depict some details of the location of the fasteners for the Co-Cured Design. In contrast, the Black-Aluminum does not feature co-cured skin and stringers, but uses additional Ti-fasteners. Therefore, two fasteners rows along the length of the stabilizer are needed to securely attach each stringer to the wing skin. Table 9.30 shows a summary of the components and their weights. The total structural weight of the main box adds up to around 1,500 lbs. not including the fasteners however.

**Table 9.30 Summary of the Component Parameters**

#	Component	Material	Weight	Comment
2	Skins	Carbon/Epoxy	323 lbs/pc.	Upper / Lower
14	Hat-Stringers	Carbon/Epoxy	40 lbs/pc.	7 Upper/ 7 Lower
2	Spars	Carbon/Epoxy	50 lbs/pc.	Front / Rear
22	Ribs	Aluminum	10 lbs/pc.	High Speed Mach.
	<b>Total (Main Box Only)</b>		<b>ca 1,500 lbs</b>	<b>w/o Fasteners</b>

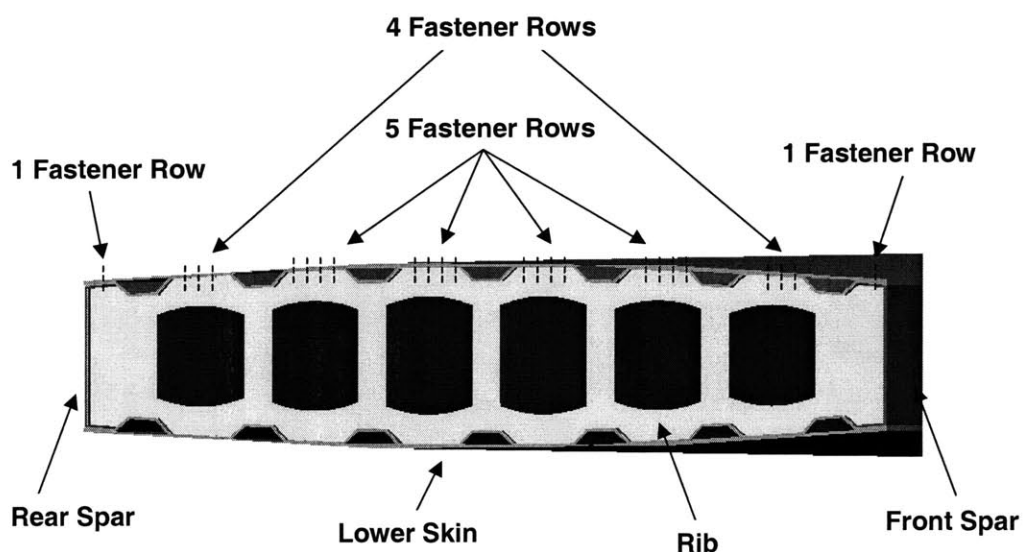


**Figure 9.31 Assembly Detail and Fasteners**

### 9.3.2 Co-Cured Design

The Co-Cured design is characterized by the integration of the stiffening stringer elements with the outer skin of the horizontal stabilizer. The following paragraphs first describe the manufacturing costs of the co-cured skin and the other components. Hereby, a process based cost estimation model is used in connection with actual data provided by the manufacturer. The chapter then discusses the actual assembly costs and the overall investment costs for tooling and fixturing.

#### Component Process Plan

The material used to produce the skin is a 6-inch wide carbon fiber prepreg tape, which costs about \$80/lb and is laid up by an automatic tape-laying machine. Because of the automatic operation, the material scrap is only around 7%. In order to tailor the wing like structure to the mechanical loads, the laminate incorporates many ply-drops as the skin thickness tapers off from 1 inch at the inboard end to about 1/8 inch at the outboard end. Figure 9.32 shows, that from the initial 200 plies only about 25 go through continuously to the tip of the stabilizer. The entire operation of laying up one skin takes about 4.5 days while working 3 shifts per day. After every shift, the plies are consolidated during a debulking step. The out-time of this special prepreg tapes exceeds 1 week and therefore premature curing is not an issue.

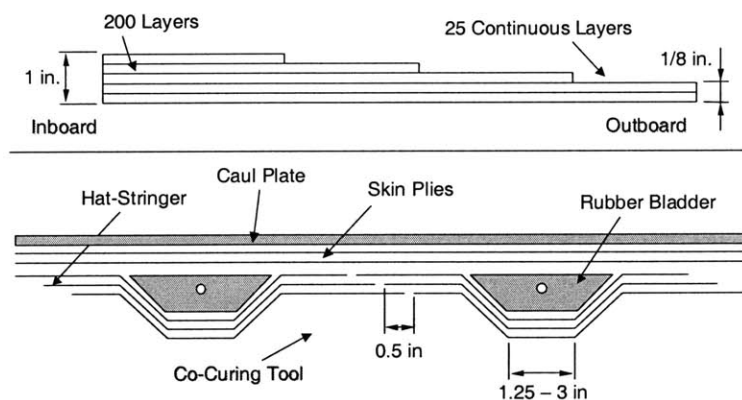


**Figure 9.32** Side & Frontal View of the Skin Cross-Section

The layup of the 14 stringers however is performed manually. The carbon prepreg are pre-cut by a Gerber CNC cutter and then draped by the operators over a layup tool as depicted in Figure 9.33. The stacking and positioning of the plies is guided by laser projection system, since the laminate structure of the stringers is quite complex. Not only does the stringer exhibit many ply-drops, but also requires a precise staggering of the plies in order to form the  $\frac{1}{2}$  inch overlaps shown in the lower part of Figure 9.32. These overlaps form lap joints, as the stringers and the skin are assembled in the co-curing tool. This feature improves the strength and the crack resistance of the structure. It takes 4 workers about 7 hours to layup one of the 14 stringers. Because of the nature of the laminate and the manual layup, the material scrap can be assumed to be around 20%.

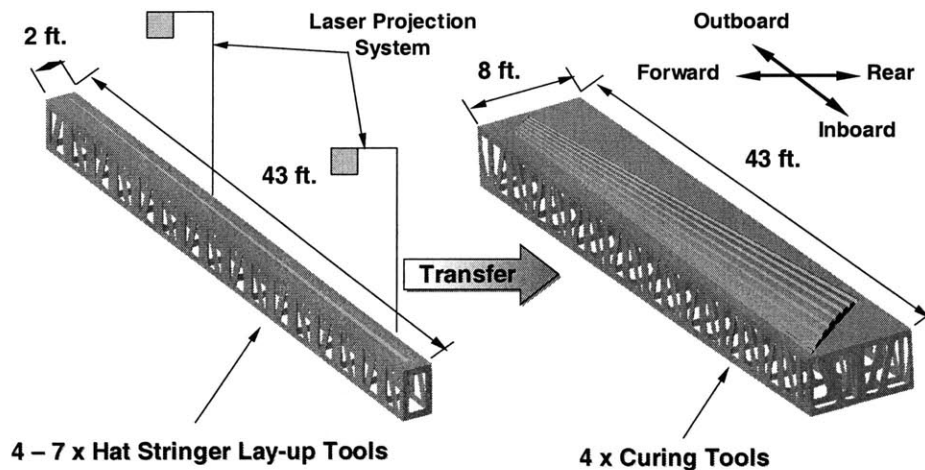


**Figure 9.33** Stringer Layup and Preparation of Skin/Stringer Co-Cure

Due to the soft overlap joints between the stringers; the parts need to be positioned precisely with respect to each other. Therefore, an IML (Inner Mold Line) co-curing tool is used to assemble the uncured stringers and the skin. As depicted in Figure 9.33, first the stringers are transferred and loaded into the co-curing mold. Figure 9.32 then shows, how stiff rubber bladders are placed in the open sections of the stiffeners. These bladders are vented to the autoclave's ambient pressure during curing, which causes them to expand and consolidate the laminate. Once all the stringers and bladders are in place the laid up skin is placed on top and fitted to the curvature of the co-curing tool. The skin is then covered by a caulk plate in order to give it a smooth and aerodynamic surface. At

last, a vacuum bag seals in the entire assembly before the curing cycle can commence inside the Autoclave. The resin is solidified and the parts are permanently baked together in a 10-hour long curing cycle. The risks of an unsuccessful cure are relatively low according to the manufacturer, since the critical time zone is with about 2 hours relatively short. Only a massive bag failure from the point where the resin has gelled to the completion of the cross-linking reactions can cause irreparable damage to the part. Small leaks are generally harmless because the hot air rushing in is either deflected by the caul plate or sucked away by one of the numerous vacuum manifolds. Therefore, dry spots and inadequate adhesive strength is rarely observed. However, to ensure quality, the entire part is subjected to a subsequent Ultrasonic Inspection scan. Any discovered flaws larger than  $\frac{1}{4}$  of an inch in diameter have to be repaired. The rework is done by peeling away the effected layers and patching the area with uncured prepreg. The structure is then vacuum bagged again and run through another cure cycle.

**Table 9.31 Consolidated Process Plan for the Skin/Stringer Co-Cure**

<i>Step</i>	<i>Description</i>
1	Skin Tape Layup
2	Hat-Stringer Hand Layup
3	Assemble Skin & Stringers in Co-Curing Mold
4	Autoclave Curing Cycle
5	Trimming & Finishing
6	Ultrasonic Inspection

Table 9.31 outlines the major fabrication steps of the integrated skin/stringer structure. Based on actual data and technical scaling models, Table 9.62 shows the actual production time for each of the major steps. The distribution of the production time is plotted in Figure 9.38 and shows that almost 60% of the time goes into the layup of the skin alone, whereas 26% of the time are spent on the fabrication of the stringers.

#### Component Manufacturing Costs

The labor costs and the costs for the usage of the Tape Laying and Autoclave equipment can be easily derived from the data on the production times. For labor, a rate of \$100/hr is assumed, whereas the Tape Laying machine costs about \$200/hr and the Autoclave

around \$30/hr. These rates are consistent with the information from the manufacturer and the previously estimated costs. The material is priced at \$80/lb and given the weights listed in Table 9.30, the material costs can be calculated while also considering any scrap due to cutting or expired material. Table 9.32 summarizes the manufacturing costs for each component separated by cost category. The total production costs for all the components add up to approximately \$250K. When looking at the cost distribution it is not surprising that the skins contribute about 41% to the total costs, followed by the Hat-stringers with 31% and the ribs with 11%.

**Table 9.32 Component Manufacturing Costs**

#	Component	Material	Labor	Machine
2	Skins	\$27,700	\$10,800	\$16,300
14	Hat-Stringers	\$4,700	\$700	\$100
2	Spars	\$4,800	\$4,000	\$1,300
22	Ribs	\$300	\$500	\$500
	Co-Cure & Inspection etc.	--	\$6,500	\$8,700
	<b>Total</b>	<b>\$ 137,400</b>	<b>\$ 56,900</b>	<b>\$ 56,100</b>

### Manufacturing Tooling Costs

As discussed in Chapter 9.2, knowledge about the tooling expenses is vital for deciding the economic viability of a particular design concept. The point where an integrated design potentially becomes more economical than its integrated counterpart is largely dependent on the tooling cost and the anticipated production volume. To determine any potential crossover points, the costs for tooling is estimated by means of the developed tooling models and backed up by actual cost data obtained from the manufacturers.

The tool on which the Tape Laying machine places the skin plies is essentially flat and made out of a Aluminum. The relatively thin face sheet is supported by a movable steel frame construction. Since, the tool is only used for layup and is not subjected to any thermal or mechanical loads, its price is only about \$20K according to the manufacturer.

The co-curing tools are the most complex tools, since they integrate all the components and exhibit all the features of the final structure. Chapter 7.8.6 discusses the estimation

process in great detail and concludes that the price of the first copy of the co-curing tool is about \$1.1M. The price for the first copy can also be estimated quickly by multiplying the 51,800 in<sup>2</sup> (360 ft<sup>2</sup>) projected area with \$21/in<sup>2</sup>, a value, which is derived from Figure 7.27. Since, the engineering costs only have to be borne once, additional copies of similar co-curing tools are priced at around \$400K a piece. In total, 4 tools are required to produce the geometrically slightly different upper, lower and port, starboard skins.

The Hat-Stringer layup tools are quite inexpensive in comparison. Since, they are only used for laying up and are not subjected to any considerable mechanical and thermal loads, the tools can be made from cast resin and structural foam. A welded support structure on casters gives additional support and allows for easy handling. In order to provide enough layup capacity and stay in-sync with the skin production, a total of 4 layup tools is required. Each of the Hat-Stringer tools only cost around \$6,000.

Table 9.33 summarizes all the tooling costs and lists the overall investment at \$2.3M.

**Table 9.33 Manufacturing Tooling Costs (Co-Cure)**

#	Co-Cured Design	Material	Size	Weight	1st Copy	Addl. Copies
1	Skin Lay-Up Tool	Alu	50,000 in <sup>2</sup>	--	\$20,000	--
4	Stringer Lay-Up Tool	Epoxy	12,500 in <sup>2</sup>	--	\$6,000	\$6,000
4	Skin Co-Curing Tool	Invar	51,800 in <sup>2</sup>	24,000 lbs	\$1,100,000	\$400,000
					<b>Total</b>	<b>\$ 2,344,000</b>

### Assembly Process Plan

The assembly of all the components, which eventually form the final wing mainbox, is easily described by means of Figure 9.34. After loading and positioning the front and rear spar onto the locators in the main assembly area, the workers start attaching the Aluminum ribs. What the schematic of the assembly fixture in Figure 9.34 does not show is the scaffolding surrounding the main assembly area. It moves up and down and allows workers good access to the entire structure. Once in place, holes are drilled through the spars into the ribs to accommodate the two-piece Ti-Fasteners. Occasionally, it becomes necessary to bridge the gap between spar and ribs with some shimming

material in order to keep any residual stresses to a minimum. After all holes are drilled and deburred, the fasteners are installed and tightened with manually operated pneumatic tools. Apparently, the low production volume does not justify the investment for an Automated Fastening System. Meanwhile, the two wing skins are loaded onto locators in the loading area. From there, each skin can be guided individually on precision rails into the assembly area. Now the workers apply a liquid shimming compound to all the interface areas between the spars, the ribs, and the skins. Before the compound starts to cure, the skins are brought in and tightly clamped onto the internal structure. The excess shim is squeezed out and removed by the workers and the remainder forms an accurate fit between skins, ribs, and spars.

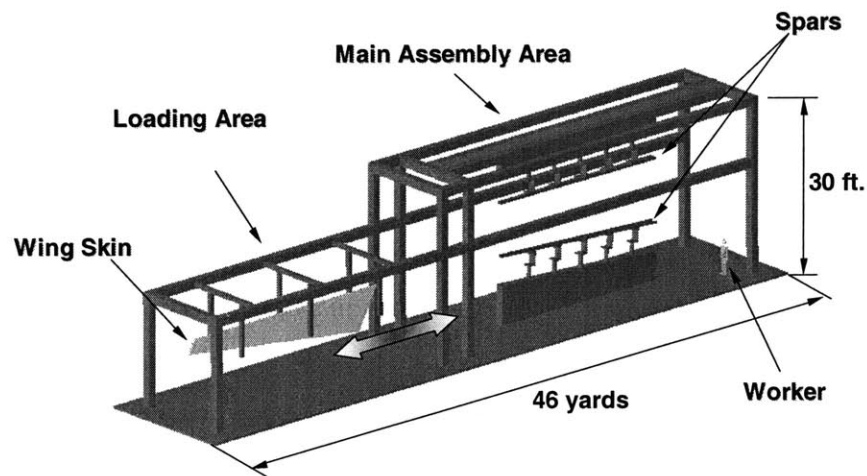


**Figure 9.34** Main Box Assembly Fixture

Following a 6 to 8 hour cure, fastener holes are drilled through the skin directly into the spars and ribs to ensure a proper line up and fit of the components and fasteners. Figure 9.31 sketches the individual locations for fasteners and holes. The skins are then unclamped and removed in order to deburr the numerous holes. Once, the deburring is completed the first skin is moved back in again and is lined up with all the previously drilled holes. This part of the process can be the most difficult one, because thermal mismatch between the tool and the skin can potentially cause some holes to be out of line. The facility is therefore air-conditioned. Fortunately, the mechanical fastening of composites does not require press fits between fasteners and the components and



therefore somewhat simplifies the lineup. Also, according to an industry source, composite skins are considerably stiffer and therefore easier to handle, since they keep their shape and therefore cause less problems when trying to line up all the holes. The first skin is then fastened by using Titanium two-piece fasteners and manually operated power tools. After completion, the process is repeated for the second skin. However, access to the inside of the structure is now restricted and therefore prohibits the use of two-piece fasteners. Instead rivets or one-piece fasteners are employed as depicted in Figure 6.17. The assembly of the main box is hereby completed and the structure is removed from the assembly fixture making room for the next main box assembly. Table 9.34 sums up the major assembly steps.

**Table 9.34 Consolidated Assembly Process Plan (Co-Cure Design)**

<i>Step</i>	<i>Description</i>
1	Load Front & Rear Spar into Fixture
2	Load Ribs into Fixture
3	Fasten Ribs & Spars
4	Apply Liquid Shim
5	Load Skins & Cure Shim
6	Drill Fastener Holes into Skins
7	Unload Skin (a)
8	Fasten Skin (b)
9	Load & Fasten Skin (a)

The production times for each of the major steps are listed in Table 9.63. The times were obtained from process based scaling laws and confirmed by the manufacturer. The details of their calculation are described in a studied carried out by Alex Gorgias [16]. About 2 to 4 workers are busy on the assembly for about 2 shifts a day, which results in an annual production volume of 64 wing boxes or 16 airplanes. Currently, one mainbox is produced every 3.5 to 4 days. The results listed in Table 9.63 illustrate, that the actual fastening is with about 47 hours the most time consuming step and accounts for about 84% of the total assembly time. It also scales almost linearly with the number of fasteners used and therefore one can already guess at this stage, that any elimination of fasteners from the design will have a significant impact on the overall production time.

Assembly Costs

Because of their high price, the costs of the Ti-fasteners drive 88% of the assembly costs. The remainder is contributed by the labor costs required to install each fastener. At \$100/hr for each worker and a total of almost 57 production hours, the labor costs amount to approximately \$5,700. Since all operations are performed manually, the charges for the use of any power tools can easily be neglected. However, because of their importance and since the material and labor costs scale directly with the number of fasteners, the following paragraphs describe the underlying calculations in more detail.

**Table 9.35 Assembly Costs (Co-Cure Design)**

#	Component	Material	Labor	Machine
1	Fasten Bolts & Rivets	\$42,480	\$3,552	manually
2	Drill Fastener Holes	--	\$1,179	manually
3	Apply Liquid Shim & Cure	negligible	\$404	--
4	Load & Unload Skins	--	\$230	--
5	Load Ribs into Fixture	--	\$185	--
6	Load Front & Rear Spar	--	\$120	--
	<b>Total</b>	<b>\$42,480</b>	<b>\$5,670</b>	<b>\$0</b>

Figure 9.31 illustrates the locations of the fasteners and which facilitates the computation of the total amount of fasteners. Six fasteners are used to connect one rib to a spar on each side. Therefore, by multiplying 22 ribs with 6 fasteners and 2 spars one gets 264 fasteners. The fasteners connecting the spars to the skin are spaced about  $\frac{3}{4}$  of an inch apart and run along the entire length of the wing box. Dividing the stabilizer length of 516 inches by  $\frac{3}{4}$  of an inch gives 688 fasteners per row. To attach the upper and lower skin to the front and rear spar, 4 rows of fasteners are needed, bringing the total to 2,752 + 264 fasteners. Now all the fasteners for tightly securing the ribs with the skin and the rest of the structure are added up. At each of the 22 ribs, around 56 fasteners are installed on average, which requires another 1,232 fasteners. Adding it all up, one requires 4,248 fasteners at \$10 a piece to complete the assembly.

Table 9.35 lists the individual cost positions for the major production steps. According to these results, the variable costs to assemble one of the two main boxes of the horizontal stabilizer amount to \$48,150.

### Assembly Tooling Costs

All other cost elements generally dwarf the costs for the large and complex assembly fixture. The tool depicted in Figure 9.34, costs around \$6M or almost \$50,000 per foot according to an industry resource [19]. The price also includes the drilling templates used to accurately position each fastener hole. Chapter 7.6 on assembly tooling discusses the features of the fixture and its costs in more detail.

### Cost Summary - Co-Cured Assembly

Adding up all the costs for material and labor one obtains an amount of almost \$300K for the production of one wing main box. These recurring costs include the costs for component production and are contrasted by about \$8.3M investment costs for tooling and fixturing. From these numbers and the expected production volume one can derive the unit costs under the consideration of depreciation period and capital costs.

### 9.3.3 Black Aluminum Design

The so-called Black Aluminum design simply replaces the Aluminum components of the initial design with parts made out of carbon fiber composites. Since, the level of integration is generally low for pure Aluminum assemblies, the Black-Aluminum design exhibits a considerably higher part count in comparison to the Co-Cured design. Consequently, more fasteners are used for the Black Aluminum design and the following paragraphs outline the impact of the difference on the overall costs. Also, any change in tooling or fixturing costs is evaluated and discussed.

#### Component Process Plan & Manufacturing Costs

The production of the components for the Black Aluminum design is similar to the component fabrication for the Co-Cured design. The Black Aluminum design also consists of 22 Aluminum ribs, 2 composites spars, 2 skins and 14 stringers. However, the major difference is that the Black Aluminum design does not integrate the Hat-Stringers and the Skin during a co-curing step. In contrast, after layup, the skin and the stringers are placed onto individual curing tools and are then vacuum bagged and readied for cure. The time saved for not having to place the stringers onto the co-curing mold is almost offset by the additional time consumed during the individual bagging of each stringer. It is also assumed, all components are cured as one batch during one curing cycle. Therefore, in this example the component production costs can be regarded identical for the two designs.

#### Manufacturing Tooling Costs

Inherently, when co-curing several parts at once, the tooling is more complex than the tooling needed to cure each component individually as it is the case here. By applying the previously developed cost estimation methods for tooling (see Chapter 7.3), a fairly accurate cost estimate can be obtained for the skin curing and for the stringer curing tools. The 4 Invar skin curing tools can be categorized as complexity 1 to 2 tools and are priced at around \$12.5/in<sup>2</sup>. For the first copy about \$665K are due, whereas the additional copies go for about \$350K each. In comparison to the co-curing tools, this is

almost \$600K less, which one has to spend on the skin curing tools alone. However, the skin curing tool is not dramatically different in complexity (only 1.5 levels difference) in comparison to the co-curing mold and therefore the difference is still moderate. For higher levels of integration and therefore more pronounced differences in complexity, one would expect a larger difference. However, for the curing of the Hat-Stringers additional tools are required. The Co-Cured approach could get away with inexpensive layup tools made of cast resin, however now that the Hat-Stringers are cured on special tools in an Autoclave, drastically more expensive Invar tools are needed. The Hat-Stringer tool can be classified as a complexity 2 tool and therefore is priced at around \$13.5/in<sup>2</sup>. The first copy then costs approximately \$155K and all additional copies \$80K each. In order to decide, which design approach requires less investment for production tooling, the necessary number of Invar Hat-Stringer tools has to be determined. When evaluating the Co-Cured design, one notes, that each of the 28 stringers is slightly different and an individually fabricated tool would be required for each stringer. However, one can assume that designers, in their efforts to minimize part variety and therefore tooling costs, would standardize the Hat-Stringer design throughout the entire stabilizer assembly. On the other hand, at least 4 curing tools have to be procured to provide enough production capacity and produce all the stringers for each main box assembly by the time the wing skins are ready. It is therefore assumed, that 7 Invar curing tools are necessary to cure half the stringers, required for one main box assembly.

**Table 9.36 Manufacturing Tooling Costs (Black Aluminum Design)**

#	<i>Black Alu Design</i>	<i>Material</i>	<i>Size</i>	<i>Weight</i>	<i>1st Copy</i>	<i>Addl. Copies</i>
1	Skin Lay-Up Tool	Alu	50,000 in <sup>2</sup>	--	\$20,000	--
7	Stringer Lay-Up Tool	Invar	12,500 in <sup>2</sup>	5,600 lbs	\$146,000	\$65,000
4	Skin Co-Curing Tool	Invar	51,800 in <sup>2</sup>	21,000 lbs	\$665,000	\$350,000
					<b>Total</b>	<b>\$ 2,271,000</b>

Table 9.36 lists the major cost details and displays the total amount invested in component production tooling. Surprisingly, the almost \$2.3M are very close to the tooling costs for the Co-Cured design. The reason is the high tooling costs for stringer fabrication. In the here presented example, the Black-Aluminum production concept

requires 3 additional and more expensive tools than the Co-Cured approach. The savings resulting from the less complex skin curing tools are unfortunately eaten up by the additional costs for the stringer tools. It appears, that in this example the costs incurred by complexity of the co-cured part is simply redistributed over several tools. However, this particular result must not be generalized, since the tooling costs can differ considerably in other assembly applications.

### Assembly Process Plan

Except for the loading and fastening of the 14 Hat-Stringers, the assembly process plan for the Black-Aluminum design is very much identical to its Co-Cured counterpart. These extra steps require a considerable amount of additional labor, because each stringer has to be loaded into the large assembly fixture, positioned, clamped, and finally attached to the wing skin. The production times listed in Table 9.64 show, that the actual loading only takes an extra 10 hours, however the major time difference results from the installation of the additional fasteners. The detailed calculation of the production times can be found in Reference [16]. Again, drilling and fastening consumes about 87% of the total assembly time, however takes now as much as 250 hours versus approximately 47 hours for the Co-Cured assembly. As outlined in the subsequent paragraph, this large difference is directly related to the number of fasteners of which the Black-Aluminum design contains about 5.5 times more. The total assembly time for one mainbox lies around 288 hours, resulting in one box produced every 12 days when working 3 shifts a day. Consequently, the annual production volume is only about 20 mainboxes or 5 airplanes. However, the current annual demand is around 15 planes and therefore insufficient capacity prevents the production of more than 5 airplanes. The Co-Cured concept is capable of producing 15 airplanes working only 2 shifts a day. If production of the Black Aluminum design would have to be ramped up to this level, at least 3 more assembly workstations would have to be installed or the fastening process would have to be automated. Both solutions are associated with considerable additional investments.

### Assembly Costs

Because of the impact of the number of fasteners on labor and material costs, the calculation is once again explained in some detail. In addition to the 4,248 fasteners required to attach ribs, spars and skin, another 19,264 fasteners are necessary to attach the 14 stringers to the skin. Each stringer is joined with the skin by 2 rows of fasteners each spaced  $\frac{3}{4}$  inch apart along the 516 inches wing length. Overall, 23,512 fasteners are used to assemble one main box when choosing the Black-Aluminum design. At \$10 per fastener, the difference in material costs amounts to \$193K in comparison to the Co-Cured design. What's more, fastener costs drive 89% the overall assembly costs. The rest is incurred by labor, as seen in Table 9.37, which adds another \$23K to the assembly costs. The total for assembling one main box is around \$263K, which is approximately \$215K more per box when compared to the Co-Cured design.

**Table 9.37 Assembly Costs (Black Aluminum Design)**

#	Component	Material	Labor	Machine
1	Fasten Bolts & Rivets	\$235,120	\$19,608	manually
2	Drill Fastener Holes	--	\$ 5,578	manually
3	Apply Liquid Shim & Cure	negligible	\$ 2,063	--
4	Load Stringers	--	\$ 963	--
5	Load & Unload Skins	--	\$ 294	--
6	Load Ribs into Fixture	--	\$ 185	--
7	Load Front & Rear Spar	--	\$ 120	--
	<b>Total</b>	<b>\$235,120</b>	<b>\$28,811</b>	<b>\$0</b>

### Assembly Tooling Costs

Again, the same assembly fixture as depicted in Figure 9.34 is used to assemble the wing mainbox. In addition, to the costs of around \$6M another \$100K are needed to pay for the additional drilling templates used to attach the stringers. However, the costs of the templates are almost negligible when compared to the overall investment costs.

### Cost Summary - Black Aluminum Assembly

When adding the costs to produce the components, \$514,331 on recurring costs have to be incurred to produce one main box of the horizontal stabilizer. This is an increase of

approximately \$200K as opposed to the recurring costs for the Co-Cured design. However, the investment costs are very similar and total \$8,371,000 including production and assembly tooling.



### 9.3.4 Design & Cost Comparison

The decision, which design approach is more economical, is based on an evaluation of the recurring costs and the total investment costs in consideration of the expected total production volume. Table 9.38 summarizes the various costs elements for the Co-Cured and the Black-Aluminum design. The recurring costs for the co-cured approach total around \$300K and the required investment for fixturing and tooling is about \$8.3M. In contrast, \$500K have to be spent for each wing box built according to the Black-Aluminum concept, while also having to invest \$8.3M into tooling and fixturing. Therefore, for this particular example it is clear that the Co-Cured design is always more economical under the given production and design assumptions.

**Table 9.38** Costs of Co-Cured vs. Black Aluminum Design

<i>Cost Elements</i>	<i>Co-Cured Skin Design</i>	<i>Black Aluminum Design</i>
Component Material Costs	\$137,400	\$137,400
Component Labor & Machine Costs	\$113,000	\$113,000
Component Tooling Costs	<b>\$2,344,000</b>	<b>\$2,271,000</b>
Assembly Material Costs	<b>\$42,480</b>	<b>\$235,120</b>
Assembly Labor Costs	<b>\$5,670</b>	<b>\$28,811</b>
Assembly Tooling Costs	\$6,000,000	\$6,100,000
<b>Investment Costs</b>	<b>\$8,344,000</b>	<b>\$8,371,000</b>
<b>Recurring Costs</b>	<b>\$298,550</b>	<b>\$514,331</b>

Overall, there are mainly three factors responsible for the outcome of this result. The first is the costs of the Ti-fastener required to join carbon fiber composites. The high fastener prices put the less integrated design at a strong disadvantage regardless of the additional labor costs for installation. Structures made off Glass- or Kevlar fibers only require less expensive Aluminum or Steel fasteners.

The second factor is the costs for production tooling. The more integrated design featuring a lower part count, generally requires fewer but more complex tools. In contrast, the modular design generally exhibits a higher part count and therefore more tools have to be procured. However, each tool features a simpler shape and is consequently less costly. The trade-off scenario is clear and the question is, whether the few complex tools or the many simple tools are more expensive. In the presented

example, it turns out, that no advantage seems to be gained from either concept and the investment in tooling is nearly identical. It appears that in order to produce a structure of a certain complexity one has to invest a certain amount of money into tooling regardless of the design approach. However, under no circumstance should this observation be generalized, because in the case of the horizontal stabilizer the large cost discrepancy between the Invar curing tools and the Epoxy layup led to the particular outcome.

The third factor is related to the costs for the assembly fixtures. Again, the overall investment into assembly fixture is nearly identical for both of the assembly methods. In general, one would have expected higher fixturing costs to join the design exhibiting the higher part count. However, in the present example, the major investment goes into the fixture itself and only a relatively small sum has to be spent on drilling templates for Black-Aluminum design.

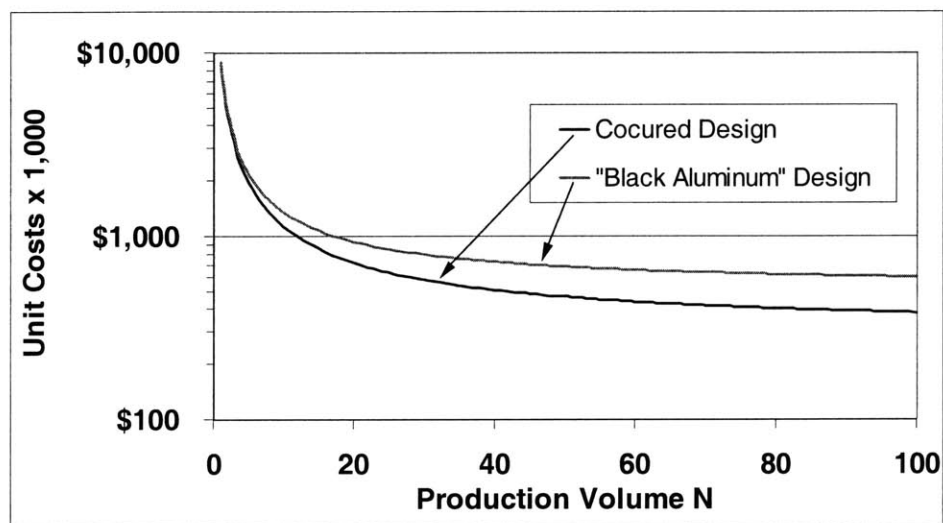


**Figure 9.35 Evolution of Unit Costs with Cumulative Production Volume**

All investment costs being equal and considering a difference of \$200K in terms of recurring costs, one can calculate the unit costs for one stabilizer main box at different cumulative production volumes. Figure 9.35 plots these unit costs and exhibits the familiar shape as the unit costs decline with the inverse of the production volume. The cost savings due to the Co-Cured design total around \$300M over a 5 year production span, considering a production rate of 30 main boxes per annum.

The obvious cost savings are undisputable in this particular scenario, but what about the economic impact of any of the involved risks. To simplify the discussion, let's only focus on the risks where there is a perceived difference between the Co-Cured and the Black Aluminum design.

The first risk, which comes to mind, is the risk associated directly with production. In general, the argument is in favor of the less integrated design, since any potential mistakes during production affect less integrated and therefore less expensive parts. In addition, any production errors might be easier to repair, since the respective component could be simply exchanged for a good one. These are valid arguments and unfortunately, there is not enough information available to determine the probability and the economic impact of these risks. Qualitatively speaking, in the present example the potential benefits are simply not large enough to close the \$200K gap between the designs. According to the manufacturer their scrap and rework rate is relatively low when it comes to the wing skins and any problems can be fixed relatively quickly by simply replacing the flawed laminate and curing the part again.

The second major risk is the risk of part failure during operation. Aircraft producers generally prefer to rely on mechanical joints, since the fatigue and long-term behavior of adhesively joint components is not entirely investigated at this point. However, as the producers obtain more data and grow more confident about the use of adhesives and co-curing techniques, one would expect to see a trend pointing away from the use of fasteners. In connection with part failure also the issue of on-site repairs comes to mind. Here a more modular design potentially can simplify and therefore reduce costs when having to replace damaged structural components.

Finally, one can say, that the question whether to integrate or not can not be answered conclusively at this point. It appears each production situation has to be assessed individually in order to determine the economical optimum degree of integration. However, the developed cost models facilitate the evaluation and help to estimate the majority of the investment and production costs.

## 9.4 References

### Composite Manufacturing

- [1] Reinhart, T. J. (Ed.), "Engineered Materials Handbook – Composites", Vol. 1, ASM International, 1988.
- [2] Tsai, S. W., Springer, G. S., Enders, M. L., "The Fiber-Placement Process", ICCM 8, Composites, Vol. 2, Sections 12-21, p. 14B1-14B11.
- [3] Willden, K., et al. "Advanced Technology Composite Fuselage - Manufacturing", NASA Report CR-4735, 1997.
- [4] Mabson, G. E., Ilcewicz, L. B., et al., "Cost Optimization Software for Transport Aircraft Design Evaluation - Overview," NASA CR-4736, 1996.
- [5] Ilcewicz, L. B. et al., "Cost Optimization Software for Transport Aircraft Design Evaluation", NASA Report CR-4737, 1996.
- [6] Neoh, E. T. "Adaptive Framework for Estimating Fabrication Time", Ph.D Thesis, MIT, 1995.
- [7] Haffner, S. M., Gutowski, T. G., "Automated Cost Estimation for Advanced Composite Materials", NSF Conference, 1998.
- [8] Marin, T., Haffner, S. M., Gutowski, T. G. "Cost Elements of Autoclave Tooling", NSF Conference Paper, 2000.
- [9] Pas, J., Haffner, S. M., Gutowski, T. G. "Web Based Cost Estimation Model for Advanced Composites", NSF Conference Paper, 2001.
- [10] Moy, E. "Design Tradeoffs for Advanced Composite Manufacturing Using Cost Modeling", M.S. Thesis, MIT, 1997.
- [11] Kang, P. J., "A Technical and Economic Analysis of Structural Composite Use in Automotive Body-in-White Applications", M.S. Thesis, MIT, June 1998.
- [12] Truslow, S., "Permanent Press, No Wrinkles: Reinforced Double Diaphragm Forming of Advanced Thermoset Composites", M.S. Thesis, MIT, 2000.
- [13] Land, I. B., "Design and Manufacture of Advanced Composite Aircraft Structures using Automated Tow Placement", M.S. Thesis, MIT, 1996.
- [14] Beresheim, G. "Part Complexity Based Time Estimation Model for the ATP Process", MIT & IVW Report, 2001.

## Assembly

- [15] Northrop Grumman, Inc., <http://www.northgrum.com/>, Interviews with Steve Rice, January 2000.
- [16] Gorgias, A., "Economic Analysis of Assembly vs. Part Integration in Composite Manufacturing", M.S. Thesis, MIT & TU Munich, 2000.
- [17] Speller, T., "A Case Study of a Product Architecture", M.S. Thesis, SD&M, MIT, 2000.
- [18] Gemcor, Inc., <http://www.gemcor.com/>, Interviews with Tom Speller, March 2002.
- [19] Paul W. Marino Gages, Inc., <http://www.pmarginage.com/>, Interviews with Gene Vaughn, April 2002.
- [20] Kassapoglou, C., "Minimum Cost and Weight Design of Fuselage Frames. Part A: Design Constraints and Manufacturing Process Characteristics", Composites, Part A, Vol. 30, 1999, pp. 887-894.
- [21] Kassapoglou, C., "Minimum Cost and Weight Design of Fuselage Frames. Part B: Cost Considerations, Optimization, and Results", Composites, Part A, Vol. 30, pp. 895-904, 1999.
- [22] Redford, A., Chal, J., "Design for Assembly: Principles and Practice", McGraw-Hill, 1994.
- [23] Keeney, R. L., Raiffa, H., "Decisions with Multiple Objectives", John Wiley, 1976.
- [24] De Fazio, T., Whitney, D., Rhee, S., "A Design-Specific Approach to Design for Assembly (DFA) for Complex Mechanical Assemblies", Proc. IEEE International Symposium on Assembly and Task Planning, 1997.
- [25] Cunningham, T. W., "Chains of Function Delivery: A Role for Product Architecture in Concept Design", Ph.D. Thesis, MIT, 1998.
- [26] Mantripragada, R., "Assembly Oriented Design: Concepts, Algorithms and Computational Tools", Ph.D. Thesis, MIT, 1998.
- [27] Lee, D., Thornton, A., "The Identification and Use of Key Characteristics in the Product Development Process", Proceedings of the ASME Design Engineering Technical Conference, Irvine, CA, 1996.
- [28] Noton, B. "Cost Drivers and Design Methodology for Automated Airframe Assembly", 31<sup>st</sup> International SAMPE Symposium, 1986.
- [29] Noton, B. "Manufacturing Cost/Design Guide (MC/DG) for Metallic and Composite Structures", Battelle's Columbus Laboratories, American Institute of Aeronautics and Astronautics, 1981.

(This page is intentionally left blank.)

## 9.5 Appendix - Results & Discussion

### 9.5.1 Prices for Tooling & Equipment

**Table 9.39** Hourly Equipment Rates at Different Capital & Maintenance Costs

<i>Composite Production Equipment (including 10% Installation Costs)</i>	<i>Investment [\$]</i>	<i>Depreciation [years]</i>	<i>Monthly Avail. [hrs]</i>	<i>Hourly Rate [\$/hr]</i>	<i>Hourly Rate [\$/hr]</i>
Autoclave	470,000	7	400	23	34
Resin Transfer Molding	88,000	5	400	6	8
Automated Tow Placement	5,500,000	10	600	145	230
Pultrusion	330,000	7	400	16	24
Double Diaphragm Forming	150,000	7	400	7	11
Automatic Fastening System	1,500,000	10	400	59	94
Maintenance & Consumables				20%	30%
Opportunity Cost of Capital (APR)				10%	20%

**Table 9.40** Price of Production Tooling

<i>Composite Production Tooling</i>	<i>Size</i>	<i>Area</i>	<i>Price</i>	<i>Annual Costs</i>
Invar Curing Tool	120 x 24 x 12 in <sup>3</sup>	2,900 in <sup>2</sup>	\$30,000	\$ 9,397
RTM Mold	120 x 20 x 12 in <sup>3</sup>	2,400 in <sup>2</sup>	\$70,000	\$21,926
ATP Tool	120 x 24 x 12 in <sup>3</sup>	5,800 in <sup>2</sup>	\$60,000	\$18,794
Pultrusion Die	36 x 20 x 6 in <sup>3</sup>	720 in <sup>2</sup>	\$42,000	\$13,156
Forming Tool	120 x 24 x 12 in <sup>3</sup>	2,900 in <sup>2</sup>	\$13,000	\$ 4,072
Assembly Fixture	134 x 24 x 12 in <sup>3</sup>	3,200 in <sup>2</sup>	\$50,000	\$15,662
Maintenance	5%			
Depreciation [yrs]	5			
Opportunity Cost of Capital (APR)	15%			

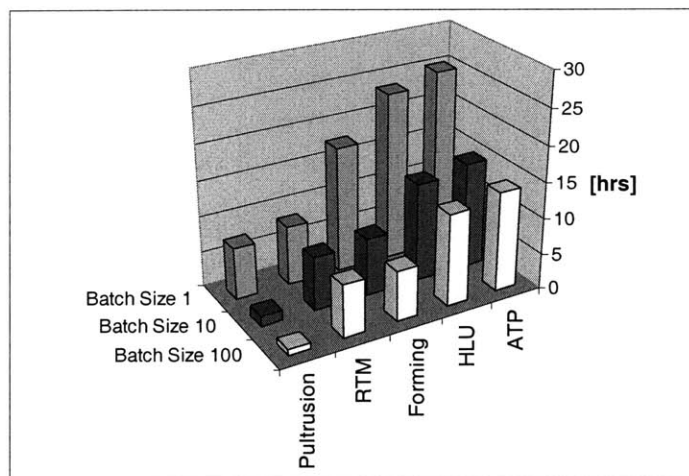


**Figure 9.36** Part Cycle Time

### 9.5.2 Hand Layup (HLU) - Manufacturing Data

**Table 9.41 Hand Layup Manufacturing Times & Performance**

<i>HLU Mfg. Time</i>	<i>Labor</i>	<i>Machine</i>	<i>Labor</i>	<i>Machine</i>	<i>Labor</i>	<i>Machine</i>	<i>Labor</i>	<i>Machine</i>
<i>[min]</i>	<i>Non-Rec.</i>	<i>Non-Rec.</i>	<i>Batch Size</i>	<i>Rec. 1</i>	<i>Batch Size</i>	<i>Rec. 10</i>	<i>Batch Size</i>	<i>Rec. 100</i>
Tool Setup	44	0	18	0	177	0	1,773	0
Material Setup	24	0	46	0	459	0	4,585	0
Layup	0	0	152	0	1,523	0	15,226	0
Debulk	1	0	371	0	3,709	0	37,089	0
Vacuum Bagging	23	0	78	0	783	0	7,826	0
Autoclave Setup	65	65	57	57	572	570	5,722	5,702
Cure	483	483	9	9	94	94	935	935
Finishing	12	0	31	0	313	0	3,133	0
Sum [hrs]	10.9	9.1	12.7	1.1	127.1	11.1	1,271.5	110.6
Overall Total [hrs]			23.6		138.0		1,282.4	
Per Part [hrs]			23.6		13.8		12.8	
Performance [lbs/hr]			0.8		1.3		1.4	

**Table 9.42 Hand Layup - Manufacturing Time Distribution**

<i>HLU Mfg. Time Distribution</i>			
<i>Batch Size</i>	<i>1</i>	<i>10</i>	<i>100</i>
Debulk	26%	45%	48%
Layup	11%	18%	20%
Vacuum Bagging	7%	10%	10%
Autoclave Setup	9%	8%	8%
Cure	35%	7%	2%
Material Setup	5%	6%	6%
Finishing	3%	4%	4%
Tool Setup	4%	3%	2%
Sum	100%	100%	100%



### 9.5.3 Resin Transfer Molding (RTM) - Manufacturing Data

**Table 9.43 RTM Tooling Costs**

<i>RTM Mold - Cost Summary</i>		
Design Costs	\$ 19,189	40%
Material Costs	\$ 12,842	27%
Manufacturing Costs	\$ 13,324	28%
Detailing Costs	\$ 2,617	5%
<b>Total Cost</b>	<b>\$ 47,972</b>	<b>100%</b>
<b>Estimated Price</b>	<b>\$ 68,531</b>	<b>30%</b>

**Table 9.44 RTM Manufacturing Times & Performance**

<i>RTM Mfg. Time</i>	<i>Labor</i>		<i>Machine</i>		<i>Labor</i>		<i>Machine</i>	
	<i>Non-Rec.</i>	<i>Non-Rec.</i>	<i>Batch Size</i>	<i>1</i>	<i>Batch Size</i>	<i>10</i>	<i>Batch Size</i>	<i>100</i>
<i>[min]</i>								
Tool Setup	8	0	15	0	153	0	1,531	0
Material Setup	2	0	12	0	124	0	1,236	0
Close Mold	15	15	40	40	401	401	4,013	4,013
Setup Machine	5	5	1	1	5	5	52	52
Inject & Cure	5	5	295	295	2,950	2,950	29,500	29,500
Demolding	12	12	43	43	426	426	4,258	4,258
Finishing	12	0	31	0	313	0	3,133	0
Sum [hrs]	1.0	0.6	7.3	6.3	72.9	63.0	728.7	630.4
Overall Total [hrs]			8.3		73.9		729.7	
<b>Per Part [hrs]</b>			<b>8.3</b>		<b>7.4</b>		<b>7.3</b>	
<b>Performance [lbs/hr]</b>			<b>2.2</b>		<b>2.5</b>		<b>2.5</b>	

**Table 9.45 RTM - Manufacturing Time Distribution**

<i>RTM Mfg. Time Distribution</i>			
<i>Batch Size</i>	<i>1</i>	<i>10</i>	<i>100</i>
Tool Setup	5%	4%	4%
Material Setup	3%	3%	3%
Close Mold	11%	9%	9%
Setup Machine	1%	0%	0%
Inject & Cure	60%	67%	67%
Demolding	11%	10%	10%
Finishing	9%	7%	7%
<b>Sum</b>	<b>100%</b>	<b>100%</b>	<b>100%</b>

### 9.5.4 Automated Tow Placement (ATP) - Manufacturing Data

**Table 9.46 ATP Tooling Costs**

<b>ATP Mold - Cost Summary</b>		
Design Costs	\$ 12,906	30%
Material Costs	\$ 12,046	28%
Manufacturing Costs	\$ 15,918	37%
Detailing Costs	\$ 2,151	5%
<b>Total Cost</b>	<b>\$ 43,023</b>	<b>100%</b>
<b>Estimated Price</b>	<b>\$ 61,462</b>	<b>30%</b>

**Table 9.47 ATP Manufacturing Times & Performance**

<b>ATP Mfg. Time</b>	<b>Labor</b>		<b>Machine</b>		<b>Labor</b>		<b>Machine</b>	
	<b>Non-Rec.</b>	<b>Non-Rec.</b>	<b>Batch Size</b>	<b>1</b>	<b>Batch Size</b>	<b>10</b>	<b>Batch Size</b>	<b>100</b>
<b>[min]</b>								
Tool Setup	84	84	15	0	154	0	1,535	0
Machine Setup	20	20	0	0	0	0	0	0
Material Setup	0	0	10	10	104	104	1,043	1,043
Layup	0	0	572	572	5,725	5,725	57,247	57,247
Part Handling	0	0	12	0	120	0	1,200	0
Part Protection	17	0	23	0	230	0	2,304	0
Vacuum Bagging	23	0	78	0	783	0	7,826	0
Autoclave Setup	65	65	57	57	572	570	5,722	5,702
Cure	483	483	9	8	94	81	935	806
Finishing	12	0	31	0	313	0	3,133	0
Sum [hrs]	11.7	10.9	13.5	10.8	134.9	108.0	1,349.1	1,080.0
Overall Total [hrs]			25.2		146.6		1,360.8	
<b>Per Part [hrs]</b>			<b>25.2</b>		<b>14.7</b>		<b>13.6</b>	
<b>Performance [lbs/hr]</b>			<b>0.7</b>		<b>1.3</b>		<b>1.4</b>	

**Table 9.48 ATP - Manufacturing Time Distribution**

<b>ATP Mfg. Time Distribution</b>	<b>1</b>	<b>10</b>	<b>100</b>
<b>Batch Size</b>			
Tool Setup	7%	3%	2%
Machine Setup	1%	0%	0%
Material Setup	1%	1%	1%
Layup	38%	65%	70%
Part Handling	1%	1%	1%
Part Protection	3%	3%	3%
Vacuum Bagging	7%	9%	10%
Autoclave Setup	8%	7%	7%
Cure	33%	7%	2%
Finishing	3%	4%	4%
<b>Sum</b>	<b>100%</b>	<b>100%</b>	<b>100%</b>

### 9.5.5 Pultrusion (PUL) - Manufacturing Data

**Table 9.49 Pultrusion Tooling Costs**

<i>Pultrusion Die - Cost Summary</i>		
Design Costs	\$ 11,653	40%
Material Costs	\$ 73	0%
Manufacturing Costs	\$ 15,817	54%
Detailing Costs	\$ 1,589	5%
<b>Total Cost</b>	<b>\$ 29,132</b>	<b>100%</b>
<b>Estimated Price</b>	<b>\$ 41,617</b>	<b>30%</b>

**Table 9.50 Pultrusion Manufacturing Times & Performance**

<i>Pultrusion Mfg. Time</i>	<i>Labor</i>		<i>Machine</i>		<i>Labor</i>		<i>Machine</i>	
<i>[min]</i>	<i>Non-Rec.</i>	<i>Non-Rec.</i>	<i>Rec.</i>	<i>Rec.</i>	<i>Rec.</i>	<i>Rec.</i>	<i>Rec.</i>	<i>Rec.</i>
			<i>Batch Size</i>	<i>1</i>	<i>Batch Size</i>	<i>10</i>	<i>Batch Size</i>	<i>100</i>
Machine Setup	232	232	0	0	0	0	0	0
Material Setup	60	60	0	0	0	0	0	0
Setup Resin Bath	5	5	1	1	5	5	52	52
Pultrusion	80	80	11	11	113	113	1,131	1,131
Finishing	12	0	31	0	313	0	3,133	0
Sum [hrs]	6.5	6.3	0.7	0.2	7.2	2.0	71.9	19.7
Overall Total [hrs]			7.2		13.7		78.4	
<b>Per Part [hrs]</b>			<b>7.2</b>		<b>1.4</b>		<b>0.8</b>	
<b>Performance [lbs/hr]</b>			<b>2.5</b>		<b>13.3</b>		<b>23.1</b>	

**Table 9.51 Pultrusion - Manufacturing Time Distribution**

<i>Pultrusion Mfg. Time Distribution</i>			
<i>Batch Size</i>	<i>1</i>	<i>10</i>	<i>100</i>
Finishing	10%	40%	67%
Machine Setup	54%	28%	5%
Pultrusion	21%	24%	26%
Material Setup	14%	7%	1%
Setup Resin Bath	1%	1%	1%
<b>Sum</b>	<b>100%</b>	<b>100%</b>	<b>100%</b>

### 9.5.6 Double Diaphragm Forming (DDF) - Manufacturing Data

**Table 9.52 DDF Manufacturing Times & Performance**

<i>Forming Mfg. Time</i>	<i>Labor</i>	<i>Machine</i>	<i>Labor</i>	<i>Machine</i>	<i>Labor</i>	<i>Machine</i>	<i>Labor</i>	<i>Machine</i>
<i>[min]</i>	<i>Non-Rec.</i>	<i>Non-Rec.</i>	<i>Batch Size</i>	<i>Rec. 1</i>	<i>Batch Size</i>	<i>Rec. 10</i>	<i>Batch Size</i>	<i>Rec. 100</i>
<i>Material &amp; Tool Setup</i>	49	49	23	23	235	235	2,349	2,349
<i>Layup</i>	0	0	152	0	1,523	0	15,226	0
<i>Machine Setup</i>	9	9	17	17	167	167	1,674	1,674
<i>Forming</i>	0	0	47	47	466	466	4,662	4,662
<i>Vacuum Bagging</i>	23	0	78	0	783	0	7,826	0
<i>Autoclave Setup</i>	65	65	57	57	572	570	5,722	5,702
<i>Cure</i>	483	483	9	8	94	81	935	806
<i>Finishing</i>	12	0	31	0	313	0	3,133	0
<i>Sum [hrs]</i>	10.7	10.1	6.9	2.5	69.2	25.3	692.1	253.2
<i>Overall Total [hrs]</i>			17.6		79.9		702.8	
<i>Per Part [hrs]</i>			17.6		8.0		7.0	
<i>Performance [lbs/hr]</i>			1.0		2.3		2.6	

**Table 9.53 DDF - Manufacturing Time Distribution**

<i>Forming Mfg. Time Distribution</i>	<i>Batch Size 1</i>	<i>Batch Size 10</i>	<i>Batch Size 100</i>
<i>Material &amp; Tool Setup</i>	7%	6%	6%
<i>Layup</i>	14%	32%	36%
<i>Machine Setup</i>	2%	4%	4%
<i>Forming</i>	4%	10%	11%
<i>Vacuum Bagging</i>	10%	17%	19%
<i>Autoclave Setup</i>	12%	13%	14%
<i>Cure</i>	47%	12%	3%
<i>Finishing</i>	4%	7%	7%
<i>Sum</i>	100%	100%	100%

### 9.5.7 Assembly - Manufacturing Data

**Table 9.54 Assembly Production Time (incl. Component Production)**

<i>Time per Part [hrs]</i>	<i>Batch Size 1</i>	<i>Batch Size 10</i>	<i>Batch Size 100</i>
<b>Mech.</b>	50	31	29
<b>Co-Bond</b>	47	28	27
<b>Co-Cure</b>	35	25	24

### 9.5.8 Co-Cure - Manufacturing Data

**Table 9.55 Co-Curing Costs w/o Tooling**

<i>Co-Curing Costs</i>			
<i>Batch Size</i>	<i>1</i>	<i>10</i>	<i>100</i>
Material	\$ 1,699	\$ 16,990	\$ 169,900
Labor	\$ 3,466	\$ 24,912	\$ 239,367
Machine	\$ 294	\$ 582	\$ 3,462
<b>Unit Costs (\$/part)</b>	<b>\$ 5,459</b>	<b>\$ 4,248</b>	<b>\$ 4,127</b>
<b>Tooling</b>	<b>\$ 30,000</b>		

### 9.5.9 Mechanical Assembly - Manufacturing Data

**Table 9.56 Mechanical Assembly Cycle Time (incl. Component Production)**

<i>Mech. Assembly Mfg. Time</i>			
<i>Batch Size</i>	<i>1</i>	<i>10</i>	<i>100</i>
Non-Recurring	1,316	1,316	1,316
Recurring	1,713	17,128	171,280
Labor [min]	3,029	18,444	172,596
Labor per Set [hrs]	50.5	30.7	28.8

**Table 9.57 Mech. Assembly - Time Distribution (w/o Component Production)**

<i>Mech. Assembly Process Plan</i>	<i>Distribution</i>
Setup Assembly	2.2%
Load Parts	16.6%
Shimming	60.9%
Drilling	5.3%
Install Fasteners	8.7%
Unload Assembly	6.3%
<b>Total</b>	<b>100%</b>

**Table 9.58 Mech. Assembly Costs (w/o Component Costs)**

<i>Mech. Assembly Costs</i>			
<i>Batch Size</i>	<i>1</i>	<i>10</i>	<i>100</i>
Components	\$ -	\$ -	\$ -
Material	\$ 1,101	\$ 11,010	\$ 110,100
Labor	\$ 1,582	\$ 5,828	\$ 48,293
Machine	\$ -	\$ -	\$ -
<b>Unit Costs [\$/part]</b>	<b>\$ 2,683</b>	<b>\$ 1,684</b>	<b>\$ 1,584</b>
Fixturing	\$ 50,000		

### 9.5.10 Adhesive Bonding - Manufacturing Data

**Table 9.59 Adhesive Bonding Cycle Time (incl. Component Production)**

<i>Co-Bonding Mfg. Time</i>			
<i>Batch Size</i>	<i>1</i>	<i>10</i>	<i>100</i>
Non-Recurring	1,259	1,259	1,259
Recurring	1,582	15,820	158,200
Labor [min]	2,841	17,079	159,459
Labor per Set [hrs]	47.4	28.5	26.6

**Table 9.60 Adhesive Bonding - Time Distribution (w/o Component Production)**

<i>Aggregated Process Plan</i>	<i>Distribution</i>
Setup Assembly	3.2%
Load Parts	24.3%
Surface Preparation	13.4%
Adhesive Bonding	49.9%
Unload Assembly	9.2%
<b>Total</b>	<b>100%</b>

**Table 9.61 Adhesive Bonding Costs (w/o Component Costs)**

<i>Co-Bonding Costs</i>			
<i>Batch Size</i>	<i>1</i>	<i>10</i>	<i>100</i>
Components	\$ -	\$ -	\$ -
Material	\$ 3	\$ 32	\$ 317
Labor	\$ 1,269	\$ 3,553	\$ 26,398
Machine	\$ -	\$ -	\$ -
<b>Unit Costs [\$ /part]</b>	<b>\$ 1,272</b>	<b>\$ 359</b>	<b>\$ 267</b>
<b>Fixturing</b>	<b>\$ 50,000</b>		

9.5.11 Horizontal Stabilizer - Component Manufacturing Data

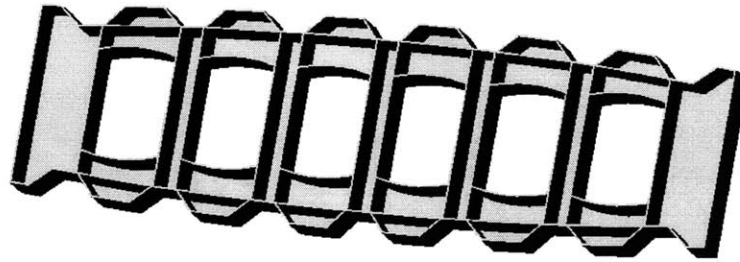


Figure 9.37 Schematic of an Aluminum Rib

Table 9.62 Manufacturing Time Distribution

Step	Description	Labor [hrs]	Distrib.
1	Skin Mfg.	216	57%
2	Hat-Stringer Mfg.	98	26%
3	US Inspection	32	8%
4	Autoclave Cure	20	5%
5	Loading parts	9.63	3%
6	Trimming	2.96	1%
7	Locator Holes	0.35	0%
	<b>Total</b>	<b>378.9</b>	<b>100%</b>

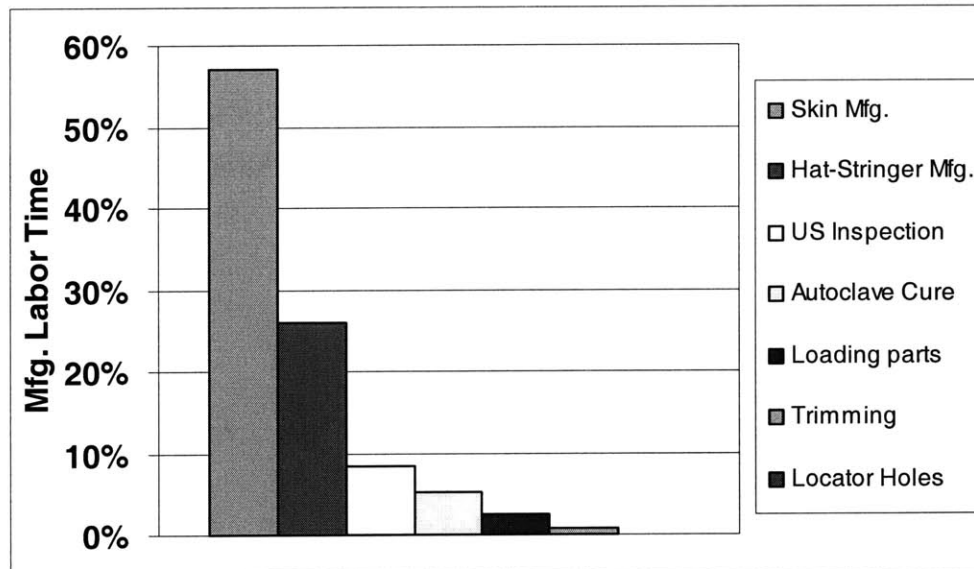


Figure 9.38 Time Driver – Component Production



9.5.12 Co-Cured Stabilizer - Assembly Data

Table 9.63 Co-Cured Design: Assembly Time Distribution

Step	Description	Labor [hrs]	Distrib.
1	Fasten Bolts & Rivets	35.5	63%
2	Drill Fastener Holes	11.8	21%
3	Apply Liquid Shim & Cure	4.0	7%
4	Load & Unload Skins	2.3	4%
5	Load Ribs into Fixture	1.9	3%
6	Load Front & Rear Spar	1.2	2%
	<b>Total</b>	<b>56.7</b>	<b>100%</b>

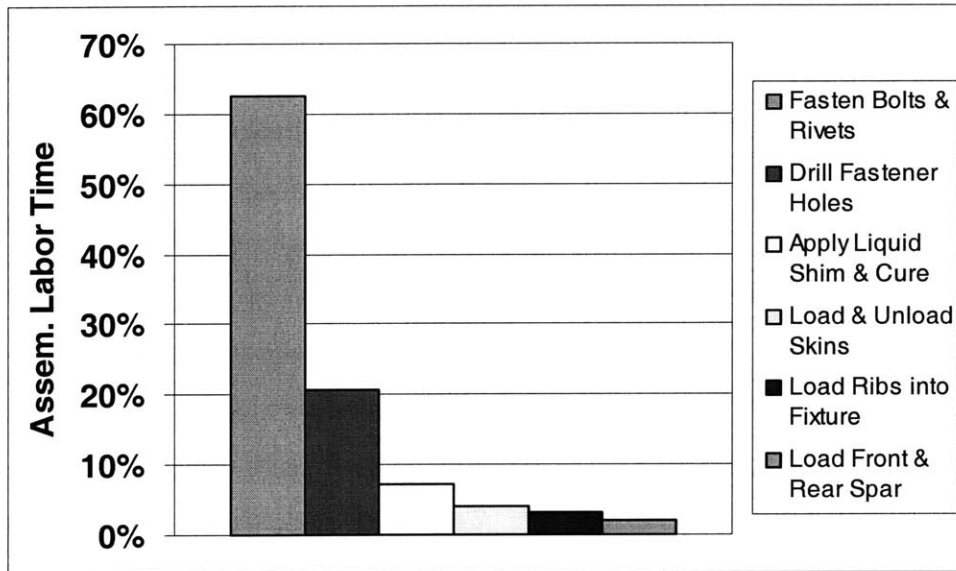


Figure 9.39 Co-Cured Design: Time Driver – Assembly

9.5.13 Black Alu Design - Assembly Data

Table 9.64 Black Alu Design: Assembly Time Distribution

Step	Description	Labor [hrs]	Distrib.
1	Fasten Bolts & Rivets	196.1	68%
2	Drill Fastener Holes	55.8	19%
3	Apply Liquid Shim & Cure	20.6	7%
4	Load Stringers	9.6	3%
5	Load & Unload Skins	2.9	1%
6	Load Ribs & Stringers	1.9	1%
7	Load Front & Rear Spar	1.2	0%
	<b>Total</b>	<b>288.1</b>	<b>100%</b>

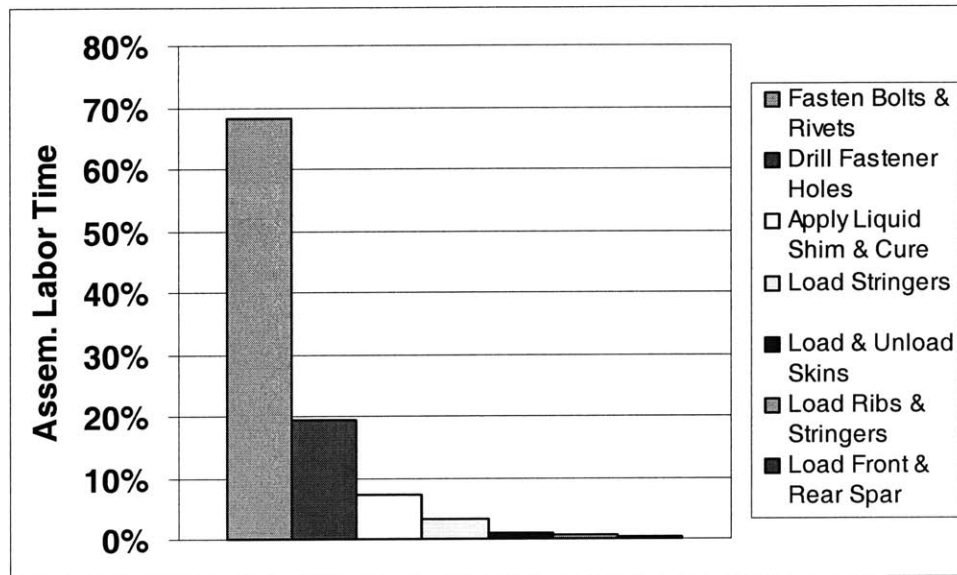
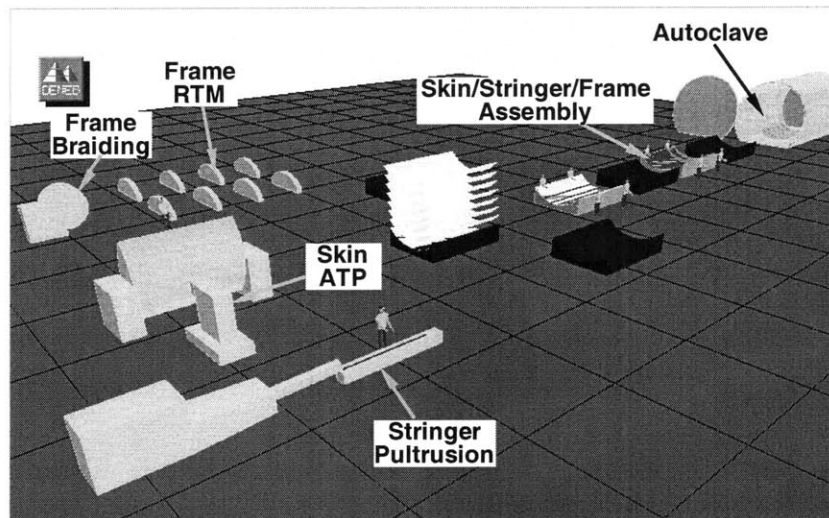


Figure 9.40 Black Alu Design: Time Driver – Assembly

## 10 Conclusions & Outlook

The results of this study further stress the importance of viable cost data to assess the economics of composite designs. In particular, cost models, which are sensitive to part size and geometry, facilitate the evaluation of the numerous trade-off scenarios between product design, process performance, and investment requirements. The analysis of the cost effectiveness of the most common composite manufacturing processes in terms of their material, labor, tooling and equipment costs certainly assists managers and engineers in their effort to reduce costs. Cost reduction is still an issue facing the composite industry today. Cost in connection with performance essentially drives the substitution of conventional materials with composites and therefore determine the success of the industry.



**Figure 10.1** Production Layout for Composite Aircraft Production

Composite materials are however inherently complex due to their non-isotropic nature. Composites even derive some of their superior performance from these non-isotropic properties. Consequently, the processes have to control the Anisotropy at some point during production and are thus more time consuming than their traditional counterparts. The industry has responded to this economic challenge with the introduction of increased process automation and part integration, in an attempt to speed up production and lower

the labor content. The study shows how the higher investments associated with automation can lead to eventual cost savings at high production volumes. The cost savings achievable through the integration of parts are probably only limited by the over proportionally increasing tooling costs and the growing inflexibility to react to changes in customer preferences and design. The question is, if these two major cost reduction efforts are able to close the cost gap between conventional materials and advanced composites. The sustainability is certainly questionable, since general advances in automation technology and part reduction strategies also trickle through to conventional metal working or plastic processes.

However, as the composite industry is attempting to close the cost gap, producers of conventional materials are vowing to catch up with the unparalleled performance of composites. The high specific strength and stiffness of advanced composites is their real competitive advantage. It allows the construction of products at equal performance but only at a fraction of the current weight. Therefore, one has to identify products where these weight savings yield potential economic benefits in order to justify the higher production costs. In general, opportunities for composites exist, where the higher costs during production and possibly during disposal are offset by cost savings during their useful life. When taking a system's wide approach, the use of composites in cars, and airplanes can definitely lead to net savings over the life span of the product. However, in contrast to airlines, customers of the car industry so far have been reluctant to accept an increase in vehicle prices for potential long term cost savings. It would actually be interesting to find out what return would consumers demand to accept the presently higher price.

Many of the raised issues are still not answerable definitively and remain the subject future studies. However, the present research provides tools, which help to evaluate each production situation individually and draw the necessary conclusions.

The large amount of feedback, which was received from industry and academia through the WEB interface of the cost model, certainly proves the strong interest to understand the overall cost implications of composite materials. As expected, smaller and medium

sized companies who do not possess the internal resources to develop their own cost models were primarily interested in the manufacturing cost models. Among the users is are part suppliers to the automotive industry (e.g. Venture Global Industries). They and others received a copy of our software so they can adopt the models to their own processes. Also a few management consulting companies (e.g. A.T. Kearney) used the WEB model to better understand the processes and the various correlation between costs and design. Large producers of aerospace technology (e.g. Lockheed Martin & Loral) who already have proprietary cost models in place were intrigued by the potentials of the 4 tooling cost models. Traditionally, tooling production has always been left to outside suppliers and therefore their costs are not commonly understood. Students and other members of academia frequently use the model to test the economic viability of their designs and concept studies.

Of course, in hindsight, one would always do a few things differently. The programming of the WEB model in its current form required considerable resources to create. However, the use of JavaScript and HTML makes it difficult for users unfamiliar with the code to adapt the model to different scenarios. Possibly a model, which is solely based on Excel spreadsheets but also available on the WEB would have been even more successful. It also would have freed up much needed manpower for the very difficult and time consuming process of collecting information and conducting case studies.

Overall however, the first publicly available and comprehensive cost library for the production of composites has been received positively.